# A Study of the Anatomy and Physiology of Sleep in the Rock Hyrax, *Procavia capensis*.

Nadine GRAVETT

This thesis is submitted in fulfilment of the requirements for the degree of Doctor of Philosophy

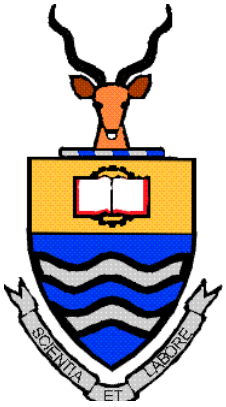


SCHOOL OF ANATOMICAL SCIENCES
UNIVERSITY OF THE WITWATERSRAND

**JOHANNESBURG**

**July, 2011**

**DECLARATION**

I declare that this thesis is my own unaided work. It is being submitted for the Degree of Doctor of Philosophy in the University of the Witwatersrand, Johannesburg. It has not been submitted before for any degree or examination in any other University.

_____

(Signature of candidate)

_____day of_____2011

**ABSTRACT**

The rock hyrax, *Procavia capensis*, is a social diurnal mammal that typically lives in colonies on rocky outcrops and is found throughout most parts of Southern Africa. The aim of this thesis was to describe the sleep phenomenology of the rock hyrax. By means of immunohistochemistry the location and distribution of the cholinergic, catecholaminergic, serotonergic, orexinergic, histaminergic, and the GABAergic systems were described. For the most part these systems and their terminal network distributions followed the general mammalian organisational plan; however, several features, potentially unique to the rock hyrax, were found. These include the presence of cholinergic neurons in the AD and AV nuclei of the dorsal thalamus, parvo- and magnocellular divisions of the cholinergic LDT and PPT nuclei. A dense orexinergic terminal network distribution was noted in the regions coincident with the AD nucleus, a feature only observed in other diurnal mammals. Parvalbumin neurons did not show any association to the sleep related nuclei, whereas calbindin and calretinin neurons were found in all sleep related areas, though with differing densities and some homogeneities. The physiological measurable parameters of sleep were recorded continuously for 72 h under both solitary and social conditions and compared to determine whether differences existed. The results revealed that no major differences existed between the social and solitary conditions, but sleep intensity and REM duration (particularly REM0) was more pronounced in the social condition. REM was ambiguous in these animals, and led to its subdivision into REM1 and REM0. It is possible that REM1 could be a form of low voltage slow wave sleep, but further investigation is required. If REM1 is a form of NonREM sleep it would imply that the rock hyrax has the lowest amount of REM sleep of any terrestrial mammal studied to date.

**ACKNOWLEGEMENTS**

I would like to take this opportunity to thank my PhD supervisor Prof Paul Manger; it has been a huge honour and privilege working with you for the last five years. I will forever be grateful for all your invaluable advice, guidance and the opportunities you presented me with. It has been an awesome five years, thank you for everything you have done, your support, encouragement and fantastic attitude. It has been an unforgettable journey. Thank you.

To my colleagues and partners in crime, Bugz, Jillani, Constance and Nina, it has been an honour to know and work with you guys. Thank you for all your support and encouragement through the crazy times. May you all be very successful in all you future endeavours. It has been fun.

Thank you, Prof. Jerome Siegel and Dr. Oleg Lyamin, from UCLA, USA for your support, invaluable advice and guidance in the understanding and analysis of the sleep physiology.

Thank you, Prof Kjell Fuxe, for your enthusiasm, assistance and advice in analysing the immunohistochemistry.

Thank you Mr. Jason Hemingway for you assistance with the statistical analysis.

Thanks to Mrs. Christopher Gravett, Simon Perry and Adhil Bhagwandin for their help with the capturing of the hyraxes.

Thank you to Dr. Wim de Wet and the staff of Klein Kariba, Mrs. Andre Momberg, Conrad Momberg and the Labuschagne's for allowing and helping with the capture of hyraxes.

Thank you to the staff of the School of Anatomical Sciences, University of the Witwatersrand, Johannesburg, for all the technical and administrative support.

Lastly, thanks to the staff of the Central Animal Services, University of the Witwatersrand, Johannesburg, for the surgical and technical support.

## DEDICATION

**This thesis is dedicated in loving memory to my dearest uncle, Willie Nortje**

**My Mom (Connie), Dad (Keith) and Brother (Christopher).**

Thank you for all your support, love, guidance and encouragement but most of all thank you for never allowing me to quit and believing in me. Everything I am today is a direct result of your hard work and sacrifices. No amount of words could ever describe how much I appreciate everything you have done for me. I love you with all my heart and more than you would ever be able to comprehend. I could not have asked for a better family. I am truly blessed!

To my family, my grannies, uncles, aunts and cousins. Thank you for your support, interest and love. I love you all.

To Simon Perry, thank you for all your support, help and words of encouragement. You mean the world to me and I love you with all my heart.

To my dear friend, Adhil Bhagwandin, you have surely made the last four years interesting to say the least. Thank you for all your help, support, and encouragement. Most importantly thank you for being such an awesome friend. You have made this a journey that I will never forget.

# CONTENTS


DECLARATION ii

ABSTRACT iii

ACKNOWLEDGMENTS iv

DEDICATION vi

**Chapter 1: Introduction**

1.1. The rock hyrax, *Procavia capensis*: An overview 1

1.2. The sleep phenomenology of the rock hyrax, *Procavia capensis* 2

1.3. Specific aims 5

1.4. Individual chapters 6

1.4.1. Chapter 2 6

1.4.2. Chapter 3 7

1.4.3. Chapter 4 8

1.4.4. Chapter 5 9

1.4.5. Chapter 6 10

**Chapter 2: Nuclear organization and morphology of cholinergic, putative catecholaminergic and serotonergic neurons in the brain of the rock hyrax, *Procavia capensis***

2.1. Introduction 11

2.2. Materials and Methods 13

2.3. Abbreviations 17

2.4. Results 22

2.4.1. Cholinergic neurons 22

2.4.1.1. Striatal cholinergic interneurons 23

2.4.1.1.1. Nucleus accumbens 23

2.4.1.1.2. Dorsal striatopallidal complex – caudate/putamen globus pallidus 23

2.4.1.1.3. Islands of Calleja and olfactory tubercle 24

2.4.1.2. Cholinergic nuclei of the basal forebrain 25

2.4.1.2.1. Medial septal nucleus 25

2.4.1.2.2. Diagonal band of Broca 25

2.4.1.2.3. Nucleus basalis 26

2.4.1.3. Diencephalic cholinergic nuclei 26

2.4.1.3.1. Medial habenular nucleus 26

2.4.1.3.2. Hypothalamic cholinergic nuclei 27

2.4.1.3.3. Cholinergic neurons in the anterodorsal and anteroventral dorsal thalamic nuclei 27

2.4.1.4. Pontomesencephalic nuclei 28

2.4.1.4.1. Parabigeminal nucleus 28

2.4.1.4.2. Pedunculopontine tegmental nucleus (PPT) – magnocellular and parvocellular nuclei 29

2.4.1.4.3. Laterodorsal tegmental nucleus (LDT) – magnocellular and parvocellular nuclei 30

2.4.1.5. Cholinergic cranial nerve motor nuclei 31

2.4.2. Putative catecholaminergic nuclei 33

2.4.2.1. Olfactory bulb (A16) 34

2.4.2.2. Diencephalic nuclei 34

2.4.2.3. Midbrain nuclei 35

2.4.2.3.1. Ventral tegmental area nuclei (VTA, A10 complex) 35

2.4.2.3.2. Substantia nigra nuclear complex (A9) 37

2.4.2.3.3. Retrorubral nucleus (A8) 38

2.4.2.4. Pontine nuclei – the locus coeruleus (LC) nuclear complex 38

2.4.2.4.1. Medullary nuclei 40

2.4.3. Serotonergic nuclei 41

2.4.3.1. Rostral cluster 42

2.4.3.1.1. Caudal linear nucleus (CLi) 42

2.4.3.1.2. Supralemniscal nucleus (B9) 42

2.4.3.1.3. Median raphe (MnR) 43

2.4.3.1.4. Dorsal raphe nuclear complex (DR) 43

2.4.3.2. Caudal cluster 45

2.4.3.2.1. Raphe magnus nucleus (RMg) 45

2.4.3.2.2. Rostral and caudal ventrolateral serotonergic medullary columns (RVL and CVL) 45

2.4.3.2.3. Raphe pallidus nucleus (RPa) 46

2.4.3.2.4. Raphe obscurus nucleus (ROb) 46

2.5. Discussion 72

2.5.1. Cholinergic neurons in the anterodorsal (AD) and anteroventral (AV) nuclei of the dorsal thalamus of the rock hyrax 73

2.5.2. Magnocellular and parvocellular divisions/nuclei of the pedunculopontine and laterodorsal tegmental nuclei in the rock hyrax 74

2.5.3. Increased numbers of preganglionic cholinergic neurons in the inferior salivatory nucleus (pIX) of the rock hyrax 77

2.5.4. Lack of TH+ neurons in compact locus coeruleus (A6c) and decreased numbers of TH+ neurons in the locus coeruleus proper (A6d) of the rock hyrax 77

2.5.5. Evolutionary and phylogenetic considerations 79

**Chapter 3: Distribution of orexin-A immunoreactive neurons and their terminal networks in the brain of the rock hyrax, *Procavia capensis***

3.1. Introduction 81

3.2. Materials and Methods 84

3.3. Abbreviations 87

3.4. Results 91

3.4.1. Orexin-A neuronal cell body distribution 91

3.4.2. Orexin-A terminal network distribution 93

3.4.2.1. Telencephalon 93

3.4.2.2. Diencephalon 93

3.4.2.3. Midbrain and Pons (Mesencephalon and Metencephalon) 94

3.4.2.4. Medulla Oblongata (Myelencephalon) 95

3.5. Discussion 110

3.5.1. Orexinergic neuronal distribution 110

3.5.2. Orexinergic terminal network distribution 113

3.5.3. Orexinergic innervation of the anterodorsal nucleus of the dorsal thalamus and diurnality? 115

**Chapter 4: Solitary sleep in the rock hyrax, *Procavia capensis***

4.1. Introduction 117

4.2. Materials and Methods 119

4.2.1. Surgical Procedure 120

4.2.2. Sleep recording 121

4.2.3. Data analysis 122

4.3. Results 124

4.3.1. Physiological Data – State Definitions 125

4.3.1.1. Total state times 126

4.3.1.2. Number of episodes 127

4.3.1.3. Duration of episodes 128

4.3.1.4. REM periodicity and slow wave activity (SWS) 129

4.3.2. Behavioural Data 130

4.4. Discussion 159

4.4.1. Comparison to previous sleep studies in Hyraxes 162

4.4.2. Comparison to sleep in other Afrotheria, Xenarthra and other mammals 162

**Chapter 5: Social contrasted with solitary sleep patterns in the rock hyrax, *Procavia capensis***

5.1. Introduction 168

5.2. Materials and Methods 170

5.2.1. Surgical Procedure 171

5.2.2. Sleep recording 172

5.2.3. Data analysis 173

5.3. Results 175

5.3.1. Physiological Data 176

5.3.1.1. Total state times 177

5.3.1.2. Number of episodes 179

5.3.1.3. Duration of episodes 180

5.3.1.4. REM periodicity and slow wave activity (SWA) 182

5.3.2. Behavioural Data 183

5.4. Discussion 208

5.4.1. Sleep fragmentation in the social condition 209

5.4.2. Reduced sleep quotas, but better sleep quality in the social condition? 211

5.4.3. The effects of social sleeping in the rock hyrax 213

**Chapter 6: The interrelations of the distribution of sleep associated nuclei and terminal networks in the brain of the rock hyrax, *Procavia capensis***

6.1. Introduction 215

6.2. Materials and Methods 218

6.3. Abbreviations 221

6.4. Results 227

6.4.1. Cholinergic nuclei 227

6.4.2. Catecholaminergic nuclei 230

6.4.3. Serotonergic nuclei 231

6.4.4. Orexinergic nuclei 233

6.4.5. Serotonergic terminal networks related to the sleep-wake nuclei 233

6.4.6. Orexinergic terminal networks related to the sleep-wake nuclei 234

6.4.7. Histaminergic terminal networks related to the sleep-wake nuclei 235

6.4.8. GABAergic inhibitory interneurons related to the sleep-wake nuclei 236

6.4.8.1. GABAergic interneurons and the cholinergic system 237

6.4.8.2. GABAergic interneurons and the catecholaminergic system 239

6.4.8.3. GABAergic interneurons and the serotonergic system 239

6.4.9.4. GABAergic interneurons and the orexinergic system 240

6.5. Discussion 269

6.5.1 The unique cholinergic and orexinergic features of the hyrax brain 269

6.5.2 GABAergic interneurons, functional aspects of relevance 270

6.5.3 GABAergic neurons and the anterior thalamic nuclei 271

6.5.4 GABAergic neurons and the pontine cholinergic nuclei 272

6.5.5 GABAergic neurons and the locus coeruleus complex 273

6.5.6 GABAergic neurons and the serotonergic dorsal raphe complex 274

6.5.7 Summary 275

**Chapter 7: Concluding Remarks**

7.1. Conclusion 276

7.2. The way forward 281

**8. References**

8.1. Chapter 1 283

8.2. Chapter 2 287

8.3. Chapter 3 297

8.4. Chapter 4 309

8.5. Chapter 5 315

8.6. Chapter 6 319

8.7. Chapter 7 325

**Outputs form Thesis** 329

**List of figures**


**Figure 2.1:** Photographs of the rock hyrax brain 48

**Figure 2.2:** Diagrams of coronal sections through the rock hyrax brain 50

**Figure 2.3:** Diagrams of sagittal section through the rock hyrax brain 54

**Figure 2.4:** Photomicrographic montage of the basal forebrain 56

**Figure 2.5:** Photomicrographs of cholinergic nuclei 58

**Figure 2.6:** Photomicrographs of cholinergic nuclei 60

**Figure 2.7:** Photomicrographs of cholinergic nuclei 62

**Figure 2.8:** Photomicrographs of catecholaminergic nuclei 64

**Figure 2.9:** Photomicrographic montage of catecholaminergic nuclei 66

**Figure 2.10:** Photomicrographic montage of serotonergic nuclei 68

**Figure 2.11:** Photomicrographs of serotonergic nuclei 70

**Figure 3.1:** Diagrams of coronal sections through the rock hyrax brain 96

**Figure 3.2:** Photomicrograph montage of the hypothalamus 100

**Figure 3.3:** Photomicrographs of orexinergic nuclei 102

**Figure 3.4:** Photomicrographs of orexinergic terminal networks 104

**Figure 3.5:** Photomicrographs of orexinergic terminal networks 106

**Figure 3.6:** Photomicrographs of orexinergic terminal networks 108

**Figure 4.1:** Examples of EEG and EMG polygraphs 131

**Figure 4.2:** EEG and EMG polygraphs demonstrating the transitions 133

**Figure 4.3:** Scatter plots of instantaneous heart rate (IHR) 135

**Figure 4.4:** Diagram illustrating the spectral power of states 137

**Figure 4.5:** Hypnograms showing transitions occurring over a 24 h 139

**Figure 4.6:** Hypnograms showing transitions occurring over a 24 h 141

**Figure 4.7:** State transition probabilities 143

**Figure 4.8:** Histograms of total time spent in each physiological state 145

**Figure 4.9:** Histograms depicting REM periodicity 149

**Figure 4.10:** Slow wave activity for the 72 h recording period 151

**Figure 4.11:** Histograms of total time spent in each behavioural state 153

**Figure 5.1:** Diagram illustrating the spectral power of states 186

**Figure 5.2:** State transition probabilities 188

**Figure 5.3:** Histograms of total time spent in each physiological state 190

**Figure 5.4:** Histograms depicting REM periodicity 194

**Figure 5.5:** Slow wave activity for the 72 h recording period 196

**Figure 5.6:** Histograms of total time spent in each behavioural state 198

**Figure 5.7:** Hypnograms showing transitions occurring over a 24 h 200

**Figure 5.8:** Hypnograms showing transitions occurring over a 24 h 202

**Figure 6.1:** Diagrams of coronal sections through the rock hyrax brain 241

**Figure 6.2:** Photomicrographs of serotonergic terminal networks 249

**Figure 6.3:** Photomicrographs of orexinergic terminal networks 251

**Figure 6.4:** Photomicrographs of histaminergic terminal networks 253

**Figure 6.5:** Photomicrographs of GABAergic neurons 255

**Figure 6.6:** Photomicrographs of the anterior thalamic nuclei 257

**Figure 6.7:** Photomicrographs of GABAergic neurons 259

**Figure 6.8:** Photomicrographs of GABAergic neurons 261

**Figure 6.9:** Photomicrographs of GABAergic neurons 263

**Figure 6.10:** Photomicrographs of GABAergic neurons 265

## LIST OF TABLES

**Table 4.1:** Total wake, sleep and REM times as a percentage of 24 hours for each individual animal as well as the species mean for the solitary condition. 155

**Table 4.2:** Illustration of where statistically significant differences ($p<0.05$) were noted between the three recording days for each state with regards to the number of epochs, episodes and episode duration for each individual animal as well as for the group for the solitary condition. 157

**Table 5.1:** Total wake, sleep and REM times as a percentage of 24 hours for each individual animal as well as the species mean for the social condition 204

**Table 5.2:** Illustration of where statistically significant differences ($p<0.05$) were noted between the three recording days for each state with regards to the number of epochs, episodes and episode duration for each individual animal as well as for the group for the social condition. 206

**Table 6.1:** Illustration of different the degrees of GABAergic neuronal and terminal network distribution in relation to the nuclei of the cholinergic, catecholaminergic, serotonergic and orexinergic systems associated with the sleep-wake cycle. 267

# Chapter 1

# Introduction

## 1.1. The rock hyrax, *Procavia capensis*: An overview on the evolutionary history, ecology and behaviour

The rock hyrax belongs to the cohort Afrotheria that consists of Proboscidea (elephant), Sirenia (manatee and dugong), Hyrocoidea (hyracoids), Macroscelidea (elephant shrew), Tubulidentata (aardvark), and Tenrecoidea (tenrecs and golden mole) (Rübsamen *et al.*, 1982; Kleinschmidt *et al.*, 1986; Carter and Enders, 2004; Greenwood *et al.*, 2004; Hakeem *et al.*, 2005; Kellogg *et al.*, 2007; Tabuce, 20008). The rock hyrax is a member of the Procavidea family, which is the only living family within the Hyracoidea order (Bothma, 1971; Skinner and Smithers, 1990). The family consists of five different species grouped into three distinct genera; *Procavia capensis* (rock hyrax, one species), *Heterohyrax* (bush hyrax, one species) and *Dendrohyrax* (tree hyrax, three species) (Hoeck, 2010). According to the fossil record the appearance of the Afrotheria dates back to the Cretaceous with the origin of the Hyrocoidea order older than the early Eocene. The fossil record also suggests that this order dominated the Afro-Arabian continent as the most diverse herbivores (Tabuce, 2008).

The rock hyrax is a small, agile, diurnal, herbivorous mammal that typically inhabits rocky outcrops or “koppies”, and they are widely distributed throughout Africa (Skinner and Chimimba, 2005; Hoeck, 2010). The average weight of the rock hyrax varies between 1.5 to 5.6 kg and they are not considered to be sexually dimorphic in terms of body mass, as body mass appears to be closely correlated to annual precipitation

(Klein and Cruz-Uribe, 1996). Morphological characteristics of the rock hyrax include: rubbery plantigrade feet with abundant sweat glands, long vibrissae distributed across the body surface, a dorsal gland surrounded by a creamy-yellowish or black circle of hair, tusk-like upper incisors, complex digestive system, abdominal testes in males and a duplex uterus in females. A low metabolic rate and a poor ability to regulate body temperature are some of the physiological characteristic associated with the rock hyrax (Hoeck, 2010).

Rock hyraxes are social animals and typically live in colonies consisting of four to sixty individuals (Olds and Shoshani, 1982; Bothma, 1971; Skinner and Smithers, 1990). Depending on the size of the rocky outcrop these colonies can consist of more than one family group. Each family group consists of one territorial male, peripheral males, dispersing males, three to seven related females, and juveniles of both sexes (Hoeck, 2010). Sexual maturity is reached between 28 to 29 months in males and 16 to 17 months in females, with seasonal mating being triggered by the photoperiod (Skinner and Chimimba, 2005). The average gestation period and number of offspring is 7.5 months and 1 to 4 respectively. Common predators of the rock hyrax include eagles, leopards, jackals and snakes (Hoeck, 2010).

### 1.2. The sleep phenomenology of the rock hyrax, *Procavia capensis*

Many studies deal with the evolutionary history, ecology and behavior of the hyrax, but when it comes to the anatomy of the brain and the associated sleep phenomenology, very little previous data is available. Previous studies that have focused on the hyrax brain have been more comparative than specific. The hyrax brain has been classified as

being macrosmatic (Hoffmeister, 1967) and from a comparative point it has been found to be similar to those of ungulates (Flower and Lydekker, 1891). Furthermore, comparative studies between the hyrax and their relatives, elephants, have revealed that both these animals have a surprisingly large hippocampus, perhaps associated with a good memory and higher cognitive functions (Hakeem *et al.*, 2005); however, a large void is still apparent in our understanding of the anatomy and associated physiology of the hyrax brain, particularly the structures involved in the production of the sleep-wake cycle. A study by Snyder in 1974 on sleep in Hyracoidea revealed that sleep in the rock could be classified as being polycyclic, that is when periods of sleep and waking are constantly interchanging with one another. The study revealed that the amount of paradoxical and transitional sleep most closely resembled those of other small vegetarian mammals and ungulates respectively. There was also no significant difference in the distribution of the different sleep stages during the day and night however the study did note that feeding predominantly took place during the night. A study by Sherwood et al. (2009) describing the neocortical distribution and morphology of calbindin, calretinin, and parvalbumin interneurons in the atlantogenatans - which the rock hyrax is a member of – in general, reported that calretinin interneurons were less common in the neocortex compared to calbindin and parvalbumin. The study also concluded that extant afrotherians showed similar morphologies to the stem eutherian mammal in contrast to other lineages that favour a larger number of derived traits.

The study of mammalian sleep evolution has sparked several debates and theories. Many theories are centered on phylogeny, and claim that below the class level sleep phenomenology may be constrained in its evolution, while others believe that this sleep

phenomena is purely adaptive brought about by specific selection pressures. However, a larger number of these studies on which the theories are based either focus on major phylogenetic transitions (e.g. Kavanau *et al*., 2002; Nicolau *et al*., 2000) or on phylogenetic unusual forms (e.g. Rattenborg *et al*., 2000; Lyamin et al., 2008) and while the adaptive theory might sound appealing it has been found that the factors (e.g. environmental, behavioral etc.) considered to be adaptive, only account for a small amount of the variance in the sleep phenomena (Siegel, 1995; 2003). Furthermore, current data and theories regarding mammalian sleep evolution have been obtained from studies comparing mammals of different sizes and orders; however, comparing mammals of different orders poses a problem. Several previous studies (reviewed by Manger, 2005) have pointed out that the neural systems implicated in the sleep-wake cycle are not consistent across different orders, thus by making such comparisons subject to false inferences regarding mammalian sleep evolution. Several trends such as the direct relationship between the amount of REM (rapid eye movement) sleep and the degree of immaturity at birth, as well as the inverse correlation between body size and total sleep time have been identified (Siegel, 2003). Yet another problem arises when making these deductions, comparisons between the sleep states and factors such as phylogenetic relationship, and brain and body size, are not clear-cut and fail to provide the necessary explanation as to what exactly changes in the sleep phenomena. Thus, no dependable predictability can be assigned to these trends.

Another issue that needs to be addressed is the dependability of the predictability of the anatomy of the somnogenic system. The phenomenon of sleep has been described as a particular state of an organism that is hierarchical in its organization. It is made up of

three distinct yet closely intertwined parts; anatomical, physiological and behavioral. The anatomical basis of sleep is comprised of the complex of neurons in the ventral portion of the brain, the somnogenic system; the physiological basis is distinguished by the global neural activity of the brain and the behavioral aspect characterized by non-responsiveness and motoric inactivity. Thus, in order to make correct inferences about evolutionary changes in the physiological and behavioral parameters of sleep one requires comprehensive insight on the topic of anatomical changes in the somnogenic system. The potential predictability of the neuronal systems controlling sleep is a major preliminary finding driving the present study (Manger, 2005). Previous studies have shown that a distinct evolutionary trend is present in the nuclear complexity of neural systems controlling sleep (Manger *et al.*, 2002a-c, 2003). This raises the question of whether knowledge of the anatomy of the somnogenic system as well as that of the brain can allow accurate predictions of the physiological measurable parameters of sleep.

### 1.3. Specific aims

The practical aims of this thesis are twofold: (1) to provide a complete description of the subcortical structures of the brain of the rock hyrax that comprise the somnogenic system; (2) to determine what may be considered the normal pattern of sleep in the hyrax under both solitary and social conditions. This is followed by a theoretical aim, which will attempt to place these findings in the broader picture of sleep evolution from an adaptive and structuralist standpoint.

## 1.4. Individual chapters

### 1.4.1. Chapter 2: Nuclear organization and morphology of cholinergic, putative catecholaminergic and serotonergic neurons in the brain of the rock hyrax, *Procavia capensis.*

The nuclear subdivisions of the cholinergic, putative catecholaminergic and serotonergic systems within the brain of the rock hyrax (*Procavia capensis*) were identified following immunohistochemistry for acetylcholinesterase, tyrosine hydroxylase and serotonin. The aim of the study was to investigate possible differences in the complement of nuclear subdivisions of these systems by comparing those of the rock hyrax to published studies of other mammals. For the most part, the nuclear organization of these three systems closely resembled that described for many other mammalian species. The nuclear organization of the serotonergic system was identical to that seen in all eutherian mammals. The nuclear organization of the putative catecholaminergic system was very similar to that seen in rodents except for the lack of a C3 nucleus and the compact division of the locus coeruleus (A6c). In addition, the diffuse locus coeruleus (A6d) appeared to contain very few tyrosine hydroxylase immunoreactive (TH+) neurons. The cholinergic system showed many features in common with that seen in both rodents and primates; however, there were three differences of note: (1) cholinergic neurons were observed in the anterior nuclei of the dorsal thalamus; (2) cholinergic parvocellular nerve cells, probably representing interneurons, forming subdivisions of the laterodorsal and pedunculopontine tegmental nuclei were observed at the midbrain/pons interface; and (3) a large number of cholinergic nerve cells in the periventricular gray of the medulla oblongata were

observed. Thus, while there are many similarities to other mammalian species, the nuclear organization of these systems in the rock hyrax show specific differences to what has been observed previously in other mammals.

### 1.4.2. Chapter 3: Distribution of orexin-A immunoreactive neurons and their terminal networks in the brain of the rock hyrax, *Procavia capensis.*

This chapter describes the distribution of orexin-A immunoreactive neurons and terminal networks in relation to the previously described catecholaminergic, cholinergic and serotonergic systems within the brain of the rock hyrax, *Procavia capensis.* Adult female rock hyrax brains were sectioned and immunohistochemically stained with an antibody to orexin-A. The staining revealed that the neurons were mainly located within the hypothalamus as with other mammals. The orexinergic terminal network distribution also resembled the typical mammalian plan. High-density orexinergic terminal networks were located within regions of the diencephalon (e.g. paraventricular nuclei), midbrain (e.g. serotonergic nuclei) and pons (locus coeruleus), while medium density orexinergic terminal networks were evident in the telencephalic (e.g. basal forebrain), diencephalic (e.g. hypothalamus), midbrain (e.g. periaqueductal grey matter), pontine (e.g. serotonergic nuclei) and medullary regions (e.g. serotonergic and catecholaminergic nuclei). Although the distribution of the orexinergic terminal networks was typically mammalian, the rock hyrax did show one atypical feature, the presence of a high-density orexinergic terminal network within the anterodorsal nucleus of the dorsal thalamus (AD). The dense orexinergic innervation of the AD nucleus has only been reported previously in the Nile grass rat, *Arvicanthis niloticus* and Syrian hamster, *Mesocricetus*

*auratus*, both diurnal mammals in nature (Syrian hamster is also known to be nocturnal and hibernating in captivity). It is possible that orexinergic innervation of the AD nucleus might be a unique feature associated with diurnal mammals. It was also noted that the dense orexinergic innervation of the AD nucleus coincided with previously identified cholinergic neurons and terminal networks in this particular nucleus of the rock hyrax brain. It is possible that this dense orexinergic innervation of the AD nucleus in the brain of the rock hyrax may act in concert with the cholinergic neurons and/or the cholinergic axonal terminals, which in turn may influence arousal states and motivational processing.

### 1.4.3. Chapter 4: Solitary sleep in the rock hyrax, *Procavia capensis.*

It is well known that the rock hyrax is a social animal that typically lives in colonies consisting of few to many individuals. In this chapter, the focus is on the effects of solitary sleep in these animals. The rock hyraxes used in this study were captured from wild populations at random. A total of three hyraxes were captured at a time and housed together in specific recording enclosures. They were allowed to acclimatize for a period of one month before any experimentation commenced. One animal was selected from the group for recording purposes and implanted with a telemetric recording device. The implanted animal was allowed to recover from surgery for a minimum period of one week and placed in a recording enclosure by itself. The physiological parameters of sleep as well as the accompanying behavior were subsequently recorded continuously for 72 hours. The aim of the study was to determine the amount of time, as a percentage of 24 hours, spent in each sleep state, i.e. SWS (slow wave sleep) and REM (rapid eye movement), as well as the number and average duration of SWS and REM epochs.

Furthermore, the study also aimed to determine the impact of sleeping "alone" as opposed to sleeping in a group. The questions to be answered was whether a naturally social animal being placed in under solitary conditions would show an increase, a decrease or no change in the total amount of time spent in each sleep state as well as the number and average duration of SWS and REM epochs.

### 1.4.4. Chapter 5: Social contrasted with solitary sleep conditions in the rock hyrax, *Procavia capensis.*

In this chapter the difference in social sleep versus solitary sleep in the rock hyrax is investigated. Following 72 hours of solitary sleep recording, the non-implanted animals were reunited with the implanted animal and allowed to familiarize themselves with each other for a period of three days after which 72 hours continuous social sleep recording commenced. The data was analyzed and the total amount of time, as a percentage of 24 hours, spent in each sleep state, i.e. SWS (slow wave sleep) or REM (rapid eye movement), as well as the number and average duration of SWS and REM epochs, was determined. The social sleep data was compared to solitary sleep data to determine whether any differences existed. Furthermore, the behavior of each of the non-implanted hyraxes were analyzed and correlated with each other as well as the implanted hyrax, to determine whether all hyraxes were in the same state at the same time or whether their behavioral states differed from one another. The aim of the study was to determine the correlation between social and solitary sleep in the rock hyrax, with regard to total amount of sleep time as well as the number and average duration of SWS and REM

epochs. What effect does the social setting have on the duration, intensity and quality of sleep in the rock hyrax and is it significantly different to the solitary scenario?

### 1.4.5. Chapter 6: Nuclear organization and morphology of GABAergic and histaminergic neurons in the brain of the rock hyrax, *Procavia capensis*, and their relation and interplay with the cholinergic, putative catecholaminergic and serotonergic neurons.

This study examined the interrelations of the distribution of sleep associated nuclei and terminal networks in the brain of the rock hyrax, *Procavia capensis*. These systems were identified following immunohistochemistry. A one in ten series of stains was made for nissl, myelin, choline acetyltransferase (ChAT) (identification of the cholinergic system), tyrosine hydroxylase (TH) (identification of the dopaminergic and noradrenergic systems), serotonin (5HT) (identification of the serotonergic system), orexin A (identification of the orexinergic system), parvalbumin (identification of a subset of the GABAergic system), calretinin (identification of a subset of the GABAergic system), calbindin (identification of a subset of the GABAergic system) and histamine (identification of the histaminergic system). The aim of the study was to describe the general organisation and distribution of the GABAergic and histaminergic systems in the brain of the rock hyrax and how it correlates to previous published data of these systems in other mammals, and secondly to examine the relation and interplay of the GABAergic interneurons to the cholinergic, dopaminergic and noradrenergic, serotonergic, and orexinergic systems.

# Chapter 2

## Nuclear organization and morphology of cholinergic, putative catecholaminergic and serotonergic neurons in the brain of the rock hyrax, *Procavia capensis*.

### 2.1. Introduction

The rock hyrax, *Procavia capensis*, is a member of the Procavidea family, which is the only living family within the Hyracoidea order (Klein and Cruz-Uribe, 1996). The family consists of three genera: *Procavia* (the rock hyrax, 1 species), *Heterohyrax* (two species) and *Dendrohyrax* (three species) (Skinner and Chimimba, 2005). The rock hyrax is a small, agile, diurnal, social, herbivorous mammal, typically weighing between 2.5 and 4.6 kg, and lives in rocky outcrops or "koppies" in most parts of Africa (Skinner and Chimimba, 2005). Sexual maturity is reached between 28 to 29 months in males and 16 to 17 months in females, with seasonal mating being triggered by the photoperiod (Skinner and Chimimba, 2005). According to the fossil record, hyraxes first appeared approximately forty million years ago and they are grouped phylogenetically with the African elephant (Proboscidea), and manatee and dugong (Sirenia). These three orders, together with the Chrysochloridea (golden moles), Macroscelidea (elephant shrews), Tubulidentata (aardvarks) and the Tenrecidea (tenrecs) form the cohort Afroplacentalia (Arnason et al., 2008).

In the present study the cholinergic, putative catecholaminergic and serotonergic systems within the brain of the rock hyrax were examined and described using immunohistochemical techniques. It is well known that these systems project to most parts of the brain and that they are associated with several functions (Woolf, 1991;

Smeets and González, 2000; Törk, 1990; Jacobs and Azmitia, 1992); for example, cognition (e.g. Bartus et al., 1982; Previc, 1999), the sleep-wake cycle (e.g. Siegel, 2006), reproduction (e.g. Tillet, 1995), and sensory-motor (e.g. Pompeiano, 2001; Fuxe et al., 2007a) functions to name but a few. The cholinergic system has an extensive distribution throughout the brain (Woolf, 1991; Reiner and Fibiger, 1995; Manger et al., 2002a; Maseko et al., 2007) while the catecholaminergic and serotonergic neuronal systems are mainly concentrated within the brainstem (Dahlström and Fuxe, 1964; Andén et al., 1964; Fuxe et al., 1969, 1970, 2006, 2007a; Diksic and Young, 2001; Manger et al., 2002b,c; Maseko et al., 2007). The nuclear organization of these systems has been studied in several mammalian species (e.g. Maseko et al., 2007; Bhagwandin et al., 2008; Limacher et al., 2008); however no studies of these systems have been done in any member of the Afroplacentalia cohort. Thus, the aim of this study is to determine the nuclear organization of these systems in the brain of the rock hyrax and extend our basis for understanding the evolutionary processes associated with the nuclear organization of these systems.

These systems have exhibited some evolutionary trends and even though these systems are quite similar across species for the most part, differences due occur. For example, the catecholaminergic C3 nucleus has only been reported to be present in the rodents (e.g. Smeets and González, 2000; Manger et al., 2002b; Maseko et al., 2007; Moon et al., 2007; Badlangana et al., 2007; Dwarika et al., 2008; Bhagwandin et al., 2008; Limacher et al., 2008). Serotonergic neurons in the mammalian hypothalamus have only been reported for monotremes (Manger et al., 2002c). These examples and other evidence has led Manger (2005) to propose that members of the same order will show the

same complement of nuclei, but this complement may differ between orders. Some predictions of the current study include: (1) the rock hyrax will have many nuclei in common with other mammals; (2) the rock hyrax may have some nuclei unique to this species; (3) the rock hyrax may exhibit nuclei found only in members of the Afroplacentalia; and (4) the rock hyrax may be missing some nuclei commonly found in other mammalian species.

### 2.2. Materials and Methods

A total of six adult female rock hyraxes, *Procavia capensis,* were used in the present study. Permits from the Limpopo and Gauteng Provincial Governments were obtained for the capture and transport of the animals from the wild. All animals were treated and used according to the guidelines of the University of the Witwatersrand Animal Ethics Committee (approval number AESC 2005/8/5), which parallel those of the NIH for the care and use of animals in scientific experimentation. Each animal was weighed, deeply anaesthetized and subsequently euthanized with weight appropriate doses of sodium pentobarbital (200mg sodium pentobarbital/kg, i.p.). Upon cessation of respiration the animals were perfused intracardially with 0.9% saline followed by 4% paraformaldehyde in 0.1M phosphate buffer (PB, pH 7.4) (approximately 1 l/kg of each solution), both solutions having a temperature of 4°C. The brains were then carefully removed from the skulls and post-fixed overnight in 4% paraformaldehyde in 0.1M PB followed by equilibration in 30% sucrose in 0.1M PB. The brains were then frozen and with the aid of a freezing microtome sectioned at 50 µm in either coronal (n = 4) or sagittal (n = 2) planes. A one in five series of stains was made for nissl, myelin, choline

acetyltransferase (ChAT) (identification of the cholinergic system), tyrosine hydroxylase (TH) (identification of the dopaminergic and noradrenergic systems), and serotonin (5HT) (identification of the serotonergic system). Sections kept for the Nissl series were mounted on 0.5% gelatine coated glass slides, cleared in a solution of 1:1 chloroform and absolute alcohol, then stained with 1% cresyl violet to reveal cell bodies. Myelin sections were stored in 5% formalin for a period of two weeks and were then mounted on 1.5% gelatine coated glass slides and subsequently stained with silver solution to reveal myelin sheaths (Gallyas, 1979).

For immunohistochemical staining each section was treated with endogenous peroxidase inhibitor (49.2% methanol: 49.2% 0.1 M PB: 1.6% of 30% $H_2O_2$) for 30 min and subsequently subjected to three 10 min 0.1 M PB rinses. The sections were then preincubated in a solution (blocking buffer) consisting of 3% normal serum (normal rabbit serum, NRS, for the ChAT sections and normal goat serum, NGS, for the TH and 5HT sections), 2% bovine serum albumin (BSA, Sigma) and 0.25% Triton X100 (Merck) in 0.1M PB, at room temperature for 2 h. This was followed by three 10 min rinses in 0.1M PB. The sections were then placed, for 48 h at 4°C under constant gentle shaking, in primary antibody solution that contained the appropriately diluted primary antibody in blocking buffer (see above). The primary antibodies used were anti-choline acetyltransferase for cholinergic neurons (AB144P, Chemicon, raised in goat, at a dilution of 1:2000), anti-tyrosine hydroxylase for putative catecholaminergic neurons (AB151, Chemicon, raised in rabbit, at a dilution of 1:7500), and anti-serotonin for serotonergic neurons (AB938, Chemicon, raised in rabbit, at a dilution of 1:10000). This was followed by another three 10 min rinses in 0.1M PB, after which the sections were

incubated for 2 h at room temperature in secondary antibody solution. The secondary antibody solution contained a 1:750 dilution of biotinylated anti-rabbit IgG (BA-1000, Vector Labs) in 3% NGS (or anti-goat IgG, BA-5000 in 3% NRS for the ChAT sections), and 2% BSA in 0.1M PB. Once this was completed, the sections were again subjected to another three 10 min rinses in 0.1M PB, followed by a 1 h incubation in AB solution (Vector Labs) and again rinsed. This was followed by a 5 min treatment of the sections in a solution consisting of 0.05% diaminobenzidine (DAB) in 0.1M PB, after which, and while still in the same solution, 3µl of 30% $H_2O_2$ per 0.5ml of solution was added. With the aid of a low power stereomicroscope the progression of the staining was visually followed and allowed to continue until a level was reached where the background staining could assist in reconstruction without obscuring the immunopositive neurons. Once this level was reached the reaction was stopped by placing the sections in 0.1M PB, followed by a final session of three 10 min rinses in 0.1M PB. All solutions used in the immunohistochemical process had a pH of 7.4. The immunohistochemically stained sections were mounted on 0.5% gelatine coated slides and left to dry overnight. The mounted sections were dehydrated by placing it in 70% alcohol for 2 h at room temperature under gentle shaking and then transferred through a series of graded alcohols, cleared in xylene and coverslipped with Depex.

The sections were observed with a low power stereomicroscope, and the architectonic borders traced according to the Nissl and myelin stained sections using a camera lucida. The corresponding immuno-stained sections were then matched to the drawings and the immuno-positive neurons marked. The drawings were scanned and redrawn with the aid of the Canvas 8 program. The drawings were made from sections

obtained from one brain, while photomicrographs were taken from representative sections of this and the five remaining brains. The nomenclature used for the cholinergic system was adopted from Woolf, (1991), Manger et al. (2002a), Maseko and Manger (2007), Maseko et al. (2007), Limacher et al. (2008) and Bhagwandin et al. (2008); the catecholaminergic system from Dahlström and Fuxe (1964), Hökfelt et al. (1984), Smeets and González (2000), Manger et al. (2002b), Maseko and Manger (2007), Maseko et al. (2007), Moon et al. (2007), Dwarika et al. (2008), Limacher et al. (2008) and Bhagwandin et al. (2008); and for the serotonergic system from Törk, (1990), Bjarkam et al. (1997), Manger et al. (2002c), Maseko and Manger (2007), Maseko et al. (2007), Moon et al. (2007), Dwarika et al. (2008), Limacher et al. (2008) and Bhagwandin et al. (2008). While we use the standard nomenclature for the catecholaminergic system in this paper, we realize that the neuronal groups we revealed with tyrosine hydroxylase immunohistochemistry may not correspond directly with those nuclei that have been described in previous studies by Dahlström and Fuxe (1964), Hökfelt et al. (1976), Meister et al. (1988), Kitahama et al. (1990, 1996), and Ruggiero et al. (1992); however, given the striking similarity of the results of the tyrosine hydroxylase immunohistochemistry to that seen in other mammals we feel this terminology is appropriate. Clearly further studies in the rock hyrax with a wider range of antibodies, such as those to phenylethanolamine-*N*-methyltransferase (PNMT), dopamine-β-hydroxylase (DBH) and aromatic L-amino acid decarboxylase (AADC) would be required to fully determine the implied homologies ascribed in this study. We address this potential problem with the caveat of putative catecholaminergic neurons where appropriate in the text.

## 2.3. Abbreviations

III – oculomotor nucleus

IV – trochlear nucleus

Vmot – motor division of trigeminal nucleus

VI – abducens nucleus

VIId – facial nerve nucleus, dorsal division

VIIv – facial nerve nucleus, ventral division

X – dorsal motor vagus nucleus

XII – hypoglossal nucleus

3V – third ventricle

4V – fourth ventricle

7n – facial nerve

A1 – caudal ventrolateral medullary tegmental nucleus

A2 – caudal dorsomedial medullary nucleus

A4 – dorsal medial division of locus coeruleus

A5 – fifth arcuate nucleus

A6c – compact portion of locus coeruleus

A6d – diffuse portion of locus coeruleus

A7d – nucleus subcoeruleus, diffuse portion

A7sc – nucleus subcoeruleus, compact portion

A8 – retrorubral nucleus

A9l – substantia nigra, lateral

A9m – substantia nigra, medial

A9pc – substantia nigra, pars compacta

A9v – substantia nigra, ventral or pars reticulata

A10 – ventral tegmental area

A10c – ventral tegmental area, central

A10d – ventral tegmental area, dorsal

A10dc – ventral tegmental area, dorsal caudal

A11 – caudal diencephalic group

A12 – tuberal cell group

A13 – zona incerta

A14 – rostral periventricular nucleus

A15d – anterior hypothalamic group, dorsal division

A15v – anterior hypothalamic group, ventral division

A16 – catecholaminergic neurons of the olfactory bulb

ac – anterior commissure

AD – anterodorsal nucleus of the dorsal thalamus

Amyg – amygdala

AP – area postrema

AV – anteroventral nucleus of the dorsal thalamus

B9 – supralemniscal serotonergic nucleus

C – caudate nucleus

C1 – rostral ventrolateral medullary tegmental group

C2 – rostral dorsomedial medullary nucleus

ca – cerebral aqueduct

Cb – cerebellum

cc – corpus callosum

Cl – claustrum

CLi – caudal linear nucleus

CN – cochlear nucleus

C/P – caudate and putamen nuclei

CP – cerebral peduncle

CVL – caudal ventrolateral serotonergic group

DCN – deep cerebellar nuclei

Diag.B – diagonal band of Broca

DR – dorsal raphe

DRc – dorsal raphe nucleus, caudal division

DRd – dorsal raphe nucleus, dorsal division

DRif – dorsal raphe nucleus, interfascicular division

DRl – dorsal raphe nucleus, lateral division

DRp – dorsal raphe nucleus, peripheral division

DRv – dorsal raphe nucleus, ventral division

DT – dorsal thalamus

EW – Edinger-Westphal nucleus

f – fornix

GC – periaqueductal grey matter

GLD – dorsal lateral geniculate nucleus

GP – globus pallidus

Hbm – medial habenular nucleus

Hip – hippocampus

Hyp – hypothalamus

Hyp.d – dorsal hypothalamic cholinergic nucleus

Hyp.l – lateral hypothalamic cholinergic nucleus

Hyp.v – ventral hypothalamic cholinergic nucleus

IC – inferior colliculus

ic – internal capsule

icp – inferior cerebellar peduncle

io – inferior olivary nuclei

IP – interpeduncular nucleus

LDTmc – magnocellular division of the laterodorsal tegmental nucleus

LDTpc – parvocellular division of the laterodorsal tegmental nucleus

LRT – lateral reticular nucleus

LV – lateral ventricle

mcp – middle cerebellar peduncle

MnR – median raphe nucleus

N.Acc – nucleus accumbens

N.Amb – nucleus ambiguus

N.Bas – nucleus basalis

NEO – neocortex

OB – olfactory bulb

OC – optic chiasm

OT – optic tract

P – putamen

pVII – preganglionic motor neurons of the superior salivatory nucleus or facial nerve

pIX – preganglionic motor neurons of the inferior salivatory nucleus

PBg – parabigeminal nucleus

PIR – piriform cortex

PPTmc – magnocellular division of the pedunculopontine nucleus

PPTpc – parvocellular division of the pedunculopontine nucleus

Pta – pretectal area

py – pyramidal tract

pyx – decussation of the pyramidal tract

R – thalamic reticular nucleus

Rmc – red nucleus, magnocellular division

RMg – raphe magnus nucleus

ROb – raphe obscurus nucleus

RPa – raphe pallidus nucleus

RVL – rostral ventrolateral serotonergic group

S – septum

SC – superior colliculus

scp – superior cerebellar peduncle

Sep.M – medial septal nucleus

TOL – olfactory tubercle

TOL/Is.Call. – olfactory tubercle/Island of Calleja

vh – ventral horn of spinal cord

VPO – ventral pontine nucleus

xscp – decussation of the superior cerebellar peduncle

ZI – zona incerta

## 2.4. Results

The present study was designed to reveal the nuclear organization of the cholinergic (ChAT), putative catecholaminergic (TH), and serotonergic systems of the rock hyrax, *Procavia capensis* through immunohistochemical methods. A total of six adult female brains were used for this purpose, and the individuals used for this study had body masses ranging from 1.14 kg to 1.52 kg and brain masses between 14.4 g and 17.5 g (Fig. 2.1). The results revealed that for the most part these systems do not differ drastically from those observed in other mammalian species; however the rock hyrax does show some unique additional nuclei, specifically within the cholinergic system, that have not been noted in other species.

### *2.4.1. Cholinergic neurons*

The general organization of the cholinergic system encompasses the striatal, basal forebrain, diencephalic, and pontomesencephalic groups together with the cranial nerve motor nuclei that extend from level of the anterior horn of the lateral ventricle to the spinomedullary junction (e.g. Woolf, 1991; Manger et al., 2002a; Maseko et al., 2007).

These groups were all present in the brain of the rock hyrax and did not show any significant differences to the general mammalian group level organization of this system (Figs. 2.2, 2.3). Despite this, some novel features, potentially unique to the rock hyrax, that have not been observed in other mammals were observed. These include the existence of cholinergic neurons in the anterior nuclei of the dorsal thalamus, the existence of magnocellular and parvocellular divisions of both the laterodorsal tegmental and pedunculopontine tegmental nuclei, and a large cell group in the dorsomedial periventricular grey of the medulla oblongata (Figs. 2.2 – 7).

*2.4.1.1. Striatal cholinergic interneurons*

*2.4.1.1.1. Nucleus accumbens*

Uniformly distributed choline acetyltransferase immunoreactive (ChAT+) nerve cell bodies were located ventrally and slightly anterior to the dorsal striatopallidal complex (caudate, putamen and the globus pallidus) (Figs. 2.2 C-F, 2.3). The anterior and posterior borders of this nucleus were adjacent to the anterior horn of the lateral ventricle and the anterior commissure respectively. This arrangement is typical to what is observed in all mammals (Woolf, 1991; Manger et al., 2002a; Maseko et al., 2007). A moderate density of ChAT+ neurons were observed throughout this nucleus, these neurons being a mixture of bipolar and multipolar types, but the majority were of the multipolar type (Fig. 2.4). The ChAT+ neurons of this nucleus showed no specific dendritic organization.

*2.4.1.1.2. Dorsal striatopallidal complex – caudate/putamen and globus pallidus*

The caudate/putamen nucleus was located lateral to the lateral ventricle and its distribution extended from the level of the anterior horn of the lateral ventricle anteriorly to the medial habenular nuclei posteriorly (Figs. 2.2 D-K, 2.3), a location typical of all mammals (Woolf, 1991; Manger et al., 2002a; Maseko et al., 2007). The boundary between the caudate and putamen was clearly defined by the internal capsule at the level of the anterior commissure, but not anterior to this level. The location of the globus pallidus was found to be ventral and somewhat medial to the putamen and it extended from the level of the anterior commissure to the habenular nuclei. A moderate density of uniformly distributed ChAT+ neurons was observed within the caudate/putamen (Fig. 2.4). The globus pallidus only exhibited a small number of ChAT+ neurons and these neurons were found to be located mostly where the globus pallidus bordered the putamen laterally and the nucleus basalis ventrally. A similar neuronal morphology was noted for the caudate/putamen and the globus pallidus, the ChAT+ neurons being a mixture of bipolar and multipolar types, however a multipolar organization predominated. No specific dendritic orientation was observed for these neurons.

*2.4.1.1.3. Islands of Calleja and olfactory tubercle*

These nuclei exhibited the typical mammalian organizational plan (Woolf, 1991; Manger et al., 2002a; Maseko et al., 2007). They were located in the ventral most portion of the cerebral hemisphere at a level ventral to the nucleus accumbens (Figs. 2.2 D-F, 2.3). These nuclei extended from the level of the anterior horn of the lateral ventricle to the level of the anterior commissure. The Islands of Calleja contained a moderate density of ChAT+ neuronal clusters and a scattered low to medium density of ChAT+ neurons

surrounding these clusters were assigned to the olfactory tubercle. The cells in these regions were intensely immunoreactive and a mixture of bipolar and multipolar neuron types with ovoid shaped somas, were observed. The neurons of the Islands of Calleja as well as those of the olfactory tubercle exhibited no specific dendritic orientation.

*2.4.1.2. Cholinergic nuclei of the basal forebrain*

*2.4.1.2.1. Medial septal nucleus*

This nucleus was identified through the presence of ChAT+ neurons located within the septal nuclear complex in the rostral half of the medial wall of the cerebral hemisphere (Figs. 2.2 G-H, 2.3). The location of this nucleus is typical of what has been observed in other mammals (Woolf, 1991; Manger et al., 2002a; Maseko et al., 2007). A moderate to high density of ChAT+ neurons, a mixture of both bipolar and multipolar types with ovoid cell shapes, was observed. It was also noted that the cells located closer to the edge of the hemisphere were smaller than those cells located a small distance from the edge. Also, the cells closer to the edge of the hemisphere were mostly bipolar with dendrites arranged parallel to the edge, whereas those further away were predominantly multipolar and exhibited no specific dendritic orientation.

*2.4.1.2.2. Diagonal band of Broca*

The diagonal band of Broca was located anterior to the hypothalamus in the ventromedial corner of the cerebral hemisphere (Fig. 2.2F). The division of this nucleus into horizontal and vertical bands appeared to be unnecessary as the neurons forming this nucleus presented as a continuous, uninterrupted band. A high density of ChAT+ neurons

was found throughout the extent of this nucleus (Fig. 2.4). The cells were intensely immunoreactive, ovoid in shape and multipolar in type with their dendrites orientated roughly parallel to the edge of the cerebral hemisphere. It was also noted that the neurons of this nucleus were larger than those found in the adjacent olfactory tubercle and islands of Calleja, a feature that can be readily used to demarcate this lateroventral boundary of the diagonal band.

*2.4.1.2.3. Nucleus basalis*

ChAT+ neurons found ventral to the globus pallidus at the level of the anterior commissure, and caudal and dorsal to the olfactory tubercle were assigned to nucleus basalis (Figs. 2.2 G-H, 2.3). A low to moderate density of ChAT+ neurons was observed throughout this nucleus, and these appear to be a continuation of the ChAT+ neurons found within the globus pallidus. These ChAT+ neurons were ovoid in shape, a mixture of bipolar and multipolar types, and exhibited a rough dorsolateral to ventromedial dendritic orientation.

*2.4.1.3. Diencephalic cholinergic nuclei*

*2.4.1.3.1. Medial habenular nucleus*

The medial habenular nucleus, which forms part of the epithalamus, was located contiguous to the third ventricle in the dorsomedial region of the diencephalon (Figs. 2.2 M, 2.3). The location of this nucleus was typical of what has been observed in other mammals (Woolf, 1991; Manger et al., 2002a; Maseko et al., 2007). A high density of small, round, ChAT+ neurons, was observed. We could not discern any specific

dendritic orientation due to the dense packing of neurons within this nucleus. The ChAT+ axons arising from this nucleus clearly outlined the fasciculus retroflexus, which was seen to end in a large swirling termination within the interpeduncular nucleus.

*2.4.1.3.2. Hypothalamic cholinergic nuclei*

Three distinct ChAT+ neuronal groups (dorsal, ventral and lateral hypothalamic nuclei) were identified within the hypothalamus (Figs. 2.2 I-L, 2.3). The dorsal hypothalamic nucleus was located between the wall of the third ventricle and the fornix within the dorsomedial region of the hypothalamus. A low density of palely stained, scattered ChAT+ neurons was observed within this nucleus. The ventral hypothalamic nucleus was identified as a cluster of palely stained, widely scattered ChAT+ neurons within the ventromedial aspect of the hypothalamus that extended ventrolaterally past the level of the fornix. Within the dorsolateral region of the hypothalamus, lateral to the fornix, a low density of palely stained ChAT+ neurons were identified as the lateral hypothalamic cholinergic nucleus. The neuronal morphology of the ChAT+ neurons within these hypothalamic cholinergic nuclei was similar. These neurons had an ovoid shape, were bipolar in type and showed no specific dendritic orientation.

*2.4.1.3.3. Cholinergic neurons in the anterodorsal and anteroventral dorsal thalamic nuclei*

Within the anterior and dorsal region of the dorsal thalamus the anterodorsal nucleus (AD) was seen to exhibit a strong cholinergic neuropil staining. Around the margins of the AD nucleus a small number of scattered ChAT+ neurons were observed

(Figs. 2.2K, 2.3). The ChAT+ neurons within this nucleus were ovoid in shape, a mixture of bipolar and multipolar types with the dendrites orientated parallel to the margins of the nucleus (Fig. 2.5). Lateral to the anterodorsal nucleus, the anteroventral nucleus (AV) exhibited a much paler neuropil ChAT+ neuropil staining, but it was clearly distinguishable from the surrounding unreactive tissue of the remainder of the dorsal thalamus. ChAT+ neurons showing a similar morphology to those found in the anterodorsal nucleus were observed along the upper medial and lateral borders of the anteroventral nucleus. The cholinergic nature of the neuropil and occasional scattered ChAT+ neurons within these nuclei might be a unique feature of the hyrax, as these observations have not been made in other mammals to date.

*2.4.1.4. Pontomesencephalic nuclei*

*2.4.1.4.1. Parabigeminal nucleus*

A prominent parabigeminal nucleus was located ventral and slightly anterior to the inferior colliculus within the lateral aspect of the midbrain tegmentum (Figs. 2.2 O-P, 2.3). A dense cluster of strongly reactive ChAT+ neurons, smaller in size to the medially located pedunculopontine tegmental nucleus, was observed. The cell bodies were circular in shape but due to the high density of the packing it was difficult to determine whether these neurons were bipolar or multipolar and if the dendrites showed any specific orientation (Fig. 2.6A).

*2.4.1.4.2. Pedunculopontine tegmental nucleus (PPT) – magnocellular and parvocellular nuclei*

In all mammals studied to date, the cholinergic neurons of the pedunculopontine tegmental nucleus display a homogenous morphology (e.g. Woolf, 1991; Manger et al., 2002a; Maseko et al., 2007; Limacher et al., 2008; Bhagwandin et al., 2008). As with most mammals within the dorsal aspect of the isthmic and pontine tegmental regions, anterior to the trigeminal motor nucleus, a group of ChAT+ neurons was identified (Figs. 2.2 O-Q, 2.3). This location, and the moderate density distribution of ChAT+ neurons in this region, is again typical. In contrast to other mammals studied, the morphology of the cholinergic neurons within this region was not homogenous, and we could readily identify magnocellular and parvocellular ChAT+ nuclei within this region (Fig. 2.6B, D). The ChAT+ neurons assigned to the magnocellular PPT nucleus were found in the location, and evinced the distribution of the more typically described PPT. These magnocellular neurons were found medial and ventral to the superior cerebellar peduncle, and in the anterior portion were found to intermingle with the fibres of the superior cerebellar peduncle. The magnocellular ChAT+ neurons were found in a moderate density throughout this nucleus, were multipolar in type, showed no specific dendritic orientation, and evinced a variety of somal shapes. In the more caudal aspects of the PPT, in a position dorsal and lateral to the magnocellular nucleus, a moderately dense cluster of small ChAT+ neurons was observed, termed the parvocellular PPT nucleus. The parvocellular PPT nucleus was sometimes clearly distinguished from the magnocellular PPT nucleus on topological grounds, as it was found lateral and dorsal to

the superior cerebellar peduncle in the posterior aspect of the midbrain tegmentum; however, the size of the soma was the most reliable distinction between these two nuclei. The ovoid shaped, parvocellular ChAT+ neurons were mostly bipolar in type, but there were some multipolar neurons in this nucleus. These neurons had dendrites that were predominantly oriented in a dorsomedial to ventrolateral direction. There was no overlap in the distribution of the magnocellular and parvocellular neurons at their border.

*2.4.1.4.3. Laterodorsal tegmental nucleus (LDT) – magnocellular and parvocellular nuclei*

In all mammals studied to date, the cholinergic neurons of the laterodorsal tegmental nucleus display a homogenous morphology (e.g. Woolf, 1991; Manger et al., 2002a; Maseko et al., 2007; Limacher et al., 2008; Bhagwandin et al., 2008). As with most mammals within the ventrolateral region of the pontine periventricular- and periaqueductal grey matter, a moderate to high density of ChAT+ neurons was identified (Figs. 2.2 P-Q, 2.3). This location and distribution of ChAT+ neurons is again typical of LDT in various mammals. In contrast to other mammals studied, the morphology of the cholinergic neurons within this region was not homogenous, and we could readily identify magnocellular and parvocellular ChAT+ nuclei within this region (Fig. 2.6B, C). At the ventrolateral border of the pontine periventricular- and periaqueductal grey matter a densely packed cluster of larger neurons with similar morphology to those constituting the magnocellular PPT nucleus was found. We have termed this cluster of ChAT+ neurons the magnocellular LDT nucleus. This magnocellular LDT nucleus appears to be typical of that seen and described as the LDT in most mammals. A second cluster of

ChAT+ neurons was found medial and dorsal to the magnocellular LDT nucleus, but still within the periventricular- and periaqueductal grey matter. These neurons were significantly smaller than those in the magnocellular LDT nucleus, thus we have termed this ChAT+ neuronal cluster the parvocellular LDT nucleus. The morphology and size of these neurons was very similar to the ChAT+ neurons forming the parvocellular PPT nucleus; however, they did not display any specific dendritic orientation. These neurons were found in a moderate to high density and had soma that were ovoid to circular in shape. The lateral border of the parvocellular LDT nucleus and the medial border of the magnocellular LDT nucleus were not clearly defined as the ChAT+ neurons from both nuclei showed a region of intermingling. In this sense, while the magnocellular and parvocellular nuclei of the LDT and PPT seem to be contiguous subdivisions of these nuclei, the distinct topological parcellation of the two nuclei in the PPT was not as strongly expressed in the LDT.

*2.4.1.5. Cholinergic cranial nerve motor nuclei*

A number of large, multipolar ChAT+, neurons forming the cranial nerve motor nuclei were identified in similar regions to those previously documented for other mammals (Woolf, 1991; Manger et al., 2002a; Maseko et al., 2007; Limacher et al., 2008; Bhagwandin et al., 2008). These nuclei were: the oculomotor nucleus (III) (Fig. 2.6A), the trochlear nucleus (IV), the motor division of the trigeminal nucleus (Vmot), the abducens nucleus (VI), the dorsal and ventral subdivisions of the facial nucleus (VIId and VIIv), the nucleus ambiguus, the dorsal motor vagus nucleus (X), the hypoglossal nucleus (XII) and the ventral horn of the spinal cord (Figs. 2.2 N-Z, 2.3). In addition to

these we were able to locate ChAT+ neurons within the Edinger-Westphal nucleus and the preganglionic motor neurons of the superior salivatory nucleus of the facial nerve (pVII) and the preganglionic motor neurons of the inferior salivatory nucleus (pIX). The ChAT+ neurons of the Edinger-Westphal nucleus were moderate in number, but were strongly immunoreactive. This nucleus primarily gives rise to the preganglionic parasympathetic fibres to the eye, constricting the pupil, and is located within the periaqueductal grey matter directly contiguous to midline, between and anterior to the oculomotor nuclei. The neuronal bodies were ovoid in shape, bipolar and the dendrites were orientated dorsoventrally. Within the rostral medullary tegmentum, dorsal to the facial nerve nuclei, the ChAT+ neurons of pVII and pIX were identified. The neurons of the pVII nucleus were slightly smaller than those of the facial nerve nucleus and exhibited a small number of scattered multipolar neurons that demonstrated the typical motor neuron morphology, probably representing the preganglionic cholinergic cell bodies of the superior salivatory nucleus (see Mitchell and Templeton, 1981; Tóth et al., 2007). The ChAT+ neurons found medial to X probably represented the ChAT+ preganglionic neurons of the inferior salivatory nucleus (pIX) (see Rezek et al., 2008). At this level of the medulla oblongata a large number of ChAT+ nerve cell bodies of moderate density were located in the medial periventricular grey (Fig. 2.7). The neurons were multipolar but smaller than the motor neurons of X and XII, with no specific dendritic orientation. The extensive number of cholinergic cells in this region appears to be unusual in comparison to other mammals.

*2.4.2. Putative catecholaminergic nuclei*

The putative catecholaminergic nuclei, in the current study being those that possess neurons that are immunoreactive to tyrosine hydroxylase (TH+), are generally divided into several nuclear complexes that extend from the level of the olfactory bulb to the spinomedullary junction. These are generally defined as: the olfactory bulb, diencephalic, midbrain, pontine, and medullary nuclear complexes. All of the aforementioned nuclear complexes were present in the brain of the rock hyrax and the location and distribution of these was essentially similar to the typical mammalian organizational plan of this particular system previously described in a range of other species (Dahlström and Fuxe, 1964; Fuxe et al., 1969, 2007b; Smeets and González, 2000; Maseko et al., 2007; Limacher et al., 2008; Bhagwandin et al., 2008). No putative catecholaminergic nuclei falling outside these defined regions, as is the case in some other vertebrates, were identified in the hyrax (Smeets and González, 2000). The standard nomenclature of Dahlström and Fuxe (1964) and Hökfelt et al. (1984) was implemented in the description of these nuclei. The putative catecholaminergic nuclei identified in the rock hyrax are essentially similar to that seen in other mammals (Figs. 2.2, 2.3); however, we did not identify the rodent specific rostral dorsal midline medullary (C3) nucleus (Smeets and González, 2000; Moon et al., 2007; Dwarika et al., 2008; Limacher et al., 2008; Bhagwandin et al., 2008) and the locus coeruleus compact, built of densely packed NA cell bodies (see Fuxe et al., 1970) did not exist. Furthermore, only a few single TH+ neurons were observed in the adjacent periventricular grey of the pons, termed A6 diffuse (A6d) in the current study.

*2.4.2.1. Olfactory bulb (A16)*

Within and around the glomerular layer a moderate number of TH+ neurons were observed (Figs. 2.2A, 2.3). This position is typical of what has been documented in other mammals for the A16 catecholaminergic nucleus (Lichtensteiger, 1966; Lidbrink et el., 1974; Smeets and González, 2000; Manger et al., 2002b; Maseko et al., 2007; Limacher et al., 2008; Bhagwandin et al., 2008). The cells were triangular in shape and a mixture of bipolar and multipolar neurons were evident. These neurons also had a weak dendritic network surrounding the glomeruli.

*2.4.2.2. Diencephalic nuclei*

In the hypothalamus six distinct putative catecholaminergic nuclei were identified. These include: the dorsal division of the anterior hypothalamic nucleus (A15d); the ventral division of the anterior hypothalamic nucleus (A15v); the rostral periventricular nucleus (A14); the zona incerta (A13); the tuberal nucleus (A12); and the caudal diencephalic nucleus (A11) (Figs. 2.2 G-L, 2.3). The A15d nucleus was located between the third ventricle and the fornix within the anterior portion of the hypothalamus. The shape of the neuronal bodies was found to be ovoid, with a mixture of bipolar and multipolar types showing no specific dendritic orientation. The A15v nucleus was located near the floor of the brain adjacent to the optic tracts within the ventrolateral region of the hypothalamus. A low density of TH+ neurons with ovoid cell bodies was observed. A mixture of bipolar and multipolar neurons with no specific dendritic orientation was evident. A moderate density of TH+ neurons close to wall of the third ventricle

throughout the hypothalamus was identified as the A14 nucleus (Fig. 2.8A). The neurons had ovoid shaped somas and were mostly of the bipolar type with some being multipolar. The dendrites were observed to be orientated roughly parallel to the ventricular wall. The A13 nucleus was identified as a moderate density of TH+ neurons located within the dorsal and lateral regions of the hypothalamus, lateral to the fornix, extending into and around the zona incerta in the ventral thalamus. The neurons exhibited morphological similarity to those within the A15d nucleus.

In the ventral portion of the hypothalamus, within and in close proximity to the arcuate nucleus, a low to moderate density of TH+ neurons was identified as the A12 nucleus. The neurons of this nucleus were located near the midline and surrounded the floor of the third ventricle. The cell bodies were ovoid and the neurons a mixture of the bipolar and multipolar types with dendrites orientated roughly parallel to the floor of the brain. Around the posterior pole of the third ventricle, in the most caudal part the hypothalamus, a low density of TH+ neurons arranged in columns on either side of the midline was identified as the A11 nucleus. The neurons of this nucleus were large and multipolar, with ovoid to polygonal shaped somas. No specific dendritic orientation was observed for these neurons. The cell bodies of the A11 neurons were larger than those of all the other neurons of the diencephalic nuclei, with this feature serving as a ready marker for delineation of this nucleus.

*2.4.2.3. Midbrain nuclei*

*2.4.2.3.1. Ventral tegmental area nuclei (VTA, A10 complex)*

The A10 nuclear complex (comprised of the following nuclei: A10 – the ventral tegmental area nucleus; A10c – ventral tegmental area, central nucleus; A10d – ventral tegmental area, dorsal nucleus; A10dc – ventral tegmental area, dorsal caudal nucleus) was located within the medial part of the midbrain tegmentum slightly anterior to the level of the oculomotor nerve nucleus (Figs. 2.2 L-O, 2.3). The nuclei forming this complex originated from the dorsal and dorsolateral areas around the interpeduncular nucleus and extended dorsally to the periaqueductal grey matter, where the aqueduct component was formed caudally. The A10 nucleus was identified as a high density of TH+ neurons located between the interpeduncular nucleus and the root of the oculomotor nerve (Fig. 2.9). The neurons were distributed dorsally and dorsolaterally to the interpeduncular nucleus. The cell bodies were ovoid in shape and the neurons were a mixture of the bipolar and multipolar types showing no specific dendritic orientation. Immediately dorsal to the interpeduncular and A10 nuclei, a moderate to high density of TH+ neurons was identified as the A10c nucleus (Fig. 2.9). The neurons of this nucleus formed a characteristically roughly triangular shaped pattern in the midline. A similar neuronal morphology as the neurons of the A10 nucleus was observed for the neurons of the A10c nucleus; however the neurons of A10c were slightly smaller in size than those of A10, this size difference serving as a marker for delineating between these two adjacent nuclei. A moderate density of TH+ neurons located dorsal and between the A10c nucleus and the periaqueductal grey matter, medial to the oculomotor nerve nucleus, was identified as A10d (Fig. 2.9). The cell bodies of these neurons were ovoid in shape, bipolar in type and showed a dorsoventral dendritic orientation. The A10dc nucleus was located within the periaqueductal grey matter around the lower half of the

cerebral aqueduct (Fig. 2.8B). The TH+ neurons forming the A10dc nucleus were small, ovoid in shape, multipolar and the dendrites were orientated roughly parallel to the edge of the cerebral aqueduct.

*2.4.2.3.2. Substantia nigra nuclear complex (A9)*

In the ventrolateral region of the midbrain tegmentum, dorsal to the cerebral peduncles, four distinct nuclei comprising the substantia nigra nuclear complex were identified. These nuclei were: the substantia nigra, pars compacta nucleus (A9pc); substantia nigra, pars lateralis nucleus (A9l); substantia nigra, ventral or pars reticulata nucleus (A9v); and the substantia nigra, pars medialis nucleus (A9m) (Figs. 2.2 K-N, 2.3). The A9pc nucleus was identified as a mediolaterally oriented band of TH+ neurons of a moderate to high density located dorsal to the cerebral peduncle (Fig. 2.9). The neurons were ovoid in shape and bipolar with a medial to lateral dendritic orientation, parallel to the direction of the band. The A9l nucleus was located within the ventrolateral region of the midbrain tegmentum, dorsolateral to the lateral border of the cerebral peduncle in a position lateral to the A9pc nucleus (Figs. 2.8D, 2.9). The somas of the TH+ neurons of this nucleus were either polygonal or triangular in shape. The neurons were multipolar and did not exhibit any specific dendritic orientation. The A9v nucleus was located in the grey matter just dorsal to the cerebral peduncle ventral to the A9pc and A9l nuclei (Fig. 2.9). The neurons were found in a low to moderate density in this region and showed a rough dorsoventral dendritic orientation. A high density of TH+ neurons located between the medial edge of the A9pc nucleus and the root of the oculomotor nerve was identified as the A9m nucleus (Fig. 2.9). The neurons of this nucleus showed a

similar neuronal morphology as A9pc, with the neurons showing no specific dendritic orientation.

*2.4.2.3.3. Retrorubral nucleus (A8)*

Within the lower half of the midbrain tegmentum a moderate number of TH+ neurons were found dorsal to the A9 complex, and ventral and caudal to the magnocellular division of the red nucleus. These neurons, which exhibited a moderate density throughout this region, were assigned to the A8 nucleus (Figs. 2.2 N-O, 2.3). The TH+ neuronal bodies were ovoid in shape, bipolar and multipolar in type, and showed no specific dendritic orientation (Fig. 2.8D).

*2.4.2.4. Pontine nuclei – the locus coeruleus (LC) nuclear complex*

The locus coeruleus complex was identified as a large aggregation of TH+ neurons within the pontine region. Five nuclei within this complex were identified, being: the subcoeruleus compact nucleus (A7sc), subcoeruleus diffuse nucleus (A7d), locus coeruleus diffuse nucleus (A6d), fifth arcuate nucleus (A5), and the dorsal medial nucleus of the locus coeruleus (A4) (Figs. 2.2 P-Q, 2.3). A7sc was located within the dorsal region of the pontine tegmentum adjacent to the periventricular grey matter. A high density of TH+ neurons with ovoid somas of the multipolar type represented this nucleus (Fig. 2.8C). The neurons of A7sc showed no specific dendritic orientation. The description of this nucleus coincides to what was previously described as the subcoeruleus (Dahlström and Fuxe, 1964). TH+ neurons ventrolateral to A7sc, anterior to the trigeminal motor nucleus, in the lateral and dorsolateral region of the pontine

tegmentum were assigned to the A7d nucleus. Some of the TH+ neurons assigned to A7d were also located medial and ventral to the superior cerebellar peduncle. The TH+ neurons in this region were found in a moderate to low density, were ovoid in shape, multipolar and showed no specific dendritic orientation. A compact A6 built of TH+ neurons was absent, and only a small number of TH+ neurons was located within the ventrolateral portion of the periventricular grey matter adjacent to A7sc, and identified as A6d (Fig. 2.8C). The neurons of A6d had a similar morphology to A7sc and showed no specific dendritic orientation. In comparison to other mammalian species, the rock hyrax had markedly reduced number of immunopositive neurons within A6d (Dahlström and Fuxe, 1964; Fuxe et al., 1969, 2007b; Smeets and González, 2000; Maseko et al., 2007; Limacher et al., 2008; Bhagwandin et al., 2008). The TH+ neurons assigned to the A5 nucleus was located lateral to the superior olivary nucleus, anterior to the facial nerve nucleus and ventral to the trigeminal motor nerve nucleus, in the ventrolateral region of the pontine tegmentum. The TH+ neurons of this nucleus were few in number and had a similar neuronal morphology to the neurons seen in the other locus coeruleus nuclei. The TH+ neurons assigned to the A4 nucleus were located adjacent to the wall of the fourth ventricle, medial to superior cerebellar peduncle, in the dorsolateral part of the caudal periventricular grey matter. This nucleus was represented by a small number of TH+ neurons with a similar morphology to the neurons seen in the other locus coeruleus nuclei.

*2.4.2.4.1. Medullary nuclei*

TH+ neurons representing five putative catecholaminergic nuclei were found within in the medulla of the rock hyrax. The nuclei identified were: the rostral ventrolateral tegmental nucleus (C1), rostral dorsomedial nucleus (C2), caudal ventrolateral tegmental nucleus (A1), caudal dorsomedial nucleus (A2) and area postrema (AP) (Figs. 2.2 R-X, 2.3). The rostral dorsal midline nucleus (C3), a feature so far only identified in rodents (Smeets and González, 2000; Maseko et al., 2007; Limacher et al., 2008; Bhagwandin et al., 2008) was not present. The neurons forming the C1 nucleus were located in the ventrolateral region of the anterior medulla and were distinguished as a column of TH+ neurons that extended from the level of the superior olivary nucleus to the level of nucleus ambiguus. In the course of its distribution this band of neurons was located lateral to superior olivary nucleus and facial nerve nucleus, and medial to nucleus ambiguus. The neurons of this nucleus were ovoid in shape, multipolar and exhibited a mesh-like dendritic network interspersed among the ascending and descending fasciculi of the medulla. A low density of TH+ neurons within the dorsal region of the medulla was identified as C2. This nucleus was located anterior and dorsal to the vagus motor nerve nucleus. The dorsal strip of C2 (Kalia, et al., 1985a, b), which is the part of the C2 nucleus that is located near the floor of the fourth ventricle above the nucleus of the vagus motor nerve, could be identified. The continuation of the dorsal strip, which is known as the rostral subdivision of the C2 nucleus (Kalia, et al., 1985a, b), was not present. The neurons of this nucleus were few in number and of low density. The somal shape was ovoid and the neurons were bipolar with dendrites orientated parallel to the floor of the fourth ventricle. The A1 nucleus was identified as a column of TH+ neurons

within the ventrolateral region of the caudal medulla. The neurons of this nucleus were distributed from the level of nucleus ambiguus to the level of the spinomedullary junction. In the course of its distribution the neurons of the A1 nucleus were located lateral to nucleus ambiguus and the lateral reticular nucleus. The distinguishing factor between the partly overlapping caudal and rostral neuronal columns of the A1 and C1 (caudal part) nucleus, respectively, was their position relative to the nucleus ambiguus. The A1 column was located lateral to nucleus ambiguus while the caudal part of the C1 column was located medial to this nucleus. The neuronal morphology and dendritic organization of the A1 nucleus was similar to that of the C1 nucleus. A number of moderately sized TH+ neurons were located between, as well as around, the nuclei of the dorsal motor vagus and hypoglossal nerves and these were assigned to the A2 nucleus; however, none were found in the nucleus tractus solitarius, which is the major location for this cell group in rodents (Dahlström and Fuxe, 1964). These neurons were ovoid in shape, bipolar in type and their dendrites exhibited a medial to lateral orientation. The area postrema (AP) was identified as a high-density cluster of small TH+ neurons. This nucleus was located just anterior to the spinomedullary junction, adjacent to the floor of the fourth ventricle and dorsal to the nucleus tractus solitarius and the central canal. The neurons were ovoid shaped, bipolar in type, and showed no specific dendritic orientation.

*2.4.3. Serotonergic nuclei*

A number of distinct serotonergic immunoreactive (5HT+) nuclei were found throughout the brainstem of the rock hyrax. These were observed from the level of the decussation of the superior cerebellar peduncle through to the spinomedullary junction

(Figs. 2.2 M-W, 2.3, 2.10, 2.11). These nuclei were readily divisible into rostral and caudal nuclear clusters and the location of the nuclei within these clusters were found to be similar to what has been described for other eutherian mammals (e.g. Törk, 1990; Manger et al., 2002c; Badlangana et al., 2007; Maseko et al., 2007; Moon et al., 2007; Dwarika et al., 2008; Limacher et al., 2008; Bhagwandin et al., 2008).

*2.4.3.1. Rostral cluster*

*2.4.3.1.1. Caudal linear nucleus (CLi)*

A moderate density of 5HT+ neurons was located within the midbrain tegmentum of the rock hyrax. A cluster of these neurons were found to be in a position immediately dorsal to the interpeduncular nucleus and anterior to the decussation of the superior cerebellar peduncle in the ventral midline of the midbrain tegmentum. This cluster was designated as the caudal linear nucleus (Figs. 2.2 M-N, 2.3). At the lateral border of the interpeduncular nucleus, the 5HT+ neurons of the CLi also extended to the ventral surface of the brain and it was noted that this nucleus was the most rostrally located nucleus of all the 5HT+ nuclei. The neurons of this nucleus had ovoid shaped somas, were bipolar in nature, and had a rough dorsoventral dendritic orientation (Fig. 2.11A, B).

*2.4.3.1.2. Supralemniscal nucleus (B9)*

The B9 nucleus was identified as a loosely packed arc of 5HT+ neurons, lateral to the interpeduncular nucleus and caudal to the A9pc nucleus (Figs. 2.2 N, 2.3). This nucleus was located superior to the medial lemniscus and was found to be in continuity

with the ventrolateral neurons of the CLi nucleus. The neurons had ovoid shaped somas, were bipolar in type, and the dendrites had no specific orientation (Fig. 2.11B).

*2.4.3.1.3. Median raphe (MnR)*

In a pararaphe position, on either side of the midline, two clear, densely packed columns of 5HT+ neurons, extending dorsal to ventral along the midbrain and pontine tegmentum, were identified as the MnR nucleus (Figs, 2 N-Q, 3). The neurons forming this nucleus extended from the caudal aspect of the superior cerebellar peduncle to the level of the anterior most aspect of the trigeminal motor nucleus. The cell bodies of the 5HT+ neurons of the MnR nucleus were ovoid, bipolar in type and the dendrites showed a rough dorsoventral orientation (Fig. 2.10).

*2.4.3.1.4. Dorsal raphe nuclear complex (DR)*

Within the 5HT+ dorsal raphe nuclear complex six distinct nuclei, extending from the level of the oculomotor nerve nucleus to the level of the trigeminal motor nerve nucleus within the periaqueductal and periventricular grey matter, were identified. These nuclei were: the dorsal raphe interfascicular (DRif) nucleus, the dorsal raphe ventral (DRv) nucleus, the dorsal raphe dorsal (DRd) nucleus, the dorsal raphe lateral (DRl) nucleus, the dorsal raphe peripheral (DRp) nucleus, and the dorsal raphe caudal (DRc) nucleus (Figs 2 O-Q, 3). A dense cluster of 5HT+ neurons within the most ventral medial portion of the periventricular grey matter, between the two medial longitudinal fasciculi, was identified as the DRif nucleus (Fig. 2.10). The neurons of this nucleus had ovoid shaped cell somas, were bipolar in type and had dendrites that were orientated

roughly dorsoventrally. Immediately dorsal to the DRif nucleus and caudal to the oculomotor nerve nuclei, a high density of 5HT+ neurons was identified as the DRv nucleus (Fig. 2.10). These neurons were ovoid in shape and bipolar with no specific dendritic orientation. The DRd nucleus was identified as a high density of 5HT+ neurons located ventral to the inferior border of the cerebral aqueduct and immediately dorsal to the DRv nucleus (Fig. 2.10). The neurons of this nucleus had a similar neuronal morphology and dendritic orientation as the neurons of the DRv nucleus. A very low density of 5HT+ neurons located lateral to the DRd and DRv nuclei, anterior to the ChAT+ neurons of the LDT, in the ventrolateral portion of the periaqueductal grey matter was identified as the DRp nucleus. In the adjacent midbrain tegmentum, a small number of 5HT+ neurons forming part of the DRp nucleus were observed (Fig. 2.10). Of all the dorsal raphe nuclei, the tegmental neurons of the DRp nucleus were the only ones not located within the periventricular and periaqueductal grey matter. The 5HT+ neurons forming the DRp were ovoid to polygonal in shape, multipolar, and showed no specific dendritic orientation. Adjacent to the ventrolateral edge of the cerebral aqueduct, in a position dorsolateral to the DRd nucleus, a group of 5HT+ neurons were assigned to the DRl nucleus (Fig. 2.10). A low density of large, ovoid, multipolar neurons with no specific dendritic orientation was observed within this nucleus. This nucleus was readily distinguished from the other dorsal raphe nuclei due to the low neuronal density and the large soma of the neurons. An arc of 5HT+ neurons across the dorsal midline of the periventricular grey matter, where the cerebral aqueduct opens into the fourth ventricle, formed by the caudal coalescences of the two lateralized clusters of the DRl nucleus, was identified as the DRc nucleus (Fig. 2.11C). The neurons of this nucleus had a similar

neuronal morphology and dendritic orientation as those of the DRl nucleus. Due to the lack of 5HT+ neurons within this region of the brain in monotremes, the DRc was classified as an independent nucleus (Manger et al., 2002c).

*2.4.3.2. Caudal cluster*

*2.4.3.2.1. Raphe magnus nucleus (RMg)*

The 5HT+ neurons forming the RMg nucleus were located within the rostral medullary tegmentum, extending from the level of the anterior border of the facial nerve nucleus to the anterior border of nucleus ambiguus (Figs. 2.2 Q-S, 2.3). These 5HT+ neurons were low in density and formed two weakly expressed columns on either side of the midline. The neurons of the RMg nucleus were large, multipolar and exhibited a weak dorsoventral dendritic orientation.

*2.4.3.2.2. Rostral and caudal ventrolateral serotonergic medullary columns (RVL and CVL)*

Within the ventrolateral medullary tegmentum a column of 5HT+ neurons were identified as the RVL and CVL nuclei. This column extended from the level of the facial nerve nucleus to the spinomedullary junction and appeared to be a lateral extension of the neurons forming the RMg nucleus (Figs. 2.2 R-W, 2.3). The part of the column extending from the facial nerve nucleus to the rostral border of nucleus ambiguus was identified as the RVL nucleus, while the part of the column extending from the rostral border of nucleus ambiguus to the spinomedullary junction was designated as the CVL nucleus. The columns of the RVL nucleus were found immediately dorsal to the pyramidal tracts

anteriorly, and it was noted that this group of neurons bifurcated around the anterior pole of the inferior olivary nucleus, giving rise to two bilateral columns. These columns extended, in a position lateral to the inferior olivary nucleus, caudally within the ventrolateral medulla. The neurons of the RVL and CVL nuclei had a similar neuronal morphology and dendritic orientation as the neurons of the RMg nucleus and decreased in density from moderate, rostrally, to low, caudally. It was observed, as with other mammalian species studied to date, that the RVL and CVL columns were continuous (e.g. Maseko and Manger, 2007; Maseko et al., 2007; Moon et al., 2007; Dwarika et al., 2008; Bhagwandin et al., 2008); however, it is possible to make the distinction between these two nuclei, as the CVL column has not been found in the opossum or the monotremes (Crutcher and Humbertson, 1978; Manger et al., 2002c).

*2.4.3.2.3. Raphe pallidus nucleus (RPa)*

A low density and number of 5HT+ neurons located between the pyramidal tracts and at the ventral most border of the inferior olivary nucleus, within the ventral surface of the midline and medial medulla, was identified as the medial and lateral component of the RPa nucleus (Figs. 2.2 R-T, 2.3). The neurons of this nucleus exhibited fusiform-shaped somas, were bipolar in type with a dorsoventral dendritic orientation parallel to the medial border of the pyramidal tracts.

*2.4.3.2.4. Raphe obscurus nucleus (ROb)*

On either side of the midline a low density of 5HT+ neurons, extending dorsal to ventral, from the level of the nucleus ambiguus to the spinomedullary junction were

identified as the RObnucleus (Figs. 2.2 T-W, 2.3). The neurons were arranged in two loosely packed columns on either side of the midline. The cell bodies of these neurons were fusiform in shape, bipolar, and had a dorsoventral dendritic orientation. Unlike in some other species studied, there were no neurons located a short distance from the central columns (e.g. Maseko and Manger, 2007; Maseko et al., 2007; Moon et al., 2007; Dwarika et al., 2008; Bhagwandin et al., 2008).

**Figure 2.1:** Photographs of the dorsal (top), lateral (middle) and ventral (bottom) aspects of the rock hyrax brain. Scale bar = 1 cm.

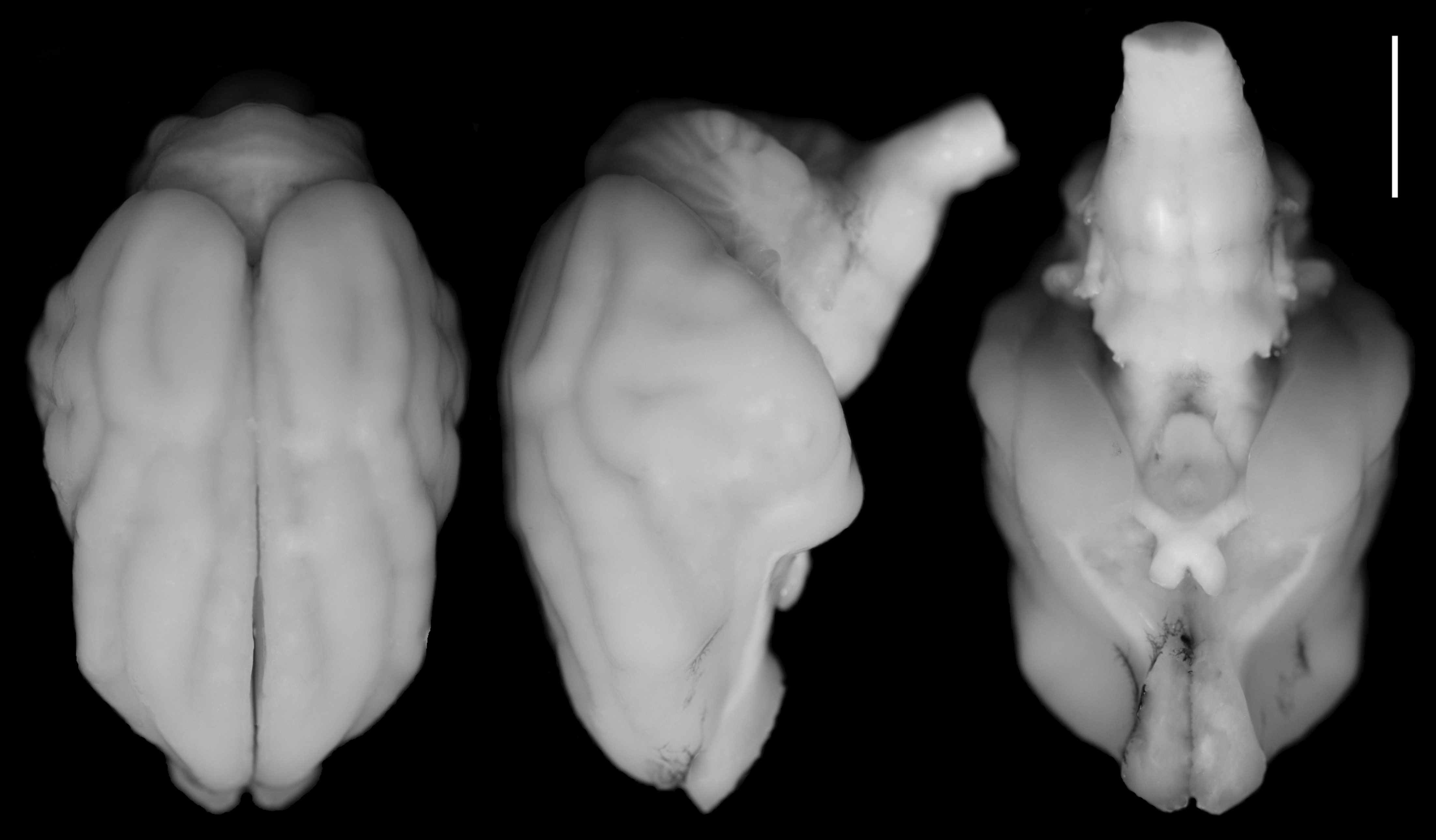

**Figure 2.2:** Diagrammatic reconstructions of a series of coronal sections through the brain of the rock hyrax illustrating the location of neurons immunohistochemically reactive for choline acetyltransferase (ChAT, black circles), tyrosine hydroxylase (TH, black triangles) and serotonin (open squares). The outlines of the architectonic regions were drawn using Nissl and myelin stains and immunoreactive neurons marked on the drawings. Drawing **A** represents the most rostral section, **Z** the most caudal. The drawings are approximately 1500 µm apart. See list for abbreviations.

A
NEO
OB
A16
B
NEO
PIR
C
NEO
LV
N.Acc
PIR
1mm
D
NEO
LV
C
P
PIR
N.Acc
TOL
E
NEO
C
ic
P
cc
PIR
N.Acc
TOL/ls.Call.
F
NEO
cc
LV
C
S
CI
ic
P
PIR
TOL/ls.Call.
N.Acc
OC
Diag.B
G
NEO
cc
C
LV
Sep.M
ic
CI
P
ac
GP
3V
A14
Hyp
PIR
OC
Amyg
A15v
N.Bas
A12
1mm
H
NEO
cc
LV
C
CI
Sep.M
f
ic
P
GP
O
OT
Amyg
PIR
A15v
A12
A14
N.Bas
I
NEO
cc
LV
f
C
ic
CI
DT
Hyp.l
R
Hyp.d
P
GP
3V
f
OT
A14
Amyg
PIR
A12
Hyp.v

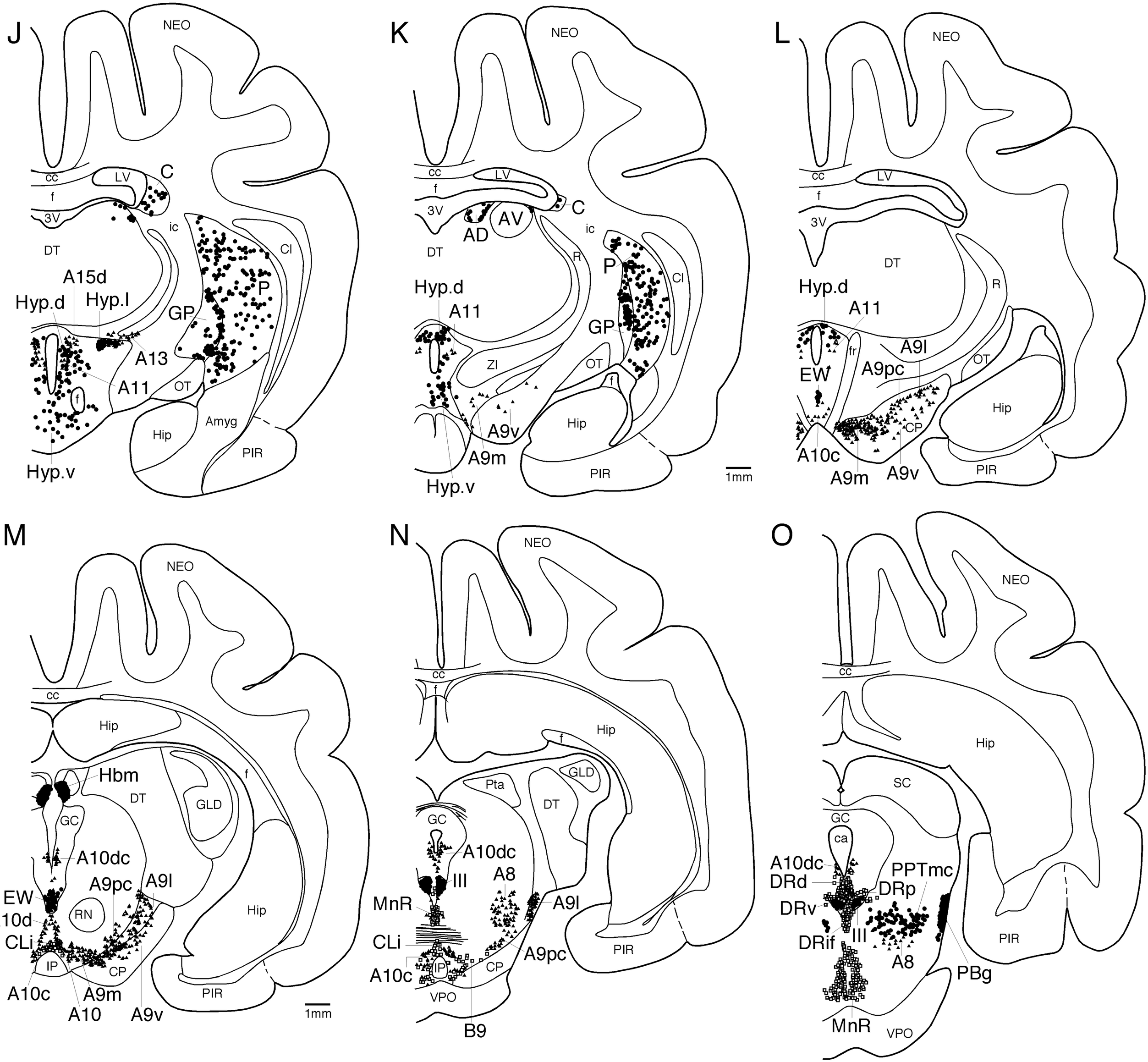
J
NEO
cc
LV
C
f
3V
ic
DT
Cl
A15d
Hyp.d
Hyp.l
P
GP
A13
A11
OT
f
Hip
Amyg
PIR
Hyp.v
K
NEO
cc
LV
f
3V
AD
AV
C
ic
DT
R
P
Cl
Hyp.d
A11
GP
ZI
OT
f
A9v
Hip
A9m
PIR
Hyp.v
1mm
L
NEO
cc
LV
f
3V
DT
R
Hyp.d
A11
fr
A9l
EW
A9pc
OT
Hip
CP
A10c
A9m
A9v
PIR
M
NEO
cc
Hip
f
Hbm
DT
GLD
GC
A10dc
A9pc
A9l
EW
RN
Hip
A10d
CLi
IP
CP
A10c
A9m
A10
A9v
PIR
1mm
N
NEO
cc
f
Hip
f
Pta
GLD
DT
GC
A10dc
III
A8
MnR
A9l
CLi
A9pc
IP
CP
A10c
VPO
PIR
B9
O
NEO
cc
Hip
SC
GC
ca
A10dc
PPTmc
DRd
DRp
DRv
III
DRif
A8
PBg
PIR
MnR
VPO

P

NEO
LV
cc
Hip
SC
PBg
LDTmc
A6d
LDTpc
IC
DRl
PIR
DRd
DRv
scp
PPTpc
DRif
mcp
MnR
PPTmc
A7d
VPO
A7sc

Q

NEO
LV
SC
PIR
IC
LDTpc
A4
PPTpc
LDTmc
PPTmc
DRc
Vmot
DRp
MnR
A7d
RMg
A5
py

1mm

R

NEO
PIR
SC
IC
Cb
icp
Vl
7n
C1
VIId
RMg
VIIv
RVL
py
RPa

S

NEO
NEO
Cb
icp
Cb
C2
CN
pIX
pVII
RMg
VIIv
C1
io
io
py
RVL
RPa

1mm

T

NEO
NEO
Cb
icp
4V
C2
pIX
X
ROb
XII
A1
io
N.Amb
C1
RPa
py
RVL/CVL

V

NEO
Cb
DCN
4V
pIX
C2
A2
X
ROb
XII
A1
io
N.Amb
py
CVL

W

NEO
Cb
DCN
Cb
AP
C2
X
A2
ROb
XII
A1
LRT
io
N.Amb
py
CVL

X

Cb
X
A2
XII
A1
vh

Y

Cb
XII
vh

Z

Cb
vh
pyx

**Figure 2.3:** Diagrams of idealized sagittal sections through the rock hyrax brain showing **A**. cholinergic, **B**. putative catecholaminergic, and **C**. serotonergic nuclei or nuclear complexes. See list for abbreviations.

A

AD
Hbm
C/P/Med.S/
N.Acc
GP
Hyp.d/l
III/EW
IV
PBg
Vmot
pIX
PPT
VI
LDT
X
VIId
pVII
XII
ls.Call/Olf.Tub
N.Bas
Hyp.v
VIIv
N.Amb
vh

B

A16
A15d
A13
A11
A10dc
A14
A10d
A8
A4
A10/9
A7
A6d
C2
A15v
A12
AP
A5
A2
C1
A1
5 mm

C

CLi
DR
MnR
RMg
B9
RPa
ROb
RVL
CVL

**Figure 2.4:** Photomicrograph montage of the basal forebrain nuclei anterior to the anterior commissure, demonstrating choline acetyletransferase (ChAT) immunoreactivity. Note the strongly ChAT+ densely packed neurons of the diagonal band of Broca (**Diag.B**) and the scattered strongly ChAT+ neurons in nucleus accumbens (**N.Acc**), caudate (**C**) and putamen (**P**). A weakly to moderately intense ChAT+ neuropil is found in these regions. Scale bar = 1 mm.

LV
C
N.Acc
ic
P
Diag.B.

**Figure 2.5:** Photomicrographs of coronal sections through the anterior nuclei of the dorsal thalamus of the rock hyrax demonstrating the location of ChAT+ neurons and neuropil in the anteroventral (**AV**) and anterodorsal nuclei (**AD**). **A**. Nissl stained section. **B**. Adjacent ChAT immunoreacted section. **C**. Higher power photomicrograph of AD showing location of ChAT+ neurons. **D**. High power photomicrograph showing ChAT+ neuron and terminals. Scale bar in B = 1 mm and applies to **A** and **B**. Scale bar in C = 100 µm Scale bar in D = 50 µm. **3V** – third ventricle.

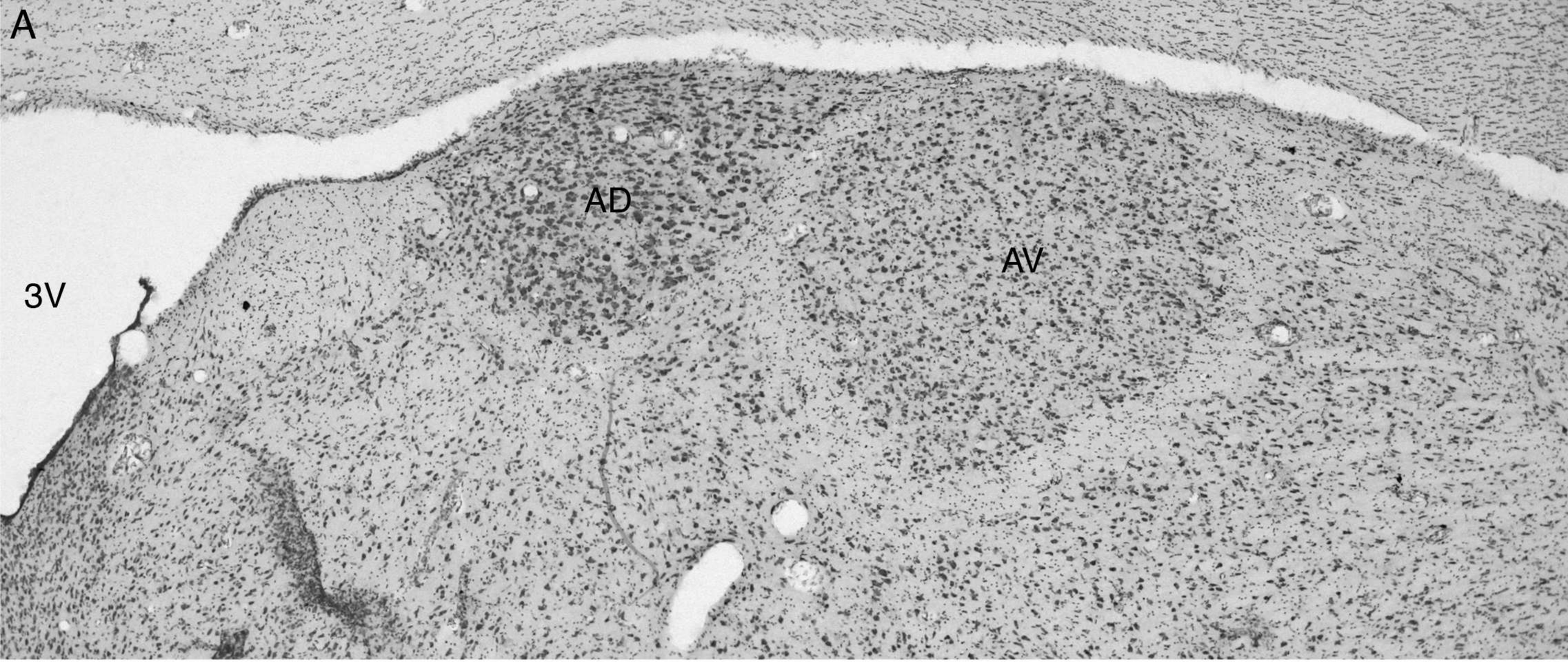
A
AD
AV
3V

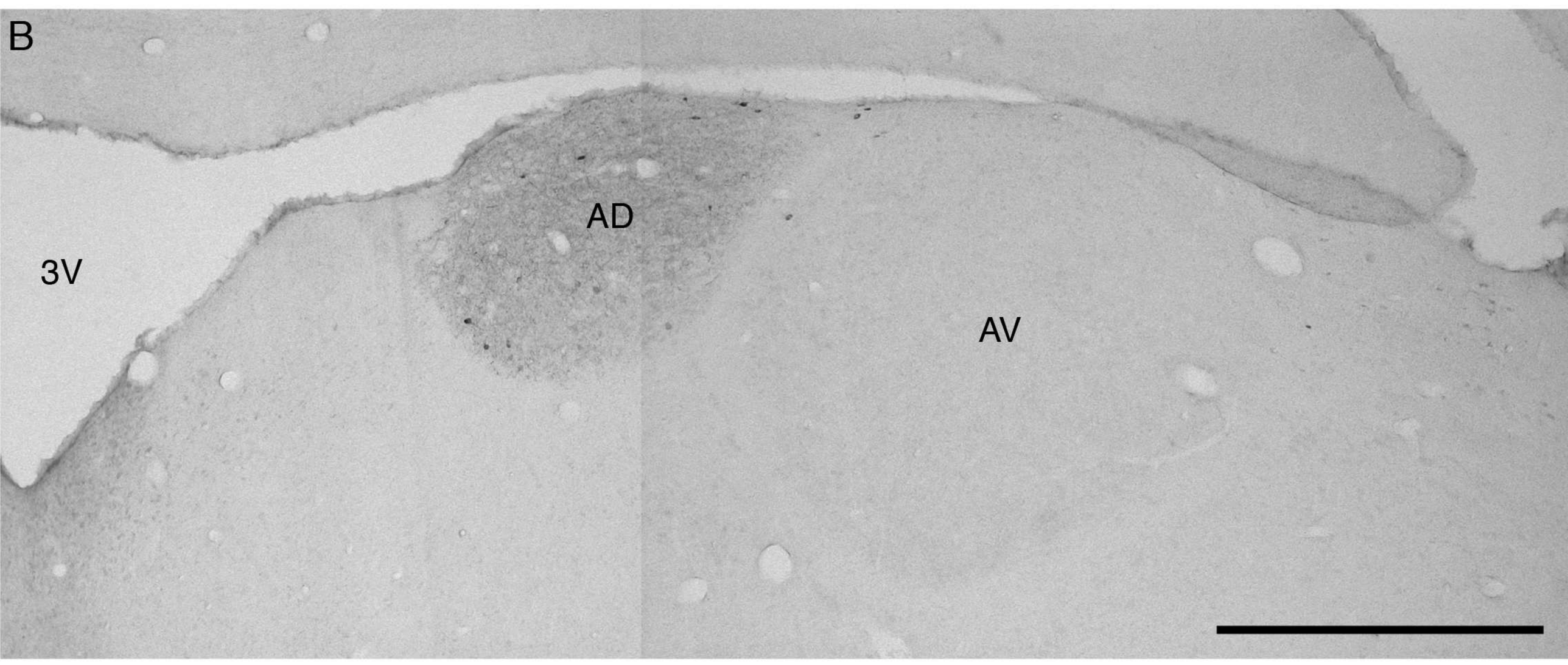
B
AD
AV
3V

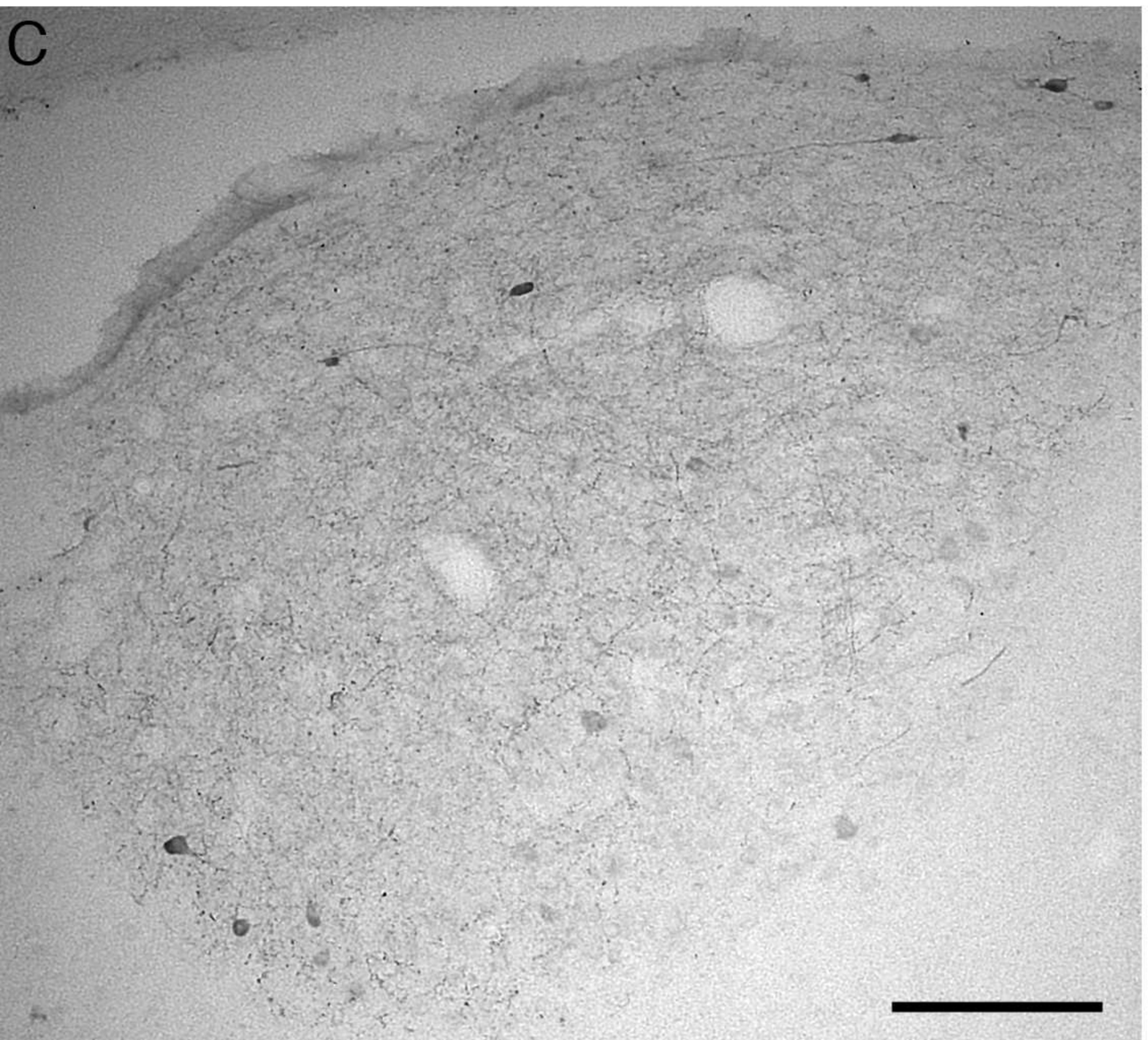
C

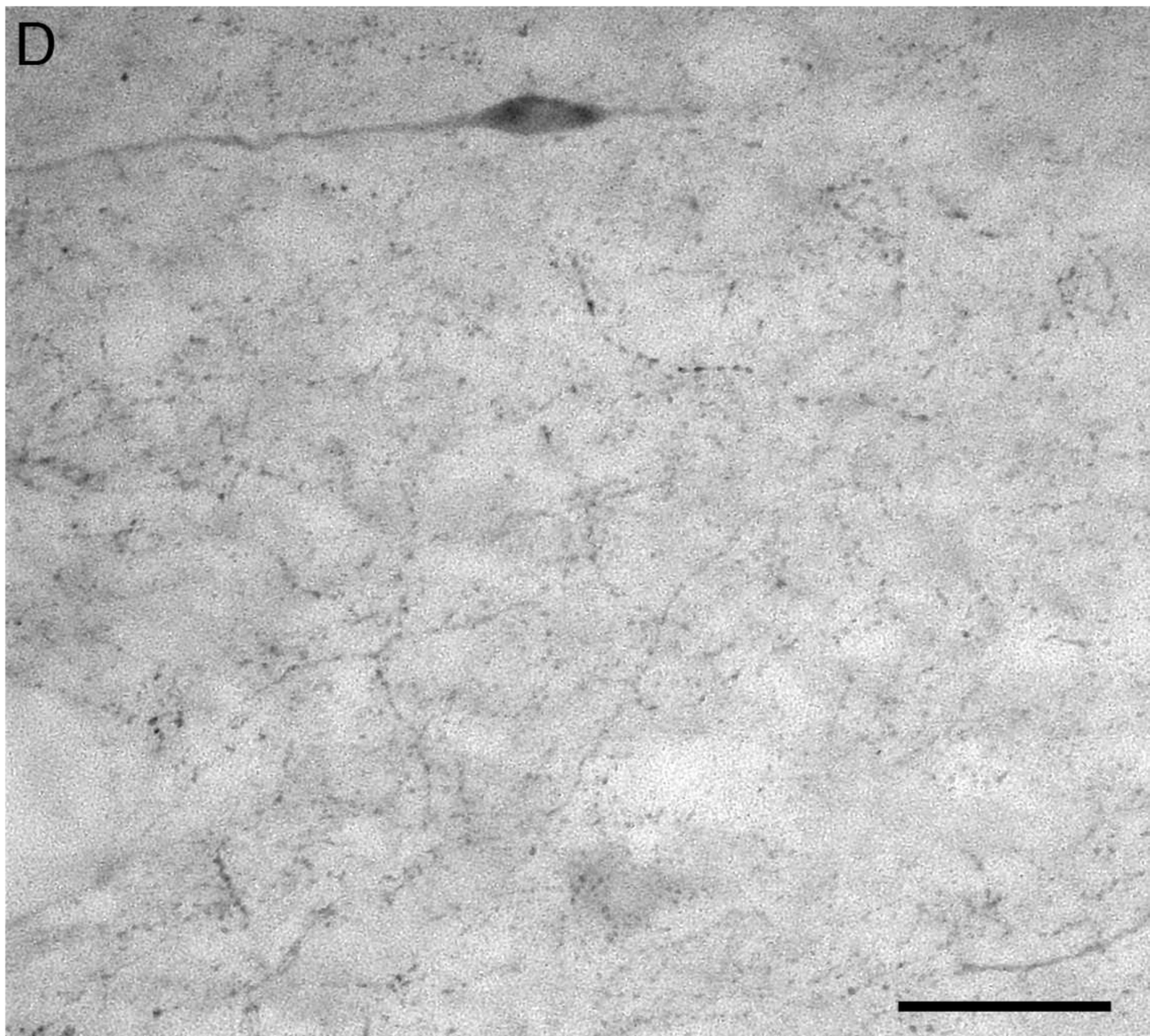
D

**Figure 2.6:** Photomicrographs of ChAT immunoreacted sections through the dorsal isthmic/pontine region of the rock hyrax brain. **A**. The magnocellular division of the pedunculopontine nucleus (**PPTmc**) at the level of the oculomotor nucleus (**III**) and the parabigeminal nucleus (**PBg**). **B**. The magnocellular and parvocellular divisions of both the laterodorsal (**LDTmc**, **LDTpc**) and pedunculopontine (**PPTmc**, **PPTpc**) nuclei at a level slightly caudal to that shown in **A**. Note the distinct clusters of small neurons (**LDTpc** and **PPTpc**) located medial to the **LDTmc** and dorsal to the **PPTmc**. The distinct clusters are shown at higher power in **C** (LDTmc and LDTpc) and **D** (**PPTmc** and **PPTpc**). Scale bar in B = 1 mm and applies to **A** and **B**. Scale bar in D = 100 µm and applies to **C** and **D**. **ca** – cerebral aqueduct.

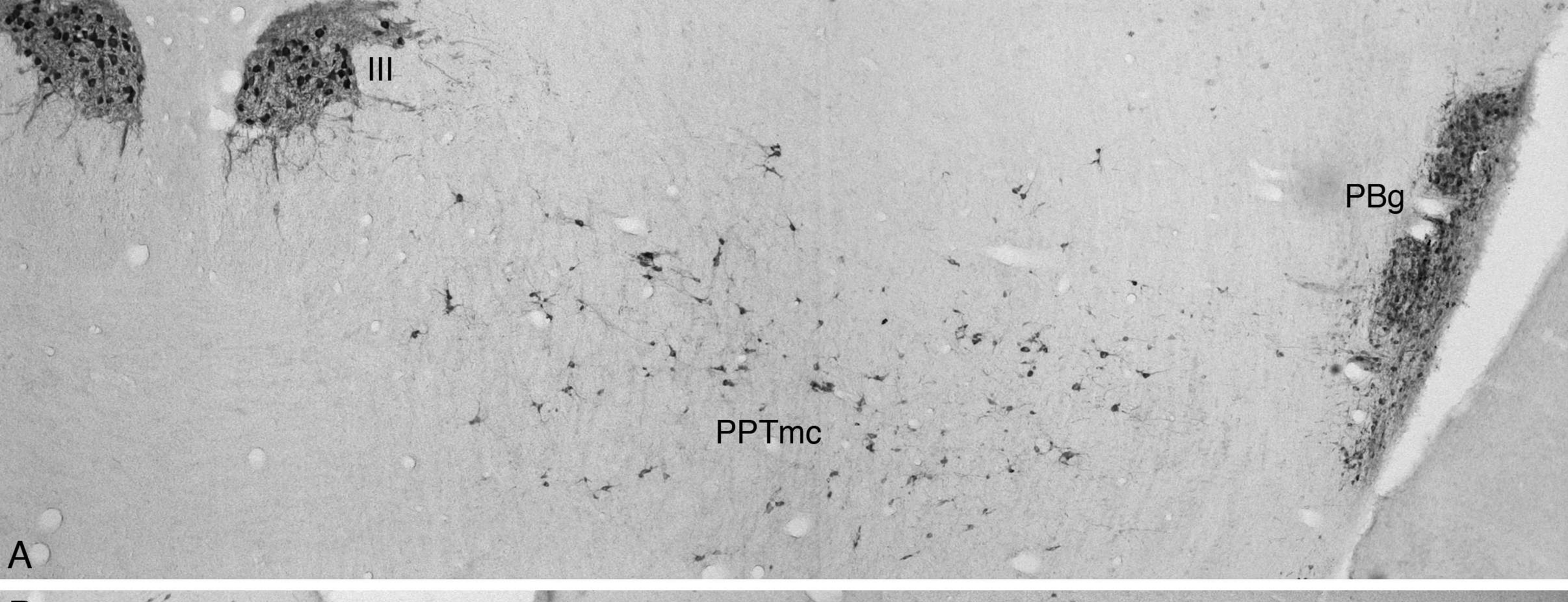
III
PBg
PPTmc
A

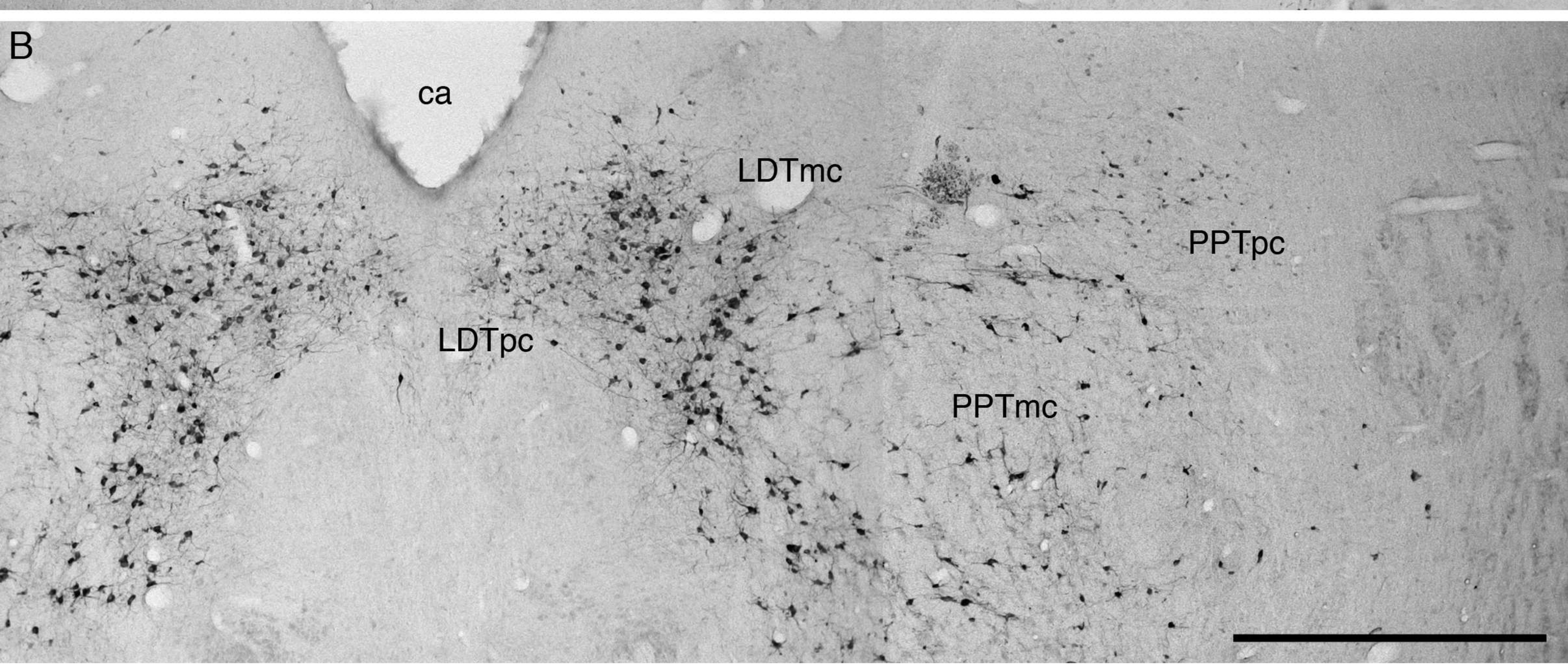
B
ca
LDTmc
PPTpc
LDTpc
PPTmc

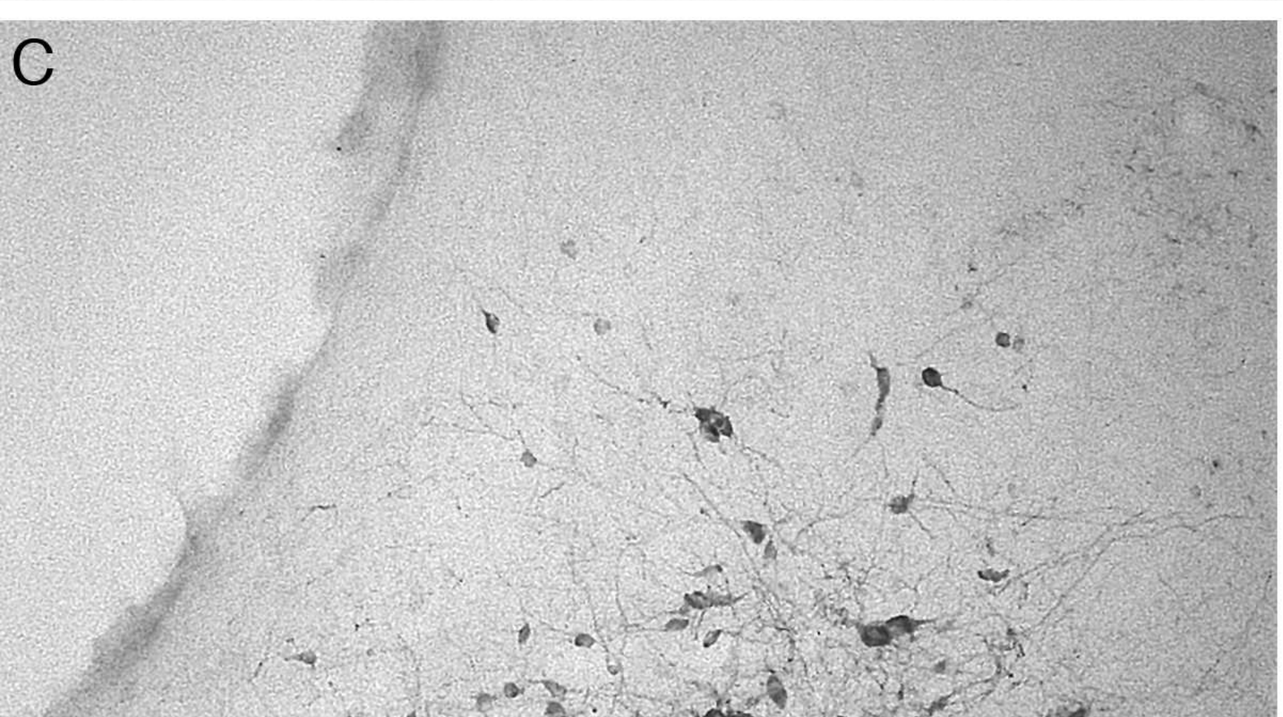
C
LDTpc
LDTmc

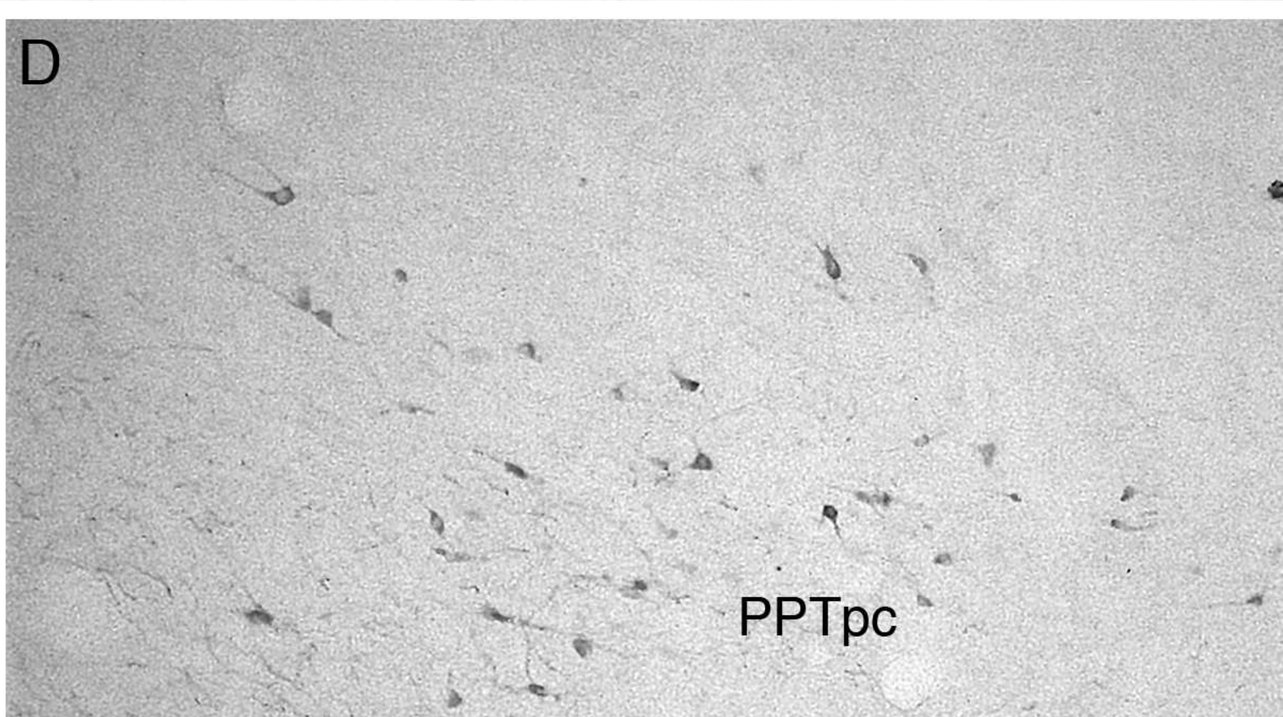
D
PPTpc
PPTmc

**Figure 2.7:** Photomicrographs of ChAT immunoreacted sections through periventricular grey matter in the dorsal caudal medullary region of the rock hyrax brain. **A**. The greatly expanded preganglionic motor neurons of the inferior salivatory nucleus (**pIX**) at a rostral level through this nucleus. **B**. The same nucleus at a more caudal level where it lies dorsal to the dorsal motor vagus (**X**) and hypoglossal (**XII**) nuclei. The Scale bar in **B** = 1 mm, applies to **A** and **B**. **4V** – fourth ventricle.

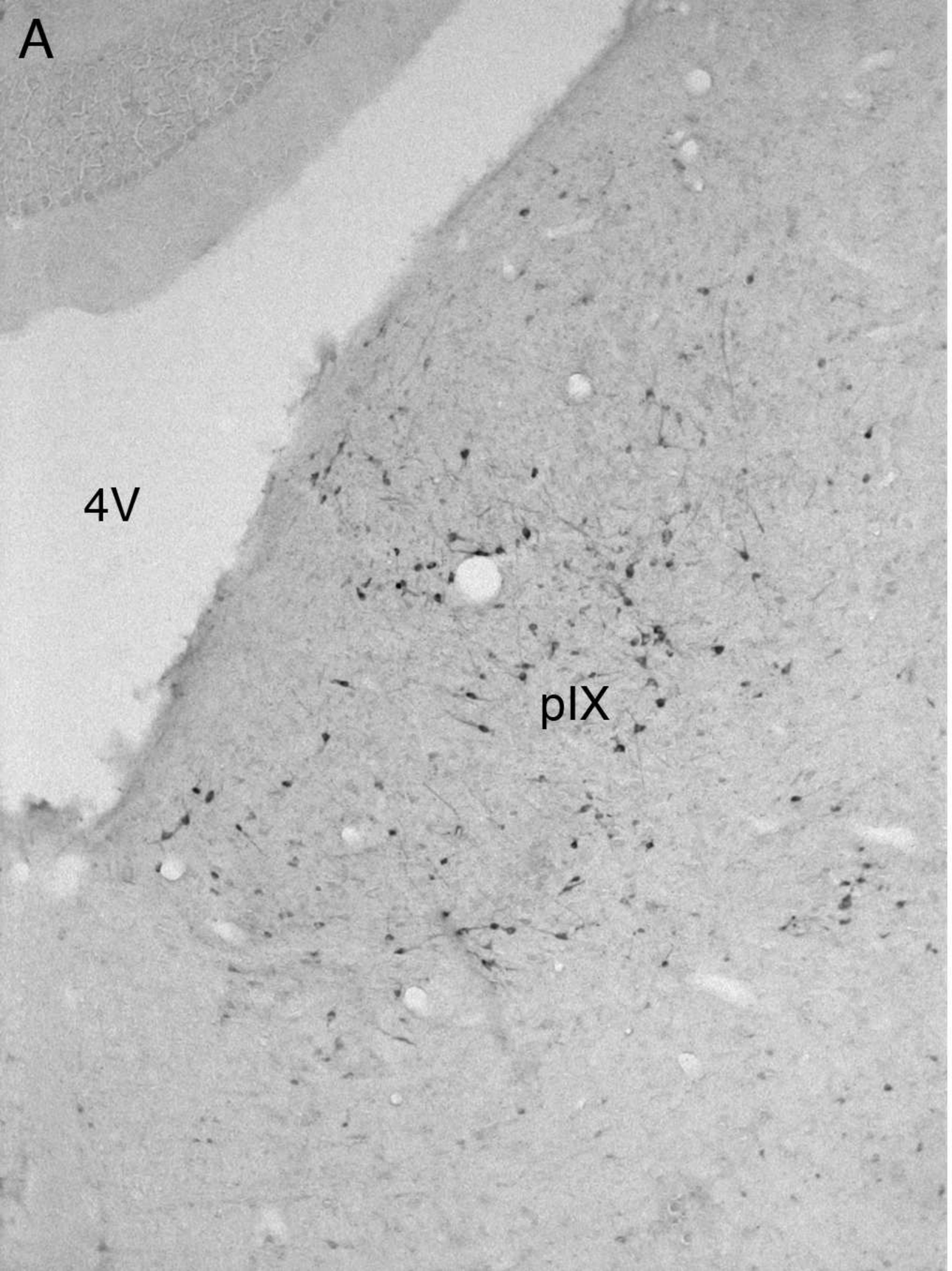
A
4V
plX

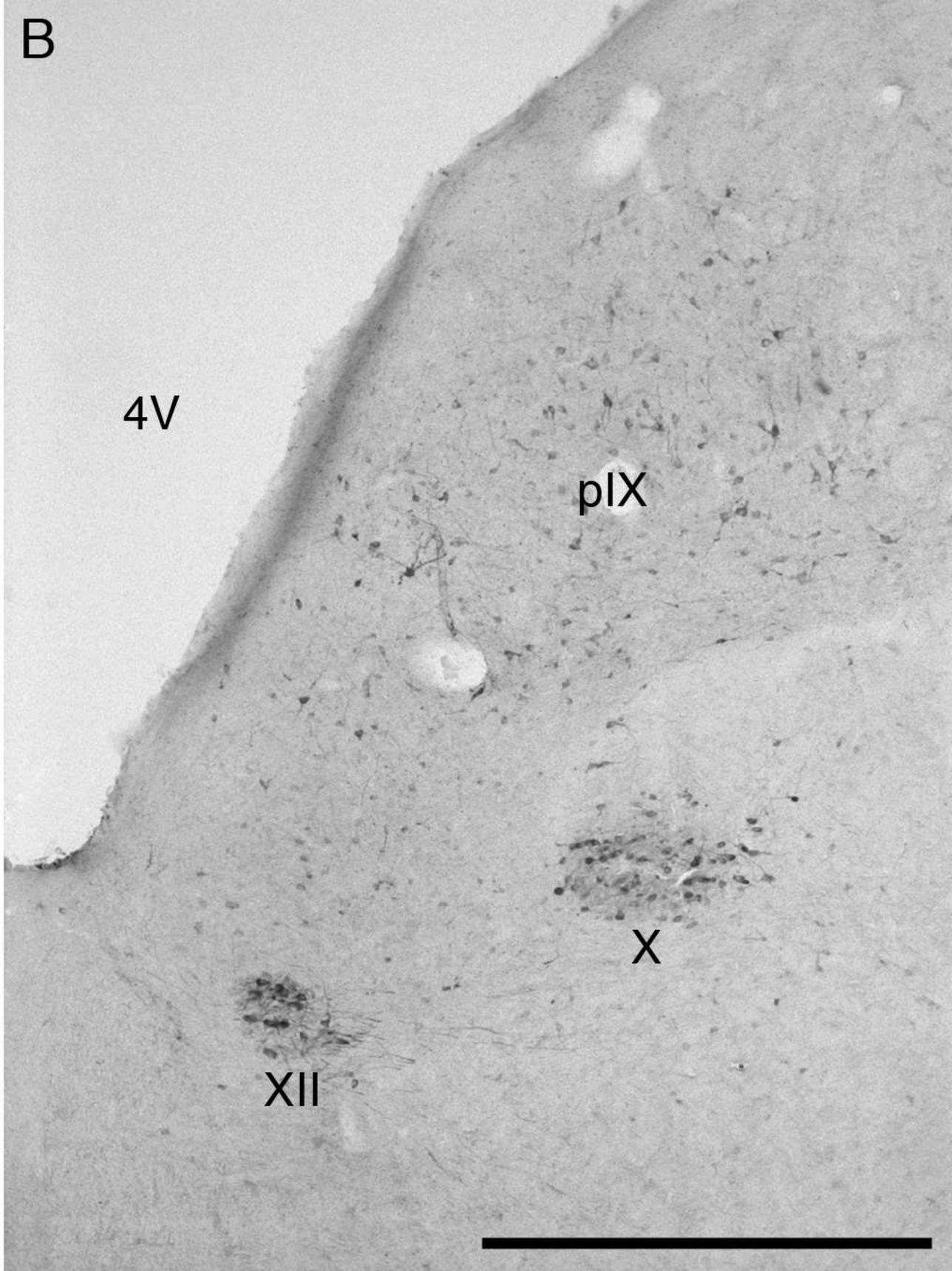
B
4V
plX
X
XII

**Figure 2.8:** Photomicrographs of selected neuronal groups immunohistochemically reactive for tyrosine hydroxylase within the brain of the rock hyrax. **A**. The rostral periventricular nucleus (**A14**) located adjacent to the walls of the third ventricle (**3V**) in the hypothalamus. **B**. The dorsal caudal nucleus of the ventral tegmental complex (**A10dc**) located around the ventral region of the cerebral aqueduct (**ca**). **C**. Very few TH+ neurons are found in the diffuse portion of the locus coeruleus (**A6d**) within the ventrolateral periaqueductal grey matter, while the compact portion of the nucleus subcoeruleus (**A7sc**) in the adjacent dorsal pontine tegmentum is rich in strongly TH+ neurons. **D**. The retrorubral nucleus (**A8**) and the lateral nucleus of the substantia nigra complex (**A9l**) in the lateral and ventral midbrain tegmentum. Scale bar in **C** = 500 µm and applies to **A**, **B**, **C**. Scale bar **D** = 1 mm.

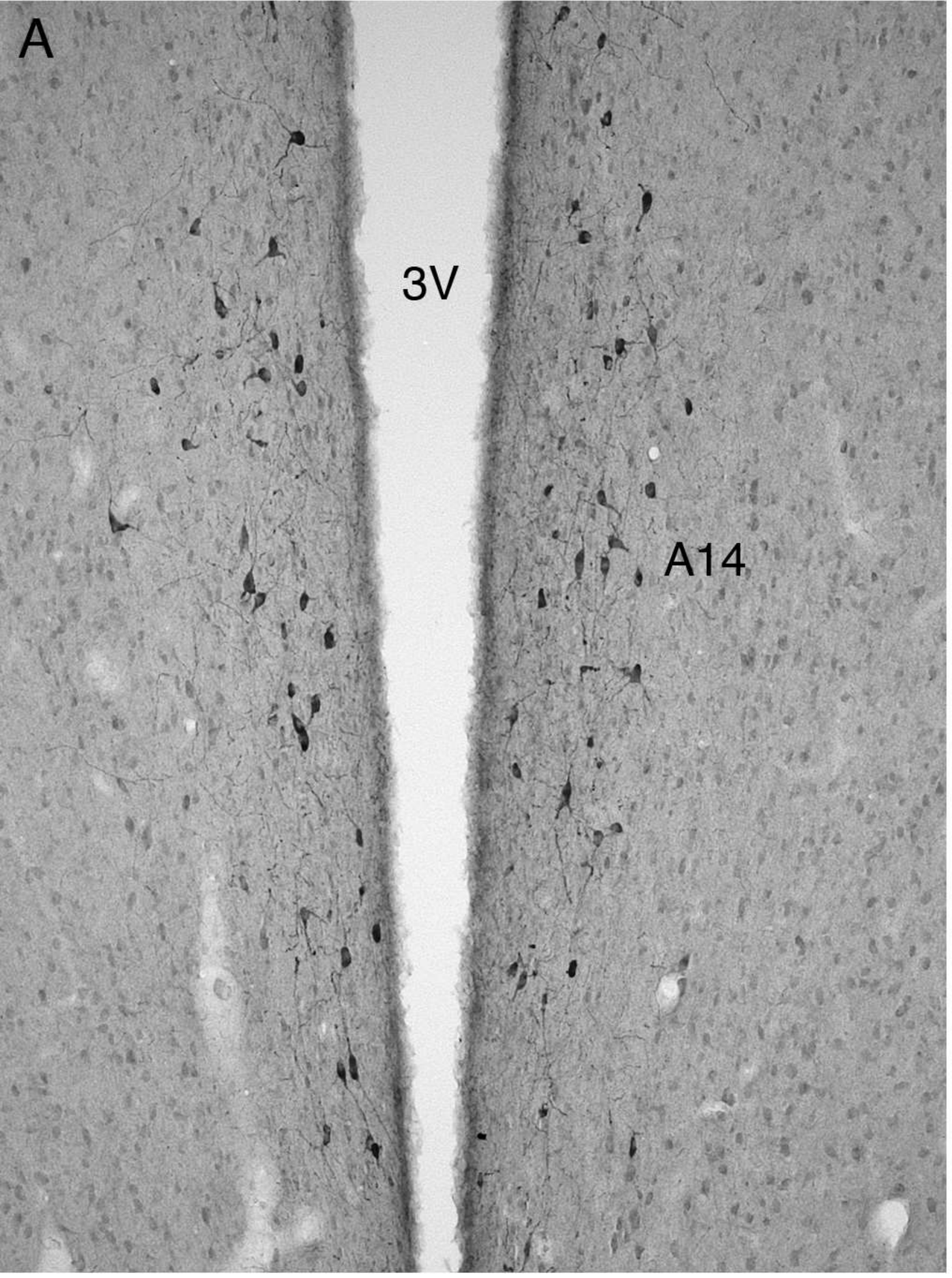
A
3V
A14

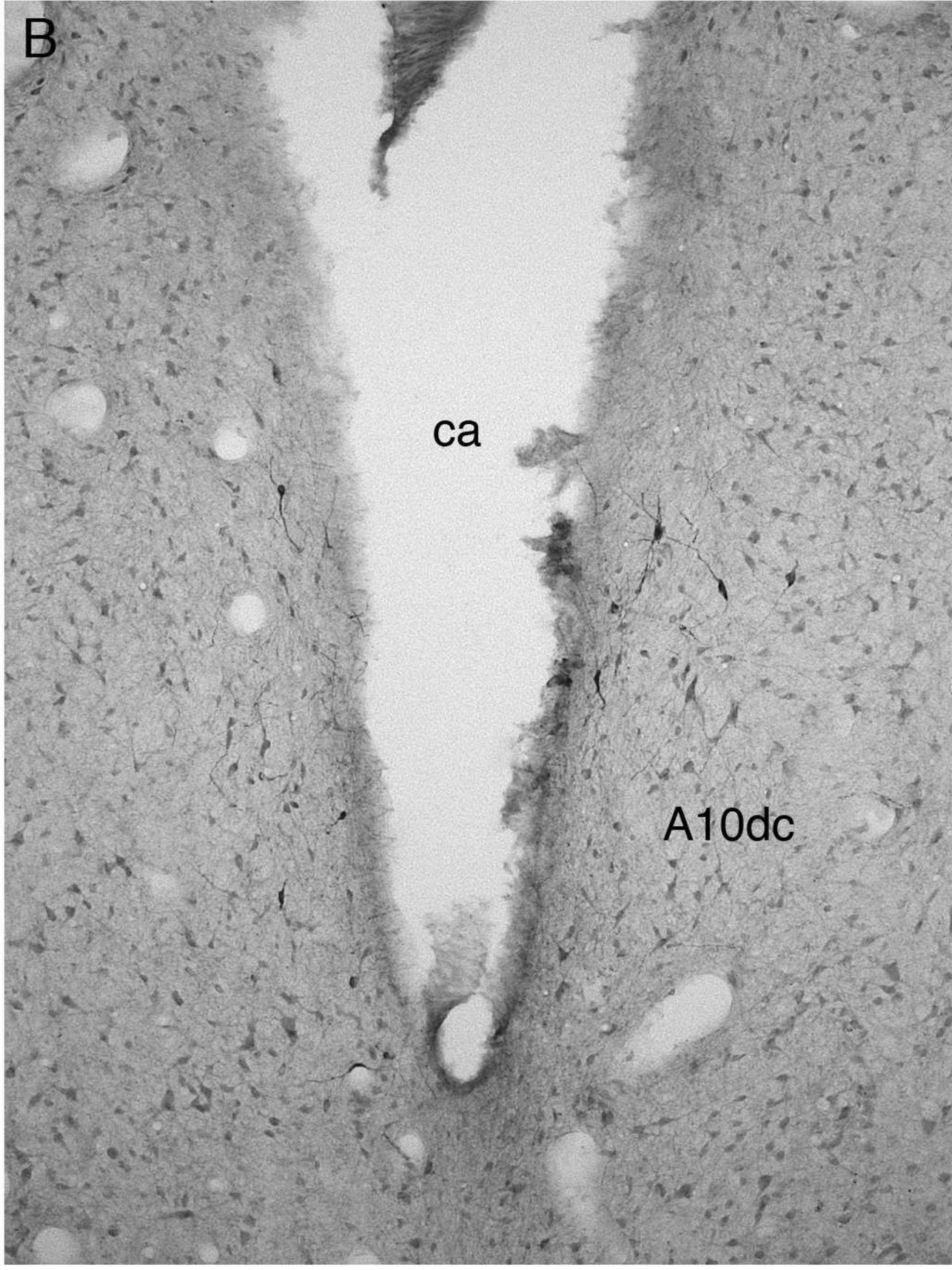
B
ca
A10dc

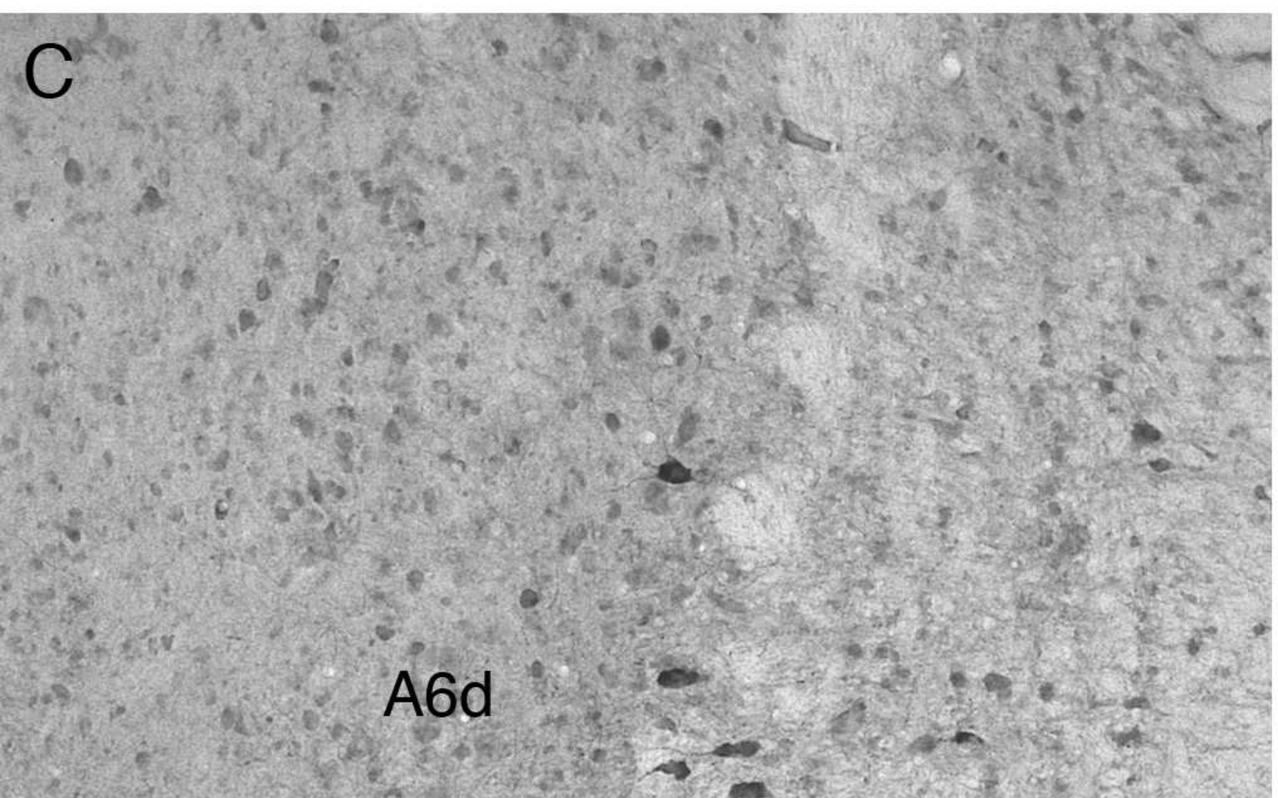
C
A6d
A7sc

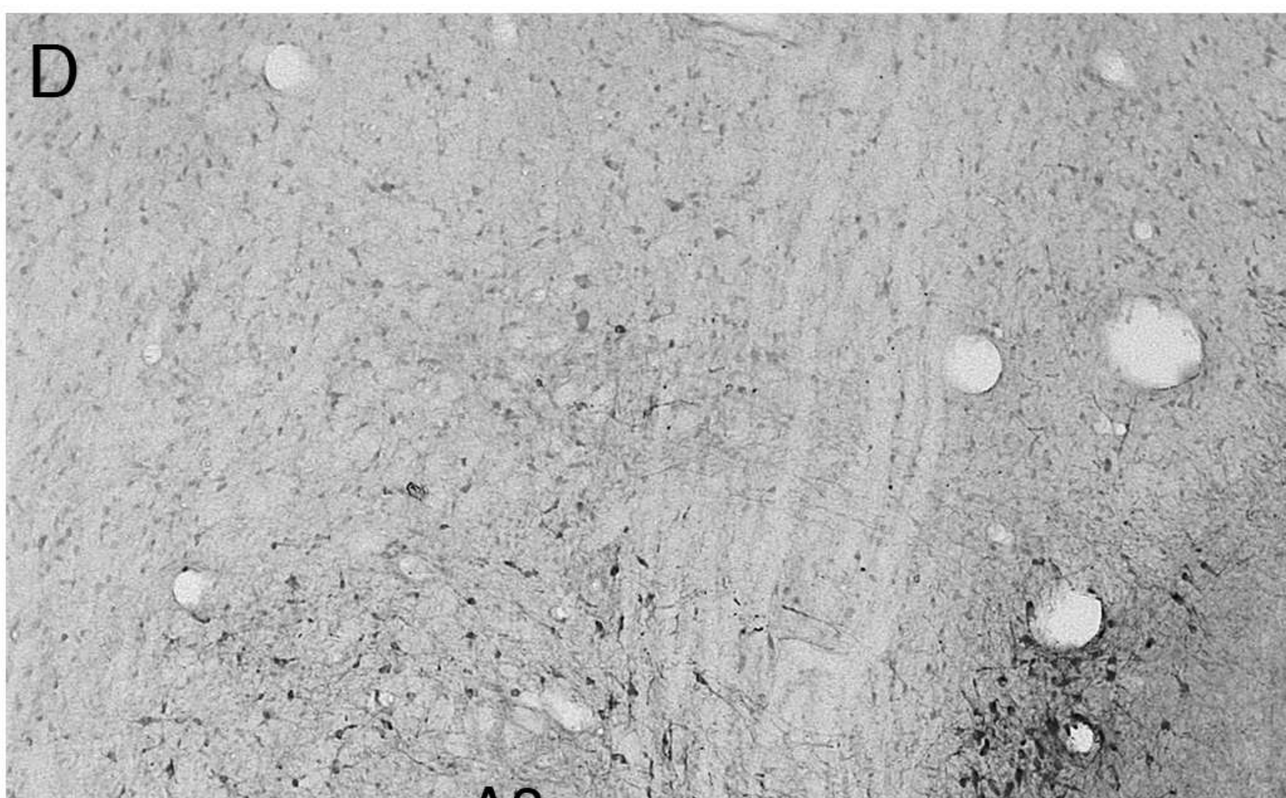
D
A8
A9l

**Figure 2.9:** Photomicrograph montage of the nuclear organization of the ventral tegmental area (**A10**, **A10c**, **A10d**) and the substantia nigra (**A9m**, **A9pc**, **A9l**, **A9v**) in the rock hyrax as revealed using tyrosine hydroxylase immunohistochemistry. Scale bar = 1 mm. **IP** – interpeduncular nucleus; **PC** – cerebral peduncle; **Rmc** – red nucleus, magnocellular division.

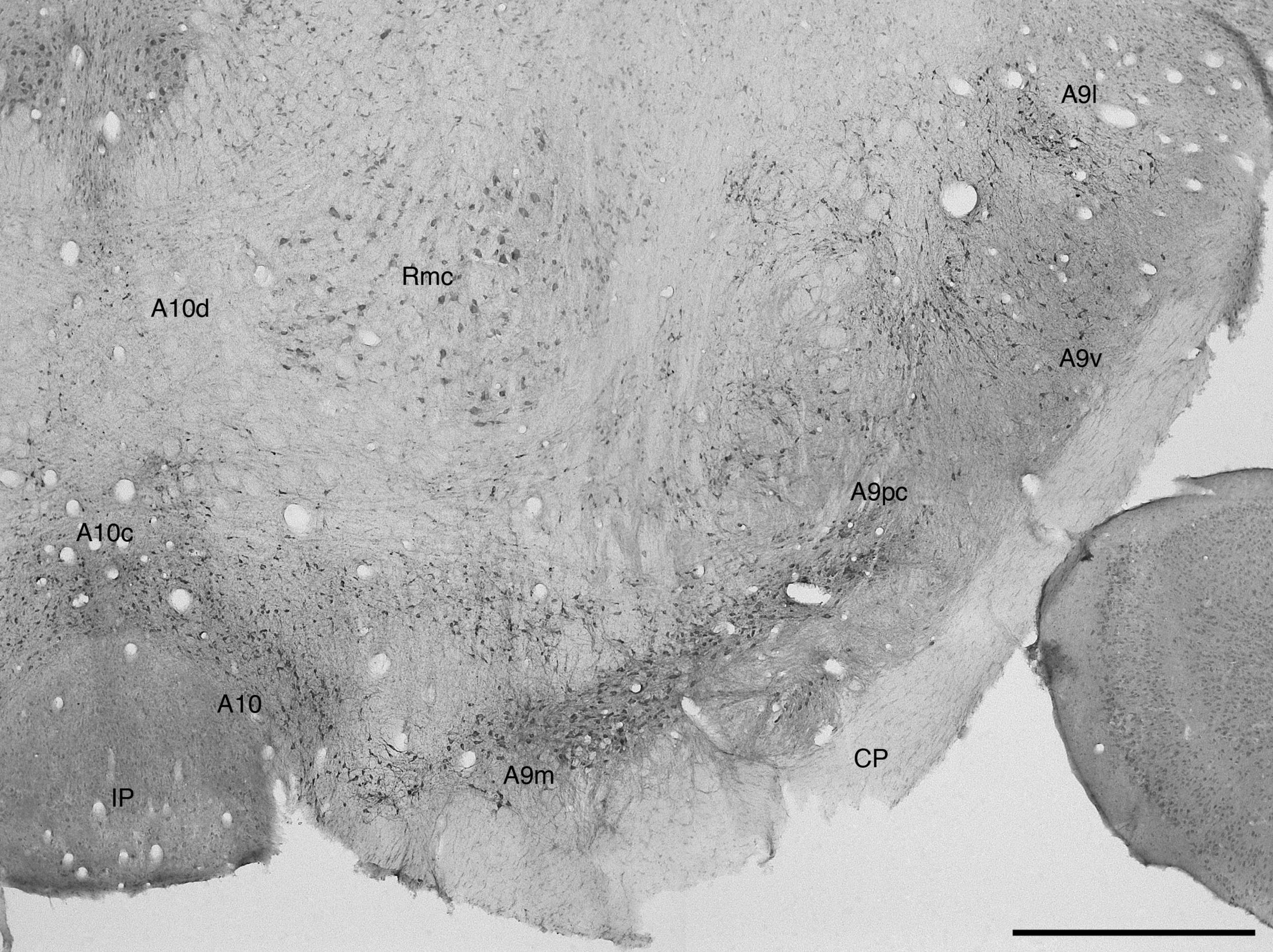
A9l
Rmc
A10d
A9v
A9pc
A10c
A10
CP
A9m
IP

**Figure 2.10:** Photomicrograph montage of the neuronal groups immunohistochemically reactive for serotonin within the dorsal raphe nuclear complex of the rock hyrax brain. Dorsal raphe lateral nucleus (**DRl**), dorsal raphe dorsal nucleus (**DRd**), dorsal raphe ventral nucleus (**DRv**), dorsal raphe interfascicular nucleus (**DRif**), dorsal raphe peripheral nucleus (**DRp**) and the median raphe nucleus (**MnR**). Scale bar = 1 mm. **ca** – cerebral aqueduct.

ca

DRI

DRd

DRp

DRv

DRif

MnR

**Figure 2.11:** Photomicrographs of selected neuronal groups immunohistochemically reactive for serotonin in the midbrain and brainstem of the rock hyrax. **A**. The caudal linear nucleus (**CLi**) at its most anterior level, immediately dorsal to the interpeduncular nucleus (**IP**). **B**. The CLi at a more posterior level, where it is located ventral to the decussation of the superior cerebellar peduncle (**xscp**), and where at its most ventral and lateral aspect it becomes continuous with the supralemniscal serotonergic nucleus (**B9**). **C**. The caudal division of the dorsal raphe nucleus (**DRc**) lying immediately ventral to the most posterior portion of the cerebral aqueduct (**ca**). Scale bar in C = 1 mm, and applies to all.

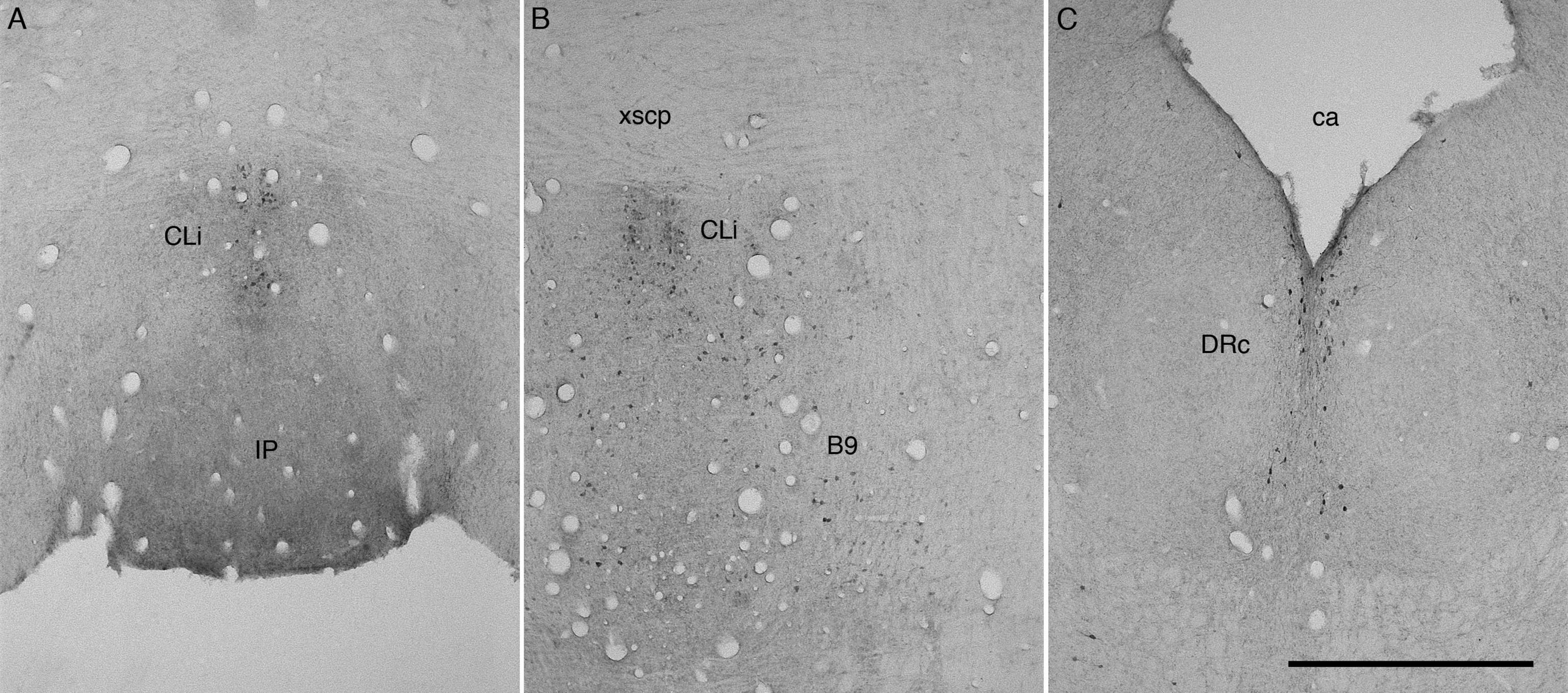
A
CLi
IP
B
xscp
CLi
B9
C
ca
DRc

## 2.5. Discussion

The aim of the current study was to reveal the nuclear organization of the cholinergic, putative catecholaminergic and serotonergic systems of the rock hyrax, *Procavia capensis.* The results revealed that these systems, for the most part, are similar to what has previously been described in other mammals; however, certain specific differences were observed regarding the nuclear organization of the cholinergic and putative catecholaminergic systems. The nuclear organization of the serotonergic system was similar to what has been documented for other eutherian mammals (e.g. Törk, 1990; Maseko et al., 2007; Moon et al., 2007; Dwarika et al., 2008; Limacher et al., 2008; Bhagwandin et al., 2008). The differences that were noted for the cholinergic system included the existence of cholinergic immunoreactive neurons in the anterior dorsal and ventral nuclei of the dorsal thalamus, the presence of parvocellular and magnocellular divisions/nuclei of both the LDT and PPT, and the presence of a large cholinergic cell group in the periventricular grey of the rostral medulla (pIX). The features of the putative catecholaminergic system that differed significantly from that seen in other mammals were the absence of a dense cluster of TH+ neurons constructing the locus coeruleus compact (A6c) and a diffuse locus coeruleus (A6d) with only few TH+ neurons. We discuss each of these unusual features in turn, and then compare the overall organization of these systems in the hyrax to prior observations of these systems across various mammalian species.

*2.5.1. Cholinergic neurons in the anterodorsal (AD) and anteroventral (AV) nuclei of the dorsal thalamus of the rock hyrax*

The AD and AV nuclei identified in the brain of the rock hyrax form part of the anterior nuclei of the dorsal thalamus and are a general feature of the mammalian dorsal thalamus (Jones, 2007). The anterior nuclear group typically consists of four distinct nuclei, the anterodorsal (AD), anteromedial (AM), anteroventral (AV), and lateral dorsal (LD) nuclei (Jones, 2007). In the rock hyrax the AD nucleus was located within the anterior and dorsal regions of the dorsal thalamus, as is typical of mammals, and exhibited a strong cholinergic neuropil staining along with ChAT immunoreactive neurons scattered around the margins of the nucleus. Lateral to the AD nucleus in the rock hyrax, a second nucleus exhibiting a weaker cholinergic neuropil staining with ChAT immunoreactive neurons along the upper medial and lateral borders was identified as the AV nucleus. While both the AD and AV nuclei are known for their strong histochemical reactivity to acetylcholinesterase, choline acetyltransferase immunoreactive neurons have not been reported in either of these nuclei in any other mammal (Jones, 2007; Maseko et al., 2007).

Afferent input to these nuclei originates largely from the hypothalamus and hippocampal formation, but also includes corticothalamic and thalamocortical connections (Jones, 2007). The AD and AV nuclei have been reported to be involved in spatial learning and memory, and navigation; however, these nuclei are not the sole contributors, but rather work in conjunction with the other anterior thalamic nuclei to achieve these functions (Segal et al., 1988; van Groen et al., 2002; Oda et al., 2003; Wolff et al., 2008). It is difficult to hypothesize on the potential effect of the presence of

cholinergic neurons within and closely surrounding these nuclei in regard to function; but given that the cholinergic system in general appears to be related to activity requiring both alertness and awareness, these neurons may have the effect of enhancing the wakefulness promoting functions of the anterior thalamic nuclei in the hyrax, possibly leading also to enhanced learning and memory functions.

Presently, it appears that these anterior thalamic cholinergic neurons are unique to the rock hyrax as they have not been observed in other mammals. Despite this, we can only tentatively conclude that they are a unique feature as no other members of the Afroplacentalia have been examined for the presence of these neurons. Thus, these anterior thalamic cholinergic neurons may be unique to the hyrax, or may be found in other members of the Afroplacentalia, especially the closely related Proboscideans and Sirenians. Until further Afroplacentalia species have been examined the uniqueness of this aspect of the cholinergic system remains uncertain.

### *2.5.2. Magnocellular and parvocellular divisions/nuclei of the pedunculopontine and laterodorsal tegmental nuclei in the rock hyrax*

Within all mammals studied to date, cholinergic neurons within the pontine tegmentum (PPT) and periventricular grey matter (LDT) have been reported (e.g. Maseko et al., 2007). In all these prior studies the morphology of the cholinergic neurons within and between the PPT and LDT nuclei have been reported to be homogeneous (e.g. Woolf, 1991; Manger et al., 2002a; Maseko and Manger, 2007; Maseko et al., 2007; Limacher et al., 2008; Bhagwandin et al., 2008). The situation observed in the current study in the rock hyrax raises a significant difference in this regard, as the cholinergic

neurons within these nuclei did not exhibit a homogenous morphology. Rather, we identified two neuronal types within each of these nuclei, and the inner spatial distribution and segregation of these two neuronal types has led to the proposal of the subdivision of these nuclei into parvocellular and magnocellular PPT and LDT nuclei. The magnocellular subdivision of both the PPT and LDT nuclei exhibited a neuronal morphology reminiscent of that described for all other mammals (Woolf, 1991; Manger et al., 2002a; Maseko et al., 2007; Limacher et al., 2008; Bhagwandin et al., 2008). For this reason, plus the topography of the neurons forming these magnocellular divisions (LDTmc being in the ventrolateral portion of the grey matter and PPTmc lying in the adjacent tegmentum), we propose that the magnocellular divisions of these nuclei in the rock hyrax are homologous to the LDT and PPT nuclei described for all other mammals. The parvocellular cholinergic subdivisions, on the other hand, have not been reported in any other mammal studied to date, although a non-cholinergic parvocellular component has at times been included as part of the PPT in rat and cat (Semba and Fibiger, 1989). The morphology of the neurons ascribed to the parvocellular divisions, being small, and bipolar with oval soma, are reminiscent of cholinergic interneurons found in the cerebral cortex (Bhagwandin et al., 2006) or superior colliculus (Tan and Harvey, 1989) in some other mammals. These putative cholinergic interneurons were found medial to the LDTmc, and dorsal to the PPTmc. It is possible that these cholinergic interneurons are also immunoreactive for GABA, forming part of the pontine GABAergic system. It has been reported by Bayraktar et al. (1997) that nearly all VIP+ and approximately 88% of ChAT+ neurons also contain GABA. A similar situation has been observed in the cortical cholinergic neurons found in certain species of mammals (Bhagwandin et al., 2006).

Potentially, a change at the molecular level of organization occurred within these neurons, such as molecular interactions, adding multiple transmission lines and thus increased functionality to this neuronal group (Agnati et al., 1986). These potentially GABAergic neurons may have acquired ChAT proteins resulting in their immunoreactivity.

The above described potential molecular change and increased transmission lines in these cholinergic interneuron groups in close apposition to the traditional cholinergic LDT and PPT could lead to interesting functional outcomes. It is well known that GABAergic neurons within the pons play a major role in the regulation of the traditional cholinergic LDT and PPT with regard to the sleep-wake cycle especially REM sleep (Maloney et al., 1999, 2000; Boissard et al., 2003; Pal and Mallick, 2006; Luppi et al., 2007). The location of the cholinergic, potentially GABAergic neurons described as the PPTpc and LDTpc in the current study makes them prime candidates forming part of a local GABAergic network involved in the switching of states during the sleep-wake cycle (Luppi et al., 2007). The added transmission line related to the production of acetylcholine in the hyrax may produce some unusual effects on the measurable physiological parameters of sleep, especially REM sleep in the hyrax.

Again it appears that these parvocellular cholinergic LDT and PPT may be unique to the rock hyrax as they have not been observed in other mammals (e.g. Maseko et al., 2007); however, as with the other currently unique aspects of the cholinergic system in the hyrax we can only tentatively conclude that they are unique features until other members of the Afrotheria have been examined for the presence of these nuclei.

*2.5.3. Increased numbers of preganglionic cholinergic neurons in the inferior salivatory nucleus (pIX) of the rock hyrax*

Cholinergic neurons within the preganglionic inferior salivatory nucleus have been identified in many mammalian species including rodents, carnivores, megachiropterans and primates, yet these are absent from the brains of other mammals studied (Maseko et al., 2007). Cholinergic neurons were identified in this nucleus in the rock hyrax; however, it appears from a qualitative comparison that the numbers of cholinergic neurons in this nucleus in the rock hyrax are far greater than that seen in the other mammals in which these neurons have been found. This qualitative impression, while impressive, needs quantitative support. The possible projections and function of this enlarged periventricular cholinergic cell group of the medulla is unknown and comparisons across other species belonging to the Afrotheria are needed to determine whether this feature of the cholinergic system of the hyrax is a feature of the Afrotherians in general.

*2.5.4. Lack of TH+ neurons in compact locus coeruleus (A6c) and decreased numbers of TH+ neurons in the locus coeruleus proper (A6d) of the rock hyrax*

The diffuse division of the locus coeruleus (A6d), or the locus coeruleus proper (Dahlström and Fuxe, 1964), has been reported in all mammals studied to date, while the compact portion has only been reported in rabbits, tree shrew, megabats and primates (e.g. Maseko et al., 2007). While the A6c is lacking in the rock hyrax, the A6d nucleus is present but was particularly low in the number of TH immunoreactive neurons. This is a qualitative impression, and further work comparing the number of neurons in this nucleus

across mammals and determining what kind of relationship may exist between neuronal number and brain mass (perhaps allometric) is required to confirm this impression; however, the qualitative impression is so dramatic as to warrant specific discussion. One interesting point to be noted is that even though the A6d nucleus showed an apparent reduction in the number of TH+ neurons, the other nuclei of the locus coeruleus complex (A7sc, A7d, A5 and A4) do not appear to be relatively more cell rich in comparison to other mammals (again a qualitative impression needing quantitative support).

This potential reduction in the number of neurons within the locus coeruleus may lead to a reduction in the amount of noradrenaline released in the specific target regions of the A6d in the hyrax. It should be noted that A6d in the rat and other mammals projects to all cortical regions of the brain, including the cerebellar cortex, as well as to the thalamus, the lower brain stem reticular formation and the dorsal and ventral horns of the spinal cord (see Fuxe et al., 1970; Ungerstedt, 1971, 2007). The neurons of the locus coeruleus represent a tonic arousal system important for vigilance and attention (see Fuxe et al., 2007). The relative absence of the catecholamine component of the locus coeruleus proper (A6d) in the hyrax is a highly interesting observation. Has the subcoeruleus (A7sc and A7d) taken over the role of the locus coeruleus (A6d) in the hyrax or does the hyrax show a lack of tonic arousal? These are major questions to be answered in future work. The reduced number of neurons found within the A6d in the hyrax may be a feature unique to this species. Further work on other members of the Afrotheria will determine whether this is indeed a species-specific feature or a feature of a broader taxonomic grouping.

*2.5.5. Evolutionary and phylogenetic considerations*

The current study extends the database that may be used for comparison across mammalian species to determine both phylogenetic and evolutionary trends of the cholinergic, putative catecholaminergic and serotonergic systems. Of these systems the serotonergic system appears to be the most conservative in terms of changes in the nuclear organization associated with different lineages. The rock hyrax, along with all other eutherian mammals studied to date and the metatherian wallaby appear to have the same nuclear organization (Maseko et al., 2007). The metatherian opossum (Crutcher and Humbertson, 1978) and the prototherian monotremes (Manger et al., 2002c) have only small comparative differences in the nuclear organization of the serotonergic system. The catecholaminergic system of the hyrax has a nuclear organization almost identical to that seen in rodents (except for the lack of a C3 nucleus, Dahlström and Fuxe, 1964; Smeets and González, 2000) and megabats and primates (except for the lack of a compact division of the locus coeruleus, A6c, Maseko et al., 2007). This nuclear organization aligns the hyrax phylogenetically most closely with the rodents and primates studied to date. The cholinergic system, for the most part, shares a similar plan of organization as that described for the rodents, megabats and primates (Maseko et al., 2007). Despite this, the hyrax does evince a degree of nuclear organizational uniqueness compared with other mammalian species through the possession of cholinergic neurons in the anterior nuclei of the dorsal thalamus and the parvocellular LDT and PPT nuclei of the pontine region. In the broader sense, the organization of these systems in the hyrax appear most similar to those seen in the rodents, rabbit, tree shrew, megabats and primates (Maseko et al., 2007). In this sense, the nuclear organizations of the neural

systems studied reflect current concepts of the phylogenetic interrelationships of mammalian lineages (Arnason et al., 2008).

The overall unique complement of nuclei of the three systems studied support the proposal of Manger (2005) that indicates each order will possess a unique nuclear complement of these systems. The current study supports the concept of placing the hyraxes into the phylogenetic grouping of an order to the exclusion of other mammals. It would be of interest to examine the cholinergic, catecholaminergic and serotonergic systems of other species of hyraxes to determine whether or not the "unique" features described in the brain of the rock hyrax are shared by all members of the Hyracoidea. It will also be of interest to examine other members of the Afrotheria and members of the Xenarthra to determine if these "unique" features are limited to this order (Hyrocoidea), cohort (Afroplacentalia), or are part of a broader phylogenetic grouping (such as the Notoplacentalia) (Arnason, 2008). The current study set out to test several potential predictions. The first prediction, that the hyrax will have many nuclei in common with other mammalian species, is supported. The second prediction, that the hyrax will have some unique features is, currently, tentatively supported. The strength of this second prediction and the third prediction can be tested by examining further species of the Afrotherian supercohort. The fourth prediction, that the hyrax may lack nuclei found in other species, is supported due to the lack of two catecholaminergic nuclei found either exclusively in rodents (C3), or seen in rabbits, tree shrews, megabats and primates (A6d). The current study then supports the usefulness of using these systems as indicators of phylogenetic relationships and supports current concepts regarding the evolution of these neural systems (Manger, 2005).

# Chapter 3

## Distribution of orexin-A immunoreactive neurons and their terminal networks in the brain of the rock hyrax, *Procavia capensis*.

### 3.1. Introduction

Orexin or hypocretin is a hypothalamic neuropeptide that consists of 130-131 amino acids in mammals and was first described in 1998 by two independent research groups. The Sutcliffe group called it hypocretin because it shared similar sequencing patterns to the secretin group of peptides and because of its hypothalamic localization (De Lecea et al., 1998; Kukkonen et al., 2002). The 130 amino acid precursor peptide they identified became known as preprohypocretin with hypocretin 1 and hypocretin 2 being the final peptides. The term orexin was coined by the Yanagisawa group who discovered that this peptide was linked to food intake (Sakurai et al., 1998; Kukkonen et al., 2002) and noted that injecting this peptide into the lateral ventricle of non-fasted rats would increase food intake. The precursor peptide thus became known as preproorexin with orexin-A and orexin B being the final peptides (Sakurai et al., 1998; Kukkonen et al., 2002).

Studies on several mammalian species have reported the location and distribution of orexinergic neurons and terminal networks (e.g. humans, Moore et al., 2001; cat, Wagner et al., 2000; Zhang et al., 2001, 2002; sheep, Iqbal et al., 2001; a variety of rodents, e.g. Broberger et al., 1998; Peyron et al., 1998; Chen et al., 1999; Cutler et al., 1999; Date et al., 1999; Nixon and Smale, 2007; microchiropterans, Kruger et al., 2010; and kangaroo, Yamamoto et al., 2006). These studies all concur regarding the location of

the orexinergic neurons and the general distribution of their major terminal networks. Orexinergic neurons have only been observed within the hypothalamus with the majority of the neurons found in the lateral hypothalamic area and the perifornical region; however, other studies have also reported isolated neurons in the region of the median eminence, posterior, anterior, dorsal and dorsomedial hypothalamus, zona incerta and ventrolateral hypothalamus. In contrast to the restricted neuronal distribution, orexinergic fibres are widely distributed throughout the brain and spinal cord and exhibit different densities of terminal networks in different regions of the brain, for example a high density network is evident in the areas immediately surrounding the third ventricle and areas involved in the regulation of the sleep-wake cycle (Chen et al., 1999; Cutler et al., 1999; Hagan et al., 1999; Wagner et al., 2000; McGranagham and Piggins, 2001; Zhang et al., 2002, 2004; Espana et al., 2005; Kruger et al., 2010). Orexinergic fibres have been reported as being both smooth and varicose, with the varicose type predominating (Peyron et al., 1998; Chen et al., 1999; Cutler et al., 1999; Kukkonen et al., 2002). Vasoactive intestinal peptide, vasopressin and neuropeptide Y terminal networks provide the main innervation to orexinergic neurons while a multitude of other neuronal circuits receive orexinergic efferents (Peyron et al., 1998; Cutler et al., 1999; Date et al., 1999; Horvath et al., 1999; Nambu et al., 1999; Abrahamson et al., 2001; Backberg et al., 2002; Kukkonen et al., 2002). Studies performed on rats to measure the release of orexin have revealed that release is closely correlated to circadian activity. These studies found that orexin concentrations in the hypothalamus were maximal around light onset and minimal at the point of light offset. Diurnal variation was also noted with similar measurements taken from the pons and intercisternal space; however, the precise time points were

shifted compared to the hypothalamus (Taheri et al., 2000; Fujiki et al., 2001; Yoshida et al., 2001; Kukkonen et al., 2002).

The diurnal variation of orexin release has an effect on food consumption, thus when orexin is released in higher concentrations (i.e. during the morning) food intake is promoted, the opposite being true of low orexin release (i.e. during the night) (Cutler et al., 1999; Hagan et al., 1999; McGranaghan and Piggins, 2001; Baldo et al., 2003; Khorooshi and Klengenspoor, 2005). Orexin regulates sleep by exciting neurons that are involved in the sleep-wake cycle, such as those of the locus coeruleus, dorsal raphe, and pontine cholinergic nuclei. This excitation causes the promotion of wakefulness and reduces sleep, especially episodes of REM (Hagan et al., 1999; Bourgin et al., 2000; Piper et al., 2000; Wagner et al., 2000; Espana et al., 2001; Huang et al., 2001; McGranaghan and Piggins, 2001; Methippara et al., 2000; Kukkonen et al., 2002; Yamanaka et al., 2002; Zang et al., 2004; Lee at al., 2005).

Although many studies deal with the location of orexinergic neurons and terminal network distribution, very few studies actually investigate the relation and interplay of these neurons and terminal networks to other neural systems. The aim of the present study is, thus, to describe the location and distribution of orexinergic neurons and terminal networks in the brain of the rock hyrax, *Procavia capensis*, based on orexin-A immunocytochemistry and to compare these to the known cholinergic, catecholaminergic and serotonergic systems (Gravett et al., 2009). This may shed light on the possible relation and interplay between the orexinergic system and these neural systems. Currently, the majority of studies reporting on orexin have made use of nocturnal laboratory rodents. Thus, the rock hyrax makes for an interesting candidate for the study

of the orexinergic system as these mammals are part of the unusual and morphologically diverse Afrotheria (Tabuce et al., 2008), for which no report of the orexinergic system is available. In addition to this the hyraxes are diurnally active and their sleep has been described as being polycyclic (Snyder, 1974). Moreover, they are poor thermoregulators (McNairn and Fairall, 1984; Brown and Downs, 2006) and orexins are known to be involved in thermoregulation and energy balance as they stimulate energy expenditure, increase food intake and suppress metabolic rate, which in turn my lead to hypothermia (Szekely et al., 2010; Teske et al., 2010).

### 3.2. Materials and Methods

The brains of six adult female rock hyraxes, *P. capensis*, were used in the present study. Permits from the Limpopo and Gauteng Provincial Governments were obtained for the capture and transport of the animals from the wild. All animals were treated and used according to the guidelines of the University of the Witwatersrand Animal Ethics Committee (approval number AESC 2005/8/5), which parallel those of the NIH for the care and use of animals in scientific experimentation. Each animal was weighed, deeply anaesthetized and subsequently euthanized with weight appropriate doses of sodium pentobarbital (200 mg sodium pentobarbital/kg, i.p.). Upon cessation of respiration the animals were perfused intracardially with 0.9% saline followed by 4% paraformaldehyde in 0.1M phosphate buffer (PB, pH 7.4) (approximately 1 l/kg of each solution), both solutions having a temperature of 4°C. The brains were then carefully removed from the skulls and post-fixed overnight in 4% paraformaldehyde in 0.1M PB followed by equilibration in 30% sucrose in 0.1M PB. The brains were then frozen in dry ice and with

the aid of a freezing microtome sectioned at 50 µm in the coronal plane. A one in three series of stains was made for Nissl, myelin, and orexin-A. Sections kept for the Nissl series were mounted on 0.5% gelatine coated glass slides, cleared in a solution of 1:1 chloroform and absolute alcohol, then stained with 1% cresyl violet to reveal cell bodies. Sections used for myelin staining were stored in 5% formalin for a period of two weeks and were then mounted on 1% gelatine coated glass slides and subsequently stained with silver solution to reveal myelin sheaths (Gallyas, 1979).

For immunohistochemical staining each section was treated with an endogenous inhibitor peroxidase (49.2% methanol: 49.2% 0.1 M PB: 1.6% of 30% $H_2O_2$) for 30 min and subsequently subjected to three 10 min 0.1 M PB rinses. The sections were then preincubated in a solution (blocking buffer) consisting of 3% normal goat serum (NGS, Chemicon), 2% bovine serum albumin (BSA, Sigma) and 0.25% Triton X100 (Merck) in 0.1M PB, at room temperature for 2 h. This was followed by three 10 min rinses in 0.1M PB. The sections were then placed for 48 h at 4°C under constant gentle shaking, in primary antibody solution, that contained the appropriately diluted primary antibody in blocking buffer (see above). The primary antibody used was anti-orexin-A (AB 3704, Millipore, raised in rabbit, dilution 1:1500). This was followed by another three 10 min rinses in 0.1M PB, after which the sections were incubated for 2 h at room temperature in secondary antibody solution. The secondary antibody solution contained a 1:1000 dilution of biotinylated anti-rabbit IgG (BA-1000, Vector Labs) in 3% normal goat serum (NGS), and 2% bovine serum albumin (BSA) in 0.1M PB. Once this was completed, the sections were again subjected to another three 10 min rinses in 0.1M PB, followed by a 1 h incubation in avidin-biotin solution (Vector Labs) and again rinsed. This was followed

by a 5 min treatment of the sections in a solution consisting of 0.05% diaminobenzidine tetrahydrochloride (DAB) in 0.1M PB, after which, and while still in the same solution, 3 µl of 30% $H_2O_2$ per 0.5 ml of solution was added. With the aid of a low power stereomicroscope the progression of the staining was visually followed and allowed to continue until a level was reached where the background staining could assist in reconstruction without obscuring the immunopositive structures. Once this level was reached the reaction was stopped by placing the sections in 0.1M PB, followed by a final session of three 10 min rinses in 0.1M PB. All solutions used in the immunohistochemical process had a pH of 7.4. The immunohistochemically stained sections were mounted on 0.5% gelatine coated slides and left to dry overnight. The mounted sections were dehydrated by placing it in 70% alcohol for 2 h at room temperature under gentle shaking and then transferred through a series of graded alcohols, cleared in xylene and coverslipped with Depex.

The sections were observed with a low power stereomicroscope, and the architectonic borders traced according to the Nissl and myelin stained sections using a camera lucida. The immunostained sections were then matched to the drawings and the immunopositive neurons marked, in addition the density of axon terminal staining was graded from low to high for each immunostained section and medium and high marked on the drawings. The drawings were scanned and redrawn with the aid of the Canvas 8 program. Location and distribution of orexin immunopositive (Orx+) neurons and terminal networks were described in relation to the general neuroanatomy of the rock hyrax brain and previously described cholinergic, catecholaminergic, and serotonergic systems (Gravett et al., 2009).

### 3.3. Abbreviations

III – oculomotor nucleus

3V – third ventricle

4V – fourth ventricle

A1 – caudal ventrolateral medullary tegmental nucleus

A2 – caudal dorsomedial medullary nucleus

A6 – locus coeruleus

A7 – subcoeruleus

A7d – nucleus subcoeruleus, diffuse portion

A7sc – nucleus subcoeruleus, compact portion

A9 – substantia nigra

A10 – ventral tegmental area

A10c – ventral tegmental area, central

A10d – ventral tegmental area, dorsal

A10dc – ventral tegmental area, dorsal caudal

A11 – caudal diencephalic group

A12 – tuberal cell group

A13 – zona incerta

A14 – rostral periventricular nucleus

A15d – anterior hypothalamic group, dorsal division

A15v – anterior hypothalamic group, ventral division

ac – anterior commissure

AD – anterodorsal nucleus of the dorsal thalamus

Amyg – amygdala

AP – area postrema

AV – anteroventral nucleus of the dorsal thalamus

B9 – supralemniscal serotonergic nucleus

C – caudate nucleus

C1 – rostral ventrolateral medullary tegmental group

C2 – rostral dorsomedial medullary nucleus

ca – cerebral aqueduct

Cb – cerebellum

cc – corpus callosum

Cl – claustrum

CLi – caudal linear nucleus

CN – cochlear nucleus

CP – cerebral peduncle

CVL – caudal ventrolateral serotonergic group

DCN – deep cerebellar nuclei

Diag.B – diagonal band of Broca

DR – dorsal raphe

DRc – dorsal raphe nucleus, caudal division

DRd – dorsal raphe nucleus, dorsal division

DRif – dorsal raphe nucleus, interfascicular division

DRl – dorsal raphe nucleus, lateral division

DRp – dorsal raphe nucleus, peripheral division

DRv – dorsal raphe nucleus, ventral division

DT – dorsal thalamus

EW – Edinger-Westphal nucleus

f – fornix

fr – fasciculus retroflexus

GC – periaqueductal grey matter

GLD – dorsal lateral geniculate nucleus

GP – globus pallidus

Hb – habenular nuclei

Hip – hippocampus

Hyp – hypothalamus

Hyp.d – dorsal hypothalamic cholinergic nucleus

Hyp.l – lateral hypothalamic cholinergic nucleus

Hyp.v – ventral hypothalamic cholinergic nucleus

IC – inferior colliculus

ic – internal capsule

icp – inferior cerebellar peduncle

IGL – intergeniculate leaflet

io – inferior olivary nuclei

IP – interpeduncular nucleus

LDT – laterodorsal tegmental nucleus

LOT – lateral olfactory tract

LRT – lateral reticular nucleus

LV – lateral ventricle

Mc – main cluster of orexinergic immunoreactive neurons

mcp – middle cerebellar peduncle

MnR – median raphe nucleus

N.Acc – nucleus accumbens

N.Bas – nucleus basalis

NEO – neocortex

OC – optic chiasm

OT – optic tract

OTc – optict tract cluster of orexinergic immunoreactive neurons

P – putamen

PV – paraventricular nucleus

PBg – parabigeminal nucleus

PIR – piriform cortex

PPT – pedunculopontine nucleus

Pta – pretectal area

py – pyramidal tract

pyx – decussation of the pyramidal tract

R – thalamic reticular nucleus

RMg – raphe magnus nucleus

RN – red nucleus

ROb – raphe obscurus nucleus

RPa – raphe pallidus nucleus

RVL – rostral ventrolateral serotonergic group

S – septum

SC – superior colliculus

SpV – spinal trigeminal tract

TOL – olfactory tubercle

vh – ventral horn of spinal cord

VPO – ventral pontine nucleus

ZI – zona incerta

ZIc – zona incerta cluster of orexinergic immunoreactive neurons

### 3.4. Results

The results revealed that the distribution of orexin-A immunopositive (Orx+) neuron cell bodies and terminal networks did not, for the most part, differ significantly from what has been described in other mammals. Despite this, an interesting difference was noted that has not been reported in most mammals studied to date, namely a strong Orx+ terminal network in the anterior dorsal nucleus of the dorsal thalamus (AD). Orx+ neurons and terminal networks are described in relation to either the general neuroanatomy of the rock hyrax brain and the cholinergic, catecholaminergic, and serotonergic systems (as described previously for this species in Gravett et al., 2009).

#### *3.4.1. Orexin-A neuronal cell body distribution*

Orx+ neuronal cell bodies were identified mainly within the hypothalamus of the brain of the rock hyrax. These cell bodies were grouped into three distinct clusters; the

main cluster, the zona incerta cluster and the optic tract cluster (Figs. 3.1-3). The main cluster was identified as a large group of densely packed Orx+ neuronal cell bodies located lateral to the third ventricle in the perifornical region, with a large number of neuronal cell bodies extending medially from this area, as well as into the dorsomedial and lateral hypothalamic areas. The majority of Orx+ neurons belonged to this cluster and they were found to be ovoid in shape, a mixture of both bipolar and multipolar types and showed no apparent regular dendritic orientation. The Orx+ neuronal cell bodies of this main cluster were intermingled with the A11 and A14 nuclear groups of the catecholaminergic system. From the main cluster a group of Orx+ neuronal cell bodies extended laterally into the region of the zona incerta. This cluster had a very low density of Orx+ neurons that were mixed with neurons of the lateral hypothalamic cholinergic nucleus and the A13 nucleus of the catecholaminergic system. The cell bodies were ovoid in shape, a mixture of bipolar and multipolar type and had no specific dendritic orientation. The third cluster extended ventrolaterally from the main cluster to the ventrolateral region of the hypothalamus adjacent to the optic tract. This cluster exhibited a low density of Orx+ neuronal cell bodies that were mostly of the bipolar type with the same cell morphology as described for the other clusters. These neurons were found to intermingle with those of the ventral hypothalamic cholinergic nucleus (Figs. 3.1 E-G, 3.2).

### *3.4.2. Orexin-A terminal network distribution*

#### *3.4.2.1. Telencephalon*

Within the telencephalon of the rock hyrax brain orexinergic terminal networks of medium density were noted. These terminal networks were mainly distributed along the medial and ventrolateral border of the telencephalon and located in and around the following structures: the nucleus accumbens, olfactory tubercle and islands of Calleja, diagonal band of Broca and the septal nuclear complex (Figs. 3.1 A-C, 3.4). It is of interest to note than in all these structures a number of cholinergic neurons were also located (Gravett et al., 2009). The remaining regions of the telencephalon had either a low density Orx+ terminal network, or no Orx+ structures could be observed.

#### *3.4.2.2. Diencephalon*

Both high and medium density orexinergic terminal networks were observed throughout the diencephalon. The high density terminal networks were located in the anterior hypothalamic area, the periventricular areas adjacent to the third ventricle in the hypothalamus (Fig. 3.2), in the paraventricular nuclei of the epithalamus (Fig. 3.5A) extending to a region surrounding the habenular nuclei, and dorsolaterally in the AD (Figs. 3.1 D-J, 3.5). The medium density terminal networks surrounded these areas of high density and were distributed through most parts of the hypothalamus (Fig. 3.2), the midline of the dorsal thalamus in the intralaminar nuclei and extended laterally to the intergeniculate leaflet (Fig. 3.5C). The high-density terminal networks overlapped with the A12, A14, and A15v nuclei of the catecholaminergic system, and the AD (Fig. 3.5B) that forms part of the cholinergic system of the rock hyrax (Gravett et al., 2009). The

Orx+ terminal networks of medium density were found to overlap the A11 and A13 nuclei of the catecholaminergic system and the dorsal, lateral, and ventral hypothalamic nuclei of the cholinergic system. The remaining regions of the diencephalon had either a low density Orx+ terminal network, or no Orx+ structures could be observed (Fig. 3.2).

*3.4.2.3. Midbrain and Pons (Mesencephalon and Metencephalon)*

Both high and medium dense orexinergic terminal networks characterized the midbrain and pontine regions; however, the medium density Orx+ terminal networks were found to dominate in these regions. The terminal networks of high density were located ventral to the cerebral aqueduct within the midline of the midbrain and pontine regions and overlapped the A10d and A10dc nuclei of the catecholaminergic system and most serotonergic nuclei of the dorsal raphe (Fig. 3.6A). The medium dense Orx+ terminal networks were coincident with the dopaminergic ventral tegmental area, the noradrenergic locus coeruleus complex (Fig. 3.6B), the cholinergic nuclei of the laterodorsal tegmental and pedunculopontine nuclei (both magno and parvocellular divisions of these nuclei, Gravett et al., 2009), the cholinergic parabigeminal and Edinger-Westphal nuclei, and the caudal linear (CLi), supralemniscal (B9), caudal nucleus of the dorsal raphe (DRc) and median raphe (MnR) serotonergic nuclei (Fig. 3.6C). In addition to this, the entire periaqueductal gray matter was observed to have a medium density Orx+ terminal network that extended outward through all layers of the superior colliculus (Figs. 3.1 K-N, 3.6). The remaining regions of the midbrain and pons had either a low density Orx+ terminal network, or no Orx+ structures could be observed.

It is worth noting that we could only find a low density Orx+ network in the inferior colliculus.

*3.4.2.4. Medulla Oblongata (Myelencephalon)*

Only medium and low-density Orx+ terminal networks were present within the medulla oblongata of the brain of the rock hyrax. The medium density networks were found in all regions where serotonergic neurons were located (i.e. the raphe magnus, rostral and caudal ventrolateral columns, raphe pallidus and raphe obscurus). Similarly, all regions that contained catecholaminergic neurons were found to have a medium density Orx+ terminal network, these being the area postrema, C1, C2, A1 and A2 nuclei. Anterior in the medulla a medium density Orx+ terminal network was found in the region of the parabrachial nuclear complex. Towards the spinal cord these medium density Orx+ networks were located in the areas surrounding the central canal and the outer edge of the dorsal horn in the spinal trigeminal tract (SpV) (Fig. 3.1 O-V). The remaining regions of the medulla had either a low density Orx+ terminal network, or no Orx+ structures could be observed.

**Figure 3.1:** Drawings of coronal sections through one half of the brain of the rock hyrax, illustrating orexin-A immunoreactive neurons and terminal network distribution. A single black dot indicates a single cell body, black and grey shaded areas indicate regions in the brain of the rock hyrax where high and medium density, respectively, orexin-A terminal networks were observed. Areas where no shading is evident represent regions of low or no orexinergic innervation. Drawing **A** represents the most rostral section, **V** the most caudal, and each drawing is approximately 1500 µm apart. See list for abbreviations.

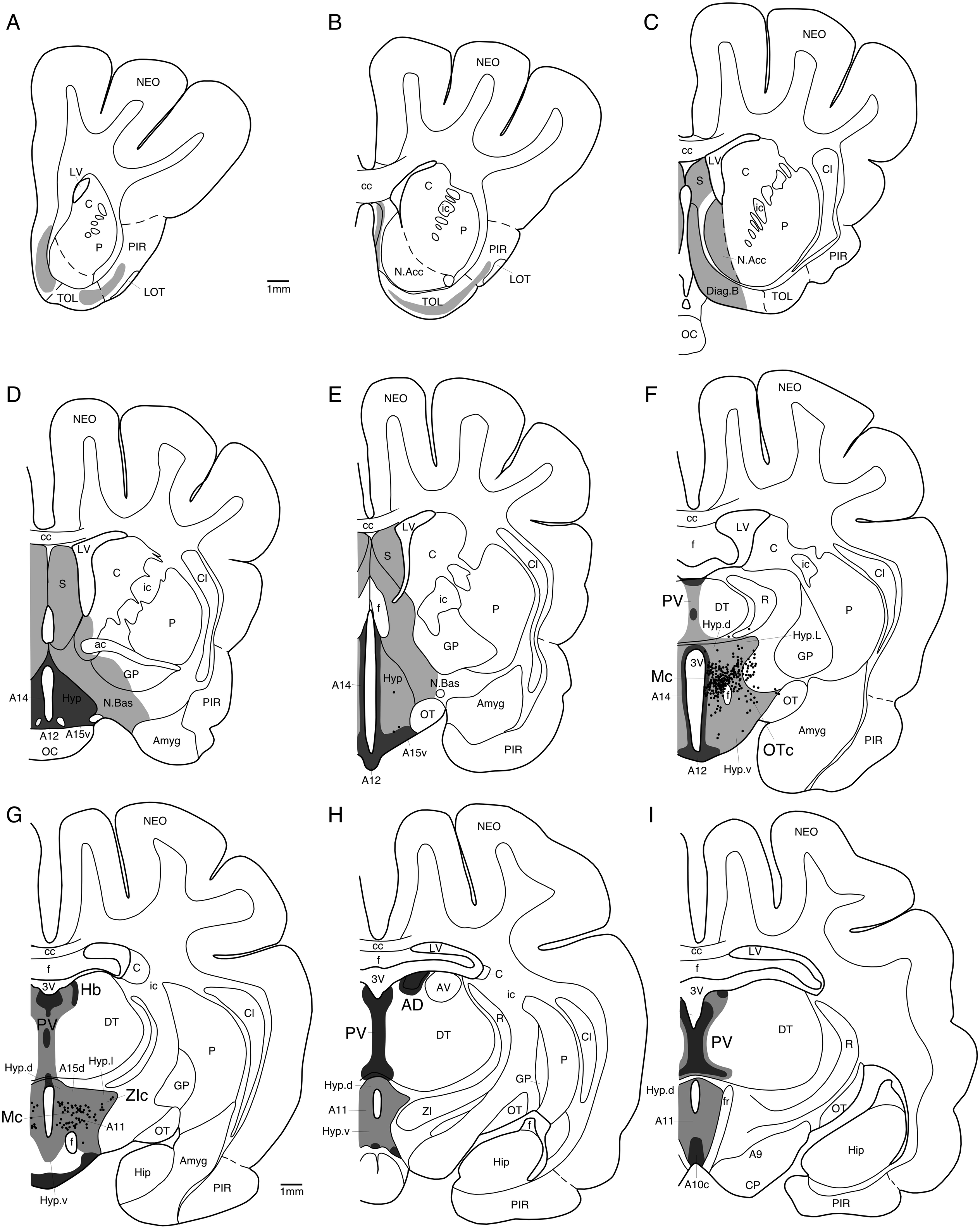
A
NEO
LV
C
P
PIR
TOL
LOT
1mm
B
NEO
cc
C
ic
P
PIR
N.Acc
LOT
TOL
C
NEO
cc
LV
S
C
Cl
ic
P
N.Acc
PIR
Diag.B
TOL
OC
D
NEO
cc
LV
S
C
ic
Cl
P
ac
GP
A14
Hyp
N.Bas
PIR
A12
A15v
OC
Amyg
E
NEO
cc
LV
S
C
Cl
f
ic
P
GP
A14
Hyp
N.Bas
OT
Amyg
A15v
PIR
A12
F
NEO
cc
LV
f
C
ic
Cl
PV
DT
R
P
Hyp.d
Hyp.L
GP
3V
Mc
A14
f
OT
Amyg
PIR
OTc
A12
Hyp.v
G
NEO
cc
f
C
3V
Hb
ic
PV
DT
Cl
P
Hyp.d
A15d
Hyp.l
GP
Zlc
Mc
A11
OT
f
Hip
Amyg
PIR
Hyp.v
1mm
H
NEO
cc
LV
f
C
3V
AV
ic
AD
PV
DT
R
Cl
P
Hyp.d
GP
A11
ZI
OT
Hyp.v
f
Hip
PIR
I
NEO
cc
LV
f
3V
PV
DT
R
Hyp.d
fr
A11
OT
A9
Hip
A10c
CP
PIR

J

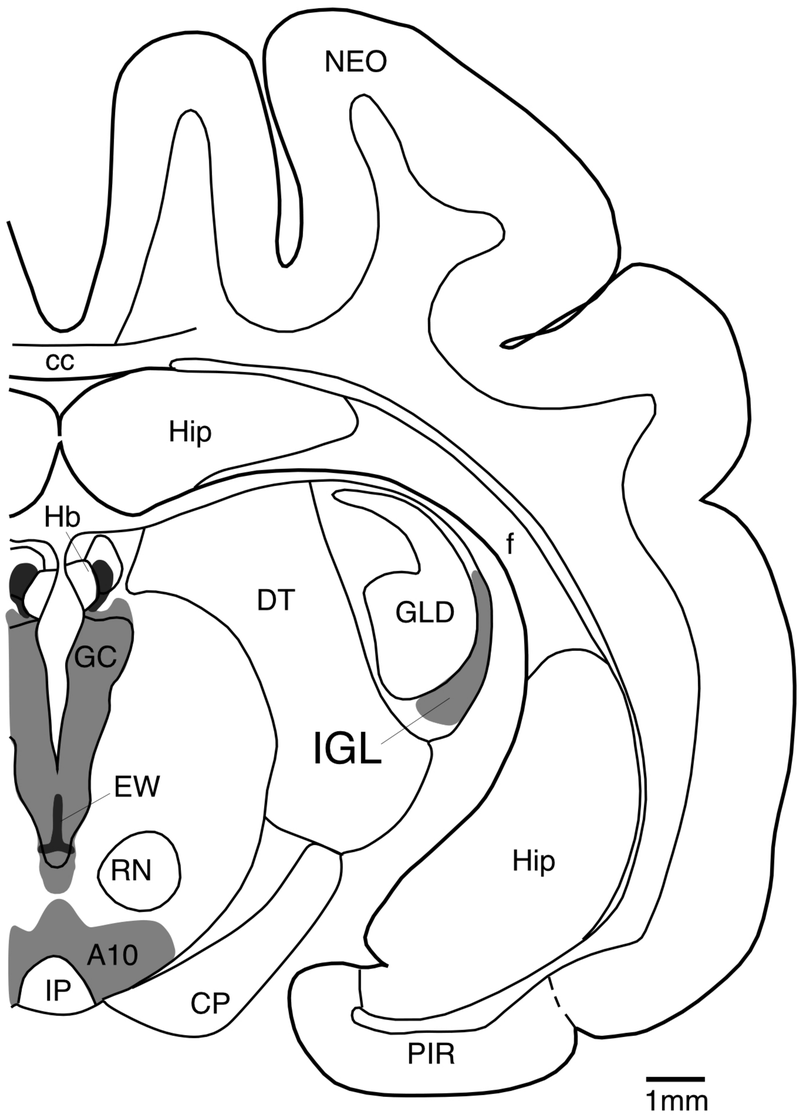
NEO
cc
Hip
Hb
f
DT
GLD
GC
IGL
EW
RN
A10
IP
CP
Hip
PIR
1mm

K

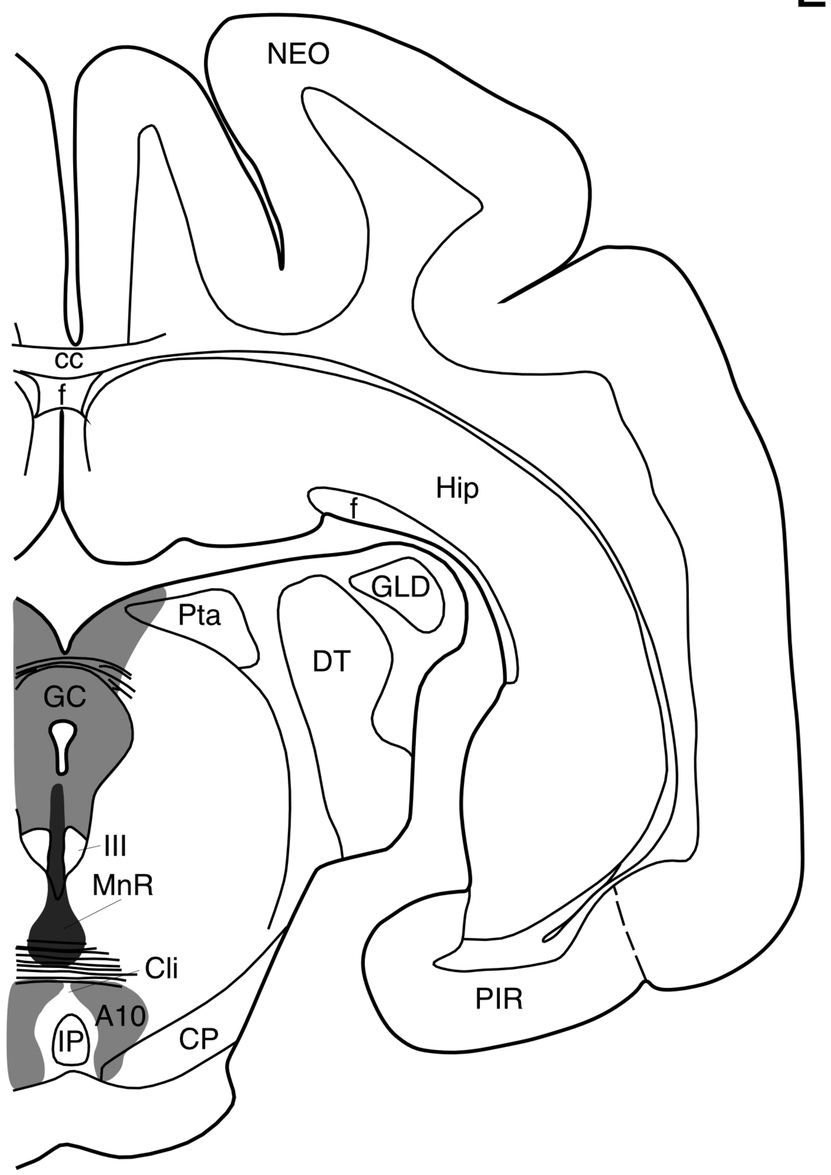
NEO
cc
f
Hip
f
GLD
Pta
DT
GC
III
MnR
Cli
A10
IP
CP
PIR

L

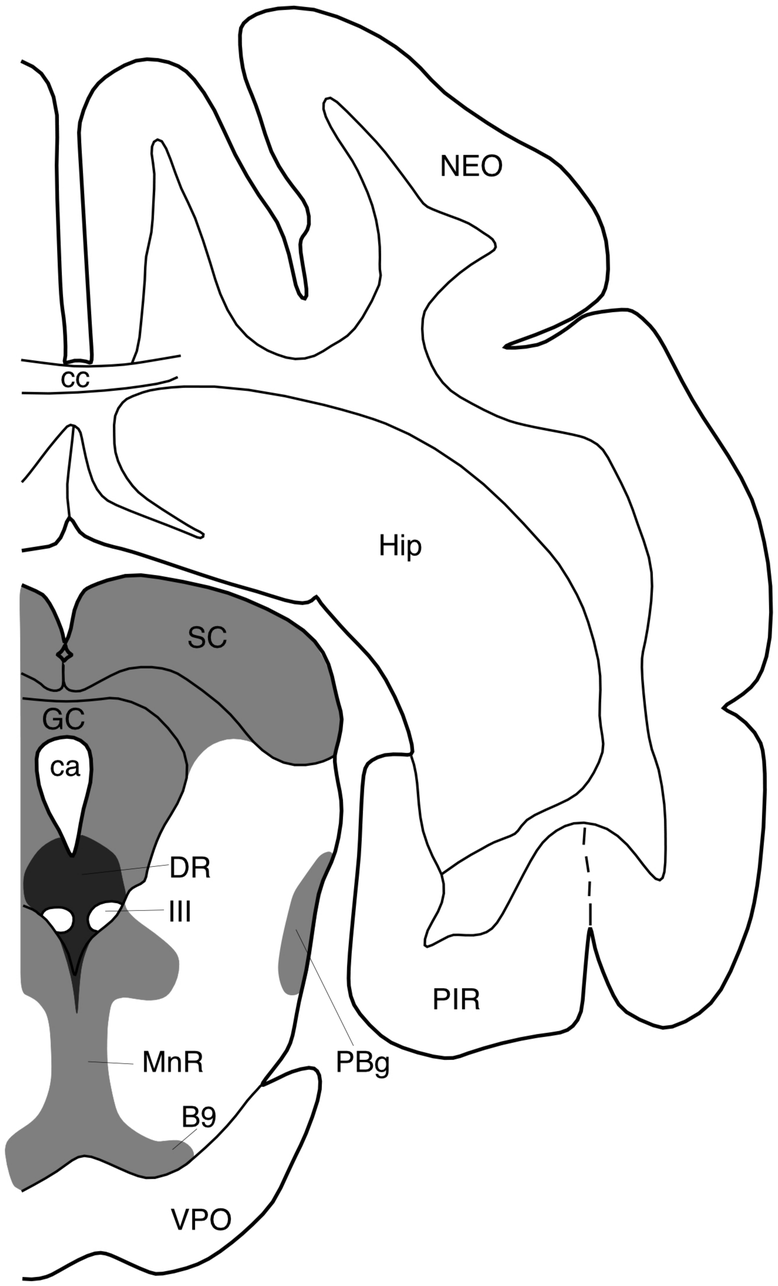
NEO
cc
Hip
SC
GC
ca
DR
III
MnR
PBg
B9
VPO
PIR

M

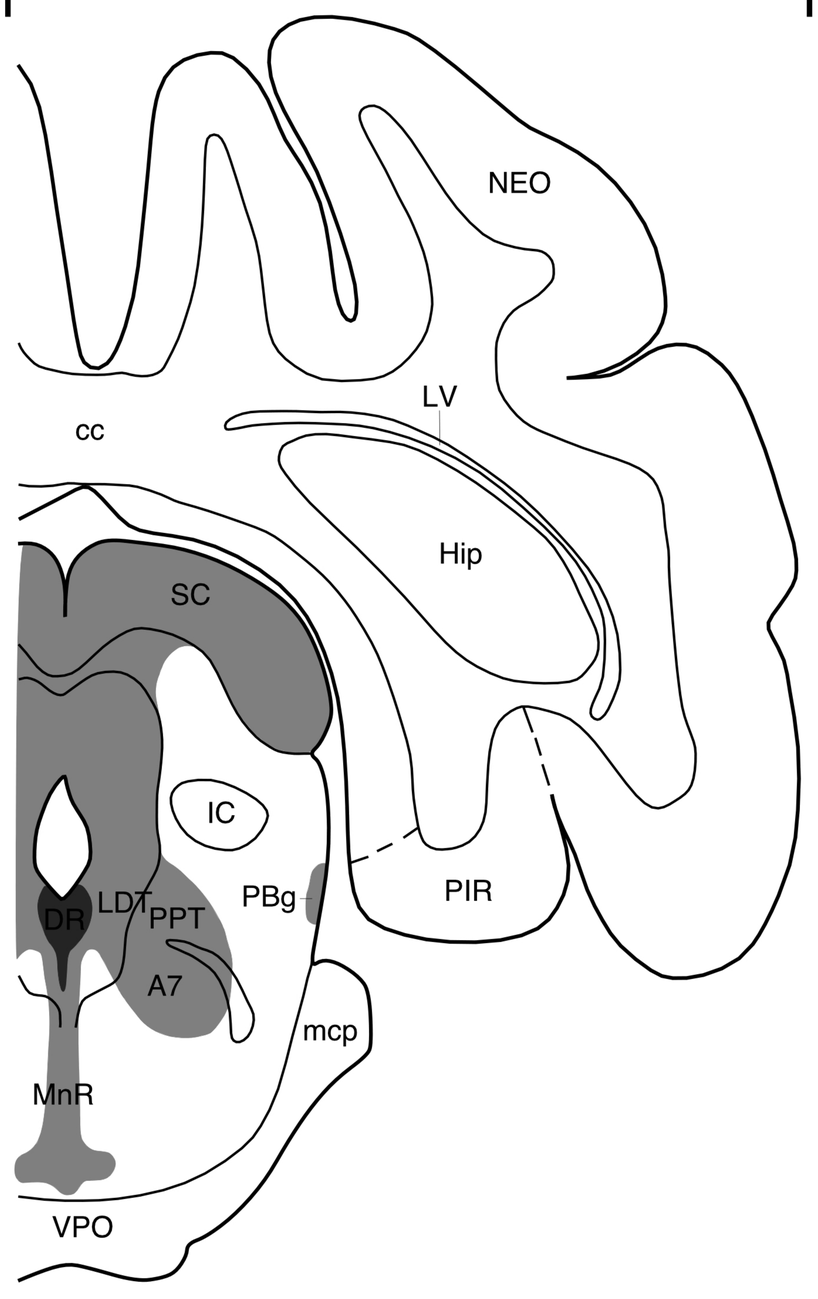
NEO
LV
cc
Hip
SC
IC
PBg
PIR
DR
LDT
PPT
A7
mcp
MnR
VPO

N

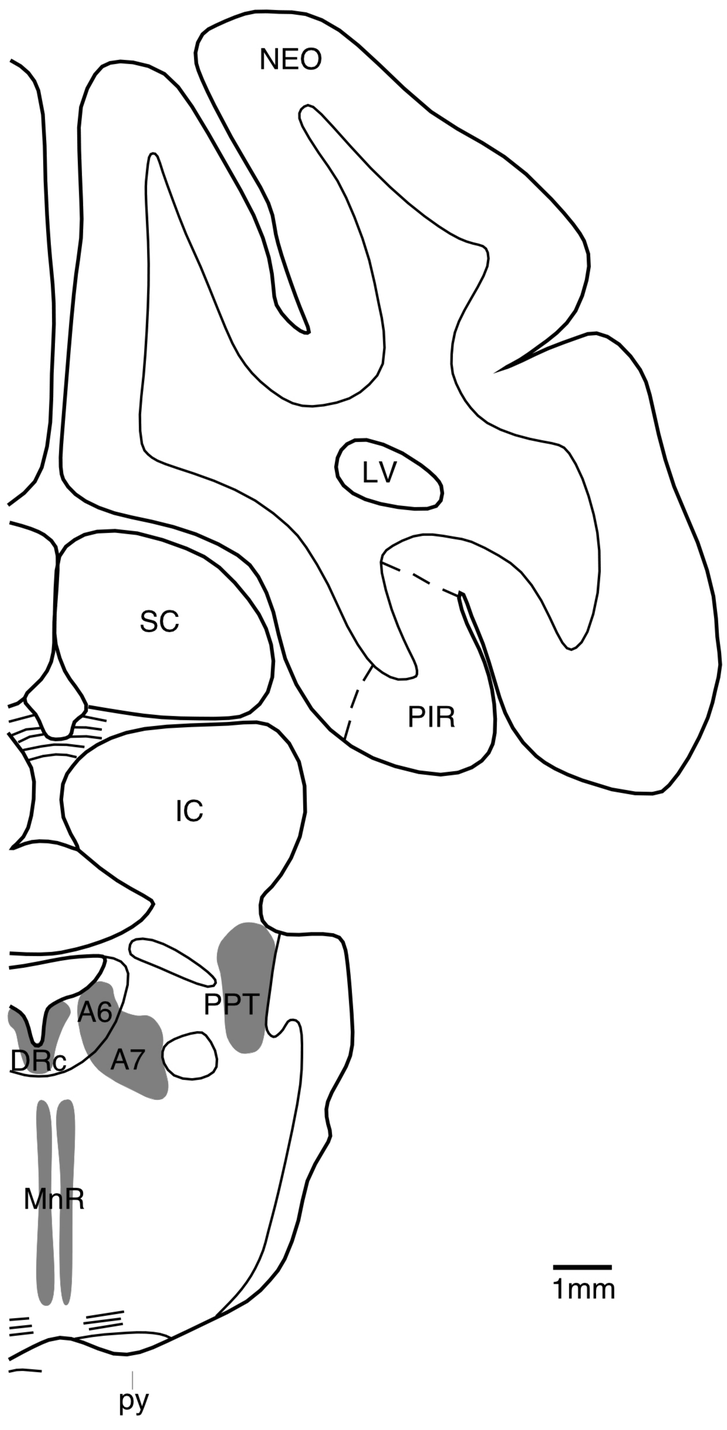
NEO
LV
SC
PIR
IC
A6
PPT
DRc
A7
MnR
py
1mm

O

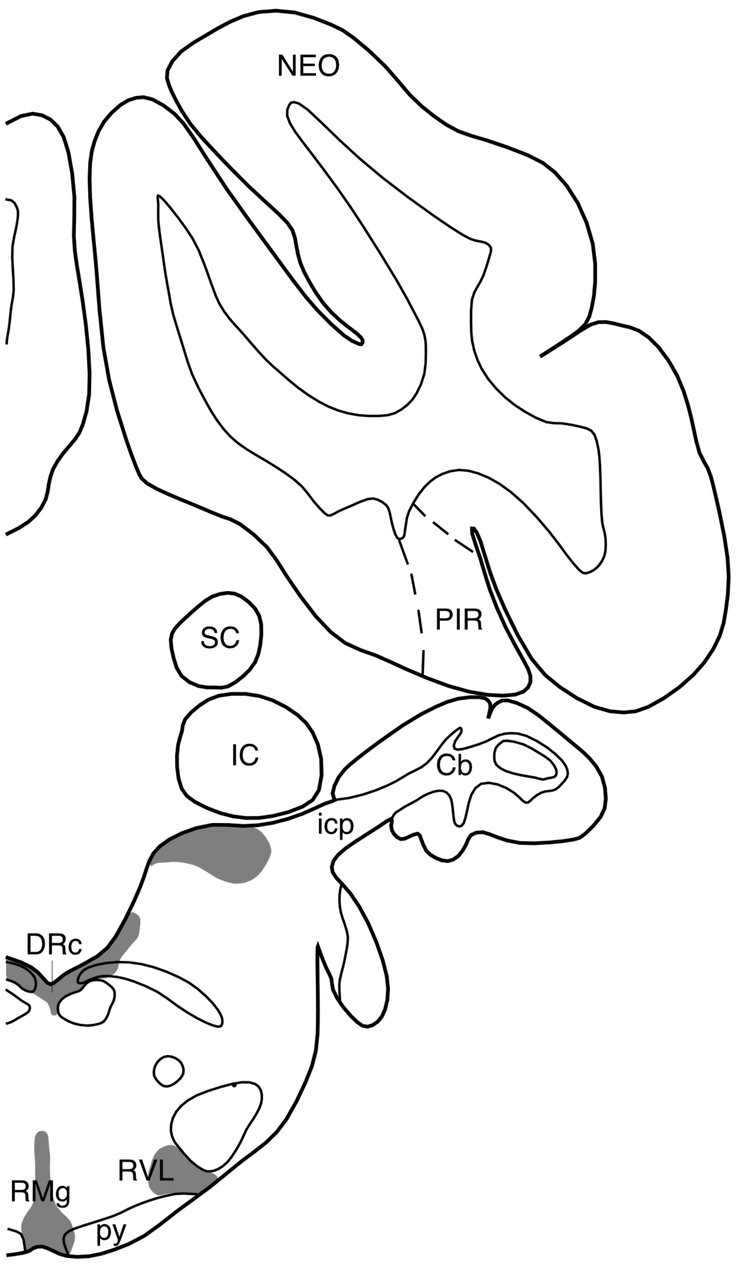
NEO
PIR
SC
IC
Cb
icp
DRc
RVL
RMg
py

P

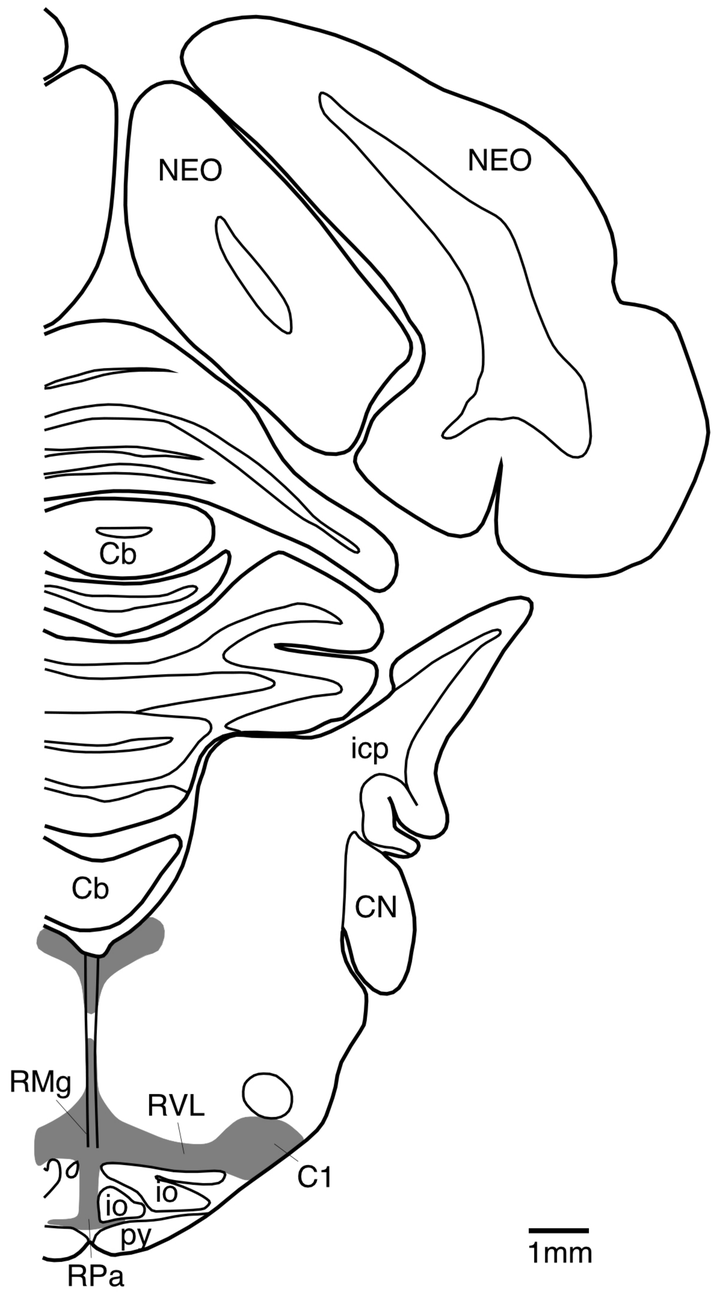
NEO
NEO
Cb
icp
Cb
CN
RMg
RVL
C1
io
io
py
RPa

1mm

Q

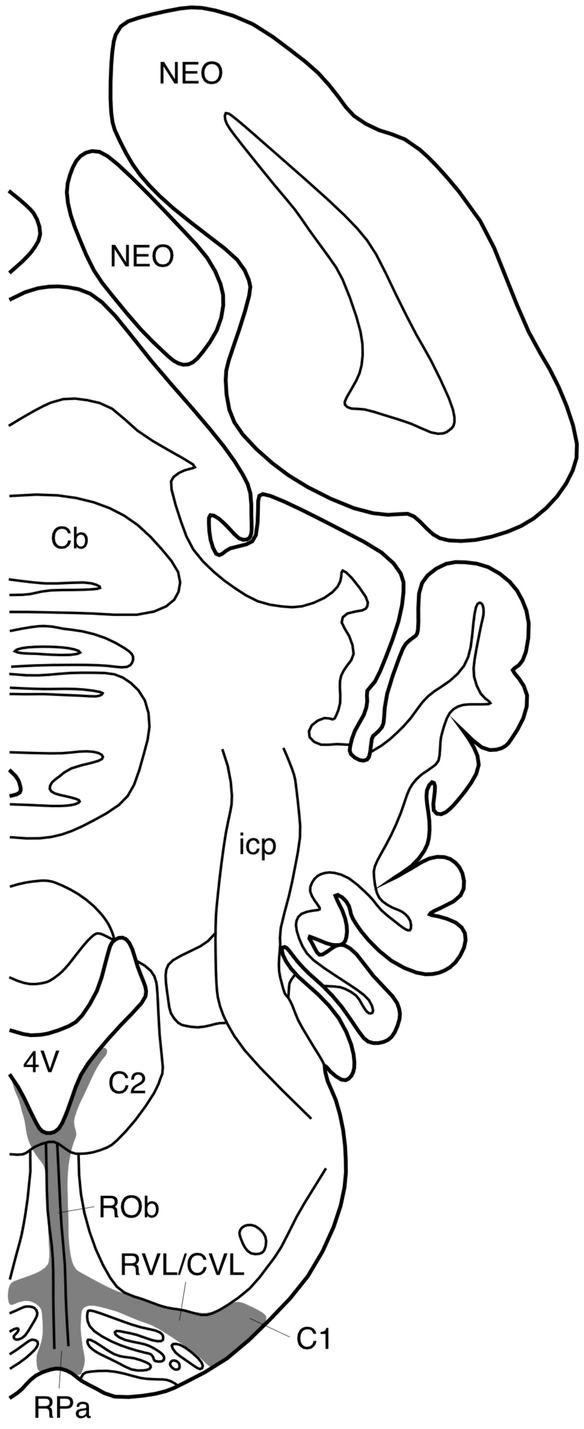
NEO
NEO
Cb
icp
4V
C2
ROb
RVL/CVL
C1
RPa

R

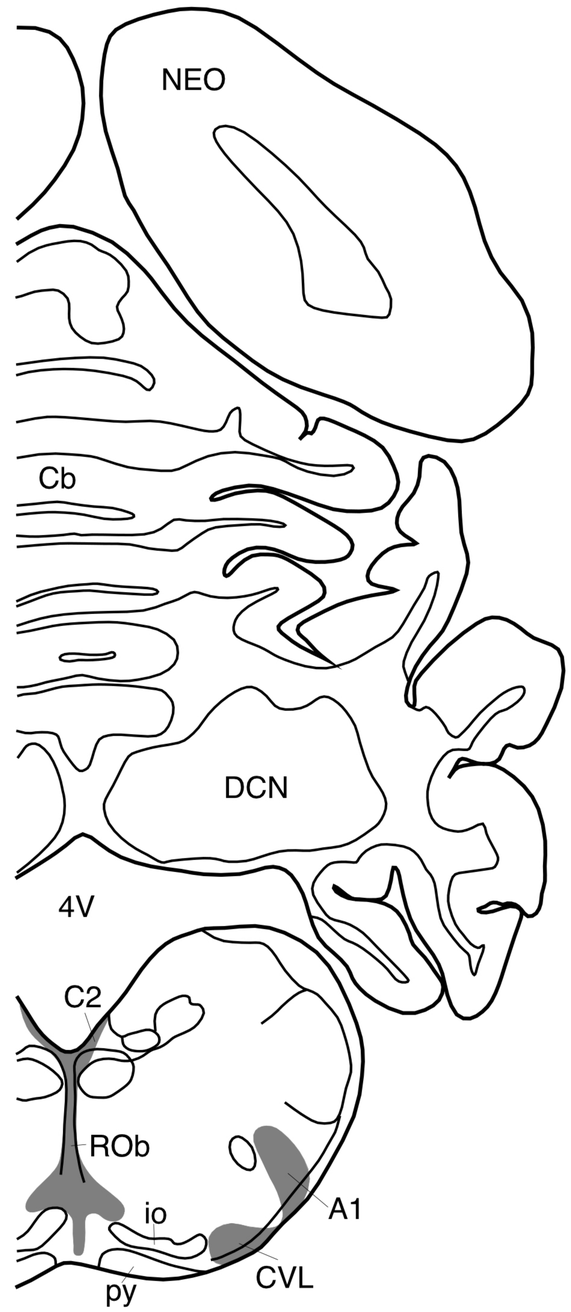
NEO
Cb
DCN
4V
C2
ROb
io
A1
py
CVL

S

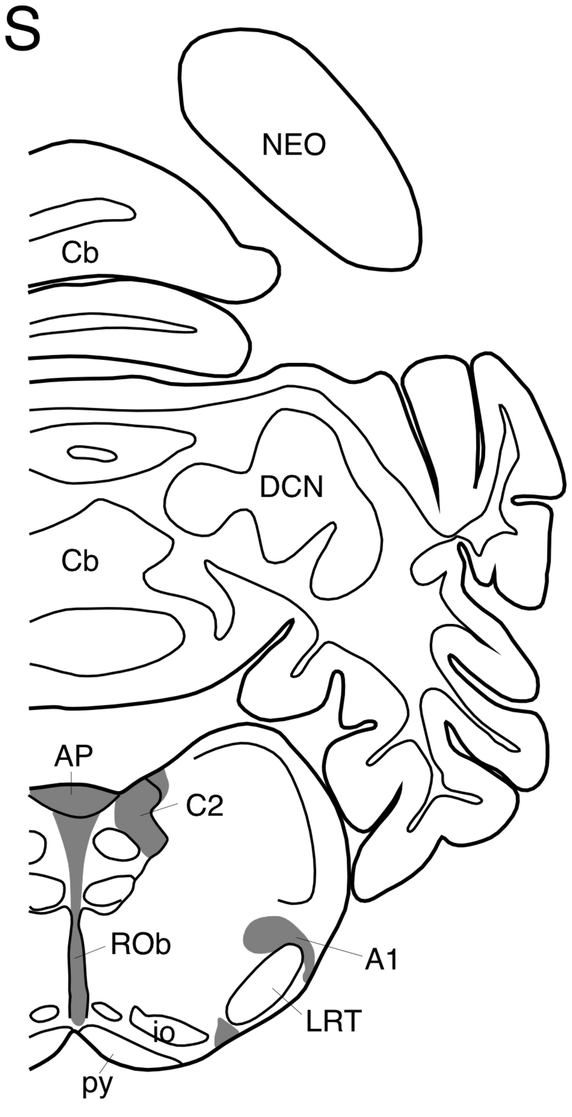
NEO
Cb
DCN
Cb
AP
C2
ROb
A1
io
LRT
py

T

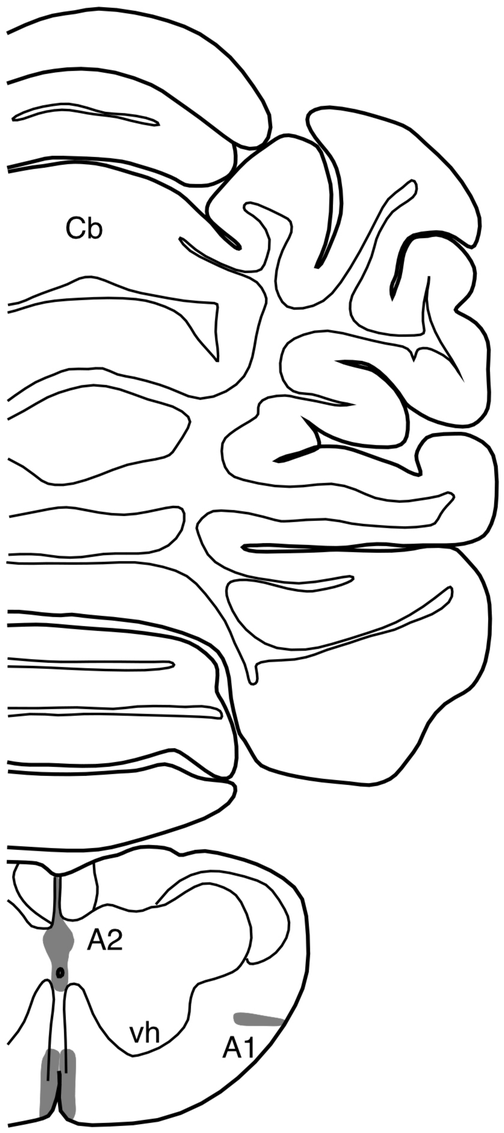
Cb
A2
vh
A1

U

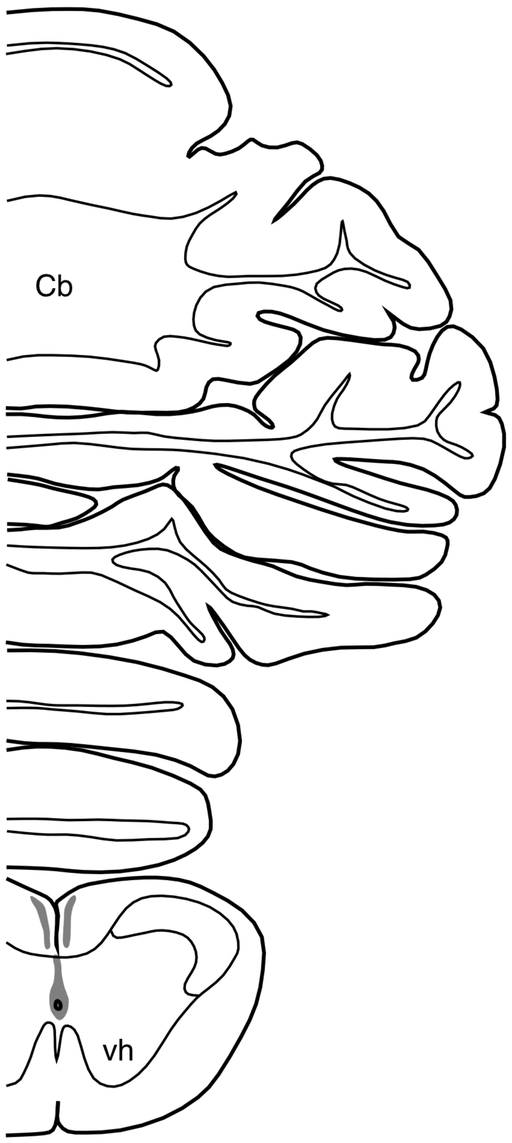
Cb
vh

V

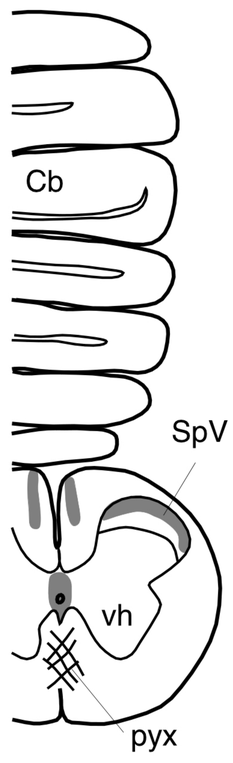
Cb
SpV
vh
pyx

**Figure 3.2:** Photomicrograph montage demonstrating the location of orexin-A immunoreactive neurons and terminal networks within the hypothalamus of the rock hyrax showing the main cluster (**Mc**), the zona incerta cluster (**ZIc**) and the optic tract cluster (**OTc**). Scale = 1 mm. **3V** – third ventricle; **f** – fornix; **OT** – optic tract.

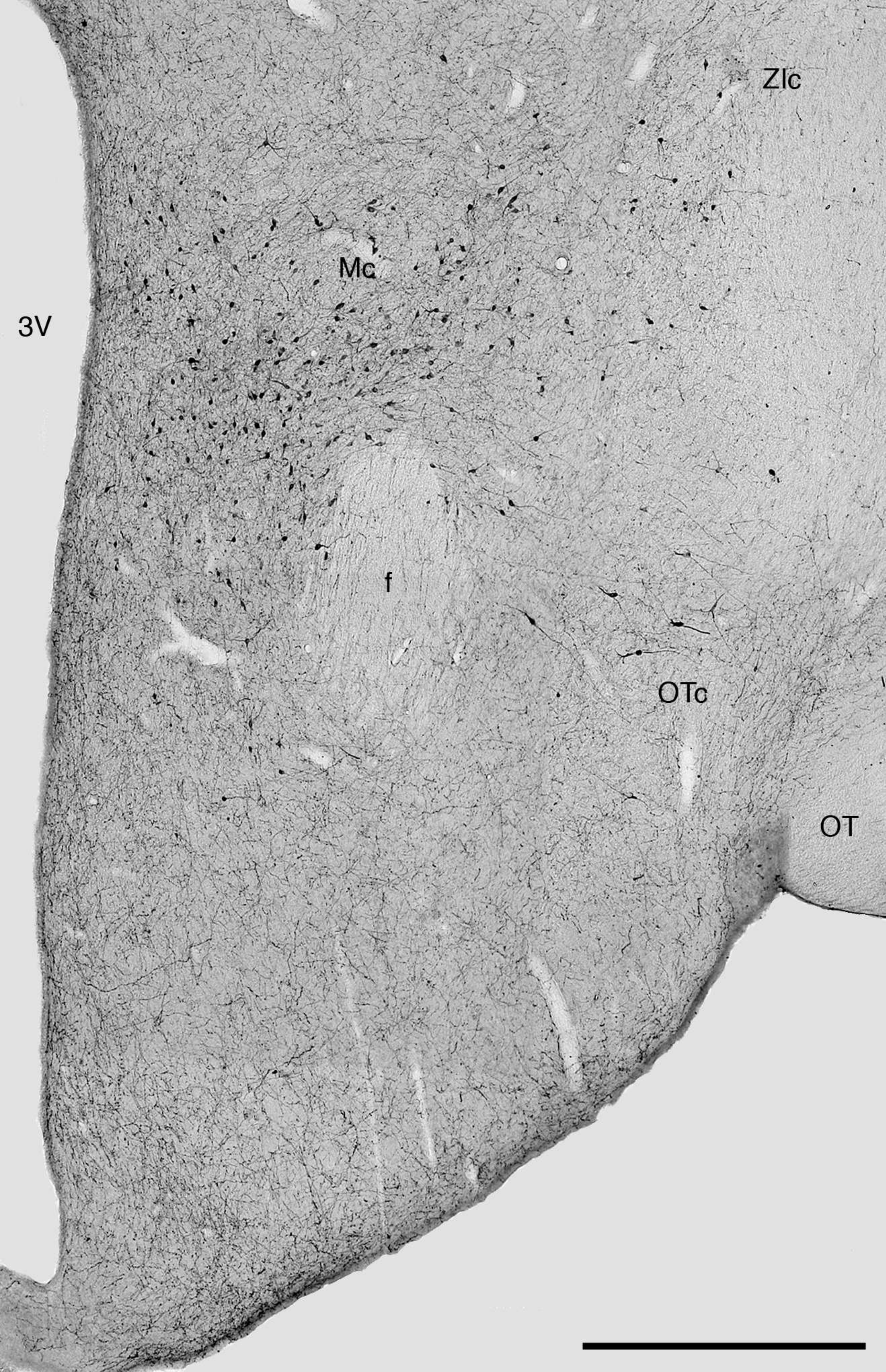
Zlc
Mc
3V
f
OTc
OT

**Figure 3.3:** Photomicrographs illustrating the neuronal morphology of the three clusters of orexin-A immunoreactive nuclear groups within the hypothalamus of the rock hyrax. **(A)** Orexin-A immunoreactive neurons of the main cluster, perifornical region. **(B)** Orexin-A immunoreactive neurons of the optic tract cluster, lateral ventral hypothalamic area. **(C)** Orexin-A immunoreactive neurons of the zona incerta cluster, lateral hypothalamic area. In all images, medial is to the left, lateral to the right, and dorsal to the top. Scale in **C** = 500 µm and applies to all.

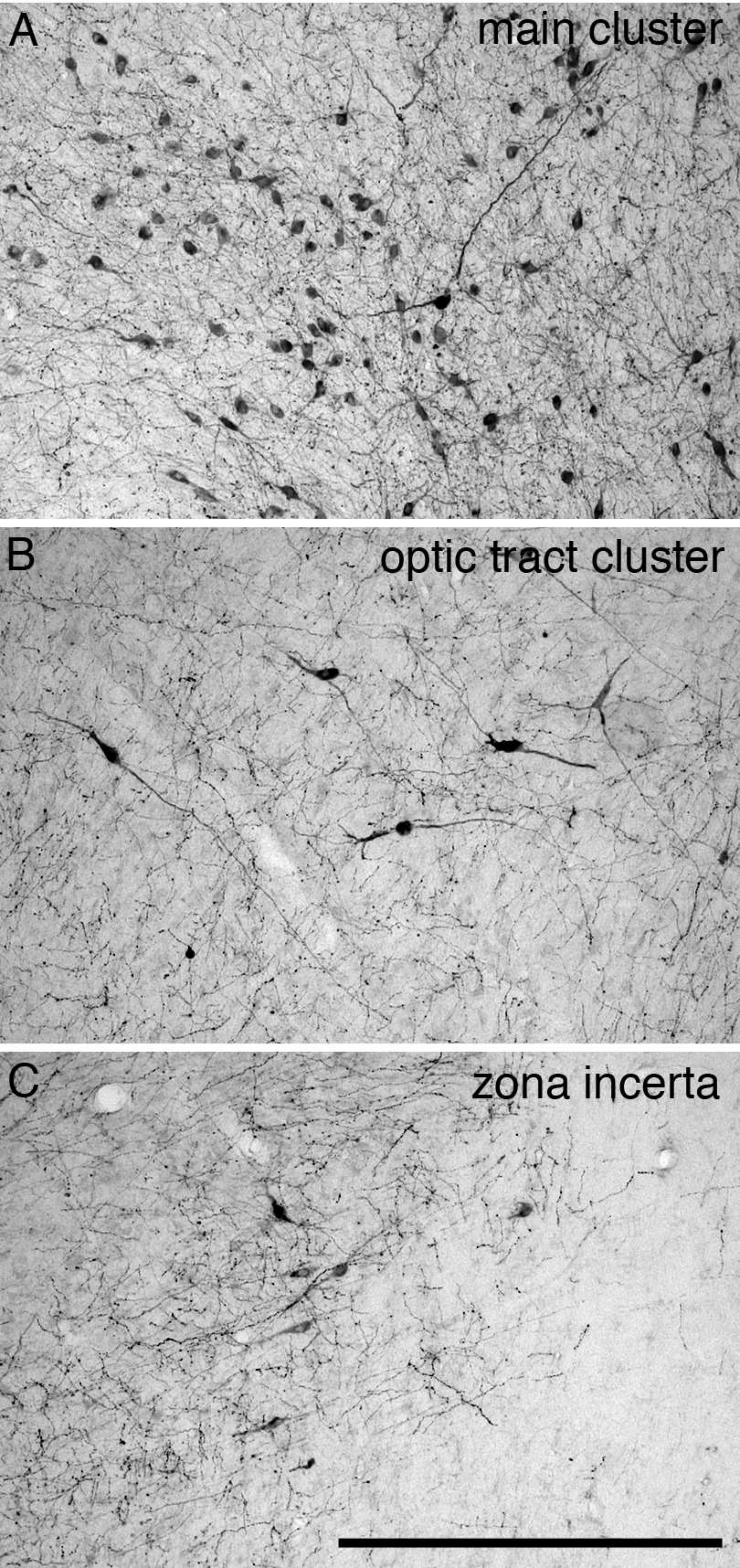
A
main cluster
B
optic tract cluster
C
zona incerta

**Figure 3.4:** Photomicrographs illustrating the distribution of orexin-A immunoreactive terminal networks within certain parts of the forebrain of the rock hyrax. **(A)** Low density orexin-A immunoreactive terminal networks within the cerebral cortex. **(B)** Medium density orexin-A immunoreactive terminal networks within the diagonal band of Broca (**Diag. B**). **(C)** Medium density orexin-A immunoreactive terminal networks within the nucleus accumbens (**N. Acc**). **(D)** Medium density orexin-A immunoreactive terminal networks within the olfactory tubercle (**TOL**). Scale in **D** = 500 µm and applies to all. Medial is to the left in all images.

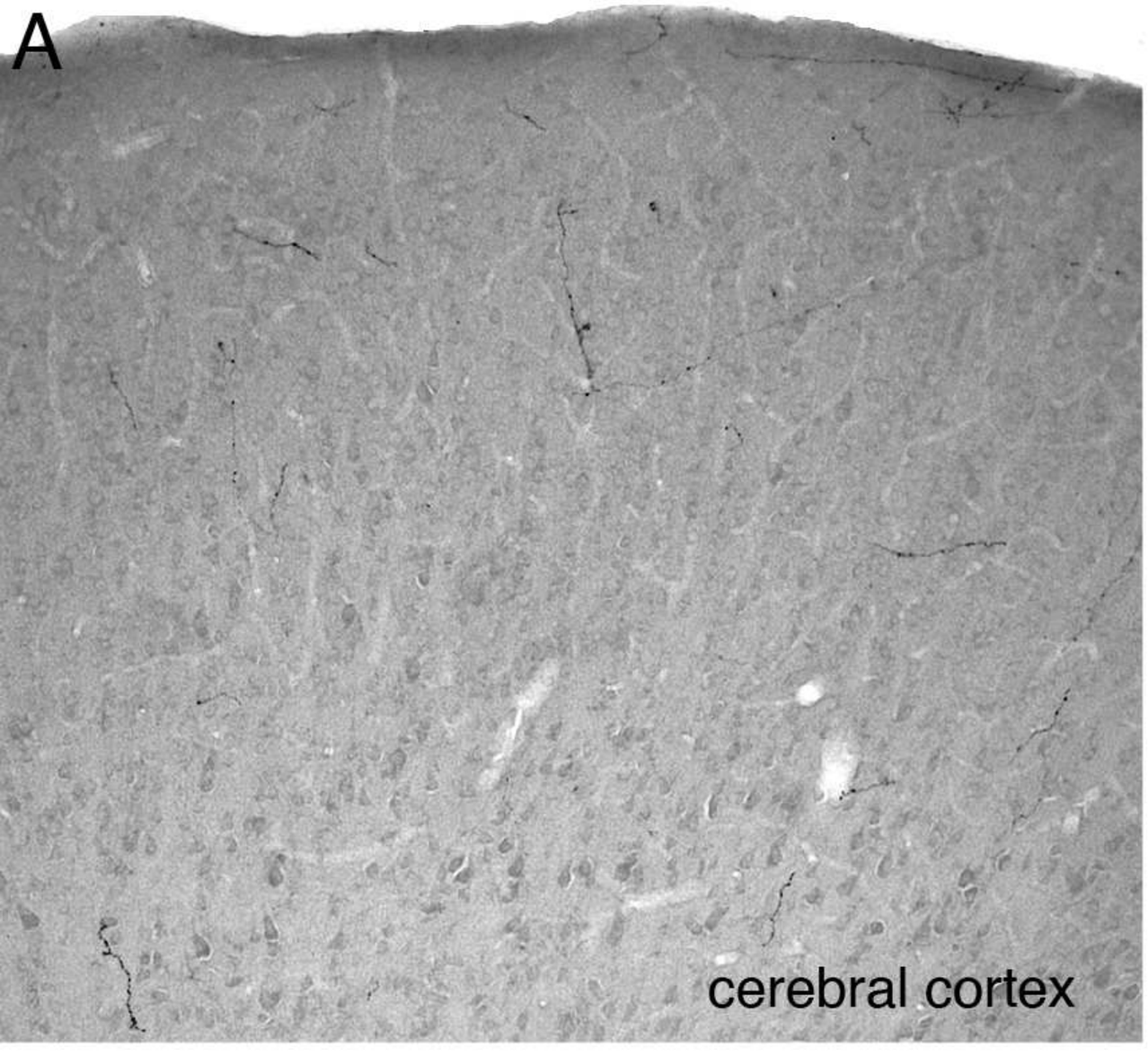
A
cerebral cortex

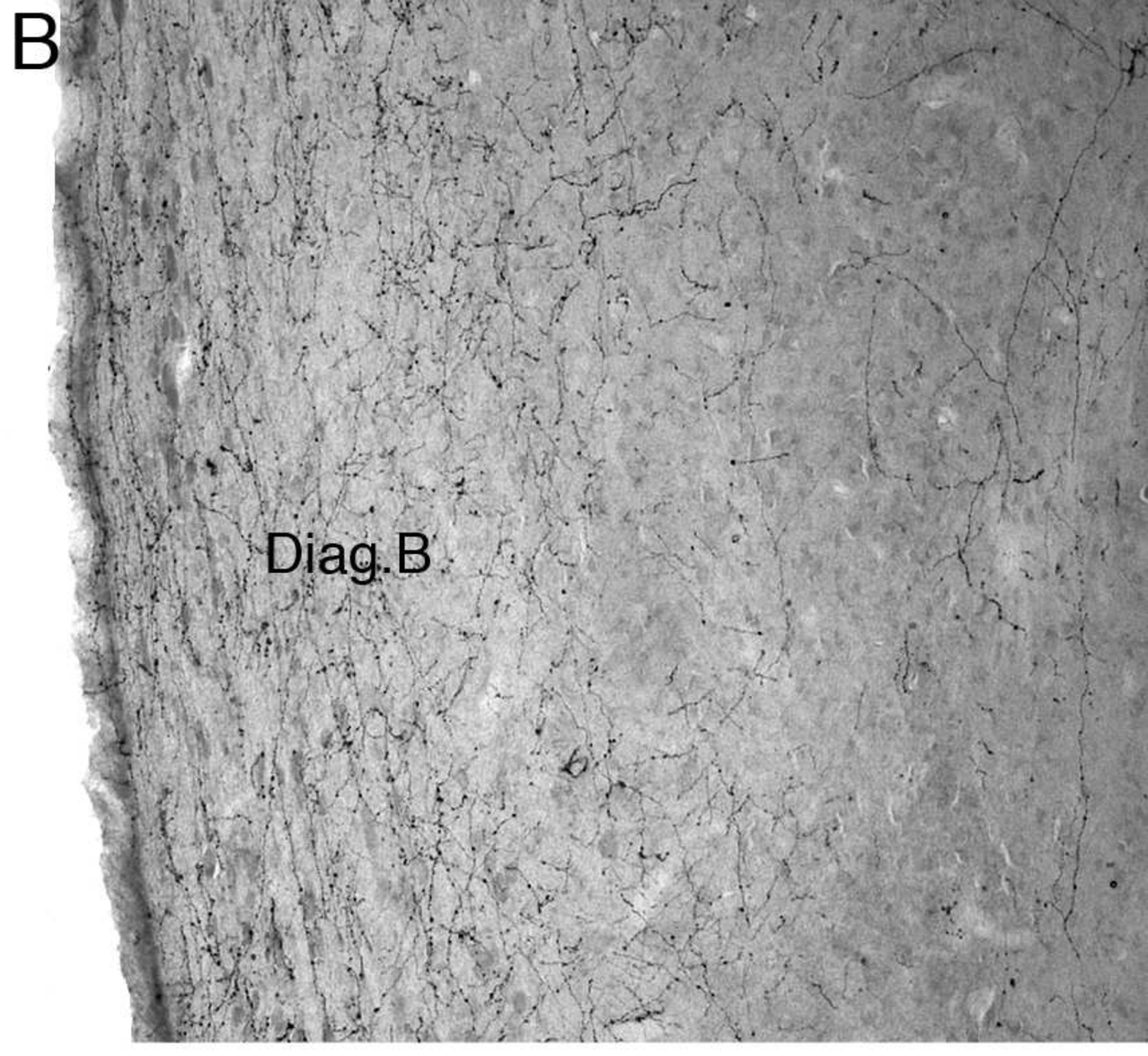
B
Diag.B

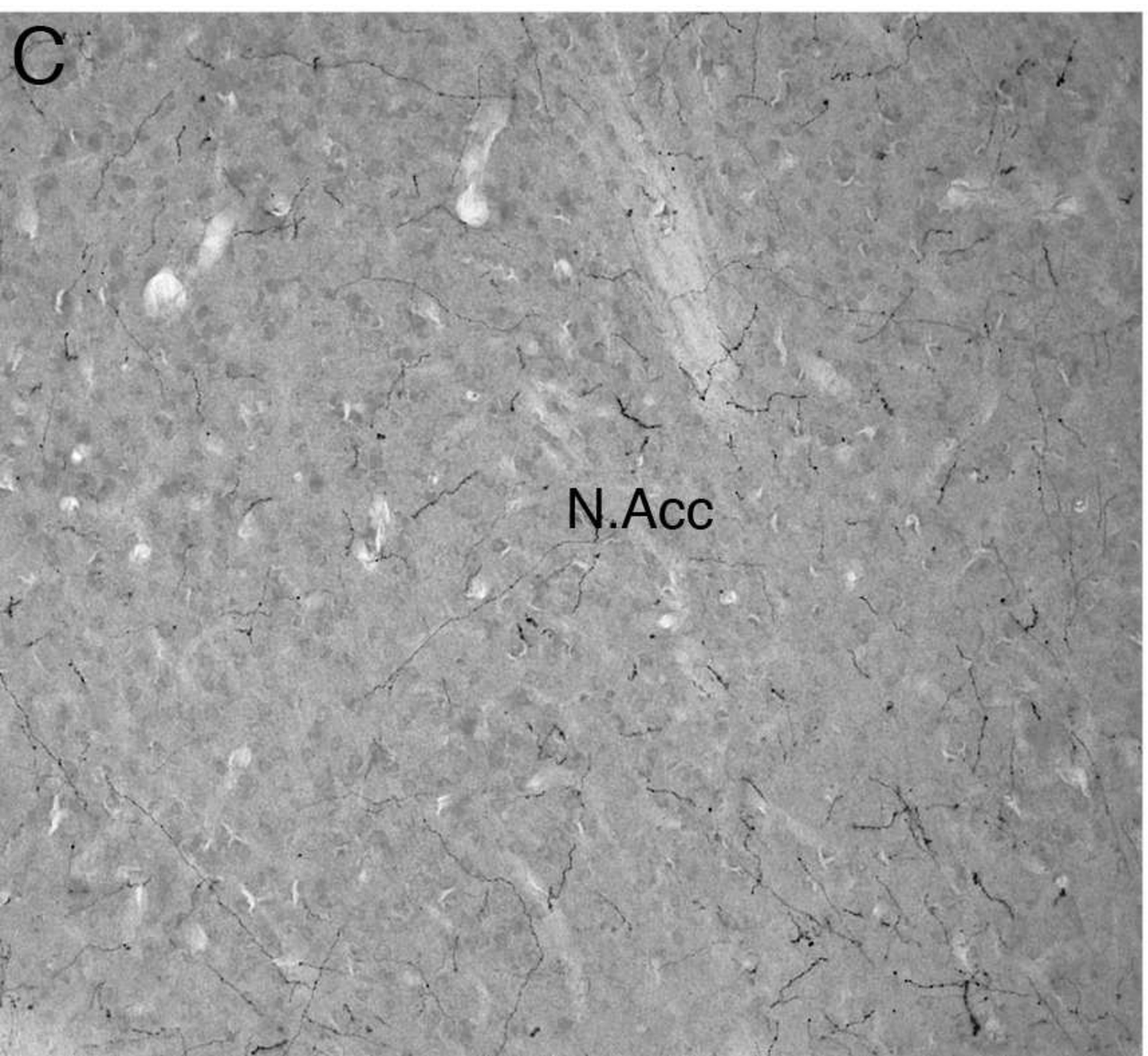
C
N.Acc

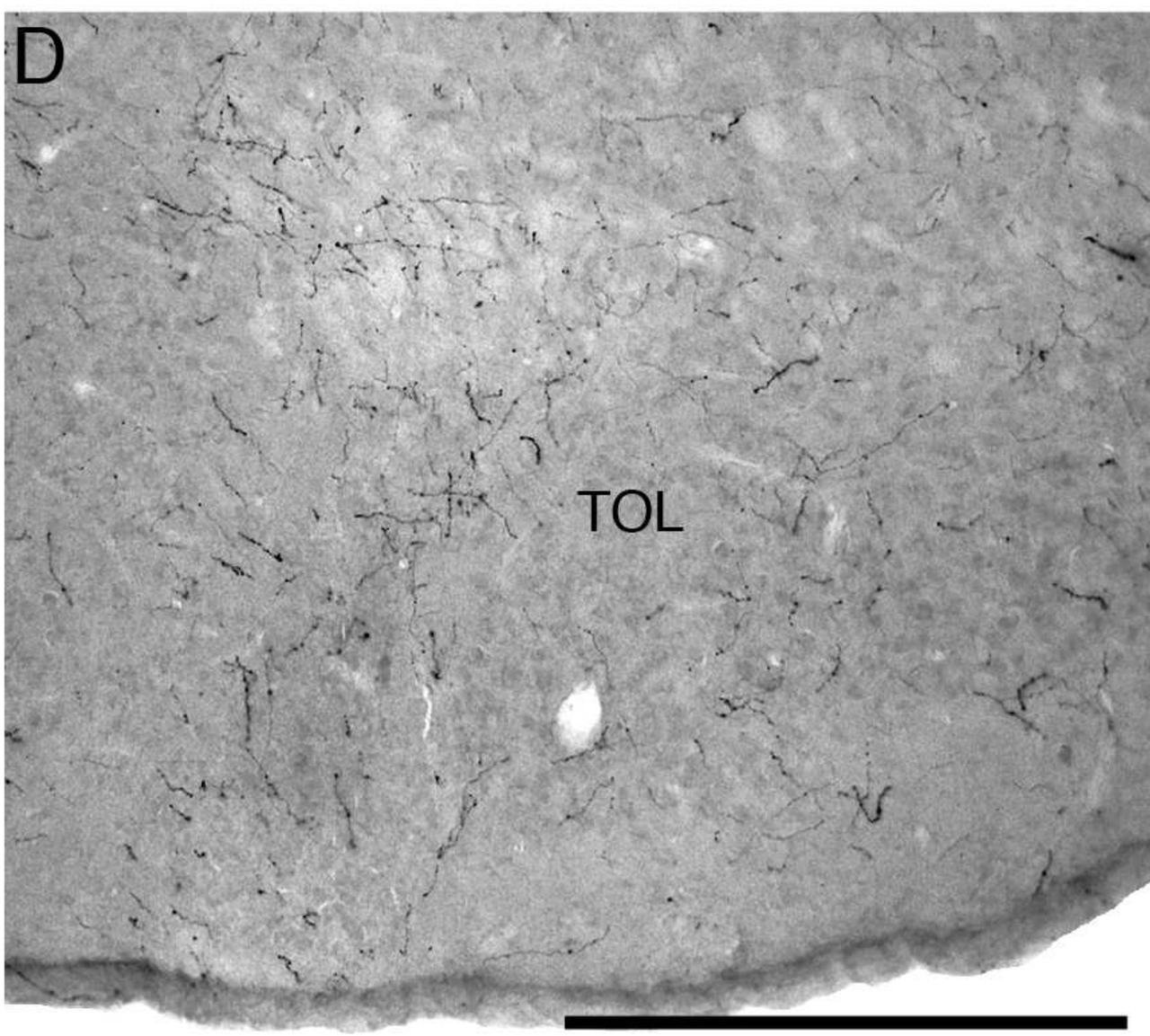
D
TOL

**Figure 3.5:** Photomicrograph illustrating the distribution of orexin-A immunoreactive terminal networks within the midbrain and pontine regions of the rock hyrax. **(A)** High density orexin-A immunoreactive terminal networks within the serotonergic dorsal raphe (DR) nuclear complex. Scale bar = 1 mm. **(B)** Medium density orexin-A immunoreactive terminal networks within the locus coeruleus nuclear complex. **(C)** Medium density orexin-A immunoreactive terminal networks within the serotonergic caudal linear nucleus (**CLi**) and supralemniscal nucleus (**B9**). Scale in **C** = 500 µm and applies to **B** and **C**. **A6** – locus coeruleus; **A7d** – subcoeruleus diffuse region; **A7sc**, subcoeruleus compact region; **ca** – cerebral aqueduct; **DRd** – dorsal division of dorsal raphe; **DRl** – lateral division of dorsal raphe; **DRp** – peripheral division of dorsal raphe; **DRv** – ventral division of dorsal raphe. Medial is to the left in all images.

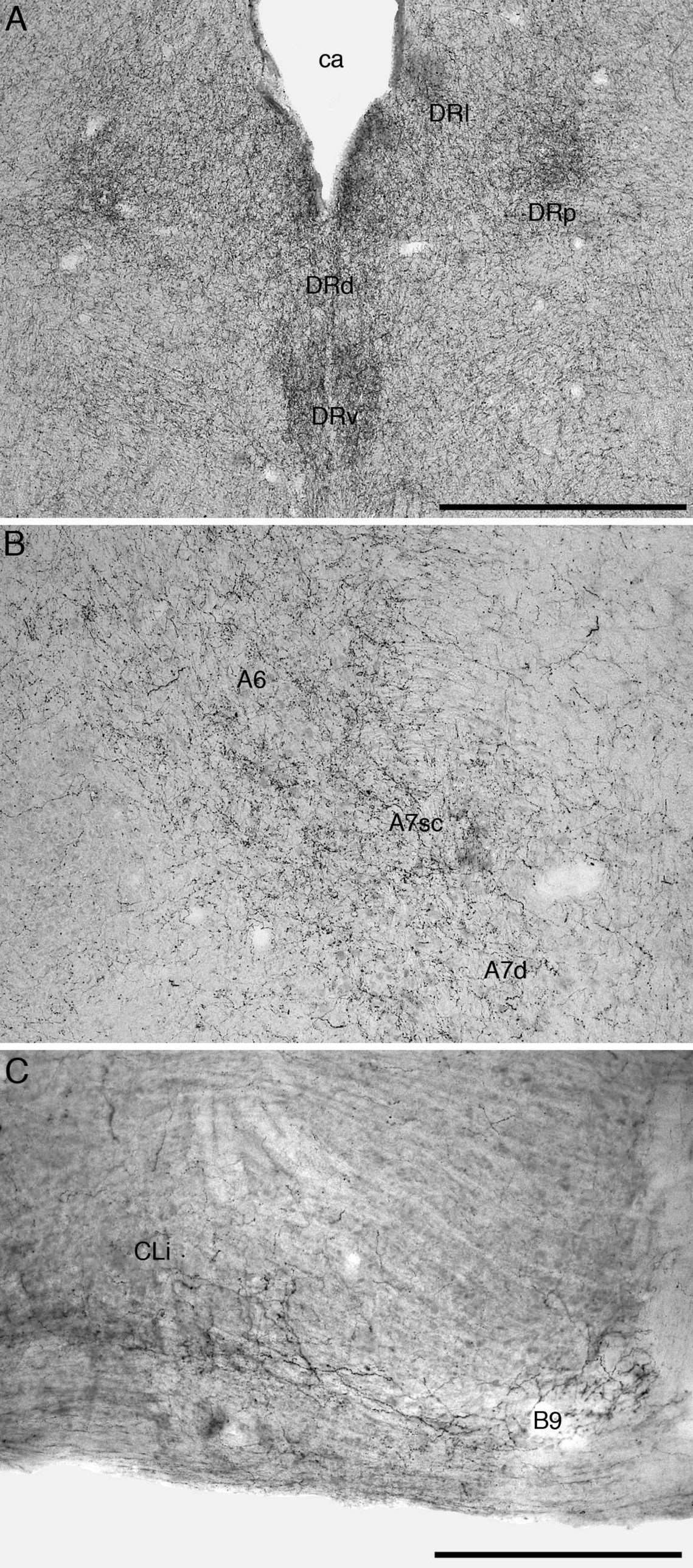
A
ca
DRl
DRp
DRd
DRv
B
A6
A7sc
A7d
C
CLi
B9

**Figure 3.6:** Photomicrograph illustrating orexin-A immunoreactive terminal networks within the diencephalon of the rock hyrax. **(A)** High density orexin-A immunoreactive terminal networks within the paraventricular thalamic nucleus (**PV**) and the lateral habenular nuclei along the border of the stria medullaris (**Hb**). Scale bar = 1 mm. **(B)** High density orexin-A immunoreactive terminal networks within the anterodorsal nucleus of the dorsal thalamus (**AD**). **(C)** Medium density orexin-A immunoreactive terminal networks within the intergeniculate leaflet (**IGL**) mainly oriented in the ventro-dorsal direction. Scale in **C** = 500 µm and applies to **B** and **C**. **AV** – anteroventral nucleus of the dorsal thalamus. Medial is to the left in all images

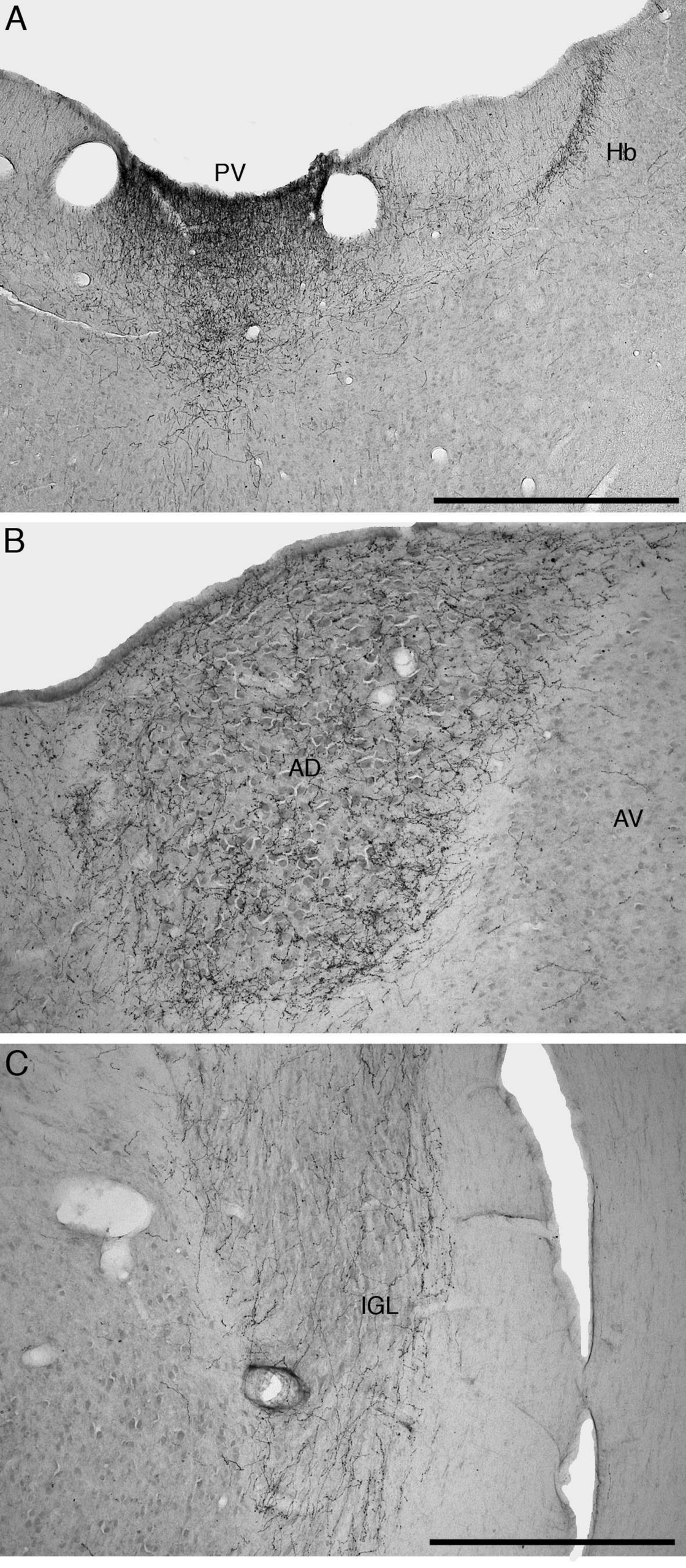
A
PV
Hb
B
AD
AV
C
IGL

## 3.5. Discussion

The aim of the present study was to identify and describe the neuronal location, nuclear organization and terminal network distribution of the orexinergic system in the brain of the rock hyrax, *Procavia capensis* by means of orexin-A immunocytochemistry. The study also examined the topological relationships of the Orx+ neurons and terminal networks with the previously described cholinergic, catecholaminergic and serotonergic systems in the brain of the rock hyrax (Gravett et al., 2009). The results revealed that the distribution and nuclear organization of the Orx+ neurons of the rock hyrax conforms closely to what has been described previously for other mammals (Broberger et al., 1998; Peyron et al., 1998; Moore et al., 2001; Zang et al., 2001, 2002; Nixon and Smale, 2007; Yamamoto., 2006; Kruger et al., 2010). The orexin-A immunoreactive terminal network distribution also showed a similar architecture as described in other mammalian species; however the anterodorsal nucleus of the thalamus was observed to have a dense orexinergic terminal network. Thus, the orexinergic system, as demonstrated with orexin-A immunoreactivity, within the rock hyrax brain is similar to what has been described in other mammals, but there is a feature of the terminal network distribution that has only been reported in a small number of other mammals.

### *3.5.1. Orexinergic neuronal distribution*

The location of orexinergic neuronal cell bodies has been described in representative species of all vertebrate classes – mammals (e.g. Wagner et al., 2000; Iqbal et al., 2001; Moore et al., 2001; Yamamoto et al., 2006; Nixon and Smale, 2007; Kruger et al., 2010; Stoyanova at al., 2010), birds (e.g. Ohkubo et al., 2002), reptiles (Domínguez

et al., 2010), amphibians (e.g. Shibahara et al., 1999; Galas et al., 2001; Singletary et al., 2005; Suzuki et al., 2008; López et al., 2009) and fish (e.g. Kaslin et al., 2004; Huesa et al., 2005; Yokogawa et al., 2007). All these studies have revealed that for the most part orexinergic neurons were located within the hypothalamus. It is clear from previous studies that this system shows a degree of variability within and between different vertebrate classes, but also a strong degree of similarity (e.g. Suzuki et al., 2008; Domínguez et al., 2010). In mammals the majority of orexinergic neurons are located within the lateral hypothalamic area and the perifornical region (which we term the main cluster, Kruger et al., 2010); however, other studies in mammals have also reported isolated neurons in the region of the median eminence, posterior, dorsal and dorsomedial hypothalamus (Chen et al., 1999; Cutler et al., 1999; Hagan et al., 1999; Wagner et al., 2000; McGranaghan and Piggins, 2001; Zhang et al., 2002, 2004; Espana et al., 2005). In the rock hyrax we could subdivide the orexinergic neurons into three distinct clusters: the main cluster, the zona incerta cluster and the optic tract cluster. While these clusters have been reported present in most mammals studied to date it has been found that microchiropterans and hamsters lack the optic tract cluster (Wagner et al., 2000; McGranaghan and Piggins, 2001; Kruger et al., 2010). The nuclear organization of the orexinergic neurons in the rock hyrax is therefore what may be described as very typically mammalian. It would seem that, apart from minor differences, the nuclear organization of the orexinergic neurons is strongly conserved across mammals. An important aspect of orexinergic nuclear parcellation relates to the connectivity of this system. For example, the zona incerta cluster specifically projects to the intergeniculate leaflet (Vidal et al., 2005) and what we term the main orexinergic cluster may be

subdivided into perifornical and lateral hypothalamic nuclei (Yoshida et al., 2006). Thus, in the hyrax we may be observing 4 specific nuclei within this system, however, further study on the specific connectivity of this system would be required to justify further nuclear parcellation than that presented here.

In conjunction with neuronal location and distribution, the present study also examined the topographical interrelationships of the orexinergic neurons with the previously described cholinergic, catecholaminergic and serotonergic systems in the brain of the rock hyrax (Gravett et al., 2009). The observations revealed that orexinergic neurons of the main cluster were topographically coincident with the A11 and A14 nuclear groups of the catecholaminergic system; the zona incerta cluster was topographically coincident with the A13 nucleus of the catecholaminergic system and the lateral hypothalamic nucleus of the cholinergic system; the optic tract cluster was topographically coincident with the cholinergic ventral hypothalamic nucleus. It has been reported that the membrane potential of orexinergic neurons are hyperpolarized by noradrenaline and serotonin and depolarized by acetylcholine (Yamanaka et al., 2003). Thus, orexinergic neurons are possibly rapidly depolarized where they intermingle with neurons from the cholinergic system. The potential intrinsic hypothalamic circuitry of these systems, due to the topological congruency, would be an avenue of interesting further study given the roles these systems play in the sleep-wake cycle, satiety and motivational states.

*3.5.2. Orexinergic terminal network distribution*

The orexinergic terminal network distribution within the brain of the rock hyrax was found to be similar to that described in other mammalian species studied to date, especially in the manner that these terminal networks are found primarily along the midline and ventricular surfaces; however, the anterodorsal nucleus of the dorsal thalamus (AD) of the rock hyrax exhibited a high-density orexinergic terminal network which is an apparent variance to most other mammals (see below).

The majority of the mammalian brain is in receipt of either very low or no orexinergic innervation, and this pattern is evident in the cerebral cortex, striatopallidal complex, hippocampal complex, amygdalar complex, the majority of the dorsal thalamus, brainstem and cerebellum of the rock hyrax brain. Medium dense orexinergic terminal networks were observed within regions of the telencephalon, diencephalon, midbrain and the medulla of the brain of the rock hyrax, whereas a high density orexinergic innervation was only evident in certain regions of the diencephalon and midbrain. This distribution of medium to high dense orexinergic terminal networks once again resembled the typical mammalian organizational plan for this system as reported in previous studies. Throughout the telencephalon, diencephalon, midbrain and medullary regions the orexinergic terminal networks were found intermingled with several nuclear complexes of the catecholaminergic, cholinergic and serotonergic systems (Gravett et al., 2009).

The regions within the telencephalon that exhibited a medium density of orexinergic terminal networks included the nucleus accumbens, the olfactory tubercle, the diagonal band of Broca, and the septal nuclear complex. This distribution of medium density orexinergic terminal networks within the telencephalon of the rock hyrax

coincides with previous reports for this system in other mammals. Within the diencephalon a medium density of orexinergic innervation was observed in the region of the intergeniculate leaflet, whereas a high density was observed in regions immediately surrounding the third ventricle, the midline of the dorsal thalamus as well as the AD nucleus (see below). The medium density orexinergic terminal networks overlapped the medial septal nucleus, dorsal, lateral and ventral hypothalamic nuclei of the cholinergic system and the A11 and A13 nuclear complexes of the catecholaminergic system. The distribution of medium to high density orexinergic terminal networks in the regions of the diencephalon of the rock hyrax brain did not differ significantly to published reports in other mammals for this region. However, it did differ to other mammals with respect to the orexinergic innervation of the AD nucleus, which has only been previously reported to occur in the Nile grass rat, *Arvicanthis niloticus* (Novak and Albers, 2002; Nixon and Smale, 2007) and the Syrian hamster, *Mesocricetus auratus* (Mintz et al., 2001). A medium density orexinergic terminal network distribution dominated the midbrain and pontine regions in the rock hyrax brain, however high density terminal networks were observed within the dopaminergic ventral tegmental area (VTA) and serotonergic dorsal raphe nuclei. A study by Nakamura et al. (2000) has reported that the calcium concentration in isolated A10 neurons is increased by orexin-A and this in turn induces hyperlocomotion, stereotypy and grooming in rats. Orexin-A has further been reported to have an excitatory effect on the serotonergic neurons of the dorsal raphe nucleus, which play an important role in the sleep-wake cycle as well as regulation of food intake and mood control (Brown et al., 2001; Matsuzaki et al., 2002; Tao et al., 2006). A moderate density of orexinergic terminal networks was identified in the noradrenergic locus

coeruleus and subcoeruleus, and cholinergic laterodorsal tegmental (LDT) and pedunculopontine tegmental (PPT) nuclei. These structures are known to play a crucial part in the sleep-wake cycle and have been reported to be activated by orexin. Orexinergic input to the cells of the locus coeruleus facilitate the waking state, whereas orexinergic innervation to the LDT and PPT play a role in the regulation of REM sleep (Ohno and Sakurai, 2008). Finally, the medullary region exhibited a medium dense orexinergic terminal network distribution in the areas ventral to the fourth ventricle and regions surrounding the central canal, whereas the remainder of this region was characterized by a low or absent orexinergic terminal network distribution. These terminal networks furthermore overlapped the RPa, RVL, RMg, ROb and CVL nuclei of the serotonergic system, the C1-2 and A1-2 nuclei of the catecholaminergic system, the nucleus ambiguus, the dorsal motor vagus and hypoglossal nuclei of the cholinergic system. Thus, for the most part the orexinergic terminal network distribution within the brain of the rock hyrax typically resembles the general mammalian organizational plan for this system.

### *3.5.3. Orexinergic innervation of the anterodorsal nucleus of the dorsal thalamus and diurnality?*

The majority of studies that describe the distribution of orexinergic terminal networks have examined nocturnal mammals. None of these studies reported either a dense or moderate orexinergic innervation of the AD. Two previous reports of moderate to dense orexinergic innervation of the AD examined the Nile grass rat, *Arvicanthis niloticus* (Novak and Albers, 2002; Nixon and Smale, 2007) and the Syrian hamster,

*Mesocricetus auratus* (Mintz et al., 2001). Novak and Albers (2002) reported a low density of orexinergic fibers in the AD nucleus and a high density in the anteroventral (AV) nucleus of the dorsal thalamus of the grass rat when the orexin B antibody was used, while Nixon and Smale (2007) reported a low density for the AV nucleus with the orexin-A antibody and a medium density in the AD nucleus with both orexin-A and B antibodies. The rock hyrax and the Syrian hamster (Mintz et al., 2001) both showed a high density of orexinergic terminals within the AD nucleus with an orexin-A antibody.

Of potential functional correlation to this is the fact that the rock hyrax (Olds and Shoshani, 1982), Nile grass rat (Novak et al., 2000) and Syrian hamster (Gatterman et al., 2008) are all diurnal species. Thus, it is possible that orexinergic innervation of the AD nucleus, the AV nucleus, or the anterior nuclear complex as a whole, might be a unique feature associated with diurnal mammals. This possibility needs to be tested across a range of mammalian species to determine whether this potentially very interesting finding is correct.

# Chapter 4

## Solitary sleep in the rock hyrax, *Procavia capensis*.

### 4.1. Introduction

Sleep is typically defined as a homeostatically regulated, easily reversible state of sustained quiescence accompanied by reduced sensory responsiveness. Mammalian sleep has been physiologically divided into non rapid eye movement sleep (NREM), often called slow wave sleep (SWS), and rapid eye movement sleep (REM) (Nicolau et al., 2000; Zepelin et al., 2005; Cirelli and Tononi, 2008; Lesku et al., 2008; Siegel, 2008). No consensus has been reached as to the functions of REM and NREM. One major clue to understanding these functions is an examination of how sleep amounts vary across species with differing physiological and ecological specializations (Tobler, 2005; Zepelin et al., 2005; Siegel, 2008; Horne, 2009; Rial et al., 2010).

A recent review (McNamara et al., 2008) detailed that sleep studies have been undertaken for approximately 127 different mammalian species representing 46 families from 17 different orders. They concluded that on average mammals sleep for approximately 12 h, with REM occupying approximately 17% of total sleep time; however, this is a generalization, as total sleep time varies significantly among different mammalian species. For instance, total sleep time (TST) in the rabbit, *Oryctolaus cuniculus*, is approximately 8.8 h (Spiess et al., 1970), TST in the laboratory mouse, *Mus musculus*, amounts to 12.8 h (Valatx and Bugat, 1974) compared to the horse, *Equus caballus*, where the TST is 2.9 h (Ruckebusch, 1972). In addition to this variation in sleep times, some mammals show some unusual forms of sleep – cetaceans exhibit

unihemispheric SWS (Lyamin et al., 2008), the ferret, armadillo and possum show unusually high amounts of REM sleep (Siegel, 2005), the fur seal has very little REM sleep while in the water compared to REM amounts when they are on land (Lyamin et al., 2008), and the platypus which has up to 8h/day of REM sleep, but lacks cortical desynchronization during much of this sleep phase (Siegel et al., 1999).

The rock hyrax belongs to the order Hyracoidea, which in turn is part of the clade Afrotheria (Tabuce et al., 2008). The Afrotherian clade is an unusual grouping, as although a strong molecular support for this clade exists, the morphological support is equivocal. The Afrotherian species show a vast range of body sizes, morphologies, life histories and ecological niches. For members of the Afrotheria, sleep has been recorded behaviourally in captive Asian and African Elephants, with TST in these animals being 4-6.5 h and 3.3 h respectively (Kurt, 1960; Tobler, 1992). EEG recordings of a fully aquatic Amazonian manatee, *Trichechus inungius*, showed that this animal spent 27% of the recorded time in SWS, which could be unihemispheric in nature, and 1% in paradoxical, or REM sleep (Mukhametov et al., 1992); however, the study was performed on a single animal and the sleep recording commenced directly after surgery and lasted only a few days. Within the Hyracoidea Snyder (1974) reports a TST of 4.9 h for *Procavia johnstoni* (rock hyrax), 5.7 h for *Heterohyrax brucei* (bush hyrax), and 4.9 h for *Dendrohyrax validus* (tree hyrax); however, only an abstract has been published for the aforementioned study and no EEG spectral evidence have been provided to support the TST reported. Reports of sleep in other Afrotherian species are not known to the authors. In the present study the physiological measurable parameters of sleep and the accompanying behaviour

were recorded using telemetry in the rock hyrax, *Procavia capensis*, a previously unstudied hyrax species.

### 4.2. Materials and Methods

A total of five adult rock hyraxes, *P. capensis*, (4 male and 1 female) with body weights ranging between 1.74 – 4.3 kg (Table 4.1), were used in the present study. Permits from the Limpopo and Gauteng Provincial Governments were obtained for the capture and transport of the animals from the wild. All animals were treated and used according to the guidelines of the University of the Witwatersrand Animal Ethics Committee (approval number AESC 2005/8/5), which parallel those of the NIH for the care and use of animals in scientific experimentation. The animals were captured at random from wild populations and thereafter allowed to acclimatize for a period of one month to the recording enclosures that had a 12-12 lighting schedule with temperature maintained between 19-21°C. Each animal was implanted with a telemetric recording devise (Data Sciences International) that allowed for the recording of physiologically measurable parameters of sleep without cables or restraint. The chamber in which recording occurred was 1.8 m x 1.5 m with a painted concrete surface that was covered with straw. The height of the chamber was approximately 1.5 m and steel mesh was placed over the chamber to prevent the animals from escaping. A wooden box (90 x 90 x 30 cm) with a Perspex roof and two entrances was placed inside the chamber and food (combinations of cucumber, tomato, sweet potato, pumpkin, apples and rabbit pellets as a source of roughage) and fresh water was supplied daily. Behaviour was also recorded with a low light CCD digital camera connected to a DVD recorder.

*4.2.1. Surgical procedure*

After acclimatization, surgical implantation of the telemetric recoding device was performed. The animals were weighed before surgery and anesthetized with weight appropriate doses of a 2:1 mixture of ketamine and xylazine (Anaket-V and Chanazine 2% Injection, Bayer HealthCare). The head and neck, left thoracic (two 2 cm x 1 cm) and abdominal (10 cm x 10 cm) regions were shaved and cleaned with CHX Chlorhexidine Disinfectant (0.5% chlorhexidine diglucunate in 75% alcohol, Kyron Laboratories (PTY) LTD) before surgery commenced. These areas correspond, respectively, to the regions were the EEG (electroencephalogram), EMG (electromyogram) and ECG (electrocardiogram) electrodes and telemeter would be implanted. The animal was placed on a heated blanket in order to maintain a constant body temperature throughout the surgery and the head was securely placed in a stereotaxic apparatus to prevent movement and allow for the accurate placement of the EEG and EMG electrodes. During the surgical procedure the animal was kept under a constant state of anaesthesia by means of isoflurane ventilation (1-2% in an oxygen/70% nitrous oxide mixture, Isofor Inhalation Anaesthetic – Safe Line Pharmaceuticals (Pty) Ltd). The animal's heart rate, body temperature and percentage oxygen saturation was monitored.

Under aseptic conditions, a mid-sagittal incision was made over the skull and the skin and temporal muscle were reflected to expose the part of the skull overlying the motor cortex. Using a dental drill, three 2 mm diameter holes were made in the cranial vault to expose the underlying dura mater. The first hole was drilled anterior to the olfactory bulbs for the placement of the indifferent electrode, while two holes were drilled approximately 5 mm apart just lateral to the sagittal sinus over the left motor

cortex for the placement of the stainless steel recording electrodes (gauge of electrode 0.457 mm, silastic outside diameter 0.9 mm and inside diameter 0.508 mm, PhysioTel ® Multiplus Transmitter, Data Sciences International). The electrodes were placed in such a manner that the tips rested firmly on the surface of the cortex but did not pierce the dura mater and were secured in place with dental cement. Two stainless steel EMG electrodes (gauge of electrode 0.457 mm, silastic outside diameter 0.9 mm and inside diameter 0.508 mm, PhysioTel ® Multiplus Transmitter, Data Sciences International) (1.5 cm apart) were sutured into the dorsal nuchal musculature, while two ECG electrodes (3 cm apart) were sutured into the subdermal tissue overlying the rib cage in the left thoracic region. A subcutaneous pocket was created (10 cm x 10 cm) over the left abdominal region, which allowed for the implantation of the telemetry unit. All skin incisions were sutured following implantation. After surgery was complete the animal was given an intramuscular analgesic (0.1 ml Tamgestic, Schering-Plough, mixed with 0.9 ml sterile water, 1 ml mixture/kg) and returned to the recording enclosure. Recovery was monitored every half hour until it could be established that the animal was able to move freely and eat/drink normally.

*4.2.2. Sleep recording*

After the surgical procedure the animal was allowed a recovery period of one week before the recording of sleep commenced. The animals were housed in the same recording enclosure for recovery as well as recording. A receiver was mounted and secured to one wall of the enclosure while a low light CCD digital camera was mounted above the enclosure. The telemetric recording system (Data Sciences International, DSI,

PhysioTel ® Multiplus Transmitter, model TL10M3-D70-EEE implant) consisted of a DEM multiplex interface to which the receiver was connected. The signal from the implanted transmitter (round, 13cm² with stainless steel electrodes, weight – 37 g, volume – 25 ml, 3 channels) detected by the receiver was relayed to the input amplifier of the Data Sciences computer system, after which it was digitally recorded (in DSI format) for analysis. After the recording was completed, data digitally saved in the DSI format was converted to text format and these files were in turn converted into the appropriate format needed for recognition and analysis by the Spike 2 computer program (version 4.2, Cambridge Electronic Design). Sleep (physiologically measurable parameters and the DVD recorded associated behaviour) was recorded continuously for a period of 72 hours. The recording enclosure was in a sound attenuating room. The animals were disturbed only once a day for approximately 5 min at the same time during each of the recording days for feeding.

*4.2.3. Data analysis*

Version 4.2.2 of the Spike 2 software (Cambridge Electronic Designs, UC) was used in order to convert the recorded data into the appropriate format, i.e. Spike 2 data format, for offline analysis. The EEG data was subsequently scored in 5 s epochs as either waking characterized by low voltage high frequency EEG and high voltage EMG, SWS characterized by high voltage low frequency EEG and EMG lower in amplitude than waking, and REM (rapid eye movement). REM in the rock hyrax was found to be ambiguous and did not resemble the classical definition of REM sleep, thus REM0, was characterized by low voltage high frequency EEG, an EMG that was almost atonic, and

an irregular ECG; whilst REM1 was characterized by a low voltage high frequency EEG, EMG amplitude characteristic of SWS and a regular ECG (Figs. 4.1-6). An epoch was only assigned to a particular state if the state occupied at least 50% of the epoch. The data obtained from the 5 s epoch scoring was analyzed to determine the modal state per minute to generate the data for the 1 min epoch scoring. An unpaired two-tailed t-test (parametric data) or Mann-Whitney (nonparametric data) test ($p<0.05$) was employed to determine if a statistically significant differences existed between the 5 s and 1 min epoch scoring methods. Behaviour was scored in 1 min epochs as either immobile – animal was completely immobile for >30 s, quiet waking – animal was immobile and only moving its head or made minor movements in the same place for >30 s, active waking – animal was actively moving around for >30 s, or eating/drinking – animal was eating and/or dinking for >30 s (Figs. 4.5-6).

All the physiologically and behaviourally scored data was tested for normality prior to any statistical testing. The Kolmogrov and Smirnov test was conducted to determine whether the data was parametric or nonparametric in nature ($p>0.05$). A one-way ANOVA was used in all comparisons where the data was parametric and a statistically significant difference between sample means were obtained in cases where $p<0.05$. Where it was found that the data was nonparametric the Kruskal-Wallis test was employed and a statistically significant difference between sample medians were obtained in all cases where $p<0.05$. Comparisons between light and dark were made by means of contingency tables, where in the case of parametric data the unpaired two-tailed T-test and in the case of nonparametric data the Mann-Whitney test was employed to

determine whether statistically significant differences existed ($p<0.05$). Microsoft Excel and GraphPad InStat computer programs were used in the analysis of the data.

### 4.3. Results

The physiologically measurable parameters of sleep, as well as the associated behaviours, were recorded in total of five hyraxes, *P. capensis*, continuously for a period of 72 h. The analysis of the data pooled across the five individuals recorded showed that 66.2% (16 h/day) of the time was spent awake, 25.1% (6 h/day) in SWS, 3% (1 h/day) in REM1 and 0.4% (6 min/day) in REM0 (the 0.9h unaccounted for can be attributed to periods where signal loss occurred). There was no statistically significant difference in the distribution of these stages between light and dark periods (Table 4.1, Figs. 4.5, 4.6, 4.8). REM in the rock hyrax was ambiguous which led to its subdivision into REM1 and REM0. REM0 was considered the definitive form of this state whereas REM1 showed mixed characteristics of both low voltage slow wave sleep as well as REM. Waking most often transitioned to SWS and SWS to waking in these animals, thus making this the most common sleep state transition. There was a 10% probability that SWS will be followed by an episode of REM1 and a 0.2% chance that it would be followed by a REM0 episode. REM1 on the other hand was most likely to transition to waking, but was also occasionally followed by REM0. In most cases REM0 was followed by waking, but it also transitioned to REM1. Both REM1 and REM0 exhibited an equal chance of transitioning to SWS. Thus the three most common state transitional pathways would be, waking → SWS → waking, waking → SWS → REM1 → waking, and waking → SWS → REM1 → REM0 → waking (Figs. 4.2 and 4.7)

*4.3.1. Physiological Data – State Definitions*

The polygraphic data was scored in 5 s epochs as waking, SWS, or REM (which was subdivided into REM0 and REM1). Waking was characterized by a low voltage, high frequency EEG with a high amplitude EMG (EMG during active waking being higher in amplitude compared to quiet waking). The ECG for this state was more regular during periods of quiet waking and more irregular during periods of active waking. SWS episodes were characterized by a high voltage, low frequency EEG, an EMG of lower amplitude when compared to waking and a regular ECG (Figs. 4.1-2). Instantaneous heart rate during waking and SWS was on average 154 bpm (SER 0.44, STDEV ± 7.79) and 158 bpm (SER 0.62, STDEV ± 10.99) respectively (Fig. 4.3). Identification of REM episodes was more ambiguous than the identification of waking and SWS episodes, due to the fact that both physiologically and behaviourally it did not follow the "textbook" definition of this state in all cases. REM is characterized as typically following a period of SWS, having an EEG that is similar to the low voltage high frequency waves of waking, an atonic EMG, an irregular ECG, muscle twitches and rapid eye movements (Desiraju et al., 1966; Elgar et al., 1988; Tobler, 1995; Siegel, 2005; Steriade, 2005; Horne, 2009). In most instances REM in the rock hyrax did not meet all of these criteria, leading to the subdivision of this stage into REM0 and REM1. In some animals the muscle twitches characteristic of REM were observed. A loss of muscle tone was evident in all of hyraxes examined where the animal would be immobile and lying down with its head on the ground and then slowly fall to one side before repositioning itself. Head dropping was also noted in cases where the animal's head was not initially placed on the ground. REM0 episodes were characterized by a low voltage, high frequency EEG

(similar to waking EEG), a noticeable drop in the EMG (in some cases it was almost completely atonic) and an irregular ECG; whereas REM1 episodes exhibited low voltage, high frequency EEG, an unaltered EMG that stayed at the same amplitude as the preceding SWS episode, and both regular and irregular ECG rates (Figs. 4.1-2). Instantaneous heart rate during REM0 and REM1 was on average 163 bpm (SER 1.52, STDEV ± 27.34) and 153 bpm (SER 0.61, STDEV ± 10.56) respectively (Fig. 4.3).

*4.3.1.1. Total state times*

The results of the 5 s epoch scoring method revealed that 66.2% (16 h/day) of the time was spent awake, 25.1% (6 h/day) in SWS, 3% (43 min/day) in REM1 and 0.4% (6 min/day) in REM0. The 1 min epoch scoring method showed similar results, 66.7% (16 h/day) of the time was spent awake, 24.8% (6 h/day) in SWS, 3.1% (45 min/day) in REM1 and 0.4% (6 min/day) in REM0 (unaccounted time can be attributed to signal loss) (Fig. 4.8A). During the light period waking was found to occupy 66.5% of time in the 5 s scoring method and 67.3% in the 1 min scoring method, SWS occupied 24.7% of the time in the 5 s scoring method and 25% in the 1 min scoring method, REM1 occupied 2.8% and 3% of the time for the 5 s and 1 min scoring method respectively and REM0 occupied 0.4% of the time for both scoring methods (Fig. 4.8B). During the dark period waking accounted for 66.1% of the time for both scoring methods, SWS 25.4% (5 s) and 24.4% (1 min), REM1 3.3% (same for both methods) and REM0 0.5% (5 s) and 0.4% (1 min) (Fig. 4.8C). Thus, no statistically significant difference was noted between the 5 s and 1 min scoring methods with regard to TST and TWT over 24 h and during the light and dark periods. No statistically significant difference was noted between the light and

dark periods with regard to TST and TWT for both scoring methods as well (Unpaired t-test for parametric data, Mann Whitney test for nonparametric data, significant $p<0.05$).

*4.3.1.2. Number of episodes*

The number of episodes per state over 24 h from each individual animal subjected to experimentation was tested for continuity between the different recording days. No statistically significant differences in the number of episodes for each particular state (Waking, SWS, REM1, and REM0) were noted overall (One-way ANOVA for parametric data, Kruskal-Wallis test for nonparametric data, significant $p<0.05$). One animal did show a difference in the number of waking, SWS and REM1 episodes, with day 1 showing more episodes of both these states compared to the remaining two days. When the group was considered as one entity no statistically significant difference was noted in the distribution of the number of episodes between the days for all stages except SWS. A greater number of SWS episodes were noted during day 1 as opposed to days 2 and 3 (Table 4.2). The average number of waking, SWS, REM1 and REM0 episodes in 24 h for the 5 s epoch scoring method amounted to 638, 559, 37 and 8 respectively whereas for the 1 min epoch scoring method it amounted to 129, 116, 27 and 4 respectively. No statistically significant difference was noted with regard to number of REM1 and REM0 episodes in 24 h, however a significant difference was noted for the number of waking and SWS episodes in 24 h when the 5 s and 1 min scoring methods were compared (average number of waking and SWS episodes in 24 h were significantly more for the 5 s scoring method) (Fig. 4.8A). The aforementioned was also observed during the light and dark periods when these two scoring methods were compared (Fig.

4.8B, C). No statistically significant difference was noted with regard to the number of episodes per state when the light and dark periods were compared for both scoring methods (Unpaired t-test for parametric data, Mann Whitney test for nonparametric data, significant $p<0.05$).

*4.3.1.3. Duration of episodes*

The average duration of each episode for a particular state was compared between the three different recording days to test for equal variances. The results revealed that there was no statistically significant difference in the average duration of an episode for a particular state between the three recording days for most of the animals tested (One-way ANOVA for parametric data, Kruskal-Wallis test for nonparametric data, significant $p<0.05$). Two animals did show a difference in the average duration of waking and SWS episodes, with the average duration of a SWS episode during the third day being much shorter than that of the two preceding days. When the entire group was compared it was found that the average duration of REM1 and REM0 episodes did not differ significantly between days; however, waking and SWS did show a statistically significant difference in their duration between days. The average duration of a waking episode was shorter during the first day of recording, whereas the average duration of a SWS episode was longer during the first day, compared to the remaining two days of recording (Table 4.2). The average duration per state over 24 h amounted to 90 s for waking, 39 s for SWS, 70 s for REM1 and 46 s for REM0 for the 5 s scoring methods whereas for the 1 min scoring method it amounted to 448 s (7 min), 185 s (3 min), 99 s (2 min) and 78 s respectively (Fig. 4.8A). A statistically significant difference for all states was noted when these two

scoring methods were compared, average episode duration for each of the states was significantly longer for the 1 min data compared to the 5 s data. The aforementioned observations were also observed during the light and dark periods when these two scoring methods were compared (Fig. 4.8B, C). No statistically significant difference was noted between the light and dark periods with regard to average episode duration per state for both of the scoring methods. No difference was noted in the average duration of REM1 episodes between the light and dark periods for the 5 s scoring method however the 1 min scoring method did show that the average REM1 episode duration was longer during the light period compared to the dark period. For both scoring methods the average REM0 episode duration was longer during the light period compared to the dark period (Unpaired t-test for parametric data, Mann Whitney test for nonparametric data, significant $p<0.05$).

*4.3.1.4. REM periodicity and slow wave activity (SWA)*

REM periodicity was calculated from the onset of one episode to the onset of the following episode and was based on the 72 h recording period for both the 5 s and 1 min scoring methods. A statistically significant difference was noted with regard to REM periodicity when the 5 s and 1 min scoring methods were compared. The modal REM periodicity for the 5 s data was 5 min whereas it was 10 min for the 1 min data. The average REM sleep cycle interval for the 5 s scoring method was 24 min whereas for the 1 min scoring method it was 33 min. When all waking episodes that lasted longer that 10 min were removed from the 1 min data, the modal sleep cycle length was found to be 15 min (Fig. 4.9).

Slow wave activity based on two-hour intervals was calculated for all states (SWA-all) and for SWS (SWA-SWS). The results revealed that the SWA was highest during SWS and showed a gradual reduction in intensity from waking to REM1 to REM0. SWA for both SWA-all and SWA-SWS remained relatively constant between the three days of recording. No statistically significant difference was noted with regard to SWA during light and dark periods for either SWA-all or SWA-SWS. A statistically significant difference (Unpaired t-test, significant $p<0.05$) was noted when the SWA-SWS was compared to SWA-all. SWA in SWA-SWS was greater than SWA-all over 24 h, as well as during both dark and light periods (Fig. 4.10).

*4.3.2. Behavioural Data*

Behaviour was recorded simultaneously with the physiological recordings and scored in 1 min epochs as immobile (animal not moving for >30 s), quiet waking (animal moving head or making minor movements in the same place for >30 s), active waking (animal was actively moving around for >30 s) or eating/drinking (animal was eating/drinking for >30 s). On average 68% (16 h/day) of the time was spent in a state of immobility, 23% (6 h/day) in quiet waking, 5% (1 h/day) in active waking and 3% (43 min/day) of the time was spent eating/drinking. When the distribution of these behavioural states was compared for dark and light periods, no statistically significant differences were noted; however, on average these animals were more active (moving, eating and drinking) during the dark compared to the light period (Unpaired t-test for parametric data, Mann Whitney test for nonparametric data, significant $p<0.05$) (Fig. 4.11).

**Figure 4.1:** Examples of EEG and EMG polygraphs demonstrating a 2 min episode of active wake, quiet wake, slow wave, REM (consisting of both REM type 1 and REM type 0), REM1 and REM0 states in the rock hyrax. Waking episodes were characterised by a low voltage high frequency EEG. The EMG for active waking exhibited higher voltages compared to the quiet waking state, and high voltage spikes that likely correspond with movements, were evident during this state. SWS was characterized by a high voltage, low frequency EEG and an EMG that was lower in amplitude than during the waking states. The EEG for both REM1 and REM0 resembled that of waking; however, during REM1 the EMG remained at the same amplitude as the preceding SWS episode, while during REM0 the EMG was reduced in amplitude.

## Active Wake

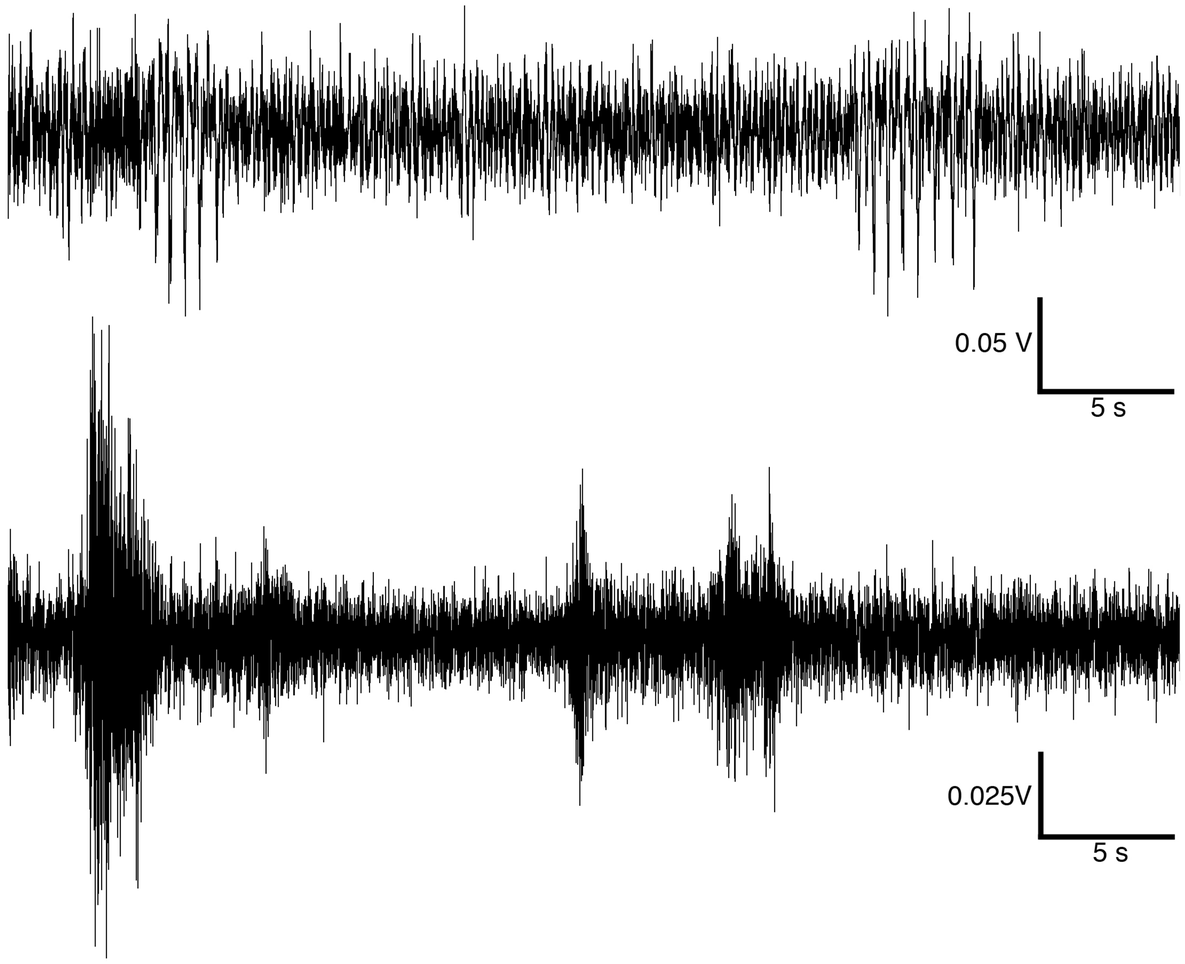


## Mixed REM Sleep

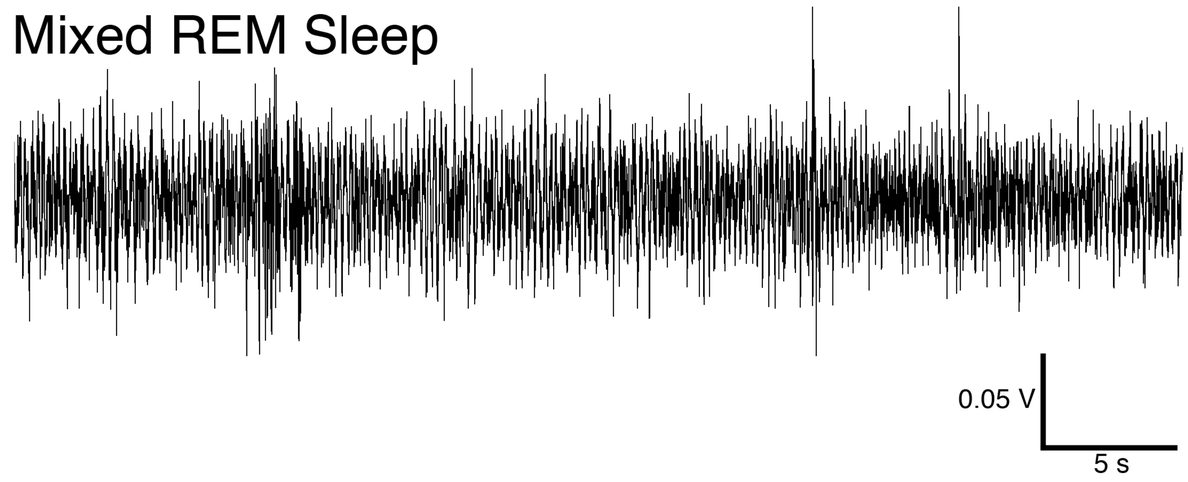


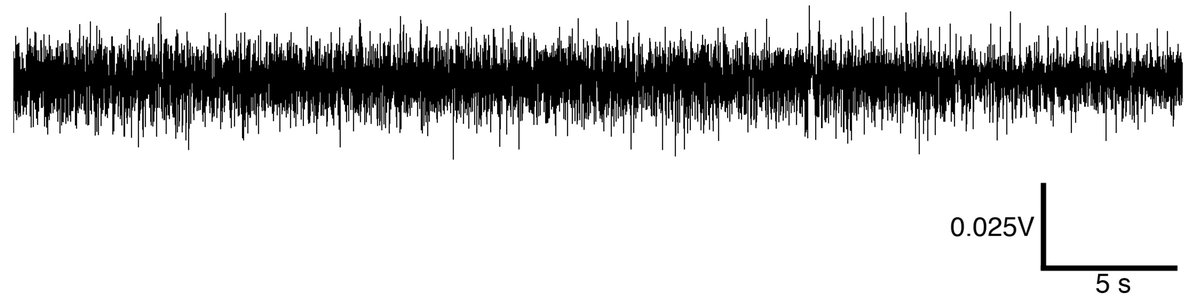


## Quiet Wake

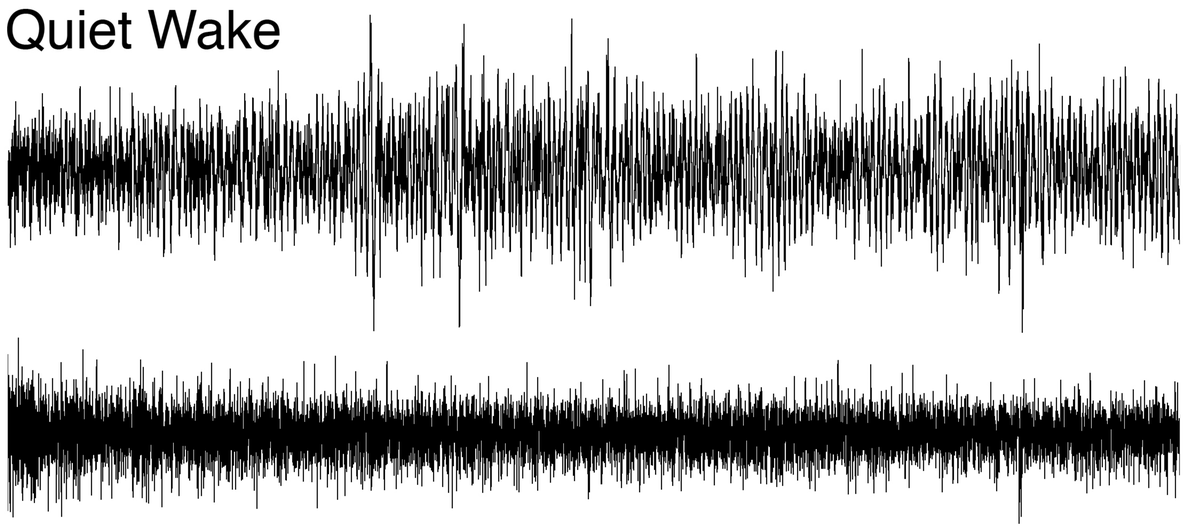


## REM Sleep type 1

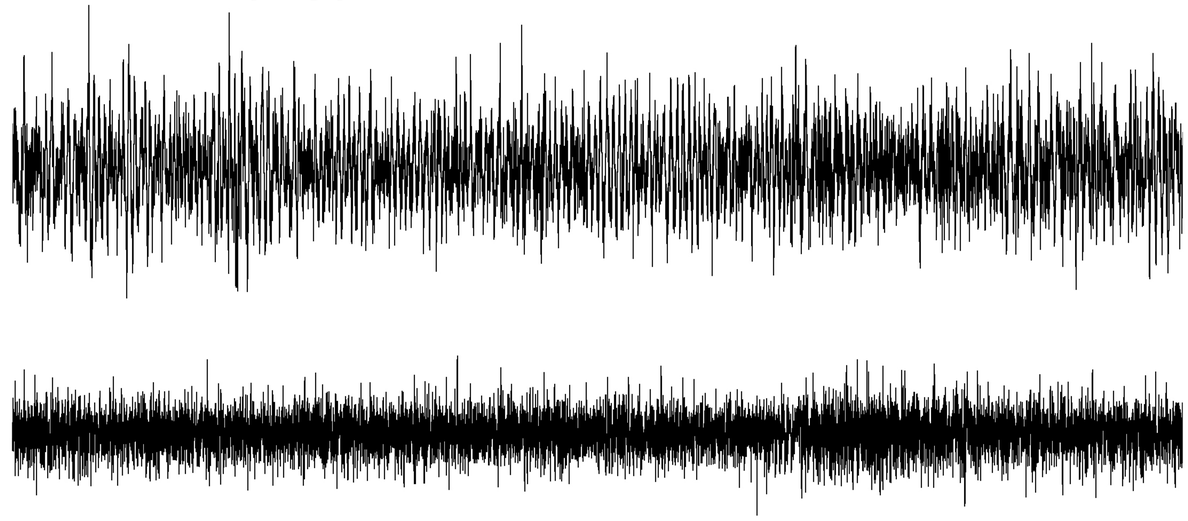


## Slow Wave Sleep

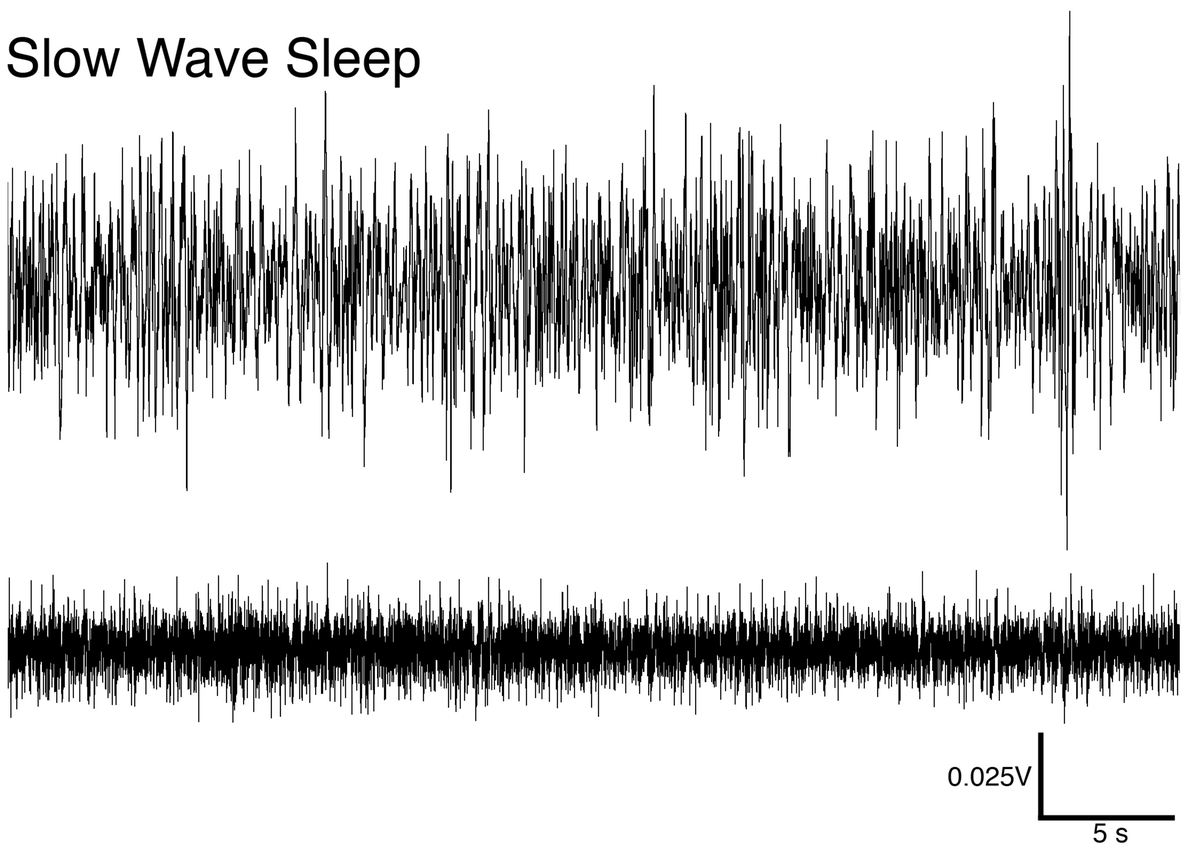


## REM Sleep type 0

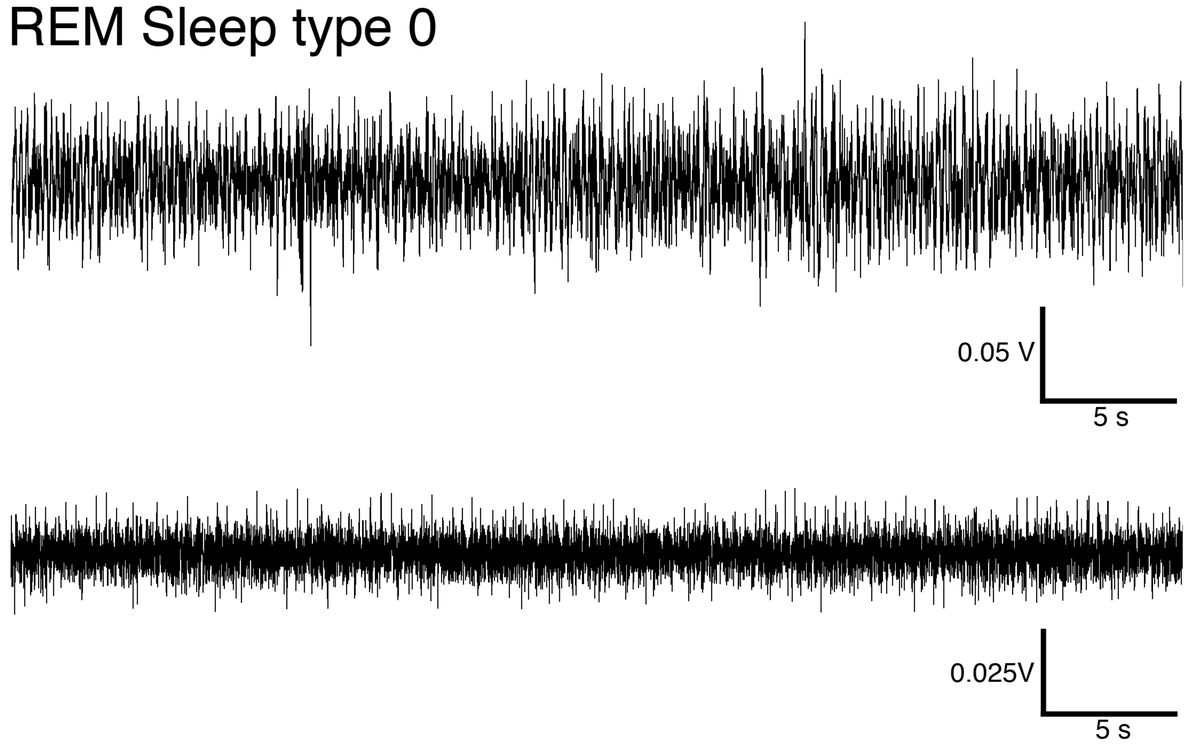

**Figure 4.2:** EEG and EMG polygraphs demonstrating the transitions that occur between the different sleep states in the rock hyrax. The first set of polygraphs is an example of SWS transitioning to REM1 which then leads into REM0 followed by waking. Note that the EMG during REM1 remains at the same amplitude as during the preceding SWS episode, and that when REM1 transitions to REM0 the EMG reduces in amplitude. The second set of polygraphs demonstrates transition from SWS to REM0 followed by waking.

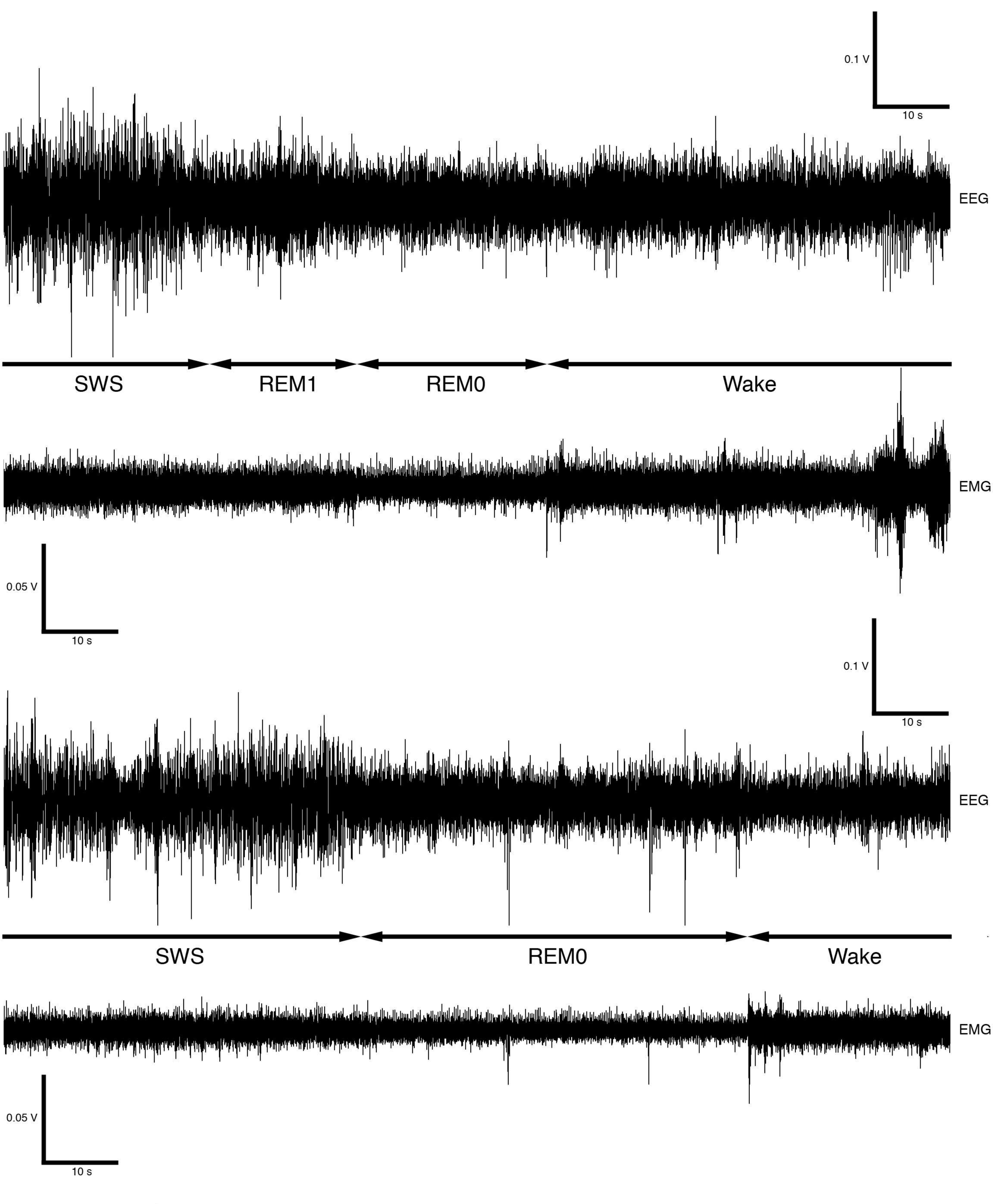
0.1 V
10 s
EEG
SWS
REM1
REM0
Wake
EMG
0.05 V
10 s
0.1 V
10 s
EEG
SWS
REM0
Wake
EMG
0.05 V
10 s

**Figure 4.3:** Scatter plots representing the instantaneous heart rate (IHR) during each of the sleep states and waking. The IHR rate during waking was irregular and more widely scattered compared to SWS that exhibited a more regular pattern. The IHR of REM1 closely resembled that of waking while REM0 was even more irregular and widely scattered compared to waking.

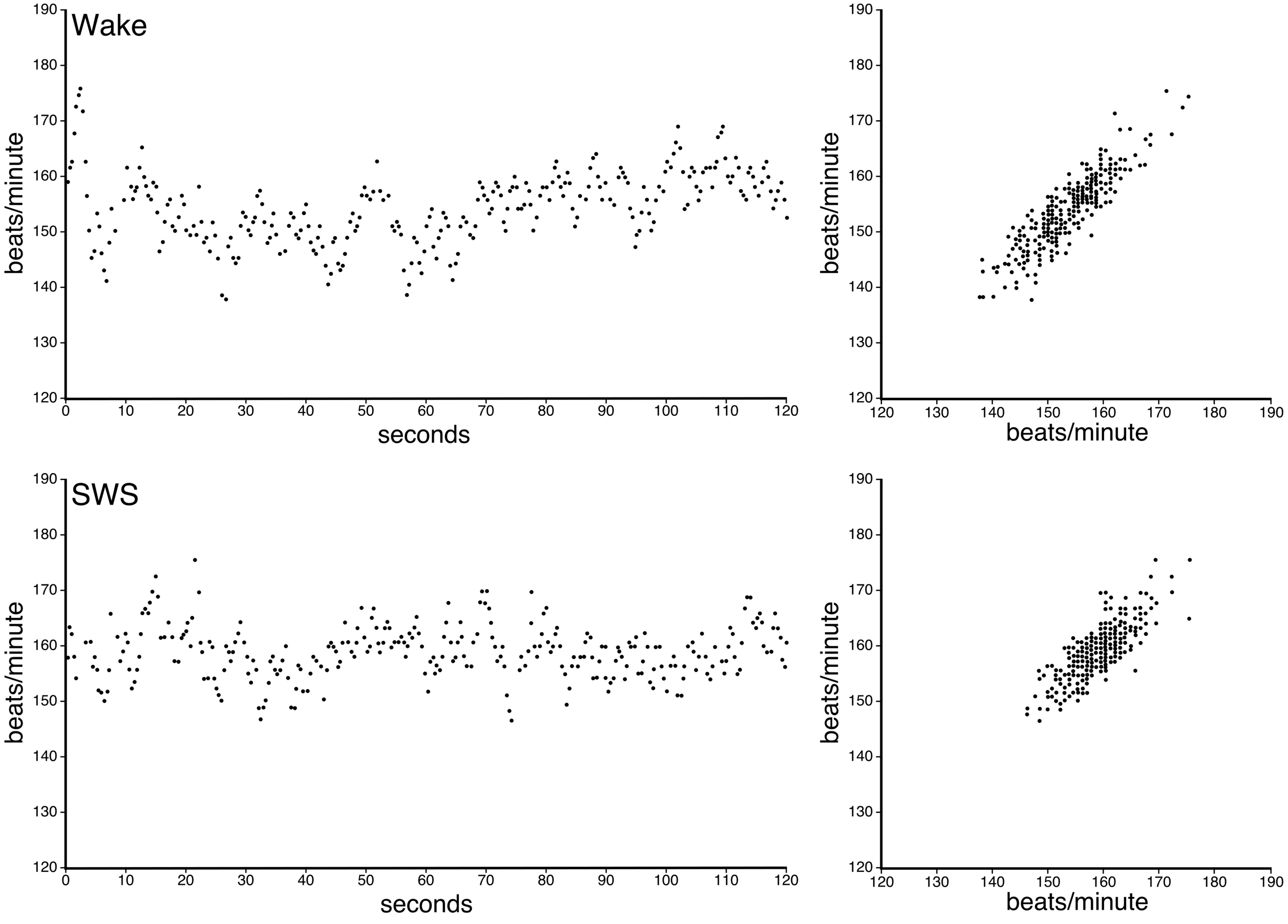
Wake
beats/minute
seconds
beats/minute
SWS
beats/minute
seconds
beats/minute
REM1
beats/minute
seconds
beats/minute
REM0
beats/minute
seconds
beats/minute

**Figure 4.4:** Diagram illustrating the spectral power and associated frequency bands characteristics of waking, SWS and REM1 and REM0 in the rock hyrax.

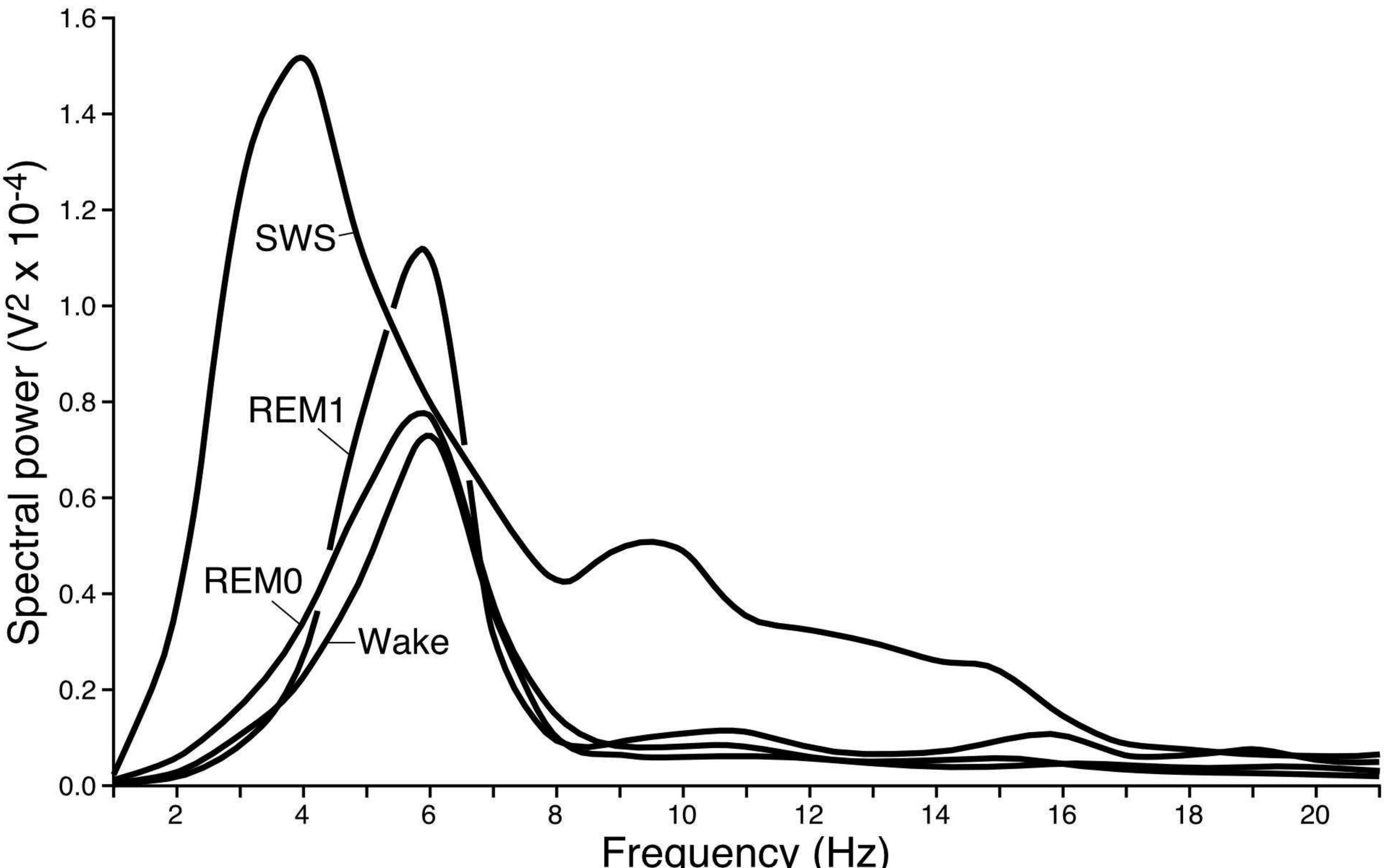
Spectral power (V2 x 10-4)
1.6
1.4
1.2
1.0
0.8
0.6
0.4
0.2
0.0
SWS
REM1
REM0
Wake
2
4
6
8
10
12
14
16
18
20
Frequency (Hz)

**Figure 4.5:** Hypnograms showing the physiological and correlated behavioral state transitions occurring over a 24 h period for H06 starting at 9 am. The shaded area is representative of the dark period. The polycyclic nature of sleep is visible in the physiological hypnogram, with SWS equally represented during both the light and dark periods; however, both REM1 and REM0 were more prevalent during the dark period. The animal also appeared to be more active and was eating more during the dark periods compared to the light periods for the 24 hours represented here.

## Physiology

REM0
REM1
SWS
Wake
Signal loss

## Behaviour

Eating/ drinking
Active wake
Quiet wake
Immobile

9:00 10:00 11:00 12:00 13:00 14:00 15:00 16:00 17:00 18:00 19:00 20:00 21:00 22:00 23:00 0:00 1:00 2:00 3:00 4:00 5:00 6:00 7:00 8:00 9:00

**Figure 4.6:** Hypnogram showing the physiological and correlated behavioral state transitions occurring over a 24 hour period for H07 starting at 9 am. The shaded area is representative of the dark period. SWS is equally represented during both the light and dark periods which is indicative of the polycyclic nature of sleep in these animals. REM1 was more prevalent during the dark period, and REM0 did not occur as frequently as in H06 (see Fig. 4.5). During this particular 24 hours active waking was distributed equally during both light and darks periods, while feeding behaviour predominated during the light period.

## Physiology

REM0
REM1
SWS
Wake
Signal loss

## Behaviour

Eating/ drinking
Active wake
Quiet wake
Immobile

9:00 10:00 11:00 12:00 13:00 14:00 15:00 16:00 17:00 18:00 19:00 20:00 21:00 22:00 23:00 0:00 1:00 2:00 3:00 4:00 5:00 6:00 7:00 8:00 9:00

**Figure 4.7:** State transition probabilities in the rock hyrax during 24 hours based on the data of two randomly selected animals. In most cases SWS was followed by waking, thus making this the most common sleep pathway observed in the rock hyrax. The next most common pathway would be when SWS is followed by r1 (REM1) which then predominantly transitions to waking; however in some cases it also transitions to r0 (REM0) which in turn is most commonly followed by waking.

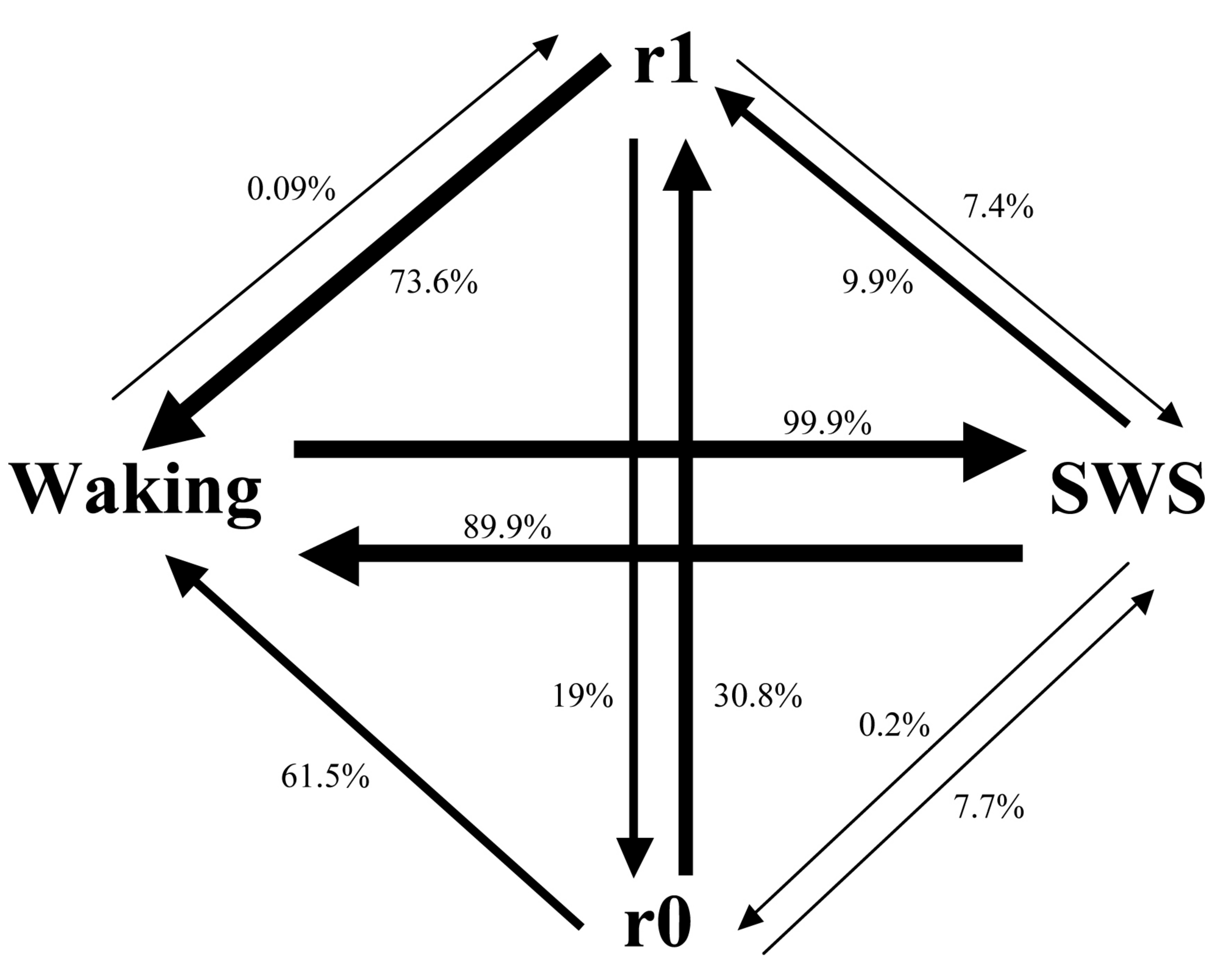
r1
0.09%
73.6%
7.4%
9.9%
99.9%
Waking
SWS
89.9%
19%
30.8%
0.2%
61.5%
7.7%
r0

**Figure 4.8:** Histograms depicting the total amount of time spent in each of the defined physiological states as well as the average number of episodes and episode duration for 24 hours **(A, first set of graphs)**, the light period **(B, second set of graphs)** and the dark period **(C, third set of graphs)** for both the 5 s (left column) and 1 min epoch (right column) scoring methods. The percentage of time occupied by each state over 24 hours and the dark period remains the same for both methods of scoring; however, a significant difference was noted in the percentage of time occupied by REM1. The number of waking and SWS episodes are significantly less in the 1 min compared to the 5 s scoring method. The average episode duration for all states was also significantly different; however, there was no significant difference in the average duration of REM0 episodes. Light shaded bars represents each of the animals studied (from left to right - H107, H03, H04, H05, H07) and the dark bars represents the species mean. The graphs also show the standard error of the mean (represented on the species mean) for the total amount of time spent in each of the defined physiological states as well as the average number of episodes and episode duration for 24 hours **(A, first set of graphs)**, the light period **(B, second set of graphs)** and the dark period for each of the physiologically defined states for both the 5 s and 1 min epoch scoring method. An unpaired two-tailed t-test was used in all statistical analyses where the data was normally distributed whereas a Mann Whitney test was used in cases where the data was not normally distributed and significance was obtained in all instances where $p<0.05$.

**A**

## 5 s epoch scoring

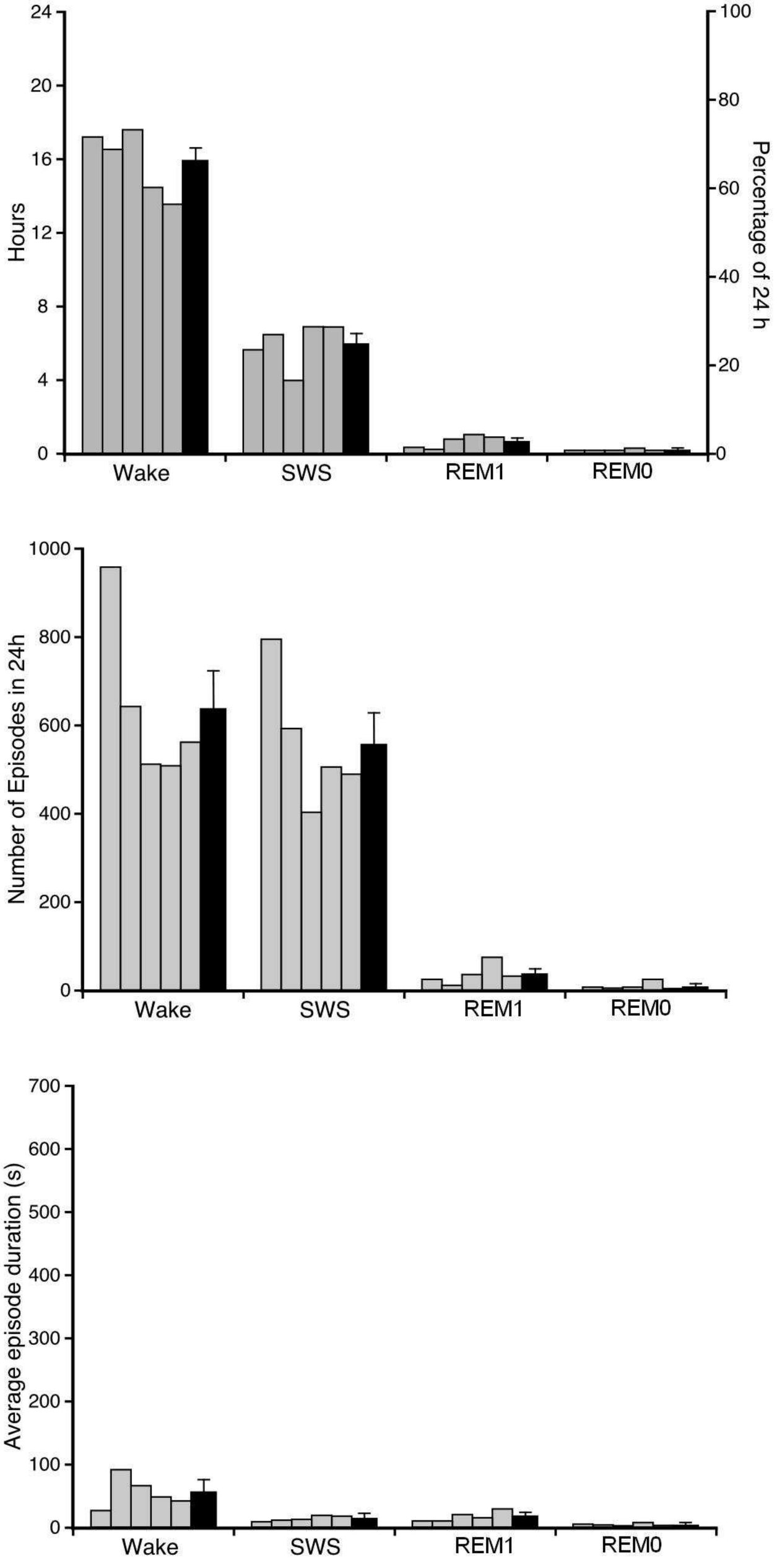


## 1 min epoch scoring

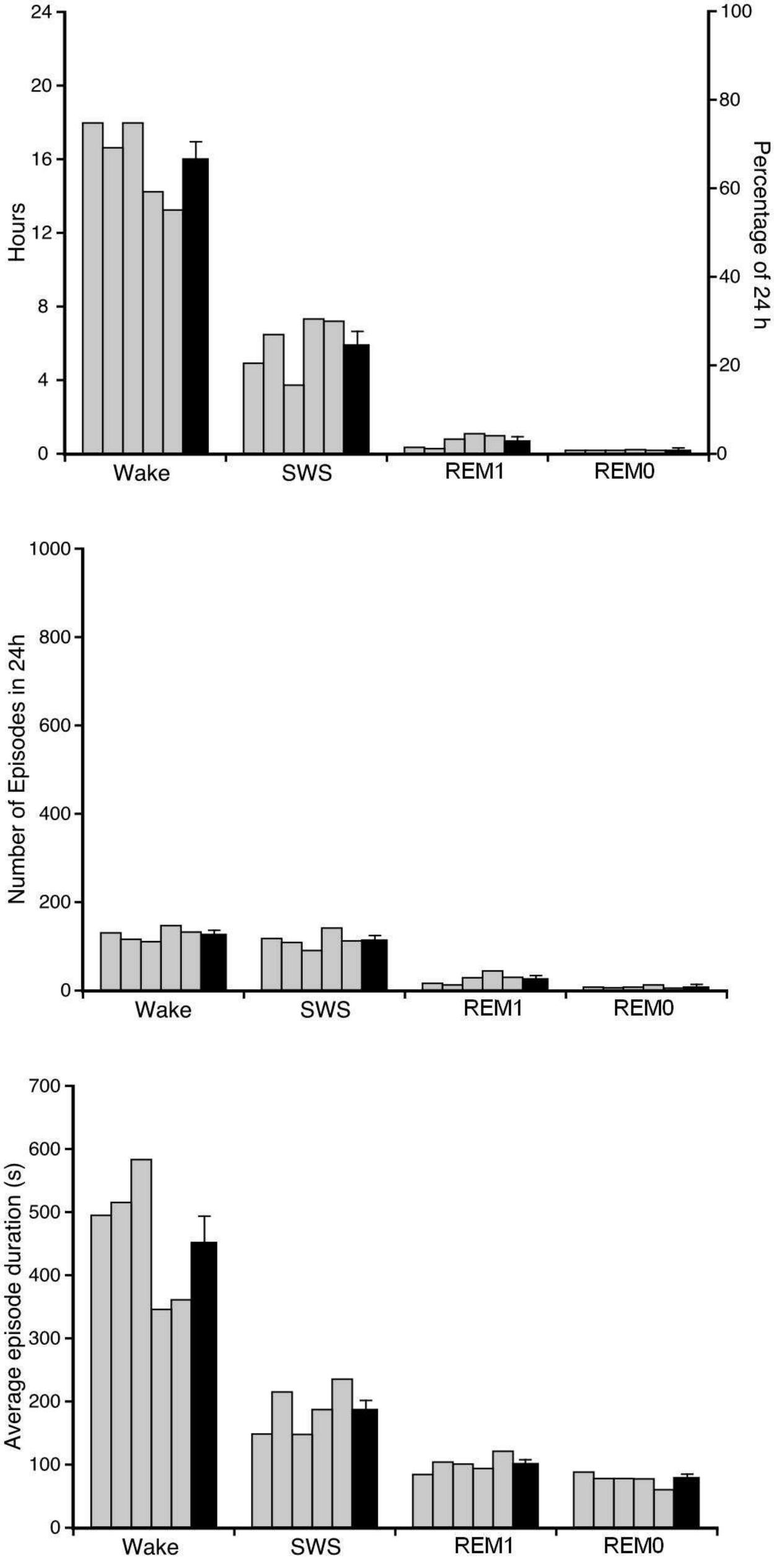

**B**

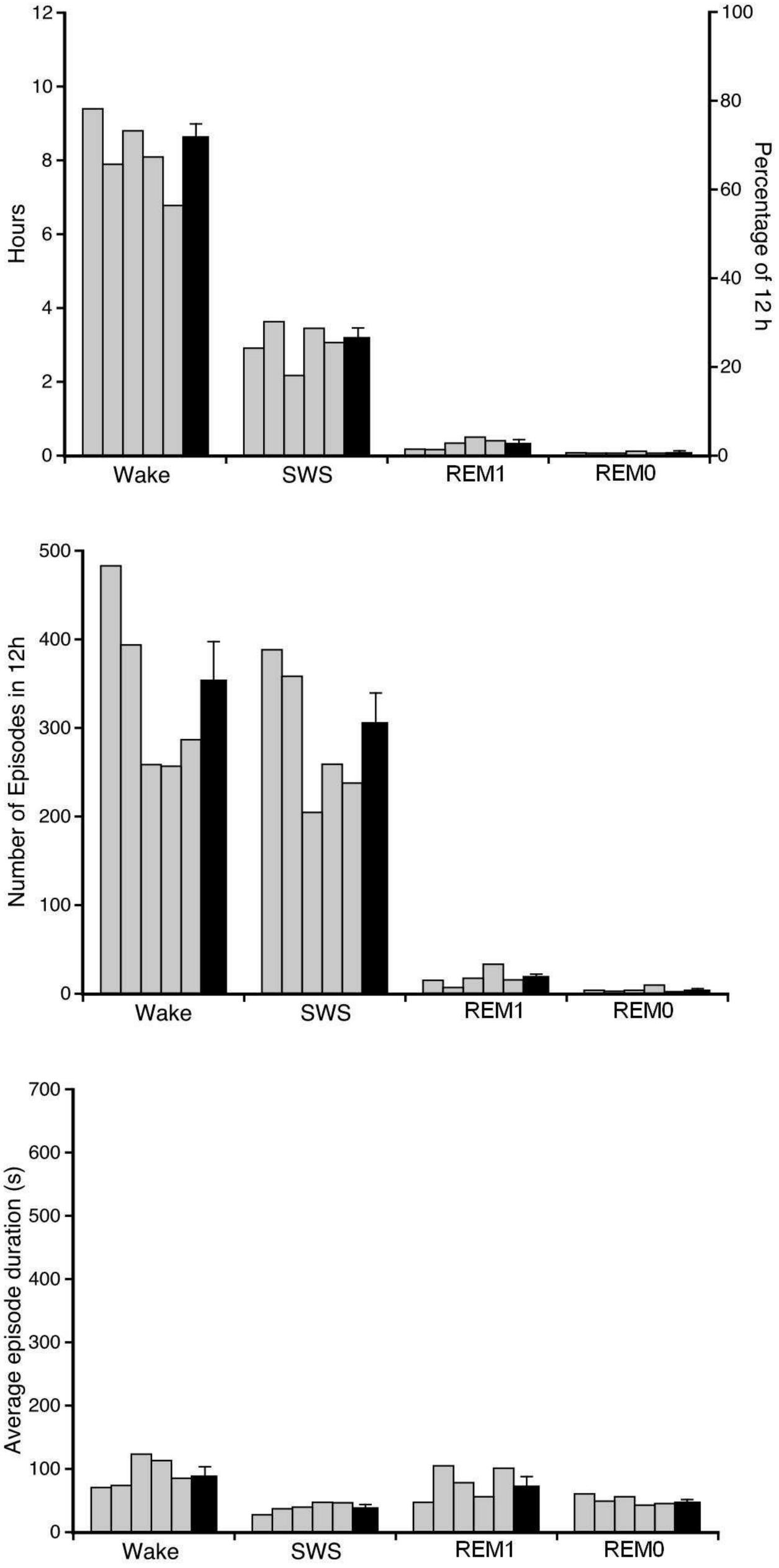
5 s epoch scoring
Hours
Percentage of 12 h
Wake
SWS
REM1
REM0
Number of Episodes in 12h
Average episode duration (s)

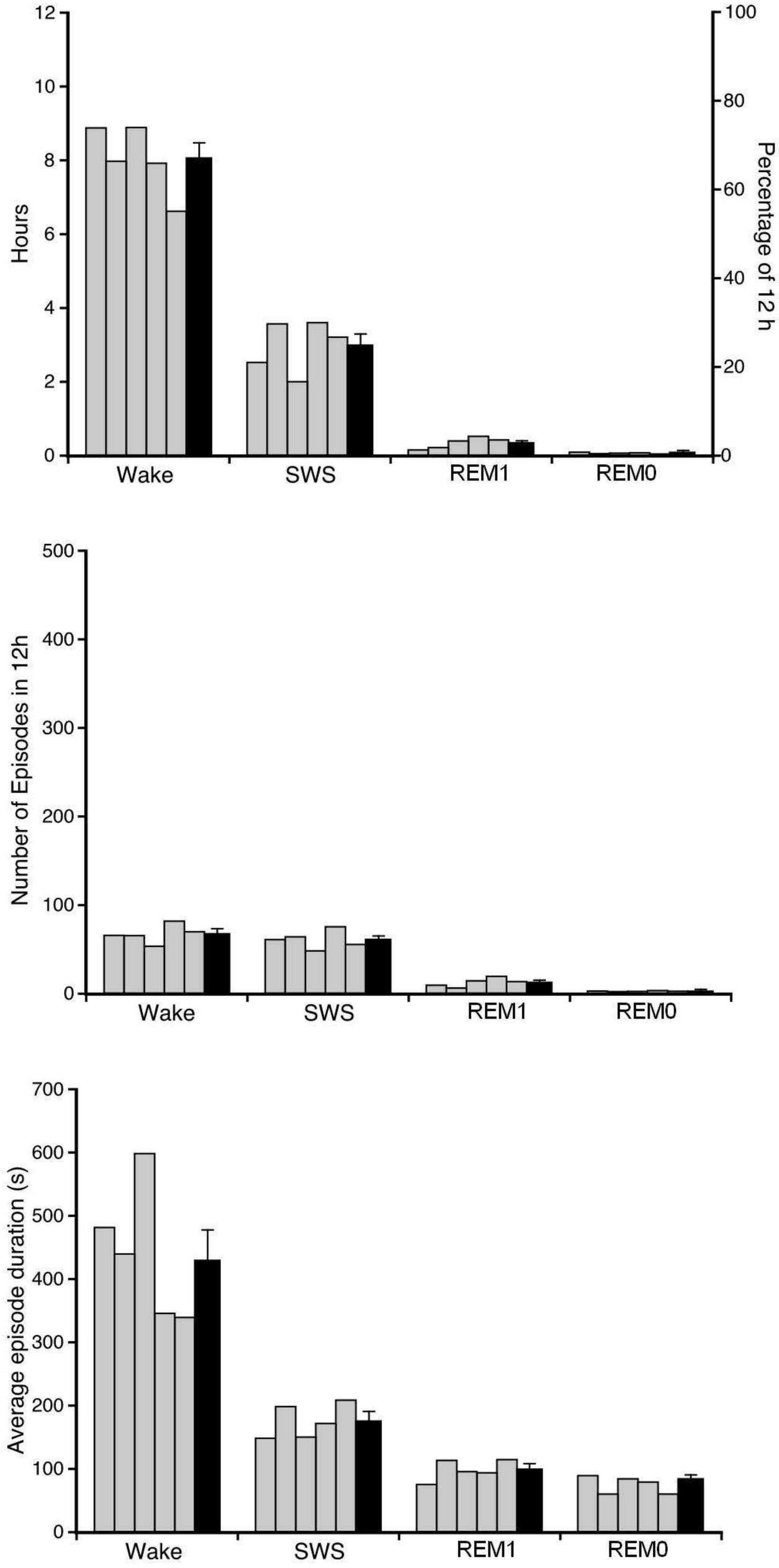
1 min epoch scoring
Hours
Percentage of 12 h
Wake
SWS
REM1
REM0
Number of Episodes in 12h
Average episode duration (s)

C

5 s epoch scoring

1 min epoch scoring

Hours

Percentage of 12 h

Wake

SWS

REM1

REM0

Number of Episodes in 12h

Average episode duration (s)

**Figure 4.9:** Histograms depicting REM periodicity for 5 s and 1 min epoch scoring methods based on a 72 h recording period as well as the REM periodicity based on the 1 min epoch data when waking episodes that lasted longer than 10 min were eliminated from the data. The modal sleep cycle for the 5 s epoch scoring method was 5 min whereas it was 10 min for the 1 min epoch scoring method. When waking episodes that lasted longer than 10 min were eliminated from the 1 min epoch data, the modal sleep cycle length was 15 min.

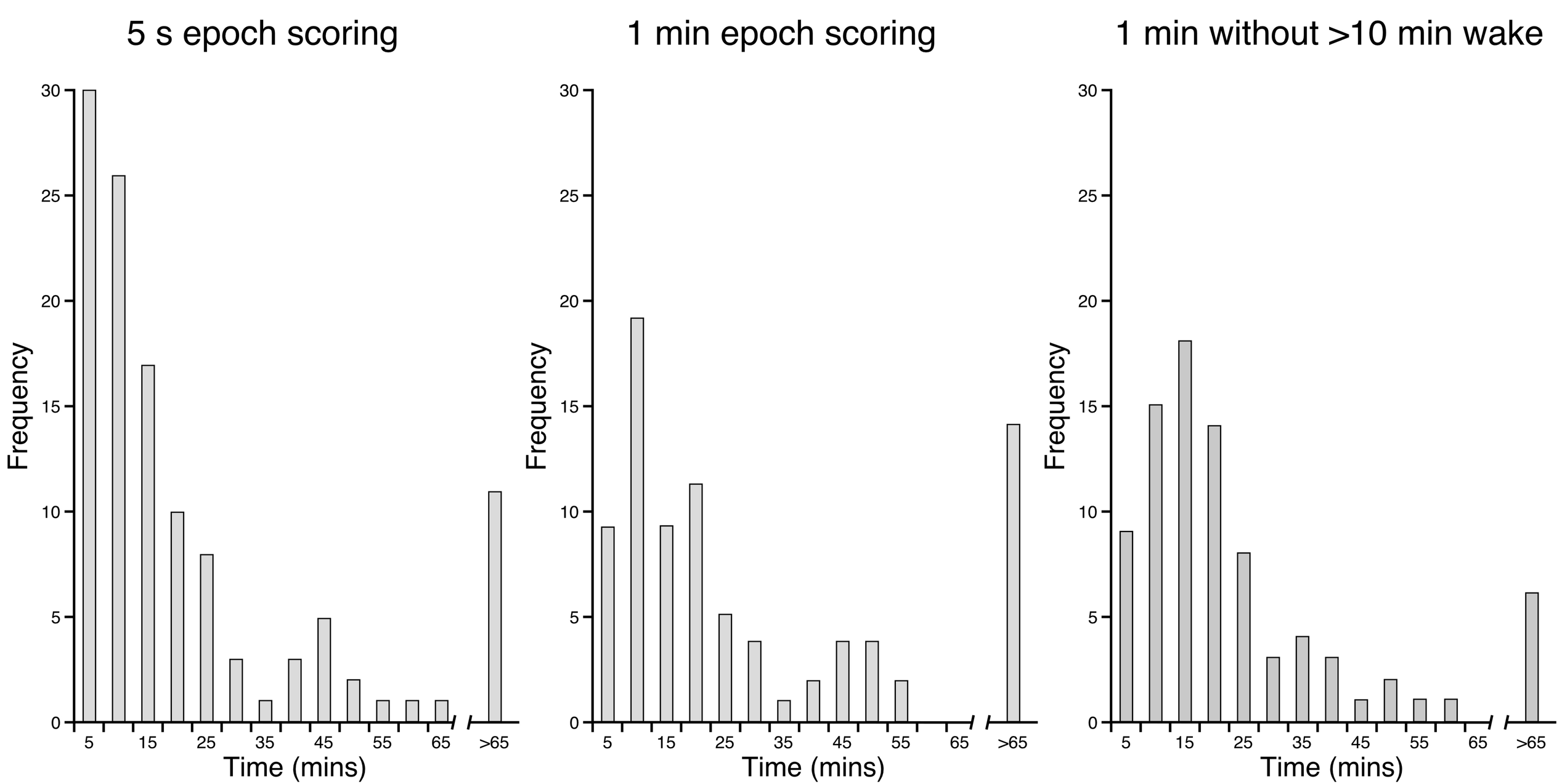
5 s epoch scoring
1 min epoch scoring
1 min without >10 min wake
Frequency
Time (mins)
0
5
10
15
20
25
30
5
15
25
35
45
55
65
>65

**Figure 4.10:** Slow wave activity (based on 2-h intervals) in three animals for the 72 h recording period during all states **(A)** and SWS **(B).** SWA remained constant during all three recording days and did not differ significantly between animals (Unpaired two-tailed t-test, $p>0.05$). **(C)** Histogram illustrating the average spectral power for the 72 h recording period for all states and SWS during the light and dark period. No significant difference (Unpaired two-tailed t-test, $p>0.05$) is evident between the light and dark periods for all states and SWS. **(D)** Line graph showing the average SWA during wake and sleep stages. SWA was the greatest during SWS and was consistently greater throughout the recording period.

A

SWA during all states (72 h)

SWA ($V^2$) x $10^{-4}$

2.0
1.8
1.6
1.4
1.2
1.0
0.8
0.6
0.4
0.2
0.0

18:00 6:00 18:00 6:00 18:00 6:00

Time (h)

B

SWA during SWS (72 h)

SWA ($V^2$) x $10^{-4}$

2.0
1.8
1.6
1.4
1.2
1.0
0.8
0.6
0.4
0.2
0.0

18:00 6:00 18:00 6:00 18:00 6:00

Time (h)

C

Total spectral power (mV)

12
10
8
6
4
2
0

SWA SWS
SWA SWS
SWA all states
SWA all states

Light period
Dark period

D

Total spectral power (mV)

10
8
6
4
2
0

SWS
Wake
REM1
REM0

Day 1
Day 2
Day 3

**Figure 4.11:** Histogram illustrating the percentage of time occupied by each behavioral state for the 72 h recording period during the light and dark period respectively. There is no significant difference in the distribution of immobile and quiet waking between the light and dark period; however, there is a tendency towards more active waking and eating/drinking behaviour during the dark period (Parametric data - Unpaired t-test, significant $p<0.05$; Nonparametric data – Mann Whitney test, significant $p<0.05$). Light shaded bars represents each of the animals studied (from left to right - H107, H03, H04, H05, H07) and the dark bars represents the species mean for each of the behavioral states.

Light period

Hours

Percentage of 12 h

0
2
4
6
8
10
12

0
20
40
60
80
100

Immobile
Quiet wake
Active wake
Eating/Drinking

Dark period

Hours

Percentage of 12 h

0
2
4
6
8
10
12

0
20
40
60
80
100

Immobile
Quiet wake
Active wake
Eating/Drinking

**Table 4.1:** Total wake, sleep and REM times as a percentage of 24 hours for each individual animal as well as the species mean. TWT – total waking time, TST – total sleep time, TSWS – total SWS time, TREM – total REM time, Tr1 – total REM1 time, Tr0 – total REM0 time.

| Animal ID | Body Weight (Kg) | Brain Weight (g) | Sex | TWT | TST | TSWS | TREM | Tr1 | Tr0 |
|---|---|---|---|---|---|---|---|---|---|
| H107 | 3.1 | 19.6 | Female | 71.6 | 25.6 | 23.5 | 2.1 | 1.6 | 0.5 |
| H03 | 3.14 | 27.1 | Male | 69 | 28.9 | 27.4 | 1.5 | 1.4 | 0.1 |
| H05 | 4.3 | 20.4 | Male | 73.4 | 20.4 | 16.7 | 3.7 | 3.4 | 0.3 |
| H06 | 1.74 | 19.5 | Male | 60.4 | 35 | 29 | 6 | 4.7 | 1.3 |
| H07 | 2.05 | 17.9 | Male | 56.4 | 32.8 | 28.7 | 4.1 | 4.1 | 0.04 |
| **Species Averages** | **2.87** | **20.9** | | **66.2** | **28.5** | **25.1** | **3.5** | **3** | **0.4** |

**Table 4.2:** Illustration of where statistically significant differences ($p<0.05$) were noted between the three recording days for each state with regards to the number of epochs, episodes and episode duration for each individual animal as well as for the group. Each of the animals subjected to experimentation was tested individually to determine whether statistically significant differences existed between each of the recording days with regard to the number of epochs and episodes as well as the episode duration for each of the physiologically defined states. Following this, the data obtained from all the animals were pooled together to determine whether any statistically significant differences existed between each of the recording days for the group. All data was tested for normality prior to any statistical analyses (Kolmogorov and Smirnov test, $p>0.05$). A one-way ANOVA was used for comparisons between parametric data (statistical significance where $p<0.05$) and a Kruskal-Wallis test was used for comparisons between nonparametric data (statistical significance where $p<0.05$). Italisized values indicate statistically significant difference between the recordings.

| Animal ID | Duration | | | | Episodes | | | | Epochs | | | |
|---|---|---|---|---|---|---|---|---|---|---|---|---|
| | **Waking** | **SWS** | **r1** | **r0** | **Waking** | **SWS** | **r1** | **r0** | **Waking** | **SWS** | **r1** | **r0** |
| H107 | 0.8736 | *0.0197* | 0.221 | 0.7002 | 0.5239 | 0.0692 | 0.1894 | 0.8531 | *0.01192* | *0.0048* | 0.074 | 0.8088 |
| H03 | *0.0257* | *1.37E-09* | 0.3069 | 0.6581 | *0.0412* | *3.04E-05* | *0.0109* | 0.3105 | *4.94E-15* | *2.87E-16* | 0.3069 | 0.5211 |
| H05 | 0.6861 | 0.5999 | 0.5173 | 0.1828 | 0.974 | 0.9506 | 0.6132 | 0.8317 | 0.2673 | 0.7823 | 0.5375 | 0.9144 |
| H06 | 0.6068 | 0.8088 | 0.4852 | 0.264 | 0.1315 | 0.1861 | 0.2254 | 0.795 | 0.484 | 0.245 | 0.1374 | 0.4525 |
| H07 | 0.2338 | 0.7018 | 0.403 | 0.304 | *0.0332* | 0.3182 | 0.8984 | 0.364 | 0.3012 | 0.7307 | 0.793 | 0.352 |
| **All** | *0.0192* | *0.0117* | 0.5138 | 0.8684 | 0.4016 | *0.0128* | 0.1914 | 0.6802 | *0.0006* | *2.42E-05* | 0.129 | 0.651 |

### 4.4. Discussion

The aim of the present study was to describe sleep in the rock hyrax, *Procavia capensis*. On average these animals spent 16 h/day in a state of waking, 6 h/day in SWS, and 50 min/day in REM (of which REM1 contributed 43 min/day and REM0 6 min/day). The polygraphic aspects of waking and SWS in the rock hyrax were characteristic of what has been described for these physiological states in many mammals (Desiraju et al., 1966; Elgar et al., 1988; Tobler, 1995; Siegel, 2005; Steriade, 2005; Horne, 2009). In this study of the rock hyrax, REM was subdivided into REM1 and REM0, as the majority of the REM episodes did not fit the conventional criteria. REM1 was characterized by an EEG similar to waking, an EMG that was the same as during SWS, and a mostly regular ECG. REM0 was characterized by an EEG similar to waking, EMG lower in amplitude than during SWS and an irregular ECG (Figs. 4.1-4). Of these two, REM0 most closely resembled what would be considered classical REM sleep (Desiraju et al., 1966; Steriade, 2005; Nicolau et al.; 2000). At present, with the data we currently have, it is difficult to determine whether REM1, which was found exhibiting all the same physiological parameters in all hyraxes studied, is a type of NREM or a type of REM. It is possible that REM1, as defined in this study, could be considered a form of low voltage slow wave sleep, a type of NREM. According to Bergmann et al. (1987) low voltage slow wave sleep (LS) is characterized by behavioural quiescence, desynchronized EEG, EMG that is at the same amplitude as during SWS and theta activity that resembles waking and is lower than during REM. In the rock hyrax REM1 exhibited some of these characteristics such as behavioural quiescence, desynchronized EEG and EMG similar to SWS. In addition to this, the ECG was not as irregular as seen during unambiguous REM

sleep in the hyrax. Thus, the data can be interpreted in such a way as to consider REM1 a type of low voltage NREM similar in structure to LS as defined by Bergmann et al. (1987) for the rat.

Despite this, it is possible that REM1 is a type of REM. The desynchronized EEG, ECG less regular in comparison to SWS, behavioural quiescence, greater amount of theta activity, and that REM1 always followed a SWS episode, all indicate that REM1 could be considered a type of REM. Clearly, this is not what would be described as typical mammalian REM sleep, but REM sleep in certain mammalian species, such as the platypus which has REM with cortical synchronization (Siegel et al., 1999), EMG in the rat and rabbit that are not always atonic in REM (e.g. Pivik et al., 1981; Gottesmann, 1992), and Tupaia in which REM has a higher amplitude EMG than in SWS (Berger and Walker, 1972), does not always fit the standard criteria determined in studies of typical laboratory animals and humans. Thus, with the currently available data REM1 might also be interpreted as a form of REM sleep.

While we do not currently have the data to resolve this issue, future studies of the rock hyrax, measuring such variables as the hippocampal theta activity, electro-oculogram, as well as single unit recordings from the sleep related brainstem nuclei could resolve whether REM1 in the rock hyrax is a form of NREM or REM. Whatever the result of such future studies, the implications of REM1 being a type of NREM or REM are of interest. If REM1 is a type of NREM, then, like many other mammals, the rock hyrax would have more than one form of NREM; however, this would mean that the rock hyrax exhibits the lowest amount of REM sleep of any terrestrial mammal studied to date, approximately 6 min/day. This is of course, an interesting possibility and may make

the hyrax an interesting animal model for the study of the function of REM sleep due to its possible paucity in this species. With the alternative view, if REM1 is a type of REM state, then the hyrax exhibits more than one type of REM, which would be unusual, and NREM of the hyrax would consist purely of SWS. This again makes the hyrax an interesting model animal for study of REM function, as if REM1 is a type of REM, then perhaps the potential benefits of REM sleep for organismal function can be derived without the expression of the full range of typical REM sleep polygraphic features. This is clearly an area that needs further investigation.

The most common sleep state transition pathway was found between waking and SWS (waking → SWS → waking), the next most common was found to be waking which leads to SWS which then transitions to REM1 followed by waking (waking → SWS → REM1 → waking) (Figs. 4.2, 4.7). When the 5 s and 1 min epoch scoring techniques were compared, no statistically significant difference was noted with regard to TST and waking times for the 24 h as well as the light and dark periods. A statistically significant difference was noted with regard to the number of episodes and episode duration for each of the states during the 24 h, light and dark periods (Fig. 4.8A-C). Thus, when drawing conclusions regarding total times over the 24h period for the different states, either the 5 s or 1 min epoch data will provide the same answers, but when determining the number of episodes and episode duration it appears to make more biological sense to use the 1 min epoch scoring method.

*4.4.1. Comparison to previous sleep studies in Hyraxes*

A previous abstract by Snyder (1974) reported sleep in three other species of hyrax, *Procavia johnstoni*, *Heterohyrax brucei and Dendrohyrax validus.* Snyder reported that TST for: *P. johnstoni* was 4.9 h (SWS contributing 4.66 h and REM 0.24 h), *H. brucei* was 5.7 h (5.24 h consisting of SWS and 0.45 h REM), and *D. vaidus* was 4.9 h (SWS contributing 4.66 h and REM 0.24 h). There was no statistically significant difference with regard to TST between light and dark periods for *P. johnstoni* and *H. brucei,* but a light/dark difference in TST was noted for *D. validus*, which was the only solitary nocturnal species studied (Kingdon, 1971; Campbell and Tobler, 1984; Elgar et al., 1988); however, as stated previously only an abstract was published for the TST reported for these species of hyrax and no spectral power analysis was performed on the data to corroborate these findings. Our results showed a 1.9 h and 1.1 h increase in TST when compared to *P. johnstoni* and *H. brucei* respectively. Total REM time, that is if we can consider REM1 to be a form of REM, in our study was also considerably greater compared to the reported values stated previously in these two species (*P. capensis* – 50 min/day, *P. johnstoni* – 14.4 min/day, *H. brucei* – 27 min/day). No statistically significant difference was noted between the light and dark periods with regard to TST in the current study as well as in the Snyder study (*P. johnstoni* and *H. brucei* only), underlining the polycyclic nature of sleep in this mammalian group.

*4.4.2. Comparison to sleep in other Afrotheria, Xenarthra and other mammals*

Hyraxes belong to the superorder Afrotheria, which includes the African and Asian elephant, the manatee and dugong, aardvark, golden moles, tenrecs, and sengis.

Observational studies have reported that TST in the Asian and African elephant amounts of approximately 3.8 h (Campbell and Tobler, 1984; Kurt, 1960), with sleep mainly occurring during the dark periods in the early morning hours (Wyatt and Eltringham, 1974). Moss (1982) reported that wild African elephant sleep a total of 3 – 5 h at night, whereas captive Asian elephants slept for approximately 4 – 6.5 h (Tobler 1992; Wilson et al., 2006). An electrophysiological study on an Amazonian manatee, *Trichechus inungius*, revealed that this animal spent approximately 27% (6.5 h) in SWS and 1% (14 min) in REM sleep over a 24 h period and that 25% of SWS was occupied by interhemispheric asymmetry (Mukhametov et al., 1992); however, it must be noted that the TST reported was based on study of a single animal and the recording of sleep was done directly after surgery, thus the TST obtained may not be representative of this species. As for the insectivoran-like afrotheres, TST in the tenrecs has been reported to be 15.6 h, with SWS contributing 13.26 h and REM 2.34 h (Campbell and Tobler, 1984; Elgar et al., 1988; Snyder, 1972).

It appears, as is clear from the aforementioned examples that sleep in the Afrotherians is just as diverse and unusual as the composition of this group, and this sleep diversity could possibly be attributed to the different lifestyles and behaviors of each of its members (Siegel, 2009). For example, some members are diurnal (e.g. elephant, manatee, rock hyrax, sengis) where others are nocturnal (e.g. tenrecs, golden moles, aardvark). Some member's offspring are precocial (e.g. rock hyrax) whereas others are altricial (e.g. stenrecs). The degree of sociality also differs greatly between the different members of this superorder, with elephants and rock hyraxes being social mammals, the manatee semi-social, some tenrecs being social, whereas the sengis live in monogamous

pairs. TST has been correlated to body size, but is only one of many factors that have been reported to be correlated to TST in mammals, and it has been reported that a negative relationship exists between these two variables (Tobler, 1995; Zepelin et al., 2005). Thus, at first glance the Afrotheres seem to adhere to this relationship, with the elephants, which has the largest body mass in this superorder, having the lowest TST, whereas the tenrecs and sengis, which have smallest body mass in this superorder, appears to have the highest TST. One would expect, purely based on body mass that the average TST for hyraxes would lie somewhat in the middle, i.e. between the TST for the manatees and the insectivore-like Afrotherians; however, we found that the TST in the rock hyrax closely resembles what has been reported in the manatee (TST in the rock hyrax – 28.5% and manatee – 28%) (Mukhametov et al., 1992). Despite this, the manatee does show a greater percentage of TSWS (27%, rock hyrax – 25.1%), whereas the rock hyrax shows a greater percentage of TREM (3.5%, manatee – 1%). This is not in accordance with the claimed inverse relation between body mass and sleep time, as the manatee has a body mass approximately 100 fold that of the rock hyrax, it leads a semi-social lifestyle whereas the rock hyrax is known to be social, their offspring are born altricially whereas the hyrax offspring are born precocially, and most probably the greatest difference between these mammals is that the manatee is an aquatic mammal whereas the rock hyrax is a terrestrial mammal. Although these two mammals share a common ancestor, they are vastly different in many respects, but spend roughly the same amount of time asleep each day. In addition, the manatee has unusual asymmetrical SWS patterns. These differences would indicate other factors, apart from body mass and state at birth (i.e. precocial *vs.* altricial) as being responsible for generating the differing sleep

times and patterns seen in these mammals. The above list of similarities and differences would appear to suggest a combination of phylogenetic constraint and adaptation to environmental factors would need to be evoked to fully explain the observed results.

Sleep has also been studied both behaviorally and electrophysiologically in the Afrotherian sister group Xenarthra which consists of armadillos, sloths and anteaters (Hallström et al., 2007). TST in the giant armadillo, *Priodontes giganteus*, has been reported to be 18.1 h (Affanni, 1972) and in the nine banded armadillo, *Dasypus novemcinctus*, 17.4 h (Van Twyver and Allison, 1974). For both species no difference was observed with regard to the distribution of TST between the light and dark periods (Campbell and Tobler, 1984). Behavioral studies conducted on the two toed sloth, *Choloepus hoffmanni*, showed that TST in these animals amounted to 16.4 h (Sunquist and Montgomery, 1973). The brown throated three toed sloth, *Bradypypus variegatus*, was found to have TST of 15. 84 h when it was recorded in captivity (Campbell and Tobler, 1984; Galvão de Moura Filho, 1983) and a TST of 9.63 h when recorded in the wild (Rattenborg et al., 2008). The rock hyrax and three toed sloth are both herbivores, whereas the giant armadillo and tenrec are insectivorous or carnivorous. When body mass is compared to the number of hours of sleep a day, the tenrec and giant armadillo sleep for a larger part of the day compared to the rock hyrax and three toed sloth. An analysis of all reported sleep times found TST in carnivores are significantly greater than that of herbivores (Siegel, 2005).

Physiological parameters such as body and brain mass, metabolic rate and state of birth have been correlated to TST in mammals; however, no consensus can be reached regarding these correlations as different studies all have opposing views. For example,

when just comparing body mass, mammals with the same dietary preference that fall within the same body mass range have different TST, the rock hyrax with an average body mass of 4 kg has a TST of approximately 7 h each day, whereas the tree toed sloth which has an average body mass of 3.5 – 4.5 kg sleeps for approximately 10 h a day in the wild and 16 h in captivity (Siegel, 2005; Rattenborg et al., 2008). It has also been shown that risk of predation as well as relative exposure of the sleeping site correlates negatively with TST (Capellini et al., 2008). Rock hyraxes have been reported to have a danger factor of 0.5 (Allison and Cicchetti, 1976) and are species that are typically heavily predated, but they sleep in relative unexposed sites. State of birth is another physiological factor that has been shown to correlate with TST. Rock hyrax offspring are born precocially, thus these animals should have a reduction in TREM time, but when compared to the manatee, a mammal whose offspring are born altricially and that has a larger body mass and lower metabolic rate, TREM is greater. Considering the evidence it is thus possible that ethological rather than physiological factors are responsible for the variations seen in TST between different mammalian species.

The current data also poses some interesting questions. The results showed that these animals were awake on average for 16 h/day, and the behavioural data suggested that active waking and eating was more predominant during the dark periods as opposed to the light periods. Thus they are not strongly diurnal or nocturnal, but can best be characterized as polycyclic without a strong circadian difference in activity or sleep patterns. In the wild rock hyraxes are rarely seen out of their dens during the night, so could the bursts of nocturnal activity that have been observed in our study be replicated when these animals are in “hiding” during the night in the wild, and what would the

relevance of this activity be when these animals sleep socially? It is furthermore also possible that the activity patterns observed in these animals in the current study could be attributed to the standardized laboratory conditions (i.e. constant ambient temperature, 12 h light/dark cycle as well as light intensity). In the wild these animals are social, they do not always experience 12 h of light followed by 12 h of dark, they are not always exposed to same light intensity, and the ambient temperature can vary greatly between day and night. It has also been shown that rock hyraxes have poor thermoregulative abilities and are often seen basking in the sun and typically sleep huddled up in groups, a possible mechanism for conserving body heat. It is therefore possible that the biology of the species can account for differences observed with regard to the phasing of sleep and activity budgets seen in the current study and that the standardized conditions might just represent a unusual condition that the will only be experienced a limited amount of time in the wild. Further studies on rock hyraxes in the wild would be required to determine to what extent these standardized laboratory conditions alter the natural phasing of sleep and activity budgets in these animals.

# Chapter 5

## Social contrasted with solitary sleep patterns in the rock hyrax, *Procavia capensis*.

### 5.1. Introduction

Sleep is a homeostatically regulated process and it is characterized by its easy reversibility, immobility and reduced responsiveness to sensory stimuli. Species specific sleep postures and sleep sites, as well as occlusion of the eyes, are typically regarded as signs of behavioral sleep. Mammalian sleep is divided into non rapid eye movement sleep (NREM) which is often but not always synonymous to slow wave sleep (SWS) and rapid eye movement sleep (REM) (Nicolau et al., 2000; Zepelin et al., 2005; Cirelli and Tononi, 2008; Lesku et al., 2008; Siegel, 2008). Many studies performed in mammals in laboratories to date have been conducted on animals housed in solitary, or asocial, conditions even though that particular animal may be social in the natural state (McNamara et al., 2008). It has been suggested that social animals sleep less, exhibit more fragmented sleep patterns and have lower NREM and REM quotas (Capellini et al., 2008). A possible reason for this is that species that sleep socially can apparently enter deeper stages of sleep as they have the security of sleeping in a group and are thus able to sleep more efficiently and acquire the benefits of sleep in a shorter time frame. It has also been hypothesized that social species have to invest more time in social interactions and relationships which in effect leave them with less time to sleep (Capellini et al., 2008). In primates, it has been proposed that hierarchy may play a role in the manifestation of sleep patterns that are observed in social mammals (Noser et al., 2003). Male Gelada baboons show no correlation between sleep duration and social rank, whereas females

and juveniles exhibit an increase in sleep duration with decreasing rank. Furthermore, dominant males have an increased amount of transitional sleep, which indicates that increasing rank leads to a decreased amount of relaxed sleep, which in effect causes an increased degree of alertness enabling these animals to react swiftly to nocturnal dangers. This study also indicated that no correlation existed between sleep fragmentation and social rank (Noser et al., 2003). It has also been shown that group or network size in primates does not correlate with sleep times (Nunn et al., 2010); however, when Drosophila were placed in a socially enriched environment they exhibited an increase in daytime, but not nighttime sleep (Ganguly-Fitzgerald et al., 2006). Studies by Meerlo et al. (1997, 2001) have also shown that in rodents social conflict affects NREM sleep by increasing electroencephalographic (EEG) slow wave activity (SWA) during the subsequent sleeping bout. Sleep duration was not affected by the social stimulus, but the rodents appeared to compensate for the socially induced sleep debt by increasing SWA during NREM. It was also noted that this increase in SWA was not only the result of the length of the preceding waking episode, but also the social nature of the preceding waking episode.

Despite these previous studies, to the authors' knowledge, no comparative physiologically monitored sleep studies have been undertaken on the same animal under freely interacting social and solitary, or asocial, conditions. Thus, in the present study sleep was telemetrically recorded in the rock hyrax, *P. capensis*, under both solitary, or asocial, and freely interacting social conditions. The aim of the present study was to determine whether a significant difference existed in wake and sleep states between the social and solitary conditions to test hypotheses regarding the effect of sleeping socially.

## 5.2. Materials and Methods

A total of five adult rock hyraxes, *P. capensis*, (4 male and 1 female) with body weights ranging between 1.74 – 4.3 kg (Table 5.1), were used in the present study. Permits from the Limpopo and Gauteng Provincial Governments were obtained for the capture and transport of the animals from the wild. All animals were treated and used according to the guidelines of the University of the Witwatersrand Animal Ethics Committee (approval number AESC 2005/8/5), which parallel those of the NIH for the care and use of animals in scientific experimentation. The animals were captured at random from wild populations and thereafter allowed to acclimatize for a period of one month in a social setting to the recording enclosures that had a 12-12 lighting schedule with temperature maintained between 19-21ºC. Each animal was implanted with a telemetric recording devise (Data Sciences International) that allowed for the recording of physiologically measurable parameters of sleep without cables or restraint. The chamber in which the recording occurred was 1.8 m x 1.5 m with a painted concrete surface that was covered with straw. The height of the chamber was approximately 1.5 m and steel mesh was placed over the chamber to prevent the animals from escaping. A wooden box (90 x 90 x 30 cm) with a Perspex roof and two entrances was placed inside the chamber and food (combinations of cucumber, tomato, sweet potato, pumpkin, apples and rabbit pellets as a source of roughage) and fresh water was supplied daily. Behaviour was also recorded with a low light CCD digital camera connected to a DVD recorder.

*5.2.1. Surgical procedure*

After acclimatization, surgical implantation of the telemetric recoding device was performed. The animals were weighed before surgery and anesthetized with weight appropriate doses of a 2:1 mixture of ketamine and xylazine (Anaket-V and Chanazine 2% Injection, Bayer HealthCare). The head and neck, left thoracic (two 2cm x 1cm) and abdominal (10cm x 10cm) regions were shaved and cleaned with CHX Chlorhexidine Disinfectant (0.5% chlorhexidine diglucunate in 75% alcohol, Kyron Laboratories (PTY) LTD) before surgery commenced. These areas correspond, respectively, to the regions were the EEG (electroencephalogram), EMG (electromyogram) and ECG (electrocardiogram) electrodes and telemeter would be implanted. The animal was placed on a heated blanket in order to maintain a constant body temperature throughout the surgery and the head was securely placed in a stereotaxic apparatus to prevent movement and allow for the accurate placement of the EEG and EMG electrodes. During the surgical procedure the animal was kept under a constant state of anaesthesia by means of isoflurane ventilation (1-2% in an oxygen/70% nitrous oxide mixture, Isofor Inhalation Anaesthetic – Safe Line Pharmaceuticals (Pty) Ltd). The animal's heart rate, body temperature and percentage oxygen saturation was monitored.

Under aseptic conditions, a mid-sagittal incision was made over the skull and the skin and temporal muscle were reflected to expose the part of the skull overlying the motor cortex. Using a dental drill, three 2 mm diameter holes were made in the cranial vault to expose the underlying dura mater. The first hole was drilled anterior to the olfactory bulbs for the placement of the indifferent electrode, while two holes were drilled approximately 5 mm apart just lateral to the sagittal sinus over the left motor

cortex for the placement of the recording electrodes (gauge of electrode 0.457 mm, silastic outside diameter 0.9 mm and inside diameter 0.508 mm, PhysioTel ® Multiplus Transmitter, Data Sciences International). The electrodes were placed in such a manner that the tips rested firmly on the surface of the cortex but did not pierce the dura mater and were secured in place with dental cement. Two EMG electrodes (gauge of electrode 0.457 mm, silastic outside diameter 0.9 mm and inside diameter 0.508 mm, PhysioTel ® Multiplus Transmitter, Data Sciences International) (1.5 cm apart) were sutured into the nuchal musculature, while two ECG electrodes (3 cm apart) were sutured into the subdermal tissue overlying the rib cage in the left thoracic region. A subcutaneous pocket was created (10 cm x 10 cm) over the left abdominal region, which allowed for the implantation of the telemeter. All skin incisions were sutured following electrode and telemeter implantation. After surgery was complete the animal was given an intramuscular analgesic (0.1 ml Tamgestic, Schering-Plough, mixed with 0.9 ml sterile water, 1 ml mixture/kg) and returned to the recording enclosure. Recovery was monitored every half hour until it could be established that the animal was fully lucid and able to move freely and eat/drink normally.

*5.2.2. Sleep recording*

After the surgical procedure the animals were allowed a recovery period of one week before the recording of sleep commenced. The animals were housed in the same recording enclosure for recovery as well as recording and during the recovery period the implanted animal was housed under solitary conditions. A receiver was mounted and secured to one wall of the enclosure while a low light CCD digital camera was mounted

above the enclosure. The telemetric recording system (Data Sciences International, DSI, PhysioTel ® Multiplus Transmitter, model TL10M3-D70-EEE implant) consisted of a DEM multiplex interface to which the receiver was connected. The signal from the implanted transmitter (round, 13cm² with stainless steel electrodes, weight – 37g, volume – 25 ml, 3 channels) detected by the receiver was relayed to the input amplifier of the Data Sciences computer system, after which it was digitally recorded (in DSI format) for analysis. Data digitally saved in the DSI format was converted to text format and these files were in turn converted into the appropriate format needed for recognition and analysis by the Spike 2 computer program (version 4.2, Cambridge Electronic Design). Asocial sleep (physiological measurable parameters and the associated behaviour) was subsequently recorded continuously for a period of 72 hours after which one or two other hyraxes were introduced to enclosure with the implanted hyrax. The hyraxes were allowed to acclimatize to their new social environment for a period of three days that was followed by the recording of sleep in this social condition for a continuous period of 72 hours. The recording enclosure was in a room that was acoustically isolated. The animals were disturbed only once a day for approximately 5 min at the same time during each of the recording days for feeding.

*5.2.3. Data analysis*

Version 4.2.2 of the Spike 2 software (Cambridge Electronic Designs, UC) was used in order to convert the recorded data into the appropriate format, i.e. Spike 2 data format, for offline analysis. The EEG data was subsequently scored in 5 s epochs as either waking characterized by low voltage high frequency EEG and high voltage EMG,

SWS characterized by high voltage low frequency EEG and EMG lower in amplitude than waking, and REM (rapid eye movement). REM in the rock hyrax was found to be ambiguous and did not resemble the classical definition of REM sleep, thus REM0, was characterized by low voltage high frequency EEG, an EMG that was almost atonic, and an irregular ECG; whilst REM1 was characterized by a low voltage high frequency EEG, EMG amplitude characteristic of SWS and a regular ECG. An epoch was only assigned to a particular state if the state occupied at least 50% of the epoch. The data obtained from the 5 s epoch scoring was analyzed to determine the modal state per minute to generate the data for the 1 min epoch scoring. An unpaired two-tailed t-test (parametric data) or Mann-Whitney (nonparametric data) test ($p<0.05$) was employed to determine if a statistically significant differences existed between the 5 s and 1 min epoch scoring methods. Behaviour was scored in 1 min epochs as either immobile – animal was completely immobile for >30 s, quiet waking – animal was immobile and only moving its head or made minor movements in the same place for >30 s, active waking – animal was actively moving around for >30 s, or eating/drinking – animal was eating and/or dinking for >30 s.

All the physiologically and behaviourally scored data was tested for normality prior to any statistical testing. The Kolmogrov and Smirnov test was conducted to determine whether the data was parametric or nonparametric in nature ($p>0.05$). A one-way ANOVA was used in all comparisons where the data was parametric and a statistically significant difference between sample means were obtained in cases where $p<0.05$. Where it was found that the data was nonparametric the Kruskal-Wallis test was employed and a statistically significant difference between sample medians were

obtained in all cases where $p<0.05$. Comparisons between light and dark were made by means of contingency tables, where in the case of parametric data the unpaired two-tailed t-test and in the case of nonparametric data the Mann-Whitney test was employed to determine whether statistically significant differences existed ($p<0.05$). Microsoft Excel and GraphPad InStat computer programs were used in the analysis of the data.

### 5.3. Results

The physiologically measurable parameters of sleep as well as the associated behaviour were recorded in five hyraxes, *P. capensis*, continuously for a period of 72 h under solitary, or asocial, conditions. This was followed by the introduction of one or two other non-implanted hyraxes to the enclosure of the implanted hyrax. The animals were allowed to acclimatize to the new social setting for a period of three days after which the physiological parameters of sleep and the accompanying behaviour was recorded continuously for 72 h. The results revealed that in the social condition 66.8% (16 h/day) of 24 h was spent awake, 24.8% (6h/day) in SWS, 2.7% (39 min/day) in REM1 and 0.6% (9 min/day) in REM0 (the 1.2h unaccounted for can be attributed to periods where signal loss occurred) (Table 5.1). These results did not differ significantly from that during the solitary, or asocial, condition in these animals (Table 5.2); however, the duration of REM0 episodes appeared to be longer under social compared to solitary conditions. Over the 24 h period REM0 was on average 20 s longer during the social condition, similar during the light period and approximately 40 s longer that the solitary condition during the dark period (Fig. 5.3). The modal and average REM periodicity was also greater during social conditions, however when waking episodes that lasted longer than 10 min

were eliminated from the data, the modal REM periodicity for both the social and solitary conditions was found to be similar (15 min) (Fig. 5.4). The average SWA was also greater during the social condition during the first two days of recording, but during the last day of recording the SWA during the social condition was lower than that recorded for the solitary condition (Fig. 5.5). The most common state transition pathway during both conditions was waking → SWS → waking. During the social condition, REM1 and REM0 never transitioned to SWS, however during the solitary condition this did occur. Furthermore waking only transitioned to SWS during the social condition whereas during the solitary condition waking was also seen to transition to REM1. REM1 transitioned more readily to REM0 during the solitary condition, whereas REM0 transitioned more readily to REM1 during the social condition (Fig. 5.2). The second most common state transition pathway during both conditions was waking → SWS → REM1 → waking.

*5.3.1. Physiological Data*

The polygraphic data was scored in 5 s epochs as waking, SWS, or REM (which was subdivided into REM0 and REM1) (see Chapter 4 for a full description of each the physiological states). Waking was characterized by a low voltage, high frequency EEG with a high amplitude EMG (EMG during active waking being higher in amplitude compared to quiet waking). The ECG for this state was more regular during periods of quiet waking and more irregular during periods of active waking. SWS episodes were characterized by a high voltage, low frequency EEG, an EMG of lower amplitude when compared to waking and a regular ECG. Identification of REM episodes were more ambiguous than the identification of waking and SWS episodes (see chapter 4) and were

subsequently subdivided into REM0 and REM1. REM0 episodes were characterized by a low voltage, high frequency EEG (similar to waking EEG), a noticeable drop in the EMG (in some cases it was almost completely atonic) and an irregular ECG; whereas REM1 episodes exhibited low voltage, high frequency EEG, an unaltered EMG that stayed at the same amplitude as the preceding SWS episode, and both regular and irregular ECG rates. The polygraphic characteristics of all states were similar during both the social and asocial condition. Instantaneous heart rate during the social condition was on average 174 bpm (STDEV ± 25.16) and 155 bpm (STDEV ± 6.85) for waking and SWS respectively whereas during REM0 and REM1 it was on average 110 bpm (STDEV ± 14.18) and 156 bpm (STDEV ± 9.18) respectively. During the solitary condition the instantaneous heart rate during waking, SWS, REM0 and REM1 was 154 bpm (STDEV ± 7.79), 158 bpm (STDEV ± 10.99), 163 bpm (STDEV ± 27.34) and 153 bpm (STDEV ± 10.56) respectively. The instantaneous heart rate during SWS and REM1 did not differ significantly between the social and solitary conditions whereas waking and REM0 did show a statistically significant difference. The instantaneous heart rate for waking during the social condition was greater compared to the solitary condition and showed the greatest amount of variation compared to all other states. The instantaneous heart rate in REM0 during the solitary condition was greater than during the social condition and showed the greatest amount of variability compared to all other states.

*5.3.1.1. Total state times*

Form the pooled data of all five hyraxes it was noted that in 24 h under social conditions, 66.8% (16 h/day) of the time was spent awake, 24.8% (6 h/day) in SWS,

2.7% (40 min/day) in REM1 and 0.6% (7min/day) in REM0. Under solitary conditions these animals spent approximately 66.2 % in 24 h (16 h/day) awake, 25.1% (6 h/day) in SWS, 3% in REM1 (43 min/day) and 0.4% in REM0 (6 min/day). No statistically significant differences exist in terms of total state times when comparing social and solitary conditions in the rock hyrax. The one state that approached statistical significance when the social and solitary conditions were compared was REM0 – the total time spent in REM0 was found to be greater during the dark period during the social condition (One-way ANOVA for parametric data, Kruskal-Wallis test for nonparametric data, significant $p<0.05$).

When social and solitary conditions were compared in each individual animal, statistically significant differences were noted between these two conditions for waking and SWS in four of the five animals examined. Half of the animals that exhibited a difference showed a greater amount of time spent awake and less time in SWS when in the social condition whereas the other half of the animals showed the same tendency but during solitary conditions. Two animals also showed a difference in the time spent in REM1, one showed an increase during the social condition whereas the other showed an increase during the solitary condition. Finally, three out of the five animals tested showed a difference in the time spent in REM0, two out of these three animals showed an increase during social conditions whereas only one showed an increase during solitary conditions (One-way ANOVA for parametric data, Kruskal-Wallis test for nonparametric data, significant $p<0.05$)

*5.3.1.2. Number of episodes*

When the data from all five animals was grouped to create a species average, it was found that the number of waking episodes was greater during the solitary condition (129 episodes over 24 h) compared to the social condition (121 episodes over 24 h). The number of SWS (solitary 116, social 111) and REM1 (solitary 27, social 26) episodes were increased, but not statistically significantly, during the solitary condition, whereas the number of REM0 episodes was greater during the social condition (solitary 4, social 5), but again this difference did not reach statistical significance. This tendency was also observed over 24 h as well as during the light period; however during the dark period the number of episodes for all states was increased during the solitary condition. The average number of waking episodes during the 12 h dark period was 61 and 59, SWS 55 and 51, REM1 14 and 13, and REM0 3 and 2 for the solitary and social conditions respectively. More waking and SWS episodes were evident during the light period for both solitary and social conditions and a statistically significant difference in the number of waking episodes were noted during the light period during the solitary condition. The number of REM1 episodes was greater during the dark period for both social and solitary conditions, whereas the number of REM0 episodes was greater during the light period during the social condition and greater during the dark period for the solitary condition (Fig. 5.3).

When comparing the number of episodes of each state during the social and solitary conditions for each animal as an individual, not all animals showed differences in the number of episodes for the same state. For example, three animals showed a statistically significant difference in the number of waking episodes, two in the number of SWS episodes, two in the number of REM1 episodes, and three in the number of REM0

episodes. In the majority of the cases, it was found that the number of episodes for waking was higher during the solitary condition. Of the two animals that showed a statistically significant difference in the number of SWS episodes, one animal showed an increase in the number of episodes of this particular state during the social conditions whereas the other animal showed an increase during the solitary condition. The same tendency was noted with regard to the two animals that exhibited a difference in the number of REM1 episodes, whereas in the majority of the animals that showed a statistically significant difference in the number of REM0 episodes it was found that during the social condition this state occurred more frequently compared to the solitary condition. No statistically significant differences were noted in the distribution of the number of episodes per state between dark and light times when the social and solitary conditions were compared within each individual animal (In all statistical analyses an ANOVA/unpaired t-test for parametric data or Kruskal-Wallis/Mann Whitney test for nonparametric data was used, significant $p<0.05$) (Table 5.2).

*5.3.1.3. Duration of episodes*

When the data from all five animals were pooled to create a species average, the average episode duration during social and solitary conditions for waking over a 24 h period was shown to be 476 s and 448 s, SWS 196 s and 185 s, REM1 94 s and 99 s, and REM0 98 s and 78 s respectively. No statistically significant differences existed between the social and solitary conditions concerning the average episode duration of the different states. While not statistically significant, the average duration of a waking, SWS and REM0 episode was greater during the social condition, but the opposite was found for

REM1. This tendency was also observed during the light as well as during the dark periods. The only state that did approach a statistically significant difference was REM0. The average REM0 episode was greater during the social condition over 24 h as well as during the dark period, but no difference was noted during the light period. On average REM0 was approximately 20 s longer during social sleep over 24 h and 40 s longer during the dark period (Fig. 5.3)

When the animals were tested separately to determine whether individuals showed a difference in the average episode duration of a state between social and solitary conditions the results revealed that all animals exhibited statistically significant differences in the average episode duration for all of the physiologically defined states; however, the differences noted for each animal did not reveal a discernable trend, as not all animals showed the same differences with regard to the average episode duration for a particular state. For example, two animals showed a difference in the average duration of waking episodes, in one case the average duration of the waking episodes were longer in the social conditions, whereas in the other case the opposite was found. Four animals showed a difference in the average duration of SWS episodes, but in this instance three out of four showed that the average duration of a SWS episode was longer during the solitary condition. Two animals exhibited a difference in the average duration of a REM1 episode, once again in one case it was found that duration of this state was longer during the social condition whereas the other case showed the opposite. Finally, three animals showed a difference in the average duration of a REM0 episode, in two of the three animals it was found that the average duration of this state was longer in the social compared to the solitary condition (In all statistical analyses an ANOVA/unpaired t-test

for parametric data or Kruskal-Wallis/Mann Whitney test for nonparametric data was used, significant $p<0.05$) (Table 5.2).

*5.3.1.4. REM periodicity and slow wave activity (SWA)*

REM periodicity was calculated from the onset of one REM episode to the onset of the following REM episode and was based on the 72 h recording period for the 1 min epoch scoring method. A statistically significant difference was noted when the modal and average REM periodicity was compared between the social and solitary conditions. The modal REM periodicity for the social condition ranged between 5-15 min whereas for the solitary condition it was 10 min. The mean REM sleep cycle interval for the social condition was 43 min whereas during the solitary condition it was 33 min. When waking episodes that lasted longer that 10 min were eliminated from the data, the REM periodicity for both the social and solitary conditions was found to be 15 min (Fig. 5.4).

SWA based on two hour intervals was calculated during waking, SWS, REM1 and REM0. The average SWA was highest during SWS and gradually declined in intensity from waking to REM1 to REM0. The SWA for all these states remained mostly constant between all three recording days (Fig. 5.5A).

During the light period, SWA during SWS (SWA-SWS) was greater than SWA in all states (SWA-all) for the solitary condition, whereas SWA-all was greater than SWA-SWS during the social condition. No statistically significant differences were noted between SWA-SWS and SWA-all for the social condition; however, in the solitary condition, SWA-SWS was statistically significantly greater than SWA-all. No statistically significant difference was noted between conditions for SWA-SWS;

however, a statistically significant difference was noted for SWA-all, where SWA-all was greater during the social condition compared to the solitary condition.

During the dark period SWA-SWS was greater than SWA-all for both social and solitary conditions. A statistically significant difference existed between SWA-SWS and SWA-all for both the social and solitary condition; however, when SWA-SWS and SWA-all was compared between conditions no statistically significant difference existed (Fig. 5.5B).

When the average SWA per day was compared between social and solitary conditions, SWA during day 1 and day 2 for SWA-SWS as well as SWA-all were higher in the social condition, but on the third day the opposite was found. Furthermore, the average SWA-SWS and SWA-all remained mostly constant between the three recording days for the solitary condition whereas during the social condition SWA-SWS and SWA during waking was significantly greater during the first recording day compared to the two remaining recording days (In all statistical analyses an unpaired t-test for parametric data or Mann Whitney test for nonparametric data was used, significant $p<0.05$) (Fig. 5.5C).

### *5.3.2. Behavioural Data*

Behaviour was recorded simultaneously with the physiologically measurable parameters of sleep and scored in 1 min epochs as either immobile (animal not moving for >30 s), quiet waking (animal moving head or making minor movements in the same place for >30 s), active waking (animal is actively moving around for >30 s) or eating/drinking (animal is eating/drinking for >30 s). During the social condition, over a

period of 24 h, on average 71% (17 hrs) of the time was spent in a state of immobility, 21% (5 h) in quiet waking, 3% (43 min) in active waking and 3% (43 min) of the time was spent eating/drinking and during the solitary condition they spent on average 68% (16 hrs) of the time immobile, 23% (5.5 hrs) in quiet waking, 5% (1 hr) in active waking and 3% (43 min) eating/drinking. When comparing the social and solitary conditions no statistically significant difference existed, however these animals spent on average about 1 h extra a day immobile in the social condition and were more active when in the solitary condition. Quiet waking showed a marginal increase during the solitary compared to social condition, whereas the time devoted to eating/drinking remained the same for both conditions.

When the distribution of these behavioural states over 24 h during the social condition was compared for the light and dark periods it was found that the animals were more immobile during the light period. Active waking and eating/drinking behaviour doubled during the dark period compared to that in the light, whereas only a slight increase was noted for the distribution of quiet waking in the dark compared to the light periods. An increased amount of quiet waking was observed during the dark period. The aforementioned light/dark distribution of these behavioural states was found to be similar to the pattern observed in the solitary condition, but a significant difference was noted for the distribution of active waking. In the solitary condition the animals were more active compared to the social condition and this active waking occurred more during the dark period than the light period (In all statistical analyses an unpaired t-test for parametric data or Mann Whitney test for nonparametric data was used, significant $p<0.05$) (Fig. 5.6).

In the social setting the behaviour of the non-implanted animals was also scored and analyzed. The results revealed that a positive correlation existed between the behaviour of the implanted and non-implanted animal/s, and in all cases the probability of the behaviour of the implanted vs. non-implanted animals being unrelated was found to approach zero. Figures 5.7 and 5.8 show behavioural hypnograms over 24 h of the same animal under social and solitary conditions as well as the behaviour of the non-implanted animal during the social condition. It is clear from these hypnograms that, in the majority of the cases, the implanted and non-implanted animals enter the same behavioural state at the same time and remain in that particular state for roughly the same amount of time.

**Figure 5.1:** Diagram illustrating the spectral power and associated frequency bands characteristics of waking, SWS and REM in the rock hyrax for both the solitary and social conditions. The spectral power for all states was slightly more increased during the solitary condition.

Solitary

Spectral power (V2) x 10-4

1.6
1.4
1.2
1.0
0.8
0.6
0.4
0.2
0.0

SWS
Wake
REM

2 4 6 8 10 12 14 16 18 20

Frequency (Hz)

Social

Spectral power (V2) x 10-4

1.6
1.4
1.2
1.0
0.8
0.6
0.4
0.2
0.0

SWS
Wake
REM

2 4 6 8 10 12 14 16 18 20

Frequency (Hz)

**Figure 5.2:** State transition probabilities in the rock hyrax during solitary (left) and social (right) sleep for 24 hours. During social sleep SWS will be followed in most cases by waking, thus making this the most common sleep pathway observed in the rock hyrax. The next most common pathway would be when SWS is followed by r1 (REM1) which then predominantly transitions to waking, however in some cases it does also transition to r0 (REM0) which in turn is most commonly followed by REM1 but it can also be followed by waking. Compared to the solitary condition REM1 and REM0 never transitioned to SWS during the social condition.

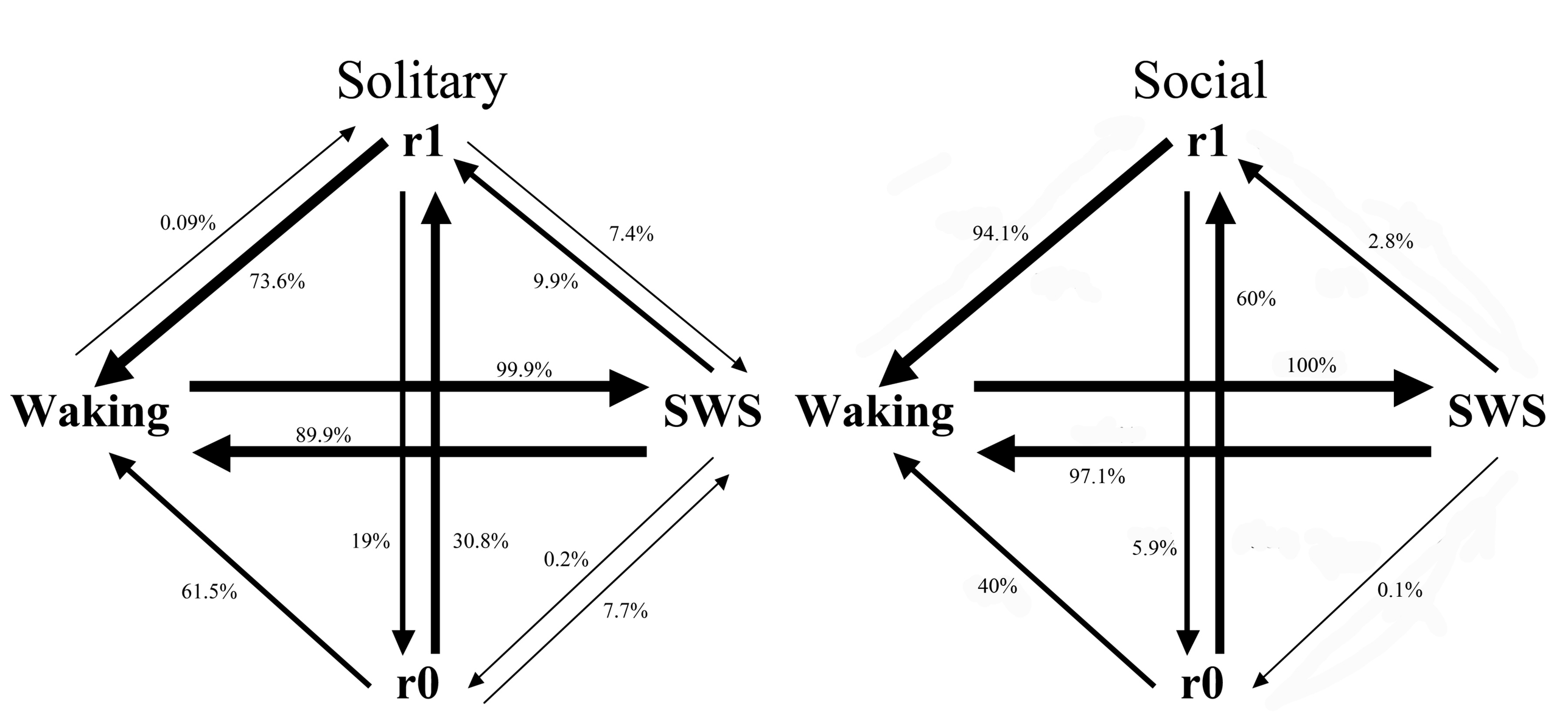
Solitary
r1
0.09%
73.6%
7.4%
9.9%
99.9%
Waking
SWS
89.9%
19%
30.8%
0.2%
61.5%
7.7%
r0
Social
r1
94.1%
2.8%
60%
100%
Waking
SWS
97.1%
5.9%
40%
0.1%
r0

**Figure 5.3:** Histograms depicting the total amount of time spent in each of the defined physiological states as well as the average number of episodes and episode duration for during solitary (left) and social sleep (right) for 24 hours **(A, first set of graphs)**, the light period **(B, second set of graphs)** and the dark period **(C, third set of graphs)**. No statistically significant difference between solitary and social sleep was noted for any of the aforementioned periods. The number wake, SWS and REM1 episodes were slightly more during solitary sleep whereas the duration of wake, SWS and REM0 was greater during social sleep (Parametric - Unpaired t-test, significant $p<0.05$; Non-parametric – Mann Whitney test, significant $p<0.05$); this pattern was observed for the 24 h, light and dark periods. Light shaded bars represents each of the animals studied (from left to right - H107, H03, H04, H05, H07) and the dark bars represents the species mean for each of the physiological states. The graphs also show the standard error of the mean (represented on the species mean) for the total amount of time spent in each of the defined physiological states as well as the average number of episodes and episode duration for 24 hours **(A, first set of graphs)**, the light period **(B, second set of graphs)** and the dark period for each of the physiologically defined states during both solitary and social sleep.

A

Solitary

Social

Hours

Percentage of 24 h

Wake

SWS

REM1

REM0

Number of Episodes in 24h

Average episode duration (s)

**B**

## Solitary

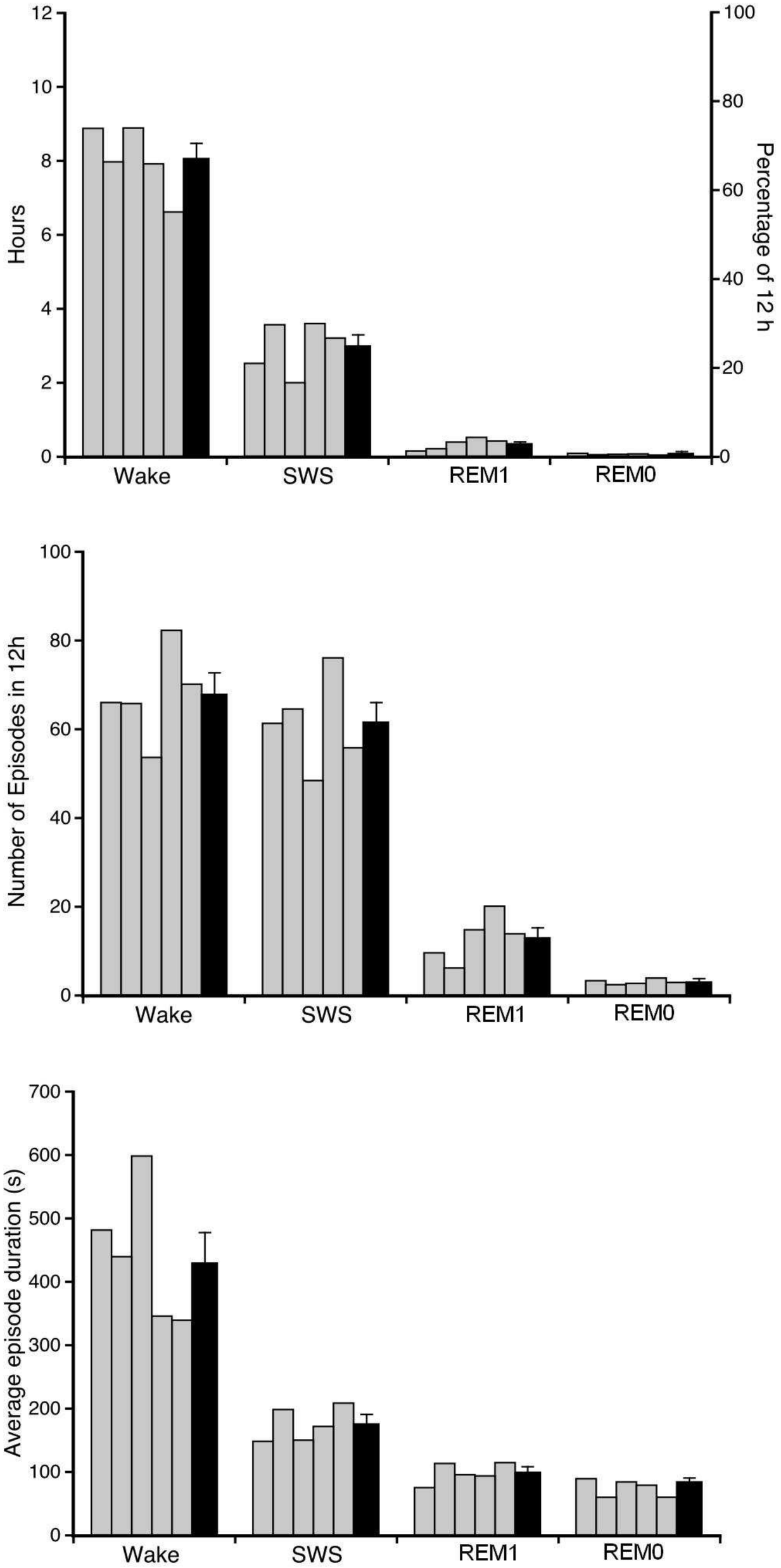


## Social

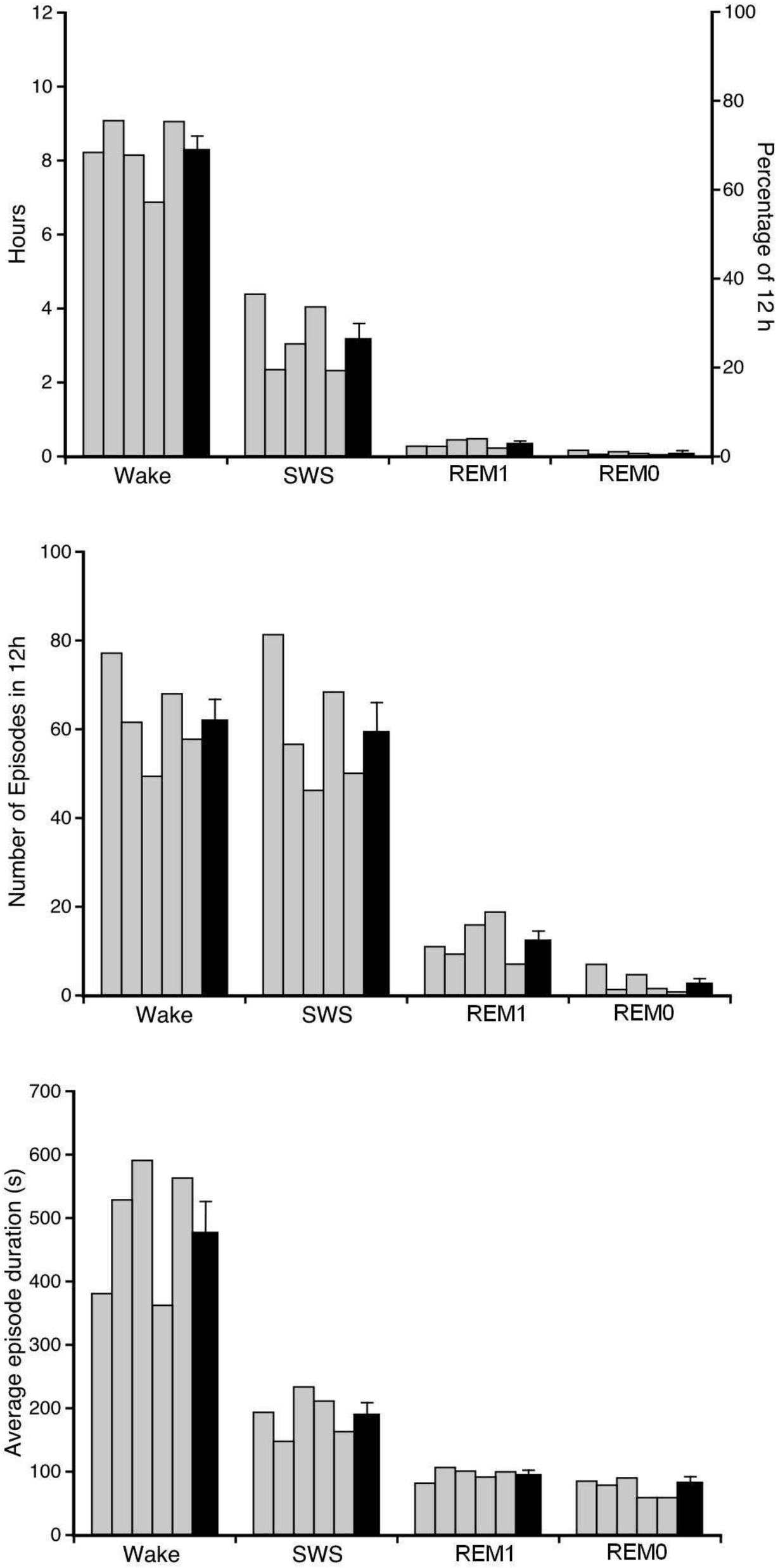

**C**

## Solitary

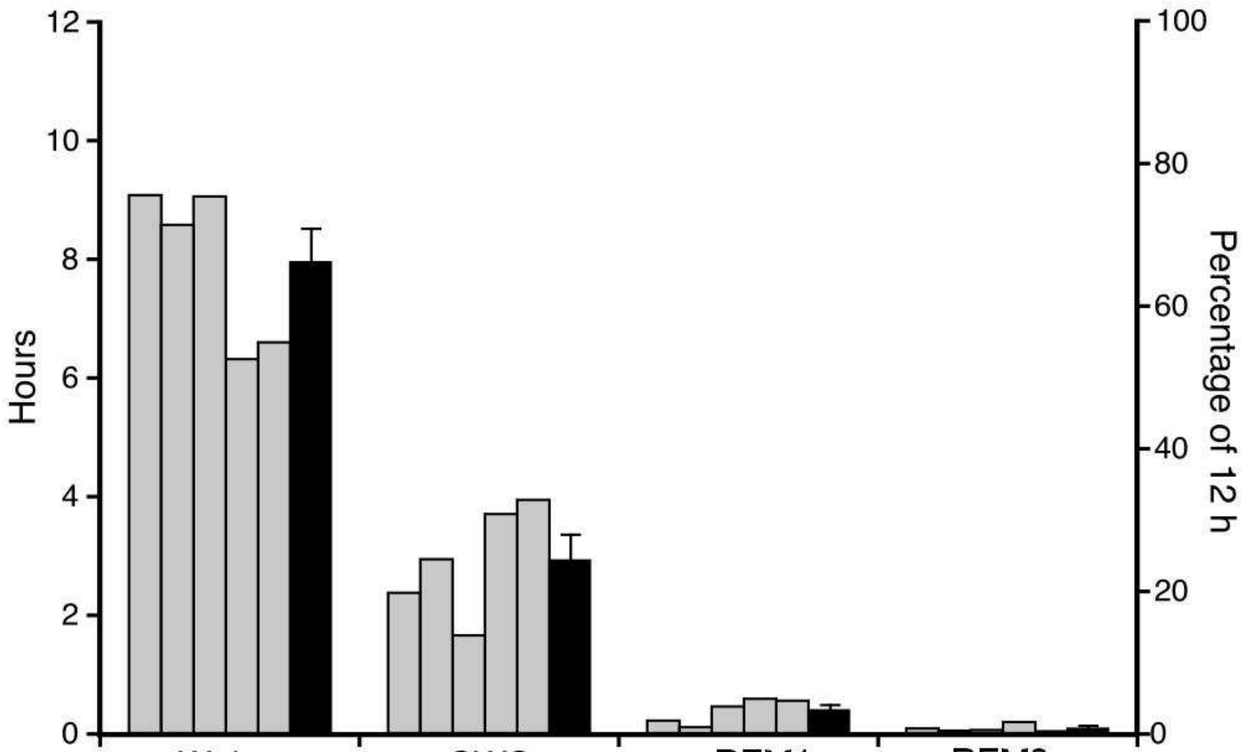


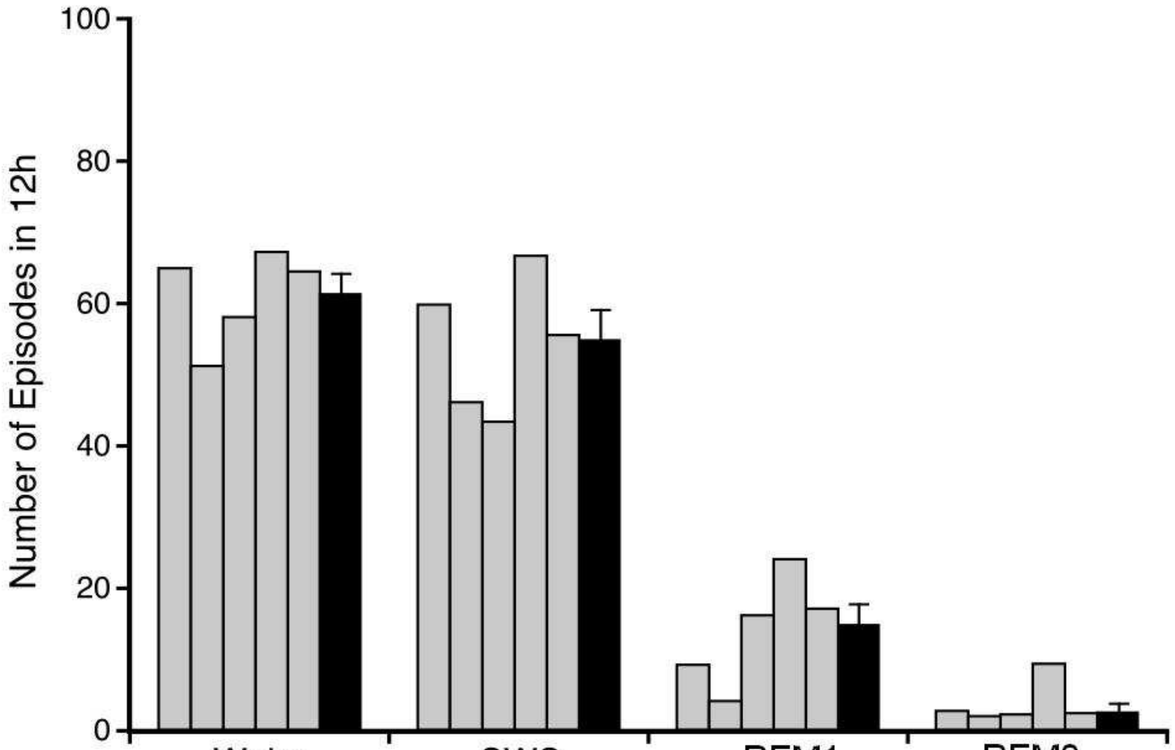


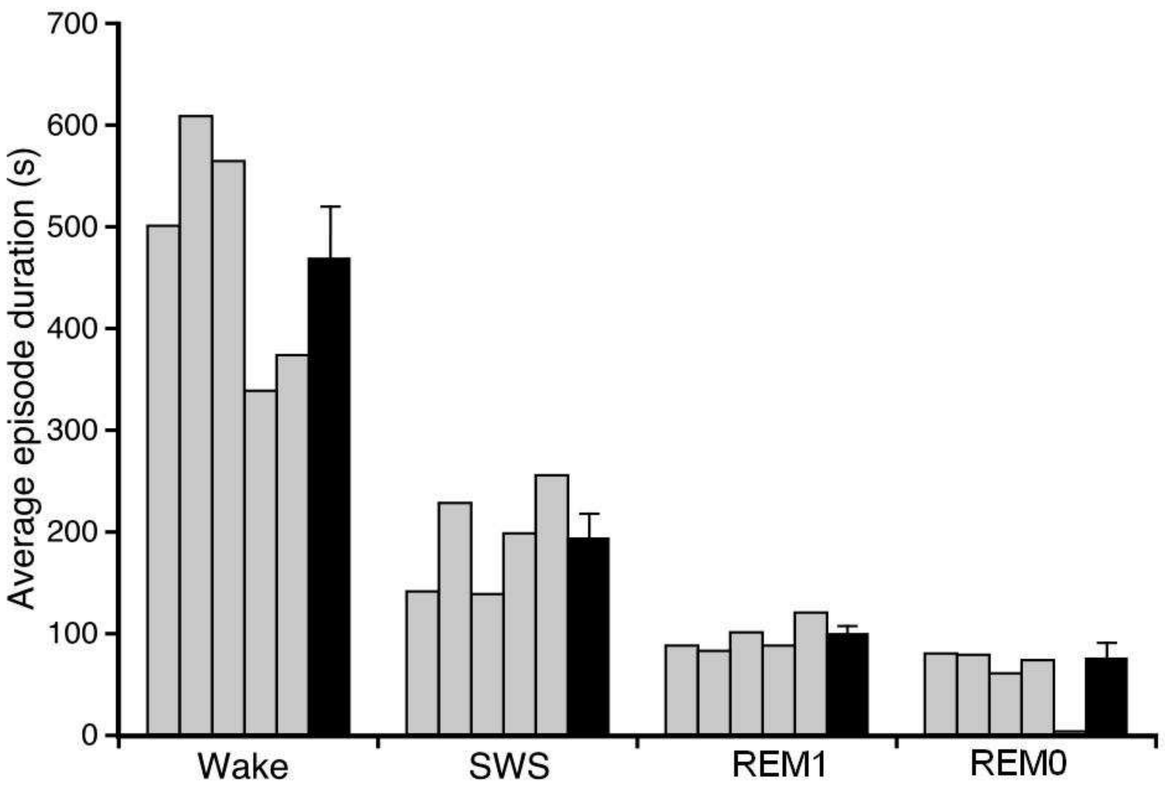


## Social

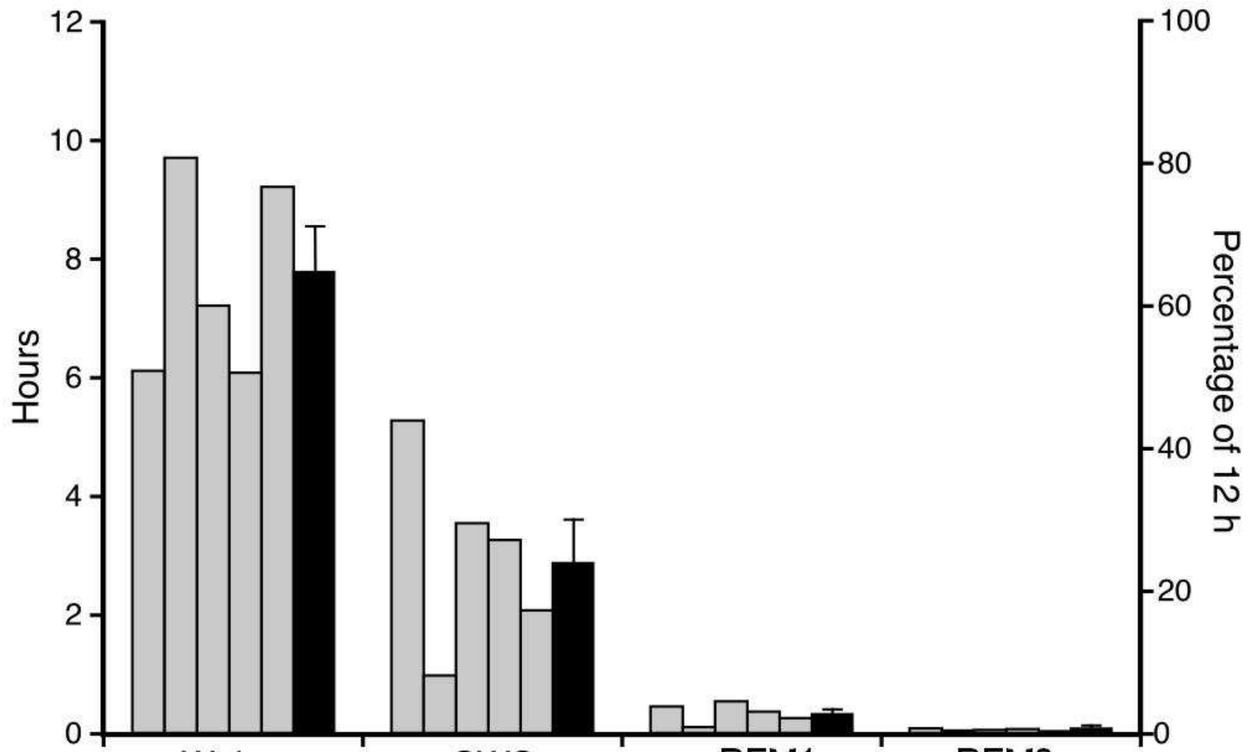


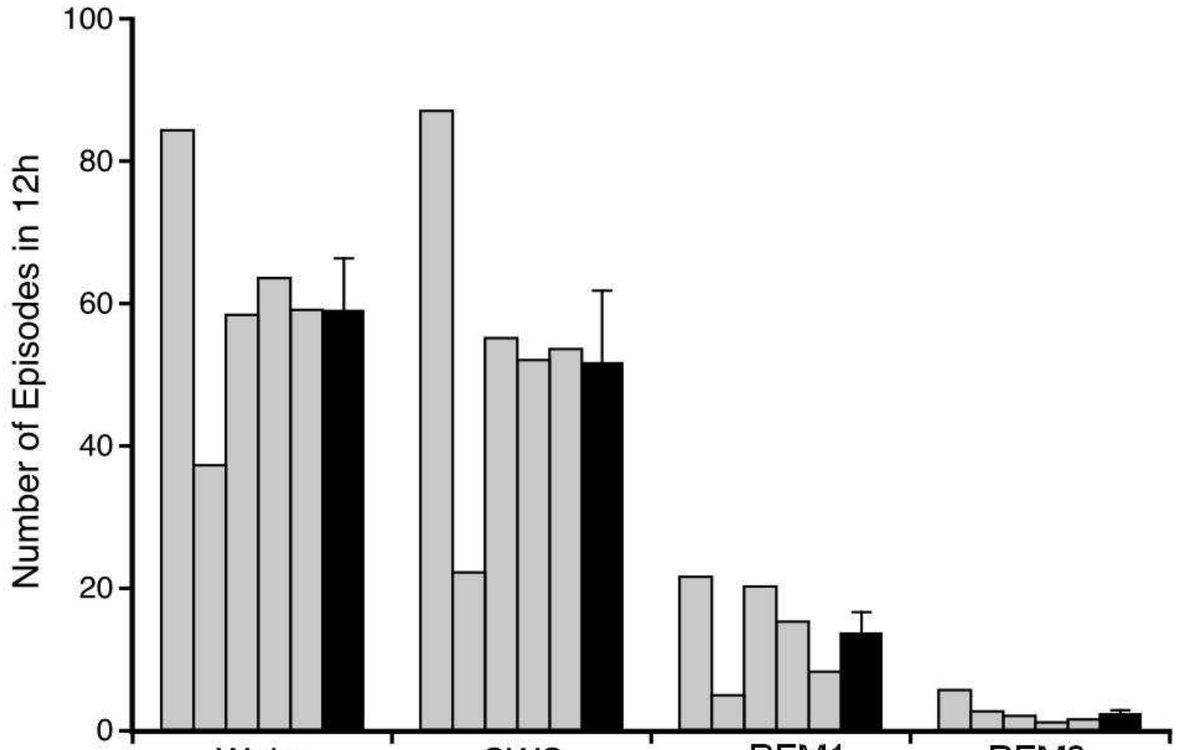


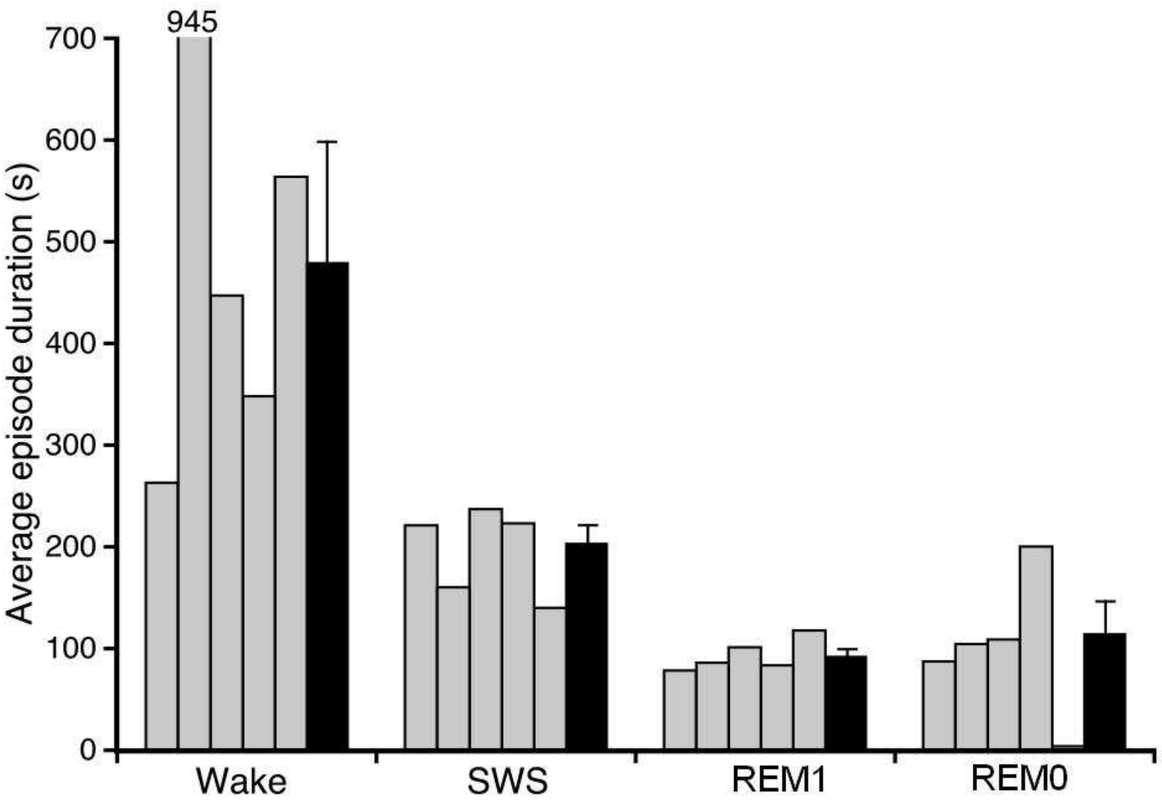

**Figure 5.4:** Histograms depicting REM periodicity for the solitary (top) and social (middle) conditions as well as the REM periodicity during the social conditions after waking episodes that lasted longer than 10 min were eliminated from the data (bottom). The REM periodicity was calculated based on a 72 hour recording period. The modal sleep cycle for the solitary sleep was 10 minutes and for social sleep it ranged between 5-15 minutes. The average REM periodicity during solitary sleep was 33min and 43 min during social sleep. A statistically significant difference was noted with regard to REM periodicity between solitary and social sleep (Unpaired t-test, significant $p<0.05$). After waking episodes that lasted longer than 10 minutes were eliminated from the data the modal REM periodicity during the social condition was 15 minutes.

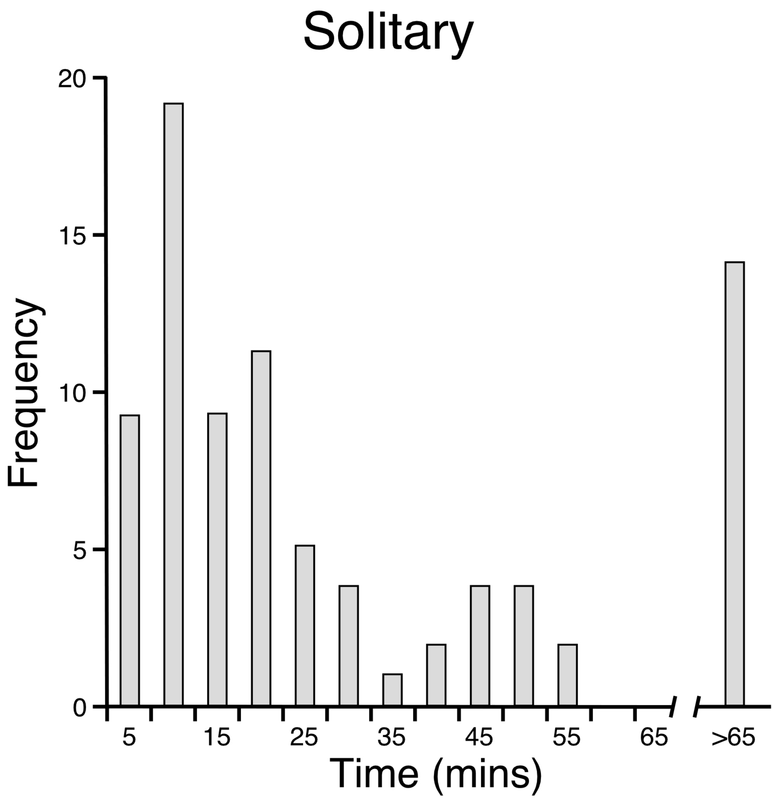
Solitary
Frequency
20
15
10
5
0
5
15
25
35
45
55
65
>65
Time (mins)

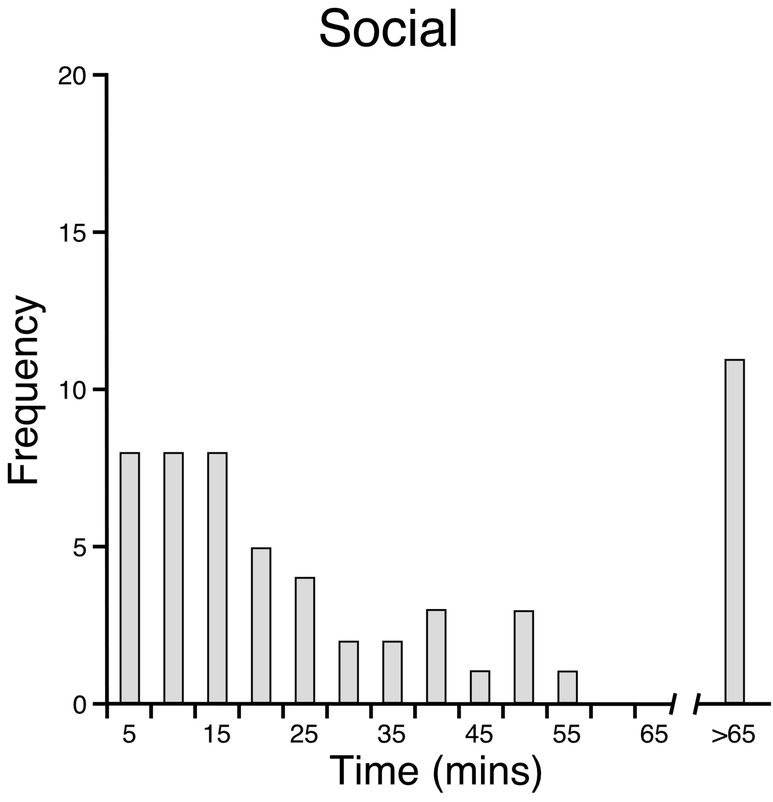
Social
Frequency
20
15
10
5
0
5
15
25
35
45
55
65
>65
Time (mins)

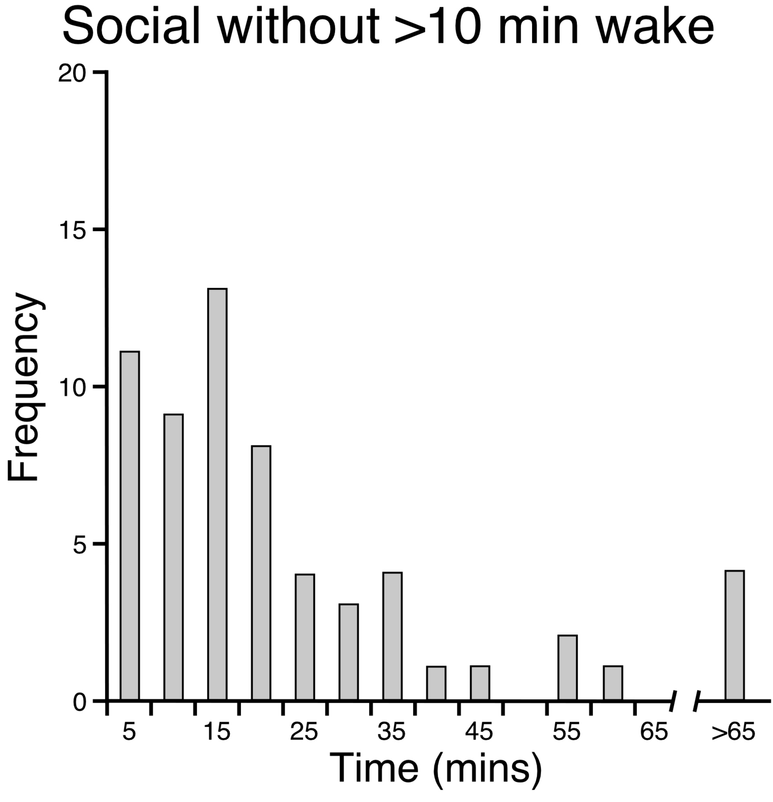
Social without >10 min wake
Frequency
20
15
10
5
0
5
15
25
35
45
55
65
>65
Time (mins)

**Figure 5.5:** Slow wave activity (based on 2-h intervals) in three animals for the 72 hour recording period during SWS for the solitary **(A)** and social **(B)** conditions. SWA was greater during the light period during the social condition, whereas during the dark period it was greater when the animals under solitary conditions. No statistically significant difference was noted between the light and dark period for the solitary condition, however such a difference was noted during the social condition **(C)**. SWA during the social condition was greater than that of the solitary condition for the first two days of recording, however during the last day of recording SWA was slightly higher during the solitary condition. Solitary SWA between the three recording days remained fairly constant, whereas during the social condition a greater variability, especially SWA during waking and SWS, between the three recording days was noted. **(D)**. Unpaired t-test used in all statistical analysis, significant $p<0.05$.

A

SWA during Solitary SWS (72 h)

SWA ($V^2$) x $10^{-4}$

2.0
1.8
1.6
1.4
1.2
1.0
0.8
0.6
0.4
0.2
0.0

18:00 6:00 18:00 6:00 18:00 6:00

Time (h)

B

SWA during Social SWS (72 h)

SWA ($V^2$) x $10^{-4}$

2.0
1.8
1.6
1.4
1.2
1.0
0.8
0.6
0.4
0.2
0.0

18:00 6:00 18:00 6:00 18:00 6:00

Time (h)

C

Total spectral power (mV)

12
10
8
6
4
2
0

solitary
social
solitary
social

SWA all states
SWA SWS
SWA all states
SWA SWS
SWA all states
SWA SWS
SWA all states
SWA SWS

Light period
Dark period

D

Total spectral power (mV)

14
12
10
8
6
4
2
0

SWS solitary
SWS social
Wake solitary
Wake social
REM1 solitary
REM1 social
REM0 solitary
REM0 social

Day 1
Day 2
Day 3

**Figure 5.6:** Histogram illustrating the percentage of time occupied by each behavioral state during the light and dark period respectively for the solitary (left) as well as social (right) conditions. For both the solitary and social conditions there is no significant difference in the distribution of waking and quiet waking between the light and dark period, however it is clear that more active waking and eating/drinking behaviour occurs during the dark period. No statistically significant difference exists between solitary and social conditions for all states except for active waking, between the light and dark periods. More active waking occurs during the dark period during the solitary condition compared to the social condition (Parametric - Unpaired t-test, significant $p<0.05$; Non-parametric – Mann Whitney test, significant $p<0.05$). Light shaded bars represents each of the animals studied (from left to right - H107, H03, H04, H05, H07) and the dark bars represents the species mean for each of the behavioral states.

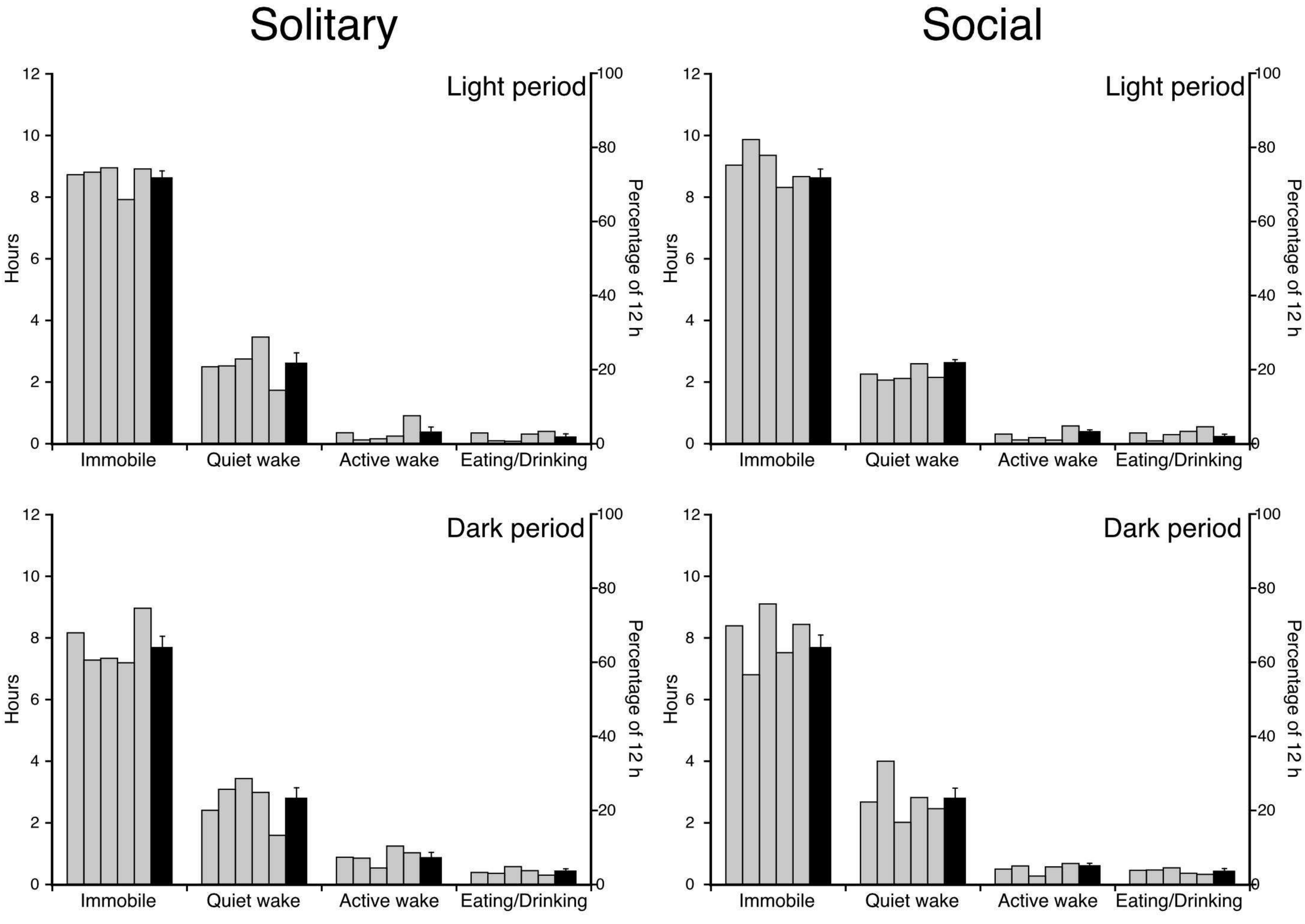
Solitary
Social
Light period
Dark period
Hours
Percentage of 12 h
0
2
4
6
8
10
12
20
40
60
80
100
Immobile
Quiet wake
Active wake
Eating/Drinking

**Figure 5.7:** Hypnograms showing the behavioral state transitions occurring over a 24 hour period for H06 starting at 9 am for the same animal during solitary and social sleep as well the non-implanted animal during the social setting. The shaded area is representative of the dark period. No statistically significant difference exists in the behaviour between the solitary and social setting, active waking appears to be more frequent in the solitary during the dark period compared to the social setting and no significant difference exists between the implanted and non-implanted animal in the social setting with regards to the distribution of each behavioral state over 24 h

## Implanted animal Solitary setting

Eating/ drinking

Active wake

Quiet wake

Immobile

## Implanted animal Social setting

Eating/ drinking

Active wake

Quiet wake

Immobile

## Non-implanted animal Social setting

Eating/ drinking

Active wake

Quiet wake

Immobile

9:00 10:00 11:00 12:00 13:00 14:00 15:00 16:00 17:00 18:00 19:00 20:00 21:00 22:00 23:00 0:00 1:00 2:00 3:00 4:00 5:00 6:00 7:00 8:00 9:00

**Figure 5.8:** Hypnograms showing the behavioral state transitions occurring over a 24 hour period for H07 starting at 9 am for the same animal during solitary and social sleep as well the non-implanted animal during the social setting. The shaded area is representative of the dark period. No statistically significant difference exists in the behaviour between the solitary and social setting, active waking appears to be more frequent in the solitary compared to the social setting and no significant difference exists between the implanted and non-implanted animal in the social setting with regards to the distribution of each behavioral state over 24 h.

## Implanted animal Solitary setting

Eating/ drinking
Active wake
Quiet wake
Immobile

## Implanted animal Social setting

Eating/ drinking
Active wake
Quiet wake
Immobile

## Non-implanted animal Social setting

Eating/ drinking
Active wake
Quiet wake
Immobile

9:00 10:00 11:00 12:00 13:00 14:00 15:00 16:00 17:00 18:00 19:00 20:00 21:00 22:00 23:00 0:00 1:00 2:00 3:00 4:00 5:00 6:00 7:00 8:00 9:00

**Table 5.1:** Total wake, sleep and REM times as a percentage of 24 hours for each individual animal as well as the species mean. TWT – total waking time, TST – total sleep time, TSWS – total SWS time, TREM – total REM time, Tr1 – total REM1 time, Tr0 – total REM0 time.

| Animal ID | Body Weight (Kg) | Brain Weight (g) | Sex | TWT | TST | TSWS | TREM | Tr1 | Tr0 |
|---|---|---|---|---|---|---|---|---|---|
| H107 | 3.1 | 19.6 | Female | 44.7 | 32 | 29 | 3 | 2 | 1 |
| H03 | 3.14 | 27.1 | Male | 78.3 | 16.2 | 14.3 | 1.9 | 1.5 | 0.4 |
| H05 | 4.3 | 20.4 | Male | 65.3 | 31.5 | 26.6 | 4.9 | 4.2 | 0.7 |
| H06 | 1.74 | 19.5 | Male | 55.8 | 32.4 | 28.4 | 4 | 3.6 | 0.4 |
| H07 | 2.05 | 17.9 | Male | 74.7 | 21.8 | 20 | 1.8 | 1.6 | 0.2 |
| **Species Averages** | **2.87** | **20.9** | | **66.8** | **28.1** | **24.8** | **3.3** | **2.7** | **0.6** |

**Table 5.2:** Illustration of where statistically significant differences ($p<0.05$) were noted between the three recording days for each state with regards to the number of epochs, episodes and episode duration during the social conditions for each individual animal, for the group as well as for the social vs. the solitary condition. Each of the animals subjected to experimentation was tested individually to determine whether statistically significant differences existed between each of the recording days with regard to the number of epochs and episodes as well as the episode duration for each of the physiologically defined states during the social setting. Following this, the data obtained from all the animals were pooled together to determine whether any statistically significant differences existed between each of the recording days for the group during the social setting. Finally the data obtained from all the individuals for the social and solitary setting were pooled together respectively and tested to determine whether statistically significant difference existed between the social and solitary conditions. All data was tested for normality prior to any statistical analyses (Kolmogorov and Smirnov test, $p>0.05$). A one-way ANOVA was used for comparisons between parametric data (statistical significance where $p<0.05$) and a Kruskal-Wallis test was used for comparisons between nonparametric data (statistical significance where $p<0.05$). Italisized values indicate statistically significant difference between the recordings.

| Animal ID | Duration | | | | Episodes | | | | Epochs | | | |
|---|---|---|---|---|---|---|---|---|---|---|---|---|
| | **Waking** | **SWS** | **r1** | **r0** | **Waking** | **SWS** | **r1** | **r0** | **Waking** | **SWS** | **r1** | **r0** |
| H107 | 0.3195 | 0.0601 | 0.8977 | 0.9488 | 0.0867 | *0.0124* | 0.2309 | 0.1328 | 0.5257 | 0.5021 | 0.8495 | 0.7861 |
| H03 | 0.6861 | 0.5999 | 0.5173 | 0.1828 | 0.6893 | 0.7271 | 0.6914 | 0.1481 | 0.5697 | 0.951 | 0.4233 | 0.1163 |
| H05 | 0.6012 | 0.3912 | 0.3947 | 0.4624 | 0.3106 | 0.4872 | 0.4056 | *0.0493* | 0.7261 | 0.8449 | 0.2467 | 0.1014 |
| H06 | 0.66 | 0.457 | 0.6263 | 0.4922 | 0.4746 | 0.9651 | 0.8269 | 0.3429 | 0.0925 | 0.661 | 0.0871 | 0.4641 |
| H07 | 0.9414 | *0.0005* | 0.0723 | 0.4579 | *0.03661* | 0.7911 | *0.0109* | 0.3492 | *0.0006* | *0.0034* | *0.02152* | 0.3624 |
| **All** | 0.8835 | 0.54 | 0.2892 | 0.2465 | 0.4034 | 0.0612 | 0.8025 | 0.2223 | 0.1827 | 0.1386 | 0.452 | 0.1487 |
| **Social vs. Solitary** | 0.0897 | 0.1163 | 0.4207 | 0.0642 | *0.0057* | 0.1826 | 0.6241 | 0.0649 | 0.4323 | 0.6818 | 0.3958 | 0.0719 |

## 5.4. Discussion

The aim of the present study was to describe the sleep-wake cycle in the rock hyrax, *Procavia capensis*, a diurnal social mammal when subjected to normal social conditions and to compare it to the results obtained during solitary, or asocial, conditions. Waking and SWS times were the same during both social and solitary conditions, but REM1 time was decreased (39 min/day – social, 43 min/day – asocial) and REM0 time was increased (9 min/day – social, 6 min/day – asocial) during the social condition (Table 5.1). No statistically significant difference was noted between conditions with regard to the number of episodes as well as the average episode duration for each of the defined physiological sates for the 24 h, light and dark periods. The number of waking, SWS and REM1 episodes was increased in the solitary condition whereas the number of REM0 episodes was greater during the social condition. The average duration of waking, SWS and REM0 episodes was greater when the animals were in the social condition, whereas the duration of a REM1 episode was greater when the animals were in the solitary condition, The aforementioned tendencies were observed during the light as well as the dark periods, with the exception of the number of REM0 episodes, which were found to be greater during the dark period under solitary conditions. The modal REM periodicity when waking episodes that lasted longer than 10 min were eliminated from the data was found to be 15 min for both conditions. The most common state transition pathway was found to be similar for both social and asocial sleep, which was waking → SWS → waking. During the solitary condition REM1 and REM0 transitioned to SWS and waking to REM1, whereas this was not the case during the social condition.

Behaviourally no statistically significant difference was noted between social and solitary conditions. Active waking and eating/drinking behaviour was more prevalent during the dark period as opposed to the light period during both conditions; however the animals were significantly more active during the dark periods when they were in the solitary condition (Fig. 5.6). The non-implanted animals also expressed the same behaviour as the implanted animal in the social condition. The results revealed a positive correlation between the implanted and non-implanted animal behaviour and the probability of the two data sets not being equal was zero in all cases (Figs. 5.7, 5.8).

*5.4.1. Sleep fragmentation in the social condition*

It has been suggested that species that sleep socially express more fragmented sleep patterns and that sleep cycle length should be shorter in solitary species based on the belief that predation risk is reduced in larger group due to detection and dilution effects (Caro, 2005; Lima et al., 2005; Capellini et al., 2008). It has also been shown that sleep cycle length and phasing of sleep were not significantly correlated with social sleep behaviour (Capellini et al., 2008); however, no studies to the authors' knowledge have been performed in the same species to examine the effects of these two sleeping conditions. In the current study no statistically significant difference was noted with regard to the number of waking, SWS, REM1 or REM0 episodes over 24 h as well as during the light and dark times when the social and solitary conditions were compared. However, during the light period a statistically significant difference was noted with regard to just the number of waking episodes during the solitary condition. This corresponds to the behavioural data that also showed that these animals exhibited more

quiet and active waking episodes during the light period in the solitary compared to the social condition. Furthermore, the average duration of SWS episodes were greater than REM1 and REM0 episodes for both the social and solitary condition, during the 24h, light and dark periods. No statistically significant difference was noted with regard to sleep cycle length or duration of episodes for all states, with the exception of REM0 (see below) between social and solitary conditions. Thus it appears that sleep does not become more fragmented during social conditions in the rock hyrax.

*5.4.2. Reduced sleep quotas, but better sleep quality in the social condition?*

In addition to sleep fragmentation, it has been proposed that NREM and REM quotas are lower in species that sleep in a social condition as they potentially sleep more efficiently and obtain all the benefits of sleep in a shorter time frame (Capellini et al., 2008). This is thought to be due to the fact that sleeping in a group provides a greater sense of security allowing the animals to enter "deeper" states of sleep. It has also been hypothesized that the shorter sleep times could be attributed to a greater amount of time that has to be devoted to social interactions which in effect results in less time available for sleep (Capellini et al., 2008). In the current study of the rock hyrax we found that no statistically significant differences existed between social and solitary conditions. Total sleep and waking times were similar during both condition, the average number of episodes for all states was not different nor was the average episode duration for all states. The one exception to this was REM0, which was on average 20 s longer during the social condition compared to the solitary condition over 24 h, and 40 s longer during the dark period.

In the present study it was also revealed that SWS during SWA-SWS as well as SWA-all was significantly greater during the social condition compared to the solitary condition (Fig. 5.5 A-C). The average SWA per day over the three recording days was also greater during the social condition during the first two days, but during the last day SWA was slightly higher during the solitary condition (Fig. 5.5C). SWA during NREM is considered a measure of sleep intensity and sleep debt as well as an indicator of NREM homeostasis (Borbély and Neuhaus, 1980; Tobler and Borbély, 1986; Daan et al., 1984; Meerlo et al., 1997, 2001; Borbély and Achermann, 1999) The studies by Meerlo et al. (1997, 2001) showed that a correlation exists between social conflict and sleep intensity. In their studies rats were subjected to a single social defeat for a 1 h period and subsequent recording revealed that SWA increased during the following NREM episode. Interestingly, the rats did not rectify the sleep debt caused by the social conflict by increasing their sleep duration, instead SWA increased and duration remained unchanged. This led to the conclusion that both the duration and the nature of the prior waking bout influence the need for sleep. It is possible that increased SWA seen during the social condition in the rock hyrax could be a result of social interactions, as an increase in this activity is only seen during the first two days of recording (although the animals were acclimatized to each other for three days prior to recording).

When comparing SWA during the light versus the dark periods between the social and solitary conditions, the results showed that SWA was highest during the light period when in the social condition, whereas during the dark period it was highest when in the solitary condition. Meerlo et al. (1997, 2001) suggested that SWA during NREM sleep is determined by the duration and nature of the previous waking experience. As the results

of the present study revealed no significant difference in the duration of waking episodes between the light and dark period in these animals, it is possible that during social sleep the nature of the waking episodes preceding NREM sleep during the light and dark periods may be different; however, no physical social conflict was noted behaviourally for all animals examined. Despite this, it is interesting though that the SWA for all states during the social condition dropped to just slightly below the SWA during the solitary condition on the third day of recording. It would have been interesting to investigate whether this trend continued if the recording period was extended for a few days longer. Extended recording would ultimately resolve the question of whether the increase in SWA during the first two days could be attributed to the animals still acclimatizing to their social environment, or whether sleep quality actually improves as a result of sleeping socially.

The average REM0 duration was also found to be significantly longer during the social compared to solitary condition over 24 h and more so during the dark period (Fig. 5.3). This increase in REM0 episode duration, plus a very slight increase in total time spent in this state, could be a result of stress induced by the social condition. REM0 is the form of REM in the rock hyrax that most closely resembles all the characteristic traits of REM sleep that has been described in most mammals studied to date. It has been hypothesized that on a behavioural level the drive for sleep might be increased by stress and many studies have shown that after restraint stress REM sleep time increased (Bonnet et al., 1997; Bouyer et al., 1997; Meerlo et al., 2001; Rampin et al., 1991). It is also possible that the increase in REM0 duration could be linked to thermoregulation. Rock hyraxes are known to be poor thermoregulators and typically sleep huddled in

groups to conserve body heat (Taylor and Sale, 1969). Horne (2009) proposed that when sleeping in a warmer environment, in the case of the rock hyrax this being several animals huddled together, body heat loss, and therefore energy expenditure and potentially feeding behaviour is reduced. Furthermore it is hypothesized that hypothalamic temperature increases, within limits, create a positive feedback loop that may result in an increase in REM.

### *5.4.3. The effects of social sleeping in the rock hyrax*

The present study provides four results of interest regarding the effects of sleeping in a social setting for the rock hyrax: (1) total time for all states is similar in both social and solitary conditions; (2) the number of episodes for each state is similar in both social and solitary conditions; (3) REM0 episode duration is longer, especially during the dark period in the social condition; (4) SWA is generally greater in the social setting. These results lead to the conclusion that when rock hyraxes sleep in a social setting, they do not sleep more or less than when they sleep alone, nor is sleep more fragmented in one condition compared to the other. The increase in REM0 duration and the increase in overall level of SWA, both indicate a better sleep quality when in the social condition. Thus, it appears possible to conclude that sleep quality may be improved when in the social setting for the rock hyrax. Whether this conclusion and the observations made in this study can be generalized to all social mammals remains an open question for further investigation of the kind undertaken here.

It is also possible that the increase in SWA seen during social sleep in the rock hyrax could be the result of social interactions creating a sleep debt alleviated by

increasing the number of slow waves. Increased REM0 duration, also seen during social sleep, could possibly be the manifestation of better thermoregulative strategies employed when sleeping socially. Thus, the differences observed in the current study between a social and a solitary condition and the effect on sleep may be related to better sleep quality, or may be related to the social and physical conditions experienced during the different states.

# Chapter 6

## The interrelations of the distribution of sleep associated nuclei and terminal networks in the brain of the rock hyrax, *Procavia capensis*

### 6.1. Introduction

The basal forebrain and hypothalamus as well as the pontomedullary junction of the brainstem has been identified as the two main regions within the brain of mammals that house the neuronal groups involved in the control and regulation of the sleep-wake cycle. The systems of interest in the current study that are involved in the sleep-wake cycle include the cholinergic, putative catecholaminergic, serotonergic, orexinergic, histaminergic and GABAergic systems. These systems have a broad distribution throughout the brain however the nuclei of these systems that are known to be involved in the sleep-wake cycle have very specific innervation patterns (Lyamin et al., 2008).

The cholinergic sleep related nuclei are mainly located within the basal forebrain, anterior hypothalamus, midbrain and the dorsal pons. These nuclei form the main arousal system of the forebrain and are responsible for the desynchronized electroencephalogram (EEG) of waking and rapid eye movement (REM) sleep. They discharge maximally during the aforementioned states however during slow wave sleep (SWS) they discharge minimally as GABAergic neurons in the vicinity of these cholinergic sleep related nuclei inhibit their excitatory actions (Steriade et al., 1990; Siegel, 2000). The cholinergic sleep related nuclei of the midbrain and dorsal pons, such as the PPT (pedunculopontine tegmental) and LDT (laterodorsal tegmental) nuclei, are selectively active during REM sleep and has been reported as being responsible for the suppression of muscle tone

during this state (Sakai and Koyama, 1996). A subgroup of these nuclei have also been identified as the driving force behind the generation of pontine-geniculate-occipital (PGO) spikes, one of the characteristics features associated with REM sleep in many mammals (Lyamin et al., 2008; Steriade et al., 1990).

One of the most well described sleep related catecholaminergic nuclear group is the locus ceroeleus (LC). The neurons of the LC complex are mainly active and fire tonically during waking, have a reduced discharge rate during the initial stages of SWS and are for the most part inactive during REM. It has also been suggested that the loss of muscle tone observed during REM sleep could be attributed to the inactivity of these neurons during this particular state (John et al., 2004; Lai et al., 2001; Lyamin et al., 2008; Siegel et al., 1991, Siegel, 2000).

The serotonergic brainstem raphe sleep related nuclei have a similar discharge pattern as that described for the LC complex and are mainly active during waking (Lyamin et al., 2008; Siegel, 2004). It has been reported that these neurons also maintain arousal, regulate muscle tone and suppress phasic waking events (Wu et al., 2004). It has also been shown that the rostral cluster of serotonergic sleep related nuclei play a role in the regulation of PGO spikes and gating the actions of REM sleep (Lyamin et al., 2008; Siegel, 2000).

Between the sleep active nuclei of the anterior hypothalamus and the wake active histamine neurons of the posterior hypothalamus the orexinergic sleep related nuclei are situated. It has been reported that these neurons have a driving effect on the other arousal systems of the brain and through their projections to the brainstems also play a role in the

regulation of muscle tone (Gerashchenko and Shiromani, 2004; Kiyashchenko et al., 2002; Lai and Siegel, 1990; Lyamin et al., 2008; Peyron et al., 1998).

As mentioned previously the histaminerigic sleep related nuclei mainly promote wakefulness and are located within the posterior hypothalamus. GABAergic inhibition of these nuclei results in sleepiness, and the desynchronized EEG associated with waking as well as arousal maintenance of the forebrain is accomplished by the tonic effects of the histaminergic, serotonergic and catecholaminergic systems in combination with the activity of the cholinergic system (Jonh et al., 2004; Lyamin et al., 2008; Saper et al., 2001).

The most potent sleep promoting neuronal groups are those of the GABAergic system located within the basal forebrain and anterior hypothalamus. Many of these neurons are maximally active during NREM sleep, less active during REM and minimally active during waking. At the onset of NREM sleep the discharge rate of these neurons is increased which also then have an inhibitory effect on the neurons involved in arousal (Lyamin et al., 2008; Szymusiak, 1995; Szymusiak et al., 2001; Siegel, 2004). The GABAergic sleep related neurons that are located in the midbrain and dorsal pontine regions have also been reported to have an inhibitory effect on the brainstem serotonergic and catecholaminergic neuronal groups (Lyamin et al., 2008; Nitz and Siegel, 1997a, b).

The aim of the present study is to describe the location and the distribution of the cholinergic, catecholaminergic, serotonergic, and orexinergic sleep related nuclear groups and the interrelation of these groups to the calcium binding GABAergic interneurons, parvalbumin (PV), calbindin (CB) and calretinin (CR), and their terminal network distributions within the brain of the rock hyrax, *Procavia capensis*

## 6.2. Materials and Methods

The brains of six adult rock hyraxes, *P. capensis*, were used in the present study. Permits from the Limpopo and Gauteng Provincial Governments were obtained for the capture and transport of the animals from the wild. All animals were treated and used according to the guidelines of the University of the Witwatersrand Animal Ethics Committee (approval number AESC 2005/8/5), which parallel those of the NIH for the care and use of animals in scientific experimentation. Each animal was weighed and then euthanized with weight appropriate doses of sodium pentobarbital (200 mg sodium pentobarbital/kg, i.p., Euthanase). Upon cessation of respiration the animals were perfused intracardially with 0.9% saline followed by 4% paraformaldehyde in 0.1M phosphate buffer (PB, pH 7.4) (approximately 1 l/kg of each solution), both solutions having a temperature of 4°C. The brains were then carefully removed from the skulls and post-fixed overnight in 4% paraformaldehyde in 0.1M PB followed by equilibration in 30% sucrose in 0.1M PB. The brains were then frozen in dry ice and with a freezing microtome sectioned at 50 µm in the coronal plane. A one in ten series of stains was made for nissl, myelin, acetylcholine esterase, tyrosine hydroxlase, serotonin, hypocretin/orexin, histamine, parvalbumin, calbindin, and calretinin. Sections kept for the Nissl series were mounted on 0.5% gelatine coated glass slides, cleared in a solution of 1:1 chloroform and absolute alcohol, then stained with 1% cresyl violet to reveal cell bodies. Myelin sections were stored in 5% formalin for a period of two weeks and were then mounted on 1% gelatine coated glass slides and subsequently stained with silver solution to reveal myelin sheaths (Gallyas, 1979).

For immunohistochemical staining each section was treated with an endogenous peroxidase inhibitor (49.2% methanol: 49.2% 0.1 M PB: 1.6% of 30% $H_2O_2$) for 30 min and subsequently subjected to three 10 min 0.1 M PB rises. The sections were then preincubated in a solution (blocking buffer) consisting of 3% normal serum (normal rabbit serum, NRS, for the sections to be stained with the CHAT antibody, or normal goat serum, NGS, for the remaining sections), 2% bovine serum albumin (BSA, Sigma) and 0.25% Triton X100 (Merck) in 0.1M PB, at room temperature for 2 h. The sections were then placed for 48 h at 4°C under constant gentle shaking, in the primary antibody solution that contained the appropriately diluted primary antibody in blocking buffer (see above). The primary antibodies used were anti-cholineacetyltransferase for cholinergic (ChAT) neurons (AB144P, Chemicon, raised in goat, at a dilution of 1:2000), anti-tyrosine hydroxylase for catecholaminergic (TH) neurons (AB151, Chemicon, raised in rabbit, at a dilution of 1:10000), anti-serotonin for serotonergic (5-HT) neurons and terminal networks (AB938, Chemicon, raised in rabbit, at a dilution of 1:10000), anti-orexin-A for orexinergic neurons and terminal networks (AB 3704, Millipore, raised in rabbit, dilution 1:3000), anti-histamine for histaminergic terminal networks (AB 5508, Millipore, raised in rabbit, dilution 1:5000, unfortunately while this antibody labels the terminal networks, it fails to labels the neurons), anti-parvalbumin for parvalbumin containing interneurons and terminal networks (PV28, Swant, raised in rabbit, dilution 1:30000), anti- calbindin for calbindin containing interneurons and terminal networks (CB38a, Swant, raised in rabbit, dilution 1:20000) and anti-calretinin for calretinin containing interneurons and terminal networks (7699/3H, Swant, raised in rabbit, dilution 1:20000). This was followed by three 10 min rinses in 0.1M PB, after which the sections

were incubated for 2 h at room temperature in secondary antibody solution. The secondary antibody solution contained a 1:1000 dilution of biotinylated anti-goat/anti-rabbit IgG (BA-5000/BA-1000, Vector Labs) in 3% NRS/NGS, and 2% BSA in 0.1M PB. Once this was completed, the sections underwent three 10 min rinses in 0.1M PB, followed by a 1 h incubation in AB solution (Vector Labs) and again rinsed. This was followed by a 5 min treatment of the sections in a solution consisting of 0.05% diaminobenzidine (DAB) in 0.1M PB, after which, and while still in the same solution, 3µl of 30% $H_2O_2$ per 1 ml of solution was added. With the aid of a low power stereomicroscope the staining was followed visually and allowed to continue until a level was reached where the background staining could assist in reconstruction without obscuring the immunopositive structures. Once this level was reached the reaction was stopped by placing the sections in 0.1M PB, followed by two 10 min rinses in 0.1M PB. All solutions used in the immunohistochemical process had a pH of 7.4. The immunohistochemically stained sections were mounted on 0.5% gelatine coated slides and left to dry overnight. The mounted sections were dehydrated by placing them in 70% alcohol for 2 h at room temperature under gentle shaking and then transferred through a series of graded alcohols, cleared in xylene and coverslipped with Depex.

The sections were observed with a low power stereomicroscope, and the architectonic borders traced according to the Nissl and myelin stained sections using a camera lucida. The corresponding immuno-stained sections were then matched to the drawings and the immuno-positive neurons (for ChAT, TH, 5-HT and orexin-A) and medium/high terminal networks (for orexin-A, 5-HT and histamine) were marked. The location and distribution of the immuno-positive neurons for parvalbumin, calbindin and

calretinin were described in relation to the previously identified nuclear groups of the cholinergic, catecholaminergic, serotonergic and orexinergic systems (Gravett et al., 2009, 2011). The drawings were scanned and redrawn with the aid of the Canvas 8 program.

### 6.3 Abbreviations

III – oculomotor nucleus

Vmot – trigeminal nucleus, motor division

3n – oculomotor nerve

3V – third ventricle

4n – trochlear nerve

5m – motor division of trigeminal nerve

5s – sensory division of trigeminal nerve

4V – fourth ventricle

A5 – fifth arcuate nucleus

A6d – locus coeruleus, diffuse portion

A7d – nucleus subcoeruleus, diffuse portion

A7sc – nucleus subcoeruleus, compact portion

A8 – retrorubral nucleus

A9 – substantia nigra

A9l – substantia nigra, lateral

A9m – substantia nigra, medial

A9pc – substantia nigra, pars compacta

A9v – substantia nigra, ventral

A10 – ventral tegmental area

A10c – ventral tegmental area, central

A10d – ventral tegmental area, dorsal

A10dc – ventral tegmental area, dorsal caudal

A11 – caudal diencephalic group

A12 – tuberal cell group

A13 – zona incerta

A14 – rostral periventricular nucleus

A15d – anterior hypothalamic group, dorsal division

A15v – anterior hypothalamic group, ventral division

APT – anterior pretectal nucleus

ac – anterior commissure

AD – anterodorsal nucleus of the dorsal thalamus

Amyg – amygdala

AV – anteroventral nucleus of the dorsal thalamus

B9 – supralemniscal serotonergic nucleus

C – caudate nucleus

ca – cerebral aqueduct

cic – commissure of the inferior colliculus

CL – central lateral thalamic nucleus

CLi – caudal linear nucleus

CM – central medial thalamic nucleus

CP – cerebral peduncle

csc – commissure of the superior colliculus

Diag.B – diagonal band of Broca

DLG – dorsal lateral geniculate nucleus

DRc – dorsal raphe nucleus, caudal division

DRd – dorsal raphe nucleus, dorsal division

DRif – dorsal raphe nucleus, interfascicular division

DRl – dorsal raphe nucleus, lateral division

DRp – dorsal raphe nucleus, peripheral division

DRv – dorsal raphe nucleus, ventral division

DTg – dorsal tegmental nucleus

EW – Edinger-Westphal nucleus

F – nucleus of the fields of Forel

f – fornix

fr – fasciculus retroflexus

GC – central grey matter

GI – gigantocellular reticular nucleus

GP – globus pallidus

Hbm – medial habenular nucleus

Hbl – lateral habenular nucleus

Hyp – hypothalamus

Hyp.d – dorsal hypothalamic cholinergic nucleus

Hyp.l – lateral hypothalamic cholinergic nucleus

Hyp.v – ventral hypothalamic cholinergic nucleus

IC – inferior colliculus

ic – internal capsule

IGL – intergeniculate leaflet

ILL – intermediate nucleus of the lateral lemniscus

IML – internal medullary lamina

IP – interpeduncular nucleus

Is.Call – island of Calleja

LDTpc – laterodorsal tegmental nucleus, parvocellular division

LDTmc – laterodorsal tegmental nucleus, magnocellular division

lfp – longitudinal fasciculus of pons

LL – lateral lemniscus

LP – lateral posterior thalamic nucleus

lp – lateral parabrachial nucleus

LT – lateral terminal nucleus of the accessory optic tract

LV – lateral ventricle

mcp – middle cerebellar peduncle

Mc – main orexinergic cluster

MD – mediodorsal thalamic nucleus

meV – mesencephalic trigeminal nucleus

MGB – medial geniculate body

ML – medial lemniscus

mlf – medial longitudinal fasciculus

MM – medial mammillary nucleus, medial part

MnR – median raphe nucleus

N.Acc – nucleus accumbens

N.Bas – nucleus basalis

oc – optic chiasm

OR – optic radiation

OT – optic tract

OTc – optic tract orexinergic cluster

P – putamen

PC – parvicellular reticular nucleus

PBg – parabigeminal nucleus

PIR – piriform cortex

Po – posterior thalamic nuclear group

PP – peripeduncular nucleus

PPT – posterior pretectal nucleus

PPTpc – pedunculopontine nucleus, parvocellular division

PPTmc – pedunculopontine nucleus, magnocellular division

PR – prerubral field

PrC – precommissural nucleus

PF – parafascicular thalamic nucleus

PVP – paraventricular thalamic nucleus, posterior part

py – pyramidal tract

R – thalamic reticular nucleus

Re – reuniens thalamic nucleus

Rmc – red nucleus, magnocellular division

RtTg – reticulotegmental nucleus of the pons

S – septal nuclear complex

SC – superior colliculus

SCN – suprachiasmatic nucleus

scp – superior cerebellar peduncle

Sep.L – lateral septal nucleus

Sep.M – medial septal nucleus

sm – stria medullaris of the thalamus

SON – supraoptic nucleus

SPO – superior olivary nuclear complex

SubB – subbrachial nucleus

TOL – olfactory tubercle

VA – ventral anterior thalamic nucleus

VLG – ventral lateral geniculate nucleus

Vmb – ventromedial basal thalamic nucleus

VPM – ventral posteromedial thalamic nucleus

VPL – ventral posterolateral thalamic nucleus

VPO – ventral pontine nucleus

xtz – decusation of the trapezoid body

xscp – decussation of the superior cerebellar peduncle

ZI – zona incerta

ZIC – zona incerta, caudal part

ZIc – zona incerta orexinergic cluster

## 6.4. Results

The aim of the present study was to reveal the locations, distributions and interactions of the neural systems controlling sleep/wake in the brain of the rock hyrax, *P. capensis*. This was achieved by immunohistochemical staining for cholineacetyltransferase (identification of cholinergic neurons), tyrosine hydroxylase (identification of catecholaminergic neurons), serotonin (identification of serotonergic neurons and terminal networks), orexin-A (identification of oerxinergic neurons and terminal networks), histamine (identification of histaminergic terminal networks) parvalbumin (identification of parvalbumin containing GABAergic interneurons and terminal networks), calbindin (identification of calbindin containing GABAergic interneurons and terminal networks) and calretinin (identification of calretinin containing GABAergic interneurons and terminal networks). The location of the GABAergic interneurons and terminal network distribution was described only in relation to the previously identified cholinergic, catecholaminergic, serotonergic and orexinergic nuclei, known to be involved in the regulation of the sleep-wake cycle, in the brain of the rock hyrax (Gravett et al., 2009, 2011, Chapters 2 and 3).

### *6.4.1. Cholinergic nuclei*

The cholinergic nuclei involved in sleep/wake in the brain of the rock hyrax were located in the basal forebrain, diencephalon and pontomesencephalon (Fig. 6.1) (Gravett

et al., 2009). These groups followed the general mammalian organizational plan for this system, however some novel features were observed that have not been described in other mammals, those being cholinergic neurons in the anterior nuclei of the dorsal thalamus, parvocellular and magnocellular divisions of the laterodorsal tegmental and pedunculopontine tegmental nuclei (Figs. 6.1 D and E, 6.6B, 6.9A) (Gravett et al., 2009).

The cholinergic neurons of the Islands of Calleja and the olfactory tubercle were located in the ventral most portion of the cerebral hemisphere at a level ventral to the nucleus accumbens. The medial septal nucleus was identified through the presence of ChAT+ neurons located within the septal nuclear complex in the rostral half of the medial wall of the cerebral hemisphere. The diagonal band of Broca was located anterior to the hypothalamus in the ventromedial corner of the cerebral hemisphere. ChAT+ neurons found ventral to the globus pallidus at the level of the anterior commissure, and caudal and dorsal to the olfactory tubercle were assigned to nucleus basalis (Fig. 6.1 A and B).

Within the diencephalon, the dorsal hypothalamic nucleus was located between the wall of the third ventricle and the fornix within the dorsomedial region of the hypothalamus. The ventral hypothalamic nucleus was identified as a cluster of palely stained, widely scattered ChAT+ neurons within the ventromedial aspect of the hypothalamus that extended ventrolaterally past the level of the fornix. Within the dorsolateral region of the hypothalamus, lateral to the fornix, a low density of palely stained ChAT+ neurons were identified as the lateral hypothalamic cholinergic nucleus (Fig 6.1 D and E) (Gravett et al., 2009). Within the anterior and dorsal region of the dorsal thalamus the anterodorsal nucleus (AD) was seen to exhibit a strong cholinergic neuropil staining. Around the margins of the AD nucleus a small number of scattered

ChAT+ neurons were observed. Lateral to the anterodorsal nucleus, the anteroventral nucleus (AV) exhibited a number of ChAT+ neurons along the upper medial and lateral borders, plus a much paler ChAT+ neuropil staining (Fig. 6.1 D and E, 6.6B).

In the pontomesencephalon cholinergic nuclei included the parabigeminal nucleus (PBg), the pedunculopontine tegmental nucleus (parvo- and magnocelluar divisions, PPTpc and PPTmc) and the laterodorsal tegmental nucleus (parvo- and magnocellular divisions, LDTpc and LDTmc) (Figs. 6.1 K-M, 6.9). A prominent parabigeminal nucleus was located ventral and slightly anterior to the inferior colliculus within the lateral aspect of the midbrain tegmentum.. Within the dorsal aspect of the isthmic and pontine tegmental regions, anterior to the trigeminal motor nucleus, a group of ChAT+ neurons was identified as the PPT. In contrast to other mammals studied, the morphology of the cholinergic neurons within this region was not homogenous, and we could readily identify magnocellular and parvocellular ChAT+ neurons within this region. The ChAT+ neurons assigned to the magnocellular PPT nucleus, PPTmc, were found medial and ventral to the superior cerebellar peduncle, and in the anterior portion were found to intermingle with the fibres of the superior cerebellar peduncle. In the more caudal aspects of the PPT, in a position dorsal and lateral to the magnocellular neurons, a moderately dense cluster of small ChAT+ interneurons, the PPTpc, was observed. The PPTpc nucleus was sometimes clearly distinguished from the PPTmc nucleus on topological grounds, as it was found lateral and dorsal to the superior cerebellar peduncle in the posterior aspect of the midbrain tegmentum; however, the size of the soma was the most reliable distinction between these two nuclei (Fig. 6.1 K and L). The LDT was identified as a moderate to high density of ChAT+ neurons within the ventrolateral region

of the pontine periventricular- and periaqueductal grey matter. The magnocellular division of the LDT, LDTmc, was located at the ventrolateral border of the pontine periventricular- and periaqueductal grey matter. The parvocellular division of the LDT, LDTpc, was found medial and dorsal to the magnocellular LDT nucleus, but still within the periventricular- and periaqueductal grey matter (Fig. 6.1 L and M) (Gravett et al., 2009).

### *6.4.2. Catecholaminergic nuclei*

The catecholaminergic nuclei involved in the sleep-wake cycle were located within the diencephalic and pontine regions of the brain and consisted of: the dorsal division of the anterior hypothalamic nucleus (A15d); the ventral division of the anterior hypothalamic nucleus (A15v); the rostral periventricular nucleus (A14); the zona incerta (A13); the tuberal nucleus (A12); and the caudal diencephalic nucleus (A11); and the locus coeruleus complex. The A15d nucleus was located between the third ventricle and the fornix within the anterior portion of the hypothalamus. The A15v nucleus was located near the floor of the brain adjacent to the optic tracts within the ventrolateral region of the hypothalamus. A moderate density of TH+ neurons close to wall of the third ventricle throughout the hypothalamus was identified as the A14 nucleus. The A13 nucleus was identified as a moderate density of TH+ neurons located within the dorsal and lateral regions of the hypothalamus, lateral to the fornix, extending into and around the zona incerta in the ventral thalamus. In the ventral portion of the hypothalamus, within and in close proximity to the arcuate nucleus, a low to moderate density of TH+ neurons was identified as the A12 nucleus. Around the posterior pole of the third ventricle, in the most

caudal part the hypothalamus, a low density of TH+ neurons arranged in columns on either side of the midline was identified as the A11 nucleus (Fig. 6.1 A-H).

A7sc (the subcoeruleus compact nucleus) was located within the dorsal region of the pontine tegmentum adjacent to the periventricular grey matter. TH+ neurons ventrolateral to A7sc, anterior to the trigeminal motor nucleus, in the lateral and dorsolateral region of the pontine tegmentum were assigned to the A7d (subcoeruleus diffuse nucleus) nucleus. Some of the TH+ neurons assigned to A7d were also located medial and ventral to the superior cerebellar peduncle. Only a small number of TH+ neurons were located within the ventrolateral portion of the periventricular grey matter adjacent to the A7sc, and these were identified as A6d (locus coeruleus diffuse nucleus) (Fig. 6.1 M and D) (Gravett et al., 2009).

*6.4.3. Serotonergic nuclei*

The serotonergic nuclei in all eutherian mammals are typically divided into a rostral and caudal cluster (e.g. Törk, 1990). The serotonergic nuclei associated with sleep/wake states are mainly located within the rostral cluster and included the caudal linear nucleus (CLi), the supralemniscal nucleus (B9), the median raphe nucleus (MnR) and the dorsal raphe nuclear complex (DR). A moderate density of 5HT+ neurons was located immediately dorsal to the interpeduncular nucleus, and anterior to the decussation of the superior cerebellar peduncle in the ventral midline of the midbrain tegmentum was designated as the caudal linear nucleus (CLi) (Fig. 6.1 J and K). The B9 nucleus was identified as a loosely packed arc of 5HT+ neurons, lateral to the interpeduncular nucleus and caudal to the A9pc nucleus. This nucleus was located superior to the medial

lemniscus and was found to be continuous with the ventrolateral neurons of the CLi nucleus (Fig. 6.1 J and K). In a pararaphe position, two densely packed columns of 5HT+ neurons, extending dorsal to ventral along the midbrain and pontine tegmentum, were identified as the MnR nucleus. The neurons forming this nucleus extended from the caudal aspect of the superior cerebellar peduncle to the level of the anterior most aspect of the trigeminal motor nucleus (Fig. 6.1 K and L).

A dense cluster of 5HT+ neurons within the most ventral medial portion of the periaqueductal grey matter, between the two medial longitudinal fasciculi, was identified as the DRif nucleus (interfascicular division of the dorsal raphe) (Fig. 6.1 K and L). Immediately dorsal to the DRif nucleus and caudal to the oculomotor nerve nuclei, a high density of 5HT+ neurons was identified as the DRv nucleus (ventral division of the dorsal raphe). The DRd nucleus (dorsal division of the dorsal raphe) was identified as a high density of 5HT+ neurons located ventral to the inferior border of the cerebral aqueduct and immediately dorsal to the DRv nucleus. A very low density of 5HT+ neurons located lateral to the DRd and DRv nuclei, anterior to the ChAT+ neurons of the LDT, in the ventrolateral portion of the periaqueductal grey matter was identified as the DRp nucleus (peripheral division of the dorsal raphe). In the adjacent midbrain tegmentum, a small number of 5HT+ neurons forming part of the DRp nucleus were observed. Adjacent to the ventrolateral edge of the cerebral aqueduct, in a position dorsolateral to the DRd nucleus, a group of 5HT+ neurons were assigned to the DRl nucleus (lateral division of the dorsal raphe. An arc of 5HT+ neurons across the dorsal midline of the periventricular grey matter, where the cerebral aqueduct opens into the fourth ventricle, formed by the caudal coalescence of the two lateralized clusters of the

DRl nucleus, was identified as the DRc nucleus (lateral division of the dorsal raphe) (Gravett et al., 2009) (Fig. 6.1 K-M).

*6.4.4. Orexinergic nuclei*

Orx+ neurons were identified mainly within the hypothalamus of the brain of the rock hyrax. These neurons were grouped into three distinct clusters; the main cluster (Mc), the zona incerta cluster (ZIc) and the optic tract cluster (OTc). The main cluster was identified as a large group of dense Orx+ neurons located lateral to the third ventricle in the perifornical region, with a large number of neurons extending medially from this area, as well as into the dorsomedial and lateral hypothalamic areas. The majority of Orx+ neurons belonged to this cluster. From the main cluster a group of Orx+ neurons extended laterally into the region of the zona incerta which was termed the zona incerta cluster. The third cluster extended ventrolaterally from the main cluster to the ventrolateral region of the hypothalamus adjacent to the optic tract (Gravett et al., 2011) (Fig. 6.1 D and E).

*6.4.5. Serotonergic terminal networks related to the sleep-wake nuclei*

A serotonergic terminal network distribution of medium density was observed projecting to all the cholinergic sleep related nuclei (see above) except for PPTpc and PPTmc where the 5HT+ terminal network was found to be very low in density (Fig. 6.1 K and L). Most of the catecholaminergic sleep nuclei were coincident with a medium density serotonergic terminal network distribution with the exception of the A7d, A7sc and A15d nuclei. The density of the serotonergic terminal networks in the region of the

subcoeruleus (A7) was found to be low to absent, whereas the serotonergic terminal network coincident with the A15d nucleus was found to be high-density around the neurons located closest to the third ventricle and medium-density around those extending laterally from the third ventricle. A medium-density serotonergic terminal network distribution was also noted in the region of the three orexinergic nuclei (Fig. 6.1 A-N, 6.2).

*6.4.6. Orexinergic terminal networks related to the sleep-wake nuclei*

Orexinergic terminal networks of medium density were found projecting to the basal forebrain and pontomesencepalic cholinergic nuclei, with the exception of PPTpc and PPTmc, where a low to very low-density orexinergic terminal network was observed (Fig. 6.1 K and L). A high density of orexinergic terminal networks was evident in the areas surrounding the third ventricle while the areas extending laterally from the ventricle and thus the majority of the hypothalamus received a medium density of orexinergic terminal networks (this gradient of density was coincident with all cholinergic, catecholaminergic and orexinergic nuclei found within the hypothalamus). The pontine catecholaminergic A6d and A7d nuclei were coincident with a medium density orexinergic terminal network, while the A7sc was coincident with a low-density orexinergic terminal network. Serotonergic nuclei coincident with orexinergic terminal networks of medium density included the MnR, DRl, CLi nuclei, the medial half of the B9 nucleus and the part of the DRc nucleus that extended laterally from the midline (Fig. 6.1 A-N) A high density of orexinergic terminal networks was observed in the midline of the pontine region and encapsulated the serotonergic DRc, DRd, DRv, and DRif nuclei.

The only serotonergic sleep related nucleus coincident with a low-density orexinergic terminal network was DRp (Fig. 6.1 K-M, 6.3, 6.6C).

*6.4.7. Histaminergic terminal networks related to the sleep-wake nuclei*

A medium density histaminergic terminal network was observed in the regions where the basal forebrain, diencephalic and pontomesencaphalic (excluding PPTpc and PPTmc) cholinergic nuclei were found. Within both divisions of the PPT a low-density to near absent histaminergic terminal network was observed. Areas of high density histaminergic terminal networks overlapping the cholinergic sleep related nuclei included the dorsal and ventral hypothalamic cholinergic nuclei, and parts of LDTpc closest to the midline. A mixture of both medium and high-density histaminergic terminal networks were observed in the areas coincident with the diencephalic catecholaminergic sleep related nuclei. Medium densities were coincident with the A11 and A13 nuclei and the lateral parts of the A15d nucleus. High densities were observed overlapping the A11 at the level of the fasciculus retroflexus, A12, A14, A15v nuclei, and the part of the A15d nucleus that was located closest to the ventricle. Within the pontine region a predominantly medium to low density histaminergic terminal network was seen. A medium density network was observed overlapping the majority of the A6d nucleus, but a high density was observed in the rostral portion of this nucleus. A low to absent histaminergic terminal network distribution was observed in the A7d and A7sc nuclei.

Serotonergic nuclei coincident with a medium density histaminergic terminal network included the B9, CLi, DRl, MnR (only part of this nucleus immediately dorsal to the interpeduncular nucleus), DRif nuclear groups and the lateral parts of the DRd, DRv,

and DRc nuclei. High density histaminergic terminal networks were observed overlapping the DRc (part located closest to the fourth ventricle) and the DRd and DRv nuclei (parts located closest to the midline). The medial half and dorsolateral region of the main cluster of orexinergic immunoreactive neurons were located in a region of high density histaminergic terminal networks while the ventrolateral region was in a region of medium density. A high density histaminergic terminal network was seen overlapping the medial two thirds of the zona incerta cluster while the remaining third of this cluster as well as the optic tract cluster were coincident with a medium density terminal network (Fig. 6.1 A-N, 6.4).

*6.4.8. GABAergic inhibitory interneurons related to the sleep-wake nuclei*

The location and distribution of the calcium binding inhibitory interneurons, containing parvalbumin (PV), calbindin (CB) and calretinin (CR), as well as their terminal network distribution in relation to the previously identified sleep related nuclei was been identified. This was done to examine the extent of the inhibitory actions produced by these GABAergic interneurons on the nuclei known to be involved in the regulation of the sleep-wake cycle. Inhibitory interneurons were found throughout all regions of the brain of the rock hyrax. Parvalbumin was found to be very specific in its distribution compared to calbindin and calretinin that generally showed a more global and homogenous distribution. These interneurons were all small, oval shaped and mostly bipolar, showing the typical appearance of GABAergic inhibitory interneurons (Table 6.1).

*6.4.8.1. GABAergic interneurons and the cholinergic system*

A low to moderate number of PV+ cells were seen in the regions of the Island of Calleja and the olfactory tubercle, but a strong PV+ terminal network was observed. No CB+ containing cells were observed within the Islands of Calleja, however within the areas surrounding this nucleus a moderate density of CB+ cells as well as a strong CB+ terminal network was noted. A moderate to high density of evenly distributed CR+ cells and a moderate CR+ terminal network was observed in the areas overlapping the Island of Calleja and the olfactory tubercle (Fig. 6.5). A few PV+ stained cells accompanied by a strongly labeled PV+ terminal network was seen in the areas overlapping the medial septal nucleus. Very few CB+ stained cells were observed in the medial septal region and the terminal network distribution was also far weaker than that observed for PV+. A moderate number of CR+ cells, accompanied by a strong CR+ terminal network, were associated with the medial septal nucleus. A low number of PV+ cells, but a strong PV+ terminal network, were observed in the region of the diagonal band of Broca. Within this region CB+ and CR+ cells had similar densities and terminal network densities as that described for PV. The areas coincident with the nucleus basalis exhibited few to no PV+ cells and a PV+ terminal network of low density. CB+ cells were moderate to low in this region and a moderate density CB+ terminal network was observed. A low number of CR+ cells and low density CR+ terminal network was noted in the region of the nucleus basalis (Table 6.1).

Numerous PV+ cells, accompanied by a dense PV+ terminal network were noted within the AD and AV nuclei where the ChAT+ neurons were located. Within the ventrolateral part of the AD nucleus no ChAT+ neurons were observed, however a

moderate number of PV+ cells and a moderate density terminal networks was noted. A dorsomedial band of CB+ cells accompanied by a moderate to high density terminal network was noted throughout the AD nucleus. Scattered CB+ cells and a low density terminal network were seen throughout the AV nucleus. A mixture of both intensely and weakly stained CB+ cells within the ventrolateral half of both the AD and AV nuclei were observed. The location and density of CR+ cells within the AD nucleus was similar to that described for CB. Within the AV nucleus very few to no CR+ cells and a low density CR+ terminal network was noted (Fig. 6.6 D-F). No PV+ cells or PV+ terminal networks were observed in any of the hypothalamic cholinergic nuclei. A moderate density of CB+ cell accompanied by intensely stained CB+ terminal networks were seen overlapping all of the hypothalamic cholinergic nuclei, whereas a moderate density of CR+ cells and medium density CR+ terminal network was observed (Table 6.1).

No PV+ cells or terminal networks were seen in the areas overlapping the PPT and LDT nuclei. A moderate number of CB+ cells and a moderate density CB+ terminal network were observed in the region of the PPT and LDT, whereas a slightly lower number of CR+ cells and low to moderate density CR+ terminal network was observed. No distinction with regard to cell number and terminal network densities for both CB and CR could be made between the parvo- and magnocellular divisions of both the PPT and LDT (Fig. 6.9). No PV+ cells or terminal networks were seen the region overlapping the PBg nucleus. A moderate number of CB+ cells and a moderate density CB+ terminal network were observed in this region. The number of CR+ cells was slightly less than that observed for CB, and the density of the CR+ terminal network was also slightly less dense than the CB+ terminal network (Table 6.1).

*6.4.8.2. GABAergic interneurons and the catecholaminergic system*

No PV+ cells or terminal networks were observed in the areas coincident with the hypothalamic catecholaminergic nuclei. A moderate density of CB+ cells and a high density CB+ terminal network was observed throughout the hypothalamus, whereas a moderate density of CR+ cells and a moderate density CR+ terminal network was observed. No PV+ cells, but a low-density PV+ terminal network were observed to overlap with the locus coeruleus complex. No CB+ cells were seen within the A6d nucleus, but in the areas immediately surrounding this nucleus a high density of CB+ cells were noted and a high density CB+ terminal network was seen within this nucleus. A moderate to high number of CB+ cells were found intermingled with the cells of the A7 nucleus and a high-density CB+ terminal network was observed. A moderate to high density of CR+ cells terminal network projections were observed throughout the entire locus coeruleus complex (Table 6.1, Figs 6.7 and 6.10)

*6.4.8.3. GABAergic interneurons and the serotonergic system*

No PV+ cells were observed in any of the regions overlapping the locations of the serotonergic nuclei. A very low PV+ terminal network was observed in the regions overlapping the CLi and B9 nuclei. A number of PV+ cells that were seen lateral to CLi did not appear to project into this nucleus. A moderate to high density of CB+ cells and terminal networks were seen overlapping all the areas corresponding to the serotonergic nuclei. A low to moderate density of CR+ cells and terminal networks were observed in the regions overlying the DRl and DRp nuclei. Within the regions overlapping the DRd, DRv and DRif nuclei a very low number of CR+ cells and a low density CR+ terminal

network was observed. A moderate number of CR+ cells and moderate density CR+ terminal network was observed coincident with the CLi and B9 nuclei. A moderate to high number of CB+ cells and a moderate to high density CB+ terminal networks were observed in the region of both the DRc and MnR nuclei, whereas a low to moderate number of CR+ cells and low to moderate density CR+ terminal network was observed (Table 6.1, Fig. 6.8).

*6.4.9.4. GABAergic interneurons and the orexinergic system*

No PV+ cells or terminal networks were observed in the areas coincident with the hypothalamic orexinergic sleep related nuclei. A moderate density of CB+ and CR+ cells were observed throughout the hypothalamus and were coincident with the distribution of the orexinergic neurons. A high-density CB+ terminal network and a moderate-density CR+ terminal network were seen in these areas (Table 6.1).

**Figure 6.1:** Diagrammatic reconstructions of a series of coronal sections through the brain of the rock hyrax illustrating from left to the right the architectonic subdivisions (based on Nissl and myelin staining), location of cholinergic immunoreactive neurons, catecholaminergic neurons, serotonergic neurons and terminal networks, orexinergic neurons and terminal networks and histaminergic terminal networks. Each dot represents a single immunoreactive neuron. Areas shaded black indicate high-density terminal networks and areas shaded grey indicate medium-density terminal networks. Drawing **A** represents the most rostral section, **N** the most caudal. The coronal sections are approximately 1 mm apart. See list for abbreviations.

**A**

## Architecture

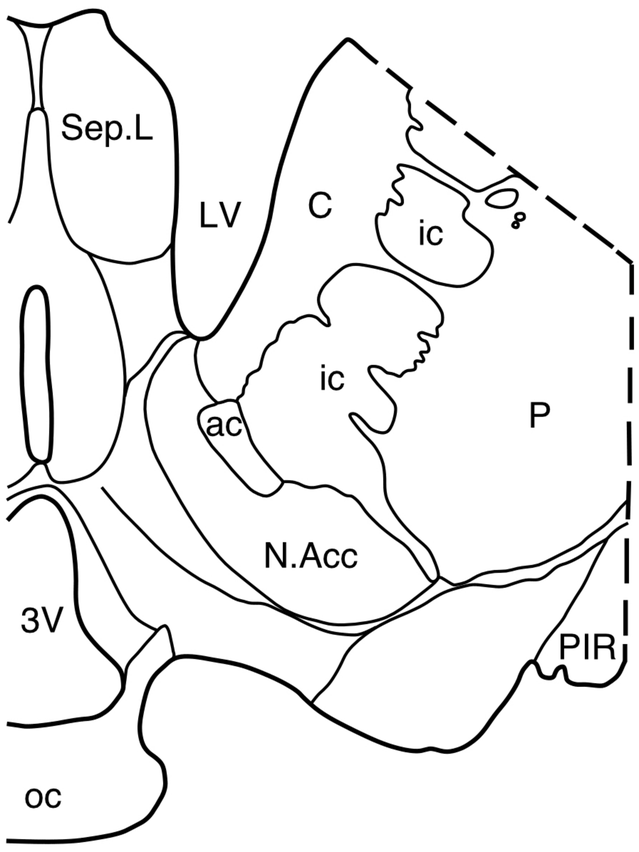


## Cholinergic

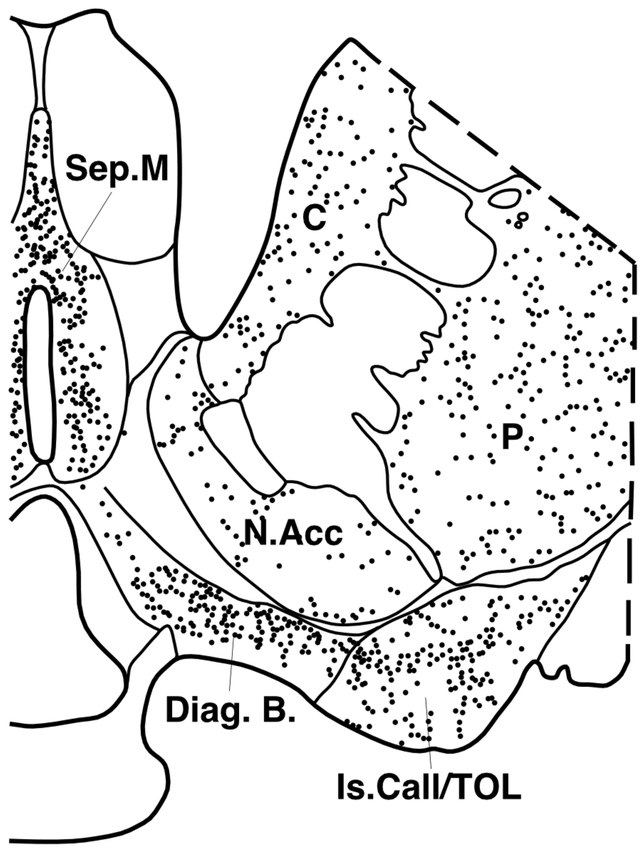


## Catecholaminergic

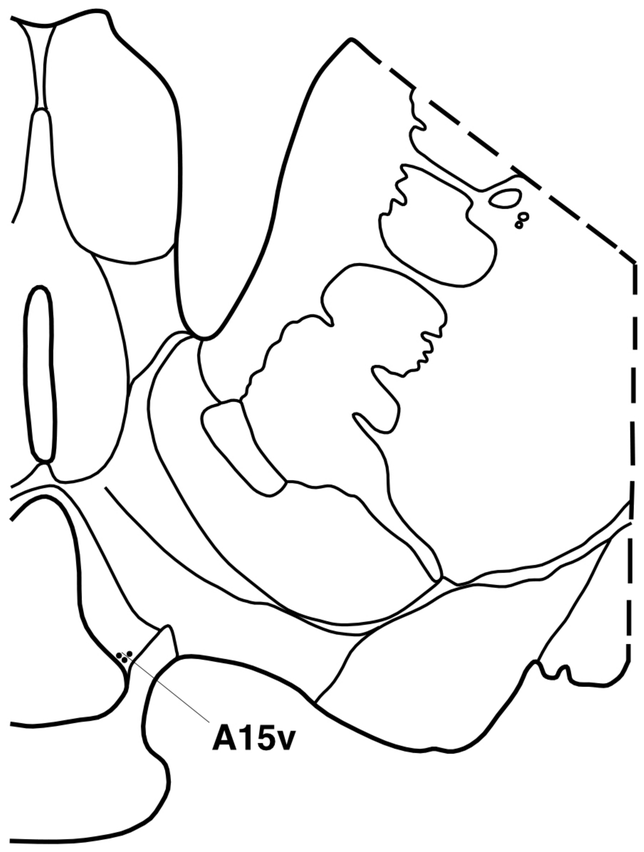


1mm

## Serotonergic

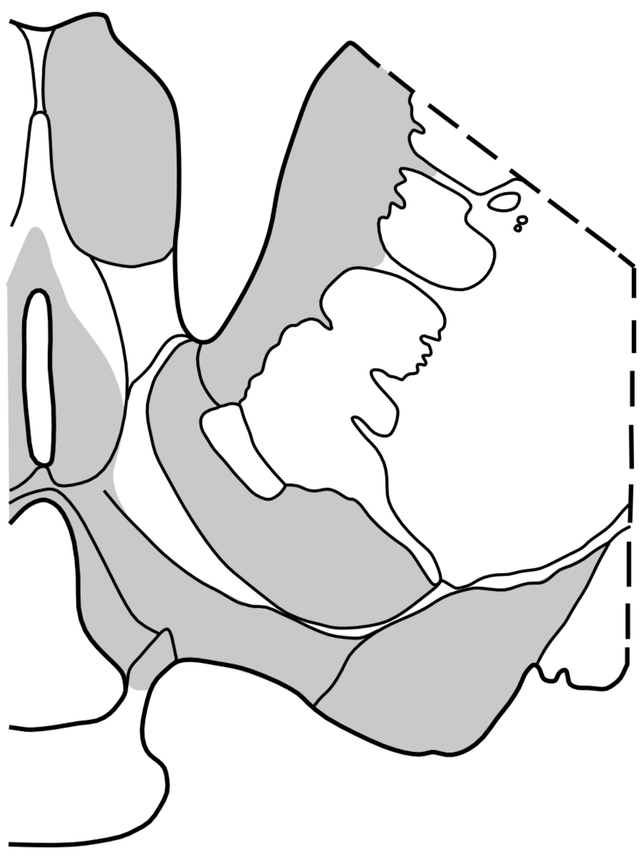

## Orexinergic

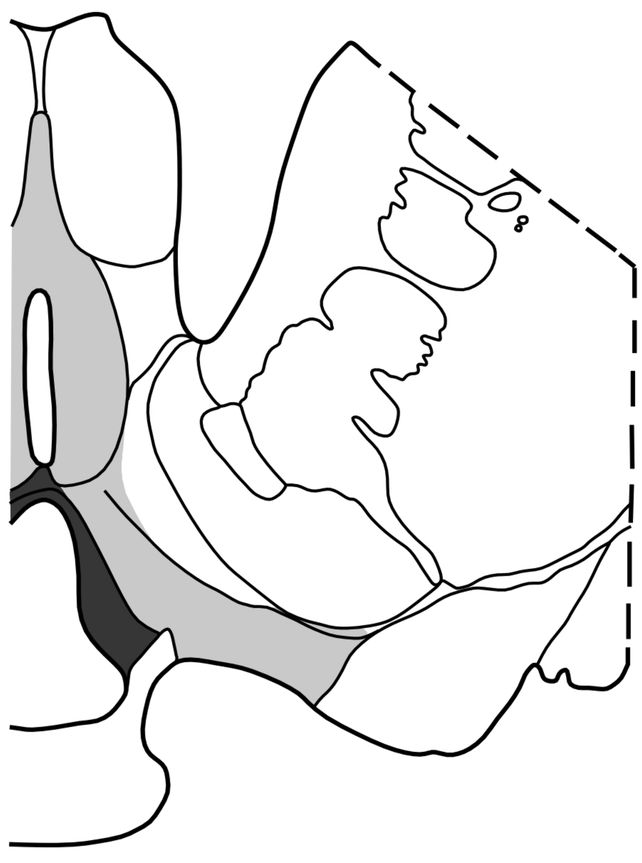

## Histaminergic

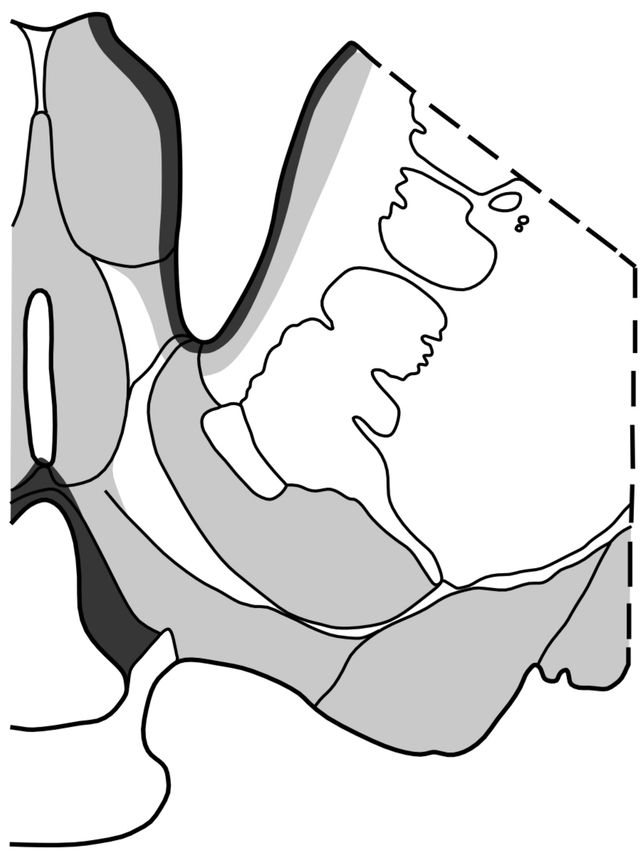

**B**

## Architecture

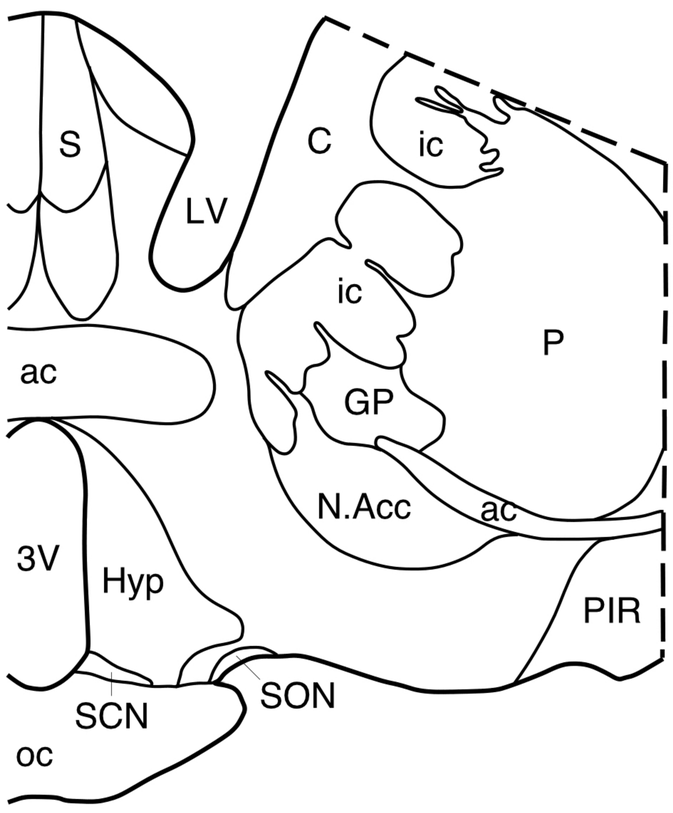


## Cholinergic

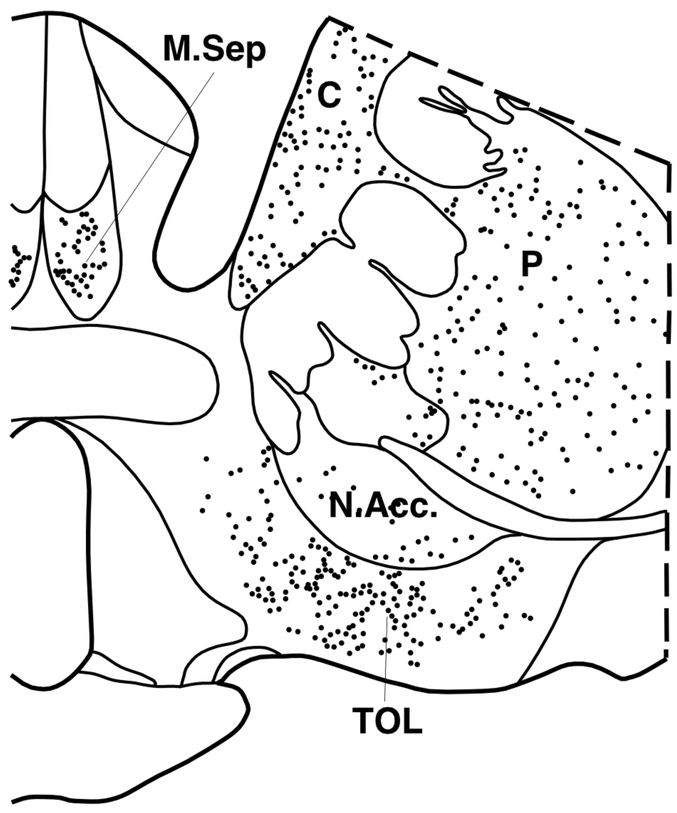


## Catecholaminergic

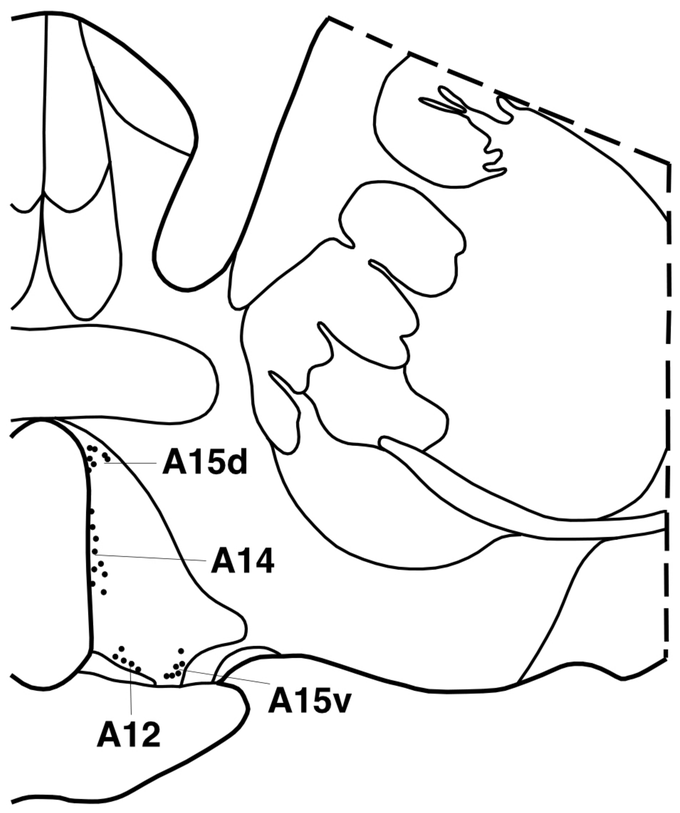


1mm

## Serotonergic

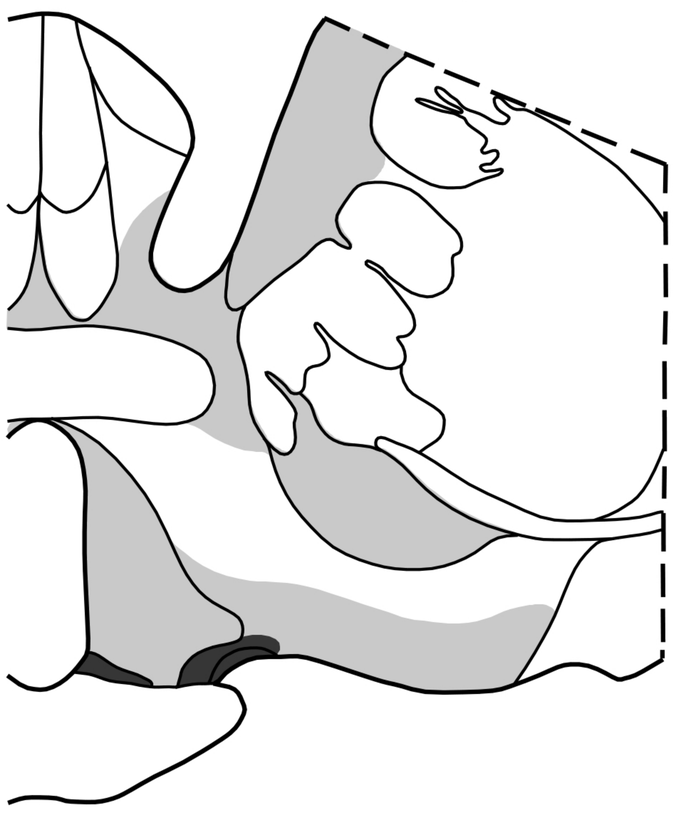

## Orexinergic

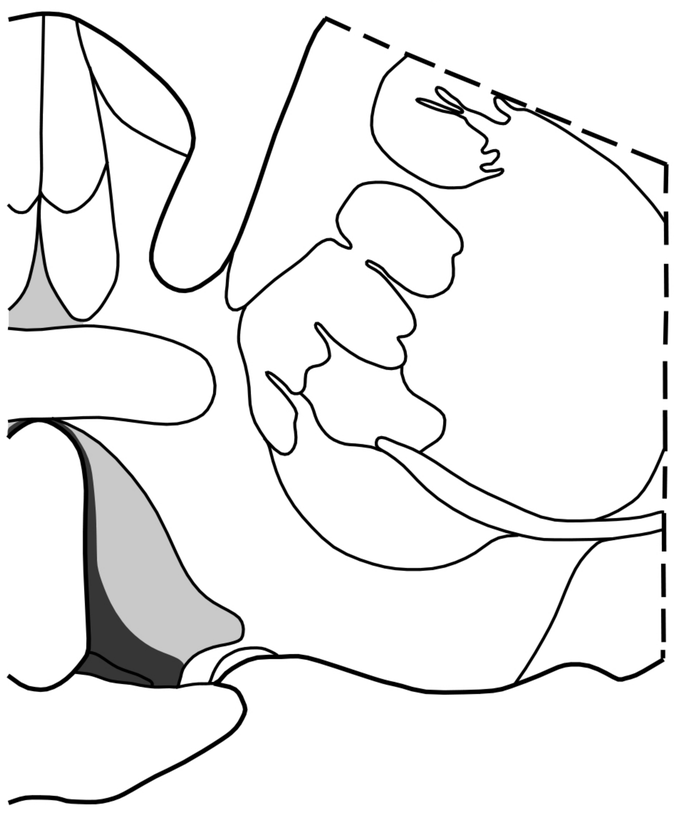

## Histaminergic

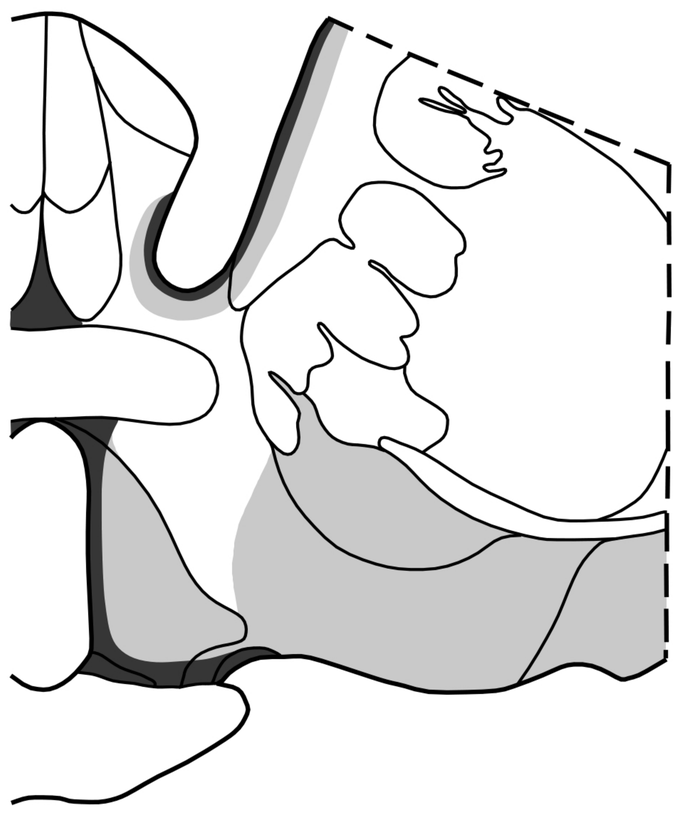

**C**

Architecture

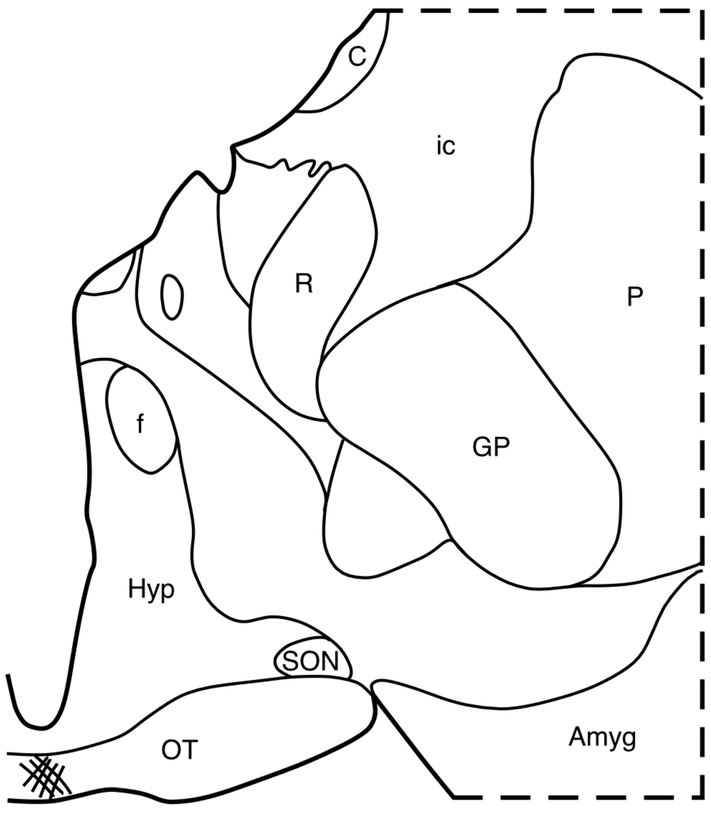


Cholinergic

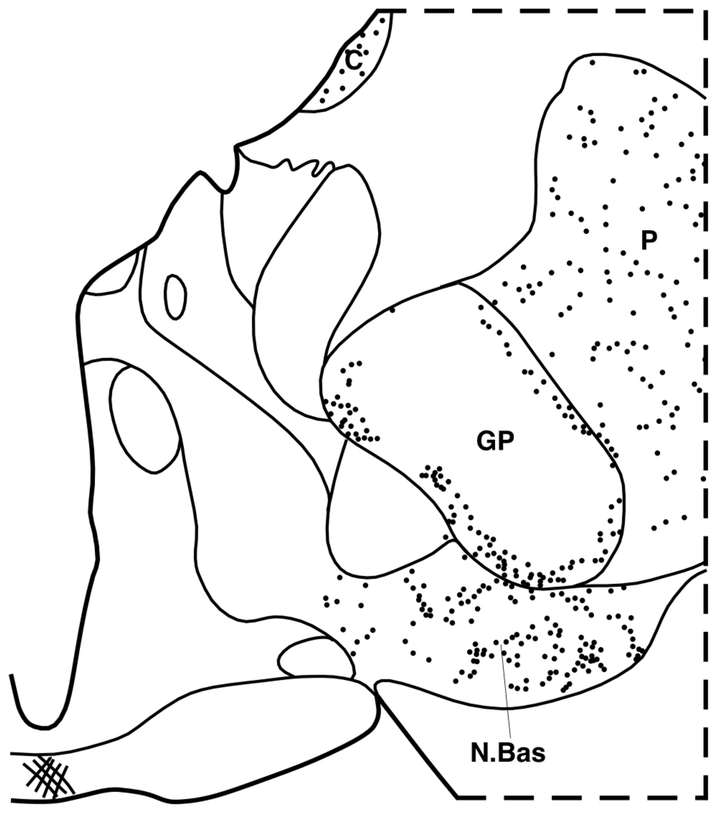


Catecholaminergic

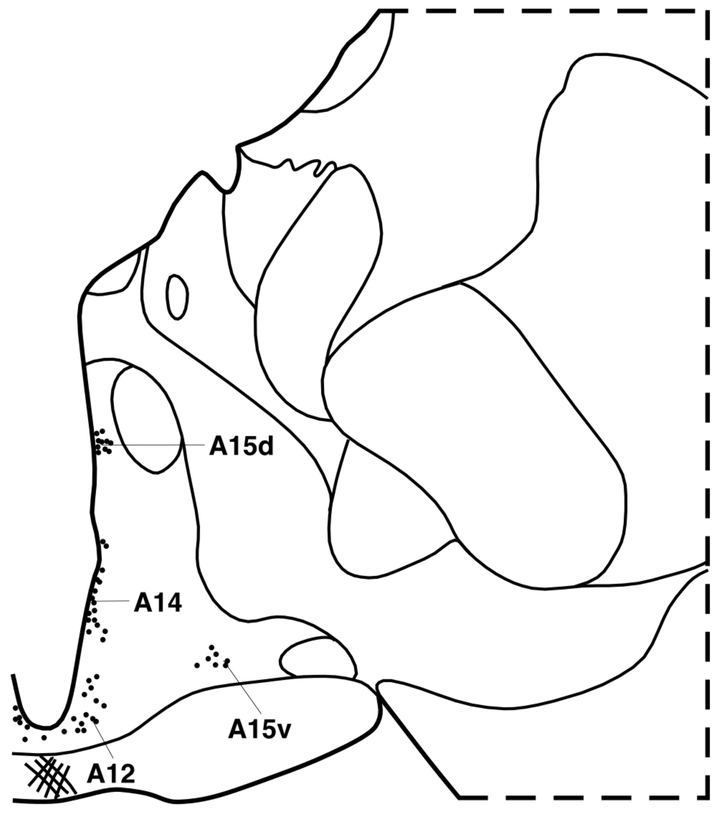


1mm

Serotonergic

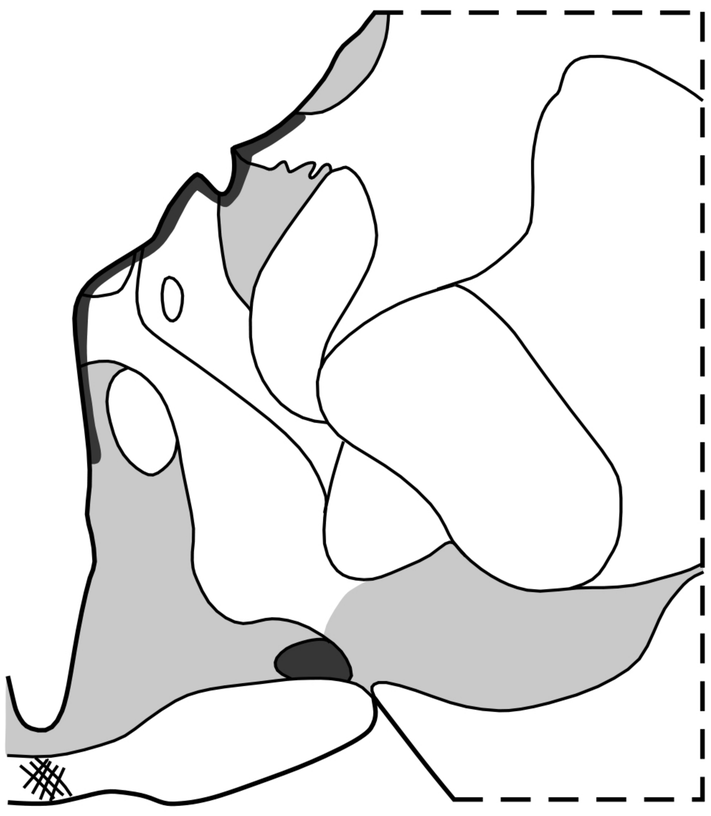

Orexinergic

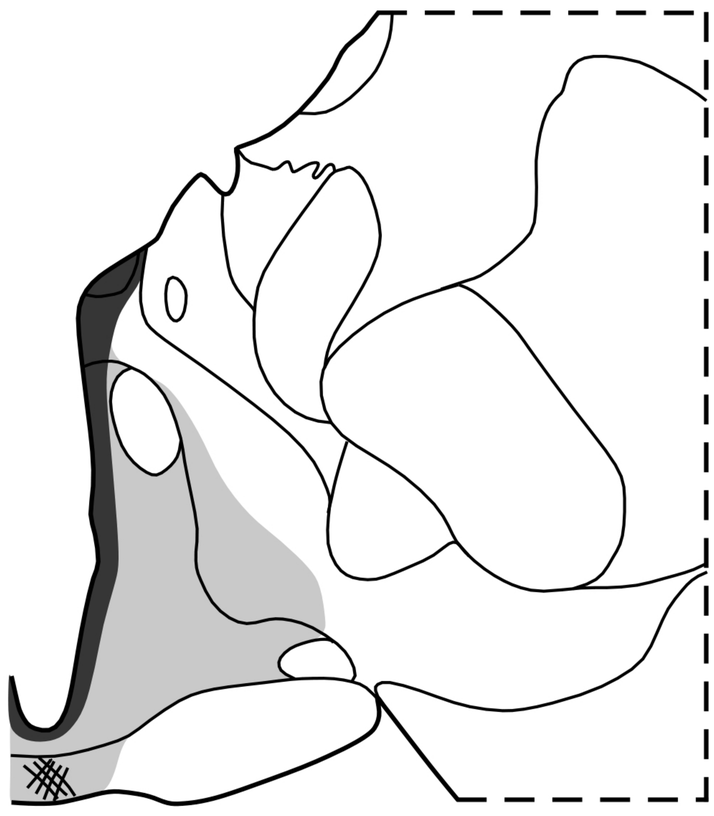

Histaminergic

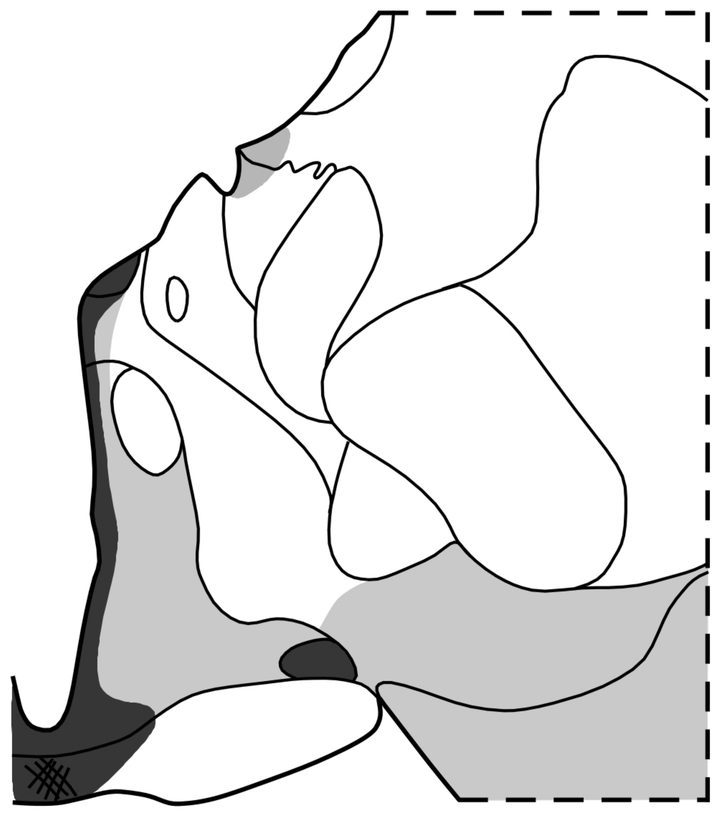

**D**

Architecture

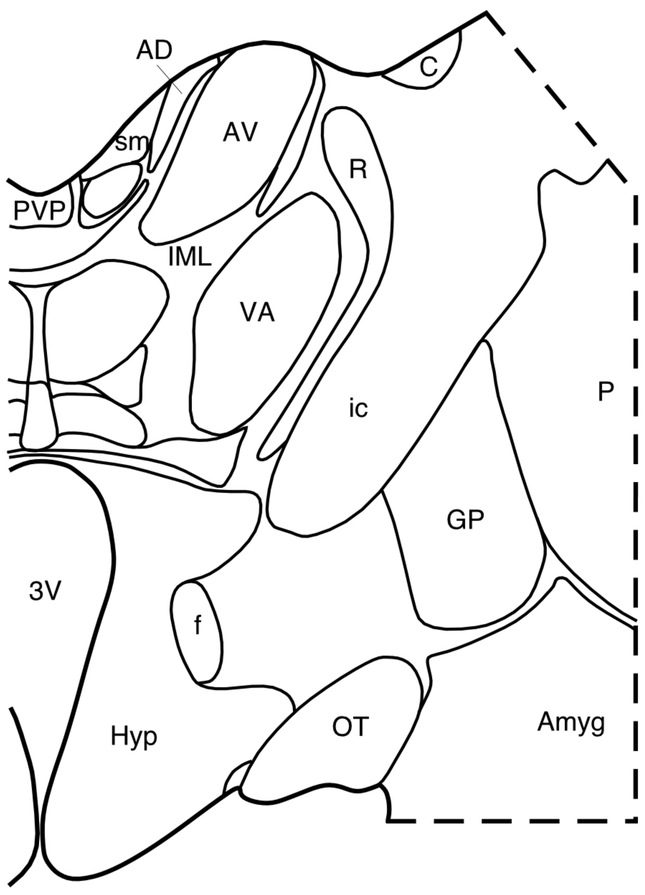


Cholinergic

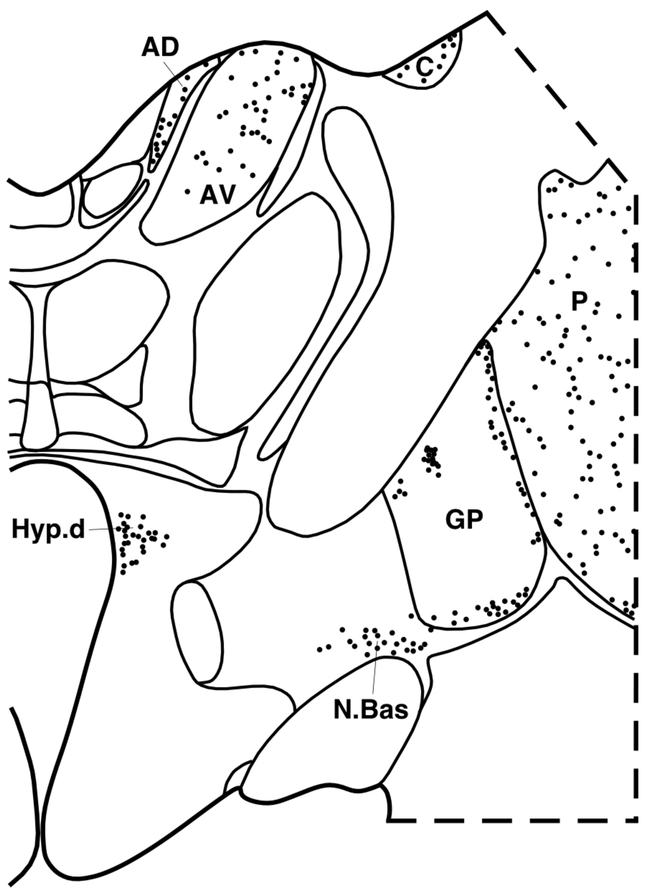


Catecholaminergic

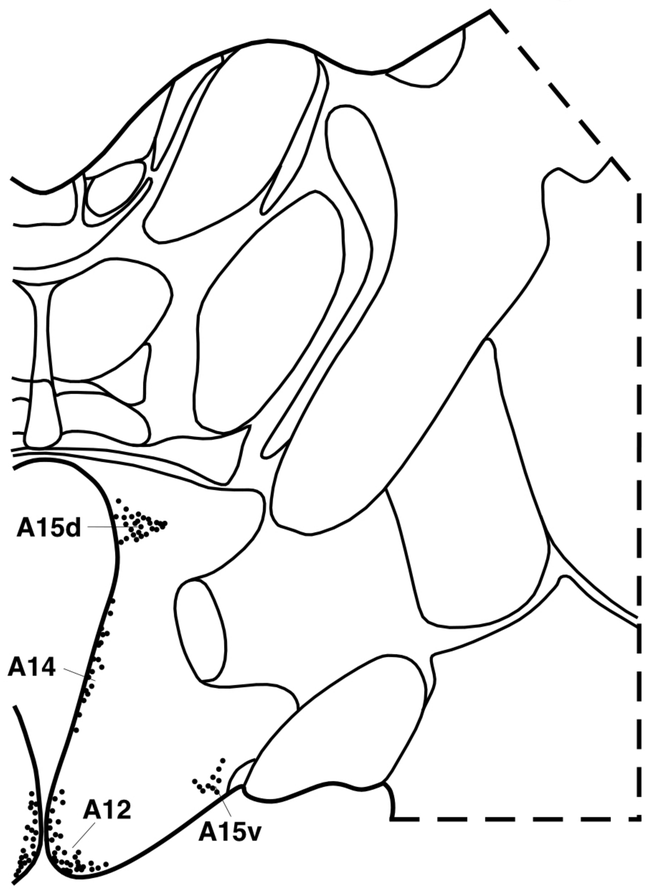


1mm

Serotonergic

Orexinergic

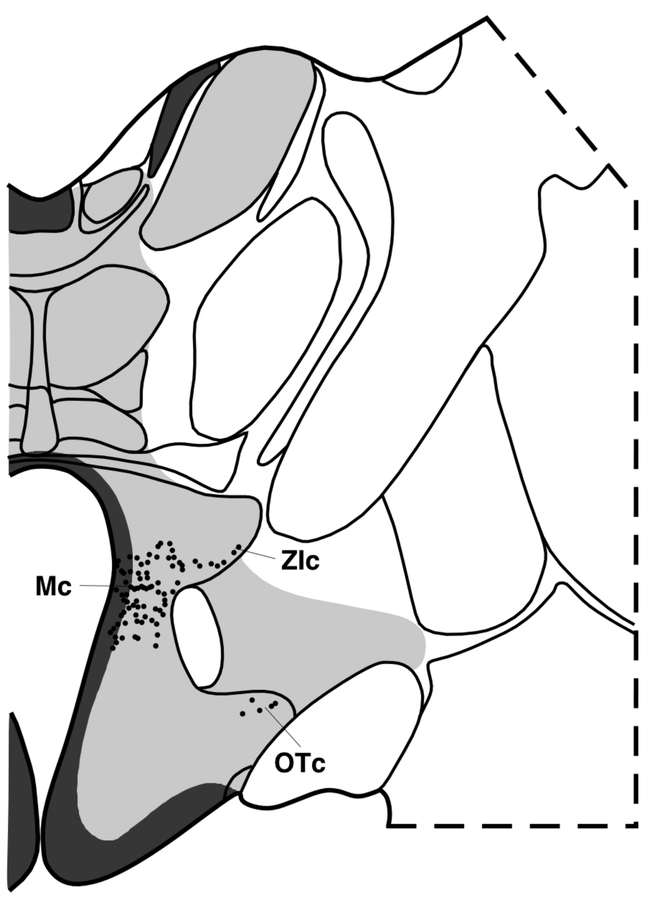


Histaminergic

**E**

## Architecture

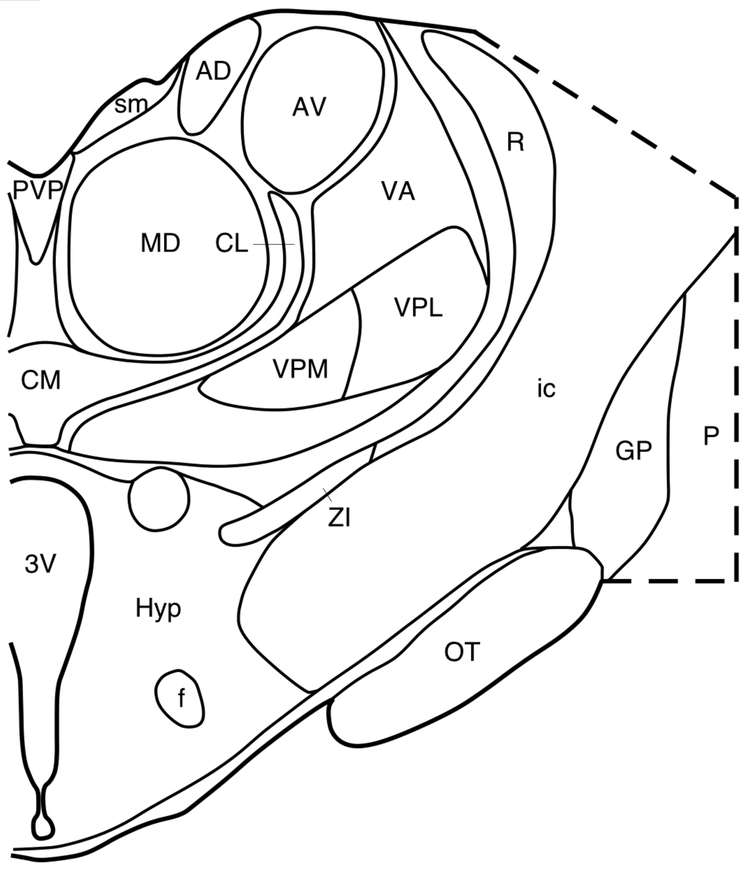


## Cholinergic

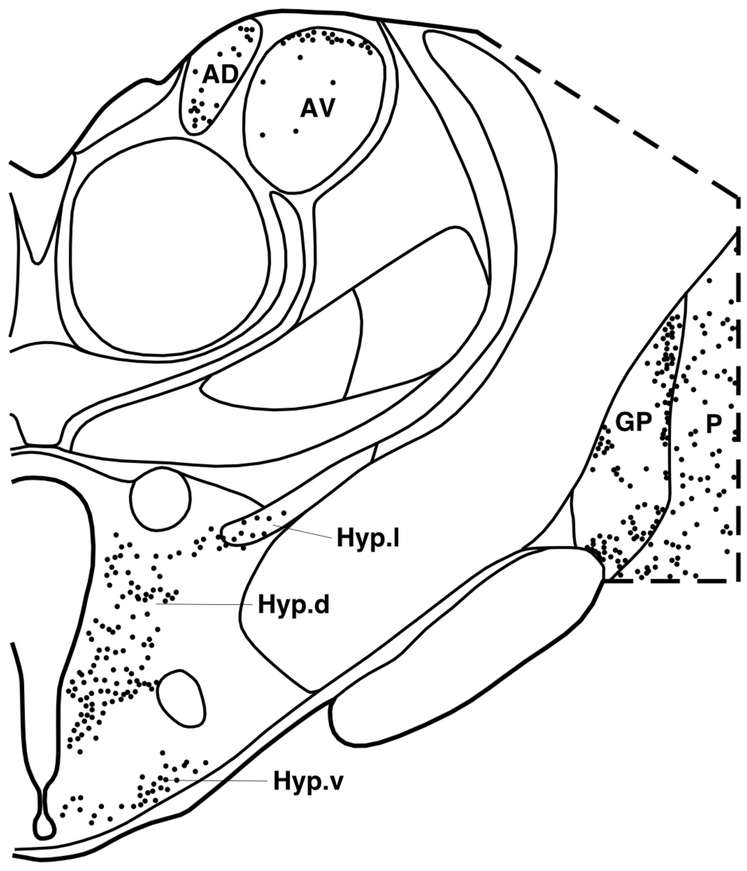


## Catecholaminergic

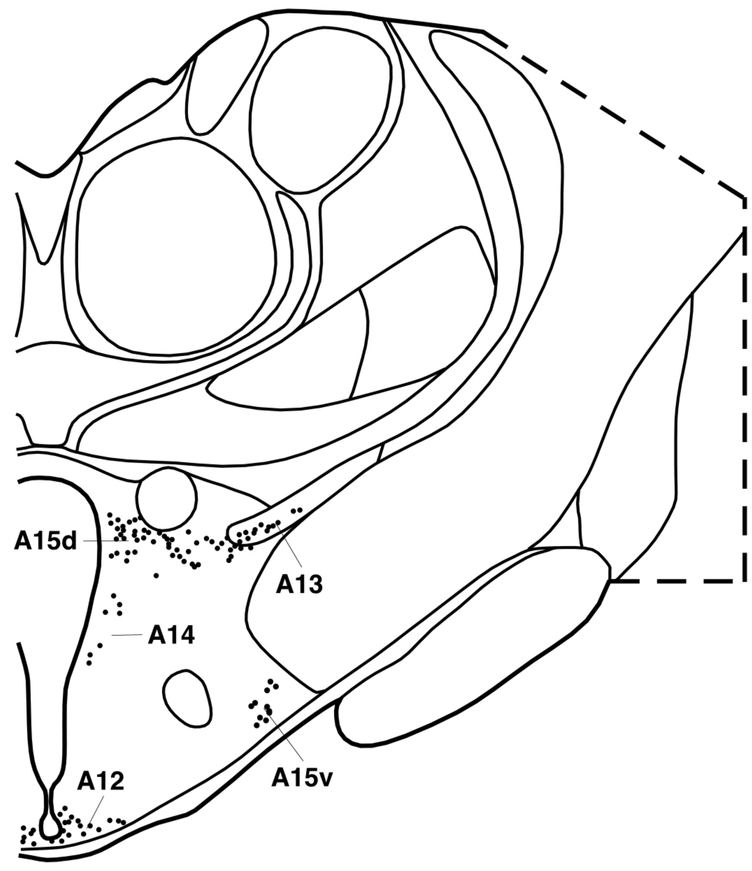


## Serotonergic

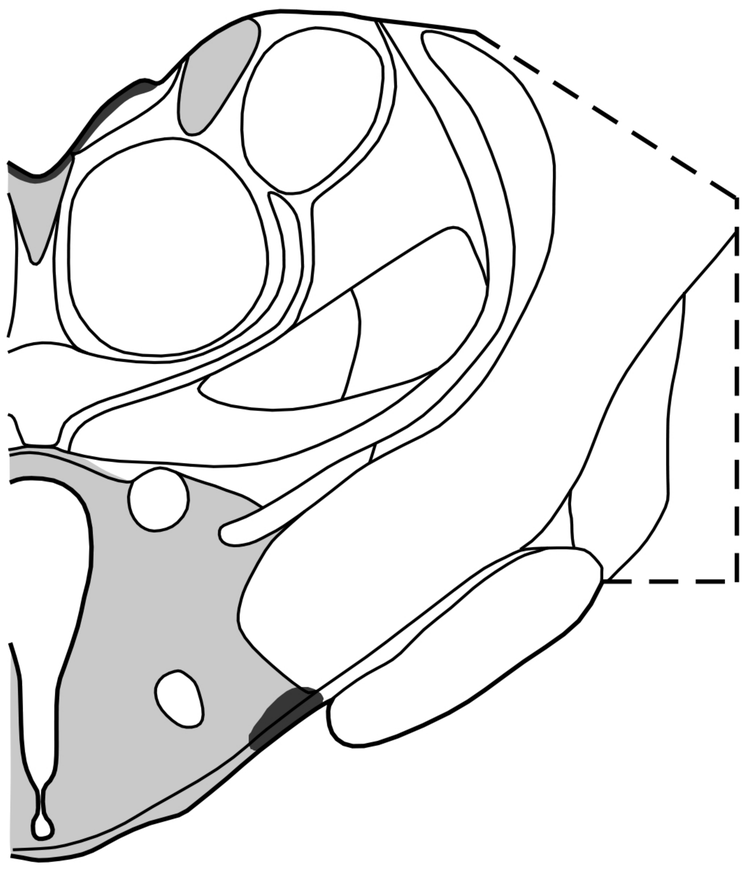

## Orexinergic

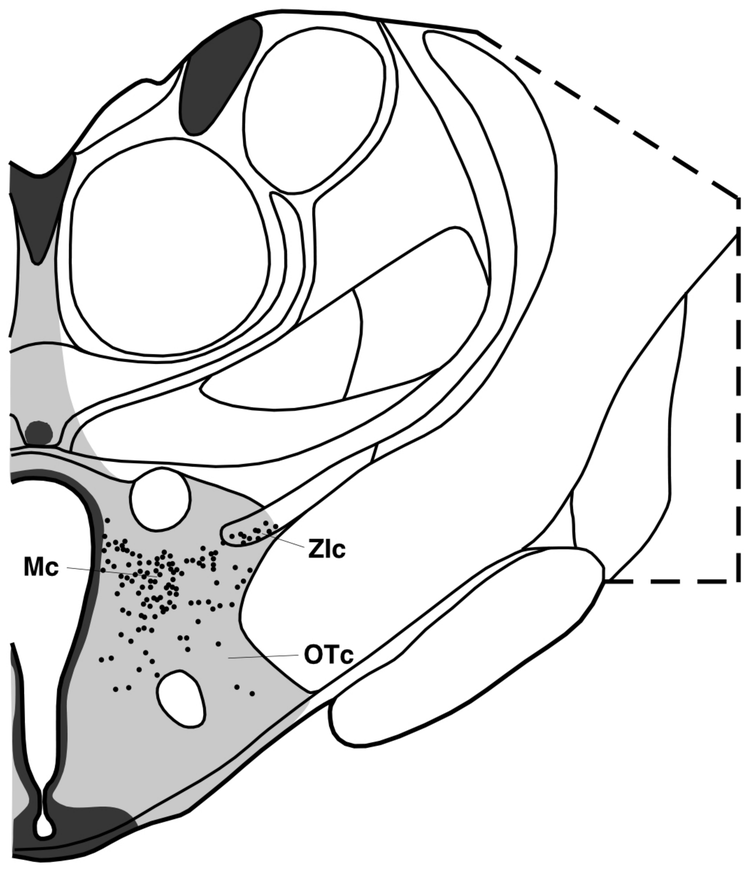


## Histaminergic

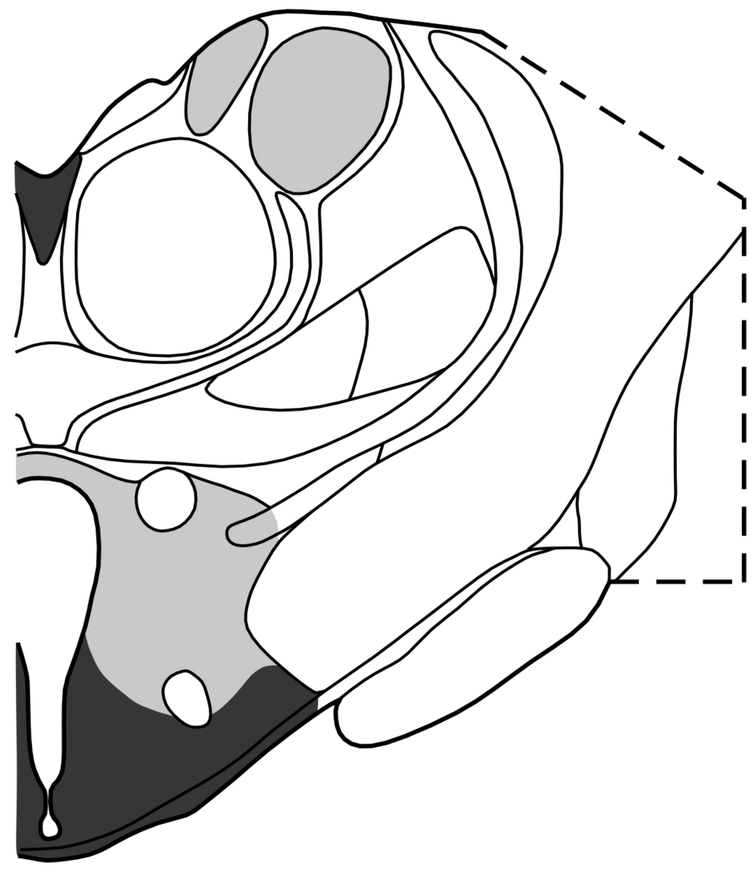

**F**

## Architecture

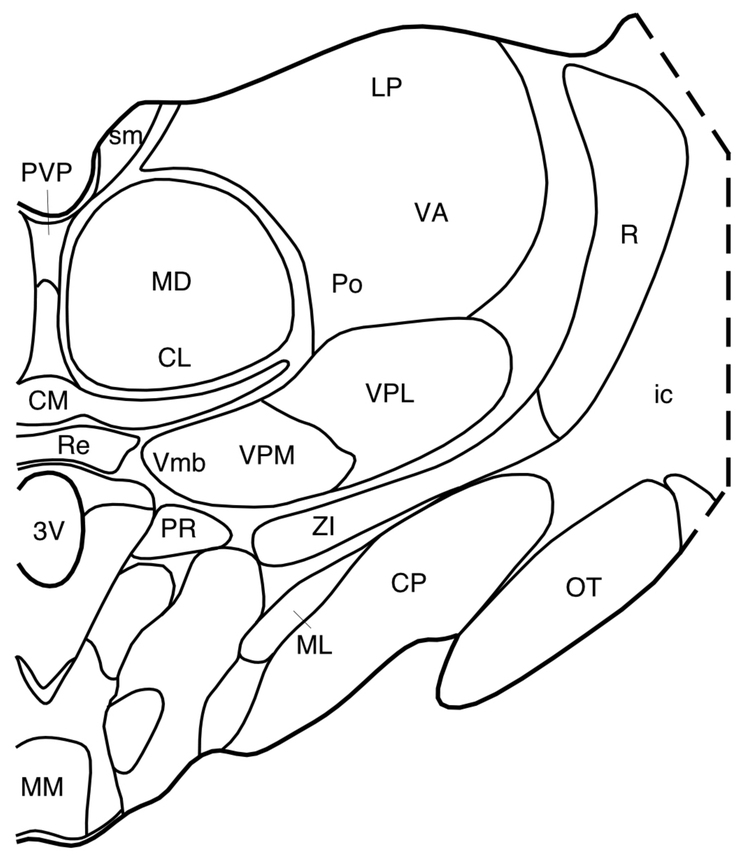


## Cholinergic

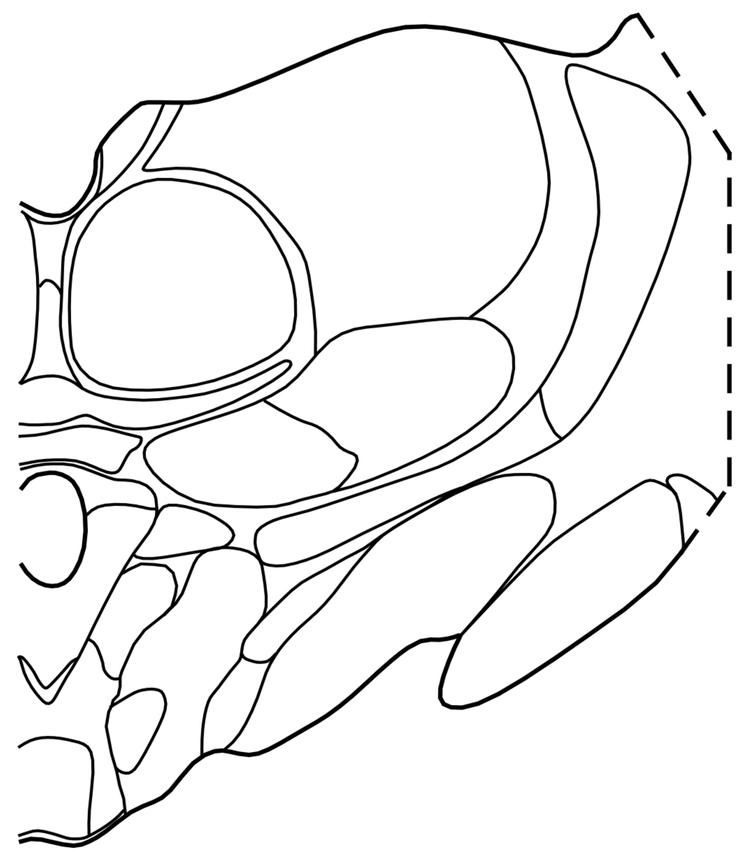

## Catecholaminergic

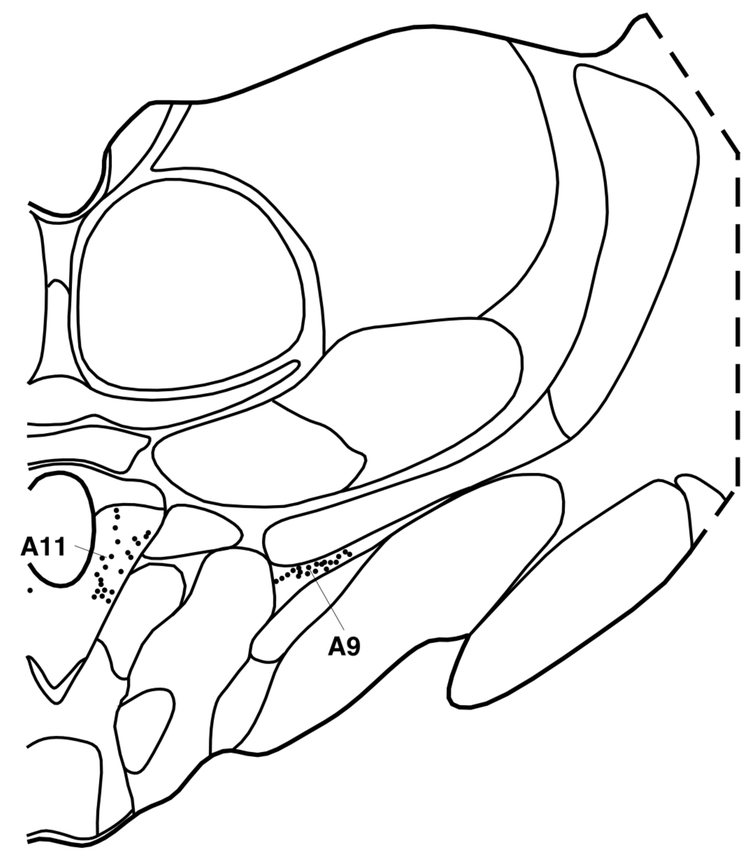


## Serotonergic

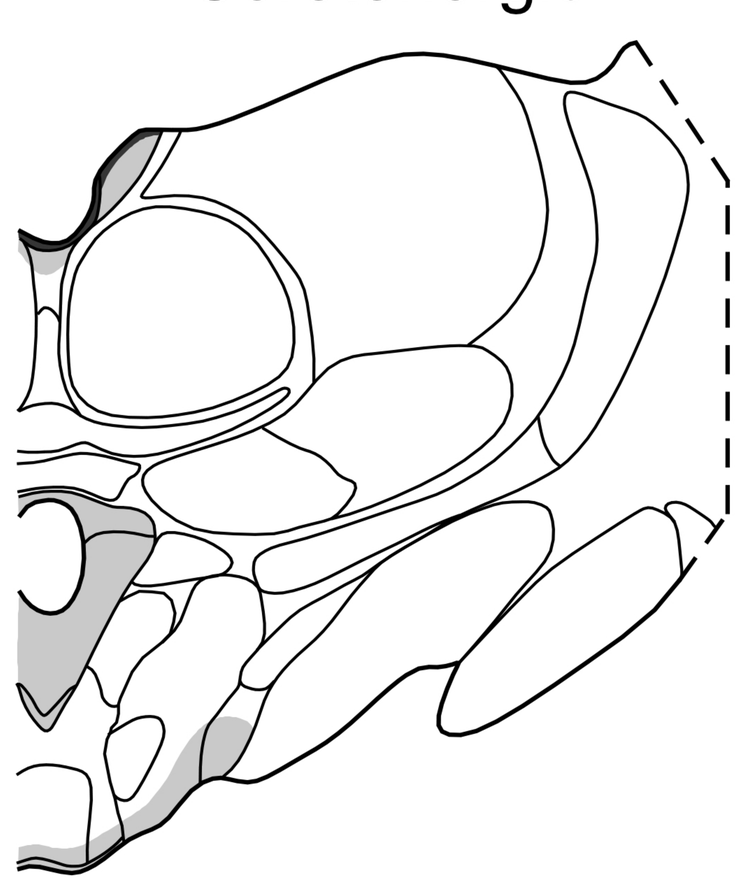

## Orexinergic

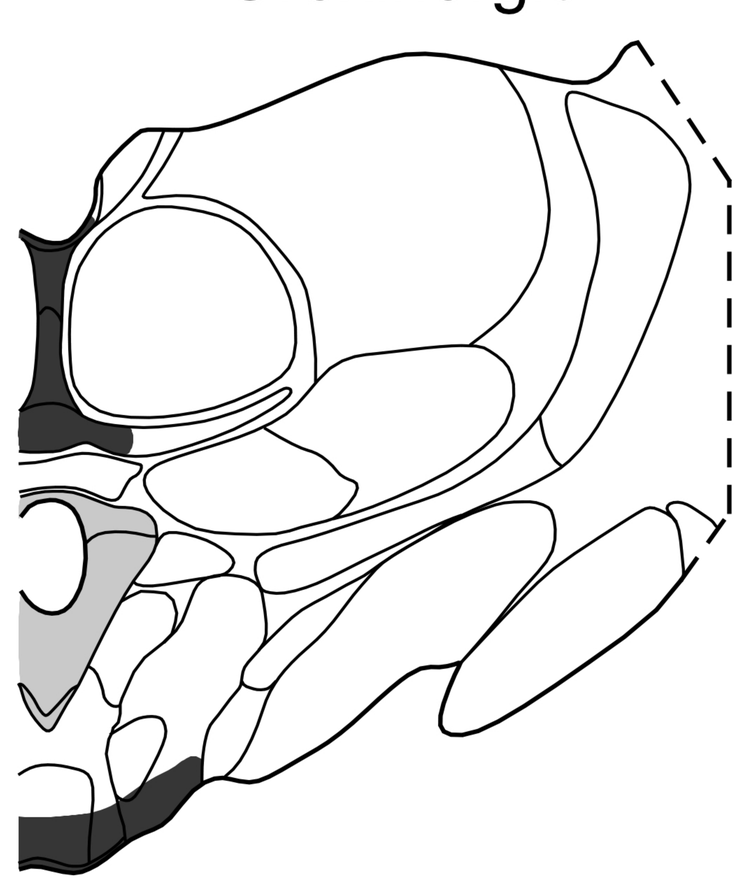

## Histaminergic

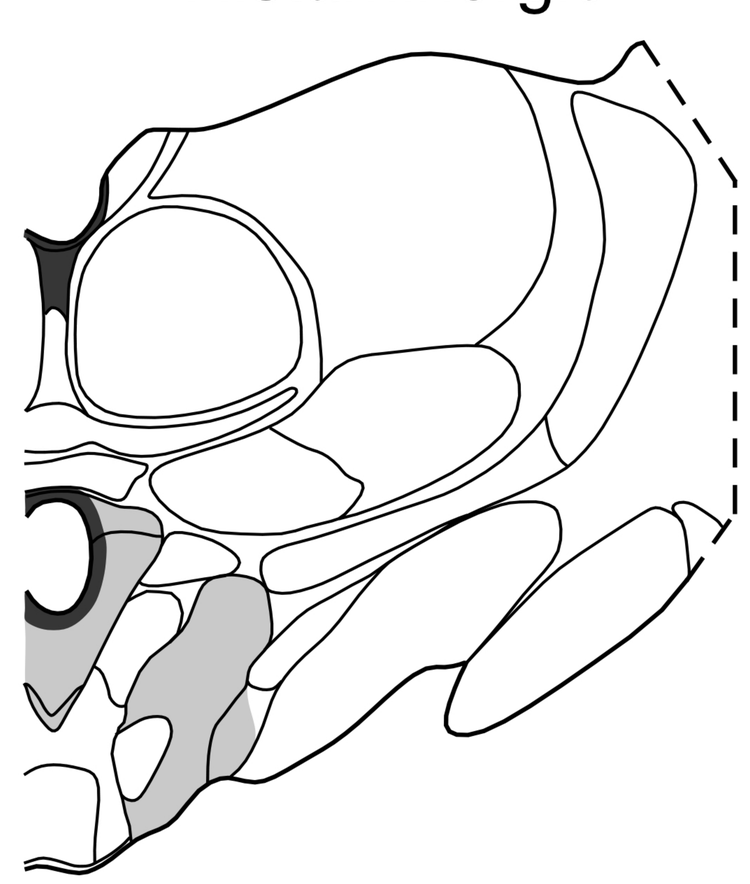

**G**

Architecture

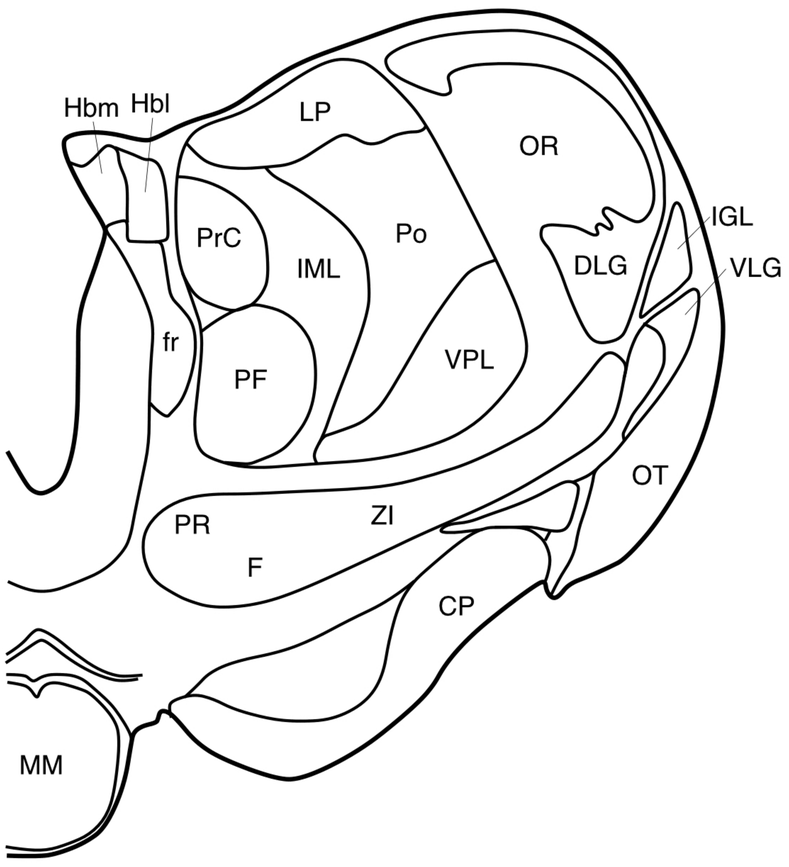


Cholinergic

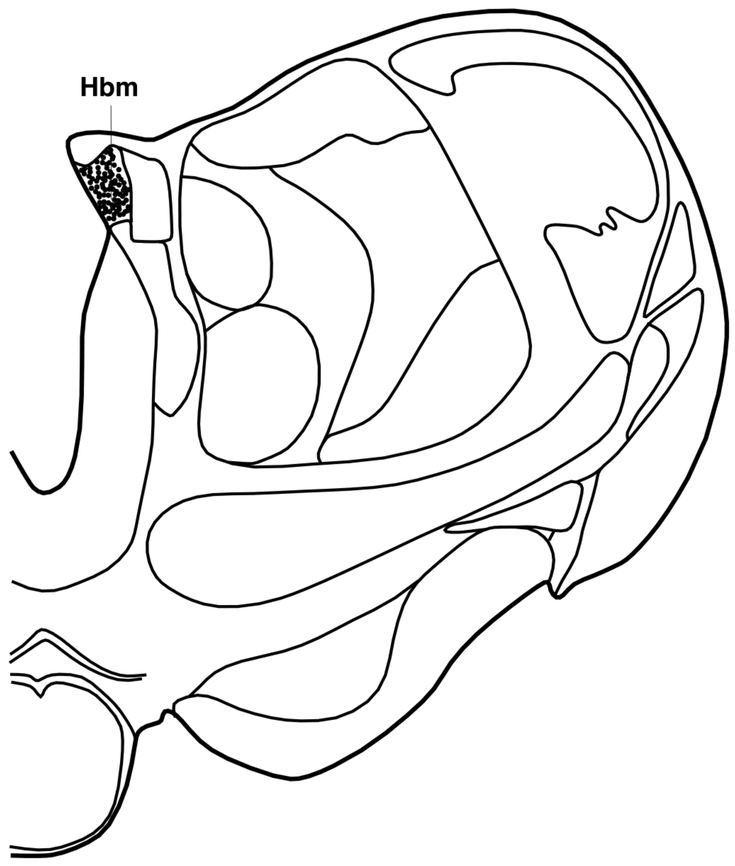


Catecholaminergic

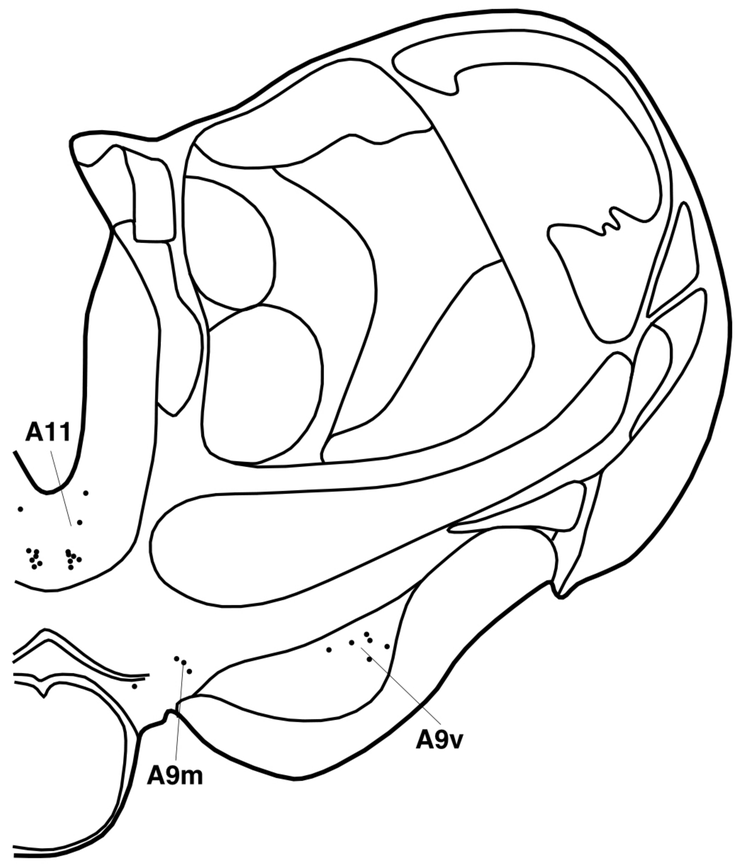


Serotonergic

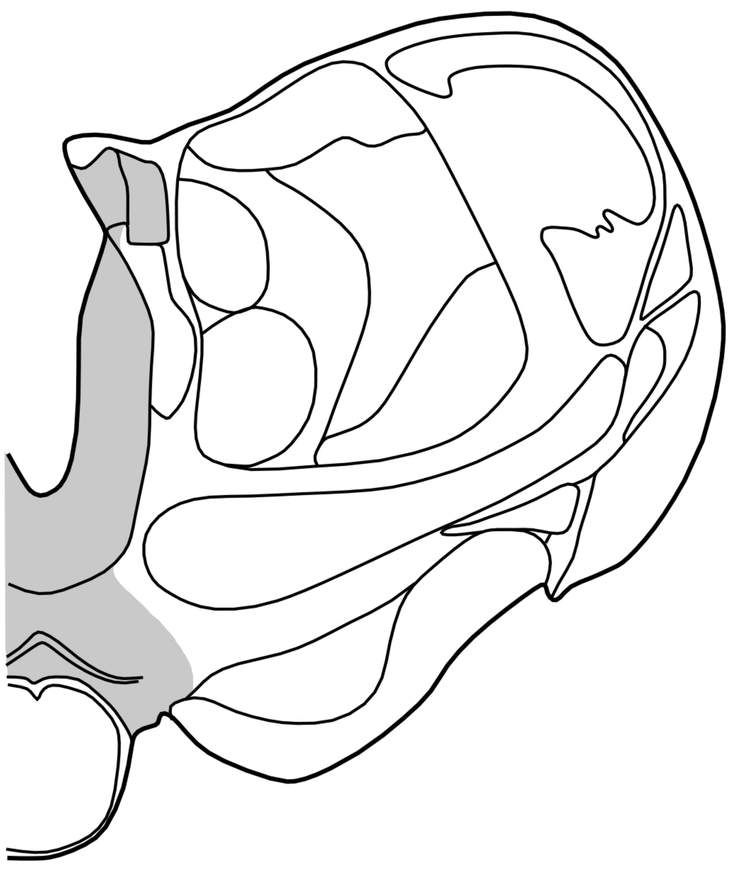

Orexinergic

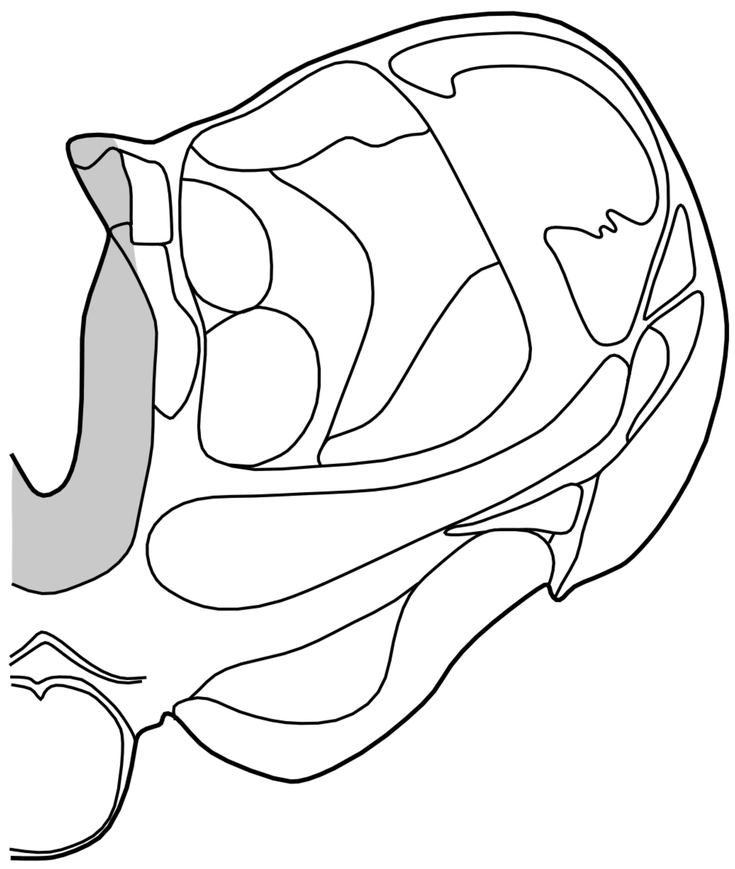

Histaminergic

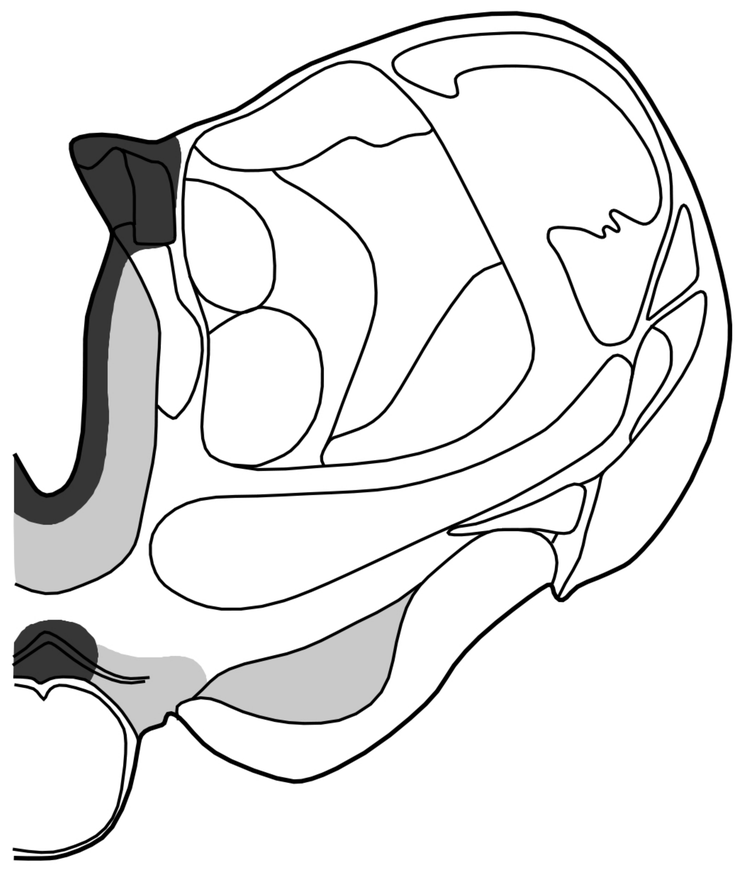

**H**

Architecture

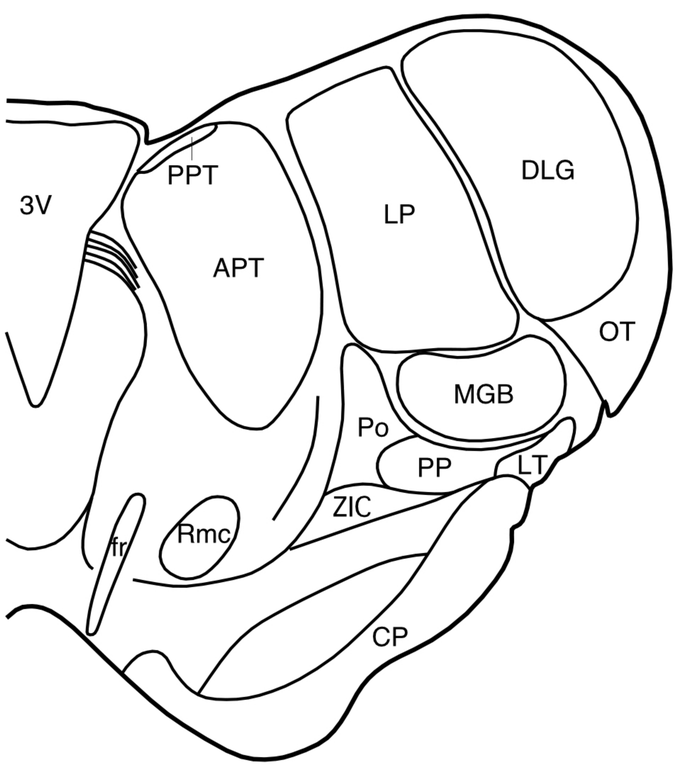


Cholinergic

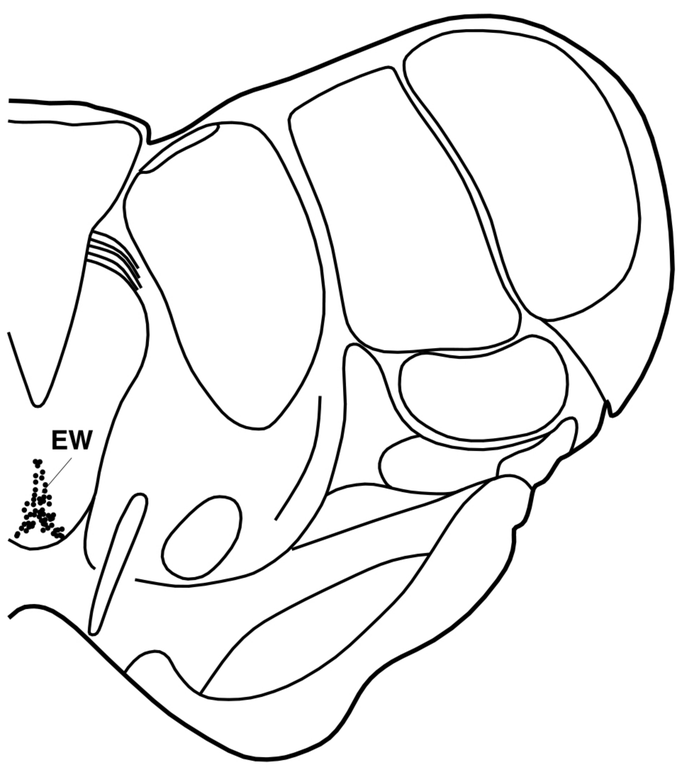


Catecholaminergic

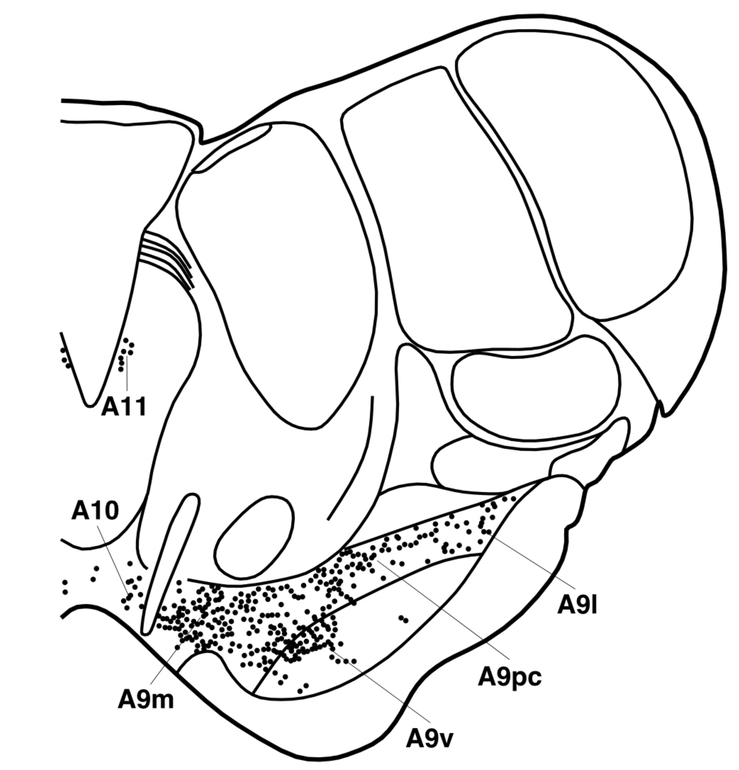


Serotonergic

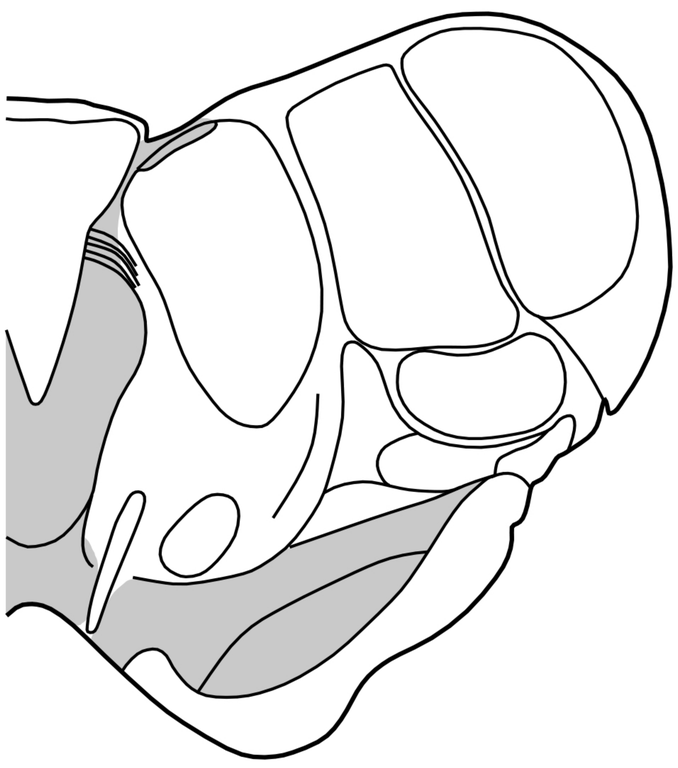

Orexinergic

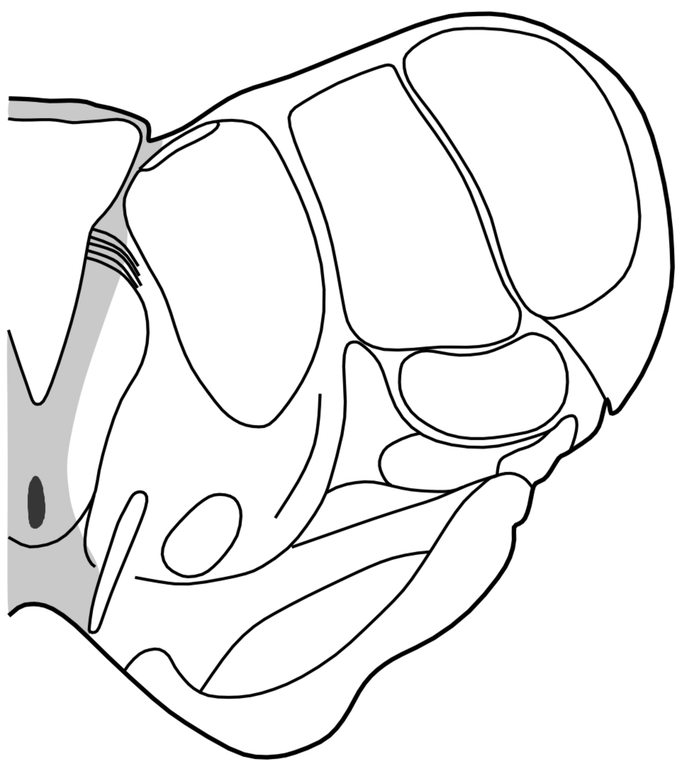

Histaminergic

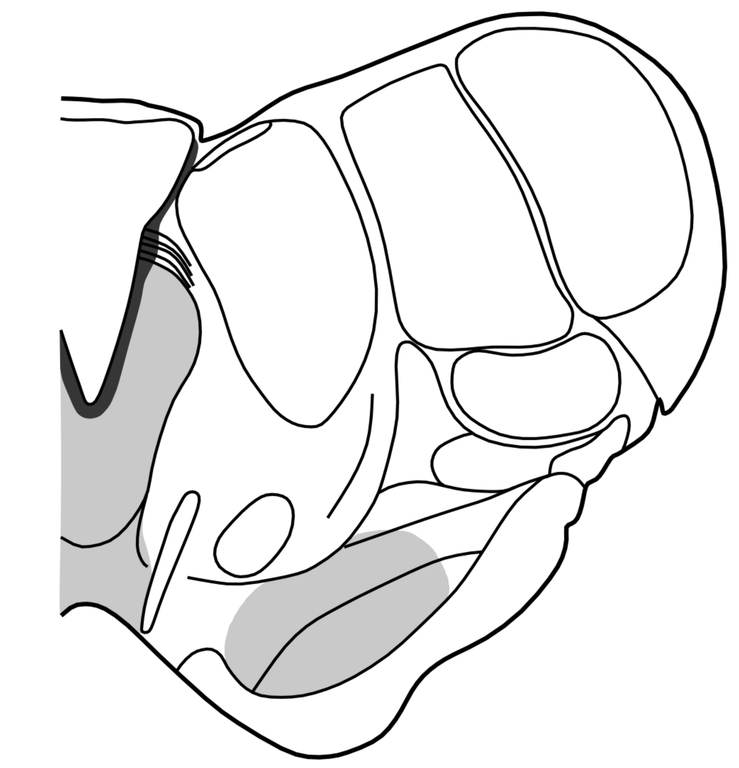

I

Architecture

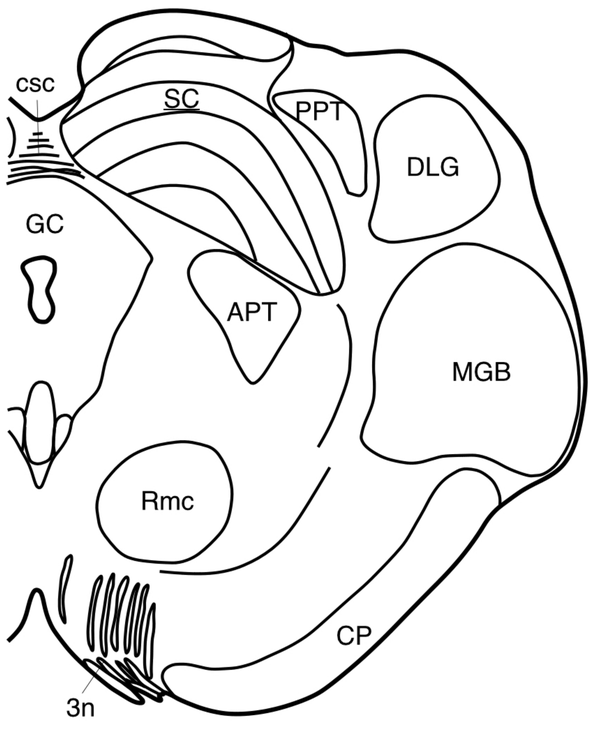


Cholinergic

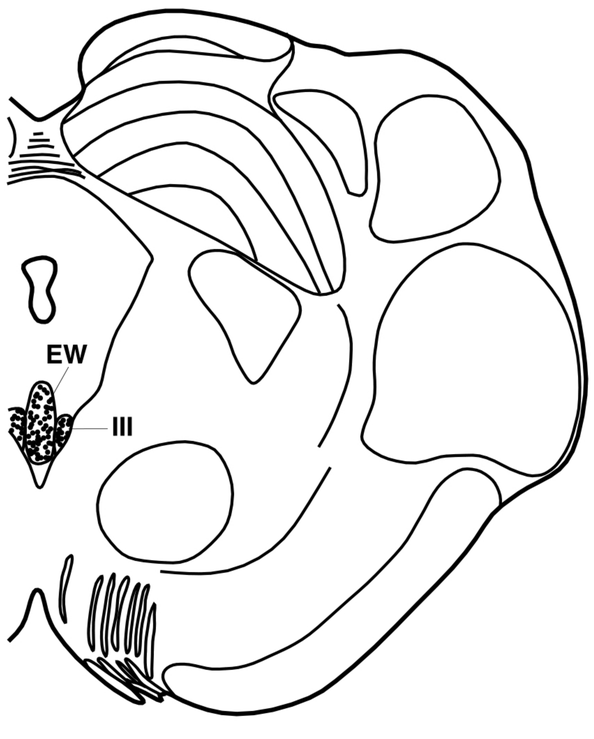


Catecholaminergic

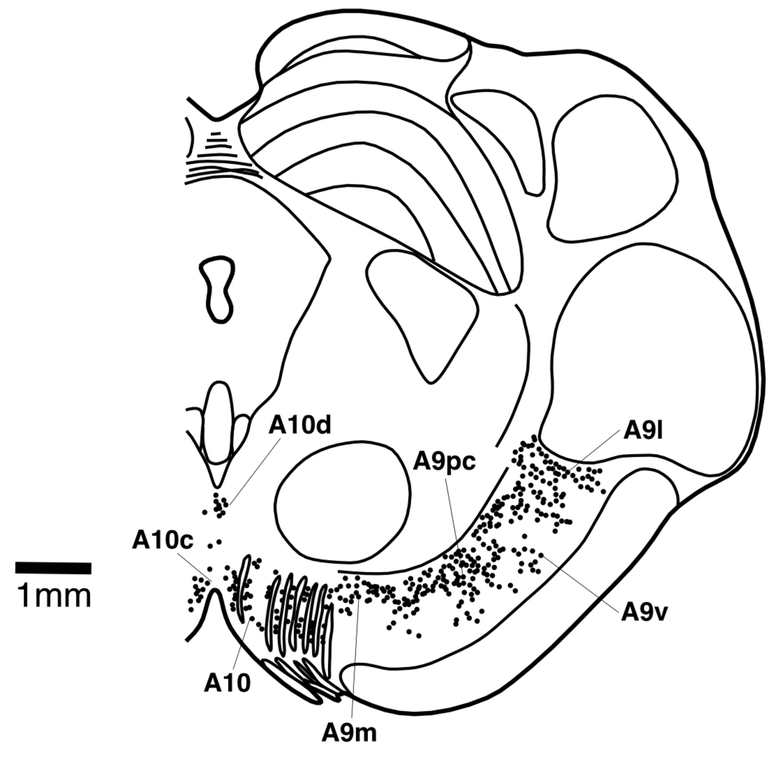


Serotonergic

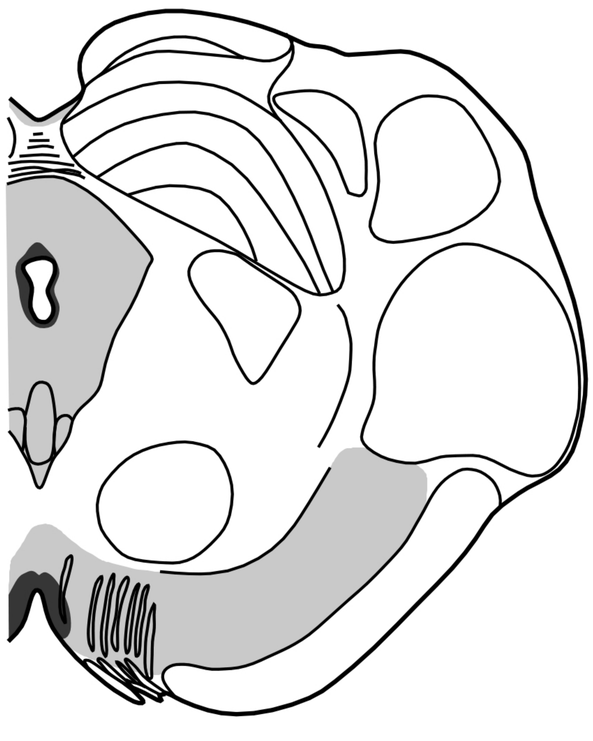

Orexinergic

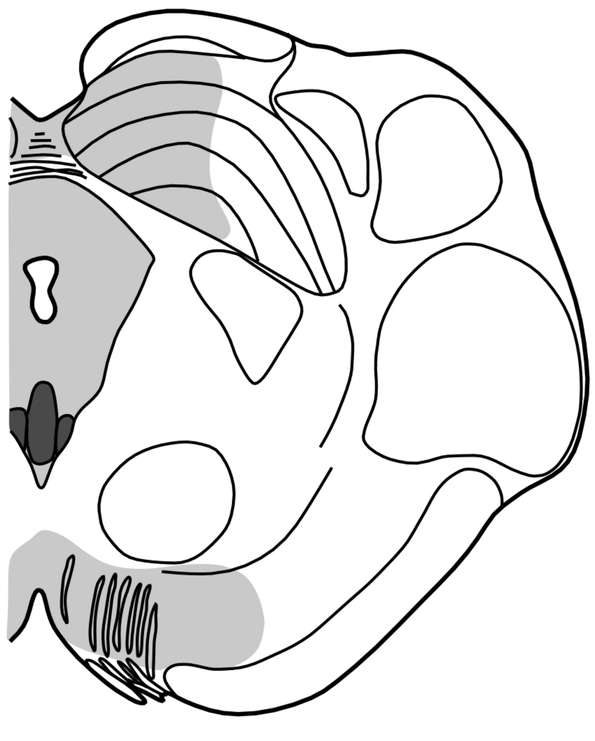

Histaminergic

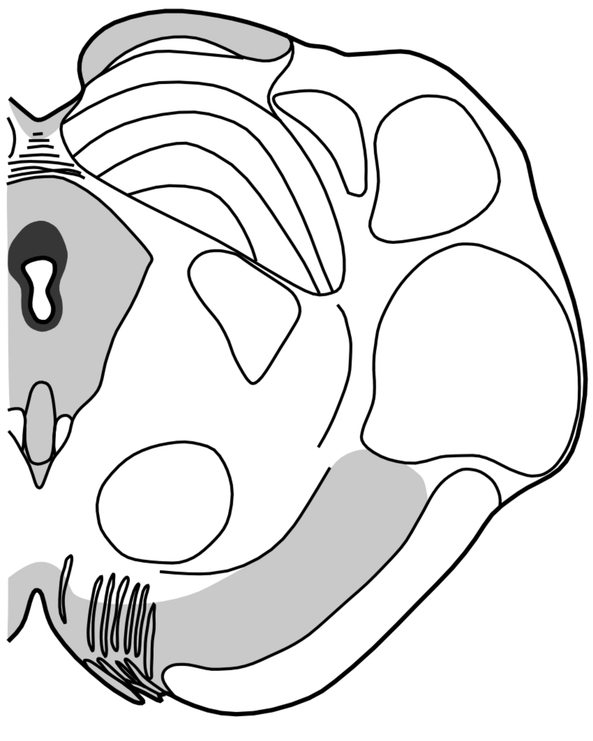

J

Architecture

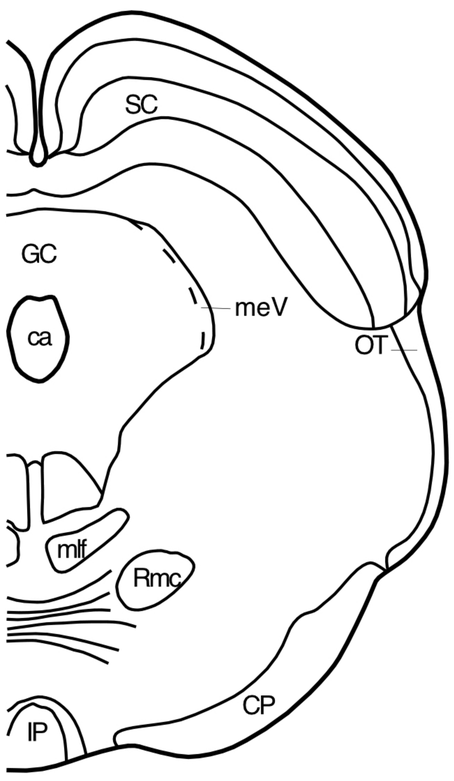


Cholinergic

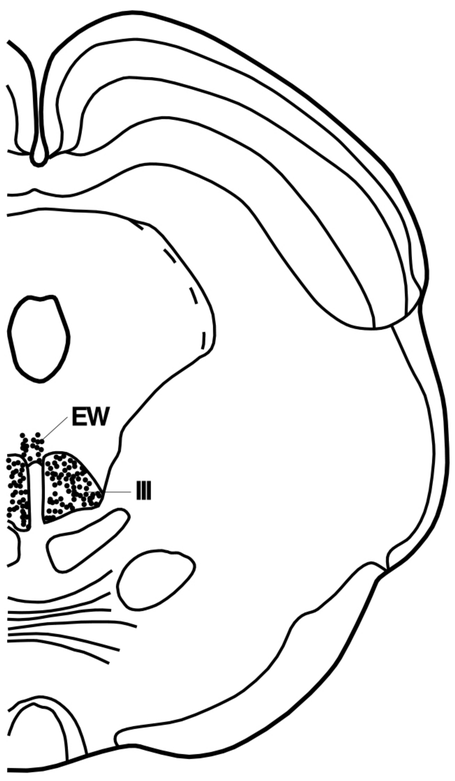


Catecholaminergic

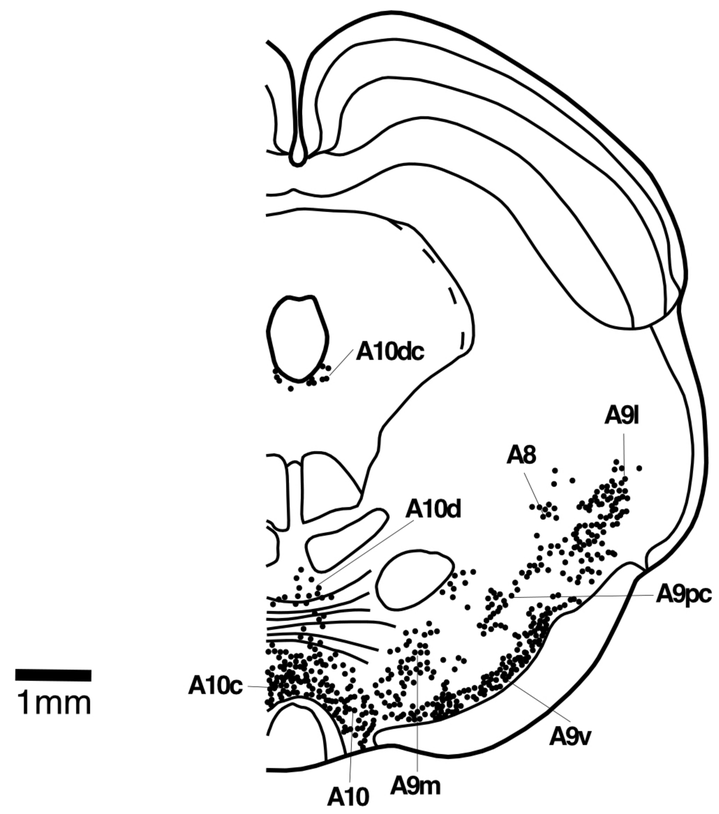


Serotonergic

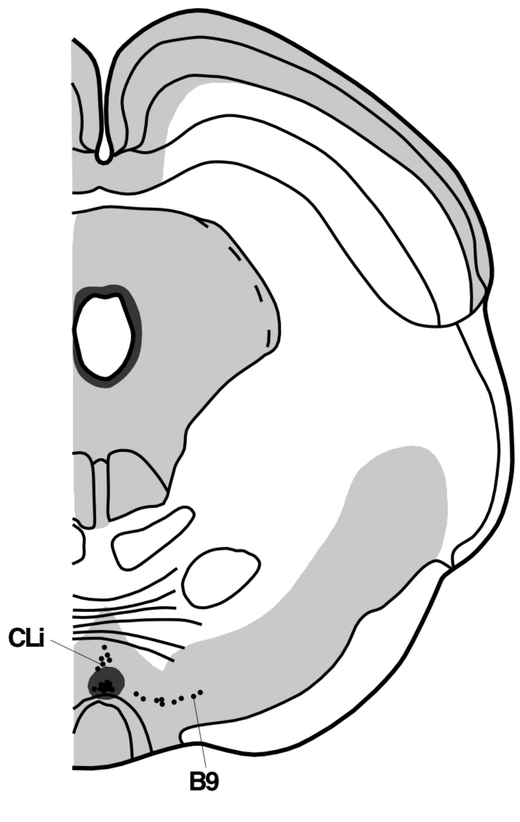


Orexinergic

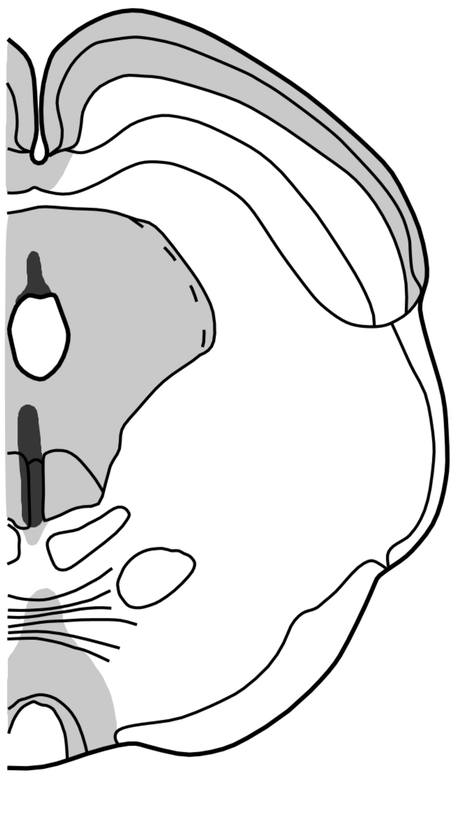

Histaminergic

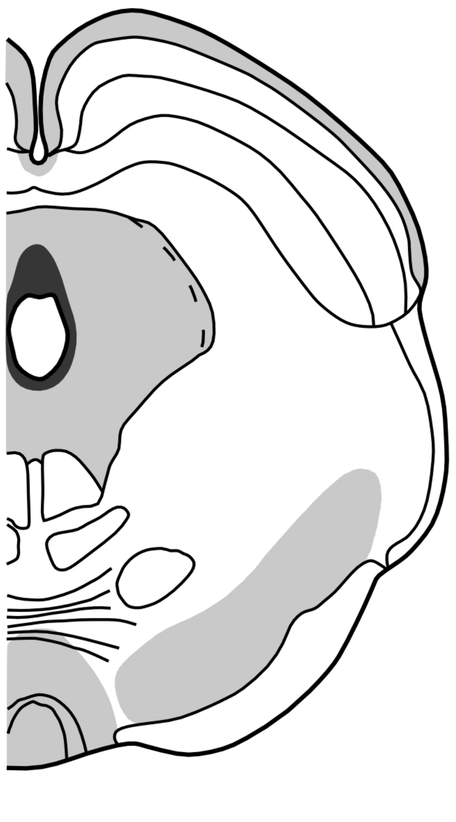

**K**

Architecture

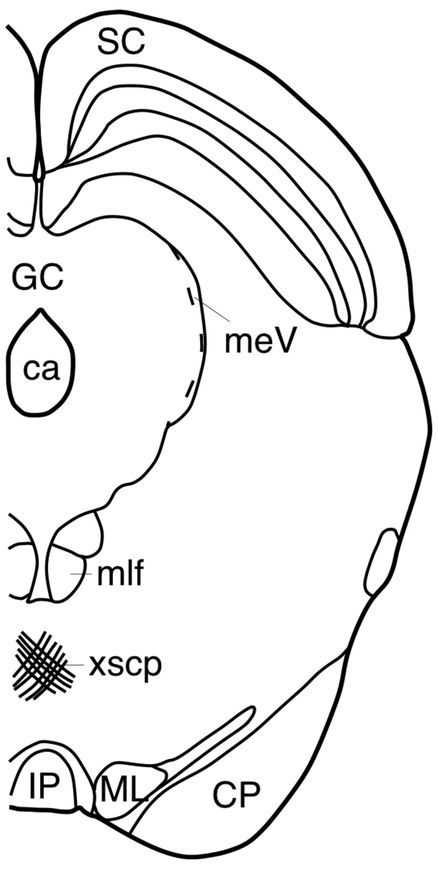


Cholinergic

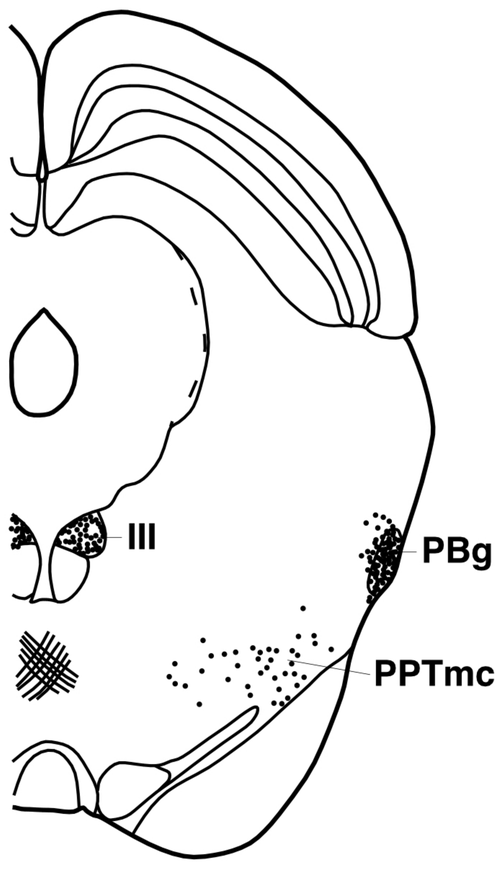


Catecholaminergic

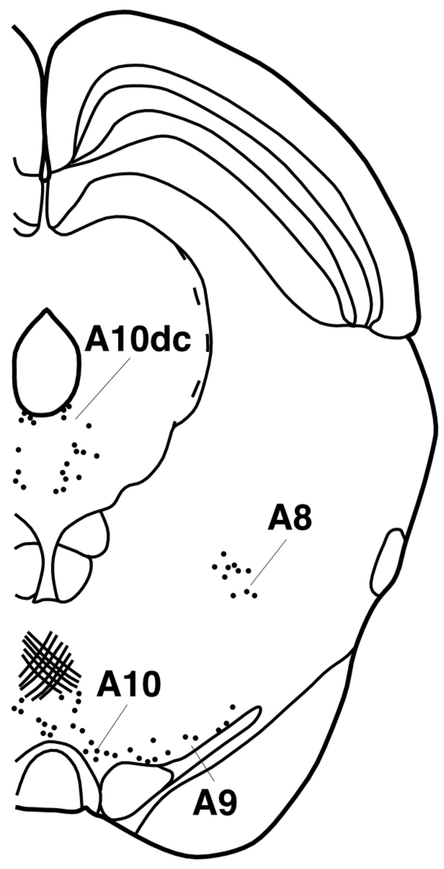


1mm

Serotonergic

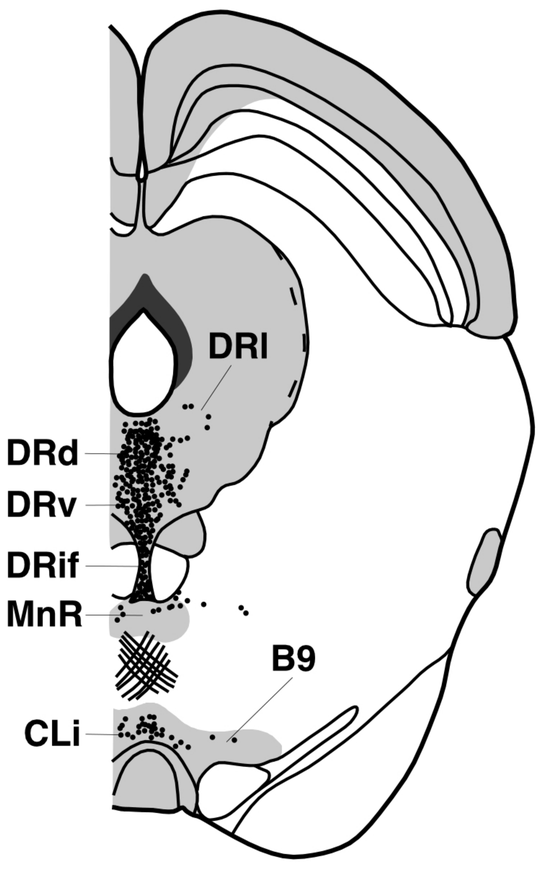


Orexinergic

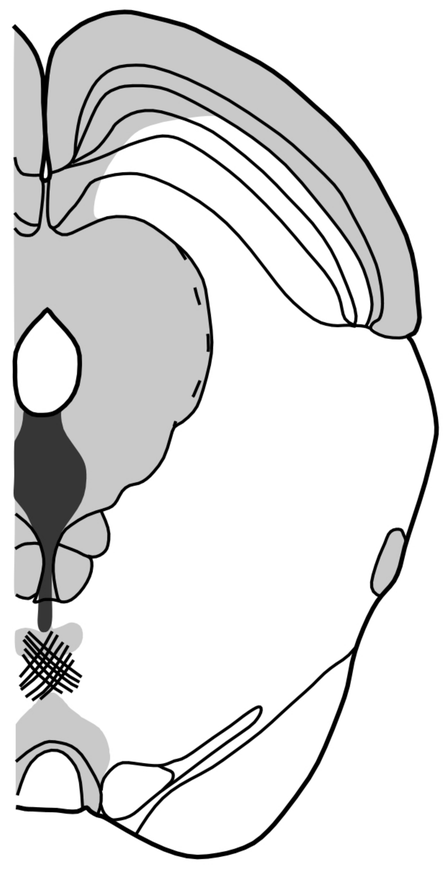

Histaminergic

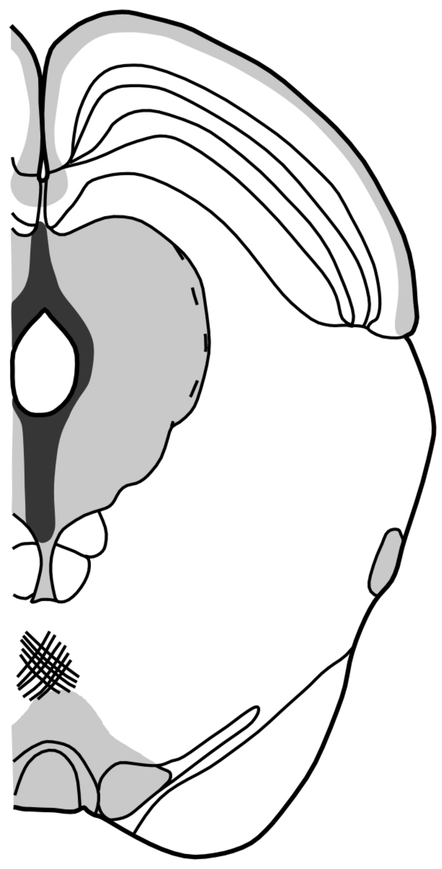

**L**

Architecture

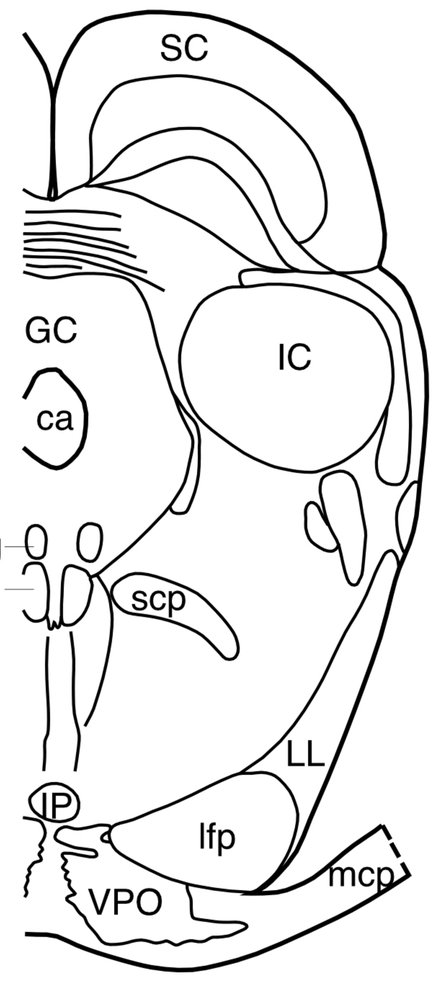


Cholinergic

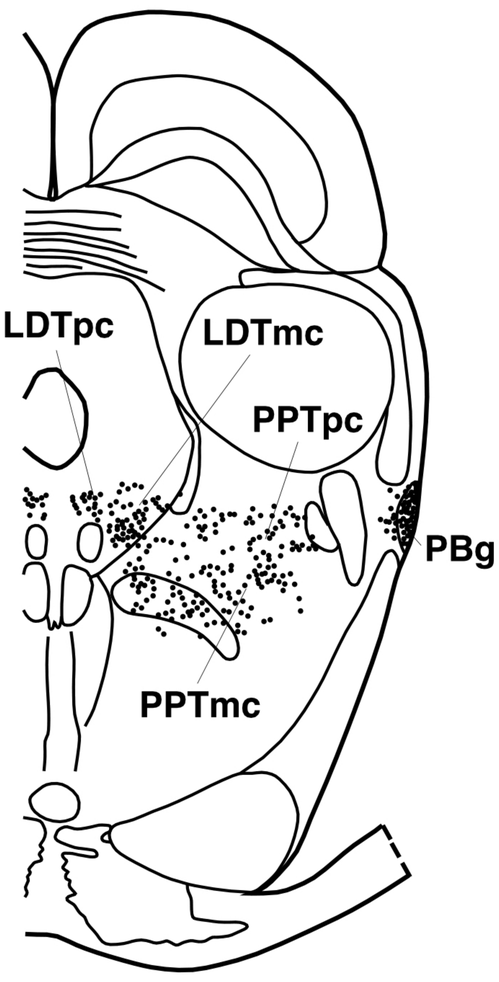


Catecholaminergic

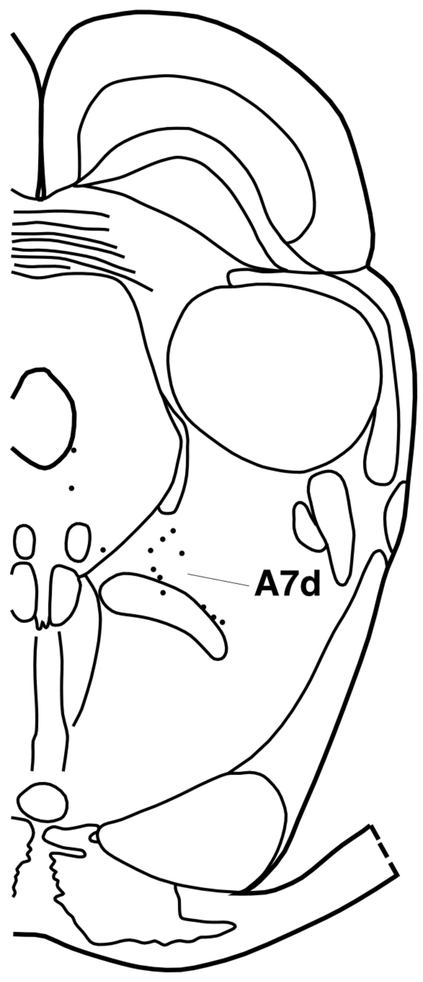


1mm

Serotonergic




Orexinergic



Histaminergic

**M**

## Architecture

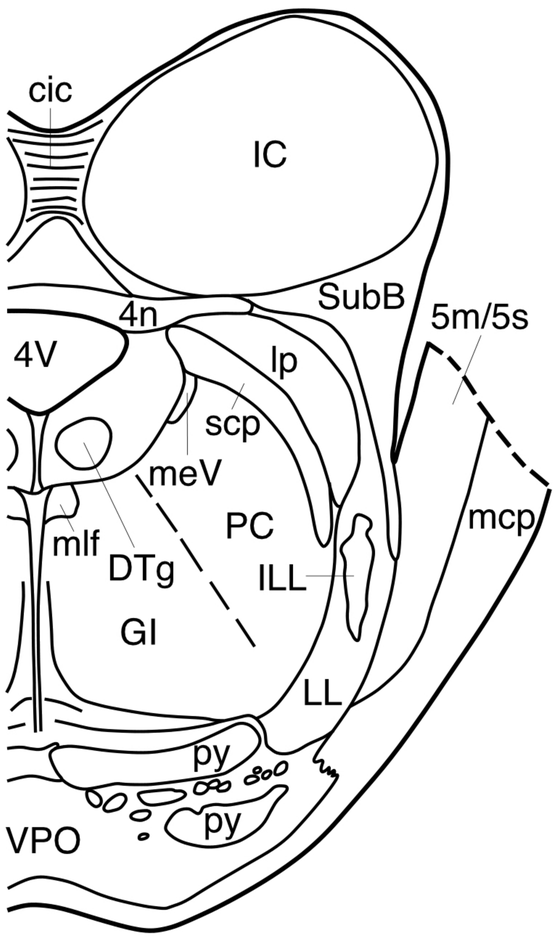


## Cholinergic

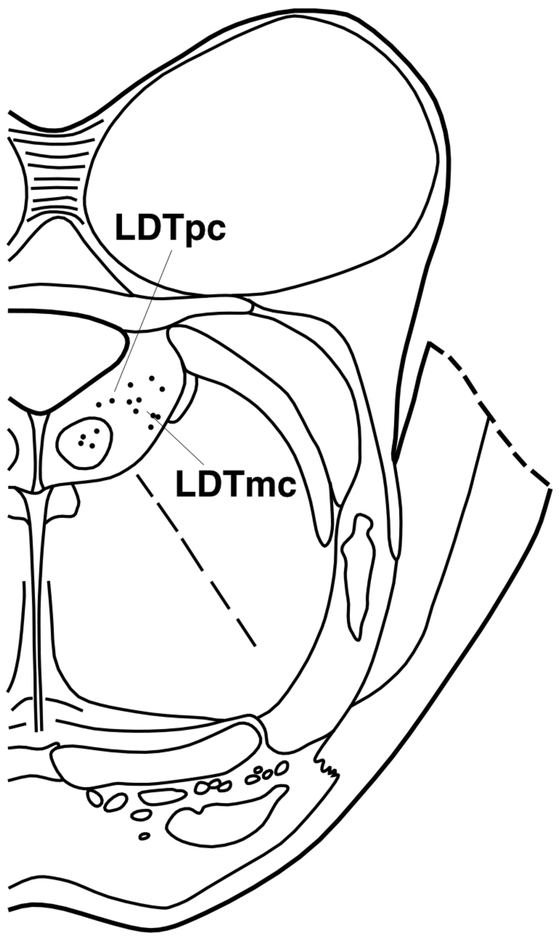


## Catecholaminergic

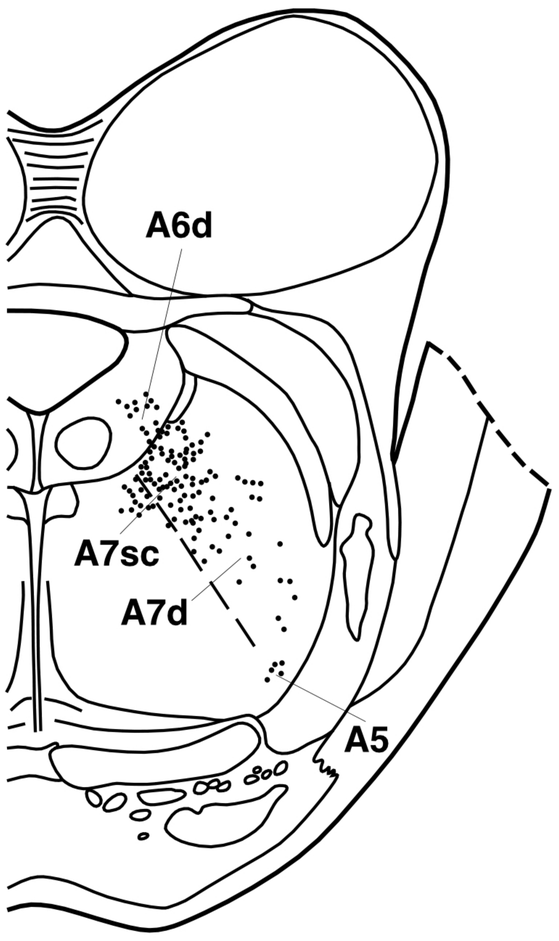


1mm

## Serotonergic

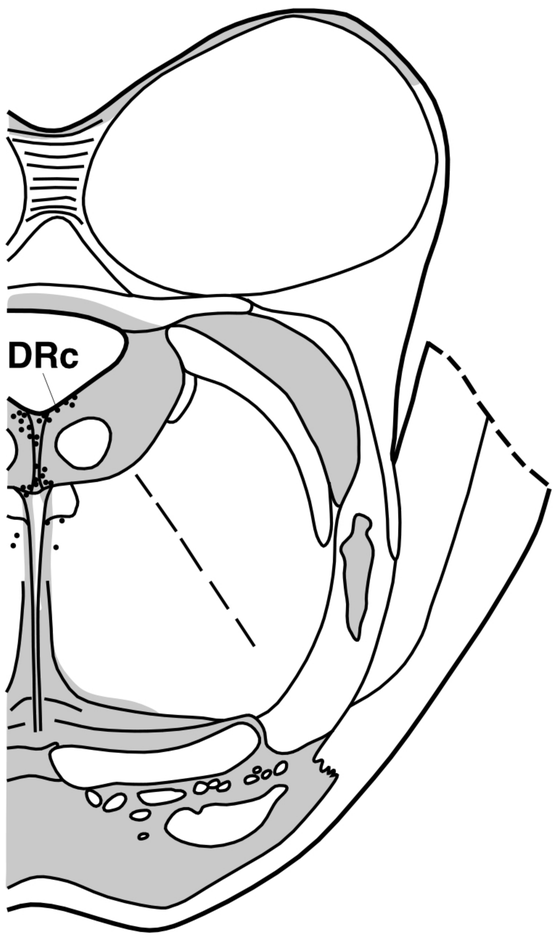


## Orexinergic

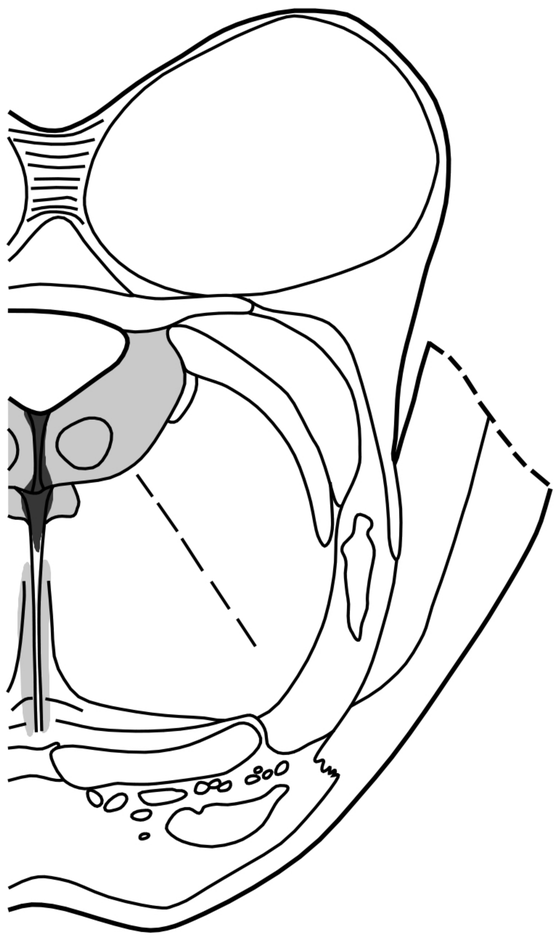

## Histaminergic

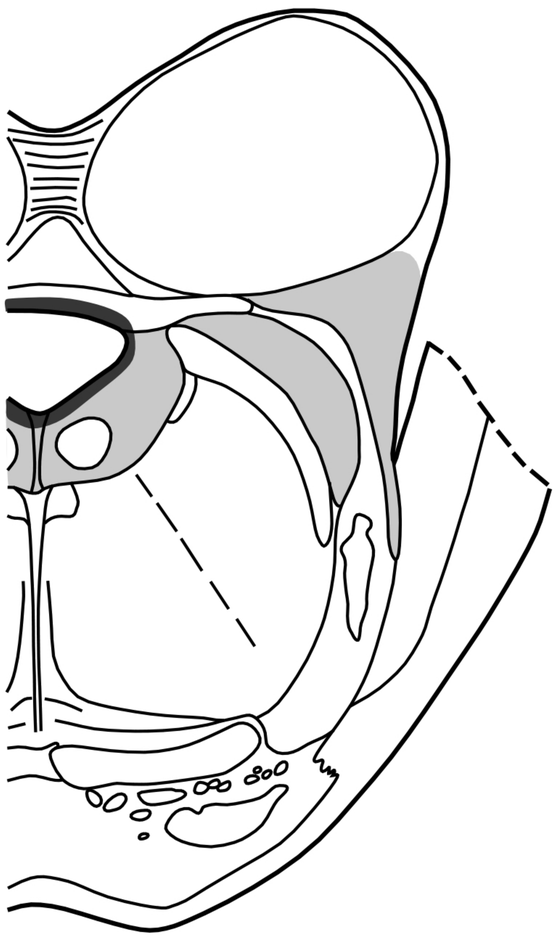

**N**

## Architecture

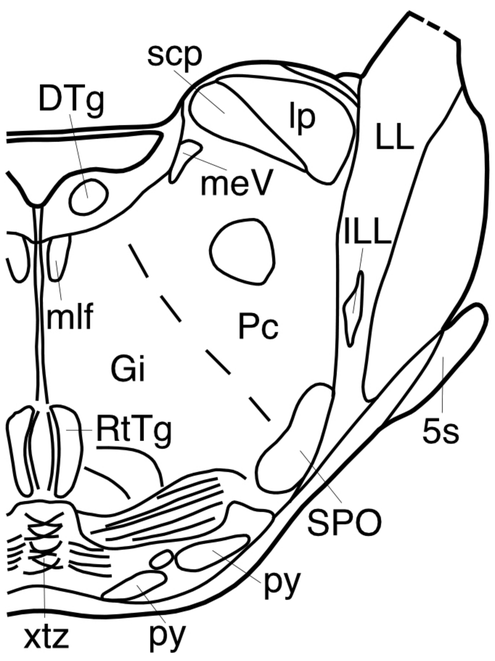


## Cholinergic

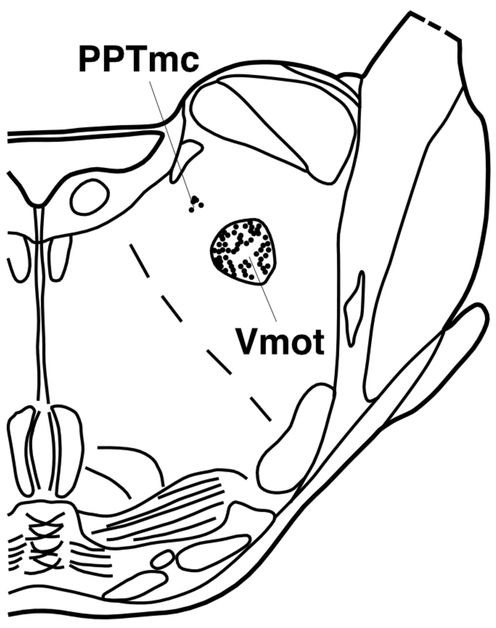


## Catecholaminergic

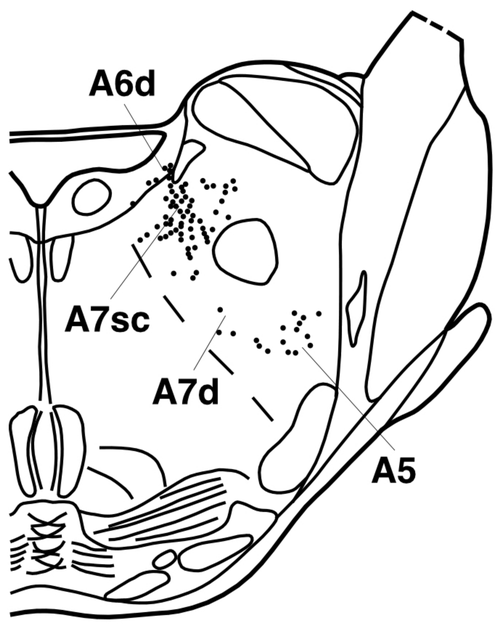


1mm

## Serotonergic

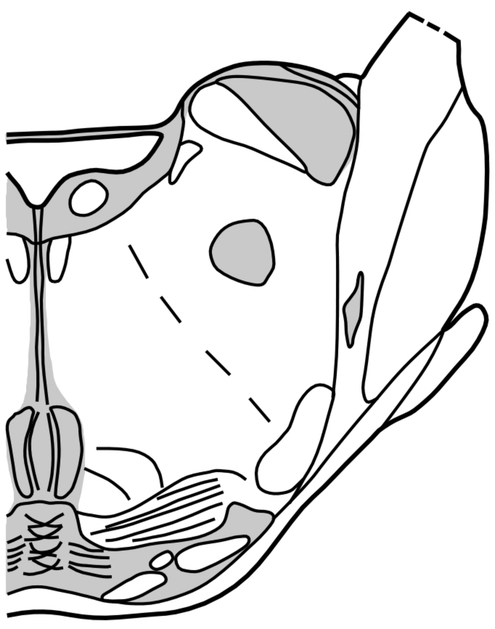

## Orexinergic

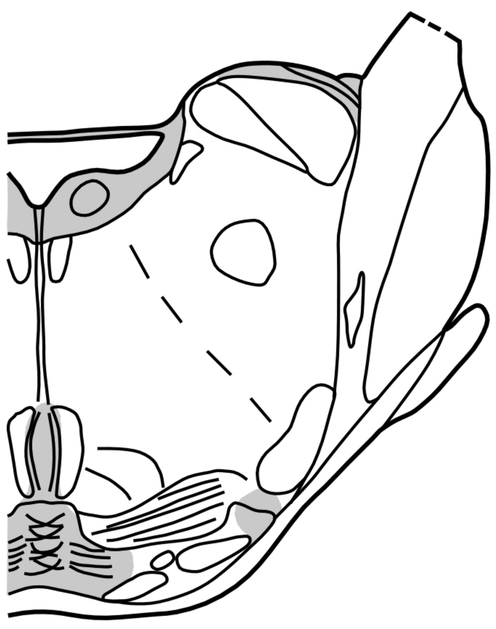

## Histaminergic

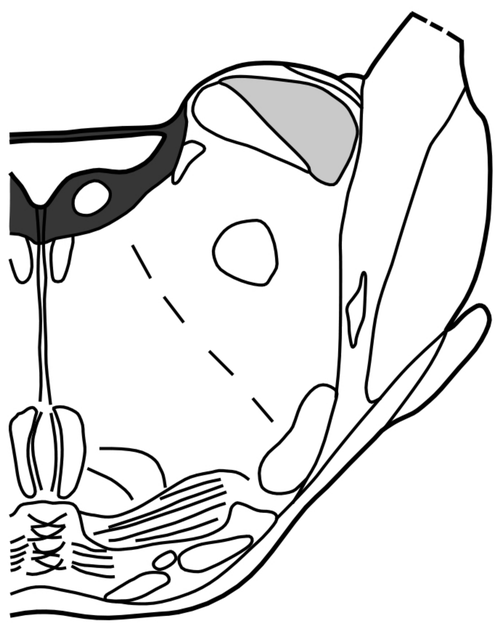

**Figure 6.2:** Photomicrographs of coronal sections through: **(A)** the ChAT immunoreactive neurons of the medial septal nucleus and **(B)** the corresponding serotonergic terminal network; **(C)** the orexinergic immunoreactive neurons of the main cluster in the hypothalamus and **(D)** the corresponding serotonergic terminal network; **(E)** the tyrosine hydroxylase immunoreactive neurons of the compact portion of the subcoeruleus (A7sc) and **(F)** the corresponding serotonergic terminal network. Note the medium serotonergic terminal network in **B** and **D** and the low serotonergic terminal network in **F**. In all figures medial is to the left and dorsal towards the top. Scale bar in F = 100 µm and applies to all.

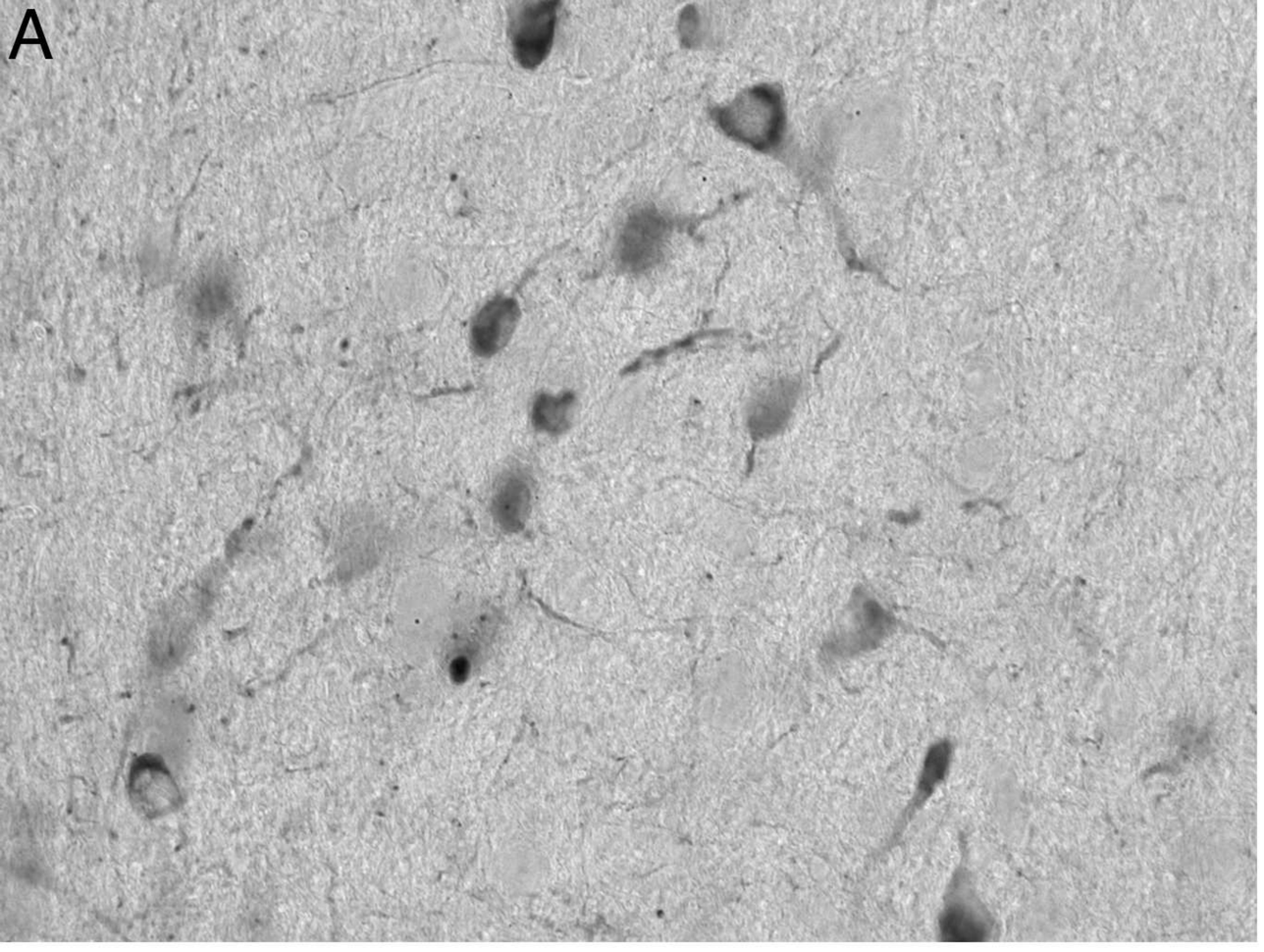
A

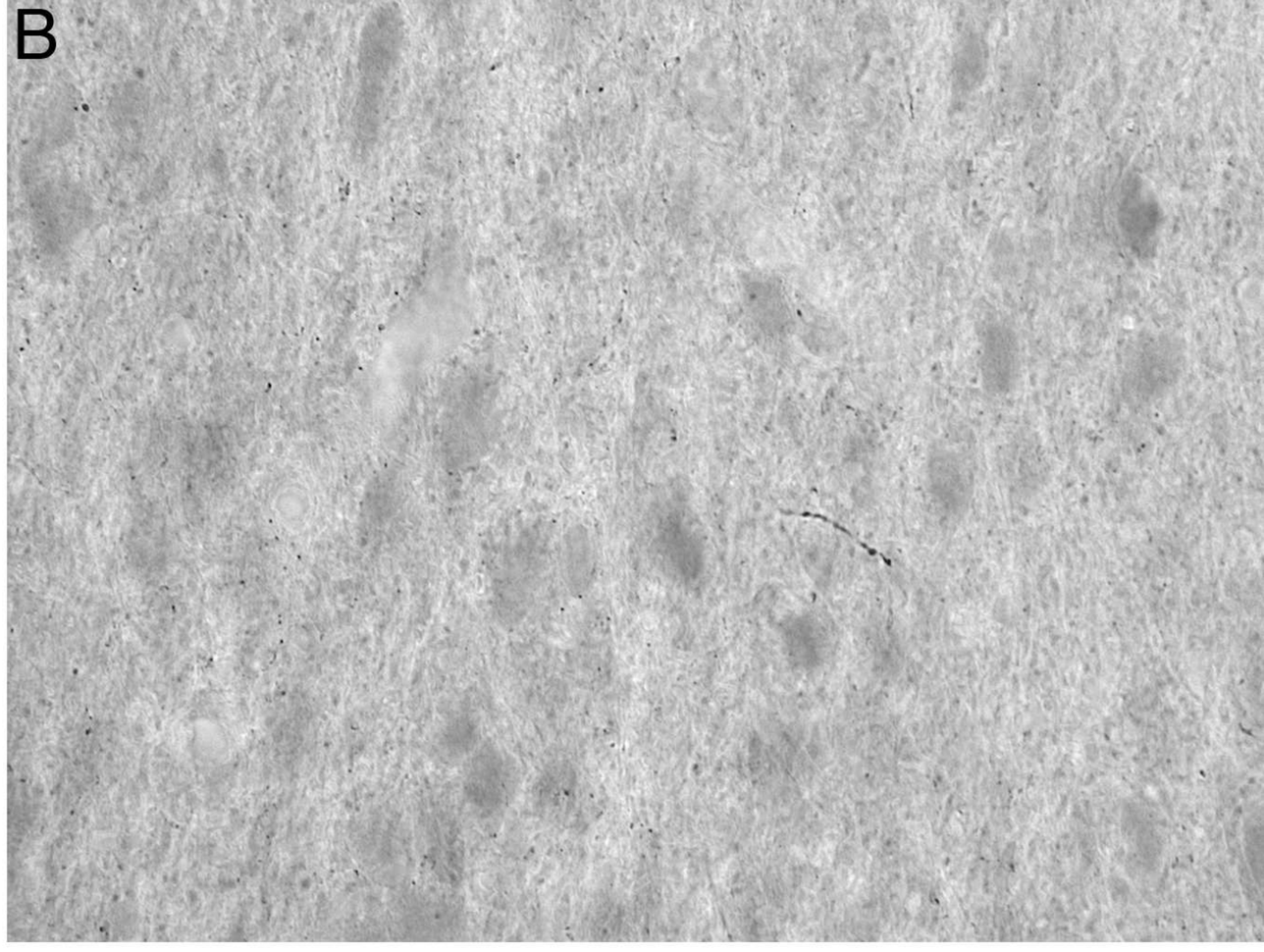
B

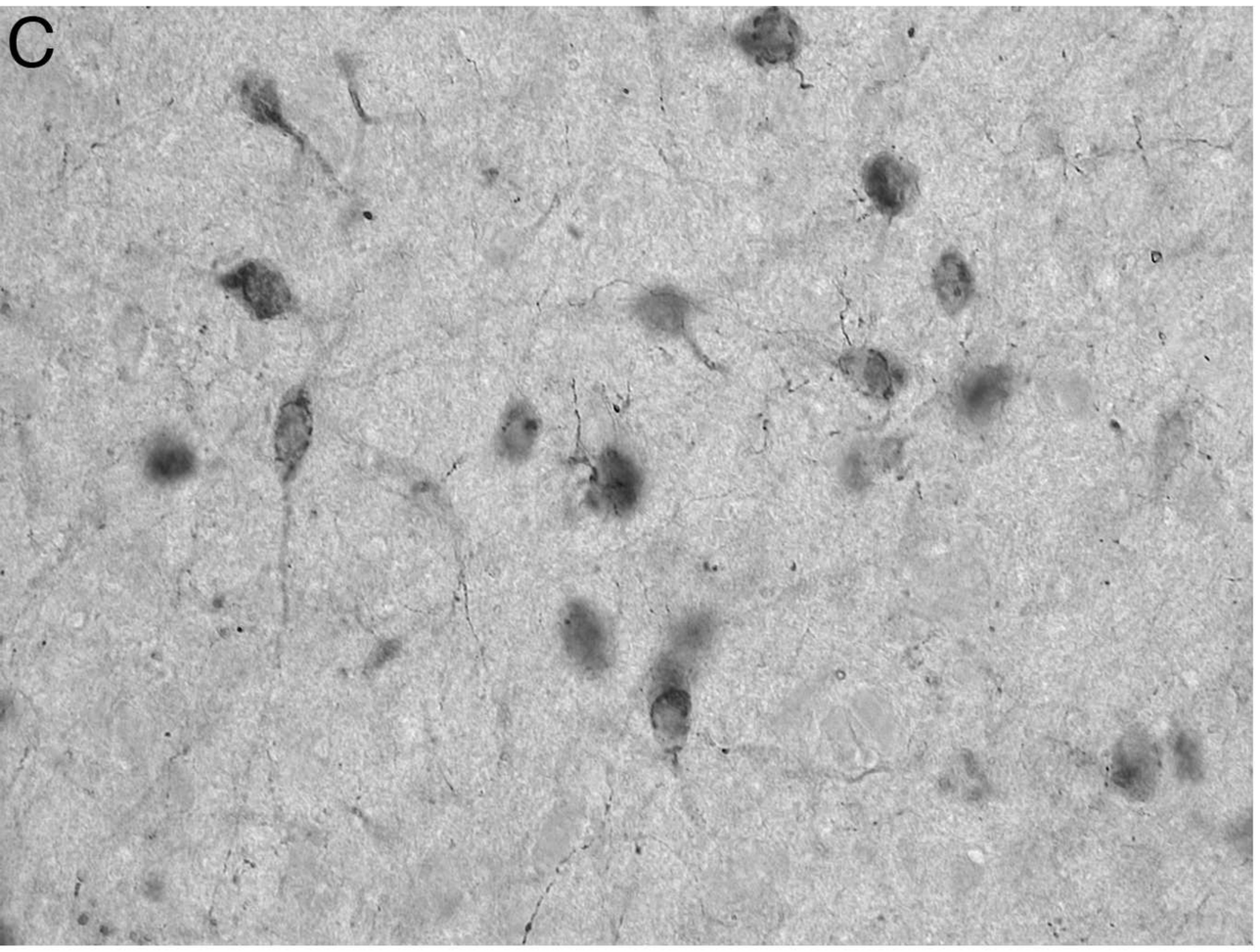
C

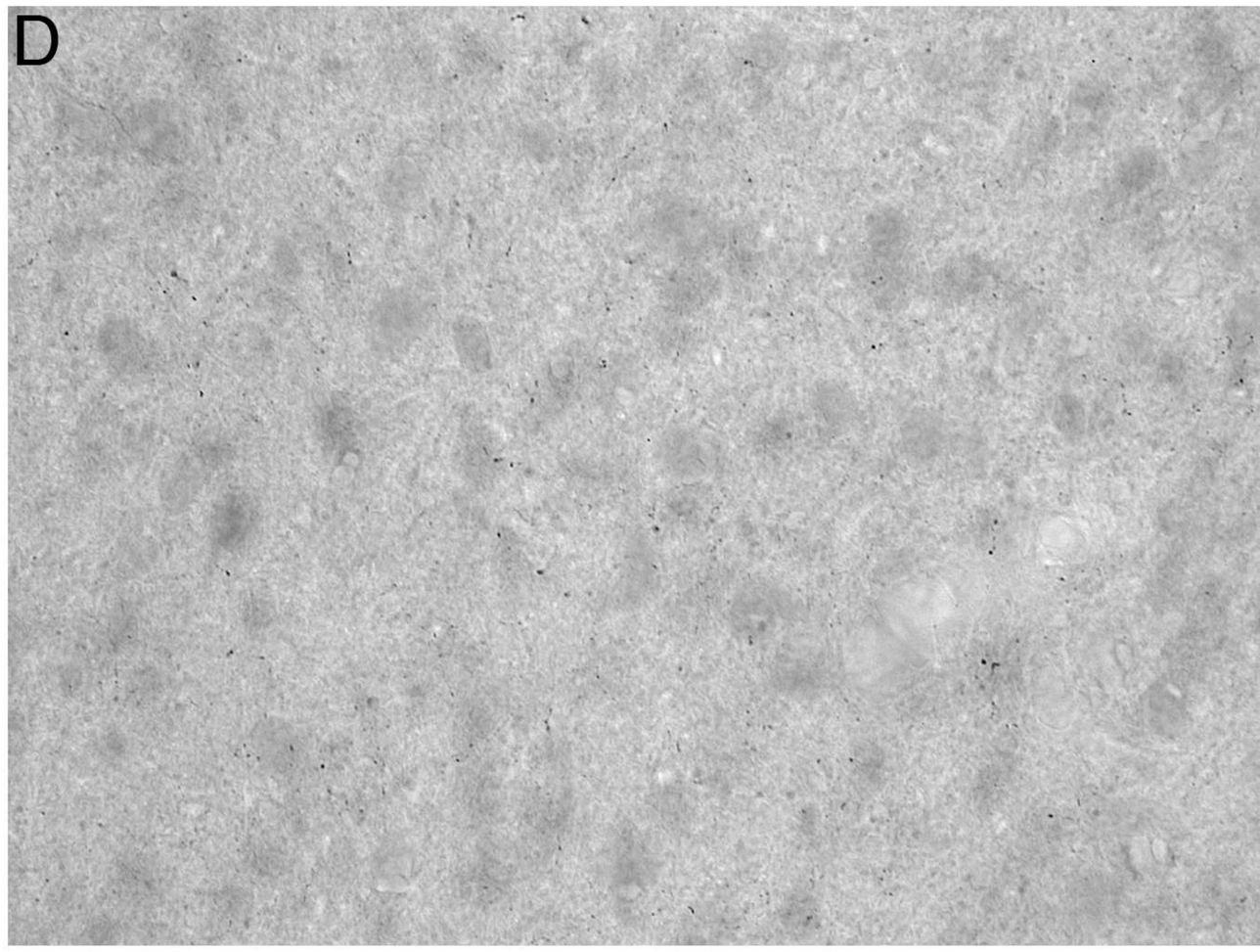
D

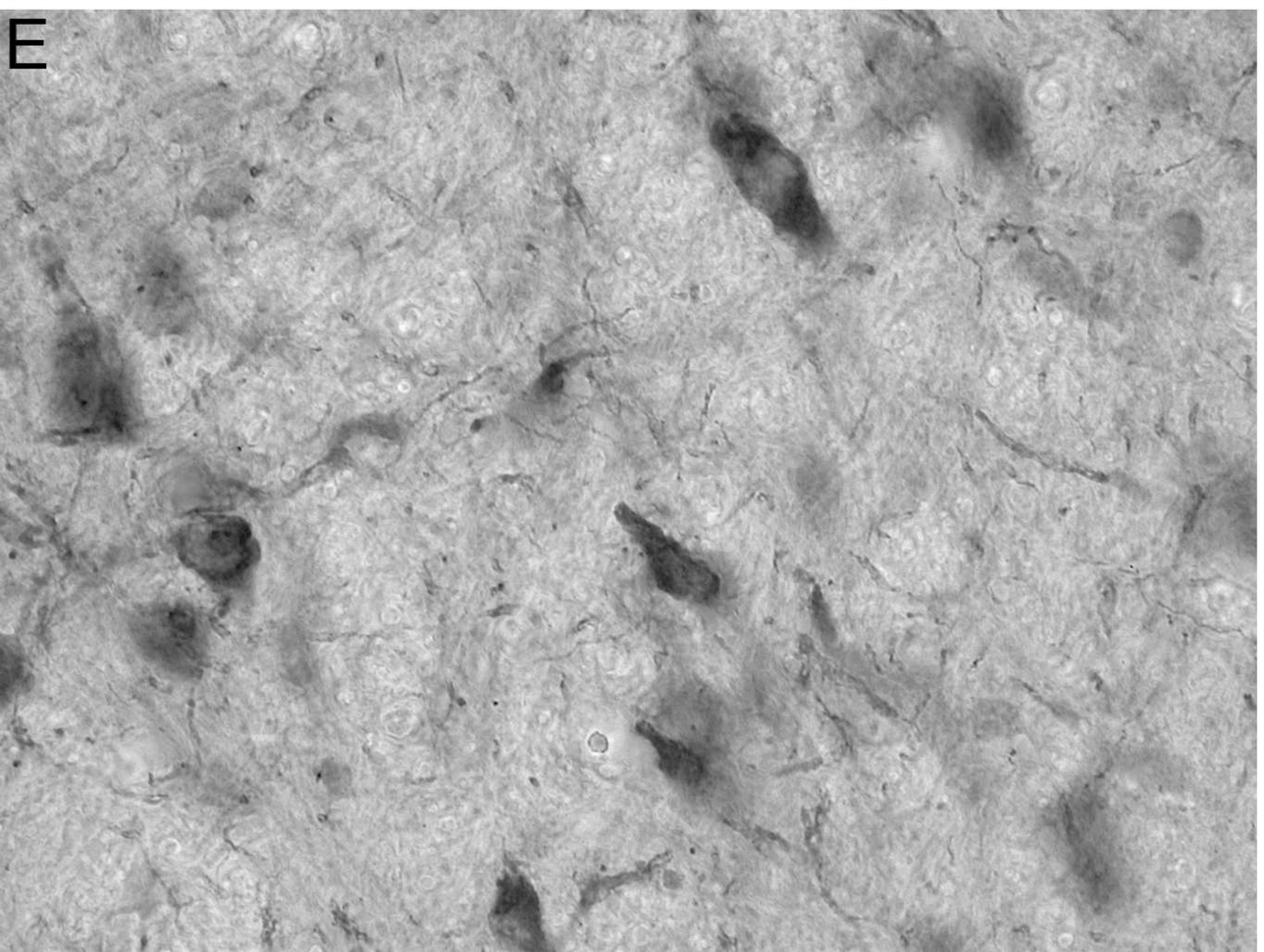
E

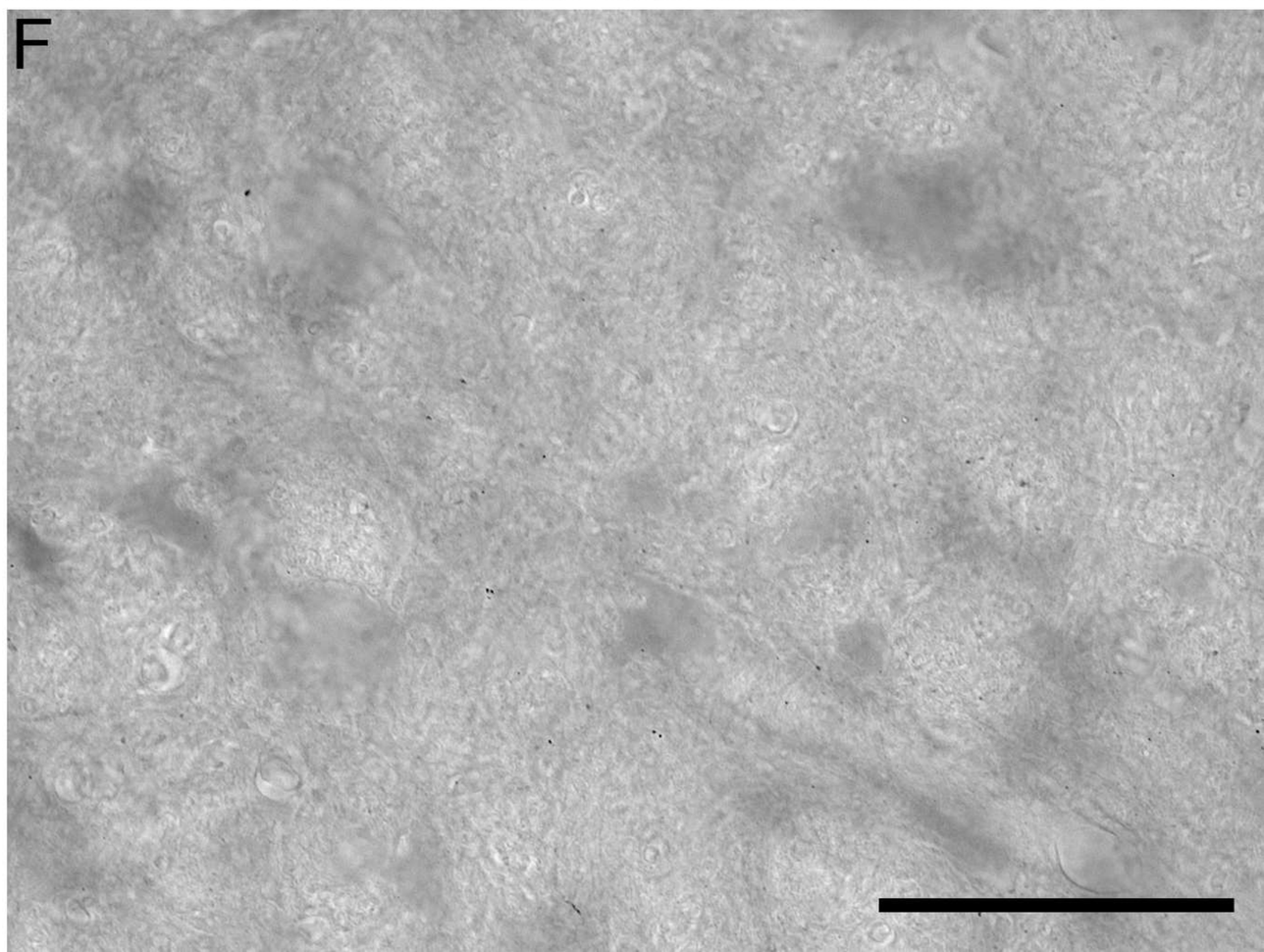
F

**Figure 6.3:** Photomicrographs of coronal sections through: **(A)** the ChAT immunoreactive neurons of the nucleus basalis and **(B)** the corresponding orexinergic terminal network; **(C)** the tyrosine hydroxylase immunoreactive neurons of the dorsal division of the anterior hypothalamic group (A15d) and **(D)** the corresponding orexinergic terminal network; **(E)** the serotonergic immunoreactive neurons of the peripheral division of the dorsal raphe nucleus (DRp) and **(F)** the corresponding orexinergic terminal network; **(G)** the tyrosine hydroxylase immunoreactive neurons of the diffuse portion of the locus coeruleus and **(H)** the corresponding orexinergic terminal network. Note the medium-density orexinergic terminal network in **D, F** and **H** and the low-density orexinergic terminal network in **B**. In all figures medial is to the left and dorsal towards the top. Scale bar in H = 100 µm and applies to all.

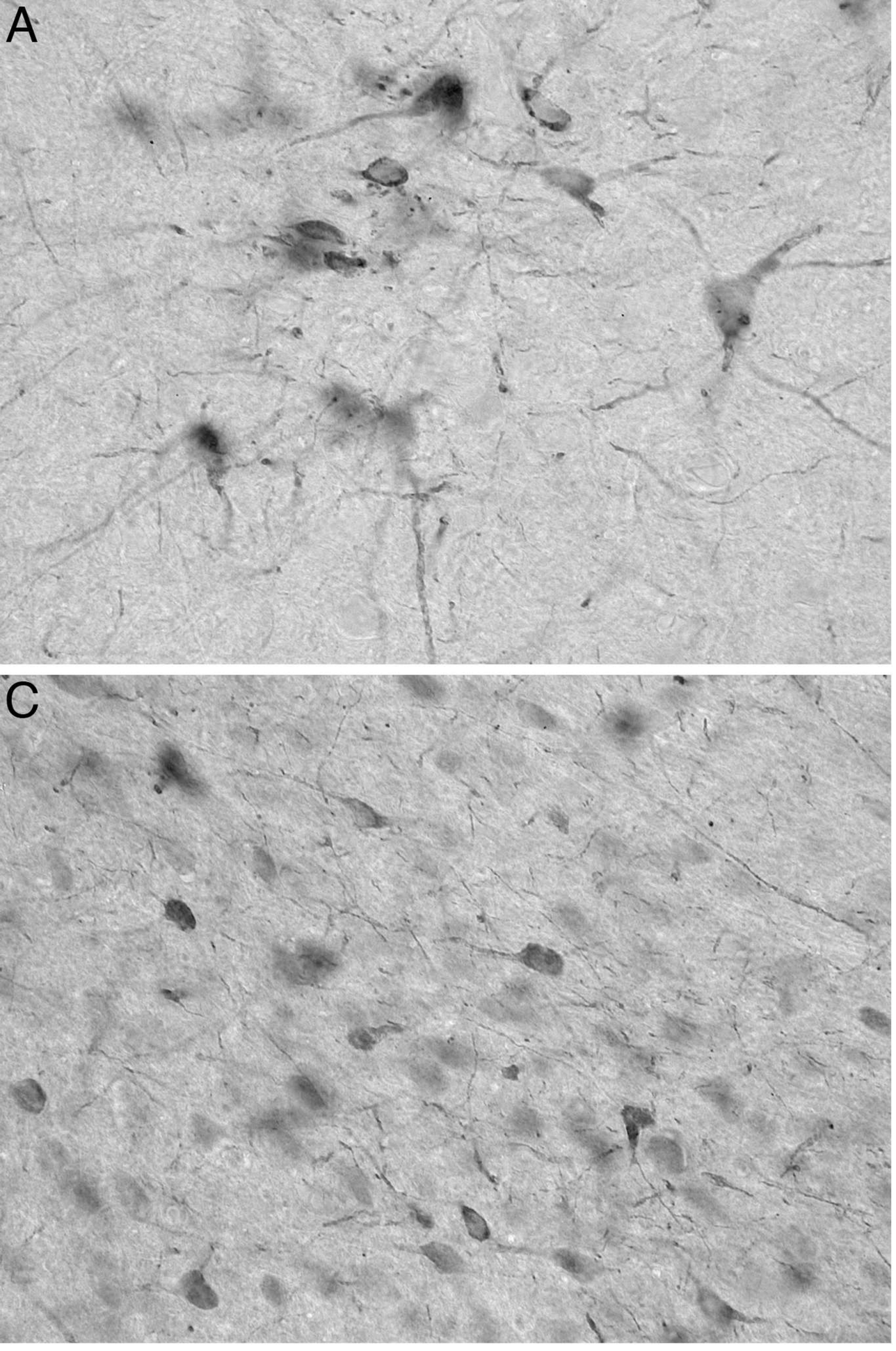
A
B
C
D
E
F
G
H

**Figure 6.4:** Photomicrographs of coronal sections through: **(A)** the ChAT immunoreactive neurons of the diagonal band of Broca and **(B)** the corresponding histaminergic terminal network; **(C)** the orexinergic immunoreactive neurons of the main cluster of the hypothalamus and **(D)** the corresponding histaminergic terminal network. Note the medium-density histaminergic terminal network distribution in **B,** and the high-density histaminergic terminal network in **D**. In all figures medial is to the left and dorsal towards the top. Scale bar in D = 100 µm and applies to all.

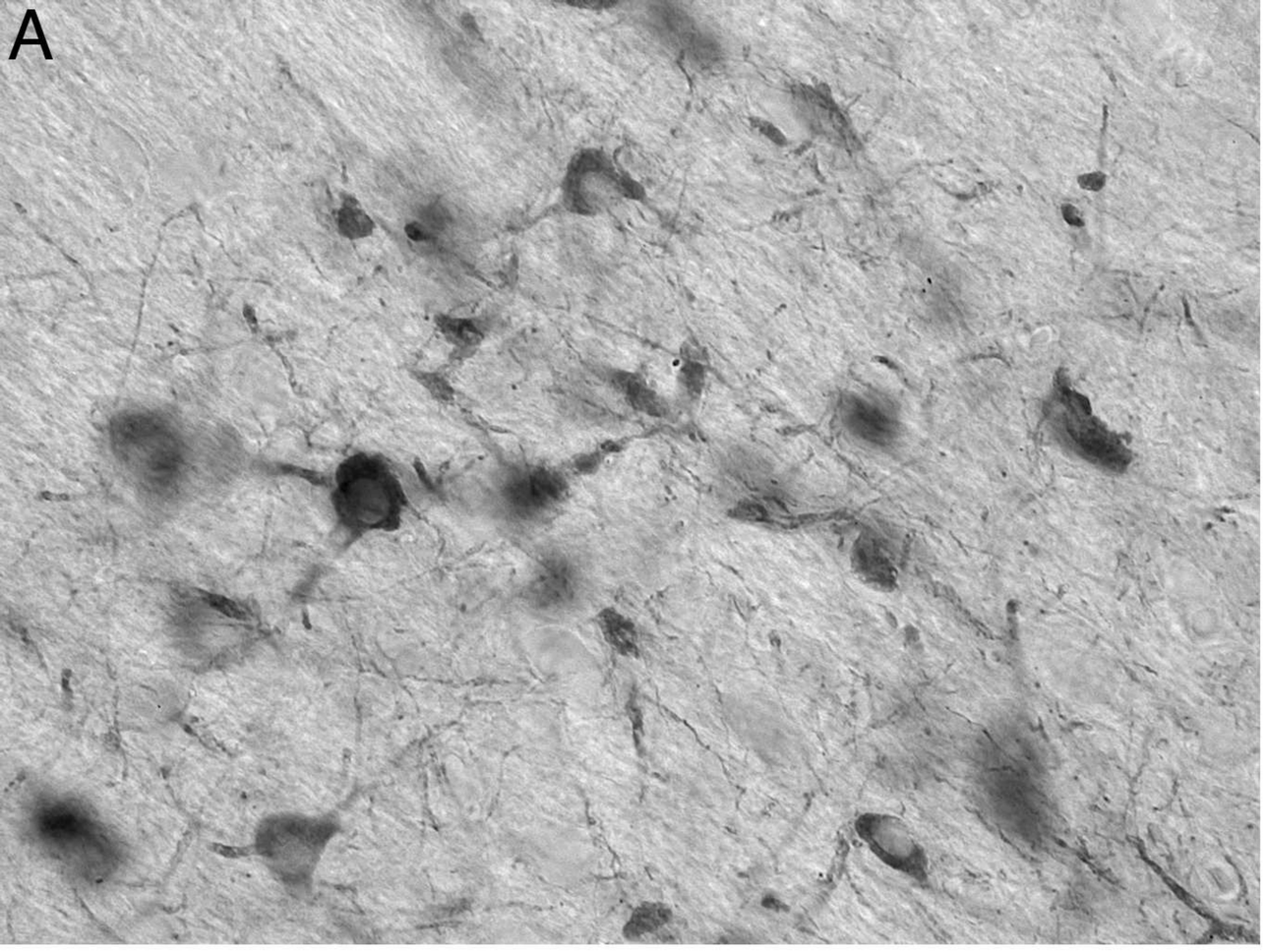
A

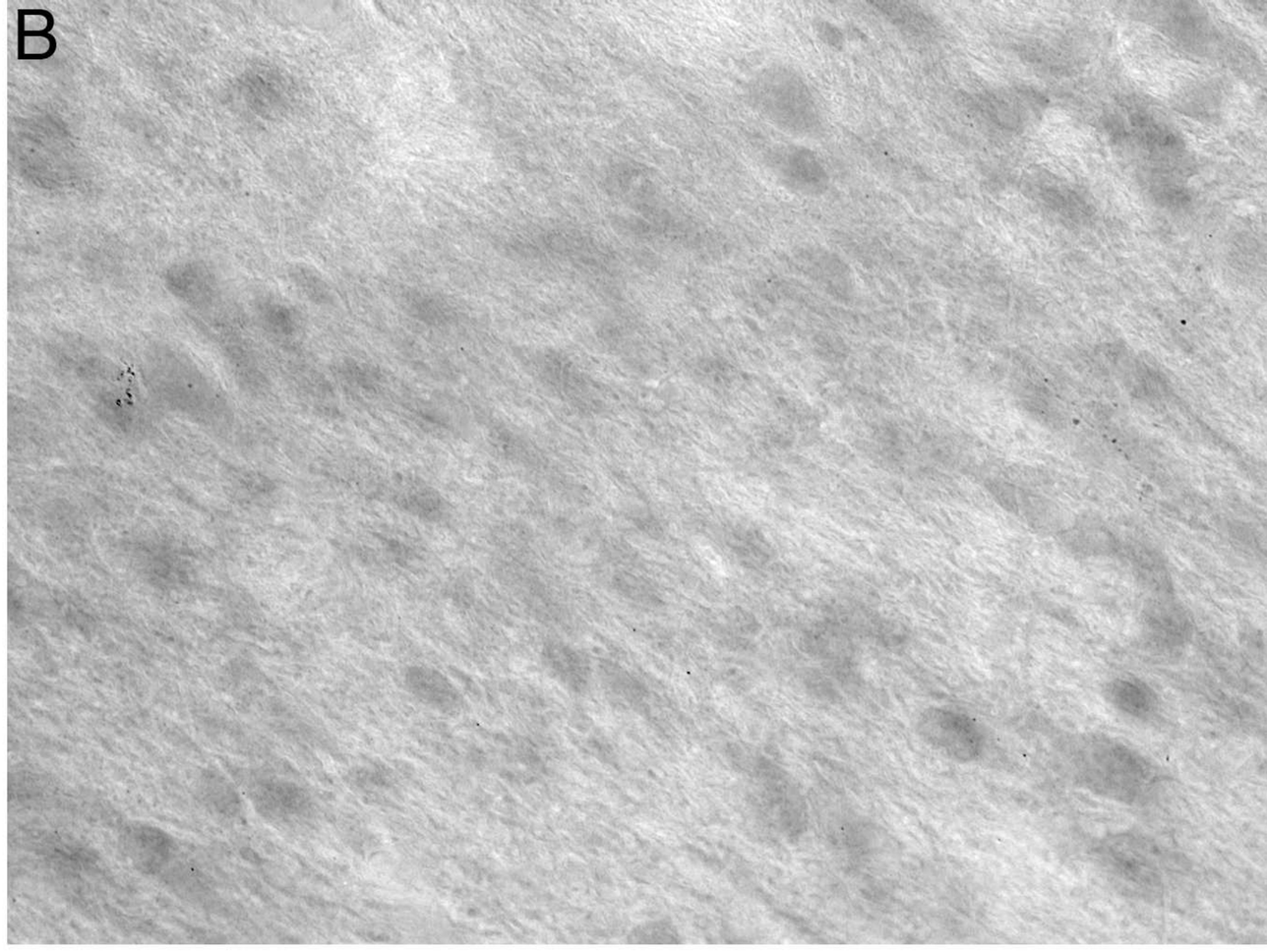
B

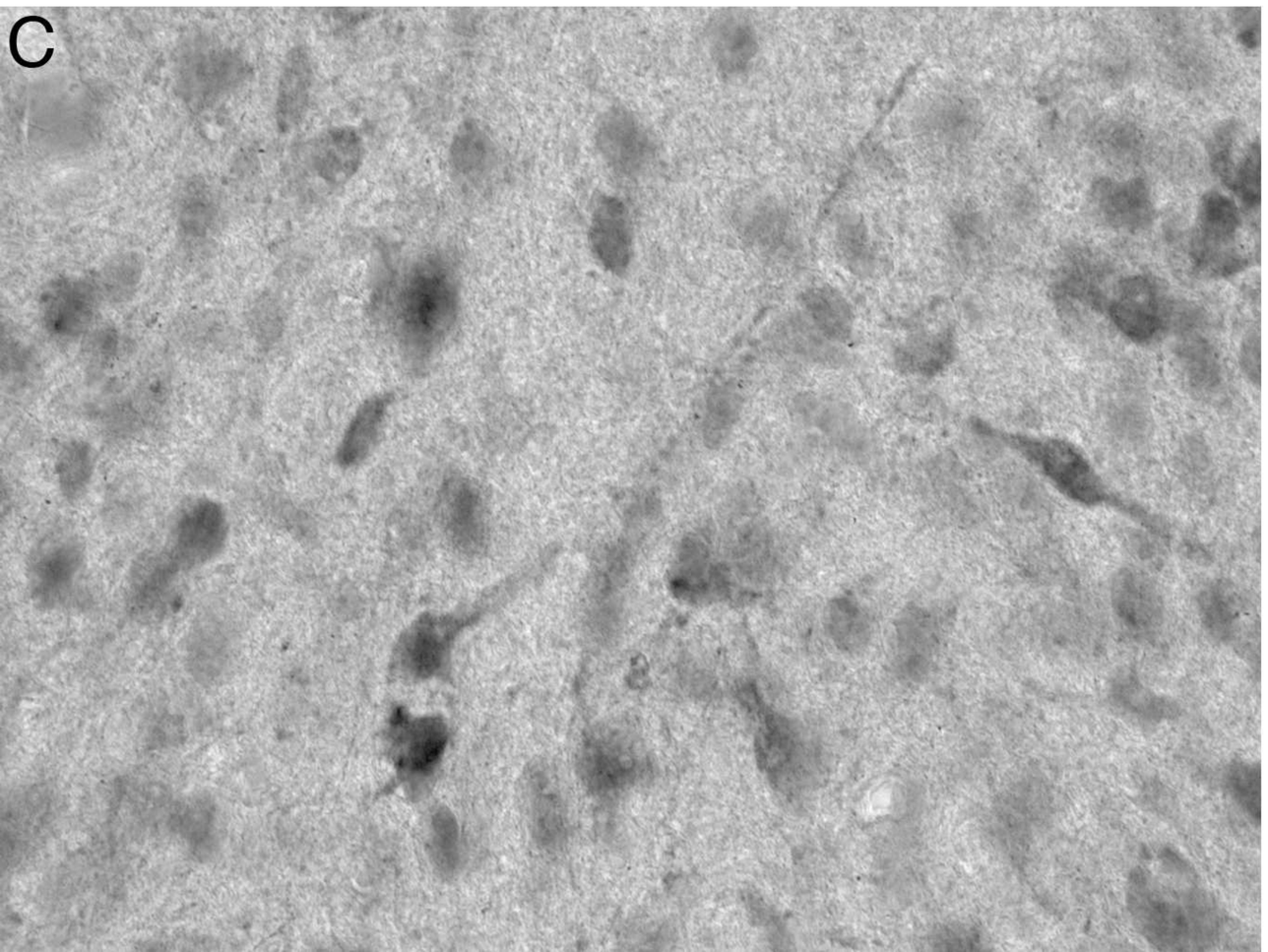
C

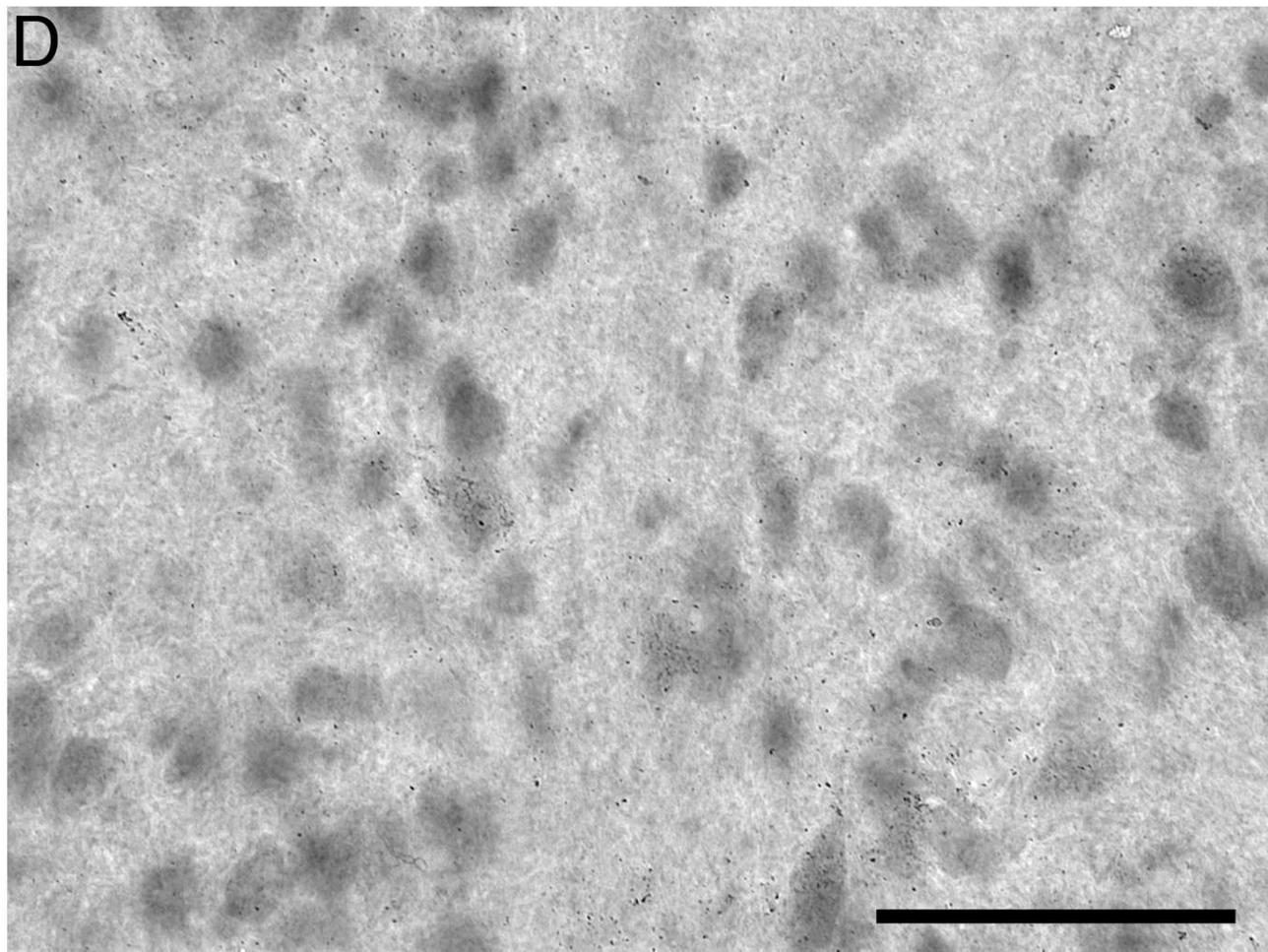
D

**Figure 6.5:** Photomicrographs of coronal sections through: **(A)** the ChAT immunoreactive neurons of the olfactory tubercle (TOL) and the corresponding **(B)** calbindin (CB), **(C)** calretinin (CR) and **(D)** parvalbumin (PV) immunoreactive neurons. A low-density of CB and PV immunoreactive neurons and a moderate density of CR immunoreactive neurons were observed in the TOL. In all figures medial is to the left and dorsal towards the top. Scale bar in D = 500 µm and applies to all.

A

B

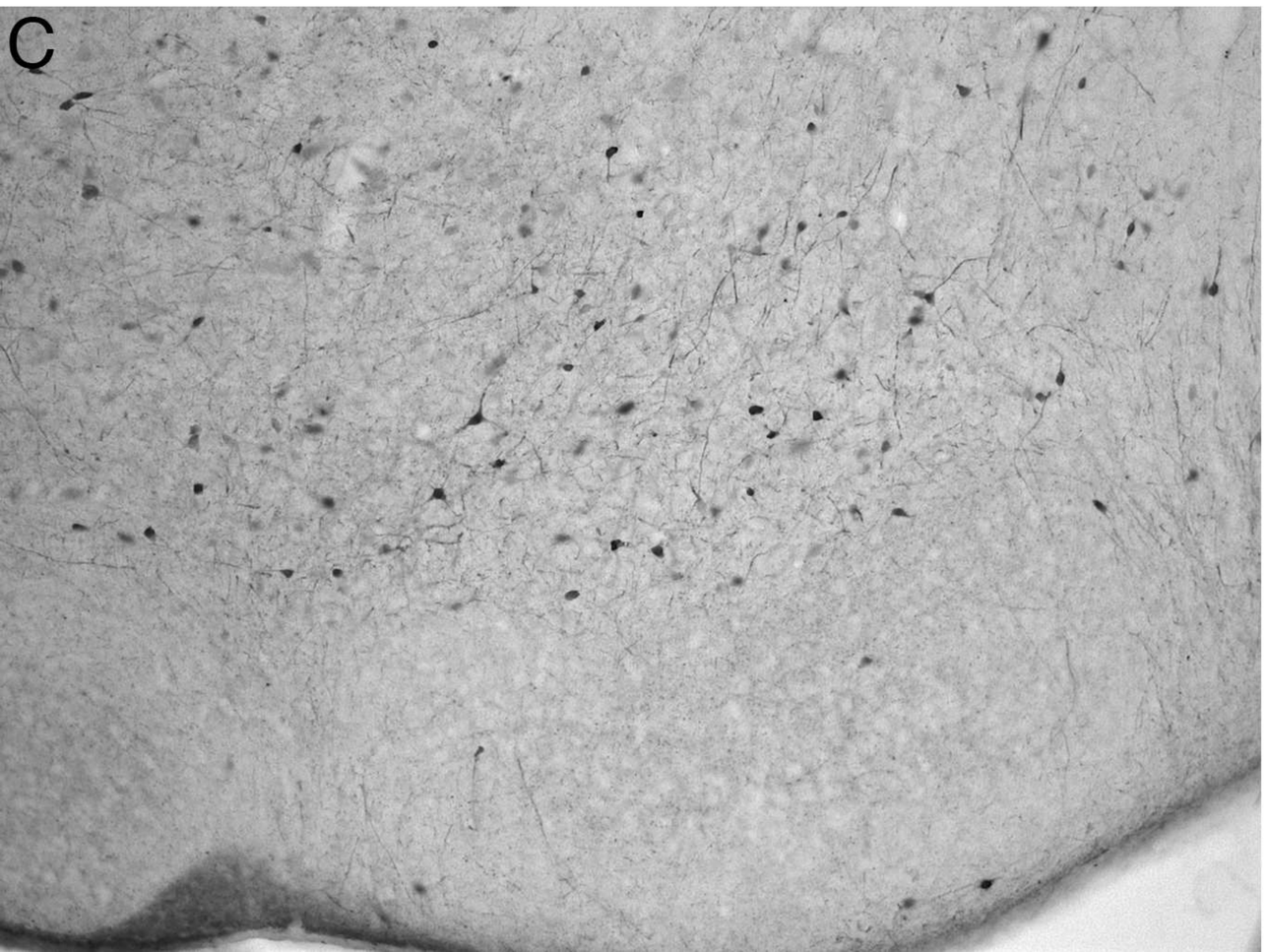
C

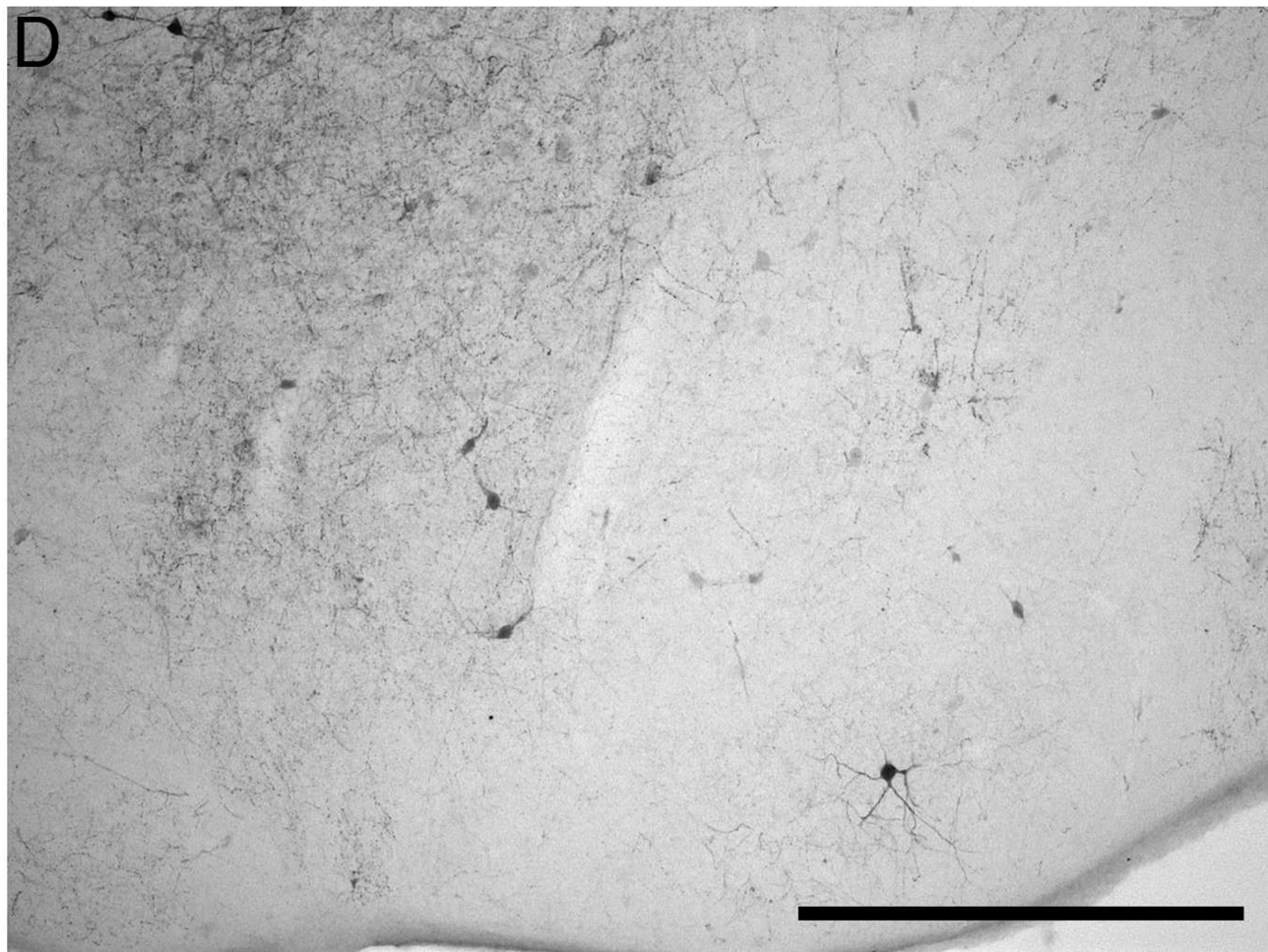
D

**Figure 6.6:** Photomicrographs of coronal sections through the anterodorsal (AD) and anteroventral (AV) nuclei of the dorsal thalamus of the rock hyrax stained for **(A)** Nissl **(B)** ChAT **(C)** Orexin-A **(D)** Calbindin (CB) **(E)** Calretinin (CR) and **(F)** Parvalbumin (PV). Note the division of the AV (**A**) into a dorsomedial and ventrolateral part. A moderate number of ChAT+ neurons are located within AD whereas only a few ChAT+ neurons mainly located on the dorsolateral periphery are seen in AV. Also note the dense orexinergic terminal network in AD, the similar morphology of the peripheral PV+ and ChAT+ cells within the AV. A moderate density of CB+ and PV+ neurons are seen within the ventrolateral region of the AV whereas few to no CR interneurons are evident. In all figures medial is to the left and dorsal towards the top. Scale bar in F = 1 mm and applies to all.

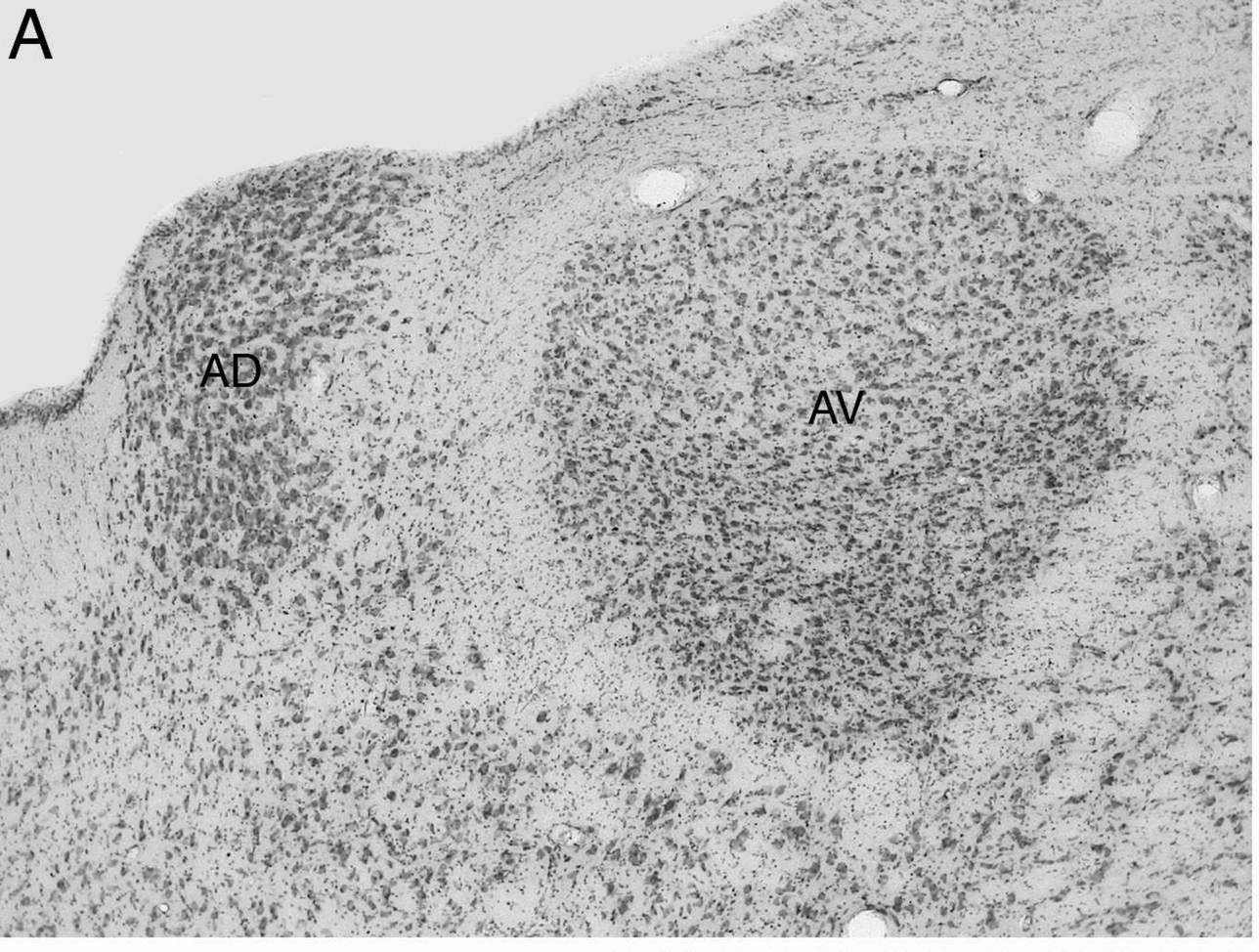
A
AD
AV

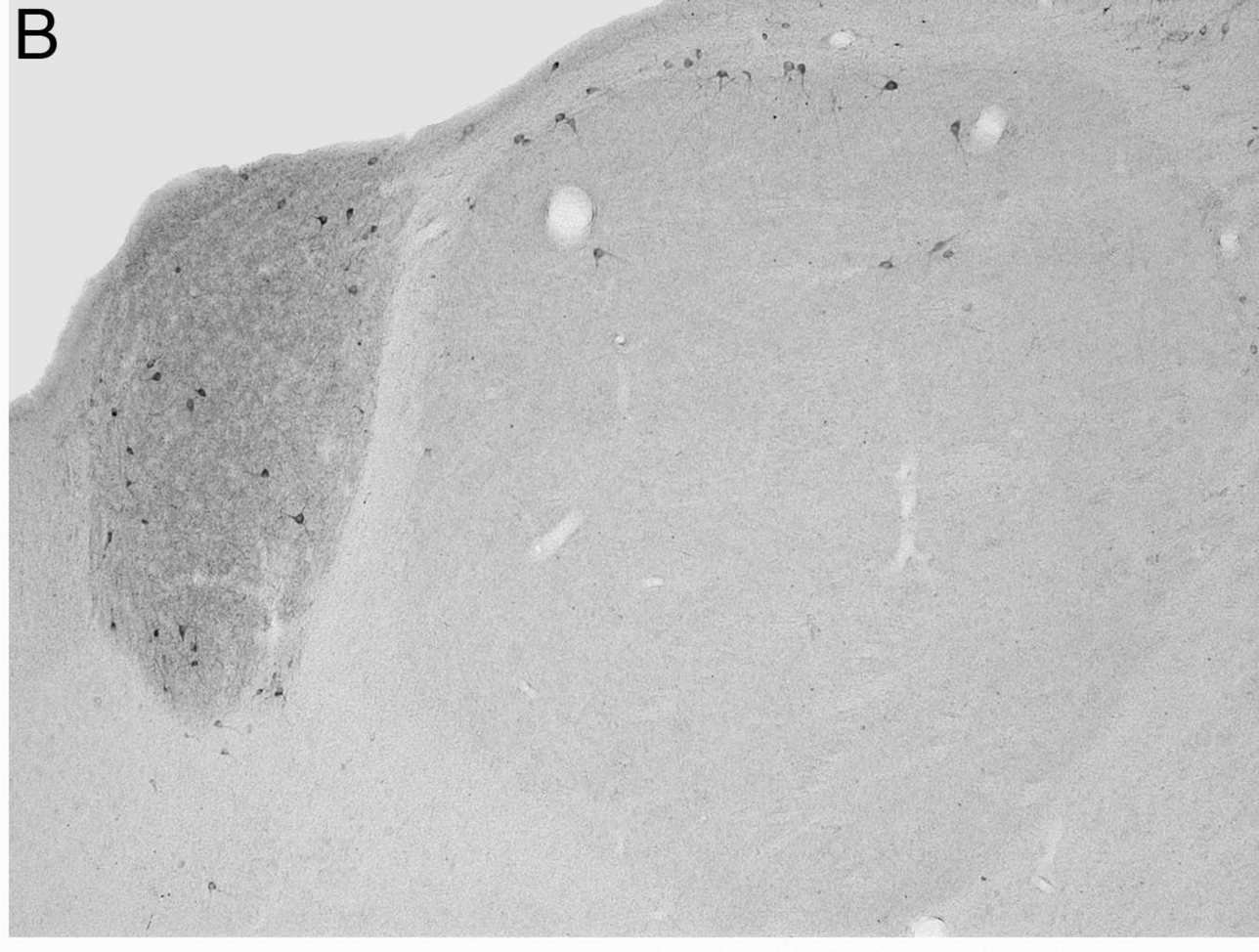
B

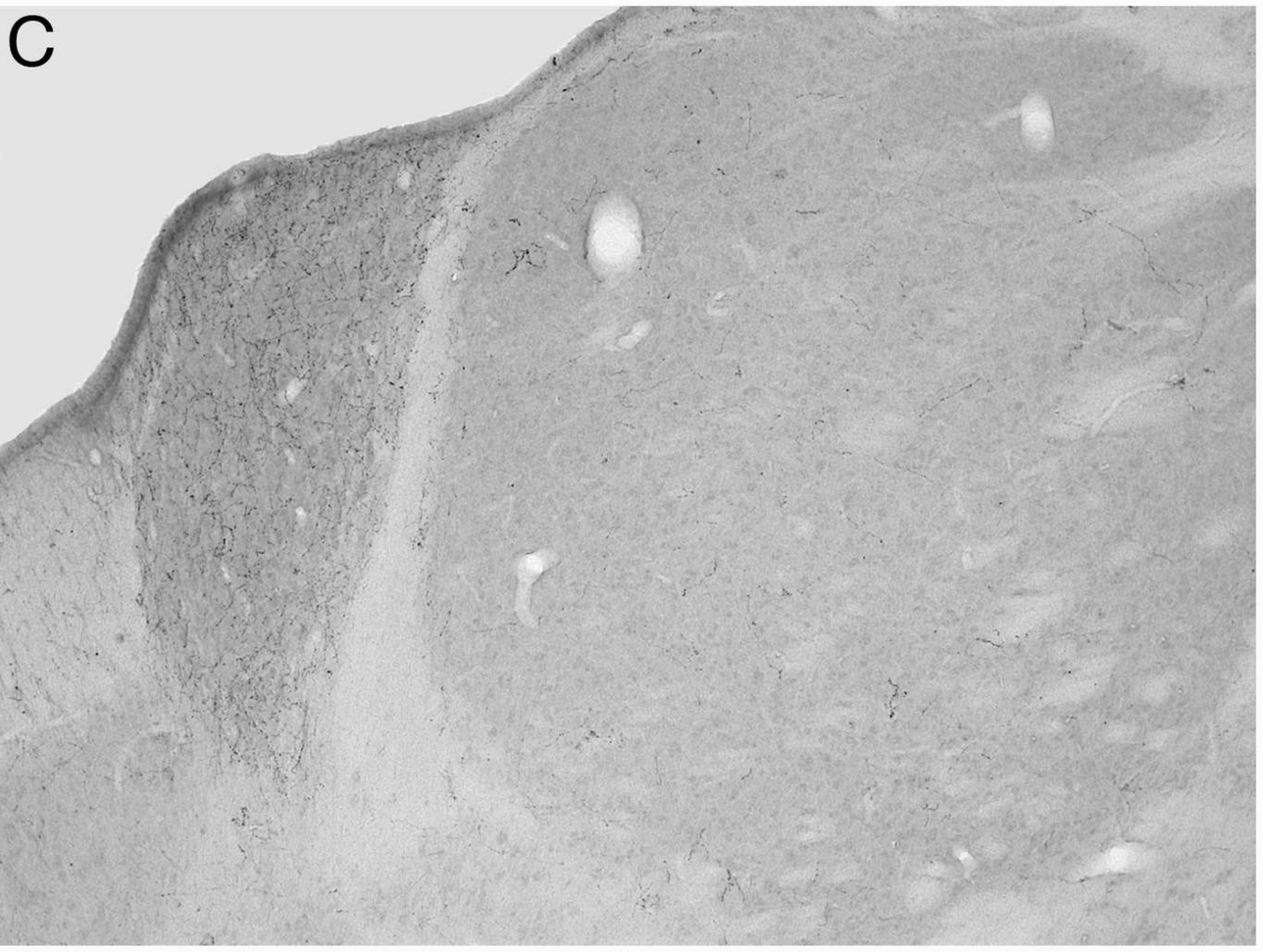
C

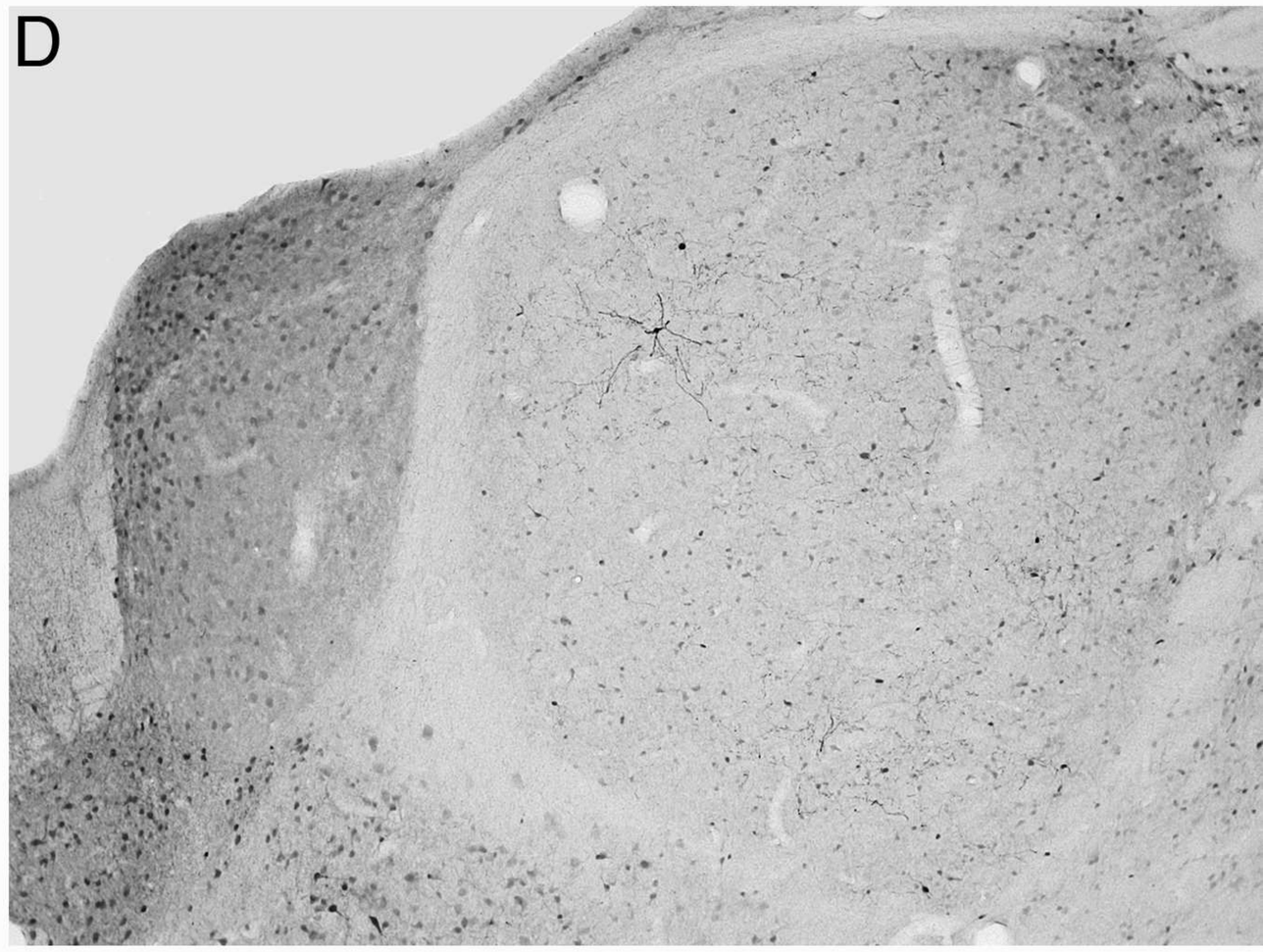
D

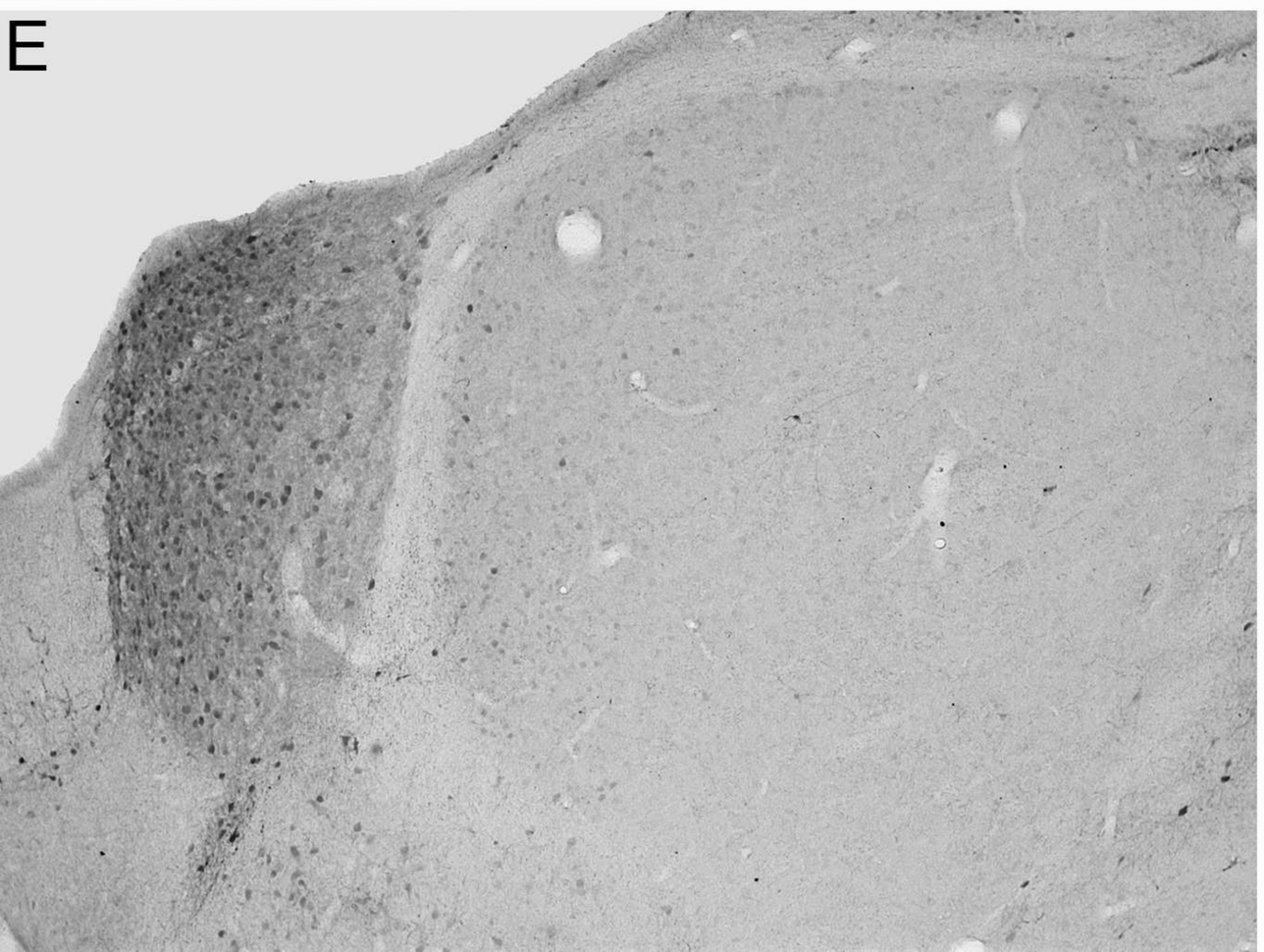
E

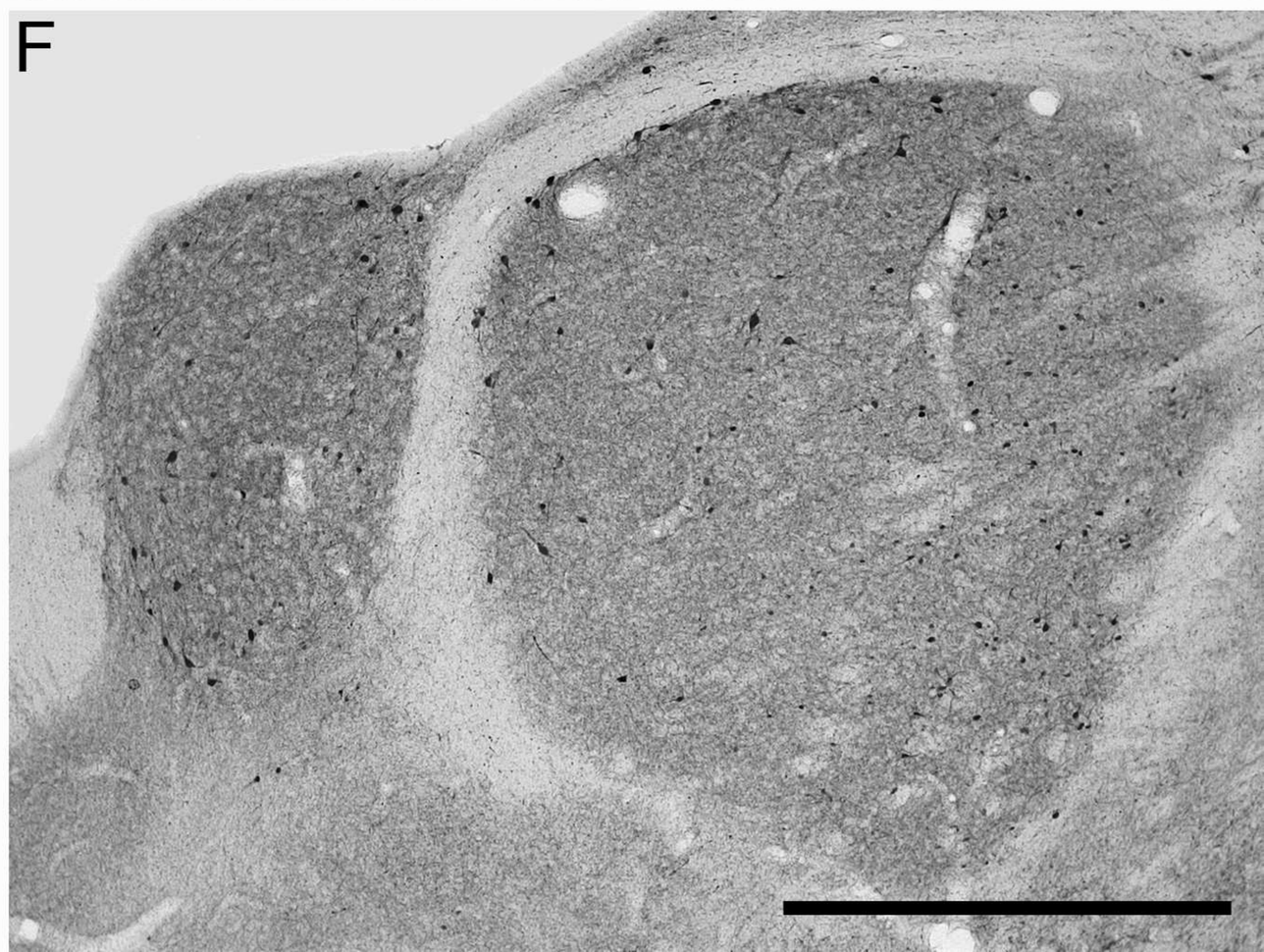
F

**Figure 6.7:** Photomicrographs of coronal sections through: **(A)** the tyrosine hydroxylase immunoreactive neurons of the caudal diencephalic group (A11) and the corresponding **(B)** calbindin (CB) **(C)** calretinin (CR) and **(D)** parvalbumin (PV) immunoreactive neurons in adjacent sections. Moderate to high-density of CB and CR immunoreactive neurons are evident, but no PV immunoreactive interneurons were observed intermingled with the TH+ neurons of the A11. In all figures medial is to the left and dorsal towards the top. Scale bar in D = 500 µm and applies to all.

A

3V

A11

fr

B

C

D

**Figure 6.8:** Photomicrographs of coronal sections through: **(A)** the serotonergic immunoreactive neurons of the dorsal raphe nuclear complex and the corresponding **(B)** calbindin (CB) **(C)** calretinin (CR) and **(D)** parvalbumin (PV) immunoreactive neurons. The midline raphe nuclei (DRd, DRv and DRif) exhibited a high density of CB+ neurons, a very low density of CR+ neurons and no PV+ neurons. A moderate density of both CB+ and CR+ neurons, but no PV+ neurons, were seen in the peripheral nuclei (DRl and DRp) of the dorsal raphe complex. In all figures medial is to the left and dorsal towards the top. Scale bar in D = 1 mm and applies to all.

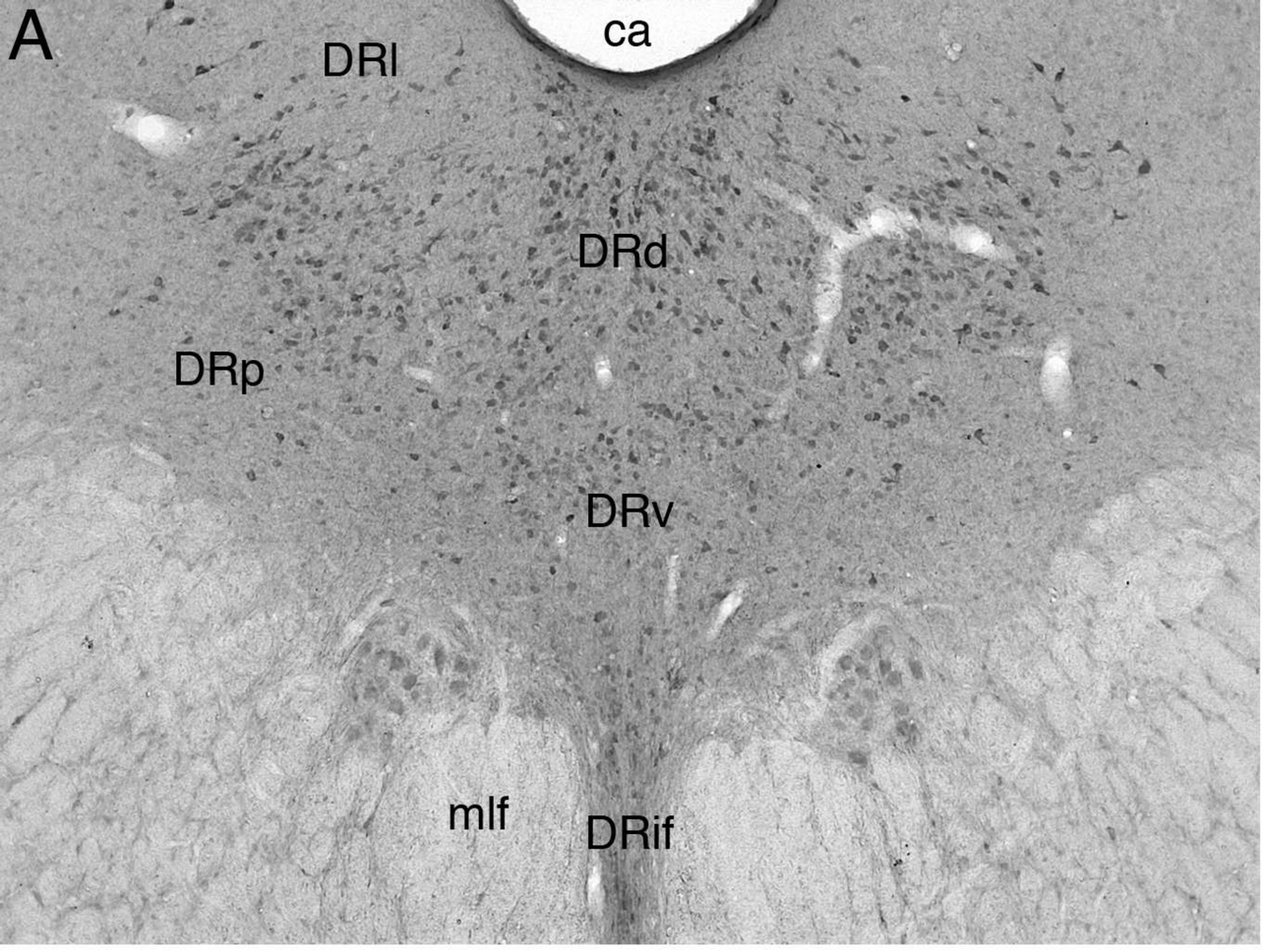
A
ca
DRl
DRd
DRp
DRv
mlf
DRif

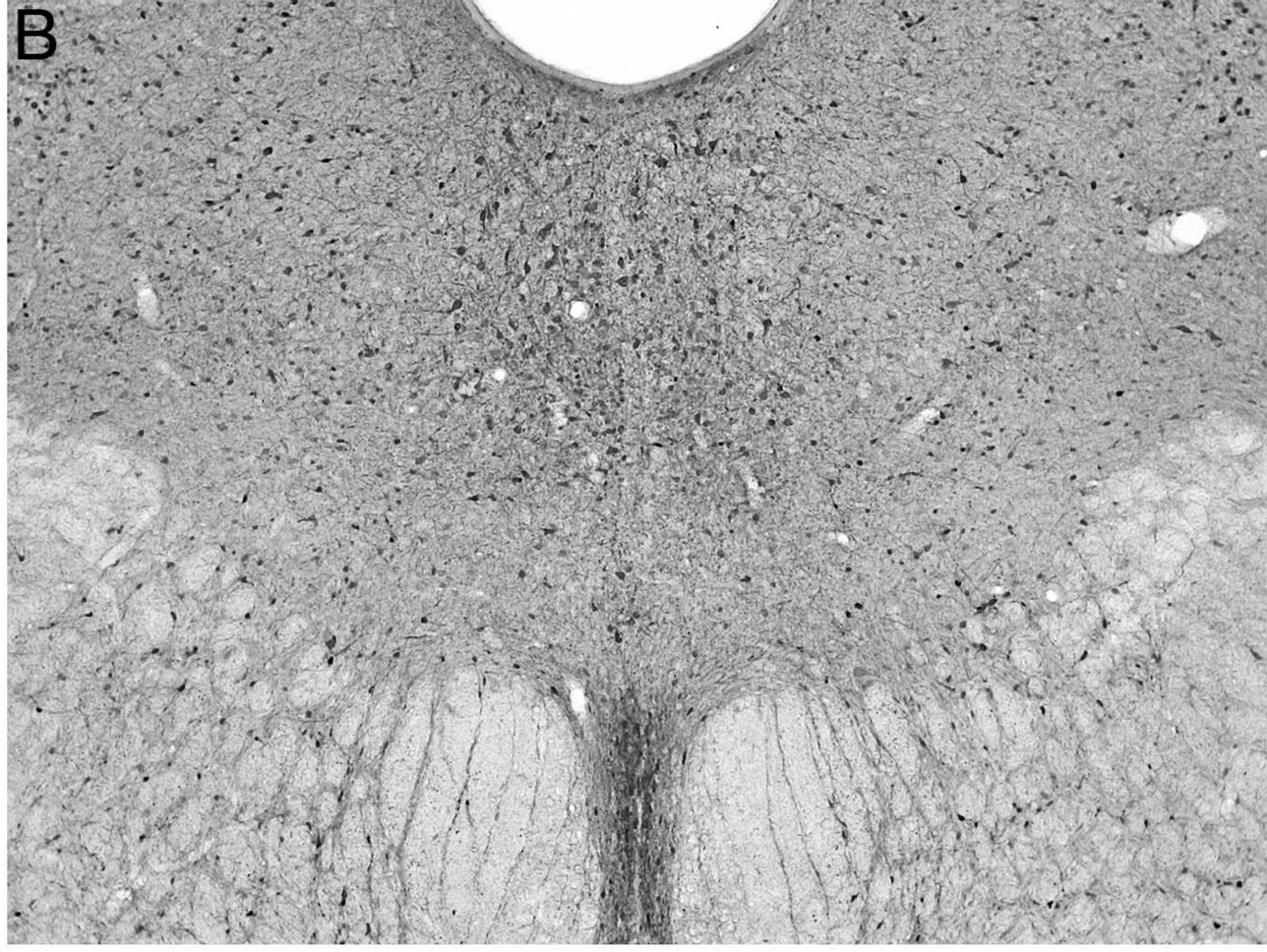
B

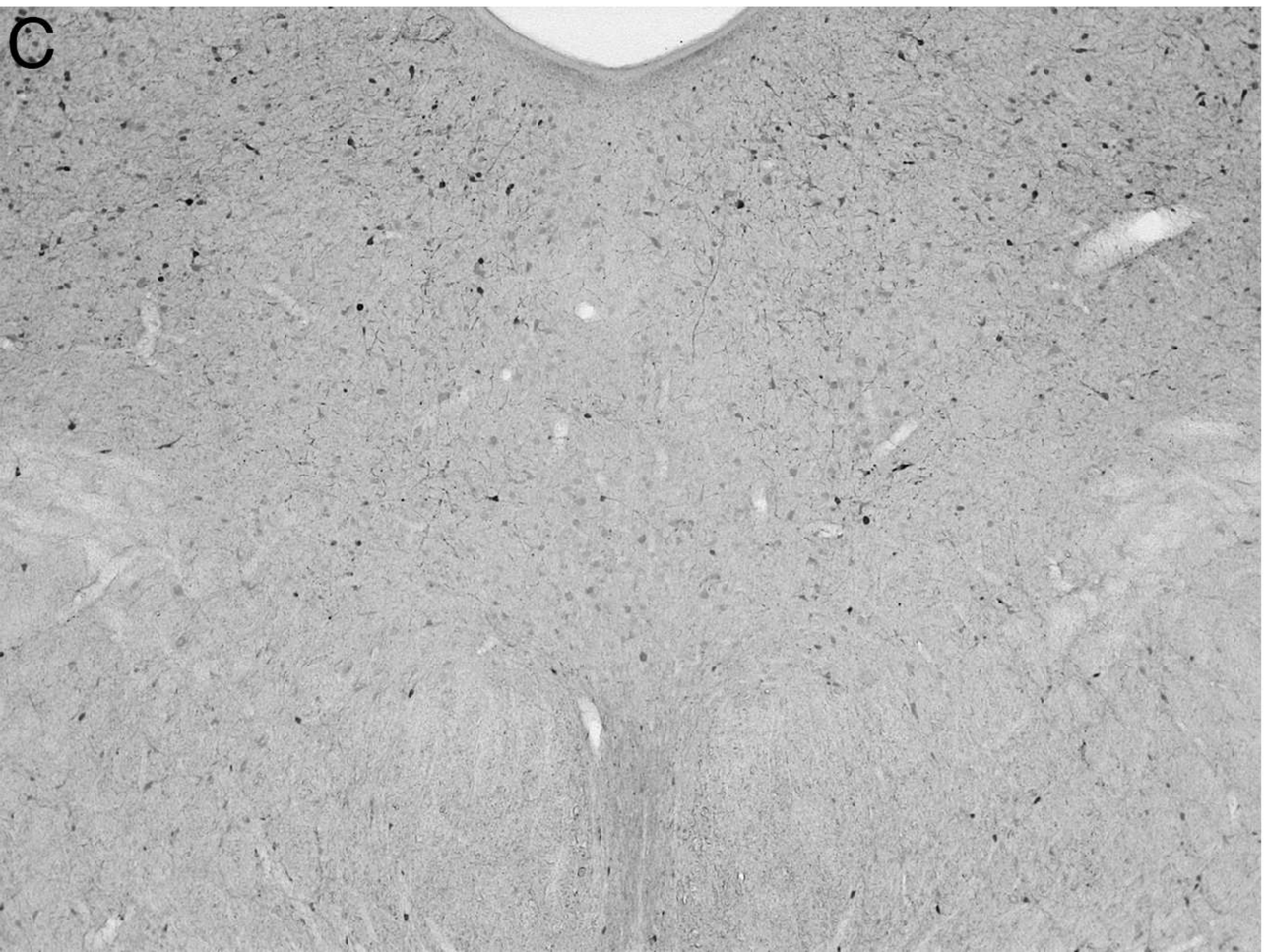
C

D

**Figure 6.9:** Photomicrographs of coronal sections through: **(A)** the ChAT immunoreactive neurons of the laterodorsal tegmental nucleus illustrating both the parvo- (LDTpc) and magnocellular (LDTmc) divisions and the corresponding **(B)** calbindin (CB) **(C)** calretinin (CR) and **(D)** parvalbumin (PV) immunoreactive neurons. A moderate density of CB+ neurons, a high density of CR+ neurons, but no PV+ neurons, were observed in the regions coincident with the LDT. Note that the CB+ and CR+ neurons are evenly distributed between the parvo- and magnocellular divisions. Also note the difference in the neuronal morphology between CB+, CR+ and ChAT+ neurons of the LDTpc, indicating that these smaller ChAT+ neurons are unlikely to be interneurons of a GABAerigic nature. In all figures medial is to the left and dorsal towards the top. Scale bar in D = 500 µm and applies to all.

A

LDTpc

LDTmc

DTg

B

C

D

**Figure 6.10:** Photomicrographs of coronal sections through: **(A)** the tyrosine hydroxylase immunoreactive neurons of the diffuse portion of the locus coeruleus (A6d) and the compact portion of the nucleus subcoeruleus (A7sc) and the corresponding **(B)** calbindin (CB), **(C)** calretinin (CR) and **(D)** parvalbumin (PV) immunoreactive neurons. A moderate density of CB+ neurons was observed in the region of the A6d, but a low density was seen in region of A7sc. CR+ neurons were seen in the region of the A6d and given the similarity in morphology it would appear that the TH+ neurons of the A6d are also CR+. A low to moderate density of CR+ neurons were seen in region of A7sc, but no PV+ neurons were observed in the regions that coincide to the A6d or A7sc. Note the high density PV+ immunoreactive terminal network overlapping the A7sc indicating PV+ input to this nucleus from a distant location. In all figures medial is to the left and dorsal towards the top. Scale bar in D = 500 µm and applies to all.

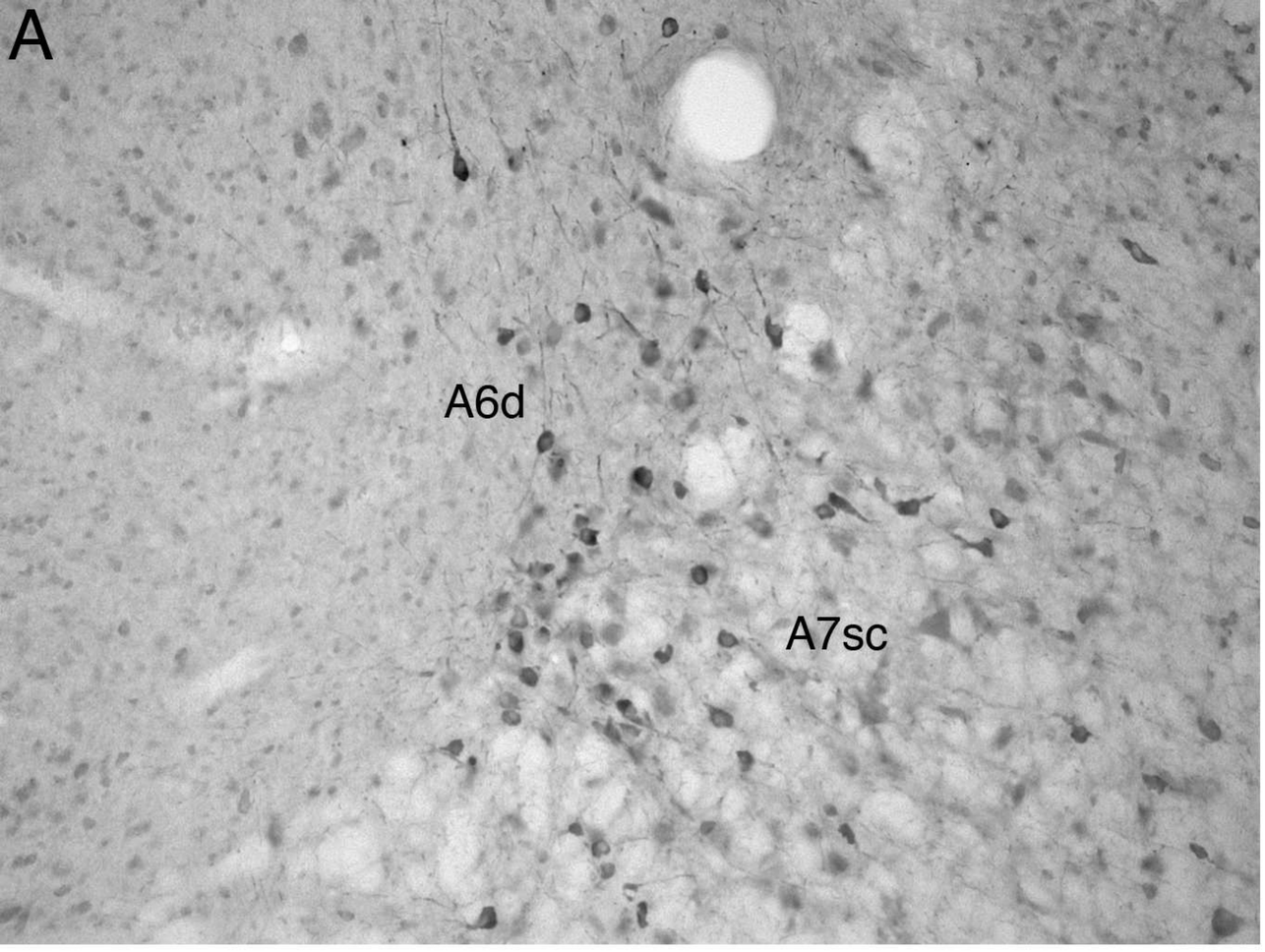
A
A6d
A7sc

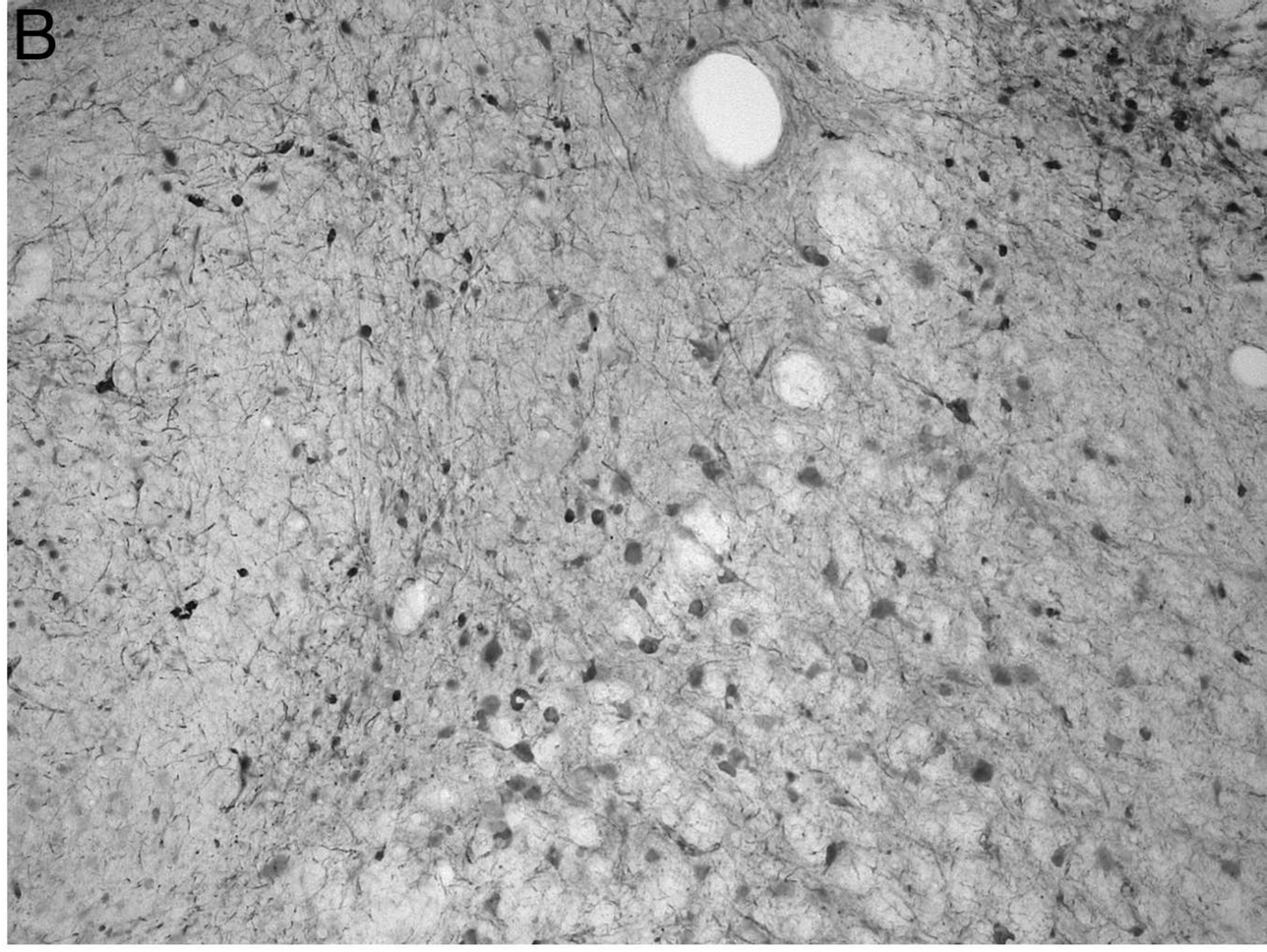
B

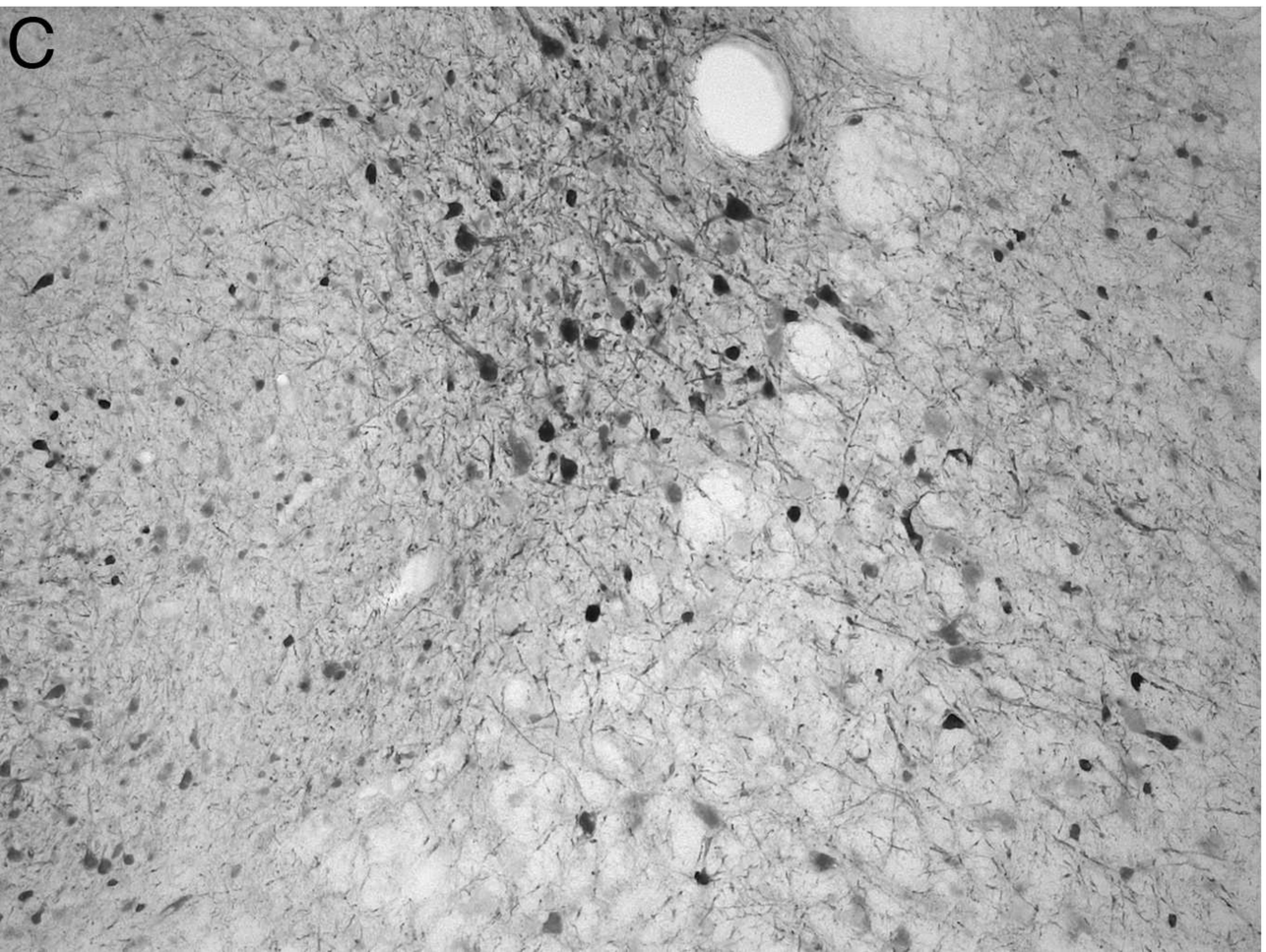
C

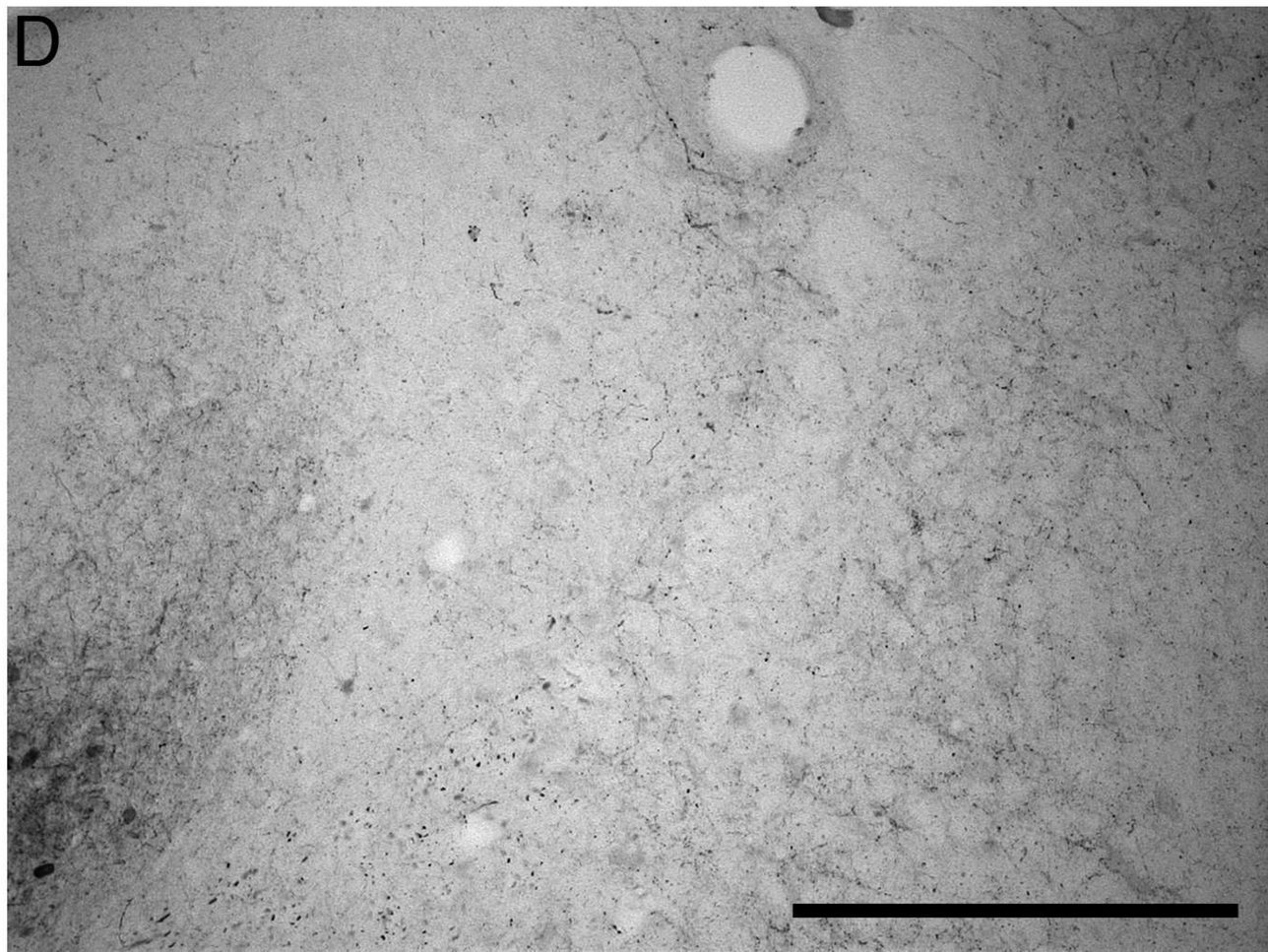
D

**Table 6.1:** Illustration of the degree of GABAergic (calbindin, calretinin and parvalbumin) neuronal and terminal network distribution in the regions of the cholinergic, catecholaminergic, serotonergic and orexinergic nuclei related to the sleep-wake cycle. In the regions where no GABAergic neurons and terminal networks were observed a (-) has been used in the table, however regions that exhibited low densities of neurons and terminal networks have been illustrated by (+), moderate densities by (++) and high densities by (+++).

| | Calbindin | | Calretinin | | Parvalbumin | |
|---|---|---|---|---|---|---|
| | **Cells** | **Terminals** | **Cells** | **Terminals** | **Cells** | **Terminals** |
| ***Cholinergic nuclei*** | | | | | | |
| Sep. M | + | + | ++ | +++ | + | +++ |
| Diag. B | + | + | ++ | +++ | -/+ | +++ |
| TOL | ++ | +++ | ++/+++ | ++ | +/++ | +++ |
| Is. Call | - | - | ++/+++ | ++ | +/++ | +++ |
| N. Bas | +/++ | ++ | + | + | -/+ | + |
| AD | +/++ | ++/+++ | +/++ | ++/+++ | ++ | ++/+++ |
| AV | + | + | -/+ | + | ++ | +++ |
| Hypothalamic nuclei | ++ | +++ | ++ | ++ | - | - |
| PPT | ++ | ++ | ++ | ++ | - | - |
| LDT | ++ | ++ | ++ | ++ | - | - |
| PBg | ++ | ++ | ++ | ++ | - | - |
| ***Catecholaminergic nuclei*** | | | | | | |
| Hypothalamic nuclei | ++ | +++ | ++ | ++ | - | - |
| A6d | - | +++ | ++/+++ | ++/+++ | - | + |
| A7 | ++/+++ | +++ | ++/+++ | ++/+++ | - | + |
| ***Serotonergic nuclei*** | | | | | | |
| CLi | ++/+++ | ++/+++ | ++ | ++ | - | + |
| B9 | ++/+++ | ++/+++ | ++ | ++ | - | + |
| MnR | ++/+++ | ++/+++ | +/++ | +/++ | - | -/+ |
| DRif | ++/+++ | ++/+++ | + | + | - | + |
| DRv | ++/+++ | ++/+++ | + | + | - | + |
| DRd | ++/+++ | ++/+++ | + | + | - | + |
| DRp | ++/+++ | ++/+++ | +/++ | +/++ | - | + |
| DRl | ++/+++ | ++/+++ | +/++ | +/++ | - | + |
| DRc | ++/+++ | ++/+++ | +/++ | +/++ | - | + |
| ***Orexinergic nuclei*** | | | | | | |
| Hypothalamic nuclei | ++ | +++ | ++ | ++ | - | - |

## 6.5. Discussion

The aim of the present study was to describe the location and the distribution of the cholinergic, catecholaminergic, serotonergic, and orexinergic sleep related nuclear groups and the interrelation of these groups to the calcium binding GABAergic interneurons, parvalbumin (PV), calbindin (CB) and calretinin (CR), and their terminal network distributions within the brain of the rock hyrax, *Procavia capensis.* The location and distribution of the nuclei involved in the control and regulation of the sleep-wake cycle was found to be similar to that previously described by Gravett et al., (2009, 2011) and followed the typical mammalian organisational plan for these systems.

### *6.5.1 The unique cholinergic and orexinergic features of the hyrax brain*

The presence of cholinergic neurons within the anterodorsal (AD) and anteroventral (AV) nuclei of the dorsal thalamus as well as the parvo- and magnocellular subdivisions of the laterodorsal tegmental (LDT) and pedunculopontine tegmental (PPT) nuclei appears to be unique to the rock hyrax and have not been described in any other mammal studied to date (Gravett et al, 2009) (Figs. 6.6 B and D, 6.9). The serotonergic, orexinergic and histaminergic terminal network distributions were similar to what has been previously described in other mammals (Leger at al., 2001, Airaksinen and Panula, 1988; Gravett et al., 2011; Inagaki et al., 1988), with the exception of the dense orexinergic innervation of the AD nucleus that has only been observed previously in the Nile grass rat, *Arvicanthis niloticus* (Novak and Albers, 2002; Nixon and Smale, 2007) and Syrian hamster, *Mesocricetus auratus*, both diurnal mammals (Mintz et al., 2001). It is possible that orexinergic innervation of the AD nucleus might be a unique feature associated with

diurnal mammals. It was also noted that the dense orexinergic innervation of the AD nucleus overlapped with cholinergic neurons and terminal networks in this nucleus. It is possible that this dense orexinergic innervation of the AD nucleus may act in concert with the cholinergic neurons and/or the cholinergic axonal terminals, which in turn may influence arousal states and motivational processing (Gravett et al., 2011).

*6.5.2 GABAergic interneurons, functional aspects of relevance*

The location and distribution of the calcium binding GABAergic interneurons in relation to the sleep related cholinergic, catecholaminergic, serotonergic and orexinergic nuclei was for the most part similar to that described in other mammals (Celio, 1990; Charara and Parent, 1998; Rogers, 1992). Of these GABAergic inhibitory interneurons PV appeared to have no direct overlap with the nuclei involved in the sleep-wake cycle although it may project to them from a distance (see Figure 6.10D), whereas CB was ubiquitous in the sleep related nuclei in both its neuronal and terminal network distribution and CR was observed to be mostly ubiquitous, but had a lower cellular number and less dense terminal network expression than CB. CB and CR inhibitory interneurons are generally involved in local processing and it is possible that those located within and adjacent to the sleep related nuclei may be involved in their circuitry. CB interneurons have a tonic or regular firing rate, whereas CR interneurons depolarize in sudden burst of activity and thus have irregular firing rates. It is possible that the regular firing rate of CB interneurons correlates to state maintenance, whereas the irregular firing rate of CR interneurons correlates to state changes (Cauli et al., 1997; Ascoli et al., 2010). Some of the functions that have been assigned to these interneuron types include the regulation of intracellular calcium homeostasis (Braun, 1990; Baimbridge et al., 1992;

Charara and Parent, 1998), while CB and CR have been reported to protect neurons against neurodegenerative processes and calcium overload (Braun, 1990; Celio, 1990; Baimbridge et al., 1992; Parent et al., 1996; Charara and Parent, 1998). Within the basal forebrain of the rock hyrax, an even distribution of both CB and CR neurons and terminal networks was observed; however, within the regions of the cholinergic AD, AV, PPT and LDT nuclei, the catecholaminergic locus coeruleus complex and the serotonergic dorsal raphe nuclear complex a heterogeneous distribution of CB and CR neurons and terminals networks was observed.

*6.5.3 GABAergic neurons and the anterior thalamic nuclei*

Within the AD nucleus a dorsomedial band of CB+ and CR+ neurons and a moderate to high-density terminal network distribution was observed. The AV nucleus contained a moderate density of scattered CB+ neurons with a low-density terminal network, whereas very few CR+ neurons and a low-density terminal network distribution were observed. It also appears from the Nissl stained sections that the AV nucleus can be architectonically subdivided into dorsomedial and ventrolateral subnuclei. Within the dorsomedial AV subnucleus, where the ChAT+ neurons were identified, PV+ neurons were also located. Both the ChAT+ and PV+ neurons in this region have similar morphologies and it is possible that these ChAT+ neurons are also PV+ neurons – It has been reported by Bayraktar et al. (1997) that nearly all VIP+ and approximately 88% of ChAT+ neurons also contain GABA. The ventrolateral AV subnucleus did not contain any ChAT+ neurons but a moderate density of smaller PV+ neurons with a different morphology was evident (Fig. 6.6). It is interesting that both these anterior thalamic nuclei exhibit a moderate density of CB+ and PV+ interneurons as both CB+ and PV+ interneurons have been described as fast spiking

cells that discharge tonically and that this discharge pattern is possibly correlated to state maintenance (Cauli et al., 1997). GABAergic neurons located within the anterior hypothalamus have also been described as being maximally active during NREM sleep and that the neurons located in this region as well as the basal forebrain could be considered as the most potent sleep promoting neurons (Szymusiak, 1995; Szymusiak et al., 2001; Siegel, 2004). Furthermore given that both the cholinergic and orexinergic systems in general appear to be related to activity requiring both alertness and awareness, the ChAT+ neurons and ChAT+ and Orx+ terminal networks observed within the AD and AV nuclei may have the effect of enhancing the wakefulness promoting functions of the anterior thalamic nuclei in the rock hyrax. It is possible that the presence of the CB+ and CR+ GABAergic interneurons within the anterior thalamic nuclei may act against the action of these wakefulness promoting cholinergic neurons and in doing so initiate and maintain NREM sleep, while the dense orexinergic terminal network (Gravett et al., 2011) may be involved in exciting the neurons and in doing so promote wakefulness (Gerashchenko and Shiromani, 2004). Double-immunohistochemical labelling as well as single unit recording studies would be required before the aforementioned possibilities could be confirmed for these anterior thalamic nuclei in the brain of the rock hyrax.

*6.5.4 GABAergic neurons and the pontine cholinergic nuclei*

An even distribution of both CB+ and CR+ neurons were observed in the regions coincident with the cholinergic parvo- and magnocellular LDT and PPT (Fig. 6.9). The ChAT+ neurons located within these nuclei had a different morphology than the intermingled CB+ and CR+ neurons, the ChAT+ neurons were larger and multipolar whereas the CB+ and CR+ neurons were smaller and bipolar. Based on the

clear difference in neuronal morphology between the cholinergic neurons and the aforementioned calcium binding inhibitory interneurons, it is likely that the parvocellular divisions of both the LDT and PPT are not inhibitory interneurons; however double-immunohistochemical labelling would be required to confirm this. If the double-immunohistochemical labelling revealed that these neurons are not inhibitory interneurons, the implication would be that the LDT and PPT within the brain of the rock hyrax would be more complexly organized than that seen in any other mammals studied to date. The complexity in the organization seen in the LDT and PPT could also possibly provide clues as to the reasons behind the peculiar aspects of REM sleep observed in these animals (see Chapters 4 and 5). Another unusual difference observed within the region of LDT was the absence of PV+ interneurons, but a dense PV terminal network within the magnocellular division. It is possible that the dense PV+ terminal network is a result of PV+ projections originating from PV+ neuronal populations located a distance away from the magnocellular division of the LDT nucleus.

*6.5.5 GABAergic neurons and the locus coeruleus complex*

A moderate to high density of CB+ and CR+ neurons were observed in the region of the locus coeruleus. The CR+ neurons appeared to have a similar neuronal morphology and were located in the same position as the TH+ neurons that define the locus coeruleus; this was not the case with the CB+ neurons (Fig. 6.10). It is possible that TH+ neurons of locus coeruleus might also be CR+ neurons, but double-immunohistochemical labelling would be needed to confirm this possibility. A low density of CB+ and CR+ neurons were also observed in the regions overlapping the subcoeruleus. The location of CB+ and CR+ neurons within the locus coeruleus

complex of the rock hyrax is thus different to that described for the rat locus coeruleus complex, where both these interneuron types were reported to be absent (Rogers, 1992).

*6.5.6 GABAergic neurons and the serotonergic dorsal raphe complex*

A heterogeneous CB+ neuronal distribution was seen in the regions of the serotonergic dorsal raphe nuclei. The median raphe nuclear groups (i.e. DRd, DRv, DRif) exhibited a higher density of CB+ neurons, whereas those located laterally (i.e. DRl and DRp) exhibited a more moderate density. CR+ neurons were present in moderate density in the lateral dorsal raphe nuclei (DRl and DRp), whereas they were observed in a low to almost absent density in the regions coincident to the midline nuclear groups (DRd, DRv and DRif). No PV+ neurons were observed overlapping the serotonergic dorsal raphe nuclear complex (Fig. 6.8). These observations are different to that described in other mammals. In primates PV+ neurons have been reported to present in all the subnuclei of the dorsal raphe, whereas CB+ and CR+ neurons were not present (Charara and Parent, 1998). The rat brain has been described as being devoid of PV+ neurons in this region, with only CB+ neurons being present in the caudal part of the dorsal raphe and CR+ neurons in the regions of the DRl and DRc nuclei (Celio, 1990; Arai et al., 1991). It has been hypothesized that in the rat some CR+ neurons in the dorsal raphe project selectively to the striatum, globus pallidus and ventrobasal thalamus (Krzywkowski et al., 1995); however, it is unknown whether CB+ and PV+ neurons are part of these projections (Charara and Parent, 1998). It is possible that some of the GABAergic interneurons overlapping these serotonergic dorsal raphe nuclei might have an inhibitory effect on the activity of the serotonergic neurons and in doing so promote sleepiness. It has also been

reported that the rostral cluster of serotonergic sleep related nuclei play a role in the gating, inhibiting or disinhibiting aspects of REM sleep (Siegel, 2000). It is possible that the lack of some the characteristic features associated with REM sleep and the peculiarity of REM sleep in particular that has been observed in the rock hyrax could be attributed to the differences noted with regard to the distribution and location of these interneuronal types and terminal networks and their specific actions in the regions coincident to the serotonergic nuclei.

### *6.5.7 Summary*

In the present study the location and distribution of the classical nuclei involved in the control and regulation of the sleep-wake cycle in the rock hyrax (cholinergic, catecholaminergic, orexinergic) was not significantly different to that described in other mammals. There appears to be a conservancy, to a degree, across most species with regard to the systems involved in the sleep-wake cycle both anatomically and physiologically. The distribution and interrelation of the GABAergic interneuron types were also, for the most part, not significantly different to that described for other mammals; however, the rock hyrax did show some unusual distributions patterns with regard to these GABAergic neurons both from a neuronal and terminal network distribution aspect. These differences could possibly provide clues as to reasons behind the unusual sleep reported, particularly REM, for the rock hyrax.

# Chapter 7

# Concluding Remarks

## *7.1. Conclusion*

The aim of the present thesis was to examine the sleep phenomenology of the rock hyrax, *Procavia capensis*. The rock hyrax is a social diurnal mammal that typically lives in colonies on rocky outcrops and is found throughout most parts of Southern Africa (Olds and Shoshani, 1982; Skinner and Chimimba, 2005). They share an interesting phylogenetic relationship with the African elephant and form part of the Afrotherian cohort which is considered the sister group to Xenarthra (Tabuce et al., 2008). Although many studies deal with the evolutionary history, ecology and behavior of these mammals, no study to date has been undertaken to examine the physiological measurable parameters of sleep as well as the accompanying neuroanatomy of the systems involved in the control and regulation of the sleep-wake cycle in the rock hyrax. An abstract by Snyder (1974) however did report total sleep times in three other species of hyrax, namely *Procavia johnstoni, Hetrohyrax brucei and Dendrohyrax validus.* Unfortunately no further information is given regarding the methodological approach used in this particular study, no polygraphic evidence is supplied to confirm the state assignation nor is there any mention of any spectral power analysis that have been performed on the data. The current study is thus to date the most complete report of the sleep phenomenology of the rock hyrax.

The first study undertaken in the process of understanding sleep in these mammals was the immunohistochemical identification of the location and distribution of the cholinergic, catecholaminergic and serotonergic systems within the brain of the rock hyrax. For the most part, the nuclear organization of these three systems closely

resembled that described for many other mammalian species (Woolf, 1991; Manger et al., 2002a; Maseko and Manger, 2007; Maseko et al., 2007; Limacher et al., 2008; Bhagwandin et al., 2008). The nuclear organization of the serotonergic system was identical to that seen in all eutherian mammals (Törk, 1990; Maseko et al., 2007; Moon et al., 2007; Dwarika et al., 2008; Limacher et al., 2008; Bhagwandin et al., 2008) while the catecholaminergic system was very similar to that seen in rodents except for the lack of a C3 nucleus and the compact division of the locus coeruleus (A6c). In addition, the diffuse locus coeruleus (A6d) appeared to contain very few tyrosine hydroxylase immunoreactive (TH+) neurons. The cholinergic system showed many features in common with that seen in both rodents and primates; however, there were three differences of note: (1) cholinergic neurons were observed in the anterior nuclei of the dorsal thalamus; (2) cholinergic parvocellular nerve cells forming subdivisions of the laterodorsal (LDT) and pedunculopontine (PPT) tegmental nuclei were observed at the midbrain/pons interface; and (3) a large number of cholinergic nerve cells in the periventricular gray of the medulla oblongata were observed. Thus, while there are many similarities to other mammalian species, the nuclear organization of these systems in the rock hyrax show specific differences to what has been observed previously in other mammals.

The second study undertaken focused on describing the distribution of orexin-A immunoreactive neurons and terminal networks in relation to the previously described catecholaminergic, cholinergic and serotonergic systems within the brain of the rock hyrax. The staining revealed that the neurons were mainly located within the hypothalamus as with other mammals (Wagner et al., 2000; McGranaghan and Piggins, 2001; Kruger et al., 2010). The orexinergic terminal network distribution also resembled the typical mammalian plan however the rock hyrax did show one atypical

feature, the presence of a high-density orexinergic terminal network within the anterodorsal nucleus of the dorsal thalamus (AD). The dense orexinergic innervation of the AD nucleus has only been reported previously in the Nile grass rat, *Arvicanthis niloticus* (Novak and Albers, 2002; Nixon and Smale, 2007) and Syrian hamster, *Mesocricetus auratus*, both diurnal mammals in nature (Mintz et al., 2001) (Syrian hamster is also known to be nocturnal and hibernating when in captivity). It is possible that orexinergic innervation of the AD nucleus might be a unique feature associated with diurnal mammals. It was also noted that the dense orexinergic innervation of the AD nucleus coincided with previously identified cholinergic neurons and terminal networks in this particular nucleus of the rock hyrax brain. It is possible that this dense orexinergic innervation of the AD nucleus in the brain of the rock hyrax may act in concert with the cholinergic neurons and/or the cholinergic axonal terminals, which in turn may influence arousal states and motivational processing.

The above studies were followed by the telemetric recording of the physiological measurable parameters of sleep in both solitary and social conditions. Sleep was firstly recorded under solitary conditions continuously for 72 hours from five wild captured rock hyraxes. The results revealed that these animals spent on average, 66.2% awake, 25.1 % in SWS and 3.5% in REM. REM in the rock hyrax was found to be ambiguous, which led to the subdivision thereof into REM1 and REM0. REM0 was considered the definitive form of this state whereas REM1 showed mixed characteristics of both low voltage slow wave sleep (LS) as well as normal REM. According to Bergmann et al. (1987) low voltage slow wave/NREM sleep (LS) is characterized by behavioural quiescence, desynchronized EEG, EMG that is at the same amplitude as during SWS and theta activity that resembles waking and lower

than during REM. In the rock hyrax REM1 did exhibit some of these characteristics such as behavioural quiescence, desynchronized EEG and EMG similar to SWS; however, theta activity could not be accurately calculated due to the placement of our EEG electrodes. If REM1 can be considered low voltage slow wave sleep, the implications would be that the rock hyrax exhibits the lowest amount of REM sleep of any terrestrial mammal studied to date. No significant differences were noted with regard to total sleep time (TST), number of episodes and episode duration for all states between the light and dark periods**.** Thus prior classification of the rock hyrax as strongly diurnal does not appear to apply to controlled laboratory conditions.

After the solitary sleep recording commenced sleep was recorded from the same individual continuously for 72 hours under social conditions. No statistically significant differences between social and solitary conditions were observed in terms of total sleep time (TST), time in waking, number of episodes of different states or episode duration for most states. The average REM0 (true REM sleep for the hyrax) episode duration was found to be greater during social conditions, and this increase in episode duration was noted across the 24 h period, but was most pronounced during the dark period. Slow wave activity (SWA) was greater during the social sleep condition, especially during SWS, for the first two days recording, but this difference was not noted for the last day of recording in the social condition. The results are thus in agreement with the notion that neither sleep cycle length nor phasing of sleep is correlated to sleeping in a social setting; however, the increased intensity of SWA during SWS and the increase in episode duration of true REM sleep (REM0) are both suggestive of better sleep quality during social conditions than solitary conditions in the rock hyrax.

Finally by means of immunohistochemistry the interrelations of the distribution of sleep associated nuclei and terminal networks in the brain of the rock hyrax were examined. The results revealed that the location and distribution of the nuclei involved in the sleep-wake cycle were typically mammalian with the exception of the cholinergic AD and AV nuclei, and the parvo- and magnocellular divisions of the PPT and LDT which appears to be specific to the rock hyrax. The terminal network distribution of the serotonergic, orexinergic and histaminergic systems was also similar to that previously described in other mammals, however a dense orexinergic terminal network distribution of the AD nucleus was noted, which as stated previously might be a specific feature of the rock hyrax and potentially diurnal mammals. Of the GABAergic calcium binding interneurons parvalbumin did not appear to be strongly related to any of the sleep related nuclei, calbindin was found to be ubiquitous in the areas immediately overlapping and surrounding the sleep related nuclei whereas calretinin was found to be less ubiquitous than calbindin. Within the basal forebrain calbindin and calretinin showed an even distribution whereas in areas such as the serotonergic dorsal raphe and catecholaminergic locus coeruleus complex these neurons were more unusual in their distribution. Other atypical features observed was the gradient like distribution of calbindin and calretinin neurons within the cholinergic AD and AV nuclei and a denser parvalbumin terminal network distribution overlapping the magnocellular division of the LDT. It is thus possible that the parvocellular divisions of both the LDT and PPT are probably not inhibitory interneurons as initially thought. It is furthermore also possible that the LDT and PPT are more complex in their organisation than any other mammal studied to date and that this difference in complexity could possibly provide clues to the reasons behind the differences observed in REM sleep in these animals.

*7.2. The way forward*

In order to put to rest the issue of the possible functions of the AD and AV nuclei as well as the parvo- and magnocellular divisions of the LDT and PPT double immuno labelling as well as single unit recording at the targeted sites would have to be performed. The double immuno labelling will enable one to determine whether the overlap observed between the different systems, for example the dense orexinergic terminal network distribution observed in the region of the cholinergic AD nucleus and the dense parvalbumin terminal network distribution overlapping the magnocellular LDT, is indicative of connectivity, whereas single unit recording at the sites of the aforementioned nuclei would provide clues to their possible functions.

REM has proven to be very unique in the rock hyrax. In order to determine whether REM1 can be classified as a REM or NREM state more sophisticated sleep recording studies have to be performed where the electrodes would be placed directly above the hippocampus in order to obtain the purest form of theta activity. In concert with the aforementioned study would have to be thermoregulative studies measuring brain (hypothalamic) as well as body temperature. The theta activity obtained from these studies will enable one to determine whether REM1 is indeed low voltage slow wave sleep or whether it can be considered a form of REM sleep. The thermoregulative studies would provide better clues as to the reasons why REM0 episode duration increases during the social condition, and whether this increase observed could be attributed to better thermoregulative strategies employed when these animals sleep socially or whether other factors such as the nature of the social interactions could be responsible as proposed. Furthermore by extending the recording period during the social conditions one would be able to determine whether the increase seen in SWA during the social condition can be attributed to social stress

or improved sleep quality. The effects of increasing group sizes would be another way forward. Does increasing group size improve sleep quality in the social condition or would it have no effect? Furthermore when group size increases would co-operative vigilance become apparent and would there be a difference in the total sleep times and fragmentation of sleep of those individuals sleeping on the periphery as opposed to those sleeping in the centre? Finally, it would be great to be able to record sleep from rock hyraxes under their natural wild conditions and to compare those results to the results obtained from the current captive studies.

# 8. References

## 8.1. Chapter 1: Introduction

Bothma, J. du P., 1971. Order Hyracoidea, Part 12. In: Meester, J., and Setzer, H.W., The mammals of Africa: An identification manual. Smithsonian Institution Press, Washington, D.C., pp. 1-8.

Carter, A.M., and Enders, A.C., 2004. Comparative aspects of trophoblast development and placentation. Reproductive Biology and Endocrinology, 2(46).

Flower, W. H., and Lydekker, R., 1891. An introduction to the study of mammals, living and extinct. Adam and Charles Black, London.

Greenwood, A.D., Englbrecht, C.C., MacPhee, R.D.E., 2004. Characterization of an endogenous retrovirus class in elephants and their relatives. BMC Evolutionary Biology, 4(38).

Hakeem, A.Y., Hof, P.R., Sherwood, C.C., Switszer III, R.C., Rasmussen, L.E.L., Allman, J.M., 2005. Brain of the African elephant (*Loxodonta africana)*: Neuroanatomy from magnetic resonance images. The anatomical record part A, 287A:1117-1127.

Hoeck, H., 2010. Hyraxes order Hyracoidea. IUCN/SSC Afrotheria Specialist Group. http://afrotheria.net/Hyracoidea.

Hoffmeister, D. F., 1967. Tubulidentates, proboscideans, and hyracoideans. In: Anderson, S., and Jones, J.K., Recent mammals of the world: A synopsis of families. The Ronald Press Co., New York, p. 355-365.

Kavanau, J.L., 2002. REM and NREM sleep as natural accompaniments of the evolution of warm-bloodedness. Neuroscience Biobehaviour Review, 26:889-906.

Kellogg, M.E., Burkett, S., Dennis, T.R., Stone, G., Gray, B.A., McGuire, P.M., Zori, R.T., Stanyon, R., 2007. Chromosome painting in the manatee supports Afrotheria and Paenungulata. BMC Evolutionary Biology, 7(6).

Klein, R. G., and Cruz-Uribe, K., 1996. Size Variation in the Rock Hyrax (*Procavia capensis*) and Late Quaternary Climatic Changes in South Africa. Quaternary Research, 46:193-207.

Kleinschmidt, T., Czelusniak, J., Goodman, M., Braunitzer, G., 1986. Paenungulata: A comparison of the hemoglobin sequences from elephant, hyrax and manatee. Molecular Biology and Evolution, 3(5):427-435.

Lyamin, O.I., Manger, P.R., Ridgway, S.H., Mukhametov, L.M., Siegel, J.M., 2008. Cetacean sleep: an unusual for of mammalian sleep. Neuroscience and Biobehavioral Reviews, 32(8):1451-84.

Manger, P.R., Fahringer, H., Pettigrew, J.D., Siegel, J.M., 2002a. Distribution and morphology of cholinergic neurons in the brain of the monotremes as revealed by ChAT immunohistochemistry. Brain Behavior and Evolution, 60:275-297.

Manger, P.R., Fahringer, H., Pettigrew, J.D., Siegel, J.M., 2002b. The distribution and morphological characteristics of catecholaminergic cells in the brain of monotremes as revealed by tyrosine hydroxylase immunohistochemistry. Brain Behavior and Evolution, 60:298-314.

Manger, P.R., Fahringer, H., Pettigrew, J.D., Siegel, J.M., 2002c. Distribution and morphology of serotonergic neurons in the brain of monotremes. Brain Behavior and Evolution, 60:315-332.

Manger, P.R., Ridgway, S.H., Siegel, J.M., 2003. The locus coeruleus complex of the bottlenose dolphin (*Tursiops truncatus*) as revealed by tyrosine hydroxylase immunohistochemistry. Journal of sleep research, 12:149-155.

Manger, P.R., 2005. Establishing order at the systems level in mammalian brain evolution. Brain Research Bulletin, 66:282-289.

Nicolau, M. C., Akaârir, M., Gamundí, A., Gonzáles, J., and Rial, R. V., 2000. Why we sleep: the evolutionary pathway to the mammalian sleep, Progress in Neurobiology, 62(4):379-406.

Olds, N., and Shoshani, J., 1982. Procavia capensis. Mammalian Species, 171:1-7.

Rattenborg, N.C., Amlaner, C.J., Lima, S.L., 2000. Behavioral, neurophysiological and evolutionary perspectives on unihemispheric sleep. Neuroscience and Biobehavioral Review, 24:817-842.

Rübsamen, K., Hume, I.D., Engelhardt, W.V., 1982. Physiology of the rock hyrax. Comparative Biochemistry and Physiology, 72A(2): 217-277.

Sherwood, C.C., Stimpson, C.D., Butti, C., Bonar, C.J., Newton, A.L., Allman, J.M., Hof, P.R., 2009. Neocortical neuron types in Xenarthra and Afrotheria: implications for brain evolution in mammals. Brain Structure and Function, 213:301-328.

Siegel, J.M., 1995. Phylogeny and the function of REM sleep. Behavioral Brain Research, 69:29-34.

Siegel, J.M., 2003. Why we sleep. Scientific American, November: 92-97.

Skinner, J.D., and Smithers, R.H.N., 1990. The Mammals of the Southern African Sub Region. University of Pretoria, Pretoria.

Skinner, J.D., Chimimba, C.T., 2005. The Mammals of the Southern African Subregion, 3rd Edition. Cambridge University Press, Cape Town.

Snyder, F., 1974. Sleep–waking patterns of Hyracoidea. Sleep Research, 3:87.

Tabuce, R., Asher, R.J., Lehmann, T., 2008. Afrotherian mammals: a review of current data. Mammalia, 72:2-14.

**8.2. Chapter 2: Nuclear organization and morphology of cholinergic, putative catecholaminergic and serotonergic neurons in the brain of the Rock Hyrax, *Procavia capensis*.**

Agnati, L.F., Fuxe, K., Zoli, M., Pich, E.M., Benfenati, F., Zini, I., Goldstein, M., 1986. Aspects on the information handling by the central nervous system: focus on cotransmission in the aged rat brain. Progress in Brain Research, 68:291-301.

Andén, N.E., Carlsson, A., Dahlström, A., Fuxe, K., Hillarp, N.Å., Larsson, K., 1964. Demonstration and mapping out of nigro-neostriatal dopamine neurons. Life Sciences, 15:523-530.

Arnason, U., Adegoke, J., Gullberg, A., Harley, E.H., Janke, A., Kullberg, M., 2008. Mitogenomic relationships of placental mammals and molecular estimates of their divergences. Gene, 421:37–51.

Badlangana, N.L., Bhagwandin, A., Fuxe. K., Manger, P.R., 2007. Distribution and morphology of putative catecholaminergic and serotonergic neurons in the medulla oblongata of a sub-adult giraffe, *Giraffa camelopardalis*. Journal of Chemical Neuroanatomy, 34:69-79.

Bartus, R.T., Dean, R.L., Beer, B., 1982. Neuropeptide effect on memory in aged monkeys. Neurobiology of Aging, 3:61-68.

Bayraktar, T., Staiger, J.F., Acsady, L., Cozzari, C., Freund, T.F., Zilles, K., 1997. Co-localization of vasoactive intestinal polypeptide, gamma-amino-butyric acid and choline acetyltransferase in the neocortical interneurons of the adult rat. Brain Res. 757, 209–217.

Bhagwandin, A., Fuxe, K., Manger, P.R., 2006. Choline acetyltransferase immunoreactive cortical interneurons do not occur in all rodents: a study of the phylogenetic occurrence of this neural characteristic. Journal of Chemical Neuroanatomy, 32:208-216.

Bhagwandin, A., Fuxe, K., Bennett, N.C., Manger, P.R., 2008. Nuclear organization and morphology of cholinergic, putative catecholaminergic and serotonergic neurons in the brains of two species of African mole-rat. Journal of Chemical Neuroanatomy, 35:371-387.

Bjarkam, C.R., Sorensen, J.C., Geneser, F.A., 1997. Distribution and morphology of serotonin-immunoreactive neurons in the brainstem of the New Zealand white rabbit. The Journal of Comparative Neurology, 380:507–519.

Boissard, R., Fort, P., Gervasoni, D., Barbagli, B., Luppi, P.H., 2003. Localization of the GABAergic and non-GABAergic neurons projecting to the sublaterodorsal

nucleus and potentially gating paradoxical sleep onset. European Journal of Neuroscience, 18:1627-1639.

Crutcher, K.A., Humbertson, A.O., 1978. The organization of monoamine neurons within the brainstem of the North American opossum (*Didelphis virginiana*). The Journal of Comparative Neurology, 179:195–222.

Dahlström, A., Fuxe, K., 1964. Evidence for the existence of monoamine-containing neurons in the central nervous system. I. Demonstration of monoamine in the cell bodies of brainstem neurons. Acta Physiologica Scandinavica, 62:1-52.

Diksic, M., Young, S.N., 2001. Study of the brain serotonergic system with labelled alpha-methyl-L-tryptophan. Journal of Neurochemistry, 78:1185-1200.

Dwarika, S., Maseko, B.C., Ihunwo, A.O., Fuxe, K., Manger, P.R., 2008. Distribution and morphology of putative catecholaminergic and serotonergic neurons in the brain of the greater canerat, *Thryonomys swinderianus*. Journal of Chemical Neuroanatomy, 35:108-122.

Fuxe, K., Hökfelt, T., Ungerstedt, U., 1969. Distribution of monoamines in the mammalian central nervous system by histochemical studies. In: Hooper, G., Metabolism of Amines in the Brain. Macmillan, London, pp. 10–22.

Fuxe, K., Hökfelt, T., Ungerstedt, U., 1970. Morphological and functional aspects of central monoamine neurons. International Review of Neurobiology, 13:93–126.

Fuxe, K., Manger, P., Genedani, S., Agnati, L., 2006. The nigrostriatal DA pathway and Parkinson's disease. Journal of Neural Transmission Supplement, 70:71-83.

Fuxe, K., Marcellino, D., Genedani, S., Agnati, L., 2007a. Adenosine A(2A) receptors, dopamine D(2) receptors and their interactions in Parkinson's disease. Movement Disorders, 22:1990-2017.

Fuxe, K., Dahlström, A., Höistad, M., Marcellino, D., Jansson, A., Rivera, A., Diaz-Cabiale, Z., Jacobsen, K., Tinner-Staines, B., Hagman, B., Leo, G., Staines, W., Guidolin, D., Kehr, J., Genedani, S., Belluardo, N., Agnati, L.F., 2007b. From the Golgi-Cajal mapping to the transmitter-based characterization of the neuronal networks leading to two modes of brain communication: wiring and volume transmission. Brain Research Reviews, 55:17-54.

Gallyas, F., 1979. Silver staining of myelin by means of physical development. Neurological Research, 1:203–209.

Hökfelt, T., Johansson, O., Fuxe, K., Goldstein, M., Park, D., 1976. Immunohistochemical studies on the localization and distribution of monoamine neuron systems in the rat brain. I. Tyrosine hydroxylase in the mes- and diencephalon. Medical Biology, 54:427-53.

Hökfelt, T., Martenson, R., Björklund, A., Kleinau, S., Goldstein, M., 1984. Distributional maps of tyrosine-hydroxylase-immunoreactive neurons in the rat brain.

In: Björklund, A., Hökfelt, T., Handbook of Chemical Neuroanatomy, vol. 2. Classical Neurotransmitters in the CNS, part 1. Elsevier, Amsterdam, pp. 277–379.

Jacobs, B.L., Azmitia, E.C., 1992. Structure and function of the brain serotonin system. Physiological Reviews, 72:165–229.

Jones, E.G., 2007. The Thalamus, 2nd Edition. Cambridge University Press, Cambridge, UK.

Kalia, M., Fuxe, K., Goldstein, M., 1985a. Rat medulla oblongata. II. Noradrenergic neurons, nerve fibers and preterminal processes. The Journal of Comparative Neurology, 233:308-332.

Kalia, M., Fuxe, K., Goldstein, M., 1985b. Rat medulla oblongata. III. Adrenergic (C1 and C2) neurons, nerve fibers and presumptive terminal processes. The Journal of Comparative Neurology, 233:333-349.

Kitahama, K., Geffard, M., Okamura, H., Nagatsu, I., Mons, N., Jouvet, M., 1990. Dopamine- and dopa-immunoreactive neurons in the cat forebrain with reference to tyrosine hydroxylase-immunohistochemistry. Brain Research, 518:83-94.

Kitahama, K., Sakamoto, N., Jouvet, A., Nagatsu, I., Pearson, J., 1996. Dopamine-beta-hydroxylase and tyrosine hydroxylase immunoreactive neurons in the human brainstem. Journal of Chemical Neuroanatomy, 10:137-146.

Klein, R.G., Cruz-Uribe, K., 1996. Size variation in the rock hyrax (*Procavia capensis*) and late quarternary climatic change in South Africa. Quaternary Research**,** 46:193-207.

Lichtensteiger, W., 1966. Uptake of norepinepherine in periglomerular cells of the olfactory bulb of the mouse. Nature, 210:955-956.

Lidbrink, P., Jonsson, G., Fuxe, K., 1974. Selective reserpine-resistant accumulation of catecholamines in central dopamine neurones after dopa administration. Brain Research, 67:439-456.

Limacher, A.M., Bhagwandin, A., Fuxe, K., Manger, P.R., 2008. Nuclear organization and morphology of cholinergic, putative catecholaminergic and serotonergic neurons in the brain of the Cape porcupine (*Hystrix afri*caeaustralis): Increased brain size does not lead to increased organizational complexity. Journal of Chemical Neuroanatomy, 36:33-52.

Luppi, P.H., Gervasoni, D., Verret, L., Goutagny, R., Peyron, C., Salvert, D., Leger, L., Fort, P., 2007. Paradoxical (REM) sleep genesis: the switch from an aminergic-cholinergic to a GABAergic-glutamatergic hypothesis. Journal of Physiology (Paris), 100:271-283.

Maloney, K.J., Mainville, L., Jones, B.E., 1999. Differential c-Fos expression in cholinergic, monoaminergic, and GABAergic cell groups of the pontomesencephalic

tegmentum after paradoxical sleep deprivation and recovery. Journal of Neurocience, 19: 3057-3072.

Maloney, K.J., Mainville, L., Jones, B.E., 2000. c-Fos expression in GABAergic, serotonergic, and other neurons of the pontomedullary reticular formation and raphe after paradoxical sleep deprivation and recovery. Journal of Neuroscience, 20:4669-4679.

Manger, P.R., 2005. Establishing order at the systems level in mammalian brain evolution. Brain Research Bulletin, 66:282-289.

Manger, P.R., Fahringer, H.M., Pettigrew, J.D., Siegel, J.M., 2002a. Distribution and morphology of cholinergic neurons in the brain of the monotremes as revealed by ChAT immunohistochemistry. Brain Behavior and Evolution, 60:275-297.

Manger, P.R., Fahringer, H.M., Pettigrew, J.D., Siegel, J.M., 2002b. Distribution and morphology of catecholaminergic neurons in the brain of monotremes as revealed by tyrosine hydroxylase immunohistochemistry. Brain Behavior and Evolution, 60:298-314.

Manger, P.R., Fahringer, H.M., Pettigrew, J.D., Siegel, J.M., 2002c. Distribution and morphology of serotonergic neurons in the brain of the monotremes. Brain Behavior and Evolution**,** 60:315-332.

Maseko, B.C., Manger, P.R., 2007. Distribution and morphology of cholinergic, catecholaminergic and serotonergic neurons in the brain of Schreiber's long-fingered bat, *Miniopterus schreibersii*. Journal of Chemical Neuroanatomy, 34:80-94.

Maseko, B.C., Bourne, J.A., Manger, P.R., 2007. Distribution and morphology of cholinergic, putative catecholaminergic and serotonergic neurons in the brain of the Egyptian Rousette flying fox, *Rousettus aegyptiacus*. Journal of Chemical Neuroanatomy, 34:108-127.

Meister, B., Hökfelt, T., Steinbusch, H.W., Skagerberg, G., Lindvall, O., Geffard, M., Joh, T.H., Cuello, A.C., Goldstein, M., 1988. Do tyrosine hydroxylase-immunoreactive neurons in the ventrolateral arcuate nucleus produce dopamine or only L-dopa? Journal of Chemical Neuroanatomy, 1:59-64.

Mitchell, J., Templeton, D., 1981. The origin of the preganglionic parasympathetic fibers to the mandibular and sublingual salivary glands in the rat: a horseradish peroxidase study. Journal of Anatomy, 132:513–518.

Moon, D.J., Maseko, B.C., Ihunwo, A., Fuxe, K., Manger, P.R., 2007. Distribution and morphology of catecholaminergic and serotonergic neurons in the brain of the highveld gerbil, *Tatera brantsii*. Journal of Chemical Neuroanatomy, 34:134-144.

Oda, S., Kuroda, M., Kakuta, S., Tanihata, S., Ishikawa, Y., Kishi, K., 2003. Ultrastructure of ascending cholinergic terminals in the anteroventral thalamic

nucleus of the rat: a comparison with the mammillothalamic terminals. Brain Research Bulletin, 59:473-483.

Pal, D., Mallick, B.N., 2006. Role of noradrenergic and GABA-ergic inputs in pedunculopontine tegmentum for regulation of rapid eye movement sleep in rats. Neuropharmocology, 51:1-11.

Pompeiano, O., 2001. Role of the locus coeruleus in the static and dynamic control of posture. Archives Italiennes de Biologie**,** 139:109-124.

Previc, F.H., 1999. Dopamine and the origins of human intelligence. Brain and Cognition**,** 41:299-350.

Reiner, P.B., Fibiger, H.C., 1995. Functional heterogeneity of central cholinergic systems. In: Bloom, F.E., Kupfer, D.J., Psychopharmacology: The Fourth Generation of Progress. Raven, New York. pp 147-153.

Rezek, O., Boldogkoi, Z., Tombácz, D., Kovágó, C., Gerendai, I., Palkovits, M., Tóth, I.E., 2008. Location of parotid preganglionic neurons in the inferior salivatory nucleus and their relation to the superior salivatory nucleus of rat. Neuroscience Letters, 440:265-269.

Ruggiero, D.A., Anwar, M., Gootman, P.M., 1992. Presumptive adrenergic neurons containing phenylethanolamine N-methyltransferase immunoreactivity in the medulla oblongata of neonatal swine. Brain Research, 583:105-119.

Segal, M., Greenberger, V., Israeli, M., Biegon, A., 1988. A correlation between regional acetylcholinesterase activity in rat brain and performance in a spatial task. Behavioral Brain Research, 30:215-219.

Semba, K., Fibiger, H.C., 1989. Organization of central cholinergic systems. Progress in Brain Research, 79:37-63.

Siegel, J.M., 2006. The stuff dreams are made of: anatomical substrates of REM sleep. Nature Neuroscience, 9:721-722.

Skinner, J.D., Chimimba, C.T., 2005. The Mammals of the Southern African Subregion, 3rd Edition. Cambridge University Press, Cape Town.

Smeets, W.J.A.J., González, A., 2000. Catecholamine systems in the brain of vertebrates: new perspectives through a comparative approach. Brain Research Reviews, 33:308-379.

Tan, M.M.L., Harvey, A.R., 1989. The cholinergic innervation of normal and transplanted superior colliculus in the rat: an immunohistochemical study. Neuroscience, 32:511-520.

Tillet, Y., 1995. Distribution of neurotransmitters in the sheep brain. Journal of Reproduction and Fertility Supplement, 49:199-220.

Törk, I., 1990. Anatomy of the serotonergic system. Annals of the New York Academy of Sciences, 600:9–35.

Tóth, I.E., Boldogkõi, Z., Medveczky, I., Palkovits, M., 1999. Lacrimal preganglionic neurons form a subdivision of the superior salivatory nucleus of rat: transneuronal labeling by pseudorabies virus. Journal of the Autonomic Nervous System, 77:45–54.

van Groen, T., Kadish, I., Micheal Wyss, J., 2002. Role of the anterodorsal and anteroventral nuclei of the thalamus in spatial memory in the rat. Behavioral Brain Research, 132:19-28.

Wolff, M., Loukavenko, E.A., Will, B.E., Dalrymple-Alford, J.C., 2008. The extended hippocampal-diencephalic memory system: enriched housing promotes recovery of the flexible use of spatial representations after anterior thalamic lesions. Hippocampus, 18:996-1007.

Woolf, N.J., 1991. Cholinergic systems in mammalian brain and spinal cord. Progress in Neurobiology, 37:475–524.

**8.3. Chapter 3: Distribution of orexin-A immunoreactive neurons and their terminal networks in the brain of the rock hyrax, *Procavia capensis*.**

Abrahamson, E.E., Leak, R.K., Moore, R.Y., 2001. The suprachiasmatic nucleus projects to posterior hypothalamic arousal systems. Neuroreport, 12:435-440.

Backberg, M., Hervieu, G., Wilson, S., Meister, B., 2002. Orexin receptor-1 (OX-R1) immunoreactivity in chemically identified neurons of the hypothalamus: focus on orexin targets involved in control of food and water intake. European Journal of Neuroscience, 15:315-328.

Baldo B.A., Daniel R.A., Berridge C.W., Kelley A.E., 2003. Overlapping distributions of orexin/hypocretin- and dopamine-β-hydroxylase immunoreactive fibers in rat brain regions mediating arousal, motivation and stress. Journal of Comparative Neurology, 464:220–237.

Bourgin, P., Huitron-Resendiz, S., Spier, A.D., Fabre, V., Morte, B., Criado, J.R., Sutcliffe, J.G., Henriksen, S.J., De Lecea, L., 2000. Hypocretin-1 modulates rapid eye movement sleep through activation of locus coeruleus neurons. Journal of Neuroscience, 20:7760-7765.

Broberger, C., De Lecea, L., Sutcliffe, J.G., Hokfelt, T., 1998. Hypocretin/orexin-And melanin-concentrating hormone-expressing cells form distinct populations in the rodent lateral hypothalamus: relationship to the neuropeptide Y and agouti gene-related protein systems. Journal of Comparative Neurology, 402:460–474.

Brown, K.J., Downs, C.T., 2006. Seasonal patterns in body temperature of free-living hyrax (*Procavia capensis*). Comparative Biochemistry and Physiology part A: Molecular and Integrative Physiology, 143:42-49.

Brown, R.E., Sergeeva, O., Eriksson, K.S., Haas, H.L., 2001. Orexin-A excites serotonergic neurons in the dorsal raphe nucleus of the rat. Neuropharmacology, 40:457–459.

Chen, C.T., Dun, S.L., Kwok, E.H., Dun, N.J., Chang, J.K., 1999. Orexin-A-like immunoreactivity in the rat brain. Neuroscience Letters, 260:161-164.

Cutler, D.J., Morris, R., Sheridhar, V., Wattam, T.A., Holmes, S., Patel, S., Arch, J.R., Wilson, S., Buckingham, R.E., Evans, M.L., Leslie, R.A., Williams, G., 1999. Differential distribution of orexin-A and orexin-B immunoreactivity in the rat brain and spinal cord. Peptides, 20:455-1470.

Date, Y., Ueta, Y., Yamashita, H., Yamaguchi, H., Matsukura, S., Kangawa, K., Sakurai, T., Yanagisawa, M., Nakazato, M., 1999. Orexins, orexigenic hypothalamic peptides, interact with autonomic, neuroendocrine and neuroregulatory systems. Proceedings of the National Academy of Sciences U.S.A., 96:748-753.

De Lecea, L., Kilduff, T.S., Peyron, C., Gao, X., Foye, P.E., Danielson, P.E., Fukuhara, C., Battenberg, E.L., Gautvik, V.T., Bartlett, F.S., Frankel, W.N., Van den Pol, A.N., Bloom, F.E., Gautvik, K.M., Sutcliffe, J.G., 1998. The hypocretins: hypothalamus-specific peptides with neuroexcitatory activity. Proceedings of the National Academy of Sciences U.S.A., 95:322-327.

Domínguez, L., Morona, R., Joven, A., González, A., López, J.M., 2010. Immunohistochemical localization of orexins (hypocretins) in the brain of reptiles and its relation to monoaminergic systems. Journal of Chemical Neuroanatomy, 39:20–34.

Espana, R.A., Baldo, B.A., Kelley, A.E., Berridge, C.W., 2001. Wake-promoting and sleep-suppressing actions of hypocretin (orexin): basal forebrain sites of action. Neuroscience, 106:699-715.

Espana, R.A., Reis, K.M., Valentino, R.J., Berridge, C.W., 2005. Organization of hypocretin/orexin efferents to locus coeruleus and basal forebrain arousal-related structures. Journal of Comparative Neurology, 481:160-178.

Fujiki, N., Yoshida, Y., Ripley, B., Honda, K., Mignot, E., Nishino, S., 2001. Changes in CSF hypocretin-1 (orexin-A) levels in rats across 24 hours and in response to food deprivation. Neuroreport, 12:993-997.

Galas, L., Vaudry, H., Braun, B., Van den Pol, A.N., De Lecea, L., Sutcliffe, J.G., Chartrel, N., 2001. Immunohistochemical localization and biochemical characterization of hypocretin/orexin-related peptides in the central nervous system of the frog *Rana ridibunda*. Journal of Comparative Neurology, 429:242–252.

Gallyas, F., 1979. Silver staining of myelin by means of physical development. Neurological Research, 1:203–209.

Gatterman, R., Johnston, R.E., Yigit, N., Fritzsche, P., Larimer, S., Ozkurt, S., Neumann, K., Song, Z., Colak, E., Johnston, J., McPhee, M.E., 2008. Golden hamsters are nocturnal in captivity but diurnal in nature. Biology Letters, 4:253-255.

Gravett, N., Bhagwandin, A., Fuxe, K., Manger, P.R., 2009. Nuclear organization and morphology of cholinergic, putative catecholaminergic and serotonergic neurons in the brain of the rock hyrax, *Procavia capensis*. Journal of Chemical Neuroanatomy, 38:57-74.

Hagan, J.J., Leslie, R.A., Patel, S., Evans, M.L., Wattam, T.A., Holmes, S., Benham, C.D., Taylor, S.G., Routledge, C., Hemmati, P., Munton, R.P., Ashmeade, T.E., Shah, A.S., Hatcher, J.P., Hatcher, P.D., Jones, D.N., Smith, M.I., Piper, D.C., Hunter, A.J., Porter, R.A., Upton, N., 1999. Orexin-A activates locus coeruleus cell firing and increases arousal in the rat. Proceedings of the National Academy of Sciences U.S.A., 96:10911–10916.

Horvath, T.L., Diano, S., Van den Pol, A.N., 1999. Synaptic interaction between hypocretin (orexin) and neuropeptide Y cells in the rodent and primate hypothalamus: a novel circuit implicated in metabolic and endocrine regulations. Journal of Neuroscience, 19:1072-1087.

Huang, Z.L., Qu, W.M., Li, W.D., Mochizuki, T., Eguchi, N., Watanabe, T., Urade, Y., Hayaishi, O., 2001. Arousal effect of orexin-A depends on activation of the histaminergic system. Proceedings of the National Academy of Sciences U.S.A., 98: 9965-9970.

Huesa, G., Van den Pol, A.N., Finger, T.E., 2005. Differential distribution of hypocretin (orexin) and melanin-concentrating hormone in the goldfish brain. Journal of Comparative Neurology, 488:476–491.

Iqbal, J., Pompolo, S., Sakurai, T., Clarke, I.J., 2001. Evidence that orexin-containing neurones provide direct input to gonadotropin-releasing hormone neurones in the ovine hypothalamus. Journal of Neuroendocrinology, 13:1033-41.

Kaslin, J., Nystedt, J.M., Östergård, M., Peitsaro, N., Panula, P., 2004. The orexin/hypocretin system in zebrafish is connected to the aminergic and cholinergic systems. Journal of Neuroscience, 24:2678–2689.

Khorooshi, R.M., Klingenspor, M., 2005. Neuronal distribution of melanin-concentrating hormone, cocaine- and amphetamineregulated transcript and orexin B in the brain of the Djungarian hamster (*Phodopus sungorus*). Journal of Chemical Neuroanatomy, 29:137-148.

Kruger, J-L., Dell, L-A., Pettigrew, J.D., Manger, P.R., 2010. Cellular location and major terminal networks of the orexinergic system in the brains of five microchiropteran species. Journal of Chemical Neuroanatomy, 40:256-262.

Kukkonen, J.P., Holmqvist, T., Ammoun, S., Åkermam, K.E.O., 2002. Functions of the orexinergic/hypocretinergic system. American Journal of Physiology: Cell Physiology, 283:C1567-C1591.

Lee, M.E., Hassani, O.K., Jones, B.E., 2005. Discharge of identified orexin/hypocretin neurons across the sleep-wake cycle. Journal of Neuroscience, 25:6716-6720.

López, J.M., Domínguez, L., Morena, N., González, A., 2009. Comparative immunohistochemical analysis of the distribution of orexins (hypocretins) in the brain of amphibians. Peptides, 30:873–887.

Matsuzaki, I., Sakurai, T., Kunii, K., Nakamura, T., Yanagisawa, M., Goto, K., 2002. Involvement of the serotonergic system in orexin-induced behavioral alterations in rat. Regulatory Peptides, 104:119–123.

McGranaghan, P.A., Piggins, H.D., 2001. Orexin-A-like immunoreactivity in the hypothalamus and thalamus of the Syrian hamster (*Mesocricetus auratus*) and Siberian hamster (*Phodopus sungorus*), with special reference to circadian structures. Brain Research, 904:234-244.

McNairn, I.S., Fairall, N., 1984. Metabolic rate and body temperature of adult and juvenile hyrax (*Procavia capensis*). Comparative Biochemistry and Physiology part A: Comparative Physiology, 79:539-545.

Methippara, M.M., Alam, M.N., Szymusiak, R., McGinty, D., 2000. Effects of lateral preoptic area application of orexin-A on sleep-wakefulness. Neuroreport, 11:3423-3426.

Mintz, E.M., Van den Pol, A.N., Casano, A.A., Albers, H.E., 2001. Distribution of hypocretin-(orexin) immunoreactivity in the central nervous system of Syrian hamsters (*Mesocricetus auratus*). Journal of Chemical Neuroanatomy, 21:225–238.

Moore, R.Y., Abrahamson, E.A., Van den Pol, A., 2001. The hypocretin neuron system: an arousal system in the human brain. Archives Italiennes de Biologie, 139:195-205.

Nakamura, T., Uramura, K., Nambu, T., Yada, T., Goto, K.,Yanagisawa, M., Sakurai, T., 2000. Orexin-induced hyperlocomotion and stereotypy are mediated by the dopaminergic system. Brain Research, 873:181–187.

Nambu, T., Sakurai, T., Mizukami, K., Hosoya, Y., Yanagisawa, M., Goto, K., 1999. Distribution of orexin neurons in the adult rat brain. Brain Research, 827:243-260.

Nixon, J.P., Smale, L., 2007. A comparative analysis of the distribution of immunoreactive orexin-A and B in the brains of nocturnal and diurnal rodents. Behavioral and Brain Functions, 13:28.

Novak, C.M., Smale, L., Nunez, A.A., 2000. Rhythms in Fos expression in brain areas related to the sleep-wake cycle in the diurnal *Arvicanthis niloticus*. American Journal of Physiology- Regulatory, Integrative and Comparative Physiology, 278:R1267-R1274.

Novak, C.M., Albers, H.E., 2002. Localization of hypocretin-like immunoreactivity

in the brain of the diurnal rodent, *Arvicanthis niloticus*. Journal of Chemical Neuroanatomy, 23:49-58.

Ohkubo, T., Boswell, T., Lumineau, S., 2002. Molecular cloning of chicken prepro-orexin cDNA and preferential expression in the chicken hypothalamus. Biochimica et Biophysica Acta, 1577:476–480.

Olds N, Shoshani J, 1982. *Procavia capensis*. Mammalian Species, 171:107.

Ohno, K., and Sakurai, T., 2008. Orexin neuronal circuitry: role in the regulation of sleep and wakefulness. Frontiers in Neuroendocrinology, 29:70–87.

Peyron, C., Tighe, D.K., Van den Pol, A.N., De Lecea, L., Heller, H.C., Sutcliffe, J.G., Kilduff, T.S., 1998. Neurons containing hypocretin (orexin) project to multiple neuronal systems. Journal of Neuroscience, 18:9996-10015.

Piper, D.C., Upton, N., Smith, M.I., Hunter, A.J., 2000. The novel brain neuropeptide, orexin-A, modulates the sleep-wake cycle of rats. European Journal of Neuroscience, 12:726-730.

Sakurai, T., Amemiya, A., Ishii, M., Matsuzaki, I., Chemelli, R.M., Tanaka, H., Williams, S.C., Richardson, J.A., Kozlowski, G.P., Wilson, S., Arch, J.R., Buckingham, R.E., Haynes, A.C., Carr, S.A., Annan, R.S., McNulty, D.E., Liu, W.S., Terrett, J.A., Elshourbagy, N.A., Bergsma, D.J., Yanagisawa, M., 1998. Orexins and

orexin receptors: a family of hypothalamic neuropeptides and G protein-coupled receptors that regulate feeding behavior. Cell, 92:573-585.

Shibahara, M., Sakurai, T., Nambu, T., Takenouchi, T., Iwaasa, H., Egashira, S., Ihara, M., Goto, K., 1999. Structure, tissue distribution, and pharmacological characterization of *Xenopus* orexins. Peptides, 20:1169–1176.

Singletary, K.G., Delville, Y., Farrell, W.J., Wilczynski, W., 2005. Distribution of orexin/hypocretin immunoreactivity in the nervous system of the green treefrog, *Hyla cinerea*. Brain Research, 1041:231–236.

Snyder, F., 1974. Sleep–waking patterns of Hyracoidea. Sleep Research, 3:87.

Stoyanova, I.I., Rutten, W.L., le Feber, J., 2010. Orexin-A and orexin-B during the postnatal development of the rat brain. Cellular and Molecular Neurobiology, 30:81-89.

Suzuki, H., Kubo, Y., Yamamoto, T., 2008. Orexin-A immunoreactive cells and fibers in the central nervous system of the axolotl brain and their association with tyrosine hydroxylase and serotonin immunoreactive somata. Journal of Chemical Neuroanatomy, 35:295-305.

Szekely, M., Petervari, E., Balasko, M., 2010. Thermoregulation, energy balance, regulatory peptides: recent developments. Frontiers in Bioscience, 2:1009-1046.

Tabuce, R., Asher, R.J., Lehmann, T., 2008. Afrotherian mammals: a review of current data. Mammalia, 72:2-14.

Taheri, S., Sunter, D., Dakin, C., Moyes, S., Seal, L., Gardiner, J., Rossi, M., Ghatei, M., Bloom, S., 2000. Diurnal variation in orexin-A immunoreactivity and prepro-orexin mRNA in the rat central nervous system. Neuroscience Letters, 279:109-112.

Tao, R., Ma, Z., McKenna, J. T., Thakkar, M. M., Winston, S., Strecker, R. E., McCarley, R. W., 2006. Differential effect of orexins (hypocretins) on serotonin release in the dorsal and median raphe nuclei of freely behaving rats. Neuroscience, 141:1101–1105.

Teske, J.A., Billington, C.J., Kotz, C.M., 2010. Hypocretin/orexin and energy expenditure. Acta Physiologica, 198:303-312.

Vidal, L., Blanchard, J., Morin, L.P., 2005. Hypothalamic and zona incerta neurons expressing hypocretin, but not melanin concentrating hormone, project to the hamster intergeniculate leaflet. Neuroscience, 134:1081-1090.

Wagner, D., Salin-Pascual, R., Greco, M.A., Shiromani, P.J., 2000. Distribution of hypocretin-containing neurons in the lateral hypothalamus and c-fos-immunoreactive neurons in the VLPO. Sleep Research, 3:35-42.

Yamamoto, Y., McKinley, M.J., Nakazato, M., Yamashita, H., Shirahata, A., Ueta, Y., 2006. Postnatal development of orexin-A and orexin-B like immunoreactivities in

the Eastern grey kangaroo (*Macropus giganteus*) hypothalamus. Neuroscience Letters, 392:124-128.

Yamanaka, A., Tsujino, N., Funahashi, H., Honda, K., Guan, J.L., Wang, Q.P., Tominaga, M., Goto, K., Shioda, S., Sakurai, T., 2002. Orexins activate histaminergic neurons via the orexin 2 receptor. Biochemical and Biophysical Research Communications, 290:1237-1245.

Yamanaka, A., Muraki,Y.,Tsujino, N., Goto, K., Sakurai, T., 2003. Regulation of orexin neurons by the monoaminergic and cholinergic systems. Biochemical and Biophysical Research Communications, 303:120–129.

Yokogawa, T., Marin, W., Faraco, J., Pe´zeron, G., Appelbaum, L., Zhang, J., Rosa, F., Mourrain, P., Mignot, E., 2007. Characterization of sleep in zebrafish and insomnia in hypocretin receptor mutants. PLoS Biology, 5(10):e277.

Yoshida, Y., Fujiki, N., Nakajima, T., Ripley, B., Matsumura, H., Yoneda, H., Mignot, E., Nishino, S., 2001. Fluctuation of extracellular hypocretin-1 (orexin-A) levels in the rat in relation to the light-dark cycle and sleep-wake activities. European Journal of Neuroscience, 14:1075-1081.

Yoshida, K., McCormack, S., Espana, R.A., Crocker, A., Scammell, T.E., 2006. Afferents to the orexin neurons of the rat brain. Journal of Comparative Neurology, 494:845-861.

Zhang, J.H., Sampogna, S., Morales, F.R., Chase, M.H., 2001. Orexin (hypocretin)-like immunoreactivity in the cat hypothlamus: a light and electron microscopic study. Sleep, 24:67–76.

Zhang, J.H., Sampogna, S., Morales, F.R., Chase, M.H., 2002. Co-localization of hypocretin-1 and hypocretin-2 in the cat hypothalamus and brainstem. Peptides, 23:1479–1483.

Zhang, J.H., Sampogna, S., Morales, F.R., Chase, M.H., 2004. Distribution of hypocretin (orexin) immunoreactivity in the feline pons and medulla. Brain Research, 995:205-217.

**8.4. Chapter 4: Solitary sleep in the rock hyrax, *Procavia capensis*.**

Allison, T., and Cicchetti, P.V., 1976. Sleep in mammals: Ecological and constitutional correlates. Science, 194(4266): 732-734.

Affanni, J. M., 1972. Observations on the sleep of some South American marsupials and edentates. In: The Sleeping Brain, edited by Chase, M., Los Angeles: Brain Information Service/Brain Research Institute, UCLA, pp. 21-23.

Berger, R.J., Walker, J.M., 1972. A polygraphic study of sleep in the tree shrew (*Tupaia glis*). Brain Behavior and Evolution 5:54-69.

Bergmann, B.M., Winter, J.B., Rosenberg, R.S., Rechtschaffen, A., 1987. NREM Sleep with Low-Voltage EEG n the Rat. Sleep, 10(1):1-11.

Campbell, S.S., and Tobler, I., 1984. Animal Sleep: A Review of Sleep Duration Across Phylogeny. Neuroscience and Behavioral Reviews, 8:296-300.

Capellini, I., Barton, R.A., McNamara, P., Preston, B.T., Nunn, C.L., 2008. Phylogenetic analysis of the ecology and evolution of mammalian sleep. Evolution, 62(7): 1764–1776.

Cirelli, C., and Tononi, G., 2008. Is sleep essential? PLOS Biology, 6(8), e216.

Desiraju, T., Anand, B.K., Singh, B., 1966. Electrographic Studies on the Nature of Sleep and Wakefulness. Physiology and Bahvior, 1:285-291.

Elgar, M.A., Pagel, M.D., Harvey, P.H., 1988. Sleep in mammals. Animal Behavior, 36:1407-1419.

Galvão de Moura Filho, A.G., Huggins, S.E., Lines, S.G., 1983. Sleep and waking in the three-toed sloth Bradypus tridactylus. Comparative Biochemistry and Physiology A., 76:345–355.

Gottesman, C., 1992. Detection of seven sleep-waking stages in the rat. Neuroscience Biobehavioral Review 16:31-38.

Hallström, B.M., Kullberg, M., Nilsson, M.A., Janke, A., 2007. Phylogenomic data analyses provide evidence that Xenarthra and Afrotheria are sister groups. Molecular Biology and Evolution, 24(9): 2059-2068.

Horne, J., 2009. Neuroscience and Biobehavioral Reviews REM sleep, energy balance and 'optimal foraging '. Biobehavioral Reviews, 33:466-474.

Kingdon, J., 1971. East African Mammals. An Atlas of evolution in Africa. Academic Press, London.

Kurt, F., 1960. Le sommeil des éléphants. Mammalia, 24: 259-272.

Lesku, J. A., Bark, R. J., Martinez-Gonzalez, D., Rattenborg, N. C., Amlaner, C. J., Lima, S. L., Planck, M., and Group, F., 2008. Predator-induced plasticity in sleep architecture in wild-caught Norway rats (*Rattus norvegicus*). Behavioural Brain Research, 189:298-305.

Lyamin, O.I., Lapierre, J.L., Kosenko, P.O., Mukhametov, L., Siegel, J.M., 2008. EEG asymmetry and spectra power during sleep in the northern fur seal. Journal of Sleep Research, 17: 154-165.

Lyamin, O.I., Manger, P.R., Ridgway, S.H., Mukhametov, L.M., Siegel, J.M., 2008. Cetacean sleep: an unusual form of mammalian sleep. Neuroscience and Biobehavioral Reviews, 32(8):1451-84.

Lyamin, O.I., Peter, O., Kosenko, P.O., Lapierre, J.L., Mukhametov, L.M., Siegel, J.M., 2008. Fur seals display a strong drive for bilateral slow wave sleep while on land. Journal of Neuroscience, 28(48):12614-12621.

McNamara, P., Capellini, I., Harris, E., Nunn, C.L., Barton, R.A., Preston, B., 2008. The Phylogeny of Sleep Database: A New Resource for Sleep Scientists. The Open Sleep Journal, 1:11-14.

Moss, C., 1982. Portraits in the wild. Chicago: University of Chicago Press, p371.

Mukhametov, L. M., Lyamin, O. I., Chetyrbok, I. S., Vassilyev, A. A., Diaz, R. P., 1992. Sleep in an Amazonian manatee, *Trichechus inunguis*. Experientia, 48:417-419.

Nicolau, M.C., Akaârir, M., Gamundí, A., Gonzáles, J., Rial, R.V., 2000. Why we sleep: the evolutionary pathway to the mammalian sleep, Progress in Neurobiology, 62: 379-406.

Pivik, R.T., Sircar, S., Braun, C., 1981. Nuchal muscle tonus during sleep, wakefulness and tonic immobility in the rabbit. Physiology and Behavior 26:13-20.

Rattenborg, N.C, Voirin, B., Vyssotski, A.L., Kays, R.W., Spoelstra, K., Kuemmeth, F., Heidrich, W., Wikelski, M. 2008. Sleeping outside the box: electroencephalographic measures of sleep in sloths inhabiting a rainforest. Biology Letters, 4:402-405.

Rial, R.V., Akaârir, M., Gamundí, A., Nicolau, C. Garau, C., Aparicio, S., Tejada, S., Gené, L., González, J., De Vera, L.M., Coenen, A.M.L., Barceló, P., Esteban, S., 2010. Evolution of wakefulness, sleep and hibernation: From reptiles to mammals. Neuroscience and Behavioral Reviews, 34:1144-1160.

Ruckebusch, Y., 1972. Comparative aspects of sleep and wakefulness in farm animals. In: M. Chase., The Sleeping Brain. Perspectives in the Brain Sciences, Los Angeles: Brain Information Service/Brain Research Institute, UCLA, pp. 23-28.

Siegel, J.M., Manger, P.R., Nienhuis, R., Fahringer, H.M., Pettigrew, J.D., 1999. Sleep in the platypus. Neuroscience, 91:391-400.

Siegel, J.M, 2005. REM Sleep. In: Kryger, M.H., Roth, R., and Dement, W.C., Principles and Practices of Sleep Medicine, 4th edition. Saunders, New York.

Siegel, J.M., 2005. Clues to the function of mammalian sleep. Nature, 437:1264-1271.

Siegel, J.M., 2008. Do all animals sleep? Trends in Neuroscience, 31(4):208-213.

Siegel, J.M., 2009. Sleep viewed as a state of adaptive inactivity. Nature Reviews Neuroscience, 10:747-753.

Snyder, F., Bugbee, N., Douthitt, T., 1972.Telemetric studies of 24-hour sleep-waking patterns in some primitive mammals. Psychophysiology, 9:122.

Snyder, F., 1974. Sleep–waking patterns of Hyracoidea. Sleep Research, 3:87.

Spiess, H. G., Whitmayer, D.I., Sawyer, C.H., 1970. Patterns of spontaneous and induced paradoxical sleep in intact and hypophysectomized rabbits. Brain Research, 18:155-164.

Steriade, M, 2005. Brain Electrical Activity and Sensory Processing during Waking and Sleeping States. In: Kryger, M.H., Roth, R., and Dement, W.C., Principles and Practices of Sleep Medicine, 4th edition. Saunders, New York.

Sunquist, M., and Montgomery, G., 1973. Activity patterns and rates of movement of two-toed and three-toed sloths, *Choloepus hoffmani* and *Bradypus infuscatus.* Journal of Mammalogy., 54: 946-954.

Tabuce, R., Asher, R.J., Lehmann, T., 2008. Afrotherian mammals: a review of current data. Mammalia, 72:2-14.

Tobler, I., 1992. Behavioral sleep in the Asian elephant in captivity. Sleep, 15:1–12.

Tobler, I., 1995. Is sleep fundamentally different between mammalian species? Behavioral Brain Research, 69:35-41.

Tobler, I., 2005. Phylogeny of Sleep Regulation. In: Kryger, M.H., Roth, R., and Dement, W.C., Principles and Practices of Sleep Medicine, 4th edition. Saunders, New York.

Valatx, J. L. and Bugat, R., 1974. Facteurs génétiques dans le déterminisme du cycle veille-sommeil chez la souris. Brain Research, 69:315-330.

Van Twyver, H., and Allison, T., 1974. Sleep in the armadillo *Dasypus novemcinctus* at moderate and low ambient temperatures. Brain Behavior and Evolution, 9:107-120.

Wilson, M.L., Bashaw, M.J., Fountain, K., Kieschnick, S., Maple, T.L., 2006. Nocturnal Behavior in a Group of Female African Elephants. Zoo Biology, 25:173–186.

Wyatt, J.R., and Eltringham, S.K., 1974. The daily activity of the elephant in the Rwenzori National Park, Uganda. East African Wildlife Journal, 12:213-289.

Zeplin, H., Siegel, J.M., Tobler, I., 2005. Mammalian Sleep. In: Kryger, M.H., Roth, R., and Dement, W.C., Principles and Practices of Sleep Medicine, 4th edition. Saunders, New York.

### 8.5. Chapter 5: Social contrasted with solitary sleep patters in the rock hyrax, *Procavia capensis*

Bonnet, C., Leger, L., Baubet, V., Debilly, G., Cespuglio, R., 1997. Influence of a 1h immobilization stress on sleep states ad corticotropin-like intermediate lobe peptide (CLIP or $ACTH_{18-39}$, Ph-$ACTH_{18-39}$) brain contents in the rat. Brain Research, 751:54-63.

Borbély. A.A., and Achermann, P., 1999. Sleep homeostasis and models of sleep regulation. Journal of Biological Rhythms, 14(6):557-68.

Borbély, A.A., and Neuhaus, H.U., 1980. Sleep-deprivation: effects on sleep and EEG in the rat. Journal of Comparative Physiology, 133:71–87.

Bouyer, J.J., Deminiere, J.M., Mayo, W., Le Moal, M., 1997. Inter-individual differences in the effects of acute stress on the sleep-wakefulness cycle in the rat. Neuroscience Letters, 225:193-6.

Capellini, I., Nunn, C.L., McNamara, P., Preston, B.T., Barton, R.A., 2008. Energetic constraints, not predation, influence the evolution of sleep patterning in mammals. Functional Ecology, 22:847-853.

Capellini, I., Barton, R.A., McNamara, P., Preston, B.T., Nunn, C.L., 2008. Phylogenetic analysis of the ecology and evolution of mammalian sleep. Evolution, 62:1764–1776.

Caro, T., 2005. Antipredator defenses in birds and mammals. University of Chicago Press, Chicago.

Cirelli, C., and Tononi, G. (2008). Is sleep essential? PLOS Biology, 6(8), e216.

Daan, S., Beersma, D.G.M., Borbély, A.A., 1984. Timing of sleep: recovery process gated by a circadian pacemaker. American Journal of Physiology, 246:R161–R187.

Ganguly-Fitzgerald, I., Donlea, J., Shaw, P. J., 2006. Waking experience affects sleep need in Drosophila. Science, 313:1775-1781.

Horne, J., 2009. Neuroscience and Biobehavioral Reviews REM sleep, energy balance and 'optimal foraging '. Biobehavioral Reviews, 33:466-474.

Lesku, J. A., Bark, R. J., Martinez-Gonzalez, D., Rattenborg, N. C., Amlaner, C. J., Lima, S. L., Planck, M., and Group, F., 2008. Predator-induced plasticity in sleep architecture in wild-caught Norway rats (*Rattus norvegicus*). Behavioural Brain Research, 189:298-305.

Lima, S.L., Rattenborg, N.C., Lesku, J.A., Amlaner, C.J., 2005. Sleeping under the risk of predation. Animal Behaviour, 70:723–736.

McNamara, P., Capellini, I., Harris, E., Nunn3, C.L., Barton, R.A., Preston, B., 2008. The Phylogeny of Sleep Database: A New Resource for Sleep Scientists. The Open Sleep Journal, 1:11-14.

Meerlo, P., Pragt, B.J., Daan, S., 1997. Social stress induces high intensity sleep in rats. Neuroscience Letters, 225:41–44.

Meerlo, P., de Bruin, E., Strijkstra, A.M., Daan, S., 2001. Social conflict increases EEG slow-wave activity during subsequent sleep. Physiology and Behavior, 73:331-335.

Meerlo, P., and Turek, F.W., 2001. Effects of social stimuli on sleep in mice: non-rapid-eye-movement (NREM) sleep is promoted by aggressive interaction but not by sexual interaction. Brain Research, 907:84–92.

Noser, R., Gygax, L., Tobler, I., 2003. Sleep and social status in captive gelada baboons (*Theropithecus gelada*). Behavioural Brain Research, 147:9–15.

Nicolau, M.C., Akaârir, M., Gamundí, A., Gonzáles, J., Rial, R.V., 2000. Why we sleep: the evolutionary pathway to the mammalian sleep, Progress in Neurobiology, 62: 379-406.

Nunn, C.L., McNamara, P., Capellini, I., Preston, B.T., Barton, R.A., 2010. Primate sleep in phylogenetic perspective. In: McNamara, P., Barton, R.A., Nunn, C.L., Evolution of sleep: Phylogenetic and functional perspectives, Cambridge, UK; New York: Cambridge University Press.

Rampin, C., Cespuglio, R., Chastrette, N., Jouvet, M., 1991. Immobilization stress induces a paradoxical sleep rebound in the rat. Neuroscience Letters, 126:113-8.

Siegel, J.M., 2008. Do all animals sleep? Trends in Neuroscience, 31(4):208-213.

Taylor, C.R., and Sale, J.B., 1969. Temperature regulation in the hyrax. Comparative Biochemistry and Physiology, 31:903-907.

Tobler, I., and Borbély, A.A., 1986. Sleep EEG in the rat as a function of prior waking. Electroencephalographic clinical Neurophysiology, 64:74–76.

Zepelin, H., 1989. Mammalian sleep. In: Kryger, M.H., Roth, T., Dement, W.C., Principles and Practices of Sleep Medicine, pp. 30–49. Saunders, Philadelphia.

### 8.6. Chapter 6: The interrelations of the distribution of sleep associated nuclei and terminal networks in the brain of the rock hyrax, *Procavia capensis*

Airaksinen, M.S., and Panula, P., 1988. The Histaminergic System in the Guinea Pig Central Nervous System: An Immunocytochemical Mapping Study Using an Antiserum Against Histamine. The Journal of Comparative Neurology, 273:163-186.

Arai, R., Winsky, L., Arai, M., Jacobowitz, D.M., 1991. Immunohistochemical localization of calretinin in the rat hindbrain. Journal of Comparative Neurology, 310:21-44.

Ascoli, G.A., Alonso-Nanclares, L., Anderson, S.A., Barrionuevo, G., Benavides-Piccione, R., Burkhalter, A., Buzsáki, G., Cauli, B., DeFelipe, J., Fairén, A., Feldmeyer, D., Fishell, G., Fregnac, Y., Freund, T.F., Gardner, D., Gardner, E.P., Goldberg, J.H., Helmstaedter, M., Hestrin, S., Karube, F., Kisvárday, Z.F., Lambolez, B., Lewis, D.A., Marin, O., Markram, H., Muñoz, A., Packer, A., Petersen, C.C.H., Rockland, K.S., Rossier, J., Rudy, B., Somogyi, P., Staiger, J.F., Tamas, G., Thomson, A.M., Toledo-Rodriguez, M., Wang, Y., West, D.C., Yuste, R., 2008.

Petilla terminology: nomenclature of features of GABAergic interneurons of the cerebral cortex. Nature Reviews Neuroscience, 9:557-568.

Baimbridge, K.G., Celio, M.R., Rogers, J.H., 1992. Calcium-binding proteins in the nervous system. Trends in Neuroscience, 15:303-308.

Bayraktar, T., Staiger, J.F., Acsady, L., Cozzari, C., Freund, T.F., Zilles, K., 1997. Co-localization of vasoactive intestinal polypeptide, gamma-amino-butyric acid and choline acetyltransferase in the neocortical interneurons of the adult rat. Brain Res. 757, 209–217.

Braun, K., 1990. Calcium-binding proteins in avian and mammalian central nervous system: localization development and possible functions. Progress in Histochemistry and Cytochemistry, 21:1-64.

Cauli, B., Audinat,E., Lambolez, B., Angulo, M.C., Ropert, N., Tsuzuki, K., Hestrin, S., Rossier, J., 1997. Molecular and Physiological Diversity of Cortical Nonpyramidal Cells. The Journal of Neuroscience, 17: 3894-3906.

Celio, M.R., 1990. Calbindin D-28k and parvalbumin in the rat nervous system. Neuroscience 35, 375-475.

Charara, A., and Parent, A., 1998. Chemoarchitecture of the primate dorsal raphe nucleus. Journal of Chemical Neuroanatomy, 15:111-127.

Gallyas, F., 1979. Silver staining of myelin by means of physical development. Neurological Research, 1:203–209.

Gerashchenko, D., Shiromani, P.J., 2004. Different neuronal phenotypes in the lateral hypothalamus and their role in sleep and wakefulness. Molecular Neurobiology, 29:41–59.

Gravett, N., Bhagwandin, A., Fuxe, K., Manger, P.R., 2009. Nuclear organization and morphology of cholinergic, putative catecholaminergic and serotonergic neurons in the brain of the rock hyrax, *Procavia capensis*. Journal of Chemical Neuroanatomy, 38:57-74.

Gravett, N., Bhagwandin, A., Fuxe, K., Manger, P.R., 2011. Dustribution of orexin-A immunoreactive neurons and their terminal networks in the brain of the rock hyrax, *Procavia capensis.* Journal of Chemical Neuroanatomy, Article in Press doi.10.1016/j.jchemneu.2010.11.005.

Inagaki, N., Yamatodani, A., Ando-Yamamoto, M., Tohyama, M., Watanabe, T., Wada, H., 1988. Organization of Histaminergic Fibers in the Rat Brain. The Journal of Comparative Neurology, 273:283-300.

John, J., Wu, M.F., Boehmer, L.N., Siegel, J.M., 2004. Cataplexy-active neurons in the hypothalamus: implications for the role of histamine in sleep and waking behavior. Neuron, 42:619–634.

Kiyashchenko, L.I., Mileykovskiy, B.Y., Maidment, N., Lam, H.A., Wu, M.F., John, J.,Peever, J., Siegel, J.M., 2002. Release of hypocretin (orexin) during waking and sleep states. Journal of Neuroscience, 22:5282–5286.

Krzywkowski, P., Jacobowitz, D.M., Lamour, Y., 1995. Calretinin-containing pathways in the rat forebrain. Brain Res. 705, 273-294.

Lai, Y.Y., Siegel, J.M., 1990. Muscle tone suppression and stepping produced by stimulation of midbrain and rostral pontine reticular formation. Journal of Neuroscience, 10:2727–2738.

Lai, Y.Y., Kodama, T., Siegel, J.M., 2001. Changes in monoamine release in the ventral horn and hypoglossal nucleus linked to pontine inhibition of muscle tone: an in vivo microdialysis study. Journal of Neuroscience, 21:7384–7391.

Leger, L., Charnay, Y., Hof, P.R., Bouras, C., Cespuglio, R., 2001. Anatomical Distribution of Serotonin-Containing Neurons and Axons in the Central Nervous System of the Cat. The Journal of Comparative Neurology, 433:157-182.

Lyamin, O.I., Manger, P.R., Ridgway, S.H., Mukhametov, L.M., Siegel, J.M., 2008. Cetacean sleep: an unusual form of mammalian sleep. Neuroscience and Biobehavioral Reviews, 32(8):1451-84.

Mintz, E.M., Van den Pol, A.N., Casano, A.A., Albers, H.E., 2001. Distribution of hypocretin-(orexin) immunoreactivity in the central nervous system of Syrian hamsters (*Mesocricetus auratus*). Journal of Chemical Neuroanatomy, 21:225–238.

Nitz, D., Siegel, J.M., 1997a. GABA release in the locus coeruleus as a function of sleep/wake state. Neuroscience, 78:795–801.

Nitz, D., Siegel, J.M., 1997b. GABA release in the dorsal raphe nucleus: role in the control of REM sleep. American Journal of Physiology, 273:R451–R455.

Nixon, J.P., Smale, L., 2007. A comparative analysis of the distribution of immunoreactive orexin-A and B in the brains of nocturnal and diurnal rodents. Behavioral and Brain Functions, 13:28.

Novak, C.M., Albers, H.E., 2002. Localization of hypocretin-like immunoreactivity in the brain of the diurnal rodent, *Arvicanthis niloticus*. Journal of Chemical Neuroanatomy, 23:49-58.

Parent, A, Fortin, M., Côté, P.-Y., Cicchetti, F., 1996. Calcium-binding proteins in primate basal ganglia. Neuroscience Research, 25:309-334.

Peyron, C., Tighe, D.K., van den Pol, A.N., De Lecea, L., Heller, H.C., Sutcliffe, J.G., Kilduff, T.S., 1998. Neurons containing hypocretin (orexin) project to multiple neuronal systems. Jornal of Neuroscience, 18:9996–10015.

Rogers, J.H., 1992. Immunohistochemical markers in the rat brain: colocalization of calretinin and calbindin-D28k with tyrosine hydroxylase. Brain Research, 587:203-210.

Sakai, K., Koyama, Y., 1996. Are there cholinergic and non-cholinergic paradoxical sleep-on neurons in the pons. Neuroreport, 7:2449–2453.

Saper, C.B., Chou, T.C., Scammell, T.E., 2001. The sleep switch: hypothalamic control of sleep and wakefulness. Trends in Neuroscience, 24:726–731.

Siegel, J.M., 2000. Brainstem mechanisms generating REM sleep. In: Kryger, M.H., Roth, T., Dement, W.C. (Eds.), Principles and Practices of Sleep Mechanisms. WB Saunders, Philadelphia, PA, pp. 112–133.

Siegel, J.M., 2004. The neurotransmitters of sleep. Journal of Clinical Psychiatry, 65 (suppl. 16):4–7.

Siegel, J.M., Nienhuis, R., Fahringer, H.M., Paul, R., Shiromani, P., Dement, W.C., Mignot, E., Chiu, C., 1991. Neuronal activity in narcolepsy: identification of cataplexy related cells in the medial medulla. Science, 252:1315–1318.

Steriade, M., Pare, D., Datta, S., Oakson, G., Curro Dossi, R., 1990. Different cellular types in mesopontine cholinergic nuclei related to ponto-geniculo-occipital waves. Journal of Neuroscience, 10:2560–2579.

Szymusiak, R., 1995. Magnocellular nuclei of the basal forebrain: substrates of sleep and arousal regulation. Sleep, 18:478–500.

Szymusiak, R., Steininger, T., Alam, N., McGinty, D., 2001. Preoptic area sleepregulating mechanisms. Archives Italiennes de Biologie, 139:77–92.

Törk, I., 1990. Anatomy of the serotonergic system. Annals of the New York Academy of Sciences, 600:9–35.

Wu, M.F., John, J., Boehmer, L.B., Nguyen, G.B., Siegel, J.M., 2004. Activity of dorsal raphe cells across the sleep-waking cycle and during cataplexy in narcoleptic dogs. Journal of Physiology, 554:202–215.

**8.7. Chapter 7: Concluding Remarks**

Bergmann, B.M., Winter, J.B., Rosenberg, R.S., Rechtschaffen, A., 1987. NREM Sleep with Low-Voltage EEG n the Rat. Sleep, 10(1):1-11.

Bhagwandin, A., Fuxe, K., Bennett, N.C., Manger, P.R., 2008. Nuclear organization and morphology of cholinergic, putative catecholaminergic and serotonergic neurons

in the brains of two species of African mole-rat. Journal of Chemical Neuroanatomy, 35:371-387.

Dwarika, S., Maseko, B.C., Ihunwo, A.O., Fuxe, K., Manger, P.R., 2008. Distribution and morphology of putative catecholaminergic and serotonergic neurons in the brain of the greater canerat, *Thryonomys swinderianus*. Journal of Chemical Neuroanatomy, 35:108-122.

Kruger, J-L., Dell, L-A., Pettigrew, J.D., Manger, P.R., 2010. Cellular location and major terminal networks of the orexinergic system in the brains of five microchiropteran species. Journal of Chemical Neuroanatomy, 40:256-262.

Limacher, A.M., Bhagwandin, A., Fuxe, K., Manger, P.R., 2008. Nuclear organization and morphology of cholinergic, putative catecholaminergic and serotonergic neurons in the brain of the Cape porcupine (*Hystrix afri*caeaustralis): Increased brain size does not lead to increased organizational complexity. Journal of Chemical Neuroanatomy, 36:33-52.

Manger, P.R., Fahringer, H., Pettigrew, J.D., Siegel, J.M., 2002a. Distribution and morphology of cholinergic neurons in the brain of the monotremes as revealed by ChAT immunohistochemistry. Brain Behavior and Evolution, 60:275-297.

Maseko, B.C., Manger, P.R., 2007. Distribution and morphology of cholinergic, catecholaminergic and serotonergic neurons in the brain of Schreiber's long-fingered bat, *Miniopterus schreibersii*. Journal of Chemical Neuroanatomy, 34:80-94.

Maseko, B.C., Manger, P.R., 2007. Distribution and morphology of cholinergic, catecholaminergic and serotonergic neurons in the brain of Schreiber's long-fingered bat, *Miniopterus schreibersii*. Journal of Chemical Neuroanatomy, 34:80-94.

McGranaghan, P.A., Piggins, H.D., 2001. Orexin-A-like immunoreactivity in the hypothalamus and thalamus of the Syrian hamster (*Mesocricetus auratus*) and Siberian hamster (*Phodopus sungorus*), with special reference to circadian structures. Brain Research, 904:234-244.

Mintz, E.M., Van den Pol, A.N., Casano, A.A., Albers, H.E., 2001. Distribution of hypocretin-(orexin) immunoreactivity in the central nervous system of Syrian hamsters (*Mesocricetus auratus*). Journal of Chemical Neuroanatomy, 21:225–238.

Moon, D.J., Maseko, B.C., Ihunwo, A., Fuxe, K., Manger, P.R., 2007. Distribution and morphology of catecholaminergic and serotonergic neurons in the brain of the highveld gerbil, *Tatera brantsii*. Journal of Chemical Neuroanatomy, 34:134-144.

Nixon, J.P., Smale, L., 2007. A comparative analysis of the distribution of immunoreactive orexin-A and B in the brains of nocturnal and diurnal rodents. Behavioral and Brain Functions, 13:28.

Novak, C.M., Albers, H.E., 2002. Localization of hypocretin-like immunoreactivity in the brain of the diurnal rodent, *Arvicanthis niloticus*. Journal of Chemical Neuroanatomy, 23:49-58.

Olds, N., and Shoshani, J., 1982. Procavia capensis. Mammalian Species, 171:1-7.

Skinner, J.D., Chimimba, C.T., 2005. The Mammals of the Southern African Subregion, 3rd Edition. Cambridge University Press, Cape Town.

Snyder, F., 1974. Sleep–waking patterns of Hyracoidea. Sleep Research, 3:87.

Tabuce, R., Asher, R.J., Lehmann, T., 2008. Afrotherian mammals: a review of current data. Mammalia, 72:2-14.

Törk, I., 1990. Anatomy of the serotonergic system. Annals of the New York Academy of Sciences, 600:9–35.

Wagner, D., Salin-Pascual, R., Greco, M.A., Shiromani, P.J., 2000. Distribution of hypocretin-containing neurons in the lateral hypothalamus and c-fos-immunoreactive neurons in the VLPO. Sleep Research, 3:35-42.

Woolf, N.J., 1991. Cholinergic systems in mammalian brain and spinal cord. Progress in Neurobiology, 37:475–524.

Journal of Chemical Neuroanatomy 38 (2009) 57–74

Contents lists available at ScienceDirect

Journal of Chemical Neuroanatomy

journal homepage: www.elsevier.com/locate/jchemneu

# Nuclear organization and morphology of cholinergic, putative catecholaminergic and serotonergic neurons in the brain of the rock hyrax, *Procavia capensis*

Nadine Gravett [a], Adhil Bhagwandin [a], Kjell Fuxe [b], Paul R. Manger [a,*]

[a] School of Anatomical Sciences, Faculty of Health Sciences, University of the Witwatersrand, 7 York Road, Parktown, 2193 Johannesburg, South Africa
[b] Department of Neuroscience, Karolinska Institutet, Retzius väg 8, S-171 77 Stockholm, Sweden

ARTICLE INFO

*Article history:*
Received 17 January 2009
Received in revised form 18 February 2009
Accepted 27 February 2009
Available online 14 March 2009

*Keywords:*
Afrotheria
Immunohistochemistry
Hyrax
Evolution
Mammalia

ABSTRACT

The nuclear subdivisions of the cholinergic, putative catecholaminergic and serotonergic systems within the brain of the rock hyrax (*Procavia capensis*) were identified following immunohistochemistry for acetylcholinesterase, tyrosine hydroxylase and serotonin. The aim of the present study was to investigate possible differences in the complement of nuclear subdivisions of these systems by comparing those of the rock hyrax to published studies of other mammals. The rock hyrax belongs to the order Hyracoidea and forms part of the Afroplacentalia mammalian cohort. For the most part, the nuclear organization of these three systems closely resembled that described for many other mammalian species. The nuclear organization of the serotonergic system was identical to that seen in all eutherian mammals. The nuclear organization of the putative catecholaminergic system was very similar to that seen in rodents except for the lack of a C3 nucleus and the compact division of the locus coeruleus (A6c). In addition, the diffuse locus coeruleus (A6d) appeared to contain very few tyrosine hydroxylase immunoreactive (TH+) neurons. The cholinergic system showed many features in common with that seen in both rodents and primates; however, there were three differences of note: (1) cholinergic neurons were observed in the anterior nuclei of the dorsal thalamus; (2) cholinergic parvocellular nerve cells, probably representing interneurons, forming subdivisions of the laterodorsal and pedunculopontine tegmental nuclei were observed at the midbrain/pons interface; and (3) a large number of cholinergic nerve cells in the periventricular grey of the medulla oblongata were observed. Thus, while there are many similarities to other mammalian species, the nuclear organization of these systems in the rock hyrax shows specific differences to what has been observed previously in other mammals. These differences are discussed in both a functional and phylogenetic perspective.

© 2009 Elsevier B.V. All rights reserved.

* Corresponding author. Tel.: +27 11 717 2497; fax: +27 11 717 2422.
*E-mail address:* Paul.Manger@wits.ac.za (P.R. Manger).

*Abbreviations:* III, oculomotor nucleus; IV, trochlear nucleus; Vmot, motor division of trigeminal nucleus; VI, abducens nucleus; VIId, facial nerve nucleus, dorsal division; VIIv, facial nerve nucleus, ventral division; X, dorsal motor vagus nucleus; XII, hypoglossal nucleus; 3V, third ventricle; 4V, fourth ventricle; 7n, facial nerve; A1, caudal ventrolateral medullary tegmental nucleus; A2, caudal dorsomedial medullary nucleus; A4, dorsal medial division of locus coeruleus; A5, fifth arcuate nucleus; A6c, compact portion of locus coeruleus; A6d, diffuse portion of locus coeruleus; A7d, nucleus subcoeruleus, diffuse portion; A7sc, nucleus subcoeruleus, compact portion; A8, retrorubral nucleus; A9l, substantia nigra, lateral; A9m, substantia nigra, medial; A9pc, substantia nigra, pars compacta; A9v, substantia nigra, ventral or pars reticulata; A10, ventral tegmental area; A10c, ventral tegmental area, central; A10d, ventral tegmental area, dorsal; A10dc, ventral tegmental area, dorsal caudal; A11, caudal diencephalic group; A12, tuberal cell group; A13, zona incerta; A14, rostral periventricular nucleus; A15d, anterior hypothalamic group, dorsal division; A15v, anterior hypothalamic group, ventral division; A16, catecholaminergic neurons of the olfactory bulb; ac, anterior commissure; AD, anterodorsal nucleus of the dorsal thalamus; Amyg, amygdala; AP, area postrema; AV, anteroventral nucleus of the dorsal thalamus; B9, supralemniscal serotonergic nucleus; C, caudate nucleus; C1, rostral ventrolateral medullary tegmental group; C2, rostral dorsomedial medullary nucleus; ca, cerebral aqueduct; Cb, cerebellum; cc, corpus callosum; Cl, claustrum; CLi, caudal linear nucleus; CN, cochlear nucleus; C/P, caudate and putamen nuclei; CP, cerebral peduncle; CVL, caudal ventrolateral serotonergic group; DCN, deep cerebellar nuclei; Diag.B, diagonal band of Broca; DR, dorsal raphe; DRc, dorsal raphe nucleus, caudal division; DRd, dorsal raphe nucleus, dorsal division; DRif, dorsal raphe nucleus, interfascicular division; DRl, dorsal raphe nucleus, lateral division; DRp, dorsal raphe nucleus, peripheral division; DRv, dorsal raphe nucleus, ventral division; DT, dorsal thalamus; EW, Edinger–Westphal nucleus; f, fornix; GC, periaqueductal grey matter; GLD, dorsal lateral geniculate nucleus; GP, globus pallidus; Hbm, medial habenular nucleus; Hip, hippocampus; Hyp, hypothalamus; Hyp.d, dorsal hypothalamic cholinergic nucleus; Hyp.l, lateral hypothalamic cholinergic nucleus; Hyp.v, ventral hypothalamic cholinergic nucleus; IC, inferior colliculus; ic, internal capsule; icp, inferior cerebellar peduncle; io, inferior olivar nuclei; IP, interpeduncular nucleus; LDTmc, magnocellular division of the laterodorsal tegmental nucleus; LDTpc, parvocellular division of the laterodorsal tegmental nucleus; LRT, lateral reticular nucleus; LV, lateral ventricle; mcp, middle cerebellar peduncle; MnR, median raphe nucleus; N.Acc, nucleus accumbens; N.Amb, nucleus ambiguus; N.Bas, nucleus basalis; NEO, neocortex; OB, olfactory bulb; OC, optic chiasm; OT, optic tract; P, putamen; pVII, preganglionic motor neurons of the superior salivatory nucleus or facial nerve; pIX, preganglionic motor neurons of the inferior salivatory nucleus; PBg, parabigeminal nucleus; PIR, piriform cortex; PPTmc, magnocellular division of the pedunculopontine nucleus; PPTpc, parvocellular division of the pedunculopontine nucleus; Pta, pretectal area; py, pyramidal tract; pyx, decussation of the pyramidal tract; R, thalamic reticular nucleus; Rmc, red nucleus, magnocellular division; RMg, raphe magnus nucleus; ROb, raphe obscurus nucleus; RPa, raphe pallidus nucleus; RVL, rostral ventrolateral serotonergic group; S, septum; SC, superior colliculus; scp, superior cerebellar peduncle; Sep.M, medial septal nucleus; TOL, olfactory tubercle; TOL/Is.Call., olfactory tubercle/island of Calleja; vh, ventral horn of spinal cord; VPO, ventral pontine nucleus; xscp, decussation of the superior cerebellar peduncle; ZI, zona incerta.

0891-0618/$ – see front matter © 2009 Elsevier B.V. All rights reserved.
doi:10.1016/j.jchemneu.2009.02.005

## 1. Introduction

The rock hyrax, *Procavia capensis*, is a member of the Procaviidae family, which is the only living family within the Hyracoidea order (Klein and Cruz-Uribe, 1996). The family consists of three genera: *Procavia* (the rock hyrax, one species), *Heterohyrax* (two species) and *Dendrohyrax* (three species) (Skinner and Chimimba, 2005). The rock hyrax is a small, agile, diurnal, social, herbivorous mammal, typically weighing between 2.5 and 4.6 kg, and lives in rocky outcrops or "koppies" in most parts of Africa (Skinner and Chimimba, 2005). Sexual maturity is reached between 28–29 months in males and 16–17 months in females, with seasonal mating being triggered by the photoperiod (Skinner and Chimimba, 2005). According to the fossil record, hyraxes first appeared approximately 40 million years ago and they are grouped phylogenetically with the African elephant (Proboscidea), and manatee and dugong (Sirenia). These three orders, together with the Chrysochloridea (golden moles), Macroscelidea (elephant shrews), Tubulidentata (aardvarks) and the Tenrecidea (tenrecs) form the cohort Afroplacentalia (Arnason et al., 2008).

In the present study the cholinergic, putative catecholaminergic and serotonergic systems within the brain of the rock hyrax were examined and described using immunohistochemical techniques. It is well known that these systems project to most parts of the brain and that they are associated with several functions (Woolf, 1991; Smeets and González, 2000; Törk, 1990; Jacobs and Azmitia, 1992); for example, cognition (e.g. Bartus et al., 1982; Previc, 1999), the sleep-wake cycle (e.g. Siegel, 2006), reproduction (e.g. Tillet, 1995), and sensory-motor (e.g. Pompeiano, 2001; Fuxe et al., 2007a) functions to name but a few. The cholinergic system has an extensive distribution throughout the brain (Woolf, 1991; Reiner and Fibiger, 1995; Manger et al., 2002a; Maseko et al., 2007) while the catecholaminergic and serotonergic neuronal systems are mainly concentrated within the brainstem (Dahlström and Fuxe, 1964; Andén et al., 1964; Fuxe et al., 1969, 1970, 2006, 2007a; Diksic and Young, 2001; Manger et al., 2002b,c; Maseko et al., 2007). The nuclear organization of these systems has been studied in several mammalian species (e.g. Maseko et al., 2007; Bhagwandin et al., 2008; Limacher et al., 2008); however no studies of these systems have been done in any member of the Afroplacentalia cohort. Thus, the aim of this study is to determine the nuclear organization of these systems in the brain of the rock hyrax and extend our basis for understanding the evolutionary processes associated with the nuclear organization of these systems.

These systems have exhibited some evolutionary trends and even though these systems are quite similar across species for the most part, differences due occur. For example, the catecholaminergic C3 nucleus has only been reported to be present in the rodents (e.g. Smeets and González, 2000; Manger et al., 2002b; Maseko et al., 2007; Moon et al., 2007; Badlangana et al., 2007; Dwarika et al., 2008; Bhagwandin et al., 2008; Limacher et al., 2008). Serotonergic neurons in the mammalian hypothalamus have only been reported for monotremes (Manger et al., 2002c). These examples and other evidence have led Manger (2005) to propose that members of the same order will show the same complement of nuclei, but this complement may differ between orders. Some predictions of the current study include: (1) the rock hyrax will have many nuclei in common with other mammals; (2) the rock hyrax may have some nuclei unique to this species; (3) the rock hyrax may exhibit nuclei found only in members of the Afroplacentalia; and (4) the rock hyrax may be missing some nuclei commonly found in other mammalian species.

## 2. Materials and methods

A total of six adult female rock hyraxes, *P. capensis*, were used in the present study. Permits from the Limpopo and Gauteng Provincial Governments were obtained for the capture and transport of the animals from the wild. All animals were treated and used according to the guidelines of the University of the Witwatersrand Animal Ethics Committee, which parallel those of the NIH for the care and use of animals in scientific experimentation. Each animal was weighed, deeply anaesthetized and subsequently euthanized with weight appropriate doses of sodium pentobarbital (200 mg sodium pentobarbital/kg, i.p.). Upon cessation of respiration the animals were perfused intracardially with 0.9% saline followed by 4% paraformaldehyde in 0.1 M phosphate buffer (PB) (approximately 1 l/kg of each solution), both solutions having a temperature of 4 °C. The brains were then carefully removed from the skulls and post-fixed overnight in 4% paraformaldehyde in 0.1 M PB followed by equilibration in 30% sucrose in 0.1 M PB. The brains were then frozen and with the aid of a freezing microtome sectioned at 50 μm in either coronal ($n = 4$) or sagittal ($n = 2$) planes. A one in five series of stains was made for nissl, myelin, choline acetyltransferase (ChAT) (identification of the cholinergic system), tyrosine hydroxylase (TH) (identification of the dopaminergic and noradrenergic systems), and serotonin (5HT) (identification of the serotonergic system). Sections kept for the Nissl series were mounted on 0.5% gelatine-coated glass slides, cleared in a solution of 1:1 chloroform and absolute alcohol, then stained with 1% cresyl violet to reveal cell bodies. Myelin sections were stored in 5% formalin for a period of two weeks and were then mounted on 1.5% gelatine-coated glass slides and subsequently stained with silver solution to reveal myelin sheaths (Gallyas, 1979).

For immunohistochemical staining each section was treated with endogenous peroxidase inhibitor (49.2% methanol:49.2% 0.1 M PB:1.6% of 30% $H_2O_2$) for 30 min and subsequently subjected to three 10 min 0.1 M PB rinses. The sections were then preincubated in a solution (blocking buffer) consisting of 3% normal serum (normal rabbit serum, NRS, for the ChAT sections and normal goat serum, NGS, for the TH and 5HT sections), 2% bovine serum albumin (BSA, Sigma) and 0.25% Triton X100 (Merck) in 0.1 M PB, at room temperature for 2 h. This was followed by three 10 min rinses in 0.1 M PB. The sections were then placed, for 48 h at 4 °C under constant gentle shaking, in primary antibody solution, that contained the appropriately diluted primary antibody in blocking buffer (see above). The primary antibodies used were anti-cholineacetyltransferase for cholinergic neurons (AB144P, Chemicon, raised in goat, at a dilution of 1:2000), anti-tyrosine hydroxylase for putative catecholaminergic neurons (AB151, Chemicon, raised in rabbit, at a dilution of 1:7500), and anti-serotonin for serotonergic neurons (AB938, Chemicon, raised in rabbit, at a dilution of 1:10000). This was followed by another three 10 min rinses in 0.1 M PB, after which the sections were incubated for 2 h at room temperature in secondary antibody solution. The secondary antibody solution contained a 1:750 dilution of biotinylated anti-rabbit IgG (BA-1000, Vector Labs) in 3% NGS (or anti-goat IgG, BA-5000 in 3% NRS for the ChAT sections), and 2% BSA in 0.1 M PB. Once this was completed, the sections were again subjected to another three 10 min rinses in 0.1 M PB, followed by a 1 h incubation in AB solution (Vector Labs) and again rinsed. This was followed by a 5 min treatment of the sections in a solution consisting of 0.05% diaminobenzidine (DAB) in 0.1 M PB, after which, and while still in the same solution, 3 μl of 30% $H_2O_2$ per 0.5 ml of solution was added. With the aid of a low power stereomicroscope the progression of the staining was visually followed and allowed to continue until a level was reached where the background staining could assist in reconstruction without obscuring the immunopositive neurons. Once this level was reached the reaction was stopped by placing the sections in 0.1 M PB, followed by a final session of three 10 min rinses in 0.1 M PB. The immunohistochemically stained sections were mounted on 0.5% gelatine-coated slides and left to dry overnight. The mounted sections were dehydrated by placing it in 70% alcohol for 2 h at room temperature under gentle shaking and then transferred through a series of graded alcohols, cleared in xylene and coverslipped with Depex.

The sections were observed with a low power stereomicroscope, and the architectonic borders traced according to the Nissl and myelin stained sections using a camera lucida. The corresponding immuno-stained sections were then matched to the drawings and the immunopositive neurons marked. The drawings were scanned and redrawn with the aid of the Canvas 8 program. The nomenclature used for the cholinergic system was adopted from Woolf (1991), Manger et al. (2002a), Maseko and Manger (2007), Maseko et al. (2007), Limacher et al. (2008) and Bhagwandin et al. (2008); the catecholaminergic system from Dahlström and Fuxe (1964), Hökfelt et al. (1984), Smeets and González (2000), Manger et al. (2002b), Maseko and Manger (2007), Maseko et al. (2007), Moon et al. (2007), Dwarika et al. (2008), Limacher et al. (2008) and Bhagwandin et al. (2008); and for the serotonergic system from Törk (1990), Bjarkam et al. (1997), Manger et al. (2002c), Maseko and Manger (2007), Maseko et al. (2007), Moon et al. (2007), Dwarika et al. (2008), Limacher et al. (2008) and Bhagwandin et al. (2008). While we use the standard nomenclature for the catecholaminergic system in this paper, we realize that the neuronal groups we revealed with tyrosine hydroxylase immunohistochemistry may not correspond directly with those nuclei that have been described in previous studies by Dahlström and Fuxe (1964), Hökfelt et al. (1976), Meister et al. (1988), Kitahama et al. (1990, 1996), and Ruggiero et al. (1992); however, given the striking similarity of the results of the tyrosine

hydroxylase immunohistochemistry to that seen in other mammals we feel this terminology is appropriate. Clearly further studies in the rock hyrax with a wider range of antibodies, such as those to phenylethanolamine-*N*-methyltransferase (PNMT), dopamine-β-hydroxylase (DBH) and aromatic L-amino acid decarboxylase (AADC) would be required to fully determine the implied homologies ascribed in this study. We address this potential problem with the caveat of putative catecholaminergic neurons where appropriate in the text.

## 3. Results

The present study was designed to reveal the nuclear organization of the cholinergic, putative catecholaminergic, and serotonergic systems of the rock hyrax, *P. capensis* through immunohistochemical methods. A total of six adult female brains were used for this purpose, and the individuals used for this study had body masses ranging from 1.14 to 1.52 kg and brain masses between 14.4 and 17.5 g (Fig. 1). The results revealed that for the most part these systems do not differ drastically from those observed in other mammalian species; however the rock hyrax does show some unique additional nuclei, specifically within the cholinergic system, that have not been noted in other species.

### 3.1. Cholinergic neurons

The general organization of the cholinergic system encompasses the striatal, basal forebrain, diencephalic, and pontomesencephalic groups together with the cranial nerve motor nuclei that extend from level of the anterior horn of the lateral ventricle to the spinomedullary junction (e.g. Woolf, 1991; Manger et al., 2002a; Maseko et al., 2007). These groups were all present in the brain of the rock hyrax and did not show any significant differences to the general mammalian group level organization of this system (Figs. 2 and 3). Despite this, some novel features, potentially unique to the rock hyrax, that have not been observed in other mammals were observed. These include the existence of cholinergic neurons in the anterior nuclei of the dorsal thalamus, the existence of magnocellular and parvocellular divisions of both the laterodorsal tegmental and pedunculopontine tegmental nuclei, and a large cell group in the dorsomedial periventricular grey of the medulla oblongata (Figs. 2–7).

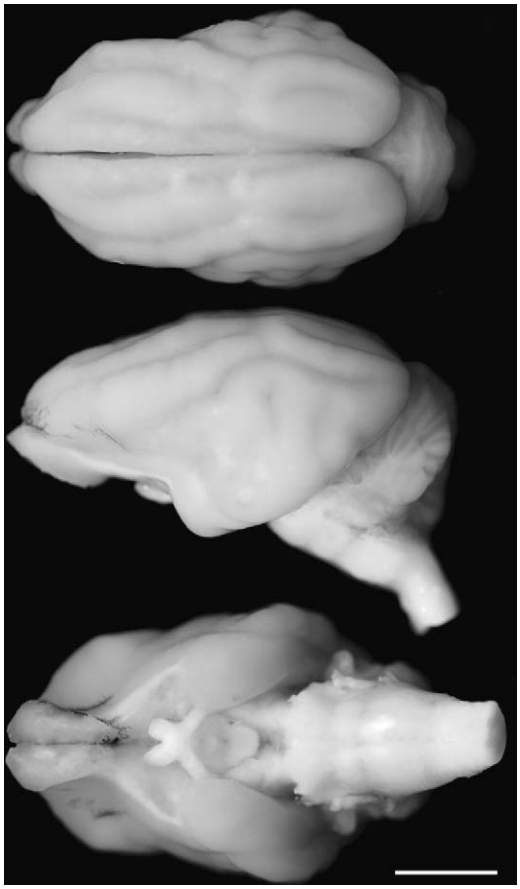

**Fig. 1.** Photographs of the dorsal (top), lateral (middle) and ventral (bottom) aspects of the rock hyrax brain. Scale bar = 1 cm.

#### 3.1.1. Striatal cholinergic interneurons

*3.1.1.1. Nucleus accumbens.* Uniformly distributed choline acetyltransferase immunoreactive (ChAT+) nerve cell bodies were located ventrally and slightly anterior to the dorsal striatopallidal complex (caudate, putamen and the globus pallidus) (Figs. 2C–F and 3). The anterior and posterior borders of this nucleus were adjacent to the anterior horn of the lateral ventricle and the anterior commissure, respectively. This arrangement is typical to what is observed in all mammals (Woolf, 1991; Manger et al., 2002a; Maseko et al., 2007). A moderate density of ChAT+ neurons was observed throughout this nucleus, these neurons being a mixture of bipolar and multipolar types, but the majority were of the multipolar type (Fig. 4). The ChAT+ neurons of this nucleus showed no specific dendritic organization.

*3.1.1.2. Dorsal striatopallidal complex – caudate/putamen and globus pallidus.* The caudate/putamen nucleus was located lateral to the lateral ventricle and its distribution extended from the level of the anterior horn of the lateral ventricle anteriorly to the medial habenular nuclei posteriorly (Figs. 2D–K and 3), a location typical of all mammals (Woolf, 1991; Manger et al., 2002a; Maseko et al., 2007). The boundary between the caudate and putamen was clearly defined by the internal capsule at the level of the anterior commissure, but not anterior to this level. The location of the globus pallidus was found to be ventral and somewhat medial to the putamen and it extended from the level of the anterior commissure to the habenular nuclei. A moderate density of uniformly distributed ChAT+ neurons was observed within the caudate/putamen (Fig. 4). The globus pallidus only exhibited a small number of ChAT+ neurons and these neurons were found to be located mostly where the globus pallidus bordered the putamen laterally and the nucleus basalis ventrally. A similar neuronal morphology was noted for the caudate/putamen and the globus pallidus, the ChAT+ neurons being a mixture of bipolar and multipolar types, however a multipolar organization predominated. No specific dendritic orientation was observed for these neurons.

*3.1.1.3. Islands of Calleja and olfactory tubercle.* These nuclei exhibited the typical mammalian organizational plan (Woolf, 1991; Manger et al., 2002a; Maseko et al., 2007). They were located in the ventral most portion of the cerebral hemisphere at a level ventral to the nucleus accumbens (Figs. 2D–F and 3). These nuclei extended from the level of the anterior horn of the lateral ventricle to the level of the anterior commissure. The islands of Calleja contained a moderate density of ChAT+ neuronal clusters, and a scattered low to medium density of ChAT+ neurons surrounding these clusters were assigned to the olfactory tubercle. The cells in these regions were intensely immunoreactive and a mixture of bipolar and multipolar neuron types with ovoid shaped somas was observed. The neurons of the islands of Calleja as well as those of the olfactory tubercle exhibited no specific dendritic orientation.

#### 3.1.2. Cholinergic nuclei of the basal forebrain

*3.1.2.1. Medial septal nucleus.* This nucleus was identified through the presence of ChAT+ neurons located within the septal nuclear

complex in the rostral half of the medial wall of the cerebral hemisphere (Figs. 2G–H and 3). The location of this nucleus is typical of what has been observed in other mammals (Woolf, 1991; Manger et al., 2002a; Maseko et al., 2007). A moderate to high density of ChAT+ neurons, comprising a mixture of both bipolar and multipolar types with ovoid cell shapes was observed. It was also noted that the cells located closer to the edge of the hemisphere were smaller than those cells located at a small distance from the edge. Also, the cells closer to the edge of the hemisphere were mostly bipolar with dendrites arranged parallel to the edge, whereas those further away were predominantly multipolar and exhibited no specific dendritic orientation.

*3.1.2.2. Diagonal band of Broca.* The diagonal band of Broca was located anterior to the hypothalamus in the ventromedial corner of the cerebral hemisphere (Fig. 2F). The division of this nucleus into horizontal and vertical bands appeared to be unnecessary as the neurons forming this nucleus presented as a continuous, uninterrupted band. A high density of ChAT+ neurons was found throughout the extent of this nucleus (Fig. 4). The cells were intensely immunoreactive, ovoid in shape and multipolar in type with their dendrites orientated roughly parallel to the edge of the cerebral hemisphere. It was also noted that the neurons of this nucleus were larger than those found in the adjacent olfactory tubercle and islands of Calleja, a feature that can be

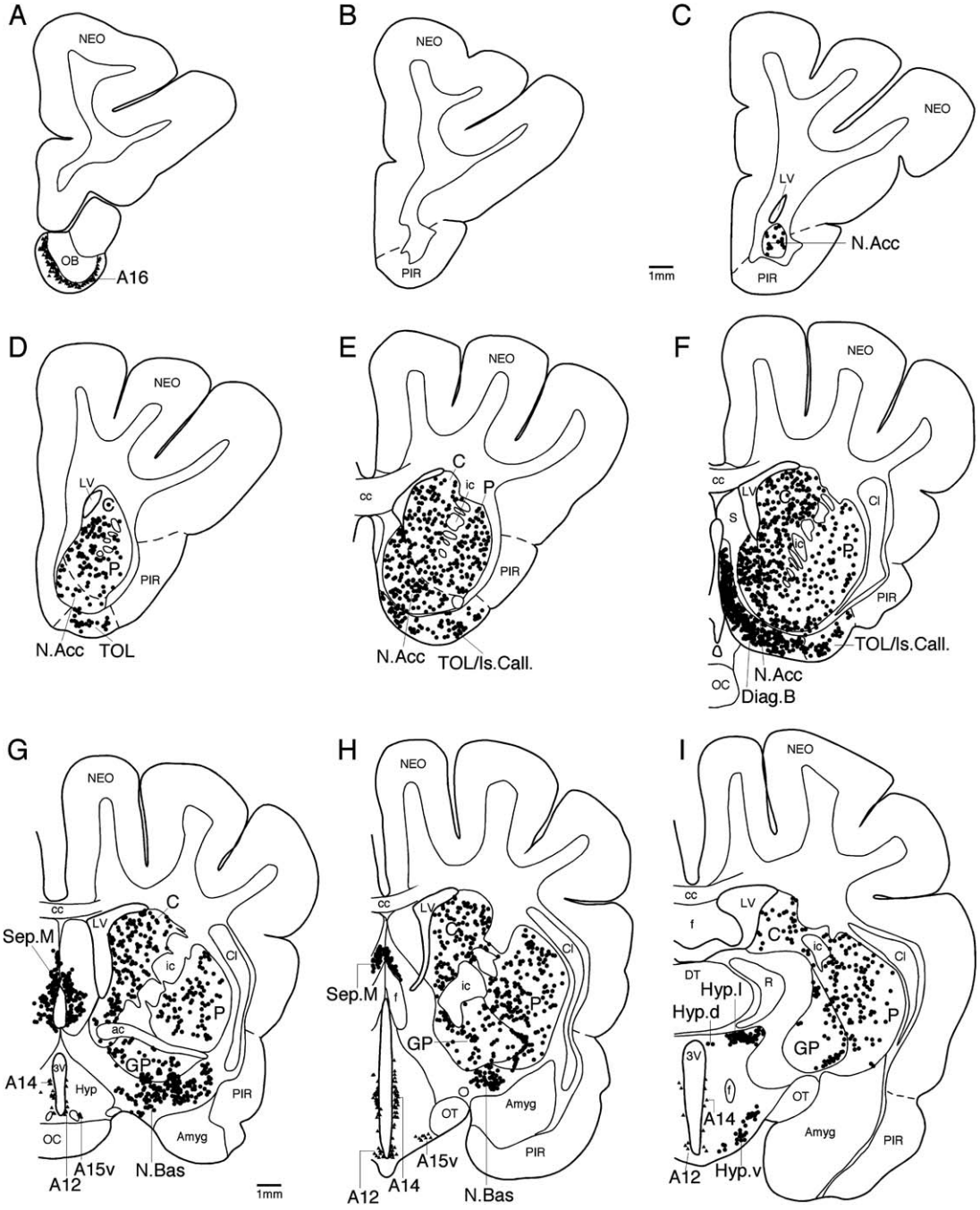


**Fig. 2.** Diagrammatic reconstructions of a series of coronal sections through the brain of the rock hyrax illustrating the location of neurons immunohistochemically reactive for cholineacetyltransferase (ChAT, black circles), tyrosine hydroxylase (TH, black triangles) and serotonin (open squares). The outlines of the architectonic regions were drawn using Nissl and myelin stains and immunoreactive neurons marked on the drawings. Drawing A represents the most rostral section, Z the most caudal. The drawings are approximately 1500 μm apart. See list for abbreviations.

readily used to demarcate this lateroventral boundary of the diagonal band.

*3.1.2.3. Nucleus basalis.* ChAT+ neurons found ventral to the globus pallidus at the level of the anterior commissure, and caudal and dorsal to the olfactory tubercle were assigned to nucleus basalis (Figs. 2G–H and 3). A low to moderate density of ChAT+ neurons was observed throughout this nucleus, and these appear to be a continuation of the ChAT+ neurons found within the globus pallidus. These ChAT+ neurons were ovoid in shape, a mixture of bipolar and multipolar types, and exhibited a rough dorsolateral to ventromedial dendritic orientation.

### 3.1.3. Diencephalic cholinergic nuclei

*3.1.3.1. Medial habenular nucleus.* The medial habenular nucleus, which forms part of the epithalamus, was located contiguous to the third ventricle in the dorsomedial region of the diencephalon (Figs. 2M and 3). The location of this nucleus was typical of what has been observed in other mammals (Woolf, 1991; Manger et al., 2002a; Maseko et al., 2007). A high density of small, round, ChAT+ neurons, was observed. We could not discern any specific dendritic orientation due to the dense packing of neurons within this nucleus. The ChAT+ axons arising from this nucleus clearly outlined the fasciculus retroflexus, which was seen to end in a large swirling termination within the interpeduncular nucleus.

*3.1.3.2. Hypothalamic cholinergic nuclei.* Three distinct ChAT+ neuronal groups (dorsal, ventral and lateral hypothalamic nuclei) were identified within the hypothalamus (Figs. 2I–L and 3). The dorsal hypothalamic nucleus was located between the wall of the third ventricle and the fornix within the dorsomedial region of the hypothalamus. A low density of palely stained, scattered ChAT+ neurons was observed within this nucleus. The ventral hypothalamic nucleus was identified as a cluster of palely stained, widely scattered ChAT+ neurons within the ventromedial aspect of the hypothalamus that extended ventrolaterally past the level of the fornix. Within the dorsolateral region of the hypothalamus, lateral to the fornix, a low density of palely stained ChAT+ neurons was identified as the lateral hypothalamic cholinergic nucleus. The neuronal morphology of the ChAT+ neurons within these hypothalamic cholinergic nuclei was similar. These neurons had an ovoid shape, were bipolar in type and showed no specific dendritic orientation.

*3.1.3.3. Cholinergic neurons in the anterodorsal and anteroventral dorsal thalamic nuclei.* Within the anterior and dorsal region of the dorsal thalamus the anterodorsal nucleus (AD) was seen to exhibit a strong cholinergic neuropil staining. Around the margins of the

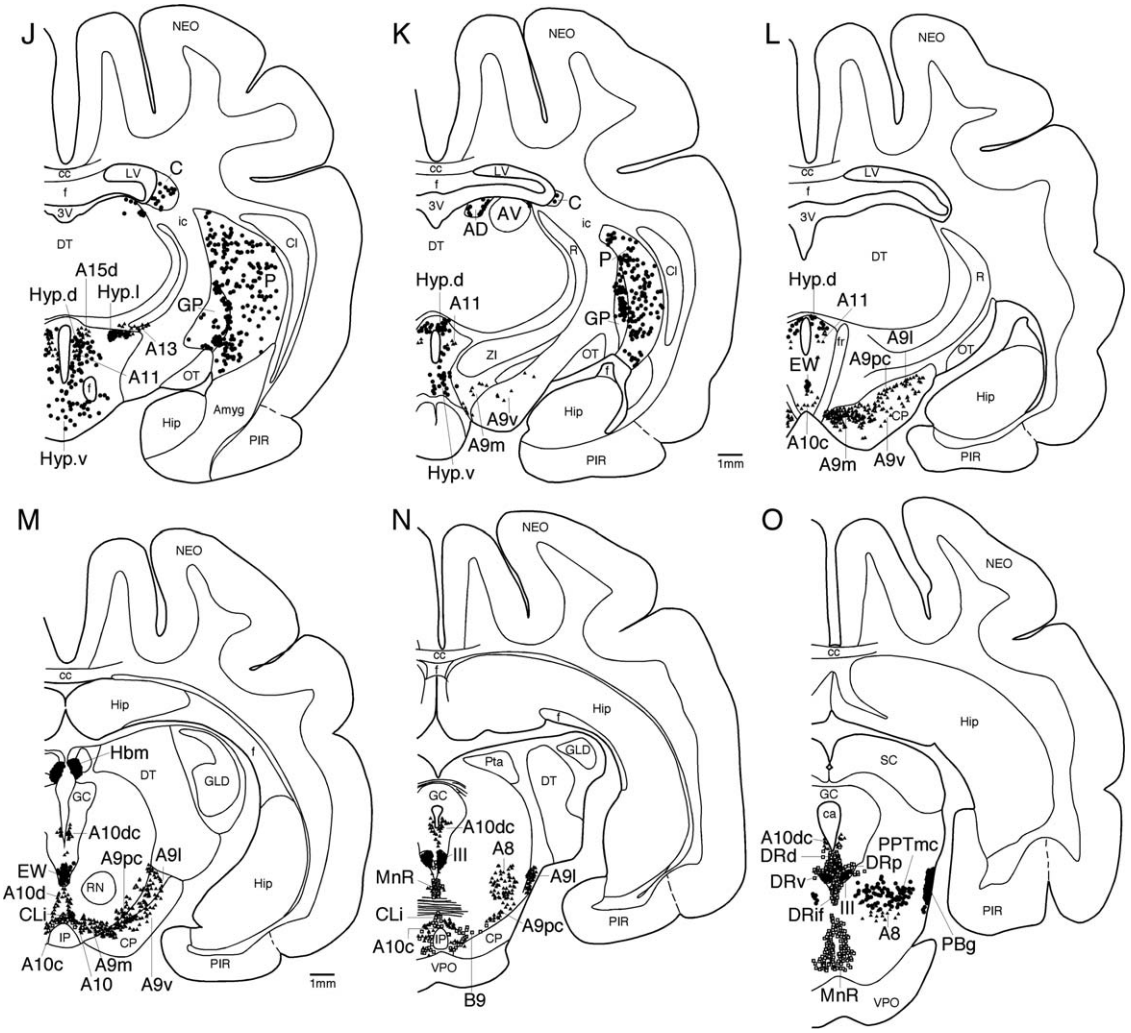


Fig. 2. (*Continued*).

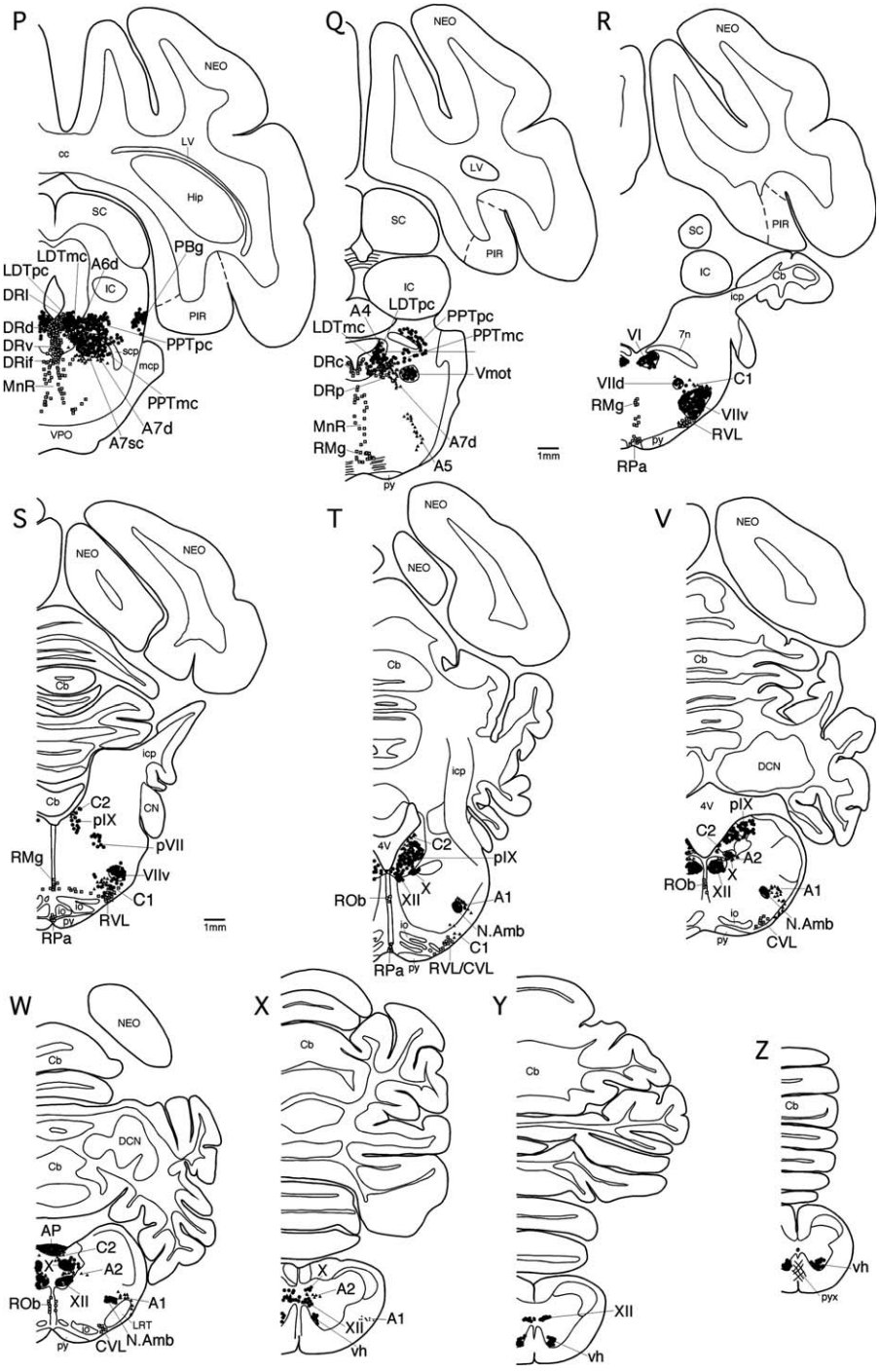


Fig. 2. (*Continued*).

AD nucleus a small number of scattered ChAT+ neurons were observed (Figs. 2K and 3). The ChAT+ neurons within this nucleus were ovoid in shape, a mixture of bipolar and multipolar types with the dendrites orientated parallel to the margins of the nucleus (Fig. 5). Lateral to the anterodorsal nucleus, the anteroventral nucleus (AV) exhibited a much paler neuropil ChAT+ neuropil staining, but it was clearly distinguishable from the surrounding unreactive tissue of the remainder of the dorsal thalamus. ChAT+ neurons showing a similar morphology to those found in the anterdorsal nucleus were observed along the upper medial and lateral borders of the anteroventral nucleus. The cholinergic nature of the neuropil and occasional scattered ChAT+ neurons within these nuclei might be a unique feature of the hyrax, as these observations have not been made in other mammals to date.

### 3.1.4. Pontomesencephalic nuclei

*3.1.4.1. Parabigeminal nucleus.* A prominent parabigeminal nucleus was located ventral and slightly anterior to the inferior colliculus within the lateral aspect of the midbrain tegmentum (Figs. 2O–P and 3). A dense cluster of strongly reactive ChAT+ neurons, smaller in size to the medially located pedunculopontine tegmental nucleus, was observed. The cell bodies were circular in shape but due to the high density of the packing it was difficult to

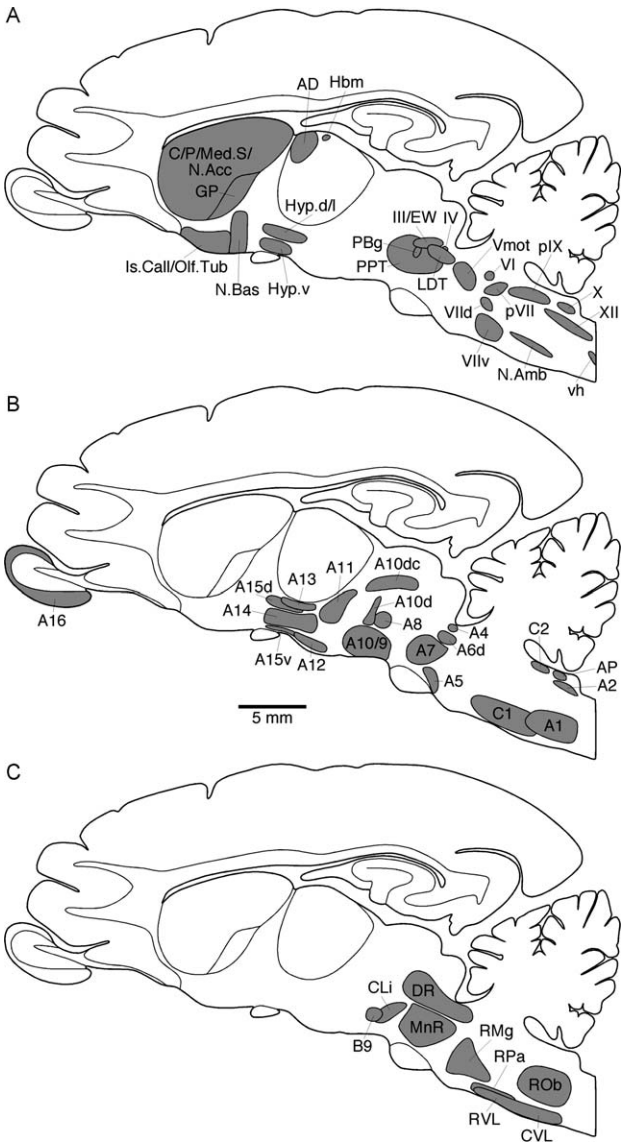


**Fig. 3.** Diagrams of idealized sagittal sections through the rock hyrax brain showing (A) cholinergic, (B) putative catecholaminergic, and (C) serotonergic nuclei or nuclear complexes. See list for abbreviations.

**Fig. 4.** Photomicrograph montage of the basal forebrain nuclei anterior to the anterior commissure, demonstrating cholineacetyletransferase (ChAT) immunoreactivity. Note the strongly ChAT+ densely packed neurons of the diagonal band of Broca (Diag.B) and the scattered strongly ChAT+ neurons in nucleus accumbens (N.Acc), caudate (C) and putamen (P). A weakly to moderately intense ChAT+ neuropil is found in these regions. Scale bar = 1 mm.

determine whether these neurons were bipolar or multipolar and if the dendrites showed any specific orientation (Fig. 6A).

*3.1.4.2. Pedunculopontine tegmental nucleus (PPT) – magnocellular and parvocellular nuclei.* In all mammals studied to date, the cholinergic neurons of the pedunculopontine tegmental nucleus display a homogenous morphology (e.g. Woolf, 1991; Manger et al., 2002a; Maseko et al., 2007; Limacher et al., 2008; Bhagwandin et al., 2008). As with most mammals within the dorsal aspect of the isthmic and pontine tegmental regions, anterior to the trigeminal motor nucleus, a group of ChAT+ neurons was identified (Figs. 2O–Q and 3). This location, and the moderate density distribution of ChAT+ neurons in this region, is again typical. In contrast to other mammals studied, the morphology of the cholinergic neurons within this region was not homogenous, and we could readily identify magnocellular and parvocellular ChAT+ nuclei within this region (Fig. 6B and D). The ChAT+ neurons assigned to the magnocellular PPT nucleus were found in the location, and evinced the distribution of the more typically described PPT. These magnocellular neurons were found medial and ventral to the superior cerebellar peduncle, and in the anterior portion were found to intermingle with the fibres of the superior cerebellar peduncle. The magnocellular ChAT+ neurons were found in a moderate density throughout this nucleus, were multipolar in type, showed no specific dendritic orientation, and evinced a variety of somal shapes. In the more caudal aspects of the PPT, in a position dorsal and lateral to the magnocellular nucleus, a moderately dense cluster of small ChAT+ neurons was observed, termed parvocellular PPT nucleus. The parvocellular PPT nucleus was sometimes clearly distinguished from the magnocellular PPT nucleus on topological grounds, as it was found lateral and dorsal to the superior cerebellar peduncle in the posterior aspect of the midbrain tegmentum; however, the size of the soma was the most reliable distinction between these two nuclei. The ovoid shaped, parvocellular ChAT+ neurons were mostly bipolar in type, but there were some multipolar neurons in this nucleus. These neurons had dendrites that were predominantly oriented in a dorsomedial to ventrolateral direction. There was no overlap in the distribution of the magnocellular and parvocellular neurons at their border.

*3.1.4.3. Laterodorsal tegmental nucleus (LDT) – magnocellular and parvocellular nuclei.* In all mammals studied to date, the cholinergic neurons of the laterodorsal tegmental nucleus display a homogenous morphology (e.g. Woolf, 1991; Manger et al., 2002a; Maseko et al., 2007; Limacher et al., 2008; Bhagwandin et al., 2008). As with most mammals within the ventrolateral region of the pontine periventricular- and periaqueductal-grey matter, a

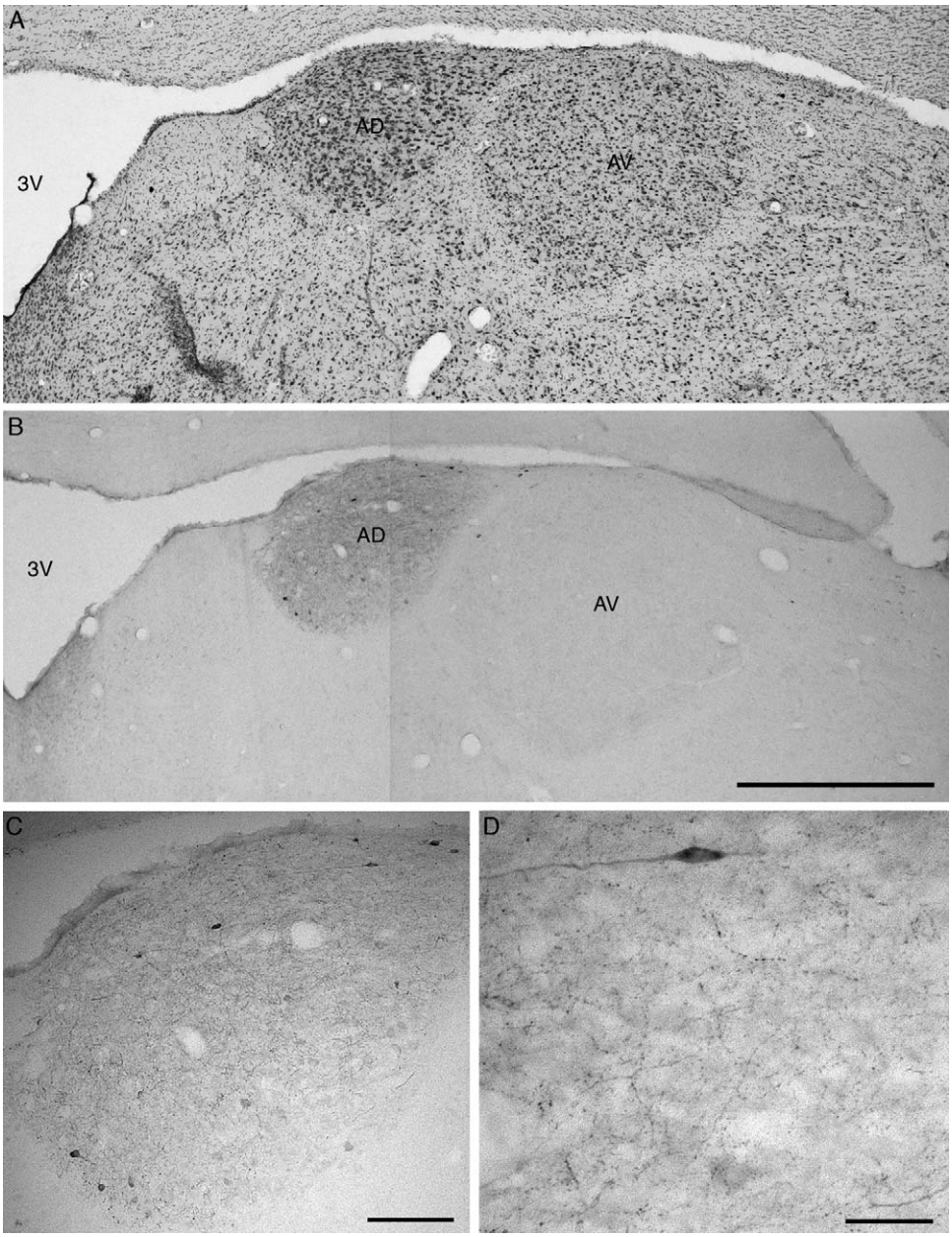


**Fig. 5.** Photomicrographs of coronal sections through the anterior nuclei of the dorsal thalamus of the rock hyrax demonstrating the location of ChAT+ neurons and neuropil in the anteroventral (AV) and anterodorsal (AD) nuclei. (A) Nissl stained section. (B) Adjacent ChAT immunoreacted section. (C) Higher power photomicrograph of AV showing location of ChAT+ neurons. (D) High power photomicrograph showing ChAT+ neuron and terminals. Scale bar in (B) = 1 mm and applies to (A and B). Scale bar in (C) = 100 μm, (D) = 50 μm. 3V – third ventricle.

moderate to high density of ChAT+ neurons was identified (Figs. 2P–Q and 3). This location and distribution of ChAT+ neurons are again typical of LDT in various mammals. In contrast to other mammals studied, the morphology of the cholinergic neurons within this region was not homogenous, and we could readily identify magnocellular and parvocellular ChAT+ nuclei within this region (Fig. 6B and C). At the ventrolateral border of the pontine periventricular- and periaqueductal-grey matter a densely packed cluster of larger neurons with similar morphology to those constituting the magnocellular PPT nucleus was found. We have termed this cluster of ChAT+ neurons the magnocellular LDT nucleus. This magnocellular LDT nucleus appears to be typical of that seen and described as the LDT in most mammals. A second cluster of ChAT+ neurons was found medial and dorsal to the magnocellular LDT nucleus, but still within the periventricular- and periaqueductal-grey matter. These neurons were significantly smaller than those in the magnocellular LDT nucleus, thus we have termed this ChAT+ neuronal cluster the parvocellular LDT nucleus. The morphology and size of these neurons were very similar to the ChAT+ neurons forming the parvocellular PPT nucleus; however, they did not display any specific dendritic orientation. These neurons were found in a moderate to high density and had soma that were ovoid to circular in shape. The lateral border of the parvocellular LDT nucleus and the medial border of the magnocellular LDT nucleus were not clearly defined as the ChAT+ neurons from both nuclei showed a region of intermingling. In this sense, while the magnocellular and parvocellular nuclei of the LDT and PPT seem to be contiguous subdivisions of these nuclei, the distinct topological parcellation of the two nuclei in the PPT was not as strongly expressed in the LDT.

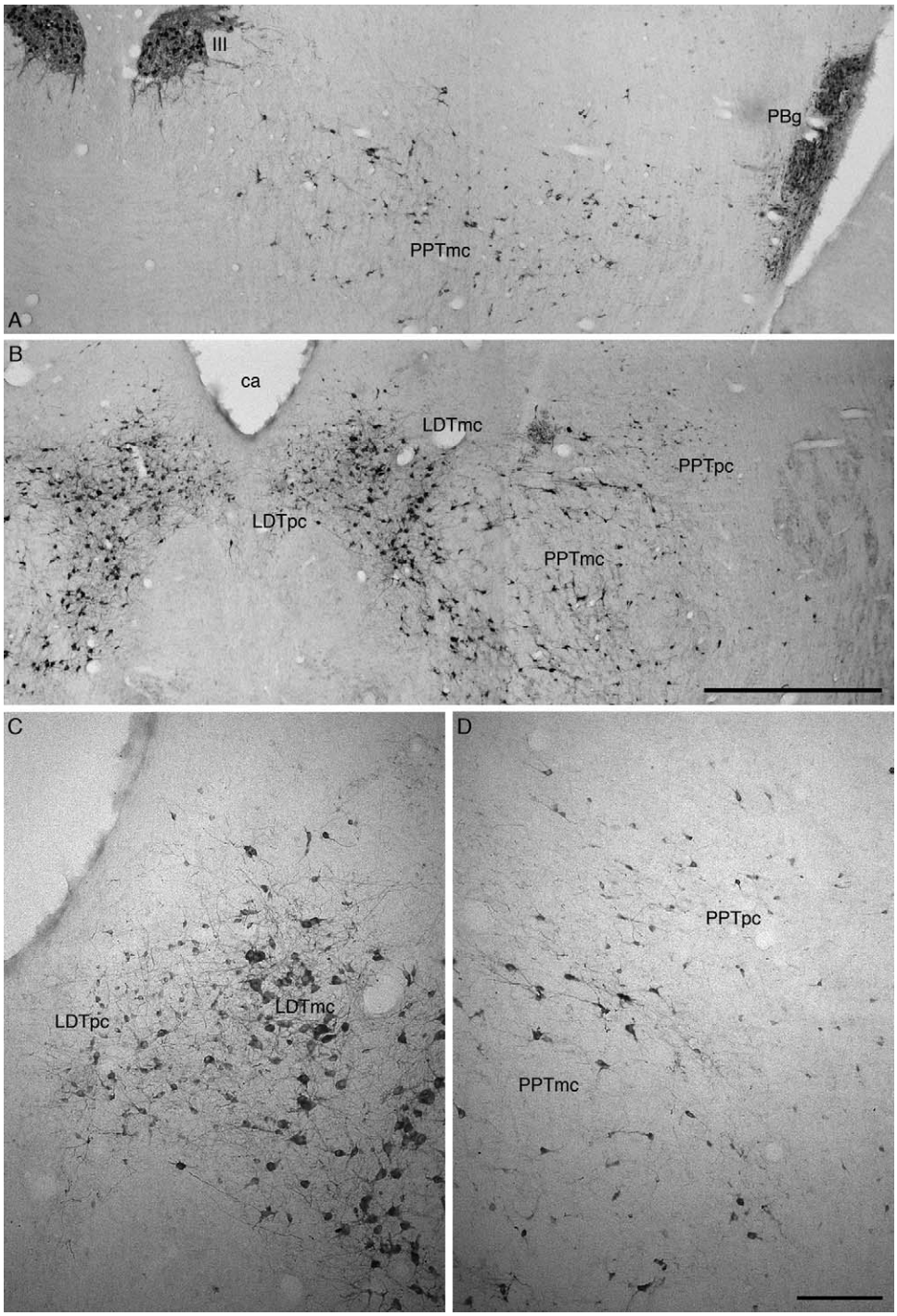


**Fig. 6.** Photomicrographs of ChAT immunoreacted sections through the dorsal isthmic/pontine region of the rock hyrax brain. (A) The magnocellular division of the pedunculopontine nucleus (PPTmc) at the level of the oculomotor nucleus (III) and the parabigeminal nucleus (PBg). (B) The magnocellular and parvocellular divisions of both the laterodorsal (LDTmc, LDTpc) and pedunculopontine (PPTmc, PPTpc) nuclei at a level slightly caudal to that shown in (A). Note the distinct clusters of small neurons (LDTpc and PPTpc) located medial to the LDTmc and dorsal to the PPTmc. The distinct clusters are shown at higher power in (C) (LDTmc and LDTpc) and (D) (PPTmc and PPTpc). Scale bar in (B) = 1 mm and applies to (A and B). Scale bar in (D) = 100 μm and applies to (C and D). ca – cerebral aqueduct.

*3.1.5. Cholinergic cranial nerve motor nuclei*

A number of large, multipolar ChAT+ neurons forming the cranial nerve motor nuclei were identified in similar regions to those previously documented for other mammals (Woolf, 1991; Manger et al., 2002a; Maseko et al., 2007; Limacher et al., 2008; Bhagwandin et al., 2008). These nuclei were: the oculomotor nucleus (III) (Fig. 6A), the trochlear nucleus (IV), the motor division of the trigeminal nucleus (Vmot), the abducens nucleus (VI), the dorsal and ventral subdivisions of the facial nucleus (VIId and VIIv), the nucleus ambiguus, the dorsal motor vagus nucleus (X), the hypoglossal nucleus (XII) and the ventral horn of the spinal cord (Figs. 2N–Z and 3). In addition to these we were able to locate ChAT+ neurons within the Edinger–Westphal nucleus and the preganglionic motor neurons of the superior salivatory nucleus of the facial nerve (pVII) and the preganglionic motor neurons of the inferior salivatory nucleus (pIX). The ChAT+ neurons of the Edinger–Westphal nucleus were moderate in number, but were strongly immunoreactive. This nucleus primarily gives rise to the

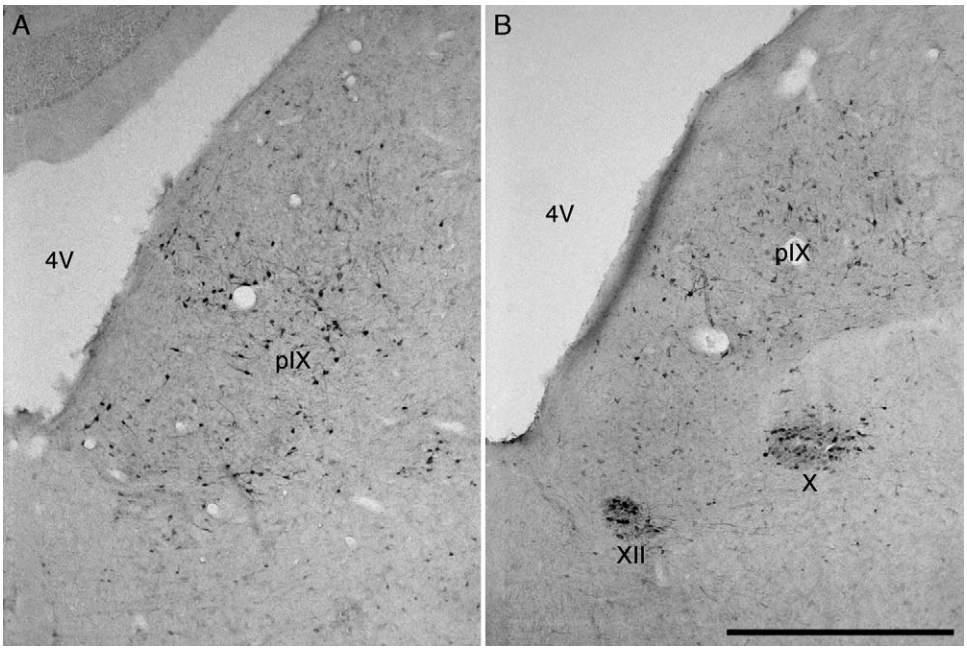


**Fig. 7.** Photomicrographs of ChAT immunoreacted sections through periventricular grey matter in the dorsal caudal medullary region of the rock hyrax brain. (A) The greatly expanded preganglionic motor neurons of the inferior salivatory nucleus (pIX) at a rostral level through this nucleus. (B) The same nucleus at a more caudal level where it lies dorsal to the dorsal motor vagus (X) and hypoglossal (XII) nuclei. The Scale bar in (B) = 1 mm, applies to (A and B). 4V – fourth ventricle.

preganglionic parasympathetic fibres to the eye, constricting the pupil, and is located within the periaqueductal grey matter directly contiguous to midline, between and anterior to the oculomotor nuclei. The neuronal bodies were ovoid in shape, bipolar and the dendrites were orientated dorsoventrally. Within the rostral medullary tegmentum, dorsal to the facial nerve nuclei, the ChAT+ neurons of pVII and pIX were identified. The neurons of the pVII nucleus were slightly smaller than those of the facial nerve nucleus and exhibited a small number of scattered multipolar neurons that demonstrated the typical motor neuron morphology, probably representing the preganglionic cholinergic cell bodies of the superior salivatory nucleus (see Mitchell and Templeton, 1981; Tóth et al., 1999). The ChAT+ neurons found medial to X probably represented the ChAT+ preganglionic neurons of the inferior salivatory nucleus (pIX) (see Rezek et al., 2008). At this level of the medulla oblongata a large number of ChAT+ nerve cell bodies of moderate density were located in the medial periventricular grey (Fig. 7). The neurons were multipolar but smaller than the motor neurons of X and XII, with no specific dendritic orientation. The extensive number of cholinergic cells in this region appears to be unusual in comparison to other mammals.

### 3.2. Putative catecholaminergic nuclei

The putative catecholaminergic nuclei, in the current study being those that possess neurons that are immunoreactive to tyrosine hydroxylase (TH+), are generally divided into several nuclear complexes that extend from the level of the olfactory bulb to the spinomedullary junction. These are generally defined as: the olfactory bulb, diencephalic, midbrain, pontine, and medullary nuclear complexes. All of the aforementioned nuclear complexes were present in the brain of the rock hyrax and the location and distribution of these were essentially similar to the typical mammalian organizational plan of this particular system previously described in a range of other species (Dahlström and Fuxe, 1964; Fuxe et al., 1969, 2007b; Smeets and González, 2000; Maseko et al., 2007; Limacher et al., 2008; Bhagwandin et al., 2008). No putative catecholaminergic nuclei falling outside these defined regions, as is the case in some other vertebrates, were identified in the hyrax (Smeets and González, 2000). The standard nomenclature of Dahlström and Fuxe (1964) and Hökfelt et al. (1984) was implemented in the description of these nuclei. The putative catecholaminergic nuclei identified in the rock hyrax are essentially similar to that seen in other mammals (Figs. 2 and 3); however, we did not identify the rodent specific rostral dorsal midline medullary (C3) nucleus (Smeets and González, 2000; Moon et al., 2007; Dwarika et al., 2008; Limacher et al., 2008; Bhagwandin et al., 2008) and the locus coeruleus compact, built of densely packed NA cell bodies (see Fuxe et al., 1970) did not exist. Furthermore, only a few single TH+ neurons were observed in the adjacent periventricular grey of the pons, termed A6 diffuse (A6d) in the current study.

#### 3.2.1. Olfactory bulb (A16)

Within and around the glomerular layer a moderate number of TH+ neurons were observed (Figs. 2A and 3). This position is typical of what has been documented in other mammals for the A16 catecholaminergic nucleus (Lichtensteiger, 1966; Lidbrink et al., 1974; Smeets and González, 2000; Manger et al., 2002b; Maseko et al., 2007; Limacher et al., 2008; Bhagwandin et al., 2008). The cells were triangular in shape and a mixture of bipolar and multipolar neurons were evident. These neurons also had a weak dendritic network surrounding the glomeruli.

#### 3.2.2. Diencephalic nuclei

In the hypothalamus six distinct putative catecholaminergic nuclei were identified. These include: the dorsal division of the anterior hypothalamic nucleus (A15d); the ventral division of the anterior hypothalamic nucleus (A15v); the rostral periventricular nucleus (A14); the zona incerta (A13); the tuberal nucleus (A12); and the caudal diencephalic nucleus (A11) (Figs. 2G–L and 3). The A15d nucleus was located between the third ventricle and the fornix within the anterior portion of the hypothalamus. The shape of the neuronal bodies was found to be ovoid, with a mixture of bipolar and multipolar types showing no specific dendritic orientation. The A15v nucleus was located near the floor of the

brain adjacent to the optic tracts within the ventrolateral region of the hypothalamus. A low density of TH+ neurons with ovoid cell bodies was observed. A mixture of bipolar and multipolar neurons with no specific dendritic orientation was evident. A moderate density of TH+ neurons close to the wall of the third ventricle throughout the hypothalamus was identified as the A14 nucleus (Fig. 8A). The neurons had ovoid shaped somas and were mostly of the bipolar type with some being multipolar. The dendrites were observed to be orientated roughly parallel to the ventricular wall. The A13 nucleus was identified as a moderate density of TH+ neurons located within the dorsal and lateral regions of the hypothalamus, lateral to the fornix, extending into and around the zona incerta in the ventral thalamus. The neurons exhibited morphological similarity to those within the A15d nucleus.

In the ventral portion of the hypothalamus, within and in close proximity to the arcuate nucleus, a low to moderate density of TH+ neurons was identified as the A12 nucleus. The neurons of this nucleus were located near the midline and surrounded the floor of the third ventricle. The cell bodies were ovoid and the neurons a mixture of the bipolar and multipolar types with dendrites orientated roughly parallel to the floor of the brain. Around the posterior pole of the third ventricle, in the most caudal part the hypothalamus, a low density of TH+ neurons arranged in columns on either side of the midline was identified as the A11 nucleus. The

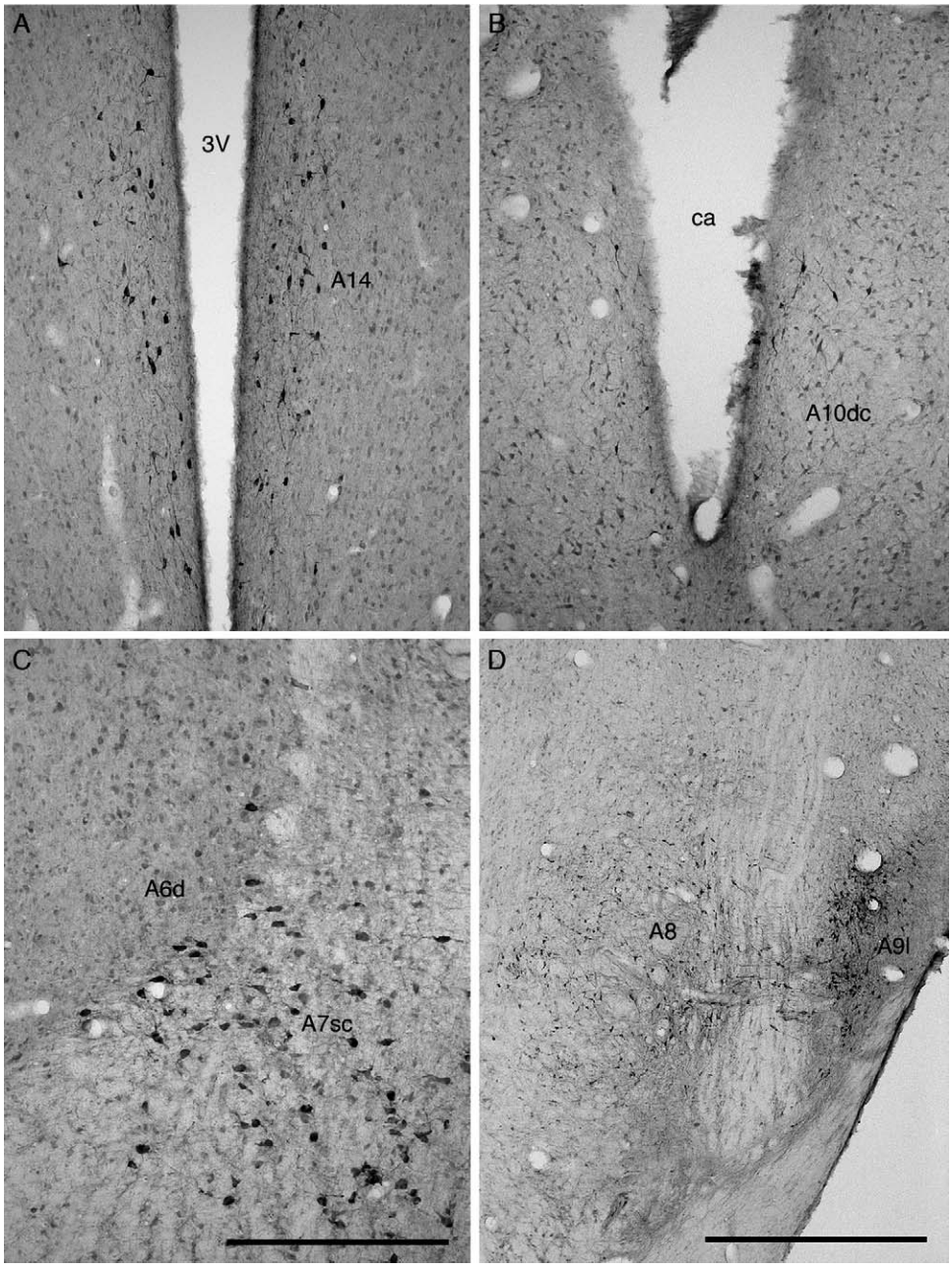


**Fig. 8.** Photomicrographs of selected neuronal groups immunohistochemically reactive for tyrosine hydroxylase within the brain of the rock hyrax. (A) The rostral periventricular nucleus (A14) located adjacent to the walls of the third ventricle (3V) in the hypothalamus. (B) The dorsal caudal nucleus of the ventral tegmental complex (A10dc) located around the ventral region of the cerebral aqueduct (ca). (C) Very few TH+ neurons are found in the diffuse portion of the locus coeruleus (A6d) within the ventrolateral periaqueductal grey matter, while the compact portion of the nucleus subcoeruleus (A7sc) in the adjacent dorsal pontine tegmentum is rich in strongly TH+ neurons. (D) The retrorubral nucleus (A8) and the lateral nucleus of the substantia nigra complex (A9l) in the lateral and ventral midbrain tegmentum. Scale bar in (C) = 500 μm and applies to (A–C). Scale bar in (D) = 1 mm.

neurons of this nucleus were large and multipolar, with ovoid to polygonal shaped somas. No specific dendritic orientation was observed for these neurons. The cell bodies of the A11 neurons were larger than those of all the other neurons of the diencephalic nuclei, with this feature serving as a ready marker for delineation of this nucleus.

### 3.2.3. Midbrain nuclei

*3.2.3.1. Ventral tegmental area nuclei (VTA, A10 complex).* The A10 nuclear complex (comprised of the following nuclei: A10 – the ventral tegmental area nucleus; A10c – ventral tegmental area, central nucleus; A10d – ventral tegmental area, dorsal nucleus; A10dc – ventral tegmental area, dorsal caudal nucleus) was located within the medial part of the midbrain tegmentum slightly anterior to the level of the oculomotor nerve nucleus (Figs. 2L–O and 3). The nuclei forming this complex originated from the dorsal and dorsolateral areas around the interpeduncular nucleus and extended dorsally to the periaqueductal grey matter, where the aqueduct component was formed caudally. The A10 nucleus was identified as a high density of TH+ neurons located between the interpeduncular nucleus and the root of the oculomotor nerve (Fig. 9). The neurons were distributed dorsally and dorsolaterally to the interpeduncular nucleus. The cell bodies were ovoid in shape and the neurons were a mixture of the bipolar and multipolar types showing no specific dendritic orientation. Immediately dorsal to the interpeduncular and A10 nuclei, a moderate to high density of TH+ neurons was identified as the A10c nucleus (Fig. 9). The neurons of this nucleus formed a characteristically roughly triangular shaped pattern in the midline. A similar neuronal morphology as the neurons of the A10 nucleus was observed for the neurons of the A10c nucleus; however the neurons of A10c were slightly smaller in size than those of A10, this size difference serving as a marker for delineating between these two adjacent nuclei. A moderate density of TH+ neurons located dorsal to and between the A10c nucleus and the periaqueductal grey matter and medial to the oculomotor nerve nucleus, were identified as A10d (Fig. 9). The cell bodies of these neurons were ovoid in shape, bipolar in type and showed a dorsoventral dendritic orientation. The A10dc nucleus was located within the periaqueductal grey matter around the lower half of the border of the cerebral aqueduct (Fig. 8B). The TH+ neurons forming the A10dc nucleus were small, ovoid in shape, multipolar and the dendrites were orientated roughly parallel to the edge of the cerebral aqueduct.

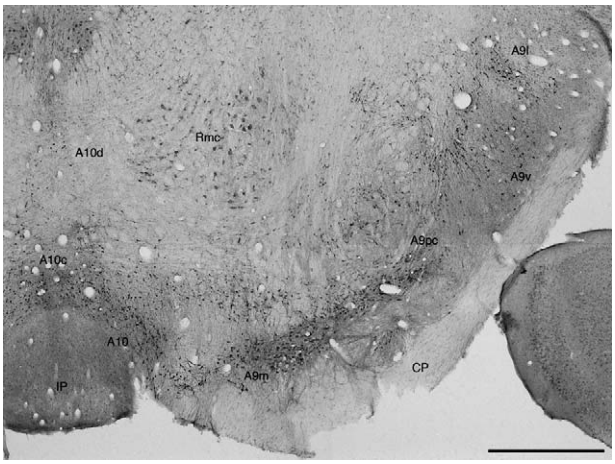


**Fig. 9.** Photomicrograph montage of the nuclear organization of the ventral tegmental area (A10, A10c, A10d) and the substantia nigra (A9m, A9pc, A9l, A9v) in the rock hyrax as revealed using tyrosine hydroxylase immunohistochemistry. Scale bar = 1 mm. IP – interpeduncular nucleus; PC – cerebral peduncle; Rmc – red nucleus, magnocellular division.

*3.2.3.2. Substantia nigra nuclear complex (A9).* In the ventrolateral region of the midbrain tegmentum, dorsal to the cerebral peduncles, four distinct nuclei comprising the substantia nigra nuclear complex were identified. These nuclei were: the substantia nigra, pars compacta nucleus (A9pc); substantia nigra, pars lateralis nucleus (A9l); substantia nigra, ventral or pars reticulata nucleus (A9v); and the substantia nigra, pars medialis nucleus (A9m) (Figs. 2K–N and 3). The A9pc nucleus was identified as a mediolaterally oriented band of TH+ neurons of a moderate to high density located dorsal to the cerebral peduncle (Fig. 9). The neurons were ovoid in shape and bipolar with a medial to lateral dendritic orientation, parallel to the direction of the band. The A9l nucleus was located within the ventrolateral region of the midbrain tegmentum, dorsolateral to the lateral border of the cerebral peduncle in a position lateral to the A9pc nucleus (Figs. 8D, 9). The somas of the TH+ neurons of this nucleus were either polygonal or triangular in shape. The neurons were multipolar and did not exhibit any specific dendritic orientation. The A9v nucleus was located in the grey matter just dorsal to the cerebral peduncle ventral to the A9pc and A9l nuclei (Fig. 9). The neurons were found in a low to moderate density in this region and showed a rough dorsoventral dendritic orientation. A high density of TH+ neurons located between the medial edge of the A9pc nucleus and the root of the oculomotor nerve was identified as the A9m nucleus (Fig. 9). The neurons of this nucleus showed a similar neuronal morphology as A9pc, with the neurons showing no specific dendritic orientation.

*3.2.3.3. Retrorubal nucleus (A8).* Within the lower half of the midbrain tegmentum a moderate number of TH+ neurons were found dorsal to the A9 complex, and ventral and caudal to the magnocellular division of the red nucleus. These neurons, which exhibited a moderate density throughout this region, were assigned to the A8 nucleus (Figs. 2N–O and 3). The TH+ neuronal bodies were ovoid in shape, bipolar and multipolar in type, and showed no specific dendritic orientation (Fig. 8D).

### 3.2.4. Pontine nuclei – the locus coeruleus (LC) nuclear complex

The locus coeruleus complex was identified as a large aggregation of TH+ neurons within the pontine region. Five nuclei within this complex were identified, being: the subcoeruleus compact nucleus (A7sc), subcoeruleus diffuse nucleus (A7d), locus coeruleus diffuse nucleus (A6d), fifth arcuate nucleus (A5), and the dorsal medial nucleus of the locus coeruleus (A4) (Figs. 2P–Q, 3). A7sc was located within the dorsal region of the pontine tegmentum adjacent to the periventricular grey matter. A high density of TH+ neurons with ovoid somas of the multipolar type represented this nucleus (Fig. 8C). The neurons of A7sc showed no specific dendritic orientation. The description of this nucleus coincides to what was previously described as the subcoeruleus (Dahlström and Fuxe, 1964). TH+ neurons ventrolateral to A7sc, anterior to the trigeminal motor nucleus, in the lateral and dorsolateral region of the pontine tegmentum were assigned to the A7d nucleus. Some of the TH+ neurons assigned to A7d were also located medial and ventral to the superior cerebellar peduncle. The TH+ neurons in this region were found in a moderate to low density, were ovoid in shape, multipolar and showed no specific dendritic orientation. A compact A6 built of TH+ neurons was absent, and only a small number of TH+ neurons were located within the ventrolateral portion of the periventricular grey matter adjacent to A7sc, and identified as A6d (Fig. 8C). The neurons of A6d had a similar morphology to A7sc and showed no specific dendritic orientation. In comparison to other mammalian species,

the rock hyrax had markedly reduced number of immunopositive neurons within A6d (Dahlström and Fuxe, 1964; Fuxe et al., 1969, 2007b; Smeets and González, 2000; Maseko et al., 2007; Limacher et al., 2008; Bhagwandin et al., 2008). The TH+ neurons assigned to the A5 nucleus was located lateral to the superior olivary nucleus, anterior to the facial nerve nucleus and ventral to the trigeminal motor nerve nucleus, in the ventrolateral region of the pontine tegmentum. The TH+ neurons of this nucleus were few in number and had a similar neuronal morphology to the neurons seen in the other locus coeruleus nuclei. The TH+ neurons assigned to the A4 nucleus were located adjacent to the wall of the fourth ventricle, medial to superior cerebellar peduncle, in the dorsolateral part of the caudal periventricular grey matter. This nucleus was represented by a small number of TH+ neurons with a similar morphology to the neurons seen in the other locus coeruleus nuclei.

#### 3.2.5. Medullary nuclei

TH+ neurons representing five putative catecholaminergic nuclei were found within in the medulla of the rock hyrax. The nuclei identified were: the rostral ventrolateral tegmental nucleus (C1), rostral dorsomedial nucleus (C2), caudal ventrolateral tegmental nucleus (A1), caudal dorsomedial nucleus (A2) and area postrema (AP) (Figs. 2R–X, 3). The rostral dorsal midline nucleus (C3), a feature so far only identified in rodents (Smeets and González, 2000; Maseko et al., 2007; Limacher et al., 2008; Bhagwandin et al., 2008) was not present. The neurons forming the C1 nucleus were located in the ventrolateral region of the anterior medulla and were distinguished as a column of TH+ neurons that extended from the level of the superior olivary nucleus to the level of nucleus ambiguus. In the course of its distribution this band of neurons was located lateral to superior olivary nucleus and facial nerve nucleus, and medial to nucleus ambiguus. The neurons of this nucleus were ovoid in shape, multipolar and exhibited a mesh-like dendritic network interspersed among the ascending and descending fasciculi of the medulla. A low density of TH+ neurons within the dorsal region of the medulla was identified as C2. This nucleus was located anterior and dorsal to the vagus motor nerve nucleus. The dorsal strip of C2 (Kalia et al., 1985a,b), which is the part of the C2 nucleus that is located near the floor of the fourth ventricle above the nucleus of the vagus motor nerve, could be identified. The continuation of the dorsal strip, which is known as the rostral subdivision of the C2 nucleus (Kalia et al., 1985a, b), was not present. The neurons of this nucleus were few in number and of low density. The somal shape was ovoid and the neurons were bipolar with dendrites orientated parallel to the floor of the fourth ventricle. The A1 nucleus was identified as a column of TH+ neurons within the ventrolateral region of the caudal medulla. The neurons of this nucleus were distributed from the level of nucleus ambiguus to the level of the spinomedullary junction. In the course of its distribution the neurons of the A1 nucleus were located lateral to nucleus ambiguus and the lateral reticular nucleus. The distinguishing factor between the partly overlapping caudal and rostral neuronal columns of the A1 and C1 (caudal part) nucleus, respectively, was their position relative to the nucleus ambiguus. The A1 column was located lateral to nucleus ambiguus while the caudal part of the C1 column was located medial to this nucleus. The neuronal morphology and dendritic organization of the A1 nucleus were similar to that of the C1 nucleus. A number of moderately sized TH+ neurons were located between, as well as around, the nuclei of the dorsal motor vagus and hypoglossal nerves and these were assigned to the A2 nucleus; however, none was found in the nucleus tractus solitarius, which is the major location for this cell group in rodents (Dahlström and Fuxe, 1964). These neurons were ovoid in shape, bipolar in type and their dendrites exhibited a medial to lateral orientation. The area postrema was identified as a high-density cluster of small TH+ neurons. This nucleus was located just anterior to the spinomedullary junction, adjacent to the floor of the fourth ventricle and dorsal to the nucleus tractus solitarius and the central canal. The neurons were ovoid shaped, bipolar in type, and showed no specific dendritic orientation.

### 3.3. Serotonergic nuclei

A number of distinct serotonergic immunoreactive (5HT+) nuclei were found throughout the brainstem of the rock hyrax. These were observed from the level of the decussation of the superior cerebellar peduncle through to the spinomedullary junction (Figs. 2M–W, 3, 10, 11). These nuclei were readily divisible into rostral and caudal nuclear clusters and the location of the nuclei within these clusters was found to be similar to what has been described for other eutherian mammals (e.g. Törk, 1990; Manger et al., 2002c; Badlangana et al., 2007; Maseko et al., 2007; Moon et al., 2007; Dwarika et al., 2008; Limacher et al., 2008; Bhagwandin et al., 2008).

#### 3.3.1. Rostral cluster

*3.3.1.1. Caudal linear nucleus (CLi).* A moderate density of 5HT+ neurons was located within the midbrain tegmentum of the rock hyrax. A cluster of these neurons was found to be in a position immediately dorsal to the interpeduncular nucleus, and anterior to the decussation of the superior cerebellar peduncle in the ventral midline of the midbrain tegmentum. This cluster was designated as the caudal linear nucleus (Figs. 2M–N, 3). At the lateral border of the interpeduncular nucleus, the 5HT+ neurons of the CLi also extended to the ventral surface of the brain and it was noted that this nucleus was the most rostrally located nucleus of all the 5HT+

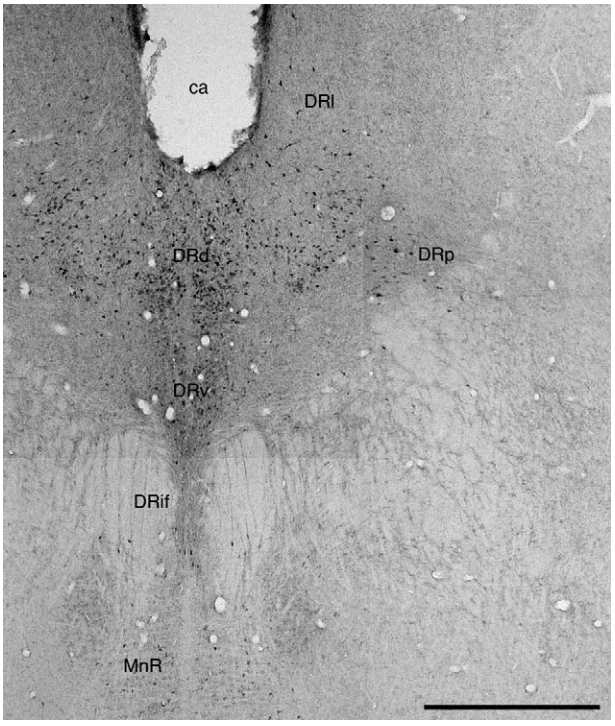


**Fig. 10.** Photomicrograph montage of the neuronal groups immunohistochemically reactive for serotonin within the dorsal raphe nuclear complex of the rock hyrax brain. Dorsal raphe lateral nucleus (DRl), dorsal raphe dorsal nucleus (DRd), dorsal raphe ventral nucleus (DRv), dorsal raphe interfascicular nucleus (DRif), dorsal raphe peripheral nucleus (DRp) and the median raphe nucleus (MnR). Scale bar = 1 mm. ca – cerebral aqueduct.

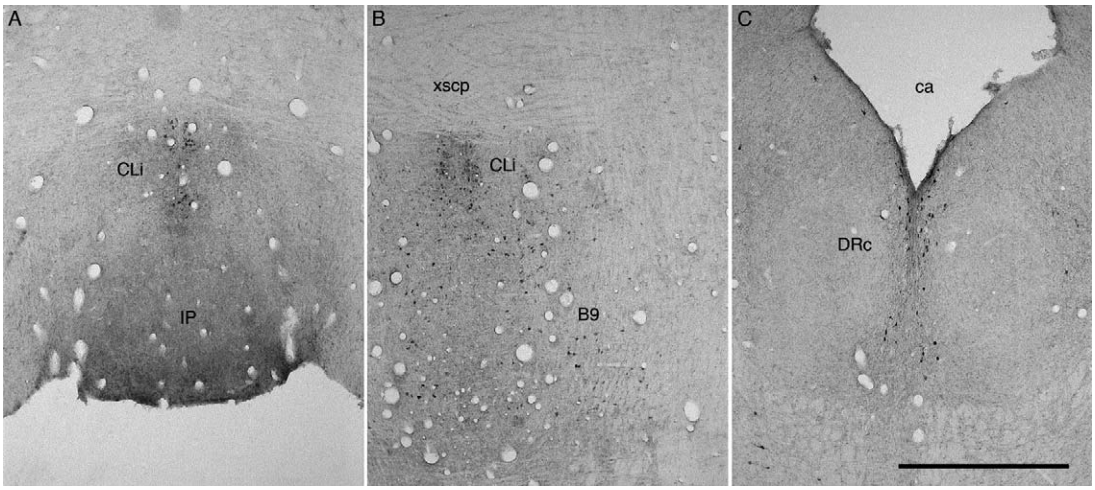


**Fig. 11.** Photomicrographs of selected neuronal groups immunohistochemically reactive for serotonin in the midbrain and brainstem of the rock hyrax. (A) The caudal linear nucleus (CLi) at its most anterior level, immediately dorsal to the interpeduncular nucleus (IP). (B) The CLi at a more posterior level, where it is located ventral to the decussation of the superior cerebellar peduncle (xscp), and where at its most ventral and lateral aspect it becomes continuous with the supralemniscal serotonergic nucleus (B9). (C) The caudal division of the dorsal raphe nucleus (DRc) lying immediately ventral to the most posterior portion of the cerebral aqueduct (ca). Scale bar in (C) = 1 mm, and applies to all.

nuclei. The neurons of this nucleus had ovoid shaped somas, were bipolar in nature, and had a rough dorsoventral dendritic orientation (Fig. 11A and B).

*3.3.1.2. Supralemniscal nucleus (B9).* The B9 nucleus was identified as a loosely packed arc of 5HT+ neurons, lateral to the interpeduncular nucleus and caudal to the A9pc nucleus (Figs. 2N and 3). This nucleus was located superior to the medial lemniscus and was found to be in continuity with the ventrolateral neurons of the CLi nucleus. The neurons had ovoid shaped somas, were bipolar in type, and the dendrites had no specific orientation (Fig. 11B).

*3.3.1.3. Median raphe (MnR).* In a pararaphe position, on either side of the midline, two clear, densely packed columns of 5HT+ neurons, extending dorsal to ventral along the midbrain and pontine tegmentum, were identified as the MnR nucleus (Figs. 2N–Q and 3). The neurons forming this nucleus extended from the caudal aspect of the superior cerebellar peduncle to the level of the anterior most aspect of the trigeminal motor nucleus. The cell bodies of the 5HT+ neurons of the MnR nucleus were ovoid, bipolar in type and the dendrites showed a rough dorsoventral orientation (Fig. 10).

*3.3.1.4. Dorsal raphe nuclear complex (DR).* Within the 5HT+ dorsal raphe nuclear complex six distinct nuclei, extending from the level of the oculomotor nerve nucleus to the level of the trigeminal motor nerve nucleus within the periaqueductal and periventricular grey matter, were identified. These nuclei were: the dorsal raphe interfascicular (DRif) nucleus, the dorsal raphe ventral (DRv) nucleus, the dorsal raphe dorsal (DRd) nucleus, the dorsal raphe lateral (DRl) nucleus, the dorsal raphe peripheral (DRp) nucleus, and the dorsal raphe caudal (DRc) nucleus (Figs 2O–Q and 3). A dense cluster of 5HT+ neurons within the most ventral medial portion of the periventricular grey matter, between the two medial longitudinal fasciculi, was identified as the DRif nucleus (Fig. 10). The neurons of this nucleus had ovoid shaped cell somas, were bipolar in type and had dendrites that were orientated roughly dorsoventrally. Immediately dorsal to the DRif nucleus and caudal to the oculomotor nerve nuclei, a high density of 5HT+ neurons was identified as the DRv nucleus (Fig. 10). These neurons were ovoid in shape and bipolar with no specific dendritic orientation. The DRd nucleus was identified as a high density of 5HT+ neurons located ventral to the inferior border of the cerebral aqueduct and immediately dorsal to the DRv nucleus (Fig. 10). The neurons of this nucleus had a similar neuronal morphology and dendritic orientation as the neurons of the DRv nucleus. A very low density of 5HT+ neurons located lateral to the DRd and DRv nuclei, anterior to the ChAT+ neurons of the LDT, in the ventrolateral portion of the periaqueductal grey matter was identified as the DRp nucleus. In the adjacent midbrain tegmentum, a small number of 5HT+ neurons forming part of the DRp nucleus were observed (Fig. 10). Of all the dorsal raphe nuclei, the tegmental neurons of the DRp nucleus were the only ones not located within the periventricular and periaqueductal grey matter. The 5HT+ neurons forming the DRp were ovoid to polygonal in shape, multipolar, and showed no specific dendritic orientation. Adjacent to the ventrolateral edge of the cerebral aqueduct, in a position dorsolateral to the DRd nucleus, a group of 5HT+ neurons was assigned to the DRl nucleus (Fig. 10). A low density of large, ovoid, multipolar neurons with no specific dendritic orientation was observed within this nucleus. This nucleus was readily distinguished from the other dorsal raphe nuclei due to the low neuronal density and the large soma of the neurons. An arc of 5HT+ neurons across the dorsal midline of the periventricular grey matter, where the cerebral aqueduct opens into the fourth ventricle, formed by the caudal coalescences of the two lateralized clusters of the DRl nucleus, was identified as the DRc nucleus (Fig. 11C). The neurons of this nucleus had a similar neuronal morphology and dendritic orientation as those of the DRl nucleus. Due to the lack of 5HT+ neurons within this region of the brain in monotremes, the DRc was classified as an independent nucleus (Manger et al., 2002c).

### 3.3.2. Caudal cluster

*3.3.2.1. Raphe magnus nucleus (RMg).* The 5HT+ neurons forming the RMg nucleus were located within the rostral medullary tegmentum, extending from the level of the anterior border of the facial nerve nucleus to the anterior border of nucleus ambiguus (Figs. 2Q–S and 3). These 5HT+ neurons were low in density and formed two weakly expressed columns on either side of the midline. The neurons of the RMg nucleus were large, multipolar and exhibited a weak dorsoventral dendritic orientation.

*3.3.2.2. Rostral and caudal ventrolateral serotonergic medullary columns (RVL and CVL).* Within the ventrolateral medullary tegmentum a column of 5HT+ neurons was identified as the RVL and CVL nuclei. This column extended from the level of the facial nerve nucleus to the spinomedullary junction and appeared to be a lateral extension of the neurons forming the RMg nucleus (Figs. 2R–W, 3). The part of the column extending from the facial nerve nucleus to the rostral border of nucleus ambiguus was identified as the RVL nucleus, while the part of the column extending from the rostral border of nucleus ambiguus to the spinomedullary junction was designated as the CVL nucleus. The columns of the RVL nucleus were found immediately dorsal to the pyramidal tracts anteriorly, and it was noted that this group of neurons bifurcated around the anterior pole of the inferior olivary nucleus, giving rise to two bilateral columns. These columns extended, in a position lateral to the inferior olivary nucleus, caudally within the ventrolateral medulla. The neurons of the RVL and CVL nuclei had a similar neuronal morphology and dendritic orientation as the neurons of the RMg nucleus and decreased in density from moderate, rostrally, to low, caudally. It was observed, as with other mammalian species studied to date, that the RVL and CVL columns were continuous (e.g. Maseko and Manger, 2007; Maseko et al., 2007; Moon et al., 2007; Dwarika et al., 2008; Bhagwandin et al., 2008); however, it is possible to make the distinction between these two nuclei, as the CVL column has not been found in the opossum or the montremes (Crutcher and Humbertson, 1978; Manger et al., 2002c).

*3.3.2.3. Raphe pallidus nucleus (RPa).* A low density and number of 5HT+ neurons located between the pyramidal tracts and at the ventral most border of the inferior olivary nucleus, within the ventral surface of the midline and medial medulla, were identified as the medial and lateral component of the RPa nucleus (Figs. 2R–T and 3). The neurons of this nucleus exhibited fusiform-shaped somas, were bipolar in type with a dorsoventral dendritic orientation parallel to the medial border of the pyramidal tracts.

*3.3.2.4. Raphe obscurus nucleus (ROb).* On either side of the midline a low density of 5HT+ neurons, extending dorsal to ventral, from the level of the nucleus ambiguus to the spinomedullary junction was identified as the ROb nucleus (Figs. 2T–W, 3). The neurons were arranged in two loosely packed columns on either side of the midline. The cell bodies of these neurons were fusiform in shape, bipolar, and had a dorsoventral dendritic orientation. Unlike in some other species studied, there were no neurons located a short distance from the central columns (e.g. Maseko and Manger, 2007; Maseko et al., 2007; Moon et al., 2007; Dwarika et al., 2008; Bhagwandin et al., 2008).

## 4. Discussion

The aim of the current study was to reveal the nuclear organization of the cholinergic, putative catecholaminergic and serotonergic systems of the rock hyrax, *P. capensis*. The results revealed that these systems, for the most part, are similar to what has previously been described in other mammals; however, certain specific differences were observed regarding the nuclear organization of the cholinergic and putative catecholaminergic systems. The nuclear organization of the serotonergic system was similar to what has been documented for other eutherian mammals (e.g. Törk, 1990; Maseko et al., 2007; Moon et al., 2007; Dwarika et al., 2008; Limacher et al., 2008; Bhagwandin et al., 2008). The differences that were noted for the cholinergic system included the existence of cholinergic immunoreactive neurons in the anterior dorsal and ventral nuclei of the dorsal thalamus, the presence of parvocellular and magnocellular divisions/nuclei of both the LDT and PPT, and the presence of a large cholinergic cell group in the periventricular grey of the rostral medulla (pIX). The features of the putative catecholaminergic system that differed significantly from that seen in other mammals were the absence of a dense cluster of TH+ neurons constructing the locus coeruleus compact (A6c) and a diffuse locus coeruleus (A6d) with only few TH+ neurons. We discuss each of these unusual features in turn, and then compare the overall organization of these systems in the hyrax to prior observations of these systems across various mammalian species.

### *4.1. Cholinergic neurons in the anterodorsal (AD) and anteroventral (AV) nuclei of the dorsal thalamus of the rock hyrax*

The AD and AV nuclei identified in the brain of the rock hyrax form part of the anterior nuclei of the dorsal thalamus and are a general feature of the mammalian dorsal thalamus (Jones, 2007). The anterior nuclear group typically consists of four distinct nuclei, the anterodorsal (AD), anteromedial (AM), anteroventral (AV), and lateral dorsal (LD) nuclei (Jones, 2007). In the rock hyrax the AD nucleus was located within the anterior and dorsal regions of the dorsal thalamus, as is typical of mammals, and exhibited a strong cholinergic neuropil staining along with ChAT immunoreactive neurons scattered around the margins of the nucleus. Lateral to the AD nucleus in the rock hyrax, a second nucleus exhibiting a weaker cholinergic neuropil staining with ChAT immunoreactive neurons along the upper medial and lateral borders was identified as the AV nucleus. While both the AD and AV nuclei are known for their strong histochemical reactivity to acetylcholinesterase, choline acetyltransferase immunoreactive neurons have not been reported in either of these nuclei in any other mammal (Jones, 2007; Maseko et al., 2007).

Afferent input to these nuclei originates largely from the hypothalamus and hippocampal formation, but also includes corticothalamic and thalamocortical connections (Jones, 2007). The AD and AV nuclei have been reported to be involved in spatial learning and memory, and navigation; however, these nuclei are not the sole contributors, but rather work in conjunction with the other anterior thalamic nuclei to achieve these functions (Segal et al., 1988; van Groen et al., 2002; Oda et al., 2003; Wolff et al., 2008). It is difficult to hypothesize on the potential effect of the presence of cholinergic neurons within and closely surrounding these nuclei in regards to function; but given that the cholinergic system in general appears to be related to activity requiring both alertness and awareness, these neurons may have the effect of enhancing the wakefulness promoting functions of the anterior thalamic nuclei in the hyrax, possibly leading also to enhanced learning and memory functions.

Presently, it appears that these anterior thalamic cholinergic neurons are unique to the rock hyrax as they have not been observed in other mammals. Despite this, we can only tentatively conclude that they are a unique feature as no other members of the Afroplacentalia have been examined for the presence of these neurons. Thus, these anterior thalamic cholinergic neurons may be unique to the hyrax, or may be found in other members of the Afroplacentalia, especially the closely related Proboscideans and Sirenians. Until further Afroplacentalia species have been examined the uniqueness of this aspect of the cholinergic system remains uncertain.

### *4.2. Magnocellular and parvocellular divisions/nuclei of the pedunculopontine and laterodorsal tegmental nuclei in the rock hyrax*

Within all mammals studied to date, cholinergic neurons within the pontine tegmentum (PPT) and periventricular grey matter (LDT) have been reported (e.g. Maseko et al., 2007). In all

these prior studies the morphology of the cholinergic neurons within and between the PPT and LDT nuclei has been reported to be homogeneous (e.g. Woolf, 1991; Manger et al., 2002a; Maseko and Manger, 2007; Maseko et al., 2007; Limacher et al., 2008; Bhagwandin et al., 2008). The situation observed in the current study in the rock hyrax raises a significant difference in this regard, as the cholinergic neurons within these nuclei did not exhibit a homogenous morphology. Rather, we identified two neuronal types within each of these nuclei, and the inner spatial distribution and segregation of these two neuronal types have led to the proposal of the subdivision of these nuclei into parvocellular and magnocellular PPT and LDT nuclei. The magnocellular subdivision of both the PPT and LDT nuclei exhibited a neuronal morphology reminiscent of that described for all other mammals (Woolf, 1991; Manger et al., 2002a; Maseko et al., 2007; Limacher et al., 2008; Bhagwandin et al., 2008). For this reason, plus the topography of the neurons forming these magnocellular divisions (LDTmc being in the ventrolateral portion of the grey matter and PPTmc lying in the adjacent tegmentum), we propose that the magnocellular divisions of these nuclei in the rock hyrax are homologous to the LDT and PPT nuclei described for all other mammals.

The parvocellular cholinergic subdivisions, on the other hand, have not been reported in any other mammal studied to date, although a non-cholinergic parvocellular component has at times been included as part of the PPT in rat and cat (Semba and Fibiger, 1989). The morphology of the neurons ascribed to the parvocellular divisions, being small, and bipolar with oval soma, is reminiscent of cholinergic interneurons found in the cerebral cortex (Bhagwandin et al., 2006) or superior colliculus (Tan and Harvey, 1989) in some other mammals. These putative cholinergic interneurons were found medial to the LDTmc, and dorsal to the PPTmc. It is possible that these cholinergic interneurons are also immunoreactive for GABA, forming part of the pontine GABAergic system. A similar situation has been observed in the cortical cholinergic neurons found in certain species of mammals (Bhagwandin et al., 2006). Potentially, a change at the molecular level of organization occurred within these neurons, such as molecular interactions, adding multiple transmission lines and thus increased functionality to this neuronal group (Agnati et al., 1986). These potentially GABAergic neurons may have acquired ChAT proteins resulting in their immunoreactivity.

The above described potential molecular change and increased transmission lines in these cholinergic interneuron groups in close apposition to the traditional cholinergic LDT and PPT could lead to interesting functional outcomes. It is well known that GABAergic neurons within the pons play a major role in the regulation of the traditional cholinergic LDT and PPT with regard to the sleep-wake cycle especially REM sleep (Maloney et al., 1999, 2000; Boissard et al., 2003; Pal and Mallick, 2006; Luppi et al., 2007). The location of the cholinergic, potentially GABAergic neurons described as the PPTpc and LDTpc in the current study makes them prime candidates forming part of a local GABAergic network involved in the switching of states during the sleep-wake cycle (Luppi et al., 2007). The added transmission line related to the production of acetylcholine in the hyrax may produce some unusual effects on the measurable physiological parameters of sleep, especially REM sleep in the hyrax.

Again it appears that these parvocellular cholinergic LDT and PPT may be unique to the rock hyrax as they have not been observed in other mammals (e.g. Maseko et al., 2007); however, as with the other currently unique aspects of the cholinergic system in the hyrax we can only tentatively conclude that they are unique features until other members of the Afrotheria have been examined for the presence of these nuclei.

### 4.3. Increased numbers of preganglionic cholinergic neurons in the inferior salivatory nucleus (pIX) of the rock hyrax

Cholinergic neurons within the preganglionic inferior salivatory nucleus have been identified in many mammalian species including rodents, carnivores, megachiropterans and primates, yet these are absent from the brains of other mammals studied (Maseko et al., 2007). Cholinergic neurons were identified in this nucleus in the rock hyrax; however, it appears from a qualitative comparison that the numbers of cholinergic neurons in this nucleus in the rock hyrax are far greater than that seen in the other mammals in which these neurons have been found. This qualitative impression, while impressive, needs quantitative support. The possible projections and function of this enlarged periventricular cholinergic cell group of the medulla are unknown and comparisons across other species belonging to the Afrotheria are needed to determine whether this feature of the cholinergic system of the hyrax is a feature of the Afrotherians in general.

### 4.4. Lack of TH+ neurons in compact locus coeruleus (A6c) and decreased numbers of TH+ neurons in the locus coeruleus proper (A6d) of the rock hyrax

The diffuse division of the locus coeruleus (A6d), or the locus coeruleus proper (Dahlström and Fuxe, 1964), has been reported in all mammals studied to date, while the compact portion has only been reported in rabbits, tree shrew, megabats and primates (e.g. Maseko et al., 2007). While the A6c is lacking in the rock hyrax, the A6d nucleus is present but was particularly low in the number of TH immunoreactive neurons. This is a qualitative impression, and further work comparing the number of neurons in this nucleus across mammals and determining what kind of relationship may exist between neuronal number and brain mass (perhaps allometric) is required to confirm this impression; however, the qualitative impression is so dramatic as to warrant specific discussion. One interesting point to be noted is that even though the A6d nucleus showed an apparent reduction in the number of TH+ neurons, the other nuclei of the locus coeruleus complex (A7sc, A7d, A5 and A4) do not appear to be relatively more cell rich in comparison to other mammals (again a qualitative impression needing quantitative support).

This potential reduction in the number of neurons within the locus coeruleus may lead to a reduction in the amount of noradrenaline released in the specific target regions of the A6d in the hyrax. It should be noted that A6d in the rat and other mammals projects to all cortical regions of the brain, including the cerebellar cortex, as well as to the thalamus, the lower brainstem reticular formation and the dorsal and ventral horns of the spinal cord (see Fuxe et al., 1970). The neurons of the locus coeruleus represent a tonic arousal system important for vigilance and attention (see Fuxe et al., 2007a,b). The relative absence of the catecholamine component of the locus coeruleus proper (A6d) in the hyrax is a highly interesting observation. Has the subcoeruleus (A7sc and A7d) taken over the role of the locus coeruleus (A6d) in the hyrax or does the hyrax show a lack of tonic arousal? These are major questions to be answered in future work. The reduced number of neurons found within the A6d in the hyrax may be a feature unique to this species. Further work on other members of the Afrotheria will determine whether this is indeed a species-specific feature or a feature of a broader taxonomic grouping.

### 4.5. Evolutionary and phylogenetic considerations

The current study extends the database that may be used for comparison across mammalian species to determine both phylogenetic and evolutionary trends of the cholinergic, putative

catecholaminergic and serotonergic systems. Of these systems the serotonergic system appears to be the most conservative in terms of changes in the nuclear organization associated with different lineages. The rock hyrax, along with all other eutherian mammals studied to date and the metatherian wallaby appear to have the same nuclear organization (Maseko et al., 2007). The metatherian opossum (Crutcher and Humbertson, 1978) and the proTótherian monotremes (Manger et al., 2002c) have only small comparative differences in the nuclear organization of the serotonergic system. The putative catecholaminergic system of the hyrax has a nuclear organization almost identical to that seen in rodents (except for the lack of a C3 nucleus, Dahlström and Fuxe, 1964; Smeets and González, 2000) and megabats and primates (except for the lack of a compact division of the locus coeruleus, A6c, Maseko et al., 2007). This nuclear organization aligns the hyrax phylogenetically most closely with the rodents and primates studied to date. The cholinergic system, for the most part, shares a similar plan of organization as that described for the rodents, megabats and primates (Maseko et al., 2007). Despite this, the hyrax does evince a degree of nuclear organizational uniqueness compared with other mammalian species through the possession of cholinergic neurons in the anterior nuclei of the dorsal thalamus and the parvocellular LDT and PPT nuclei of the pontine region. In the broader sense, the organization of these systems in the hyrax appears most similar to those seen in the rodents, rabbit, tree shrew, megabats and primates (Maseko et al., 2007). In this sense, the nuclear organizations of the neural systems studied reflect current concepts of the phylogenetic interrelationships of mammalian lineages (Arnason et al., 2008).

The overall unique complement of nuclei of the three systems studied supports the proposal of Manger (2005) that indicates each order will possess a unique nuclear complement of these systems. The current study supports the concept of placing the hyraxes into the phylogenetic grouping of an order to the exclusion of other mammals. It would be of interest to examine the cholinergic, catecholaminergic and serotonergic systems of other species of hyraxes to determine whether or not the "unique" features described in the brain of the rock hyrax are shared by all members of the Hyracoidea. It will also be of interest to examine other members of the Afrotheria and members of the Xenarthra to determine if these "unique" features are limited to this order (Hyrocoidea), cohort (Afroplacentalia), or are part of a broader phylogenetic grouping (such as the Notoplacentalia) (Arnason et al., 2008). The current study sets out to test several potential predictions. The first prediction, that the hyrax will have many nuclei in common with other mammalian species, is supported. The second prediction, that the hyrax will have some unique features, is currently, tentatively supported. The strength of this second prediction and the third prediction can be tested by examining further species of the Afrotherian supercohort. The fourth prediction, that the hyrax may lack nuclei found in other species, is supported due to the lack of two catecholaminergic nuclei found either exclusively in rodents (C3), or seen in rabbits, tree shrews, megabats and primates (A6d). The current study then supports the usefulness of using these systems as indicators of phylogenetic relationships and supports current concepts regarding the evolution of these neural systems (Manger, 2005).

## Acknowledgments

This work was supported by funding from the South African National Research Foundation (PRM) and SIDA (KF). The authors wish to extend their gratitude to the members of the Central Animal Services of the University of the Witwatersrand for their enthusiastic and expert assistance with animal handling and care during this project.

## References

Agnati, L.F., Fuxe, K., Zoli, M., Pich, E.M., Benfenati, F., Zini, I., Goldstein, M., 1986. Aspects on the information handling by the central nervous system: focus on cotransmission in the aged rat brain. Prog. Brain Res. 68, 291–301.

Andén, N.E., Carlsson, A., Dahlström, A., Fuxe, K., Hillarp, N.Å., Larsson, K., 1964. Demonstration and mapping out of nigro-neostriatal dopamine neurons. Life Sci. 15, 523–530.

Arnason, U., Adegoke, J., Gullberg, A., Harley, E.H., Janke, A., Kullberg, M., 2008. Mitogenomic relationships of placental mammals and molecular estimates of their divergences. Gene 421, 37–51.

Badlangana, N.L., Bhagwandin, A., Fuxe, K., Manger, P.R., 2007. Distribution and morphology of putative catecholaminergic and serotonergic neurons in the medulla oblongata of a sub-adult giraffe, *Giraffa camelopardalis*. J. Chem. Neuroanat. 34, 69–79.

Bartus, R.T., Dean, R.L., Beer, B., 1982. Neuropeptide effect on memory in aged monkeys. Neurobiol. Aging 3, 61–68.

Bhagwandin, A., Fuxe, K., Manger, P.R., 2006. Choline acetyltransferase immunoreactive cortical interneurons do not occur in all rodents: a study of the phylogenetic occurrence of this neural characteristic. J. Chem. Neuroanat. 32, 208–216.

Bhagwandin, A., Fuxe, K., Bennett, N.C., Manger, P.R., 2008. Nuclear organization and morphology of cholinergic, putative catecholaminergic and serotonergic neurons in the brains of two species of African mole-rat. J. Chem. Neuroanat. 35, 371–387.

Bjarkam, C.R., Sorensen, J.C., Geneser, F.A., 1997. Distribution and morphology of serotonin-immunoreactive neurons in the brainstem of the New Zealand white rabbit. J. Comp. Neurol. 380, 507–519.

Boissard, R., Fort, P., Gervasoni, D., Barbagli, B., Luppi, P.H., 2003. Localization of the GABAergic and non-GABAergic neurons projecting to the sublaterodorsal nucleus and potentially gating paradoxical sleep onset. Eur. J. Neurosci. 18, 1627–1639.

Crutcher, K.A., Humbertson, A.O., 1978. The organization of monoamine neurons within the brainstem of the North American opossum (*Didelphis virginiana*). J. Comp. Neurol. 179, 195–222.

Dahlström, A., Fuxe, K., 1964. Evidence for the existence of monoamine-containing neurons in the central nervous system. I. Demonstration of monoamine in the cell bodies of brainstem neurons. Acta Physiol. Scand. 62, 1–52.

Diksic, M., Young, S.N., 2001. Study of the brain serotonergic system with labelled alpha-methyl-L-tryptophan. J. Neurochem. 78, 1185–1200.

Dwarika, S., Maseko, B.C., Ihunwo, A.O., Fuxe, K., Manger, P.R., 2008. Distribution and morphology of putative catecholaminergic and serotonergic neurons in the brain of the greater canerat, *Thryonomys swinderianus*. J. Chem. Neuroanat. 35, 108–122.

Fuxe, K., Hökfelt, T., Ungerstedt, U., 1969. Distribution of monoamines in the mammalian central nervous system by histochemical studies. In: Hooper, G. (Ed.), Metabolism of Amines in the Brain. Macmillan, London, pp. 10–22.

Fuxe, K., Hökfelt, T., Ungerstedt, U., 1970. Morphological and functional aspects of central monoamine neurons. Int. Rev. Neurobiol. 13, 93–126.

Fuxe, K., Manger, P., Genedani, S., Agnati, L., 2006. The nigrostriatal DA pathway and Parkinson's disease. J. Neural. Transm. Suppl. 70, 71–83.

Fuxe, K., Marcellino, D., Genedani, S., Agnati, L., 2007a. Adenosine A(2A) receptors, dopamine D(2) receptors and their interactions in Parkinson's disease. Mov. Disord. 22, 1990–2017.

Fuxe, K., Dahlström, A., Höistad, M., Marcellino, D., Jansson, A., Rivera, A., Diaz-Cabiale, Z., Jacobsen, K., Tinner-Staines, B., Hagman, B., Leo, G., Staines, W., Guidolin, D., Kehr, J., Genedani, S., Belluardo, N., Agnati, L.F., 2007b. From the Golgi–Cajal mapping to the transmitter-based characterization of the neuronal networks leading to two modes of brain communication: wiring and volume transmission. Brain Res. Rev. 55, 17–54.

Gallyas, F., 1979. Silver staining of myelin by means of physical development. Neurolog. Res. 1, 203–209.

Hökfelt, T., Johansson, O., Fuxe, K., Goldstein, M., Park, D., 1976. Immunohistochemical studies on the localization and distribution of monoamine neuron systems in the rat brain. I. Tyrosine hydroxylase in the mes- and diencephalon. Med. Biol. 54, 427–453.

Hökfelt, T., Martenson, R., Björklund, A., Kleinau, S., Goldstein, M., 1984. Distributional maps of tyrosine-hydroxylase-immunoreactive neurons in the rat brain. In: Björklund, A., Hökfelt, T. (Eds.), Handbook of Chemical Neuroanatomy, Vol. 2. Classical Neurotransmitters in the CNS, Part 1. Elsevier, Amsterdam, pp. 277–379.

Jacobs, B.L., Azmitia, E.C., 1992. Structure and function of the brain serotonin system. Physiol. Rev. 72, 165–229.

Jones, E.G., 2007. 2nd ed. The Thalamus, 2nd ed., Cambridge University Press, Cambridge, UK.

Kalia, M., Fuxe, K., Goldstein, M., 1985a. Rat medulla oblongata. II. Noradrenergic neurons, nerve fibers and preterminal processes. J. Comp. Neurol. 233, 308–332.

Kalia, M., Fuxe, K., Goldstein, M., 1985b. Rat medulla oblongata. III. Adrenergic (C1 and C2) neurons, nerve fibers and presumptive terminal processes. J. Comp. Neurol. 233, 333–349.

Kitahama, K., Geffard, M., Okamura, H., Nagatsu, I., Mons, N., Jouvet, M., 1990. Dopamine- and dopa-immunoreactive neurons in the cat forebrain with reference to tyrosine hydroxylase-immunohistochemistry. Brain Res. 518, 83–94.

Kitahama, K., Sakamoto, N., Jouvet, A., Nagatsu, I., Pearson, J., 1996. Dopamine-beta-hydroxylase and tyrosine hydroxylase immunoreactive neurons in the human brainstem. J. Chem. Neuroanat. 10, 137–146.

Klein, R.G., Cruz-Uribe, K., 1996. Size variation in the rock hyrax (*Procavia capensis*) and late quarternary climatic change in South Africa. Quat. Res. 46, 193–207.
Lichtensteiger, W., 1966. Uptake of norepinepherine in periglomerular cells of the olfactory bulb of the mouse. Nature 210, 955–956.
Lidbrink, P., Jonsson, G., Fuxe, K., 1974. Selective reserpine-resistant accumulation of catecholamines in central dopamine neurones after dopa administration. Brain Res. 67, 439–456.
Limacher, A.M., Bhagwandin, A., Fuxe, K., Manger, P.R., 2008. Nuclear organization and morphology of cholinergic, putative catecholaminergic and serotonergic neurons in the brain of the Cape porcupine (*Hystrix afric*aeaustralis): increased brain size does not lead to increased organizational complexity. J. Chem. Neuroanat. 36, 33–52.
Luppi, P.H., Gervasoni, D., Verret, L., Goutagny, R., Peyron, C., Salvert, D., Leger, L., Fort, P., 2007. Paradoxical (REM) sleep genesis: the switch from an aminergic-cholinergic to a GABAergic-glutamatergic hypothesis. J. Physiol. (Paris) 100, 271–283.
Maloney, K.J., Mainville, L., Jones, B.E., 1999. Differential c-Fos expression in cholinergic, monoaminergic, and GABAergic cell groups of the pontomesencephalic tegmentum after paradoxical sleep deprivation and recovery. J. Neurosci. 19, 3057–3072.
Maloney, K.J., Mainville, L., Jones, B.E., 2000. c-Fos expression in GABAergic, serotonergic, and other neurons of the pontomedullary reticular formation and raphe after paradoxical sleep deprivation and recovery. J. Neurosci. 20, 4669–4679.
Manger, P.R., 2005. Establishing order at the systems level in mammalian brain evolution. Brain Res. Bull. 66, 282–289.
Manger, P.R., Fahringer, H.M., Pettigrew, J.D., Siegel, J.M., 2002a. Distribution and morphology of cholinergic neurons in the brain of the monotremes as revealed by ChAT immunohistochemistry. Brain Behav. Evol. 60, 275–297.
Manger, P.R., Fahringer, H.M., Pettigrew, J.D., Siegel, J.M., 2002b. Distribution and morphology of catecholaminergic neurons in the brain of monotremes as revealed by tyrosine hydroxylase immunohistochemistry. Brain Behav. Evol. 60, 298–314.
Manger, P.R., Fahringer, H.M., Pettigrew, J.D., Siegel, J.M., 2002c. Distribution and morphology of serotonergic neurons in the brain of the monotremes. Brain Behav. Evol. 60, 315–332.
Maseko, B.C., Manger, P.R., 2007. Distribution and morphology of cholinergic, catecholaminergic and serotonergic neurons in the brain of Schreiber's long-fingered bat, *Miniopterus schreibersii*. J. Chem. Neuroanat. 34, 80–94.
Maseko, B.C., Bourne, J.A., Manger, P.R., 2007. Distribution and morphology of cholinergic, putative catecholaminergic and serotonergic neurons in the brain of the Egyptian Rousette flying fox, *Rousettus aegyptiacus*. J. Chem. Neuroanat. 34, 108–127.
Meister, B., Hökfelt, T., Steinbusch, H.W., Skagerberg, G., Lindvall, O., Geffard, M., Joh, T.H., Cuello, A.C., Goldstein, M., 1988. Do tyrosine hydroxylase-immunoreactive neurons in the ventrolateral arcuate nucleus produce dopamine or only L-dopa? J. Chem. Neuroanat. 1, 59–64.
Mitchell, J., Templeton, D., 1981. The origin of the preganglionic parasympathetic fibers to the mandibular and sublingual salivary glands in the rat: a horseradish peroxidase study. J. Anat. 132, 513–518.
Moon, D.J., Maseko, B.C., Ihunwo, A., Fuxe, K., Manger, P.R., 2007. Distribution and morphology of catecholaminergic and serotonergic neurons in the brain of the highveld gerbil, *Tatera brantsii*. J. Chem. Neuroanat. 34, 134–144.
Oda, S., Kuroda, M., Kakuta, S., Tanihata, S., Ishikawa, Y., Kishi, K., 2003. Ultrastructure of ascending cholinergic terminals in the anteroventral thalamic nucleus of the rat: a comparison with the mammillothalamic terminals. Brain Res. Bull. 59, 473–483.
Pal, D., Mallick, B.N., 2006. Role of noradrenergic and GABA-ergic inputs in pedunculopontine tegmentum for regulation of rapid eye movement sleep in rats. Neuropharmocology 51, 1–11.
Pompeiano, O., 2001. Role of the locus coeruleus in the static and dynamic control of posture. Arch. Ital. Biol. 139, 109–124.
Previc, F.H., 1999. Dopamine and the origins of human intelligence. Brain Cogn. 41, 299–350.
Reiner, P.B., Fibiger, H.C., 1995. Functional heterogeneity of central cholinergic systems. In: Bloom, F.E., Kupfer, D.J. (Eds.), Psychopharmacology: The Fourth Generation of Progress. Raven, New York, pp. 147–153.
Rezek, O., Boldogkoi, Z., Tombácz, D., Kovágó, C., Gerendai, I., Palkovits, M., Tóth, I.E., 2008. Location of parotid preganglionic neurons in the inferior salivatory nucleus and their relation to the superior salivatory nucleus of rat. Neurosci. Lett. 440, 265–269.
Ruggiero, D.A., Anwar, M., Gootman, P.M., 1992. Presumptive adrenergic neurons containing phenylethanolamine N-methyltransferase immunoreactivity in the medulla oblongata of neonatal swine. Brain Res. 583, 105–119.
Segal, M., Greenberger, V., Israeli, M., Biegon, A., 1988. A correlation between regional acetylcholinesterase activity in rat brain and performance in a spatial task. Behav. Brain Res. 30, 215–219.
Semba, K., Fibiger, H.C., 1989. Organization of central cholinergic systems. Prog. Brain Res. 79, 37–63.
Siegel, J.M., 2006. The stuff dreams are made of: anatomical substrates of REM sleep. Nat. Neurosci. 9, 721–722.
Skinner, J.D., Chimimba, C.T., 2005. 3rd ed. The Mammals of the Southern African Subregion, 3rd ed., Cambridge University Press, Cape Town.
Smeets, W.J.A.J., González, A., 2000. Catecholamine systems in the brain of vertebrates: new perspectives through a comparative approach. Brain Res. Rev. 33, 308–379.
Tan, M.M.L., Harvey, A.R., 1989. The cholinergic innervation of normal and transplanted superior colliculus in the rat: an immunohistochemical study. Neuroscience 32, 511–520.
Tillet, Y., 1995. Distribution of neurotransmitters in the sheep brain. J. Reprod. Fertil. Suppl. 49, 199–220.
Törk, I., 1990. Anatomy of the serotonergic system. Ann. N. Y. Acad. Sci. 600, 9–35.
Tóth, I.E., Boldogkõi, Z., Medveczky, I., Palkovits, M., 1999. Lacrimal preganglionic neurons form a subdivision of the superior salivatory nucleus of rat: transneuronal labeling by pseudorabies virus. J. Auton. Nerv. Syst. 77, 45–54.
van Groen, T., Kadish, I., Micheal Wyss, J., 2002. Role of the anterodorsal and anteroventral nuclei of the thalamus in spatial memory in the rat. Behav. Brain Res. 132, 19–28.
Wolff, M., Loukavenko, E.A., Will, B.E., Dalrymple-Alford, J.C., 2008. The extended hippocampal-diencephalic memory system: enriched housing promotes recovery of the flexible use of spatial representations after anterior thalamic lesions. Hippocampus 18, 996–1007.
Woolf, N.J., 1991. Cholinergic systems in mammalian brain and spinal cord. Prog. Neurobiol. 37, 475–524.

Journal of Chemical Neuroanatomy 41 (2011) 86–96

Contents lists available at ScienceDirect

Journal of Chemical Neuroanatomy

journal homepage: www.elsevier.com/locate/jchemneu

# Distribution of orexin-A immunoreactive neurons and their terminal networks in the brain of the rock hyrax, *Procavia capensis*

Nadine Gravett [a], Adhil Bhagwandin [a], Kjell Fuxe [b], Paul R. Manger [a,*]

[a] School of Anatomical Sciences, Faculty of Health Sciences, University of the Witwatersrand, 7 York Road, Parktown 2193, Johannesburg, South Africa
[b] Department of Neuroscience, Karolinska Institutet, Retzius väg 8, S-171 77 Stockholm, Sweden

ARTICLE INFO

*Article history:*
Received 9 October 2010
Received in revised form 21 November 2010
Accepted 21 November 2010
Available online 30 November 2010

*Keywords:*
Afrotheria
Orexin
Hypocretin
Diurnal
Comparative neuroanatomy

ABSTRACT

The present study describes the distribution of orexin-A immunoreactive neurons and terminal networks in relation to the previously described catecholaminergic, cholinergic and serotonergic systems within the brain of the rock hyrax, *Procavia capensis*. Adult female rock hyrax brains were sectioned and immunohistochemically stained with an antibody to orexin-A. The staining revealed that the neurons were mainly located within the hypothalamus as with other mammals. The orexinergic terminal network distribution also resembled the typical mammalian plan. High-density orexinergic terminal networks were located within regions of the diencephalon (e.g. paraventricular nuclei), midbrain (e.g. serotonergic nuclei) and pons (locus coeruleus), while medium density orexinergic terminal networks were evident in the telencephalic (e.g. basal forebrain), diencephalic (e.g. hypothalamus), midbrain (e.g. periaqueductal gray matter), pontine (e.g. serotonergic nuclei) and medullary regions (e.g. serotonergic and catecholaminergic nuclei). Although the distribution of the orexinergic terminal networks was typically mammalian, the rock hyrax did show one atypical feature, the presence of a high-density orexinergic terminal network within the anterodorsal nucleus of the dorsal thalamus (AD). The dense orexinergic innervation of the AD nucleus has only been reported previously in the Nile grass rat, *Arvicanthis niloticus* and Syrian hamster, *Mesocricetus auratus*, both diurnal mammals. It is possible that orexinergic innervation of the AD nucleus might be a unique feature associated with diurnal mammals. It was also noted that the dense orexinergic innervation of the AD nucleus coincided with previously identified cholinergic neurons and terminal networks in this particular nucleus of the rock hyrax brain. It is possible that this dense orexinergic innervation of the AD nucleus in the brain of the rock hyrax may act in concert with the cholinergic neurons and/or the cholinergic axonal terminals, which in turn may influence arousal states and motivational processing.

© 2010 Elsevier B.V. All rights reserved.

*Abbreviations:* III, oculomotor nucleus; 3V, third ventricle; 4V, fourth ventricle; A1, caudal ventrolateral medullary tegmental nucleus; A2, caudal dorsomedial medullary nucleus; A6, locus coeruleus; A7, subcoeruleus; A7d, nucleus subcoeruleus, diffuse portion; A7sc, nucleus subcoeruleus, compact portion; A9, substantia nigra; A10, ventral tegmental area; A10c, ventral tegmental area, central; A10d, ventral tegmental area, dorsal; A10dc, ventral tegmental area, dorsal caudal; A11, caudal diencephalic group; A12, tuberal cell group; A13, zona incerta; A14, rostral periventricular nucleus; A15d, anterior hypothalamic group, dorsal division; A15v, anterior hypothalamic group, ventral division, acanterior commissure; AD, anterodorsal nucleus of the dorsal thalamus; Amyg, amygdala; AP, area postrema; AV, anteroventral nucleus of the dorsal thalamus; B9, supralemniscal serotonergic nucleus; C, caudate nucleus; C1, rostral ventrolateral medullary tegmental group; C2, rostral dorsomedial medullary nucleus; ca, cerebral aqueduct; Cb, cerebellum; cc, corpus callosum; Cl, claustrum; CLi, caudal linear nucleus; CN, cochlear nucleus; CP, cerebral peduncle; CVL, caudal ventrolateral serotonergic group; DCN, deep cerebellar nuclei; Diag.B, diagonal band of Broca; DR, dorsal raphe; DRc, dorsal raphe nucleus, caudal division; DRd, dorsal raphe nucleus, dorsal division; DRif, dorsal raphe nucleus, interfascicular division; DRl, dorsal raphe nucleus, lateral division; DRp, dorsal raphe nucleus, peripheral division; DRv, dorsal raphe nucleus, ventral division; DT, dorsal thalamus; EW, Edinger-Westphal nucleus; f, fornix; fr, fasciculus retroflexus; GC, periaqueductal grey matter; GLD, dorsal lateral geniculate nucleus; GP, globus pallidus; Hb, habenular nuclei; Hip, hippocampus; Hyp, hypothalamus; Hyp.d, dorsal hypothalamic cholinergic nucleus; Hyp.l, lateral hypothalamic cholinergic nucleus; Hyp.v, ventral hypothalamic cholinergic nucleus; IC, inferior colliculus; ic, internal capsule; icp, inferior cerebellar peduncle; IGL, intergeniculate leaflet; io, inferior olivary nuclei; IP, interpeduncular nucleus; LDT, laterodorsal tegmental nucleus; LOT, lateral olfactory tract; LRT, lateral reticular nucleus; LV, lateral ventricle; Mc, main cluster of orexinergic immunoreactive neurons; mcp, middle cerebellar peduncle; MnR, median raphe nucleus; N.Acc, nucleus accumbens; N.Bas, nucleus basalis; NEO, neocortex; OC, optic chiasm; OT, optic tract; OTc, optict tract cluster of orexinergic immunoreactive neurons; P, putamen; PV, paraventricular nucleus; PBg, parabigeminal nucleus; PIR, piriform cortex; PPT, pedunculopontine nucleus; Pta, pretectal area; py, pyramidal tract; pyx, decussation of the pyramidal tract; R, thalamic reticular nucleus; RMg, raphe magnus nucleus; RN, red nucleus; ROb, raphe obscurus nucleus; RPa, raphe pallidus nucleus; RVL, rostral ventrolateral serotonergic group; S, septum; SC, superior colliculus; SpV, spinal trigeminal tract; TOL, olfactory tubercle; vh, ventral horn of spinal cord; VPO, ventral pontine nucleus; ZI, zona incerta; ZIc, zona incerta cluster of orexinergic immunoreactive neurons.

* Corresponding author. Tel.: +27 11 717 2497; fax: +27 11 717 2422.
*E-mail address:* Paul.Manger@wits.ac.za (P.R. Manger).

0891-0618/$ – see front matter © 2010 Elsevier B.V. All rights reserved.
doi:10.1016/j.jchemneu.2010.11.005

## 1. Introduction

Orexin or hypocretin is a hypothalamic neuropeptide that consists of 130–131 amino acids in mammals and was first described in 1998 by two independent research groups. The Sutcliffe group called it hypocretin because it shared similar sequencing patterns to the secretin group of peptides and because of its hypothalamic localization (De Lecea et al., 1998; Kukkonen et al., 2002). The 130 amino acid precursor peptide they identified became known as preprohypocretin with hypocretin 1 and hypocretin 2 being the final peptides. The term orexin was coined by the Yanagisawa group who discovered that this peptide was linked to food intake (Sakurai et al., 1998; Kukkonen et al., 2002) and noted that injecting this peptide into the lateral ventricle of non-fasted rats would increase food intake. The precursor peptide thus became known as preproorexin with orexin-A and orexin B being the final peptides (Sakurai et al., 1998; Kukkonen et al., 2002).

Studies on several mammalian species have reported the location and distribution of orexinergic neurons and terminal networks (e.g. humans, Moore et al., 2001; cat, Wagner et al., 2000; Zhang et al., 2001, 2002; sheep, Iqbal et al., 2001; a variety of rodents, e.g. Broberger et al., 1998; Peyron et al., 1998; Chen et al., 1999; Cutler et al., 1999; Date et al., 1999; Nixon and Smale, 2007; microchiropterans, Kruger et al., 2010; and kangaroo, Yamamoto et al., 2006). These studies all concur regarding the location of the orexinergic neurons and the general distribution of their major terminal networks. Orexinergic neurons have only been observed within the hypothalamus with the majority of the neurons found in the lateral hypothalamic area and the perifornical region; however, other studies have also reported isolated neurons in the region of the median eminence, posterior, anterior, dorsal and dorsomedial hypothalamus, zona incerta and ventrolateral hypothalamus. In contrast to the restricted neuronal distribution, orexinergic fibres are widely distributed throughout the brain and spinal cord and exhibit different densities of terminal networks in different regions of the brain, for example a high density network is evident in the areas immediately surrounding the third ventricle and areas involved in the regulation of the sleep–wake cycle (Chen et al., 1999; Cutler et al., 1999; Hagan et al., 1999; Wagner et al., 2000; McGranaghan and Piggins, 2001; Zhang et al., 2002, 2004; Espana et al., 2005; Kruger et al., 2010). Orexinergic fibres have been reported as being both smooth and varicose, with the varicose type predominating (Peyron et al., 1998; Chen et al., 1999; Cutler et al., 1999; Kukkonen et al., 2002). Vasoactive intestinal peptide, vasopressin and neuropeptide Y terminal networks provide the main innervation to orexinergic neurons while a multitude of other neuronal circuits receive orexinergic efferents (Peyron et al., 1998; Cutler et al., 1999; Date et al., 1999; Horvath et al., 1999; Nambu et al., 1999; Abrahamson et al., 2001; Backberg et al., 2002; Kukkonen et al., 2002). Studies performed on rats to measure the release of orexin have revealed that release is closely correlated to circadian activity. These studies found that orexin concentrations in the hypothalamus were maximal around light onset and minimal at the point of light offset. Diurnal variation was also noted with similar measurements taken from the pons and intercisternal space; however, the precise time points were shifted compared to the hypothalamus (Taheri et al., 2000; Fujiki et al., 2001; Yoshida et al., 2001; Kukkonen et al., 2002).

The diurnal variation of orexin release has an effect on food consumption, thus when orexin is released in higher concentrations (i.e. during the morning) food intake is promoted, the opposite being true of low orexin release (i.e. during the night) (Cutler et al., 1999; Hagan et al., 1999; McGranaghan and Piggins, 2001; Baldo et al., 2003; Khorooshi and Klingenspor, 2005). Orexin regulates sleep by exciting neurons that are involved in the sleep–wake cycle, such as those of the locus coeruleus, dorsal raphe, and pontine cholinergic nuclei. This excitation causes the promotion of wakefulness and reduces sleep, especially episodes of REM (Hagan et al., 1999; Bourgin et al., 2000; Piper et al., 2000; Wagner et al., 2000; Espana et al., 2001; Huang et al., 2001; McGranaghan and Piggins, 2001; Methippara et al., 2000; Kukkonen et al., 2002; Yamanaka et al., 2002; Zhang et al., 2004; Lee et al., 2005).

Although many studies deal with the location of orexinergic neurons and terminal network distribution, very few studies actually investigate the relation and interplay of these neurons and terminal networks to other neural systems. The aim of the present study is, thus, to describe the location and distribution of orexinergic neurons and terminal networks in the brain of the rock hyrax, *Procavia capensis*, based on orexin-A immunocytochemistry and to compare these to the known cholinergic, catecholaminergic and serotonergic systems (Gravett et al., 2009). This may shed light on the possible relation and interplay between the orexinergic system and these neural systems. Currently, the majority of studies reporting on orexin have made use of nocturnal laboratory rodents. Thus, the rock hyrax makes for an interesting candidate for the study of the orexinergic system as these mammals are part of the unusual and morphologically diverse Afrotheria (Tabuce et al., 2008), for which no report of the orexinergic system in available. In addition to this the hyraxes are diurnally active and their sleep has been described as being polycyclic (Snyder, 1974). Moreover, they are poor thermoregulators (McNairn and Fairall, 1984; Brown and Downs, 2006) and orexins are clearly involved in thermoregulation and energy balance (Szekely et al., 2010; Teske et al., 2010).

## 2. Materials and methods

The brains of six adult female rock hyraxes, *P. capensis*, were used in the present study. Permits from the Limpopo and Gauteng Provincial Governments were obtained for the capture and transport of the animals from the wild. All animals were treated and used according to the guidelines of the University of the Witwatersrand Animal Ethics Committee, which parallel those of the NIH for the care and use of animals in scientific experimentation. Each animal was weighed, deeply anaesthetized and subsequently euthanized with weight appropriate doses of sodium pentobarbital (200 mg sodium pentobarbital/kg, i.p.). Upon cessation of respiration the animals were perfused intracardially with 0.9% saline followed by 4% paraformaldehyde in 0.1 M phosphate buffer (PB) (pH 7.4, approximately 1 l/kg of each solution), both solutions having a temperature of 4 °C. The brains were then carefully removed from the skulls and post-fixed overnight in 4% paraformaldehyde in 0.1 M PB followed by equilibration in 30% sucrose in 0.1 M PB. The brains were then frozen in dry ice and with the aid of a freezing microtome sectioned at 50 μm in the coronal plane. A one in three series of stains was made for Nissl, myelin, and orexin-A. Sections kept for the Nissl series were mounted on 0.5% gelatine coated glass slides, cleared in a solution of 1:1 chloroform and absolute alcohol, then stained with 1% cresyl violet to reveal cell bodies. Sections used for myelin staining were stored in 5% formalin for a period of two weeks and were then mounted on 1% gelatine coated glass slides and subsequently stained with silver solution to reveal myelin sheaths (Gallyas, 1979).

For immunohistochemical staining each section was treated with an endogenous inhibitor peroxidase (49.2% methanol: 49.2% 0.1 M PB: 1.6% of 30% $H_2O_2$) for 30 min and subsequently subjected to three 10 min 0.1 M PB rinses. The sections were then preincubated in a solution (blocking buffer) consisting of 3% normal goat serum (NGS, Chemicon), 2% bovine serum albumin (BSA, Sigma) and 0.25% Triton X100 (Merck) in 0.1 M PB, at room temperature for 2 h. This was followed by three 10 min rinses in 0.1 M PB. The sections were then placed for 48 h at 4 °C under constant gentle shaking, in primary antibody solution, that contained the appropriately diluted primary antibody in blocking buffer (see above). The primary antibody used was anti-orexin-A (AB 3704, Millipore, raised in rabbit, dilution 1:1500). This was followed by another three 10 min rinses in 0.1 M PB, after which the sections were incubated for 2 h at room temperature in secondary antibody solution. The secondary antibody solution contained a 1:1000 dilution of biotinylated anti-rabbit IgG (BA-1000, Vector Labs) in 3% normal goat serum (NGS), and 2% bovine serum albumin (BSA) in 0.1 M PB. Once this was completed, the sections were again subjected to another three 10 min rinses in 0.1 M PB, followed by a 1 h incubation in avidin-biotin solution (Vector Labs) and again rinsed. This was followed by a 5 min treatment of the sections in a solution consisting of 0.05% diaminobenzidine tetrahydrochloride (DAB) in 0.1 M PB, after which, and while still in the same solution, 3 μl of 30% $H_2O_2$ per 0.5 ml of solution was added. With the aid of a low power stereomicroscope the progression of the staining was visually followed and allowed to continue until a level was reached where the background staining could assist in reconstruction without obscuring the immunopositive structures. Once

this level was reached the reaction was stopped by placing the sections in 0.1 M PB, followed by a final session of three 10 min rinses in 0.1 M PB. The immunohistochemically stained sections were mounted on 0.5% gelatine coated slides and left to dry overnight. The mounted sections were dehydrated by placing it in 70% alcohol for 2 h at room temperature under gentle shaking and then transferred through a series of graded alcohols, cleared in xylene and coverslipped with Depex.

The sections were observed with a low power stereomicroscope, and the architectonic borders traced according to the Nissl and myelin stained sections

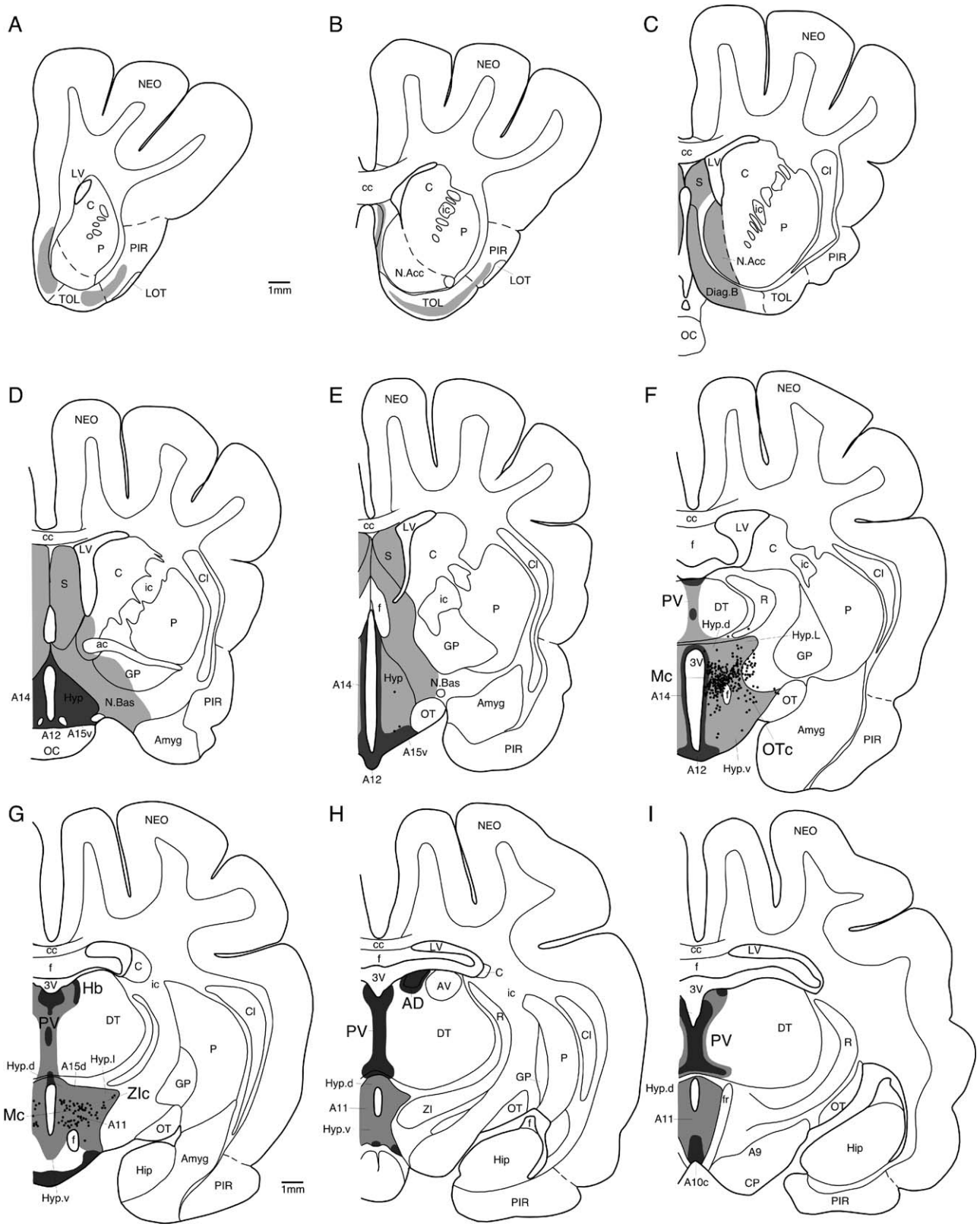


**Fig. 1.** Drawings of coronal sections through one half of the brain of the rock hyrax, illustrating orexin-A immunoreactive neurons and terminal network distribution. A single black dot indicates a single cell body, black and gray shaded areas indicate regions in the brain of the rock hyrax where high and medium density, respectively, orexin-A terminal networks were observed. Areas where no shading is evident represent regions of low or no orexinergic innervation. Drawing **A** represents the most rostral section, **V** the most caudal, and each drawing is approximately 1500 μm apart. See list for abbreviations.

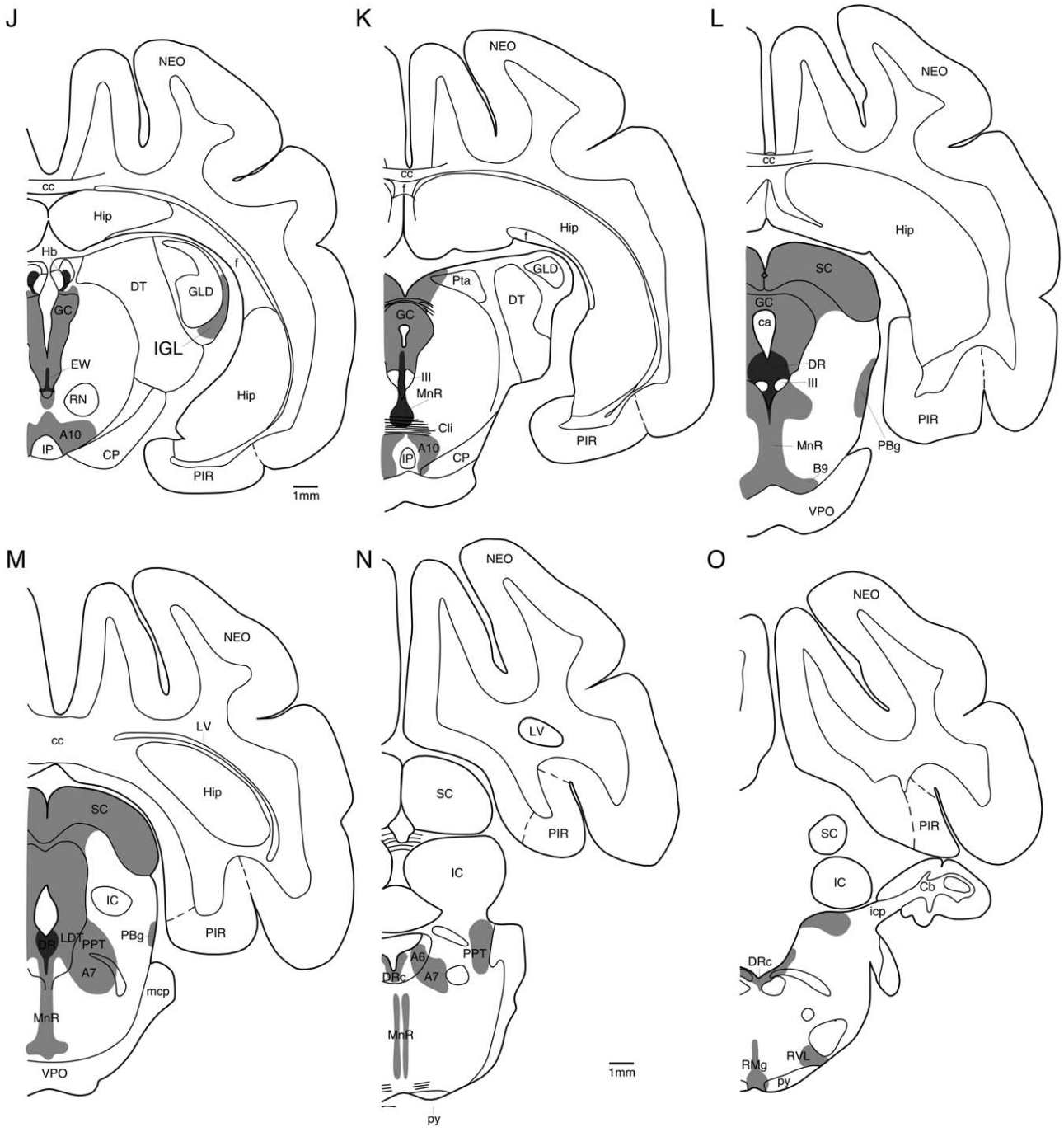


Fig. 1 (*Continued*)

using a camera lucida. The immunostained sections were then matched to the drawings and the immunopositive neurons marked, in addition the density of axon terminal staining was graded from low to high for each immunostained section and medium and high marked on the drawings. The drawings were scanned and redrawn with the aid of the Canvas 8 program. Location and distribution of orexin immunopositive (Orx+) neurons and terminal networks were described in relation to the general neuroanatomy of the rock hyrax brain and previously described cholinergic, catecholaminergic, and serotonergic systems (Gravett et al., 2009).

## 3. Results

The results revealed that the distribution of orexin-A immunopositive (Orx+) neuron cell bodies and terminal networks did not, for the most part, differ significantly from what has been described in other mammals. Despite this, an interesting difference was noted that has not been reported in most mammals studied to date, namely a strong Orx+ terminal network in the anterior dorsal nucleus of the dorsal thalamus (AD). Orx+ neurons and terminal networks are described in relation to either the general neuroanatomy of the rock hyrax brain and the cholinergic, catecholaminergic, and serotonergic systems (as described previously for this species in Gravett et al., 2009).

### 3.1. Orexin-A neuronal cell body distribution

Orx+ neuronal cell bodies were identified mainly within the hypothalamus of the brain of the rock hyrax. These cell bodies were grouped into three distinct clusters; the main cluster, the zona incerta cluster and the optic tract cluster (Figs. 1–3). The main

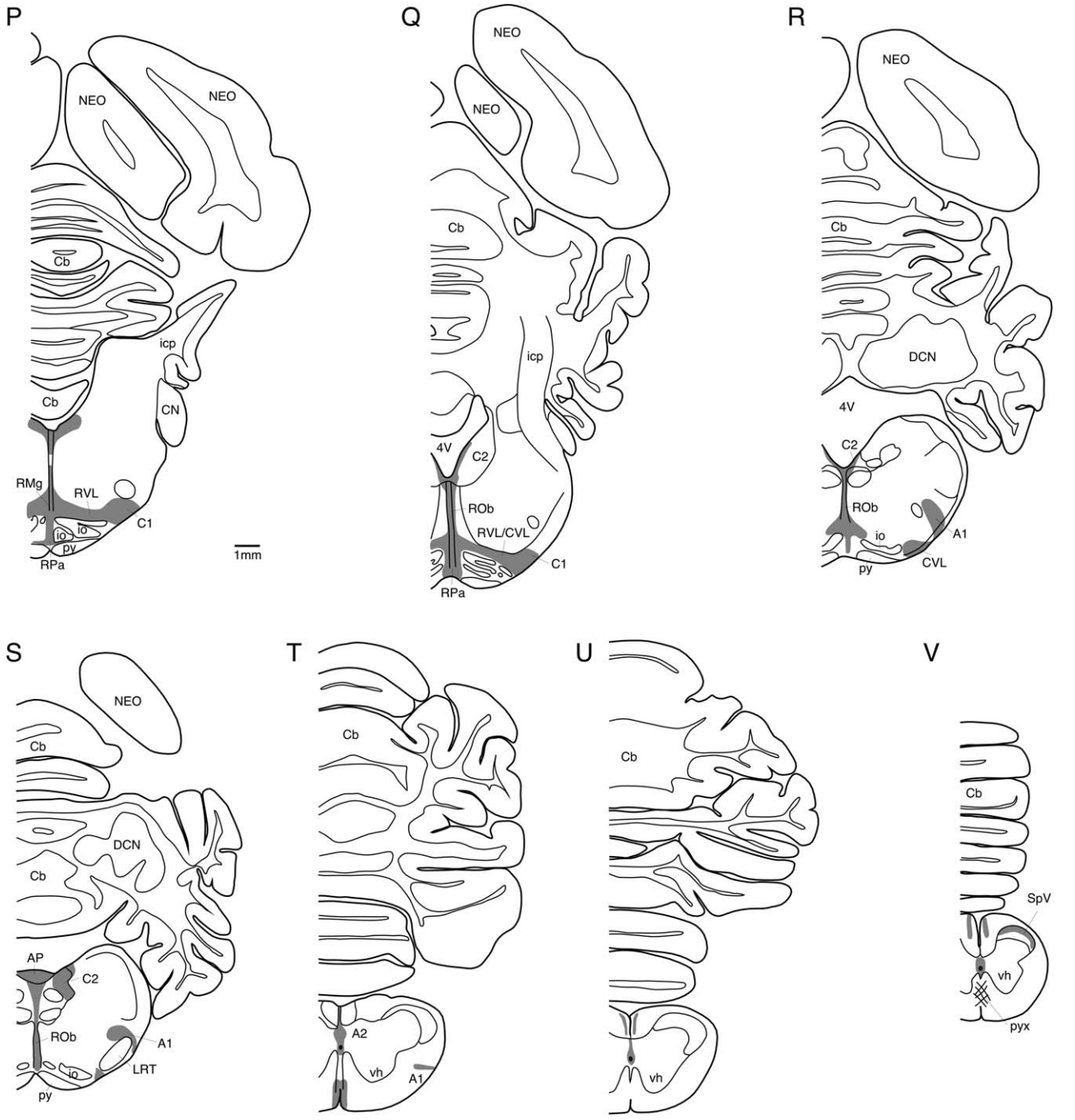


Fig. 1 (*Continued*).

cluster was identified as a large group of densely packed Orx+ neuronal cell bodies located lateral to the third ventricle in the perifornical region, with a large number of neuronal cell bodies extending medially from this area, as well as into the dorsomedial and lateral hypothalamic areas. The majority of Orx+ neurons belonged to this cluster and they were found to be ovoid in shape, a mixture of both bipolar and multipolar types and showed no apparent regular dendritic orientation. The Orx+ neuronal cell bodies of this main cluster were intermingled with the A11 and A14 nuclear groups of the catecholaminergic system. From the main cluster a group of Orx+ neuronal cell bodies extended laterally into the region of the zona incerta. This cluster had a very low density of Orx+ neurons that were mixed with neurons of the lateral hypothalamic cholinergic nucleus and the A13 nucleus of the catecholaminergic system. The cell bodies were ovoid in shape, a mixture of bipolar and multipolar type and had no specific dendritic orientation. The third cluster extended ventrolaterally from the main cluster to the ventrolateral region of the hypothalamus adjacent to the optic tract. This cluster exhibited a low density of Orx+ neuronal cell bodies that were mostly of the bipolar type with the same cell morphology as described for the other clusters. These neurons were found to intermingle with those of the ventral hypothalamic cholinergic nucleus (Figs. 1E–G and 2).

### 3.2. Orexin-A terminal network distribution

#### 3.2.1. Telencephalon

Within the telencephalon of the rock hyrax brain orexinergic terminal networks of medium density were noted. These terminal

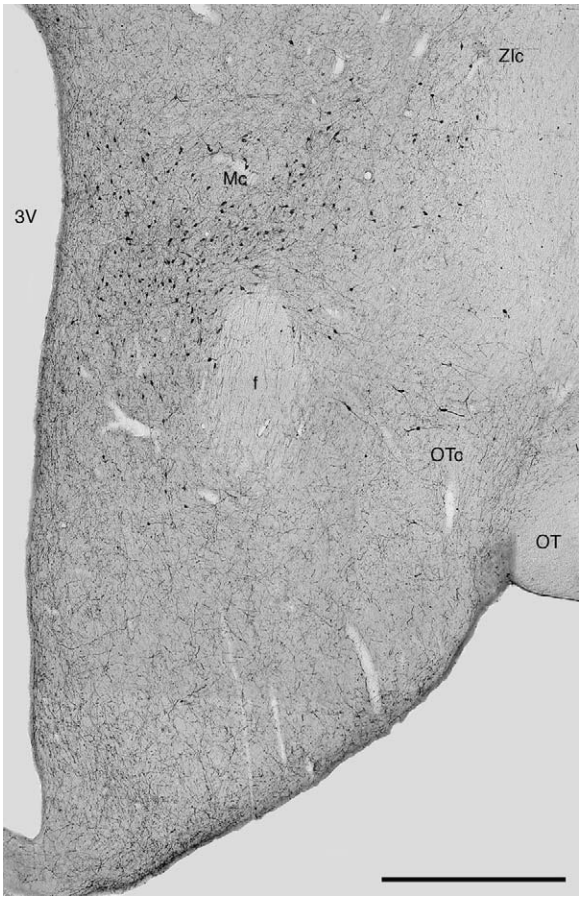


**Fig. 2.** Photomicrograph montage demonstrating the location of orexin-A immunoreactive neurons and terminal networks within the hypothalamus of the rock hyrax showing the main cluster (**Mc**), the zona incerta cluster (**ZIc**) and the optic tract cluster (**OTc**). Scale = 1 mm. **3V**: third ventricle; **f**: fornix; **OT**: optic tract.

networks were mainly distributed along the medial and ventrolateral border of the telencephalon and located in and around the following structures: the nucleus accumbens, olfactory tubercle and islands of Calleja, diagonal band of Broca and the septal nuclear complex (Figs. 1A–C and 4). It is of interest to note than in all these structures a number of cholinergic neurons were also located (Gravett et al., 2009). The remaining regions of the telencephalon had either a low density Orx+ terminal network, or no Orx+ structures could be observed.

*3.2.2. Diencephalon*

Both high and medium density orexinergic terminal networks were observed throughout the diencephalon. The high density terminal networks were located in the anterior hypothalamic area, the periventricular areas adjacent to the third ventricle in the hypothalamus (Fig. 2), in the paraventricular nuclei of the epithalamus (Fig. 5A) extending to a region surrounding the habenular nuclei, and dorsolaterally in the AD (Figs. 1D–J and 5). The medium density terminal networks surrounded these areas of high density and were distributed through most parts of the hypothalamus (Fig. 2), the midline of the dorsal thalamus in the intralaminar nuclei and extended laterally to the intergeniculate leaflet (Fig. 5C). The high-density terminal networks overlapped with the A12, A14, and A15v nuclei of the catecholaminergic system, and the AD (Fig. 5B) that forms part of the cholinergic system of the rock hyrax (Gravett et al., 2009). The Orx+ terminal networks of medium density were found to overlap the A11 and A13 nuclei of the catecholaminergic system and the dorsal, lateral, and ventral hypothalamic nuclei of the cholinergic system. The remaining regions of the diencephalon had either a low density Orx+ terminal network, or no Orx+ structures could be observed (Fig. 2).

*3.2.3. Midbrain and Pons (Mesencephalon and Metencephalon)*

Both high and medium dense orexinergic terminal networks characterized the midbrain and pontine regions; however, the medium density Orx+ terminal networks were found to dominate in these regions. The terminal networks of high density were located ventral to the cerebral aqueduct within the midline of the midbrain and pontine regions and overlapped the A10d and A10dc nuclei of the catecholaminergic system and most serotonergic nuclei of the dorsal raphe (Fig. 6A). The medium dense Orx+ terminal networks were coincident with the dopaminergic ventral tegmental area, the noradrenergic locus coeruleus complex (Fig. 6B), the cholinergic nuclei of the laterodorsal tegemental and pedunculopontine nuclei (both magno and parvocellular divisions of these nuclei, Gravett et al., 2009), the cholinergic parabigeminal and Edinger-Westphal nuclei, and the caudal linear (CLi), supralemniscal (B9), caudal nucleus of the dorsal raphe (DRc) and median raphe (MnR) serotonergic nuclei (Fig. 6C). In addition to this, the entire periaqueductal gray matter was observed to have a medium density Orx+ terminal network that extended outward through all layers of the superior colliculus (Figs. 1K–N and 6). The remaining regions of the midbrain and pons had either a low density Orx+ terminal network, or no Orx+ structures could be observed. It is worth noting that we could only find a low density Orx+ network in the inferior colliculus.

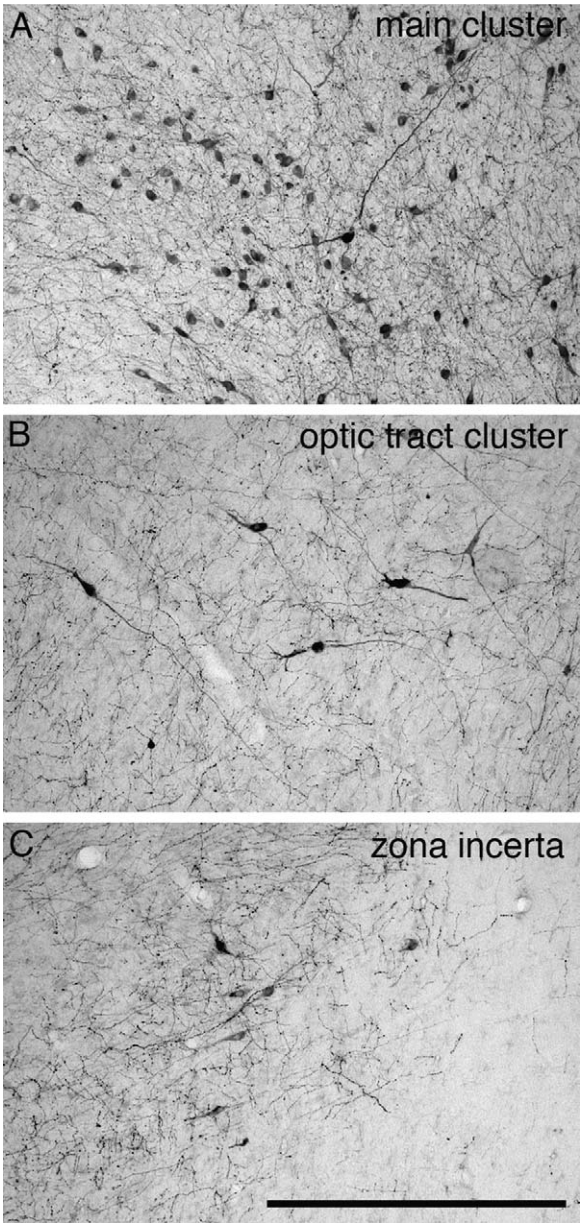


**Fig. 3.** Photomicrographs illustrating the neuronal morphology of the three clusters of orexin-A immunoreactive nuclear groups within the hypothalamus of the rock hyrax. (**A**) Orexin-A immunoreactive neurons of the main cluster, perifornical region. (**B**) Orexin-A immunoreactive neurons of the optic tract cluster, lateral ventral hypothalamic area. (**C**) Orexin-A immunoreactive neurons of the zona incerta cluster, lateral hypothalamic area. In all images, medial is to the left, lateral to the right, and dorsal to the top. Scale in *C* = 500 μm and applies to all.

#### 3.2.4. Medulla oblongata (Myelencephalon)

Only medium and low-density Orx+ terminal networks were present within the medulla oblongata of the brain of the rock hyrax. The medium density networks were found in all regions where serotonergic neurons were located (i.e. the raphe magnus, rostral and caudal ventrolateral columns, raphe pallidus and raphe obscurus). Similarly, all regions that contained catecholaminergic neurons were found to have a medium density Orx+ terminal network, these being the area postrema, C1, C2, A1 and A2 nuclei. Anterior in the medulla a medium density Orx+ terminal network was found in the region of the parabrachial nuclear complex. Towards the spinal cord these medium density Orx+ networks were located in the areas surrounding the central canal and the outer edge of the dorsal horn in the spinal trigeminal tract (SpV) (Fig. 1O–V). The remaining regions of the medulla had either a low density Orx+ terminal network, or no Orx+ structures could be observed.

## 4. Discussion

The aim of the present study was to identify and describe the neuronal location, nuclear organization and terminal network distribution of the orexinergic system in the brain of the rock hyrax, *Procavia capensis* by means of orexin-A immunocytochemistry. The study also examined the topological relationships of the Orx+ neurons and terminal networks with the previously described cholinergic, catecholaminergic and serotonergic systems in the brain of the rock hyrax (Gravett et al., 2009). The results revealed that the distribution and nuclear organization of the Orx+ neurons of the rock hyrax conforms closely to what has been described previously for other mammals (Broberger et al., 1998; Peyron et al., 1998; Moore et al., 2001; Zhang et al., 2001, 2002; Nixon and Smale, 2007; Yamamoto et al., 2006; Kruger et al., 2010). The orexin-A immunoreactive terminal network distribution also showed a similar architecture as described in other mammalian species; however the anterodorsal nucleus of the thalamus was observed to have a dense orexinergic terminal network. Thus, the orexinergic system, as demonstrated with orexin-A immunoreactivity, within the rock hyrax brain is similar to what has been described in other mammals, but there is a feature of the terminal network distribution that has only been reported in a small number of other mammals.

### 4.1. Orexinergic neuronal distribution

The location of orexinergic neuronal cell bodies has been described in representative species of all vertebrate classes – mammals (e.g. Wagner et al., 2000; Iqbal et al., 2001; Moore et al., 2001; Yamamoto et al., 2006; Nixon and Smale, 2007; Kruger et al., 2010; Stoyanova et al., 2010), birds (e.g. Ohkubo et al., 2002), reptiles (Domínguez et al., 2010), amphibians (e.g. Shibahara et al., 1999; Galas et al., 2001; Singletary et al., 2005; Suzuki et al., 2008; López et al., 2009) and fish (e.g. Kaslin et al., 2004; Huesa et al., 2005; Yokogawa et al., 2007). All these studies have revealed that for the most part orexinergic neurons were located within the hypothalamus. It is clear from previous studies that this system shows a degree of variability within and between different vertebrate classes, but also a strong degree of similarity (e.g. Suzuki et al., 2008; Domínguez et al., 2010). In mammals the majority of orexinergic neurons are located within the lateral hypothalamic area and the perifornical region (which we term the main cluster, Kruger et al., 2010); however, other studies in mammals have also reported isolated neurons in the region of the median eminence, posterior, dorsal and dorsomedial hypothalamus (Chen et al., 1999; Cutler et al., 1999; Hagan et al., 1999; Wagner et al., 2000; McGranaghan and Piggins, 2001; Zhang et al., 2002, 2004; Espana et al., 2005). In the rock hyrax we could subdivide the orexinergic neurons into three distinct clusters: the main cluster, the zona incerta cluster and the optic tract cluster. While these clusters have been reported present in most mammals studied to date it has been found that microchiropterans and hamsters lack the optic tract cluster (Wagner et al., 2000; McGranaghan and Piggins, 2001; Kruger et al., 2010). The nuclear organization of the orexinergic neurons in the rock hyrax is therefore what may be described as very typically mammalian. It would seem that, apart from minor differences, the nuclear organization of the orexinergic neurons is strongly conserved across mammals. An important aspect of orexinergic nuclear parcellation relates to the connectivity of this system. For example, the zona incerta cluster specifically projects to the intergeniculate

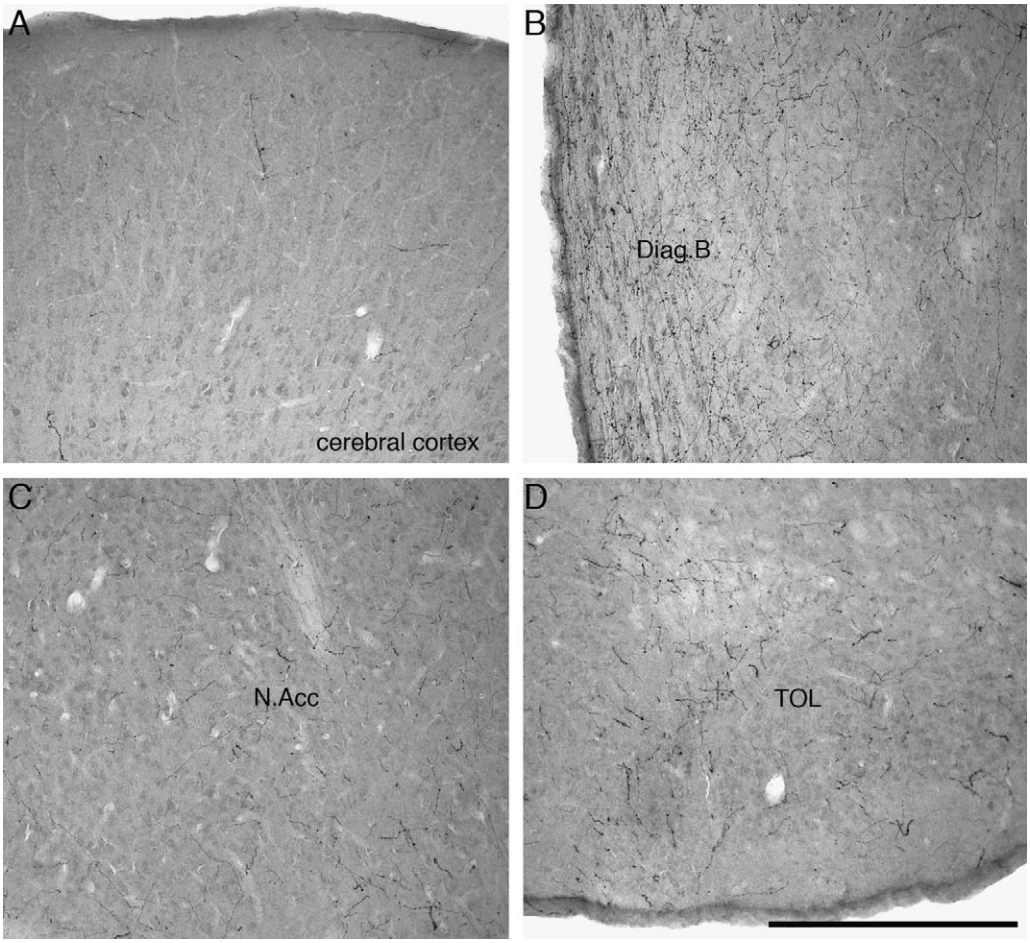


**Fig. 4.** Photomicrographs illustrating the distribution of orexin-A immunoreactive terminal networks within certain parts of the forebrain of the rock hyrax. (**A**) Low density orexin-A immunoreactive terminal networks within the cerebral cortex. (**B**) Medium density orexin-A immunoreactive terminal networks within the diagonal band of Broca (**Diag. B**). (**C**) Medium density orexin-A immunoreactive terminal networks within the nucleus accumbens (**N. Acc**). (**D**) Medium density orexin-A immunoreactive terminal networks within the olfactory tubercle (**TOL**). Scale in *D* = 500 μm and applies to all. Medial is to the left in all images.

leaflet (Vidal et al., 2005) and what we term the main orexinergic cluster may be subdivided into perifornical and lateral hypothalamic nuclei (Yoshida et al., 2006). Thus, in the hyrax we may be observing 4 specific nuclei within this system, however, further study on the specific connectivity of this system would be required to justify further nuclear parcellation than that presented here.

In conjunction with neuronal location and distribution, the present study also examined the topographical interrelationships of the orexinergic neurons with the previously described cholinergic, catecholaminergic and serotonergic systems in the brain of the rock hyrax (Gravett et al., 2009). The observations revealed that orexinergic neurons of the main cluster were topographically coincident with the A11 and A14 nuclear groups of the catecholaminergic system; the zona incerta cluster was topographically coincident with the A13 nucleus of the catecholaminergic system and the lateral hypothalamic nucleus of the cholinergic system; the optic tract cluster was topographically coincident with the cholinergic ventral hypothalamic nucleus. It has been reported that the membrane potential of orexinergic neurons are hyperpolarized by noradrenaline and serotonin and depolarized by acetylcholine (Yamanaka et al., 2003). Thus, orexinergic neurons are possibly rapidly depolarized where they intermingle with neurons from the cholinergic system. The potential intrinsic hypothalamic circuitry of these systems, due to the topological congruency, would be an avenue of interesting further study given the roles these systems play in the sleep–wake cycle, satiety and motivational states.

### 4.2. Orexinergic terminal network distribution

The orexinergic terminal network distribution within the brain of the rock hyrax was found to be similar to that described in other mammalian species studied to date, especially in the manner that these terminal networks are found primarily along the midline and ventricular surfaces; however, the anterodorsal nucleus of the dorsal thalamus (AD) of the rock hyrax exhibited a high-density orexinergic terminal network which is an apparent variance to most other mammals (see below).

The majority of the mammalian brain is in receipt of either very low or no orexinergic innervation, and this pattern is evident in the cerebral cortex, striatopallidal complex, hippocampal complex, amygdalar complex, the majority of the dorsal thalamus, brainstem and cerebellum of the rock hyrax brain. Medium dense orexinergic terminal networks were observed within regions of the telencephalon, diencephalon, midbrain and the medulla of the brain of the rock hyrax, whereas a high density orexinergic innervation was only evident in certain regions of the diencephalon and midbrain. This distribution of medium to high dense orexinergic terminal networks once again resembled the typical mammalian organizational plan for this system as reported in previous studies. Throughout the telencephalon, diencephalon, midbrain and medullary regions the orexinergic terminal networks were found intermingled with several nuclear complexes of the catecholaminergic, cholinergic and serotonergic systems (Gravett et al., 2009).

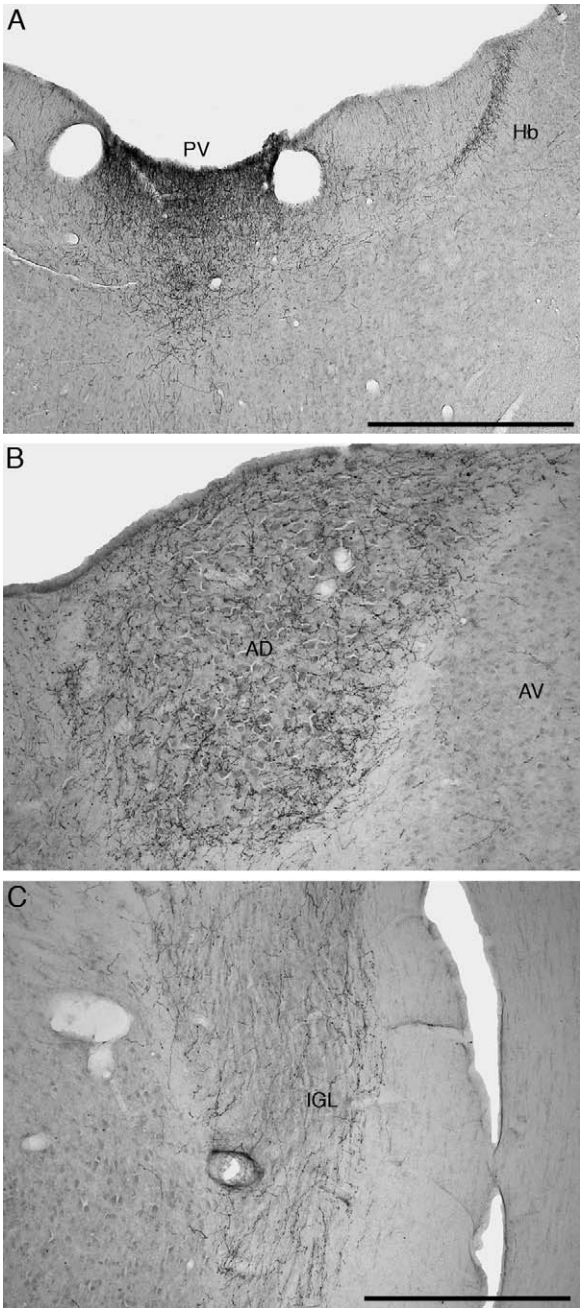


**Fig. 5.** Photomicrograph illustrating orexin-A immunoreactive terminal networks within the diencephalon of the rock hyrax. (**A**) High density orexin-A immunoreactive terminal networks within the paraventricular thalamic nucleus (**PV**) and the lateral habenular nuclei along the border of the stria medullaris (**Hb**). Scale bar = 1 mm. (**B**) High density orexin-A immunoreactive terminal networks within the anterodorsal nucleus of the dorsal thalamus (**AD**). (**C**) Medium density orexin-A immunoreactive terminal networks within the intergeniculate leaflet (**IGL**) mainly oriented in the ventro-dorsal direction. Scale in *C* = 500 μm and applies to **B** and **C**. **AV**: anteroventral nucleus of the dorsal thalamus. Medial is to the left in all images.

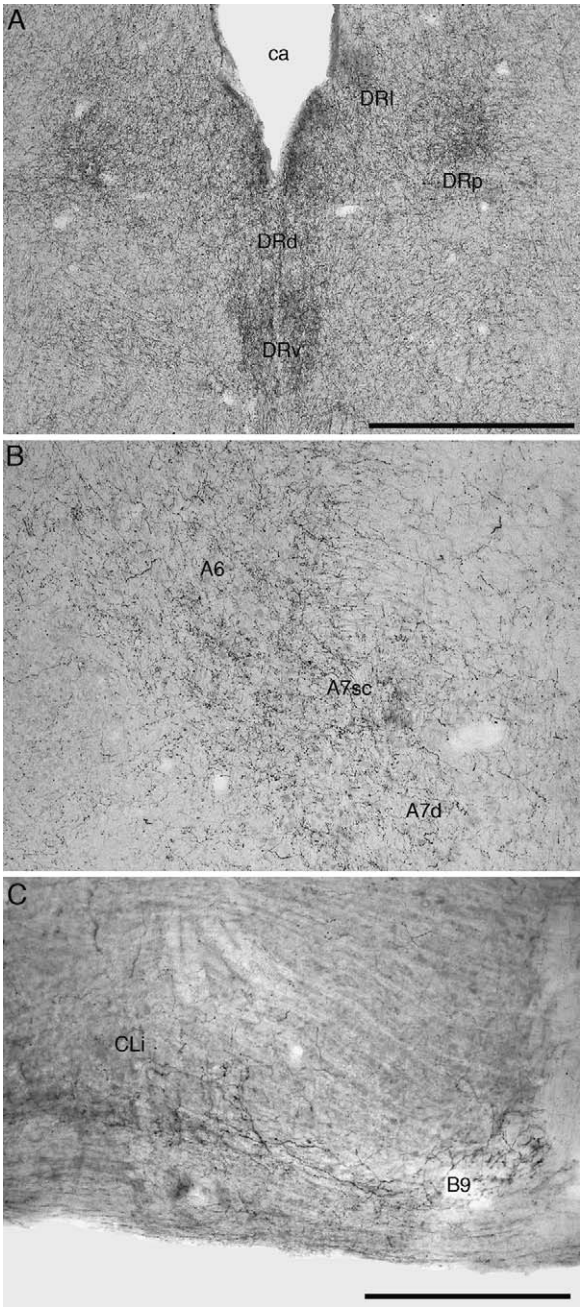


**Fig. 6.** Photomicrograph illustrating the distribution of orexin-A immunoreactive terminal networks within the midbrain and pontine regions of the rock hyrax. (**A**) High density orexin-A immunoreactive terminal networks within the serotonergic dorsal raphe (DR) nuclear complex. Scale bar = 1 mm. (**B**) Medium density orexin-A immunoreactive terminal networks within the locus coeruleus nuclear complex. (**C**) Medium density orexin-A immunoreactive terminal networks within the serotonergic caudal linear nucleus (**CLi**) and supralemniscal nucleus (**B9**). Scale in *C* = 500 μm and applies to **B** and **C**. **A6**: locus coeruleus; **A7d**: subcoeruleus diffuse region; **A7sc**, subcoeruleus compact region; **ca**: cerebral aqueduct; **DRd**: dorsal division of dorsal raphe; **DRl**: lateral division of dorsal raphe; **DRp**: peripheral division of dorsal raphe; **DRv**: ventral division of dorsal raphe. Medial is to the left in all images.

The regions within the telencephalon that exhibited a medium density of orexinergic terminal networks included the nucleus accumbens, the olfactory tubercle, the diagonal band of Broca, and the septal nuclear complex. This distribution of medium density orexinergic terminal networks within the telencephalon of the rock hyrax coincide with previous reports for this system in other mammals. Within the diencephalon a medium density of orexinergic innervation was observed in the region of the intergeniculate leaflet, whereas a high density was observed in regions immediately surrounding the third ventricle, the midline of the dorsal thalamus as well as the AD nucleus (see below). The medium density orexinergic terminal networks overlapped the medial septal nucleus, dorsal, lateral and ventral hypothalamic nuclei of the cholinergic system and the A11 and A13 nuclear complexes of the catecholaminergic system. The distribution of medium to high density orexinergic terminal networks in the

regions of the diencephalon of the rock hyrax brain did not differ significantly to published reports in other mammals for this region. However, it did differ to other mammals with respect to the orexinergic innervation of the AD nucleus, which has only been previously reported to occur in the Nile grass rat, *Arvicanthis niloticus* (Novak and Albers, 2002; Nixon and Smale, 2007) and the Syrian hamster, *Mesocricetus auratus* (Mintz et al., 2001). A medium density orexinergic terminal network distribution dominated the midbrain and pontine regions in the rock hyrax brain, however high density terminal networks were observed within the dopaminergic ventral tegmental area (VTA) and serotonergic dorsal raphe nuclei. A study by Nakamura et al. (2000) has reported that the calcium concentration in isolated A10 neurons is increased by orexin-A and this in turn induces hyperlocomotion, stereotypy and grooming in rats. Orexin-A has further been reported to have an excitatory effect on the serotonergic neurons of the dorsal raphe nucleus, which play an important role in the sleep–wake cycle as well as regulation of food intake and mood control (Brown et al., 2001; Matsuzaki et al., 2002; Tao et al., 2006). A moderate density of orexinergic terminal networks was identified in the noradrenergic locus coeruleus and subcoeruleus, and cholinergic laterodorsal tegmental (LDT) and pedunculopontine tegmental (PPT) nuclei. These structures are known to play a crucial part in the sleep–wake cycle and have been reported to be activated by orexin. Orexinergic input to the cells of the locus coeruleus facilitate the waking state, whereas orexinergic innervation to the LDT and PPT play a role in the regulation of REM sleep (Ohno and Sakurai, 2008). Finally, the medullary region exhibited a medium dense orexinergic terminal network distribution in the areas ventral to the fourth ventricle and regions surrounding the central canal, whereas the remainder of this region was characterized by a low or absent orexinergic terminal network distribution. These terminal networks furthermore overlapped the RPa, RVL, RMg, ROb and CVL nuclei of the serotonergic system, the C1-2 and A1-2 nuclei of the catecholaminergic system, the nucleus ambiguus, the dorsal motor vagus and hypoglossal nuclei of the cholinergic system. Thus, for the most part the orexinergic terminal network distribution within the brain of the rock hyrax typically resembles the general mammalian organizational plan for this system.

### 4.3. Orexinergic innervation of the anterodorsal nucleus of the dorsal thalamus and diurnality?

The majority of studies that describe the distribution of orexinergic terminal networks have examined nocturnal mammals. None of these studies reported either a dense or moderate orexinergic innervation of the AD. Two previous reports of moderate to dense orexinergic innervation of the AD examined the Nile grass rat, *Arvicanthis niloticus* (Novak and Albers, 2002; Nixon and Smale, 2007) and the Syrian hamster, *Mesocricetus auratus* (Mintz et al., 2001). Novak and Albers (2002) reported a low density of orexinergic fibres in the AD nucleus and a high density in the anteroventral (AV) nucleus of the dorsal thalamus of the grass rat when the orexin B antibody was used, while Nixon and Smale (2007) reported a low density for the AV nucleus with the orexin-A antibody and a medium density in the AD nucleus with both orexin-A and B antibodies. The rock hyrax and the Syrian hamster (Mintz et al., 2001) both showed a high density of orexinergic terminals within the AD nucleus with an orexin-A antibody.

Of potential functional correlation to this is the fact that the rock hyrax (Olds and Shoshani, 1982), Nile grass rat (Novak et al., 2000) and Syrian hamster (Gatterman et al., 2008) are all diurnal species. Thus, it is possible that orexinergic innervation of the AD nucleus, the AV nucleus, or the anterior nuclear complex as a whole, might be a unique feature associated with diurnal mammals. This possibility needs to be tested across a range of mammalian species to determine whether this potentially very interesting finding is correct.

## References


Abrahamson, E.E., Leak, R.K., Moore, R.Y., 2001. The suprachiasmatic nucleus projects to posterior hypothalamic arousal systems. Neuroreport 12, 435–440.

Backberg, M., Hervieu, G., Wilson, S., Meister, B., 2002. Orexin receptor-1 (OX-R1) immunoreactivity in chemically identified neurons of the hypothalamus: focus on orexin targets involved in control of food and water intake. Eur. J. Neurosci. 15, 315–328.

Baldo, B.A., Daniel, R.A., Berridge, C.W., Kelley, A.E., 2003. Overlapping distributions of orexin/hypocretin- and dopamine-β-hydroxylase immunoreactive fibers in rat brain regions mediating arousal, motivation and stress. J. Comp. Neurol. 464, 220–237.

Bourgin, P., Huitron-Resendiz, S., Spier, A.D., Fabre, V., Morte, B., Criado, J.R., Sutcliffe, J.G., Henriksen, S.J., De Lecea, L., 2000. Hypocretin-1 modulates rapid eye movement sleep through activation of locus coeruleus neurons. J. Neurosci. 20, 7760–7765.

Broberger, C., De Lecea, L., Sutcliffe, J.G., Hokfelt, T., 1998. Hypocretin/orexin-and melanin-concentrating hormone-expressing cells form distinct populations in the rodent lateral hypothalamus: relationship to the neuropeptide Y and agouti gene-related protein systems. J. Comp. Neurol. 402, 460–474.

Brown, K.J., Downs, C.T., 2006. Seasonal patterns in body temperature of free-living hyrax (*Procavia capensis*). Comp. Biochem. Physiol. A. Mol. Integr. Physiol. 143, 42–49.

Brown, R.E., Sergeeva, O., Eriksson, K.S., Haas, H.L., 2001. Orexin-A excites serotonergic neurons in the dorsal raphe nucleus of the rat. Neuropharmacology 40, 457–459.

Chen, C.T., Dun, S.L., Kwok, E.H., Dun, N.J., Chang, J.K., 1999. Orexin-A-like immunoreactivity in the rat brain. Neurosci. Lett. 260, 161–164.

Cutler, D.J., Morris, R., Sheridhar, V., Wattam, T.A., Holmes, S., Patel, S., Arch, J.R., Wilson, S., Buckingham, R.E., Evans, M.L., Leslie, R.A., Williams, G., 1999. Differential distribution of orexin-A and orexin-B immunoreactivity in the rat brain and spinal cord. Peptides 20, 1455–1470.

Date, Y., Ueta, Y., Yamashita, H., Yamaguchi, H., Matsukura, S., Kangawa, K., Sakurai, T., Yanagisawa, M., Nakazato, M., 1999. Orexins, orexigenic hypothalamic peptides, interact with autonomic, neuroendocrine and neuroregulatory systems. Proc. Natl. Acad. Sci. U.S.A. 96, 748–753.

De Lecea, L., Kilduff, T.S., Peyron, C., Gao, X., Foye, P.E., Danielson, P.E., Fukuhara, C., Battenberg, E.L., Gautvik, V.T., Bartlett, F.S., Frankel, W.N., Van den Pol, A.N., Bloom, F.E., Gautvik, K.M., Sutcliffe, J.G., 1998. The hypocretins: hypothalamus-specific peptides with neuroexcitatory activity. Proc. Natl. Acad. Sci. U.S.A. 95, 322–327.

Domínguez, L., Morona, R., Joven, A., González, A., López, J.M., 2010. Immunohistochemical localization of orexins (hypocretins) in the brain of reptiles and its relation to monoaminergic systems. J. Chem. Neuroanat. 39, 20–34.

Espana, R.A., Baldo, B.A., Kelley, A.E., Berridge, C.W., 2001. Wake-promoting and sleep-suppressing actions of hypocretin (orexin): basal forebrain sites of action. Neuroscience 106, 699–715.

Espana, R.A., Reis, K.M., Valentino, R.J., Berridge, C.W., 2005. Organization of hypocretin/orexin efferents to locus coeruleus and basal forebrain arousal-related structures. J. Comp. Neurol. 481, 160–178.

Fujiki, N., Yoshida, Y., Ripley, B., Honda, K., Mignot, E., Nishino, S., 2001. Changes in CSF hypocretin-1 (orexin-A) levels in rats across 24 hours and in response to food deprivation. Neuroreport 12, 993–997.

Galas, L., Vaudry, H., Braun, B., Van den Pol, A.N., De Lecea, L., Sutcliffe, J.G., Chartrel, N., 2001. Immunohistochemical localization and biochemical characterization of hypocretin/orexin-related peptides in the central nervous system of the frog *Rana ridibunda*. J. Comp. Neurol. 429, 242–252.

Gallyas, F., 1979. Silver staining of myelin by means of physical development. Neurol. Res. 1, 203–209.

Gatterman, R., Johnston, R.E., Yigit, N., Fritzsche, P., Larimer, S., Ozkurt, S., Neumann, K., Song, Z., Colak, E., Johnston, J., McPhee, M.E., 2008. Golden hamsters are nocturnal in captivity but diurnal in nature. Biol. Lett. 4, 253–255.

Gravett, N., Bhagwandin, A., Fuxe, K., Manger, P.R., 2009. Nuclear organization and morphology of cholinergic, putative catecholaminergic and serotonergic neurons in the brain of the rock hyrax, *Procavia capensis*. J. Chem. Neuroanat. 38, 57–74.

Hagan, J.J., Leslie, R.A., Patel, S., Evans, M.L., Wattam, T.A., Holmes, S., Benham, C.D., Taylor, S.G., Routledge, C., Hemmati, P., Munton, R.P., Ashmeade, T.E., Shah, A.S., Hatcher, J.P., Hatcher, P.D., Jones, D.N., Smith, M.I., Piper, D.C., Hunter, A.J., Porter, R.A., Upton, N., 1999. Orexin-A activates locus coeruleus cell firing and increases arousal in the rat. Proc. Natl. Acad. Sci. U.S.A. 96, 10911–10916.

Horvath, T.L., Diano, S., Van den Pol, A.N., 1999. Synaptic interaction between hypocretin (orexin) and neuropeptide Y cells in the rodent and primate hypothalamus: a novel circuit implicated in metabolic and endocrine regulations. J. Neurosci. 19, 1072–1087.

Huang, Z.L., Qu, W.M., Li, W.D., Mochizuki, T., Eguchi, N., Watanabe, T., Urade, Y., Hayaishi, O., 2001. Arousal effect of orexin-A depends on activation of the histaminergic system. Proc. Natl. Acad. Sci. U.S.A. 98, 9965–9970.

Huesa, G., Van den Pol, A.N., Finger, T.E., 2005. Differential distribution of hypocretin (orexin) and melanin-concentrating hormone in the goldfish brain. J. Comp. Neurol. 488, 476–491.

Iqbal, J., Pompolo, S., Sakurai, T., Clarke, I.J., 2001. Evidence that orexin-containing neurones provide direct input to gonadotropin-releasing hormone neurones in the ovine hypothalamus. J. Neuroendocrinol. 13, 1033–1041.
Kaslin, J., Nystedt, J.M., Östergård, M., Peitsaro, N., Panula, P., 2004. The orexin/hypocretin system in zebrafish is connected to the aminergic and cholinergic systems. J. Neurosci. 24, 2678–2689.
Khorooshi, R.M., Klingenspor, M., 2005. Neuronal distribution of melanin- concentrating hormone, cocaine- and amphetamineregulated transcript and orexin B in the brain of the Djungarian hamster (*Phodopus sungorus*). J. Chem. Neuroanat. 29, 137–148.
Kruger, J.-L., Dell, L.-A., Pettigrew, J.D., Manger, P.R., 2010. Cellular location and major terminal networks of the orexinergic system in the brains of five microchiropteran species. J. Chem. Neuroanat. 40, 256–262.
Kukkonen, J.P., Holmqvist, T., Ammoun, S., Åkermam, K.E.O., 2002. Functions of the orexinergic/hypocretinergic system. Am. J. Physiol. Cell Physiol. 283, C1567–C1591.
Lee, M.E., Hassani, O.K., Jones, B.E., 2005. Discharge of identified orexin/hypocretin neurons across the sleep–wake cycle. J. Neurosci. 25, 6716–6720.
López, J.M., Domínguez, L., Morena, N., González, A., 2009. Comparative immunohistochemical analysis of the distribution of orexins (hypocretins) in the brain of amphibians. Peptides 30, 873–887.
Matsuzaki, I., Sakurai, T., Kunii, K., Nakamura, T., Yanagisawa, M., Goto, K., 2002. Involvement of the serotonergic system in orexin-induced behavioral alterations in rat. Regul. Pept. 104, 119–123.
McGranaghan, P.A., Piggins, H.D., 2001. Orexin-A-like immunoreactivity in the hypothalamus and thalamus of the Syrian hamster (*Mesocricetus auratus*) and Siberian hamster (*Phodopus sungorus*), with special reference to circadian structures. Brain Res. 904, 234–244.
McNairn, I.S., Fairall, N., 1984. Metabolic rate and body temperature of adult and juvenile hyrax (*Procavia capensis*). Comp. Biochem. Physiol. A. Comp. Physiol. 79, 539–545.
Methippara, M.M., Alam, M.N., Szymusiak, R., McGinty, D., 2000. Effects of lateral preoptic area application of orexin-A on sleep–wakefulness. Neuroreport 11, 3423–3426.
Mintz, E.M., Van den Pol, A.N., Casano, A.A., Albers, H.E., 2001. Distribution of hypocretin-(orexin) immunoreactivity in the central nervous system of Syrian hamsters (*Mesocricetus auratus*). J. Chem. Neuroanat. 21, 225–238.
Moore, R.Y., Abrahamson, E.A., Van den Pol, A., 2001. The hypocretin neuron system: an arousal system in the human brain. Arch. Ital. Biol. 139, 195–205.
Nakamura, T., Uramura, K., Nambu, T., Yada, T., Goto, K., Yanagisawa, M., Sakurai, T., 2000. Orexin-induced hyperlocomotion and stereotypy are mediated by the dopaminergic system. Brain Res. 873, 181–187.
Nambu, T., Sakurai, T., Mizukami, K., Hosoya, Y., Yanagisawa, M., Goto, K., 1999. Distribution of orexin neurons in the adult rat brain. Brain Res. 827, 243–260.
Nixon, J.P., Smale, L., 2007. A comparative analysis of the distribution of immunoreactive orexin-A and B in the brains of nocturnal and diurnal rodents. Behav. Brain Funct. 13, 28.
Novak, C.M., Albers, H.E., 2002. Localization of hypocretin-like immunoreactivity in the brain of the diurnal rodent Arvicanthis niloticus. J. Chem. Neuroanat. 23, 49–58.
Novak, C.M., Smale, L., Nunez, A.A., 2000. Rhythms in Fos expression in brain areas related to the sleep–wake cycle in the diurnal Arvicanthis niloticus. Am. J. Physiol. Regul. Integr. Comp. Physiol. 278, R1267–R1274.
Ohkubo, T., Boswell, T., Lumineau, S., 2002. Molecular cloning of chicken prepro-orexin cDNA and preferential expression in the chicken hypothalamus. Biochim. Biophys. Acta 1577, 476–480.
Ohno, K., Sakurai, T., 2008. Orexin neuronal circuitry: role in the regulation of sleep and wakefulness. Front. Neuroendocrinol. 29, 70–87.
Olds, N., Shoshani, J., 1982. *Procavia capensis*. Mammalian Species 171, 107.
Peyron, C., Tighe, D.K., Van den Pol, A.N., De Lecea, L., Heller, H.C., Sutcliffe, J.G., Kilduff, T.S., 1998. Neurons containing hypocretin (orexin) project to multiple neuronal systems. J. Neurosci. 18, 9996–10015.
Piper, D.C., Upton, N., Smith, M.I., Hunter, A.J., 2000. The novel brain neuropeptide, orexin-A, modulates the sleep–wake cycle of rats. Eur. J. Neurosci. 12, 726–730.
Sakurai, T., Amemiya, A., Ishii, M., Matsuzaki, I., Chemelli, R.M., Tanaka, H., Williams, S.C., Richardson, J.A., Kozlowski, G.P., Wilson, S., Arch, J.R., Buckingham, R.E., Haynes, A.C., Carr, S.A., Annan, R.S., McNulty, D.E., Liu, W.S., Terrett, J.A., Elshourbagy, N.A., Bergsma, D.J., Yanagisawa, M., 1998. Orexins and orexin receptors: a family of hypothalamic neuropeptides and G protein-coupled receptors that regulate feeding behavior. Cell 92, 573–585.
Shibahara, M., Sakurai, T., Nambu, T., Takenouchi, T., Iwaasa, H., Egashira, S., Ihara, M., Goto, K., 1999. Structure, tissue distribution, and pharmacological characterization of *Xenopus orexins*. Peptides 20, 1169–1176.
Singletary, K.G., Delville, Y., Farrell, W.J., Wilczynski, W., 2005. Distribution of orexin/hypocretin immunoreactivity in the nervous system of the green treefrog, *Hyla cinerea*. Brain Res. 1041, 231–236.
Snyder, F., 1974. Sleep–waking patterns of Hyracoidea. Sleep Res. 3, 87.
Stoyanova, I.I., Rutten, W.L., le Feber, J., 2010. Orexin-A and orexin-B during the postnatal development of the rat brain. Cell Mol. Neurobiol. 30, 81–89.
Suzuki, H., Kubo, Y., Yamamoto, T., 2008. Orexin-A immunoreactive cells and fibers in the central nervous system of the axolotl brain and their association with tyrosine hydroxylase and serotonin immunoreactive somata. J. Chem. Neuroanat. 35, 295–305.
Szekely, M., Petervari, E., Balasko, M., 2010. Thermoregulation, energy balance, regulatory peptides: recent developments. Front. Biosci. 2, 1009–1046.
Tabuce, R., Asher, R.J., Lehmann, T., 2008. Afrotherian mammals: a review of current data. Mammalia 72, 2–14.
Taheri, S., Sunter, D., Dakin, C., Moyes, S., Seal, L., Gardiner, J., Rossi, M., Ghatei, M., Bloom, S., 2000. Diurnal variation in orexin-A immunoreactivity and prepro-orexin mRNA in the rat central nervous system. Neurosci. Lett. 279, 109–112.
Tao, R., Ma, Z., McKenna, J.T., Thakkar, M.M., Winston, S., Strecker, R.E., McCarley, R.W., 2006. Differential effect of orexins (hypocretins) on serotonin release in the dorsal and median raphe nuclei of freely behaving rats. Neuroscience 141, 1101–1105.
Teske, J.A., Billington, C.J., Kotz, C.M., 2010. Hypocretin/orexin and energy expenditure. Acta Physiol. 198, 303–312.
Vidal, L., Blanchard, J., Morin, L.P., 2005. Hypothalamic and zona incerta neurons expressing hypocretin, but not melanin concentrating hormone, project to the hamster intergeniculate leaflet. Neuroscience 134, 1081–1090.
Wagner, D., Salin-Pascual, R., Greco, M.A., Shiromani, P.J., 2000. Distribution of hypocretin-containing neurons in the lateral hypothalamus and c-fos-immunoreactive neurons in the VLPO. Sleep Res. 3, 35–42.
Yamamoto, Y., McKinley, M.J., Nakazato, M., Yamashita, H., Shirahata, A., Ueta, Y., 2006. Postnatal development of orexin-A and orexin-B like immunoreactivities in the Eastern grey kangaroo (Macropus giganteus) hypothalamus. Neurosci. Lett. 392, 124–128.
Yamanaka, A., Tsujino, N., Funahashi, H., Honda, K., Guan, J.L., Wang, Q.P., Tominaga, M., Goto, K., Shioda, S., Sakurai, T., 2002. Orexins activate histaminergic neurons via the orexin 2 receptor. Biochem. Biophys. Res. Commun. 290, 1237–1245.
Yamanaka, A., Muraki, Y., Tsujino, N., Goto, K., Sakurai, T., 2003. Regulation of orexin neurons by the monoaminergic and cholinergic systems. Biochem. Biophys. Res. Commun. 303, 120–129.
Yokogawa, T., Marin, W., Faraco, J., Pézeron, G., Appelbaum, L., Zhang, J., Rosa, F., Mourrain, P., Mignot, E., 2007. Characterization of sleep in zebrafish and insomnia in hypocretin receptor mutants. PLoS Biol. 5 (10), e277.
Yoshida, Y., Fujiki, N., Nakajima, T., Ripley, B., Matsumura, H., Yoneda, H., Mignot, E., Nishino, S., 2001. Fluctuation of extracellular hypocretin-1 (orexin-A) levels in the rat in relation to the light-dark cycle and sleep–wake activities. Eur. J. Neurosci. 14, 1075–1081.
Yoshida, K., McCormack, S., Espana, R.A., Crocker, A., Scammell, T.E., 2006. Afferents to the orexin neurons of the rat brain. J. Comp. Neurol. 494, 845–861.
Zhang, J.H., Sampogna, S., Morales, F.R., Chase, M.H., 2001. Orexin (hypocretin)-like immunoreactivity in the cat hypothlamus: a light and electron microscopic study. Sleep 24, 67–76.
Zhang, J.H., Sampogna, S., Morales, F.R., Chase, M.H., 2002. Co-localization of hypocretin-1 and hypocretin-2 in the cat hypothalamus and brainstem. Peptides 23, 1479–1483.
Zhang, J.H., Sampogna, S., Morales, F.R., Chase, M.H., 2004. Distribution of hypocretin (orexin) immunoreactivity in the feline pons and medulla. Brain Res. 995, 205–217.